Genetic regulation and biological function of the novel antimicrobial target gene *samA* in *Pseudomonas aeruginosa*

Thesis submitted to the University of Nottingham for the degree of
Doctor of Philosophy, November 2022

Ioanna Chatzigianni, MSc

14248394

Supervised by

Prof Miguel Cámara
Dr Stephan Heeb
Prof Paul Williams

Declaration

Unless otherwise acknowledged, the work presented in this thesis is my own. No part has been submitted for another degree at the University of Nottingham or any other institute of learning.



Ioanna Chatzigianni, November 2022

Disability and Covid-19 Statement

During the progress of this PhD, several experiments were affected by two serious injuries affecting my left arm and by the Covid-19 pandemic. The two injuries resulted on me taking a lot of time off to recover. After the second injury of one of my tendons I was diagnosed as disabled, which meant I could not undertake any more laboratory work. After long discussions with different departments within the University in order to come up with a resolution, a lot of time was lost. Unfortunately, the Covid-19 pandemic disrupted these complicated discussions and that had a strong impact on the amount of work that could be completed.

Among the biggest issues, was identifying an individual to take on the physical work of the project under my direct supervision. However, due to Covid-19 this possibility was deemed risky. Finally, after more discussions we identified Sam Fenn, a colleague, that had agreed to take on the work as he was familiar with many techniques that I used in my project. During that time Sam and me were always in contact and we were usually having meetings with our supervisors, Prof Miguel Cámara and Dr Stephan Heeb.

Sam had to work under conditions that also affected the number of daily hours that could be worked. Namely, restrictive access to BDI, with 8 hours long shifts available to do laboratory work (without including the cleaning times prior and after every shift). Also, no weekend access for several months as well as some weeks that were mandatory “work from home” only. Meanwhile, the waiting times for arrival of reagents and supplies were extended, not to mention at times the shortage of essential laboratory equipment.

More specifically to the outstanding work of this project, we had a necessity of growing strains under anaerobic conditions, which takes a lot of time. This it was delayed due to the lack of access to an anaerobic cabinet placed in other areas of the Biodiscovery Institute building.

For the reasons mentioned above the western blot analysis of FdhG protein production could not be performed, and thus, several aspects of this study remain inconclusive. This type of experiment requires extensive optimizations and due to limited time, this experiment was abandoned in order to carry out the validations of the RNA-seq results by RT-qPCR, in order to at least be able to conclude that part of the work.

Acknowledgments

First and foremost, I would like to thank my supervisors, Miguel Cámara and Stephan Heeb whose guidance has been outstanding. Miguel has mentored me throughout my project and his enthusiasm and motivation were key in this journey. Stephan has provided wonderful advice which have been very useful for the completion of this thesis. Both Miguel and Stephan are wonderful human beings, beyond supervisors, that cared about my wellbeing and offered me support in a myriad ways!

Special thanks to James McInerney, Vincent Wilson, Maria Murphy, Jennie Phillips, Tom Bagley, Dan Pitt and Owen Butler for their collective efforts to make this project completion possible despite all the unfortunate circumstances faced.

I would like to aknowledge the BBSRC Impact Acceleration Account (IAA) for funding SamA structure determination and Simon Caulton for demonstrating most of the techniques used for that part of the study.

To Sam, you have my deepest appreciation. Thank you for making this possible.

To Edu my guardian angel, your presence is the primary reason why I am here today able to write these acknowledgments and about to conclude this journey. You know how much I love you.

To the two brightest lights in my life in Nottingham, my sisters Nati and Maria E, thank you for keeping me from crashing time and time again. You are so precious to me chicas de mi corazon!

To the most crazy labmates that I am lucky to call my friends Manu, Elena, Celia, Nati and Edu… the list could go on. Thank you for all the funny moments in the lab, Jam Café & Bodega. I am walking away with the best memories that I will cherish forever!

To my precious partner, Marco your importance simply cannot be put in words alone! Ti voglio un mondo di bene!

Finally, to my ever caring family for there endless love and sacrifices and my friends from back home (Markella, Eirini, Rena, Maria T, Maria D , Evagoras & Michalis) for their love. THANK YOU.

This is especially for you grandpa Yianni, I miss you more every day.

Abstract

Pseudomonas aeruginosa is an opportunistic pathogen causing life-threatening infections due to the array of virulence factors it produces, in addition to being a multidrug-resistant organism for which conventional antibiotics fail to be adequate for treatment.

Therefore, the challenges posed by the global issue of drug-resistant bacterial infections call on the development of new strategies to tackle those infections. Non-biocidal approaches, that aim at 'disarming' the pathogens from virulence are in the spotlight.

The gene of interest investigated in this study, *samA* was uncovered by an integrated whole genome screening using several disease models as a promising antimicrobial target gene.

Hence, one aim of this PhD project, reported in Chapter 3 was to advance the knowledge of the *samA* gene's impact on the growth and production of virulence traits in *P. aeruginosa*, among others. The most striking finding was the twitching impairment in the *samA* gene deletion mutant and a possible role of *samA* in *P. aeruginosa* surface attachment.

Interestingly, *samA* is located upstream of a unique tRNA gene in *P. aeruginosa*, which is predicted to incorporate a unique aminoacid in proteins via a dedicated codon system. It was hypothesised that SamA might be acting as a methyltransferase adding a modification on this tRNA, ultimately aiding adaptation to anaerobiosis through a mechanism similar to the one described in *E. coli*.

Chapter 4 primarily sought to analyse SamA bioinformatically and, secondly, to assess the catalytic activity of SamA in *P. aeruginosa*. The main finding from this chapter was that the predicted secondary structure of SamA indicates that it could be a putative tRNA methyltransferase, though further work remains to be done in this direction.

Since it was hypothesized that SamA modifies this unique tRNA, Chapter 5 reports the *in silico* analysis of this unique tRNA and the unique modified protein sequences from *P. aeruginosa* to assess their potential in roles equivalent to those described in *E. coli.* Overall, the findings from the bioinformatic analysis supported this hypothesis, which constitutes a starting point for future work on the elucidation of these mechanisms in *P. aeruginosa.*

To get a broader view of the functions and unravel the roles of SamA and this tRNA's in *P. aeruginosa*, Chapter 6 sought to use transcriptomics. The results indicate that *samA* has a greater effect under anaerobic compared to aerobic conditions, which suggests a more important role for SamA under those conditions. This is in line with the hypothesis that SamA plays a role in *P. aeruginosa* adaptation to anaerobic growth.

However, the most striking finding was that in the tRNA-deficient mutant the equivalents of two homologous genes involved in this decoding mechanism in *E.coli* were found downregulated.

All in all, this study paved the way towards the elucidation of the roles played by SamA and the unique tRNA in the lifestyle of *P. aeruginosa.* The results otained have also suggested a possible involvement of these uniquely modified proteins in the virulence of *P. aeruginosa*. These findings have therefore highlighted the importance of further characterising these proteins since they may be exploited as potential targets for preventing *P. aeruginosa* infections.

Table of Contents

CHAPTER 1 General Introduction 18

1.1 *Pseudomonas aeruginosa* overview 18

1.2 Relevance of studying *P. aeruginosa* 19
1.2.1 *P. aeruginosa* as a pathogen 19
1.2.1.1 *P. aeruginosa* in Cystic Fibrosis 20
1.2.2 *P. aeruginosa* virulence and colonisation mechanisms 22
1.2.3 Pyocyanin 24
1.2.4 Proteases 25
1.2.5 Other colonisation factors 27

1.3 Colonization mechanisms 28
1.3.1 Motility 28
1.3.2 Biofilm 32

1.4 Regulatory mechanisms of pathogenicity in *P. aeruginosa* 36
1.4.1 Quorum sensing systems in *P. aeruginosa* 36
1.4.1.1 *las* and *rhl* systems 38
1.4.1.2 *Pseudomonas* Quinolone Signal (PQS) QS 39

***1.5* Antibiotic resistance in *P. aeruginosa* 43**
1.5.1 Intrinsic resistance 44
1.5.2 Acquired resistance 44
1.5.3 Adaptive resistance 45
1.5.4 Biofilm-associated resistance 45

***1.6* . Non-traditional strategies to target Bacterial Infections with a focus on *P. aeruginosa* 46**
1.6.1 Introduction: Challenges in fighting bacterial infections 46
1.6.2 The concept of antivirulence strategies, the potential targets 47
1.6.3 New antipseudomonal antibiotics 49
1.6.4 Virulence factor secretion targeting 50
1.6.4.1 Immunotherapy 51
1.6.5 Adhesion and Biofilm formation targeting 52
1.6.6 Bacterial communication targeting 53
1.6.7 Counteraction of Immune evasion 54
1.6.8 Phage therapy (eg. As carriers, using phage-derived products) 54
1.6.9 Novel therapeutic strategies for *P. aeruginosa* treatment 55
1.6.9.1 Lectin inhibitors 55
1.6.9.2 Iron chelation 55
1.6.9.3 Efflux pumps 55
1.6.9.4 Vaccines 56
1.6.9.5 Pseudolysin 56
1.6.9.6 Immunotherapy 56
1.6.9.7 Antisense RNA 57
1.6.10 Conclusions 57

1.7 *P. aeruginosa* model strain genomic background 59

1.8 Identification of novel putative antimicrobial targets in *P. aeruginosa* 59

1.9 Aims of this study 60

CHAPTER 2 Materials and methods 61

2.10 Bacterial strains and growth conditions 61
2.10.1 Media and antibiotic concentrations 61
2.10.1.1 Chemically defined medium (CDM) 61
2.10.1.2 Minimal M9 medium 61
2.10.1.3 Nutrient Broth 61
2.10.1.4 *Pseudomonas* isolation agar 62
2.10.1.5 Terrific Broth 62
2.10.1.6 Roswell Park Memorial Institute (RPMI) 1640 Medium 62
2.10.2 Culture growth 62
2.10.3 Bacterial storage/ Bacteria preservation 62

2.11 General chemicals 62

2.12 DNA manipulation 63
2.12.1 Strains and plasmids 63
2.12.2 Molecular procedures 68
2.12.3 Construction of biosensors 71
2.12.3.1 Construction of PA4802.1 transcriptional gene fusion reporter 71
2.12.4 Construction of deletion mutants and their complementation plasmids 72
2.12.4.1 Construction of the *P. aeruginosa* PA4802.1 deletion mutant. 72
2.12.4.2 Construction of *samA* gene complementation plasmid 75
2.12.4.3 Construction of PA4802.1 gene complementation plasmid 76
2.12.4.4 Construction of *samA* and PA4802.1 gene complementation plasmid 77
2.12.5 Construction of the *P. aeruginosa* conditional mutant PA4803ind (samA*Ind*) strain 78
2.12.6 Construction of chromosomal His-tagged *fdhG* gene strain in *P. aeruginosa.* 80

2.13 Phenotypic characterization assays 81
2.13.1 Growth assays 81
2.13.2 Construction of strains by conjugation 81
2.13.3 Motility assays 82
2.13.3.1 Swarming motility 82
2.13.3.2 Twitching motility 82
2.13.4 Exoproduct quantification assays 82
2.13.4.1 Pyocyanin 83
2.13.4.2 Alkaline protease, AprA 83
2.13.4.3 Elastase, LasB 83
2.13.5 Alkyl quinolone extractions and LC-MS/MS quantification analysis 83

2.14 Transposon mutagenesis 84
2.14.1 Transposon insertion locations 84

2.15 Gene expression analysis 84
2.15.1 Biosensor based gene expression assays / Microtiter plate assay 84
2.15.2 RNA isolation (and reverse transcription) 84

2.15.3 (q)RT-PCR 85
2.15.4 RNA-Seq library construction and sequencing 86
2.15.5 RNA-seq analysis 86

2.16 Bioinformatics/structure determination of PA4803 and PA4802.1 genes 86
2.16.1 Alignment of primary and secondary structures / Secondary structure predictions 86
2.16.2 Prediction of tertiary structures (and ligand binding sites) 86

2.1 PA4803 protein production, purification and crystallization 88
2.16.3 PA4803 *(samA)* gene expression 88
2.16.4 Sample preparation and expression analysis by SDS-PAGE and Western Blotting 89
2.16.5 Purification of MBP and/or Hexahistidine tagged PA4803 (SamA) 89
2.16.6 Size exclusion chromatography/Gel filtration 90
2.16.7 Crystallization trials and Optimization of conditions 90
2.16.8 Pull down assays 90

2.17 Results analysis 93
2.17.1 Pixel integration analysis 93
2.17.2 Statistical analysis 93

CHAPTER 3 Initial characterisation of the impact of PA4803 (*samA*) and PA4802.1 in the biology of *P. aeruginosa* 94

3.1 Introduction 94
3.1.1 Discovery of PA4803 (*samA*) as a putative antimicrobial target 94
3.1.2 Background information on PA4803 (*samA*) gene 96
3.1.3 Discovery of PA4802.1 in the vicinity of PA4803 (*samA*). 98
3.1.4 Aims of the study 98

3.2 Results 100
3.2.1 Phenotypic characterization of an in-frame *samA* deletion mutant 100
3.2.1.1 Impact of *samA* on *P. aeruginosa* growth 100
3.2.1.1.1 Aerobic conditions 100
3.2.1.1.2 Anaerobic conditions 103
3.2.1.2 Effect of *samA* deletion on motility and exoproduct production of *P. aeruginosa* 103
3.2.1.2.1 Swarming and Twitching 103
3.2.1.2.2 Pyocyanin, Elastase and Alkaline Protease production 105
3.2.1.3 Initial investigation of the *samA* regulon 105
3.2.1.3.1 *samA* and quorum sensing (QS) 105
3.2.1.3.2 Modulation of quorum sensing signalling molecules (QSSMs) production by SamA 108
3.2.1.4 Identification of genes impacting on samA expression using a Tn*5*-based approach and study of their impact on virulence trait production. 109
3.2.2 Phenotypic characterization of *PA4802.1* deletion mutant strain 113
3.2.2.1 Impact of PA4802.1 on *P. aeruginosa* growth 113
3.2.2.2 Effect of a *PA4802.1* deletion on the motility of *P. aeruginosa* 114
3.2.2.2.1 Swarming and Twitching 114
3.2.2.3 Initial investigation of PA4802.1 regulon 115
3.2.2.3.1 PA4802.1 and QS 115
3.2.3 Impact of SamA on PA4802.1 expression 116

3.3 Discussion 117

CHAPTER 4 SamA protein crystallization and functionality 126

4.1 Introduction 126
4.1.1 S-adenosylmethionine (SAM) and its metabolism in bacteria 126
4.1.2 The versatility of S-adenosylmethionine (SAM) and the SAM-binding proteins 127
4.1.3 SAM-dependent methyltransferases classifications 128
4.1.4 SAM-dependent methyltransferases in the biology of *P. aeruginosa* 130
4.1.4.1 HemK (PrmC), a universally conserved SAM-dependent methyltransferase 130
4.1.4.2 PrmC and SamA relations 131
4.1.5 Aims of the study 132

4.2 Results 133
4.2.1 *In silico* characterization of *P. aeruginosa* SamA protein 133
4.2.2 PA4803 expression, protein purification and crystallization 137
4.2.2.1 PA4803 production and protein purification 137
4.2.2.2 Size exclusion chromatography 139
4.2.2.3 Crystallization trials 143
4.2.2.4 Pull down assays 146

4.3 Discussion 148
4.3.1 PA4803 production, purification and crystallization 148
4.3.2 Pull down assays 150
4.3.3 Conclusion and Future directions 151

CHAPTER 5 Possible link between the selenocysteine-tRNA in *P. aeruginosa* encoded by PA4802.1 and SamA 152

5.1 Introduction 152
5.1.1 The unique process of selenocysteine incorporation into selenoproteins 152
5.1.2 The (bacterial) SECIS element and SECIS search-based identification of selenoproteins 153
5.1.3 Biosynthesis and Identity of the $tRNA^{Sec}$ in *E. coli* 155
5.1.4 The SECIS-like element function in *E. coli* 156
5.1.5 Phylogenetic analysis of the selenocysteine decoding trait in bacteria 158
5.1.6 Prokaryotic selenoproteins functions 159
5.1.6.1 Selenoproteins and Anaerobiosis 159
5.1.7 Modification of tRNA 161
5.1.7.1 tRNA methytransferases and tRNA methylation 161
5.1.8 Selenocysteine-inserting tRNAs 162
5.1.8.1 Bacterial selenocysteine-inserting tRNAs 162
5.1.8.2 Eukaryal selenocysteine-inserting tRNAs 162
5.1.9 Main Hypothesis 164
5.1.10 Aims of the study 166

5.2 Results 167
5.2.1 *In silico* characterisation of *P. aeruginosa* $tRNA^{sec}$ 167
5.2.1.1 Alignment of the $tRNA_{sec}$ from *E. coli* with that from *P. aeruginosa* 167
5.2.2 Biological function and regulation of PA4802.1 171
5.2.2.1 In silico characterisation of the regulatory elements involved in selenocysteine incorporation in *P. aeruginosa* 171
5.2.2.2 *In silico* characterisation of the suspected *P. aeruginosa* selenoprotein FdoG 172

5.3 Discussion 178
5.3.1 Future directions 181

CHAPTER 6 Impact of samA and PA4802.1 on global gene expression in *P. aeruginosa* 183

6.1 Introduction 183
6.1.1 Aims of this research 185

6.2 Results 186
6.2.1 Impact of *samA* on global gene expression in *P. aeruginosa* grown under aerobic and anaerobic conditions 189
6.2.1.1 Impact of *samA* on global gene expression in *P. aeruginosa* by RNA-seq grown under aerobic conditions. 190
6.2.1.1.1 Identification of Downregulated DEGs by *samA* deletion under aerobic conditions 192
6.2.1.1.2 Identification of Upregulated DEGs by *samA* deletion under aerobic conditions 193
6.2.1.1.3 Functional classification of downregulated and upregulated DEGs found under aerobic conditions, identified due to *samA* deletion 196
6.2.1.2 Impact of *samA* on global gene expression in *P. aeruginosa* by RNA-seq grown under anaerobic conditions. 198
6.2.1.2.1 Identification of Downregulated DEGs by the *samA* deletion under anaerobic conditions 198
6.2.1.2.2 Identification of Upregulated DEGs by PA4803 (*samA*) deletion under anaerobic conditions 202
6.2.1.2.3 Functional classification of downregulated and upregulated DEGs found under anaerobic conditions, identified due to *samA* deletion 205
6.2.2 Impact of PA4802.1 on global gene expression in *P. aeruginosa* by RNAseq grown under both aerobic and anaerobic conditions. 207
6.2.2.1 Impact of PA4802.1 on global gene expression in *P. aeruginosa* by RNAseq under both aerobic conditions 207
6.2.2.1.1 Identification of Downregulated DEGs by PA4802.1 deletion under aerobic conditions 208
6.2.2.1.2 Identification of Upregulated DEGs by PA4802.1 deletion under aerobic conditions 209
6.2.2.1.3 Functional classification of downregulated and upregulated DEGs found under aerobic conditions, identified due to the PA4802.1 deletion 211
6.2.2.2 Impact of PA4802.1 on global gene expression in *P. aeruginosa* by RNAseq grown under anaerobic conditions 211
6.2.2.2.1 Identification of Downregulated DEGs by PA4802.1 deletion under anaerobic conditions 211
6.2.2.2.2 Identification of Upregulated DEGs by PA4802.1 deletion under anaerobic conditions 212
6.2.2.2.3 Functional classification of downregulated and upregulated DEGs found under anaerobic conditions in the PA4802.1 deletion mutant 212
6.2.3 qRT-PCR Validation of the RNA-seq data 213

6.3 Discussion 217
6.3.1 Impact of SamA and PA4802.1 under aerobic conditions 218
6.3.2 Impact of SamA and PA4802.1 under anaerobic conditions 220
6.3.3 Impact of PA4802.1 on *fdnH* and *fdhI* 224

6.4 Future directions 225

6.5 Summary 225

6.6 Conclusions 226

CHAPTER 7 General Discussion 227

BIBLIOGRAPHY 235

List of Figures

Figure 1.1. Flagellum and Type 4 pili (T4P) structures in *P. aeruginosa*.....31
Figure 1.2. Schematic representation of AHL-dependent and AQ-dependent QS systems in *P. aeruginosa*. 42
Figure 1.3 The virulence factors of *P. aeruginosa* discussed in this thesis.....43

Figure 2.1. Schematic of the strategy used to construct the PA4802.1 biosensor. 72
Figure 2.2. Schematic of the strategy used to construct the *P. aeruginosa* PA4802.1 deletion mutant. 74
Figure 2.3. Schematic of the strategy used to construct the *P. aeruginosa samA* gene complementation vector. 75
Figure 2.4. Schematic of the strategy used to construct the *P. aeruginosa* PA4802.1 gene complementation vector 76
Figure 2.5. Schematic of the strategy used to construct the *P. aeruginosa samA* and PA4802.1 gene complementation vector. 77
Figure 2.6. Schematic of the strategy used to construct the *P. aeruginosa samA*Ind strain 79
Figure 2.7. FdhG protein tagging through a chromosomal insertion – Cloning strategy 81
Figure 2.8. Protein purification protocol flowchart. 88
Figure 2.9. Pull down assay schematic. 92
Figure 2.3. Schematic of the strategy used to construct the *P. aeruginosa samA* gene complementation plasmid. 75
Figure 2.4. Schematic of the strategy used to construct the *P. aeruginosa* PA4802.1 gene complementation plasmid 76
Figure 2.5. Schematic of the strategy used to construct the *P. aeruginosa samA* and PA4802.1 gene complementation plasmid. 77

Figure 3.1. Schematic of the process followed to identify putative antimicrobial target genes. 95
Figure 3.2. Genetic context of PA4803 (*samA*).....97
Figure 3.3. PA4803 (*samA*) predicted network by STRING.....98
Figure 3.4. Growth curves determined manually for the wt and the *samA* mutant (*ΔsamA*) under aerobic conditions in several growth media.....101
Figure 3.5. Growth curves determined automatically for the wt and the *samA* deletion (*ΔsamA*) under aerobic conditions in several growth media. 102
Figure 3.6. Growth curves determined manually for the wt and the *ΔsamA* under aerobic conditions and anaerobic conditions. 103
Figure 3.7. Effect of samA deletion on *P. aeruginosa* PAO1-L motilities.....104
Figure 3.8. Impact of samA deletion on exoproduct production of *P. aeruginosa* PAO1-L. 105
Figure 3.9. Effect of quorum sensing genes (*lasI, rhlI, pqsA and vfr*) on *samA* gene expression. 106
Figure 3.10. Promoter activity of the *lasI, rhlI* and *pqsA* quorum sensing genes in the *samA* mutant and the samAInd background. 107
Figure 3.11. Quantitative profiling of QSSMs by LC-MS/MS. 108
Figure 3.12. Effect of selected Tn*5* chromosomal insertions on samA gene expression. 109
Figure 3.13. Motility profiles of selected *P. aeruginosa* PAO1-L Tn5 mutants.....112
Figure 3.14. The effect of selected Tn5 insertions on *P. aeruginosa* PAO1-L pyocyanin production and proteolytic activity. 113

Figure 3.15. ManualGrowth curves for the WT, the ΔsamA and PA4802.1 mutant (aka ΔtRNA^{sec}) under aerobic conditions and anaerobic conditions. 114
Figure 3.16. Role of PA4802.1 in *P. aeruginosa* PAO1-L swarming and twitching motilities. 115
Figure 3.17. Effect of quorum sensing genes (*lasI, rhlI, pqsA* and *vfr*) on PA4802.1 gene expression. 116
Figure 3.18. Role of *samA* on PA4802.1 promoter activity**.** 117

Figure 4.1. The S-adenosylmethionine (SAM) metabolism in bacteria. 127
Figure 4.2. The tertiary structures of the five classes of SAM-dependent methyltransferases (MTases)..... 129
Figure 4.3. SamA (PA4803) and PrmC (PA4664) gene expression profiles under oxygen limitation conditions..... 132
Figure 4.4. A graphical output of the predicted secondary structure of the SamA protein. 133
Figure 4.5. Schematic representation of the putative topology of SamA protein following the Class I methyltransferases fold. 134
Figure 4.6. SamA predicted 3D protein structures as determined by the iterative threading assembly refinement**.** 136
Figure 4.7. Western blot analysis of the SamA C-terminal His-tagged protein overexpressed using the pSK67 expression vector. 137
Figure 4.8. Schematic of the recombinant fusion constructs Histag-SamA-(MBP) products. 138
Figure 4.9. Expression analysis of the *samA*–MBP fusion C-terminal His-tagged protein overexpressed using the pMALX(E) vector. 139
Figure 4.10. Gel filtration of the SamA-MBP fusion C-terminal His-tagged protein with no-cleavable tags overexpressed using the pIC14. 140
Figure 4.11. Gel filtration of the SamA-MBP fusion C-terminal His-tagged protein with cleavable MBP, overexpressed using the pIC15. 140
Figure 4.12. Additive Gel filtration of SamA-MBP fusion C-terminal His-tagged protein overexpressed using the pMALX(E). 141
Figure 4.13. Summary of C-terminal His-tagged protein with cleavable MBP overexpressed using the pIC15 vector processing. 142
Figure 4.14. Gel filtration of the Histag-SamA overproduced using the pIC13 (pCOLD1::samA) vector. 143
Figure 4.15. Pull down assays using SamA fusion His-tagged protein (with and without linker region) overproduced using the pMALX(E) and/or pCOLD1 vectors. 147
Figure 4.13. Summary of C-terminal His-tagged protein with cleavable MBP overexpressed using the pIC15 plasmid processing. 142
Figure 4.14. Gel filtration of the Histag-SamA overproduced using the pIC13 (pCOLD1::samA) plasmid. 143

Figure 5.1. Interactions involved in the assembly of a functional quaternary complex SelB • GTP • mRNA • Sec-tRNA^{Sec} complex. 153
Figure 5.2. bSECIS consensus structural model and minimum ORF constraints. 154
Figure 5.3. Reactions involved in the biosynthesis of selenocysteine tRNA in *E. coli.* 155
Figure 5.4. Interaction of SelB with the SECIS and the SECIS-like of the fdhF mRNA of the *selAB* mRNA, respectively. 157
Figure 5.5. Secondary structure of tRNA^{Sec} from *E. coli.* 162

Figure 5.6. Cloverleaf tRNA(ser)sec models of *E. coli* (left panel) and mammalian (right panel). 163
Figure 5.7. Current hypothesis. 165
Figure 5.8. A model of UGA decoding during selenoprotein synthesis....166
Figure 5.9. Sequence alignment between the tRNA-Sec of *E. coli* (encdoded by selC) and the tRNA-Sec of *P. aeruginosa* PAO1 (encoded by PA4802.1). 169
Figure 5.10. The different cloverleaf predicted structures of PA4802.1 $tRNA^{sec.}$....170
Figure 5.11. SECIS alignment of PA4808/*selA* from *P. aeruginos*a upstream region and selA SECIS-like element from *E. coli*. 171
Figure 5.12. *P. aeruginosa* PA4808/*selA* SECIS-like element secondary structure predictions**.** 172
Figure 5.13. Primary sequence of the *P. aeruginosa* PA4812/fdhG protein. 173
Figure 5.14. SECIS alignment of the *fdnG*, *fdhF* and *fdoG* genes of *E. coli*, encoding formate dehydrogenase isoenzymes. 173
Figure 5.15. *E. coli fdnG*, *fdhF* and *fdoG* SECIS elements secondary structure predictions. 174
Figure 5.16. SECIS alignment of PA4812/*fdhG* from *P. aeruginosa* and *fdoG* from *E. coli.* 175
Figure 5.17. Comparison of *P. aeruginosa* PA4812/*fdhG* and *E. coli fdoG* SECIS elements secondary structure predictions. 175
Figure 5.18. SECIS element component organization of the *P. aeruginosa fdhG* gene (upper schematic) and *E. coli fdoG* gene (lower schematic). 176
Figure 5.19. SDS-PAGE and Western blot analysis of the chromosomally His-tagged FdhG protein under aerobic and anaerobic conditions**.** 177
Figure 5.20. Experimental design for the identification of modifications on the specific tRNAsec under investigation. 181

Figure 6.1. Volcano plot of RNA-seq transcriptome data displaying the pattern of gene expression values for *ΔsamA***.** 190
Figure 6.2. Venn diagram showing the overlap of DEGs among the four comparisons....191
Figure 6.3. Volcano plot of RNA-seq transcriptome data displaying the pattern of gene expression**.** 207
Figure 6.4. Expression analysis for *cdrA* gene....215
Figure 6.5. Expression analysis for *pscQ* and *oprM* genes....216
Figure 6.6. Expression analysis for *fdhG a*nd *fdhH* genes....217

List of Tables

Table 1.1. Main Virulence factors in *P. aeruginosa* that are discussed within this thesis[a] 23

Table 2.1. Overview of antibiotic concentration usage in this study. 61
Table 2.2. Bacterial strains and plasmids used in this study. 63
Table 2.3. Primers used in this study. 68
Table 2.4. Detailed PCR amplification programs used in this study. 70
Table 2.5. Primers used in this study for qRT-PCR purposes. 85
Table 2.6. Summary of online servers and tools used for Protein and RNA Bionformatic analysis[a] 87

Table 3.1. Identification of Tn*5* disrupted genes probably involved in the regulation of *samA* gene expression. 110

Table 4.1 Summary of Crystallization screen conditions set up during this study. 143

Table 5.1. Summary of BLASTN hits for PA4802.1 (tRNA-Sec, from PAO1 reference strain) which overlapped with the 104 ortholog list for the samA gene (hypothetical protein, from PAO1 reference strain), which were all *P. aeruginosa* strains 167

Table 6.1. Strain nomenclature. 186
Table 6.2. Data Quality Control Summary. 187
Table 6.3. Overview of Mapping Status. 188
Table 6.4. Numbers of DEGs affected in each comparison between strains, performed by RNA-seq. 189
Table 6.5. Summary of genes found downregulated due to *samA* deletion under aerobic conditions. 192
Table 6.6. Summary of genes found upregulated due to *samA* deletion under aerobic conditions. 193
Table 6.7. KEGG Pathway Enrichment Summary of downregulated and upregulated DEGs found under aerobic conditions, identified due to *samA* deletion. 196
Table 6.8. Summary of genes found downregulated due to *samA* deletion under anaerobic conditions 198
Table 6.9. Summary of genes found upregulated due to *samA* deletion under anaerobic conditions**.** 202
Table 6.10. KEGG Pathway Enrichment Summary of downregulated and upregulated DEGs found under anaerobic conditions, identified due to *samA* deletion**.** 205
Table 6.11. Summary of genes found downregulated due to PA4802.1 deletion under aerobic conditions. 208
Table 6.12. Summary of genes found upregulated due to PA4802.1 deletion under aerobic conditions 209
Table 6.13. Summary of genes found downregulated due to the PA4802.1 deletion under anaerobic conditions. 211
Table 6.14. Summary of genes found upregulated due to PA4802.1 deletion under anaerobic conditions 212

Table 6.15. KEGG Pathway Enrichment Summary of downregulated and upregulated DEGs found under anaerobic conditions, identified due to PA4802.1 deletion. 212

Abbreviations used in this thesis

ºC	Degrees Celsius
3-oxo-C12-HSL	*N*-(3-oxododecanoyl)-L-homoserine lactone
AHL	*N*-acyl-L-homoserine lactone
Ap	Ampicillin
AQ	2-alkyl-4-quinolones
AUC	Area under the curve
bp	Base pair
C4-HSL	*N*-butanoyl-L-homoserine lactone
Cb	Carbenicillin
CDM	Chemically defined media
CF	Cystic fibrosis
CFTR	Cystic fibrosis transmembrane conductance regulator
Cm	Chloramphenicol
DNA	Deoxyribonucleic acid
EPS	Extracellular polymeric substances
g	Grams
GFP	Green fluorescent protein
Gm	Gentamicin
h	Hour
HCl	Hydrochloric acid
HHQ	2-heptyl-4-quinolone
IPTG	Isopropyl-1-thio-(β-D-galactopyranoside)
kb	Kilobase
kDa	kilo Daltons
Km	Kanamycin
kV	Kilovolts
L	Litre
LB	Lysogeny broth
LC-MS/MS	Liquid chromatography-tandem mass spectrometry
MBP	Maltose Binding Protein
Min	Minute
mL	Millilitre
mM	Millimolar concentration
MOPS	3-(N-morpholino)propanesulfonic acid
Nal	Nalidixic acid
NB	Nutrient Broth medium
Nm	Nanometre
nM	Nanomolar concentration
OD	Optical density
ORF	Open reading frame
PCR	Polymerase chain reaction
PDB	Protein Data Bank
PIA	Pseudomonas isolation agar

PQS	Pseudomonas quinolone signal, 2-heptyl-3-hydroxy-4-quinolone
QS	Quorum sensing
QSSMs	Quorum sensing signal molecules
RLU	Relative luminescent units
RMSD	Root mean square deviation
RNA	Ribonucleic acid
rpm	Revolutions per minute
RPMI	Roswell park memorial institute media
s	Second
Sm	Streptomycin
T4P	Type IV pili
Tc	Tetracycline
TCS	Two component systems
UV	Ultraviolet light
v/v	Volume per volume
w/v	Weight per volume
µg	Microgram
µL	Microliter
µM	Micromolar concentration

Chapter 1 General Introduction

1.1 *Pseudomonas aeruginosa* overview

Pseudomonas spp. are Gram-negative bacteria that are widespread in the environment (Girard and Bloemberg, 2008). The most studied of the *Pseudomonas* species is *Pseudomonas aeruginosa* which, belongs to the phylum of Proteobacteria and is classified as Gammaproteobacterium (Girard and Bloemberg, 2008). *P. aeruginosa* bacteria can be found in various aquatic and terrestrial habitats, as well as on plant and animal tissues (Girard and Bloemberg, 2008; Stover *et al*., 2000). *P. aeruginosa* can colonize and cause infections in a wide range of host organisms, including plants, nematodes, insects, and vertebrates (Ozer *et al.*, 2014). It is an opportunistic human pathogen in patients with compromised immune defence capable of causing a wide array of life-threatening acute and chronic infections (Moradali *et al.*, 2017). *P. aeruginosa* is able to survive in the unfavourable conditions encountered in these diverse environments due to the arsenal of virulence factors it produces and secretes but also due to the formation of biofilm structures (Stover *et al.*, 2000; Trunk *et al.*, 2010). However, despite the pathogenic capacity of *P. aeruginosa* some of its strains can be beneficial in terms of plant growth (Sulochana *et al.*, 2014).

The striking environmental versatility of *P. aeruginosa* is attributed to its relatively large genome size, which is 6.3 Mb for *P. aeruginosa* PAO1, (Girard and Bloemberg, 2008; Breidenstein *et al.*, 2011; Stover *et al.*, 2000; Ozer *et al.*, 2014). It is also attributed to its very high proportion of regulatory genes, 8.4% in strain PAO1, compared to 5.8 % in *E. coli* for example (Girard and Bloemberg, 2008; Breidenstein *et al.*, 2011). For a large proportion of the genome (45.8% of ORFs) no function has yet been assigned (confidence level 4).

Interestingly, there is a high degree of genomic conservation between *P. aeruginosa* clinical and environmental isolates which is still difficult to explain but with high levels of recombination (Silby *et al.*, 2011; Wolfgang *et al.*, 2003; Grosso-Beccera *et al.*, 2014; Mansfeld *et al.*, 2010). Therefore, it could be that clinical strains could survive and persist in natural environments and that environmental strains could easily become pathogens. This phenomenon observed in *P. aeruginosa* strains makes it a difficult to design strategies, based on vaccination or hygiene measures, for treatment of infections caused by these bacteria. This highlights once again the need to design strategies that target the virulence traits expressed by *P. aeruginosa*.

Biofilms and microcolonies are important growth forms for survival under these unfavourable conditions (Costerton *et al.*, 1995; Stoodley *et al*., 2002; Hassett *et al*., 2009). It has been shown that microaerobic to anaerobic conditions dominate in *P. aeruginosa* biofilms (Hassett *et al.*, 1999; Worlitzsch *et al.*, 2002; Yoon *et al.*, 2002). In the absence of oxygen and the presence of nitrate or nitrite *P. aeruginosa* is able to grow by denitrification, or in the presence of arginine by substrate-level phosphorylation.

1.2 Relevance of studying *P. aeruginosa*

1.2.1 *P. aeruginosa* as a pathogen

P. aeruginosa is a commensal microorganism of plants and animals (Paulsen *et al.*, 2005; Cogen *et al.*, 2009). However, it can cause infections in various plant species, protozoa, and animals. Non-mammals affected by *P. aeruginosa* infections include *Caernorhabditis elegans* and *Drosophila* sp. and mammals (Cogen *et al.*, 2009) include dogs, bovines and small ruminants (Matz *et al.*, 2009; Scaccabarozzi *et al.*, 2015; Argenio *et al.*, 2001; Tan, 1999). These bacteria can evolve to survive and compete effectively in numerous environments (generalists) or in a particular niche (specialists)(Folkesson *et al.*, 2012).

P. aeruginosa is a human skin commensal, and it can also be found in the stool, urine, and axilla of healthy individuals (Morrison and Wenzel, 1984). However, it can easily become pathogenic if the skin barrier is weakened or broken or the person is immunocompromised, causing both acute and chronic infections (Cogen *et al.*, 2009). *P. aeruginosa* is categorized as an opportunistic pathogen because it can infect immunocompromised human hosts (Balasubramanian *et al.*, 2014). It is a significant source of bacteraemia in burn victims, urinary-tract infections in catheterized patients, and hospital-acquired pneumonia in patients on respirators (Bodey *et al.*, 1983). Overall, *P. aeruginosa* is the leading cause of nosocomial infections especially for cystic fibrosis patients and is rising as a major public health problem (Ball *et al.*, 2000).

P. aeruginosa produces an array of virulence factors, which sustain the acute infections. They change accordingly and contribute to the establishment of chronic infections (Jimenez *et al*., 2012; Breidenstein *et al*., 2011). Significant changes in the phenotypes between acute and chronic infections of *P. aeruginosa* are observed. The high intrinsic antibiotic resistance of this bacterium (Mah *et al.*, 2003; Lewis, 2007) together with biofilm formation which protects the cells from antimicrobials and the immune system, render chronic infections virtually impossible to eradicate (Lopes *et al.*, 2012; Mann and Wozniak, 2012; Harmsen *et al.*, 2010). Obviously, very high antibiotic concentrations are required to kill bacteria organized in biofilms (Oliver *et al.*, 2017). Taken together, the use of antibiotics as well as the host's immune response create a harsh environment which imposes selective pressure

on *P. aeruginosa* resulting in increased emergence of resistant strains (Raidt, 2015). Therefore, there is a need for alternative treatment strategies which do not pose this type of pressure such as anti-virulence strategies which do not kill the pathogen but instead prevent it from thriving in the host's environment (Zhu and Kaufmann, 2013).

As mentioned, bacteria change their phenotype during the transition between infection states. For example, they limit virulence factor secretion and they generally become less active as a way to become less immunogenic. However, some bacterial components are still immunogenic which causes an inflammatory response resulting in extensive tissue damage (Jensen *et al.*, 2010; Høiby *et al.*, 2015). To add on the complexity of this organism, the dispersed cells present a distinct phenotype from biofilm or planktonic (Chua *et al.*, 2014).

P. aeruginosa can infect a vast range of plant hosts such as lettuce, *Arabidopsis* leaves and roots, sweet basil as well as the rhizosphere of wheat and tomato (Starkey *et al.*, 2009; Walker *et al.*, 2004; Mendes *et al.*, 2013). Plant infections are getting a lot of attention because of its economic impact, although domestic animals and fish can also be infected posing a significant economic burden in aquaculture as well (Tripathy *et al.*, 2007; Thomas *et al.*, 2014; Haenni *et al.*, 2015).

1.2.1.1 *P. aeruginosa* in Cystic Fibrosis

Cystic fibrosis (CF) is a recessively inherited disorder caused by mutations in the cystic fibrosis transmembrane conductance regulator (CFTR) gene. This gene encodes a cyclic AMP-regulated chloride ion channel and it is mainly produced in the epithelium of multiple tissues and blood cells. Loss-of-function of CFTR results in impaired electrolyte transport across epithelial cell surfaces (Burns *et al*., 2001). This impacts the periciliary fluid quality, which in turn affects the mucociliary clearance of inhaled microorganisms in the lungs and this allows *P. aeruginosa* colonization (Burns *et al.*, 2001; O'Sullivan and Freedman, 2009).

Most infections caused by *P. aeruginosa* in the airways of patients transition from early, recurrent intermittent colonization (which can last for years) to chronic infections (Folkesson *et al.*, 2012). Therefore, this bacterium is a major cause of mortality and morbidity in CF patients and the predisposition to infection in these patients has been studied extensively (Folkesson *et al.*, 2012). Several factors were proposed so far to contribute to the aforementioned predisposition to infection. Firstly, the breach of the mechanical barriers plays a crucial role in the initial colonization of *P. aeruginosa* due to the lack of clearance. The viscous mucus layer creates heterogeneous distribution of antibiotics, nutrients and oxygen which *P. aeruginosa* takes advantage of. Secondly, another factor that favours the establishment is the unbalanced immune response of the host

(Voynow, 2009; Williams *et al.*, 2010). In detail, a neutrophil-mediated response is employed which promotes chronic inflammation that damages the lung architecture contributing to respiratory failure and death (Cantin *et al.*, 2015; Bjarnsholt *et al.*, 2005). To add on that, a Th2-type polarized response (instead of a Th1) is observed in CF patients which leads in the production of non-protective antibodies (Williams *et al.*, 2010). Last and thirdly, *P. aeruginosa* grows in biofilms all over the lung lumen, which then becomes virtually impossible to clear out (Jensen *et al.*, 2010; Bjarnsholt *et al.*, 2009). Unfortunately, aggressive antibiotic therapy can only substantially delay the onset of subsequent chronic infection (Folkesson *et al.*, 2012).

When *P. aeruginosa* moves from the environment into the CF airway it is confronted with highly stressful conditions and is called to adapt and survive. The various types of stresses are important evolutionary forces that drive selection of genetic variants tailored to survive and proliferate in the CF environment. The immune response of the host, the constant presence of antibiotics, the oxidative and osmotic stress as well as competition with other microorganisms are some of those factors. Hence, in order for colonization to develop into chronic infection state *P. aeruginosa* undergoes a shift, which involves both nutritional and physicochemical changes, which have an impact on its evolution. Obviously, a fundamental shift in the gene expression profile precedes these changes, which is governed by the *algU* regulon. This results in upregulation of genes affecting membrane permeability and efflux but downregulation of central metabolism, motility and virulence (Anderson *et al.*, 2008; Aspedon *et al.*, 2006; Bagge *et al.*, 2004; Cirz *et al.*, 2006; Jones *et al.*, 2010; Wu *et al.*, 2004).

Another challenge faced by *P. aeruginosa* is the changes caused in the CF airway environment itself due to the progressing infection. For instance, the extensive structural changes to the airway caused by inflammation in response to the infecting bacteria (Regamey *et al.*, 2011).

The production of reactive oxygen species (ROS) and reactive nitrogen intermediates (RNI) by the host imposes stresses on *P. aeruginosa* which is forced to grow microaerobically or anaerobically due to oxygen consumption (Worlitzsch *et al.*, 2002; Kolpen *et al.*, 2009). Interestingly, *the* oxidative and nitrosative stresses *P. aeruginosa* encounters in the CF airway can increase bacterial mutation rates (as a result of the increased DNA damage) and select for variants that are able to survive in this environment.

Stress imposed by the presence of antibiotics follows the same principle as the above stress in terms of selection of variants that developed antibiotic resistance.

One great example of *P. aeruginosa* adaptation in the CF lung caused by the general envelope stress response is conversion to a mucoid phenotype, characterized by excessive production of alginate which involves the *algU* regulon (Anderson *et al.*, 2008; Aspedon *et al.*, 2006; Bagge *et al.*, 2004; Cirz *et al.*, 2006; Jones *et al.*, 2010; Wu *et al.*, 2004). Alginate is an extracellular polysaccharide and it forms a glycocalyx all over the surface of the bacterium, thus providing protection from adverse environmental stresses such as desiccation (Costerton *et al.*, 1981).

A model of the typical course of *P. aeruginosa* colonization and infection in the CF airway suggests that colonization can occur both in the paranasal sinuses and in the lungs. Aggressive antibiotic therapy can eradicate *P. aeruginosa* from the lungs only temporarily. It seems like the sinuses act as reservoirs of *P. aeruginosa* and facilitate its adaptation until it recolonizes the lung (Hansen *et al.*, 2012). Based on this model there is a delay in the onset of the chronic infection state, which is defined as the continuous presence of the bacterium over a 6 month-period and/ or the presence of at least two precipitating antibodies against *P. aeruginosa* in the serum. It has become evident that the adaptive changes in the bacterial population required for transition to chronic state might occur long before the clinical criteria are detectable. Hence, there is a need to revisit the definition of chronic infection (Johansen *et al.*, 2012).

Importantly, large-scale changes in both the gene expression profile and the catabolic capacity of the bacterium, can be brought about by only few genetic changes in important global regulators. Such changes that affect the ecology and lifestyle of microorganisms can assist an evolutionary transition of an opportunistic pathogen into a persistent pathogen.

The evolutionary dynamics of *P. aeruginosa* during adaptation to the CF lung have been described as non-linear in an *in vitro* experimental approach (Yang *et al.*, 2011a; Cooper and Lenski, 2000; Silander *et al.*, 2007; Holder and Bull, 2001). Basically, that indicates that when bacteria are exposed to a new environment, early mutations have the largest impact on fitness, and that magnitude of the mutational effects reaches a plateau over time. However, still little is known about the evolutionary dynamics of microbial adaptation in non-defined settings, such as the human host.

1.2.2 *P. aeruginosa* virulence and colonisation mechanisms

P. aeruginosa has evolved to be really efficient at nutrient scavenging and surface colonisation, the colonization niche can be the rhizosphere, water pipes or the human host (Rohmer, 2012; Peterson, 1996; Botzenhart and Doring, 1947). In these niches, *P. aeruginosa* is called to either coexist or compete with other microorganisms found in the environment but also to avoid or inhibit defence mechanisms from the hosts that it invades. Virulence factors are specific molecules or structures

produced by *P. aeruginosa* and are the tools by which the bacterium can thrive under limiting conditions (inorganic settings, e.g. water pipes) and in such diverse environments. Some of the main virulence factors of *P. aeruginosa* are summarized in **Table 1.1** and **Figure 1.3**. Several virulence factors are adapted for certain environments and are used when those are encountered, but a significant fraction is used regardless of the colonised environment. However, *P. aeruginosa* employs the standard DNA repair mechanisms and an enhanced oxidative stress response for long term survival (Ochsner, 2000).

Table 1.1. Main Virulence factors in *P. aeruginosa* that are discussed within this thesis[a]

Categories	Virulence factor name(s)	Function(s)	References
Secreted Factors			
Exopolysacharide	Pel and Psl	Bacterial adhesion, immune evasion, biofilm formation	(Colvin *et al.*, 2011, 2013), (Ma *et al.*, 2007)
Siderophores	Pyoverdin	Chelation of ions, promotion of bacterial growth.	(Ravel and Cornelis, 2003)(Bonneau *et al.*, 2020; Sass *et al.*, 2020)
Protease	Alkaline protease (AprA)	Protection of bacterial from host defence	(Matsumoto *et al.*, 1998; Casilag *et al.*, 2016)
	Elastase A and B (LasA and LasB)	Degradation of proteins in host tissues, causes tissue damage	(Mariencheck *et al.*, 2003)(Kessler *et al.*, 1998)
Toxin	T3SS Effectors (ExoS,ExoT,ExoU and ExoY)	induction of host cell apoptosis, disruption of host actin-cytoskeleton	(Sundin *et al.*, 2001; Yahr *et al.*, 1996, 1998),(Sato *et al.*, 2003)
	Exolysin (ExlA)	Pore-formation on the host cell membrane	(Michalska and Wolf, 2015; Basso, 2017)
	Pyocyanin	Supression of host immune responses, cytotoxic to host cells	(Bianchi *et al.*, 2008; Hall *et al.*, 2016)
Bacterial Surface Structures			
Surface appendages	Type 4 Pili (T4P)	Attachment to host cells, bacterial motilities (swarming and twitching)	(Whitchurch *et al.*, 2004), (Overhage *et al.*, 2008), (Burrows, 2012)
	Flagella	Swarming motility, bacterial adhesion	(Sampedro *et al.*, 2015)
Secretion systems	Type 3 Secretion System (T3SS)	Injection of virulence effectors directly into the host cell	(Cornelis, 2010; Notti and Stebbins, 2016)
Bacterial Cell-to-cell Interactions			

Quorum Sensing (QS)		Regulation of virulence factor production by integrating environmental stilumi	(Hemmati *et al.*, 2020; Rutherford and Bassler, 2012)

[a]This table was adapted from (Liao *et al*., 2022).

1.2.3 Pyocyanin

Pyocyanin is a blue pigmented phenazine, specifically 5-methyl-1-hydroxyphenzine and two almost identical operons named *phzA1B1C1D1E1F1G1* (phz1) and *phzA2B2C2D2E2F2G2* (phz2) are involved its biosynthesis (Mavrodi *et al*., 2001). Modifying enzymes, PhzM and PhzS, along with PhnAB are responsible to covert phenazine-1-carboxylic acid (PCA) to pyocyanin (Mavrodi *et al*., 2001). The *pqs* system strongly regulates the expression of the genes encoding the modifying enzymes, especially *phnAB* which is found in the proximity of the *pqsABCDE* operon (Cao *et al.*, 2001; Lau *et al.*, 2004). Other regulators involved in pyocyanin production are the two-component regulatory system (TCS) GacA /GacS and the virulence regulator Vfr (Fuqua *et al.*, 2001).

Pyocyanin is a virulence factor for *P. aeruginosa* and it has multifaceted role, mainly due to its ability to transfer electrons. Hence, as an electron acceptor it serves as an important mediator of redox reactions under limiting conditions (oxygen-depletion) (Wang *et al.*, 2010). It can assist *P. aeruginosa* colonisation of the human host, by increasing mucin glycosylation which in turn facilitates the binding of this bacterium to airway epithelial cells (Jeffries *et al.*, 2016). Pyocyanin also increases mucus production in these cells and is able to generate reactive oxygen species (ROS) which cause widespread cellular damage in multiple hosts (Caci *et al.*, 2015; Lau *et al.*, 2004).

In the CF context pyocyanin exhibits toxic effects further categorized as redox, physical or immunomodulatory and correlates with periods of pulmonary exacerbation (Mowat *et al.*, 2010). The redox effects refer to the ability of pyocyanin to dysregulate enzymes such as catalase and superoxide dismutase, which are responsible for counteracting oxidative stress. Hence, widespread cellular damage is evident in the CF lung (O'Malley *et al*., 2004). The physical effects of pyocyanin refer to its effect on the ciliary function, blocking clearance mucus which seems beneficial to the early infection stages (Jackowski, 1996; Jackowski *et al.*, 1991). Lastly, the immunomodulatory effects of pyocyanin assist *P. aeruginosa* immune evasion. Interestingly, in a low oxygen environment like the CF lung it seems that pyocyanin is acting as electron acceptor thereby assisting adaptability of *Pseudomonas* in the particular setting (Price-whelan *et al.*, 2007). Overall, pyocyanin seems to be important during acute infections and only have a transient role on the first stages of chronic infections (Cullen *et al.*, 2019; Schaber *et al.*, 2004).

The link between pyocyanin production and biofilm formation has been controversial. On one hand a negative correlation between biofilm and pyocyanin was observed in several *P. aeruginosa* strains (Cullen *et al.*, 2019). On the other hand, its binding to eDNA seems to be important during the later steps in biofilm establishment (Das and Manefield, 2012; Das *et al.*, 2015, 2013).

Phenazines also interact with plants, with both positive and negative consequences for plant hosts (Vleesschauwer *et al.*, 2006). Pyocyanin can assist *P. aeruginosa* to displace competitors in plant host, through antibiotic effects due to the production of reactive oxygen species (Briard *et al.*, 2015; Baron and Rowe, 1981)

1.2.4 Proteases

P. aeruginosa secretes a wide range of proteases, from which four play an important role for the virulence of this bacterium (Hoge *et al.*, 2010). Proteases are divided into 6 types based on the active residues involved in the cleavage or the mode of action: Aspartic-proteases, cysteine-proteases, glutamic-proteases, metalloproteases, serine-proteases and threonine-proteases. From the main four, LasA, LasB, AprA are the metalloproteases and protease IV is a serine protease.

Proteases act by degrading complex macromolecules into usable nutrients, facilitating nutrients retrieval. Specifically, in the host environment they can degrade extracellular matrix components such as collagen and laminin (Heck, 1986; Heck *et al.*, 1986) causing tissue damage, as well as molecules from the immune system such as complement components (Hong, 1992; Schultz and Miller, 1974) and cytokines (Parmely *et al.*, 1990), amongst others. Therefore, offering advantage to *P. aeruginosa* in many environments. For instance, the main four proteases (elastase B (LasB), alkaline protease, protease IV and PasP) are detected in the CF lungs. It is suggested that for the survival of *P. aeruginosa* in such a hostile and competitive environment as the CF lung production of these proteases is prerequisite (Hoge *et al.*, 2010). Moreover, high levels of proteases are detected in biofilms, and their secretion is somehow maintained even under treatment with antibiotics which actively target metabolism (Ołdak and Trafny, 2005).

Elastases are proteases with the ability to cleave elastin, a proteinaceous component present in tissues, which offers supports/which plays a role in supportive role. In *P. aeruginosa* elastases are among the main extracellular proteases secreted.

LasB, is a metalloprotease encoded by *lasB* (PA3724) and it has a wide range of substrates (Casilag *et al.*, 2016). LasB acts in conjunction with the LasA zinc metalloendopeptidase to cleave elastin. In more detail, LasA cleaves elastin which increases its availability to LasB, resulting in a synergistic increase in

activity (Peters *et al.*, 1992; Kessler *et al.*, 1997). LasB is also able to degrade collagen, another proteinaceous structural component and IgG, an immune system component (Hoge *et al.*, 2010). Hence, LasB can cause tissue damage and it can also present immune-modulating properties (Casilag *et al.*, 2016). Moreover, LasB is highly immunogenic due to its strong activity and that triggers an inflammatory response during acute infections and the recruitment of polymorphonuclear leukocytes such as neutrophils (Kon *et al.*, 1999). Quorum sensing seems to be the main regulator of *lasB* expression. Namely, the *las* system in tandem with the *rhl* system regulate LasB during acute infections and the early stages of chronicity (Pearson *et al.*, 1997). The effect of the *pqs* system on *lasB* expression is indirect and it is *rhl* system dependent (McKnight and Iglewski, 2000; Farrow *et al.*, 2008). LasA also presents antistaphyloccocal activity by targeting the pentaglycine bridge in the *Staphylococcus aureus* peptidoglycan, granting *P. aeruginosa* a competitive advantage in CF patient's lung (Kessler *et al.*, 1993). The type 2 secretion system (T2SS) Xcp is responsible for the translocation of both LasA and LasB proteolytic enzymes (Bleves *et al.*, 2010).

AprA, aeruginolysin or the alkaline protease is a metallo-endoprotease, which uses zinc as co-factor and is encoded by the *aprA* gene (Pearson *et al.*, 1994). A type 1 secretion system (T1SS) encoded by *aprDEF* is responsible for its secretion (Wagner *et al.*, 2016; Häse and Finkelstein, 1993). It can cleave a number of substrates, including casein, gelatin and laminin as well as immune system components such as IFN-γ, TNF-α and IL-6. It can also interfere with the complement factors C3b and C5a (Laarman *et al.*, 2019). Hence, it presents several immunomodulatory properties which helps *P. aeruginosa* immune evasion (Hoge *et al.*, 2010). Moreover, AprA can act together with elastase to degrade exogenous flagellin, resulting in limited immune recognition without affecting bacterial motility (Casilag *et al.*, 2016). Similarly to *lasB*, the expression of *aprA* is subject to regulation by quorum sensing (QS), mainly the *las* system, since the *rhl* alone seems insufficient by itself to promote *aprA* expression (Casilag *et al.*, 2016). Lastly, expression of *aprA* is also iron-regulated and therefore coordinated with the conditions found within the host (Shigematsu *et al.*, 2001).

Protease IV, encoded by the *prpL* gene, is a serine endoprotease which cleaves the carboxyl-side of lysine residues (Andrejko *et al.*, 2013; Elliott *et al.*, 1986). The type 2 secretion system (T2SS) Xcp is responsible for its secretion (Bleves *et al.*, 2010). It can cleave a number of substrates, like fibrinogen, an important coagulation element in the blood that is recruited in the inflammatory response. Other substrates include the complement or IgG components of the innate and adaptive immune response, respectively (Engel *et al.*, 1998). Hence, its effects are similar to the proteases mentioned previously. Interestingly, Protease IV can degrade lactoferrin and transferrin (Wilderman *et al.*, 2001), increases chelated iron, which in turn activates the Fur system and inhibits Protease IV production in order to

prevent the toxic accumulation of intracellular iron. Hence, protease IV is involved in a negative feedback loop though substrate degradation. Also, Protease IV production is inhibited in higher iron concentrations through the control of PvdS, which is regulated by Fur (Hoge *et al.*, 2010; Wilderman *et al.*, 2001).

Overall, all the main *P. aeruginosa* proteases described here share similar roles, they possess tissue-damaging activity and are capable of degrading various plasma proteins such as complement causing extensive tissue damage meanwhile degrading immune systems components helps the bacteria to evade the immune defences (Pavlovskis *et al.*, 1981). Furthermore, all these proteases are subjected to regulation by QS or iron-mediated responses, both of which are associated with acute infections. Therefore, protease secretion is more relevant for acute infections, as when establishment of chronic infection occurs, they become less important.

1.2.5 Other colonisation factors

Besides motility appendages, peptidases or iron scavenging mechanisms discussed so far *P. aeruginosa* presents an arsenal of other factors that also facilitate successful colonisation in a competitive environment.

Exotoxin A (ToxA), an enzyme that catalyzes the transfer of the adenosine diphosphate-ribosyl moiety from nicotinamide-adenine dinucleotide to elongation factor 2 single-chain polypeptide (Pollack, 1983). This function makes it is a potent inhibitor of protein synthesis by actively inducing cell death through apoptosis (Michalska and Wolf, 2015).

Secretion systems, are machineries used by *P. aeruginosa* to transport all these elements to the extracellular environment and they constitute other important elements for its virulence. Six systems, namely T1SS-T6SS, have been described, but only five are found in *P. aeruginosa*, with T4SS being the exception. Importantly, these secretion systems used for the correct secretion of their specific substrates are crucial for *P. aeruginosa* virulence and without them this bacterium is unable to establish any infection. The relevance of these systems is further highlighted by the fact that they exist in multiple copies, in the *P. aeruginosa* genome (Bleves *et al.*, 2010).

The T3SS forms a needle-like structure, which works as a syringe mechanism that injects its substrates (at least 4 effectors) directly into the cytosol of the target, often eukaryotic cells. The T3SS resembles the flagellum assembly machinery. Substrates are transported unassembled through a 7 nm wide channel after recognition occurs through a non-cleavable N-terminal signal. These effectors are four: ExoS, ExoT, ExoU and ExoY after injection they trigger cell death by necrosis and apoptosis. Cytotoxic

P. aeruginosa isolates harbour ExoU, ExoT which cause rapid cell death whereas invasive isolates of *P. aeruginosa* harbour ExoS, ExoT, which cause a slower cellular death. Effector ExoY is often used by both types of isolates, and *exoY* gene is never found together with *exoU* gene in the same strain, the reason remains unknown (Bleves *et al.*, 2010).

The T6SS, is the latest discovered system in *P. aeruginosa* that works as an injection system like T3SS. It secretes several effectors directly into neighbouring eukaryotic or bacterial cells which results in their killing, providing a fitness advantage to *P. aeruginosa*. An intricated multi-layered regulation (including QS) is in place for T6SS (Chen *et al.*, 2015).

Interestingly, T3SS gene expression is usually inhibited by QS, suggesting a limited role for this system in acute infections. However, it may be more relevant for the chronic establishment of the pathogen (Bleves *et al.*, 2010) like the T6SS which is the major secretion mechanism used by *P. aeruginosa* during chronic infections.

1.3 Colonization mechanisms

1.3.1 Motility

Various types of bacterial motility have been described to date, assist *P. aeruginosa* to find new niches to colonize biotic or abiotic surfaces, and allow for the establishment of biofilms (Henrichsen, 1972). The interplay between a variety of factors such as physical surface properties, bacterial cell signalling and the nutritional supply in the environment shape surface motility (Yeung *et al.*, 2012). *P. aeruginosa* is capable of three major forms of motility: twitching, swimming and swarming motility. Other forms of translocation described are sliding and surfing. The different strategies employed by *P. aeruginosa* to move in the milieu will be reviewed in this section (Murray and Kazmierczak, 2008; Chow *et al.*, 2011). Three of these motility modes, swarming, swimming and twitching require functional appendages whereas gliding and sliding motility are appendage-independent (Shrout *et al.*, 2006).

Both the flagella and type IV pili are key motility appendages for the irreversible attachment *of P. aeruginosa* onto surfaces, the subsequent biofilm development and maturation (Barken *et al.*, 2008; Shrout *et al.*, 2006; Chow *et al.*, 2011). *P. aeruginosa* has a single polar flagellum that can rotate to help this bacterium move in liquid and low-density media necessary for swimming and swarming.

The flagellum is made of a chain of flagellin proteins classically divided in serotypes a and b (Campodonico *et al.*, 2010). However, the whole flagellar system/apparatus including the sophisticated flagellar motor is formed by more than 20 proteins.

Hence, building and moving the flagellum is metabolically expensive. This structure is highly immunogenic and pro-inflammatory and it is considered a virulence factor of this bacterium (Feuillet *et al.*, 2006). No virulence was detected in a murine model of pneumonia for *fliC* mutants, coding for the filament protein (Feldman *et al.*, 1998).

The flagellum has three morphologically distinguishable regions: the basal structure embedded in the cell membranes which contains the motor, the hook that emerges from the outer membrane, and a long flexible external filament which allows for high speed movement (Dasgupta *et al.*, 2004; Silverman and Simon, 1974).

The flagellum system is tightly regulated by multiple regulators to allow for changes in rotation and for the switch between planktonic and sessile lifestyles. Expression of most of the flagellar structural genes is controlled by the transcriptional regulator, FleQ. While, FleN has a negative regulatory effect. The two-component system (TCS) FleSR controls the transcription of *flgBCDEFGHIJKL*, of *fliK*, and of *fliA*, while chemotaxis is regulated by FliA and CheY (Kato *et al.*, 2008; Guttenplan and Kearns, 2014; Dasgupta *et al.*, 2004). FliA is a sigma factor inhibited by the anti-sigma factor FlgM (Dasgupta *et al.*, 2004), while CheY directly interacts with the structural protein FliM and control changes in the flagellum rotation. Finally, both the *pqs* and *rhl* QS systems have been shown to control the expression of the genes required for the production of the rhamnolipid biosurfactants (Williams and Camara, 2009). The Che chemotaxis in *P. aeruginosa* PAO1 counts more than 20 *che* genes which control flagellar rotation control and the swimming direction according to the various stimuli system, which allows *P. aeruginosa* to get closer to attractants and away from repellents (Kato *et al.*, 2008). *P. aeruginosa* was thought to swim in straight runs which alternated with reverses with angular changes of the swimming direction, this model was named "run and reverse". However, new insights support that the flagellar filament cab be wrapped around the cell body and induce a large fluctuation of the body orientation. This model was named "wrap mode" during which the bacterium explored its environment with more efficiency (Tian *et al.*, 2022).

The flagellum, apart from its primary role in motility, plays an important role in adherence, biofilm establishment and the transition from motility to sessility (Sauer *et al.*, 2002; Guttenplan and Kearns, 2014). On the other hand, the absence of flagellar motility is important to develop mature biofilm structures (Klausen *et al*., 2003; Shrout *et al*., 2006).

Swarming is a more complex form of motility used by *P. aeruginosa*, which depends on the flagellum (***Figure 1.1***). In addition, swarming uses biosurfactants, and presents characteristic dendritic patterns in *P. aeruginosa* because bacteria migrate as defined groups, referred to as tendrils (Deziel *et al.*,

2003). A wide range of mutations affect this phenotype, indicating a high complexity in the regulation of swarming in *P. aeruginosa* (Yeung *et al.*, 2009; Dubern *et al.*, 2015). A post-transcriptional level of swarming control exists and is exerted via the RNA binding proteins RsmA and RsmN, which positively influence swarming motility (Heurlier *et al.*, 2004).

Rhamnolipids are glycolipidic surface-active molecules that play an important role in motility and biofilm formation of *P. aeruginosa* (Soberón-Chávez *et al.*, 2005)(Deziel *et al.*, 2003). The rhamnolipids from *P. aeruginosa* are relevant in both clinical and industrial settings. In industry, surfactants are useful because they can minimize energy loss and improve processes by reducing abrasiveness caused by the interphase tension between the liquid and the surface. The production of rhamnolipids is regulated by the sigma factors RpoN and RpoS, as well as by the *las* and *rhl* QS systems (Dobler *et al.*, 2016). The *rhlAB* operon encode enzymes that are responsible for mono-rhamnolipid synthesis, which are further modified in di-rhamnolipids by the enzyme encoded by *rhlC* (Rahim *et al.*, 2001). In motility, rhamnolipids mediate effective migration and seem to guide bacterial expansion through swarming, by controlling the swarming patterns (Déziel *et al.*, 2003; Tremblay *et al.*, 2007).

In biofilms, rhamnolipids play a critical role for the structural integrity of biofilms, their architecture and the dispersal mechanisms (Davey *et al.*, 2003; Boles *et al.*, 2005; Schooling *et al.*, 2013; Bhattacharjee *et al.*, 2016). Interestingly, they can provide an advantage by creating an anti-adherent layer that prevents attachment of other competitor colonizers to that surface (Nickzad *et al.*, 2015). Rhamnolipids have additional roles such as inducing the death of polymorphonuclear leukocytes *in vitro,* the disruption of epithelial cell barriers, which assist colonization, and the inhibition of ciliary beating (Read *et al.*, 1992; Zulianello *et al.*, 2006; Van Gennip *et al.*, 2009).

The other motility appendage of *P. aeruginosa* are type 4a pili (T4P) (***Figure 1.1***) and their synthesis and assembly require at least 40 genes are located in several unlinked regions on the chromosome (Hobbs and Mattick, 1993). T4P are also tightly regulated, with *pilA* expression being controlled by the super regulator RpoN. Both PilR/S and AlgR/FimS two component systems are involved in the regulation, with the latter controlling production of LecB lectin which is required for PilJ, involved in pilus synthesis (Sonawane *et al.*, 2006). General regulators such as Vfr and c-di- GMP also play a role in the regulation

T4P is important as an initial attachment tool, very much like the flagellum in the correct development of microcolonies for biofilm formation (Klausen *et al.*, 2003; Barken *et al*., 2008). There is an overlap between the elements that regulate the T4P and those that regulate twitching motility, as expected.

Twitching constitutes a distinct motility that requires functional T4P and is independent of the flagella or the QS (Beatson *et al.*, 2002b). T4P is the only type of pilus involved in twitching as well as in swarming motilities (Burrows, 2012). Extension and retraction of T4P promotes a worm-like movement, cells align and move together like in a raft in high humidity and on low viscosity surfaces (Bradley, 1980; Skerker and Berg, 2001; Burrows, 2012). T4P mediate the first contact with the host and are important for host pathogenicity during acute infections (Mahenthiralingam *et al.*, 1994). Whereas, a lack of T4P is characteristic of chronic infections. Moreover, T4P have also been involved in alternative motility mechanisms and systems useful to detach from surfaces (Gibiansky *et al.*, 2010).

The role of T4P in swarming was shown to be dual, by slowing swarming progression and promoting cell-to-cell interactions of swarmers to orchestrate chemotactic movements (Anyan *et al.*, 2014). Swarmer cells have shown differential properties that differentiate them from their planktonic counterparts (Overhage *et al.*, 2008; Nogales *et al.*, 2010). Kohler *et al*. observed that swarmer cells at the edge of the tendrils are elongated and present hyperflagellation (Kohler *et al.*, 2000). The importance of T4P for swarming motility of *P. aeruginosa* has been controversial.

The host immune system detects and recognizes these motility appendages and in turn induces signalling pathways which trigger inflammatory responses and phagocytosis by murine or human macrophages (Amiel *et al.*, 2010). Over the course of the infection *P. aeruginosa* switches to a sessile lifestyle which lowers the virulence and offers a survival advantage against stresses and adverse conditions (Moradali *et al.*, 2017).

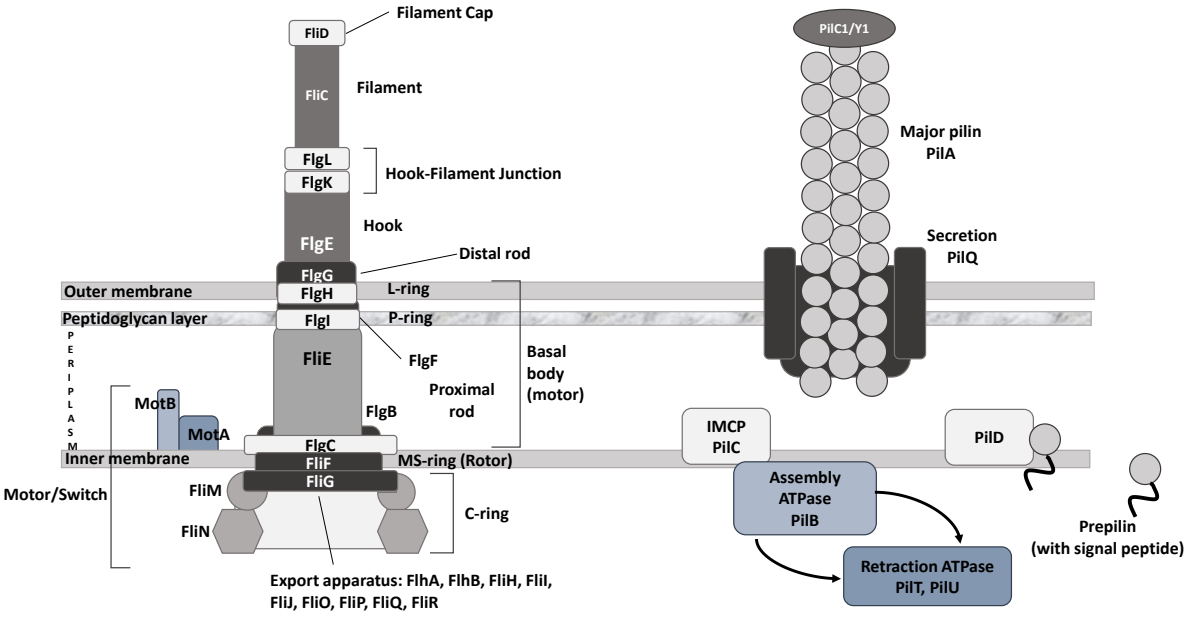


Figure 1.1. Flagellum and Type 4 pili (T4P) structures in *P. aeruginosa.*
The flagellum **(left)** is a representation drawn from information available in a publicaton by (Kanehisa *et al.*, 2017). The T4P **(right)** is an adaptation of the figure available in a publication by (Melville and Craig, 2013). An in-depth review of both

systems and their mechanism of action will not be given in this thesis, but if further information is required it can be found in a publication by (Van Gerven *et al.*, 2011). Note that, The flagella, T4P, the inner and outer membranes, and peptidoglycan layer are not drawn to scale. The flagellum is subdivided in different parts, the filament, the hook, the basal body and the rotor which are all depicted on the schematic. The T4P has a more summarised schematic which shows only the major components of the system. IMCP stands for inner membrane core protein, which are PilC accessory proteins and are not shown separately for simplification purposes.

1.3.2 Biofilm

A microbial biofilm consists of clusters or aggregates of microbial cells in a structured manner which are enclosed in a self-produced polymer matrix (Trunk *et al.*, 2010). Biofilms may consist of one microorganism or be polymicrobial (Trunk *et al.*, 2010; Colwell, 1964; Haynes, 2009; Hilker *et al.*, 2015), they may form on natural or artificial surfaces and can be prevalent in natural, industrial or hospital settings (Hall-Stoodley *et al.*, 2004).

The hallmark of chronic infections caused by *P. aeruginosa* is the formation of mucoid biofilm, which confers long-term persistence. Biofilm associated infections caused by *P. aeruginosa* include CF lung infection, chronic wound infection, chronic otitis media, chronic rhinosinusitis, catheter-associated urinary tract infection, and contact lens-related keratitis (Balsalobre, 2012). The search for biofilms in clinical samples may be difficult because biofilms are small *in vivo*, in tissues 4–200 μm, on foreign bodies 5–1,200 μm (Scaccabarozzi *et al.*, 2015). If the samples are not representative of the focus of the biofilm infection that may result in false-negative results (Høiby *et al.*, 2015). Therefore, the treatment is made even more difficult if a proper diagnosis method is not in place.

The *P. aeruginosa* biofilm matrix consists of extracellular polymeric substances (EPS) which are mainly polysaccharides, proteins, extracellular DNA (eDNA) and lipids (Strempel *et al.*, 2013). Additional host-derived components may be integrated into the biofilm matrix such as dead immune cells, eDNA, fibrin, platelets or immunoglobulins (Høiby *et al.*, 2015).

This matrix works as a shield against adverse conditions, it also creates a favourable environment for cell-cell interaction and for growth due to the reservoir of metabolic substances and nutrients it contains (Flemming and Wingender, 2010; Ghafoor *et al.*, 2011; Gellatly and Hancock, 2013; Strempel *et al.*, 2013). Physiological and biochemical gradients (nutrients, oxygen, growth rate, genetics) exist in a biofilm from the surface to its deeper layers due to its structure. Degradation of organic matter packs the matrix with high quantities of carbohydrates, humic and uronic acids (Frølund, 1996).

P. aeruginosa produces three predominant exopolysaccharides as components of the biofilm matrix: Psl, Pel, and alginate, which have an important role in enhancing surface adhesion. The ratios between these polysaccharides within the matrix vary across *P. aeruginosa* strains and this has an impact on structural stability (Colvin *et al.*, 2013). Also, it was shown that these exopolysaccharides in concert

with eDNA act as determinants of the biofilm architecture (Ghafoor *et al.*, 2011). Analysis of each EPS revealed differential roles depending on the stage of biofilm development. The presence of various EPS exhibiting different physiochemical properties confers a survival strategy for increasing the flexibility and stability of biofilms under various conditions (Jennings *et al.*, 2015).

Psl has a pentasaccharide subunit that consists of D-glucose, D-mannose and L-rhamnose in a 3:1:1 ratio with neutral net charge at slightly acidic pH (Byrd *et al.*, 2009; Ma *et al*., 2007; Friedman and Kolter, 2004). Psl is predicted to be synthesized by the *psl* gene cluster which contains 15 co-transcribed genes named *pslA* to *pslO* (Ma *et al.*, 2009; Byrd *et al.*, 2009; Franklin *et al.*, 2011; Friedman and Kolter, 2004; Jackson *et al.*, 2004). Psl exists in both soluble and cell-associated forms that might have different roles. During the very early stage of biofilm formation Psl is found anchored on the cells in a helical pattern from where it plays a key role by augmenting cell migration, cell-cell interactions and cell-surface adhesion (Overhage *et al.*, 2005), whereas, in mature biofilms Psl is found accumulated at the periphery of 3D- mushroom shaped microcolonies (Ma *et al.*, 2009; Zhao *et al*., 2014). It protects cells against phagocytosis and oxidative stress during infection (Mishra *et al.*, 2015). Psl acts by reducing phagocyte killing and by limiting complement-mediated opsonisation (Mishra *et al.*, 2015; Wei and Ma, 2013). It is also involved in several antibiotic resistance mechanisms hence conferring resistance to a broad spectrum of antibiotics particularly at early stage of biofilm development (Zegans *et al.*, 2012; Billings *et al.*, 2013). Interestingly, Psl may be maintaining the inflammatory response during chronic infections through indirect stimulation of NFκB (Byrd *et al.*, 2009). In summary, Psl provides *P. aeruginosa* with a survival advantage during pathogenesis.

Pel, is a polymer of 1,4 partially acetylated N-acetylglucosamine and N-acetylgalactosamine linked together by glycosidic bonds (Jennings *et al.*, 2015). The structure of the Pel polysaccharide was only recently described by Jennings *et al*., 2015, and it was surprisingly found to be positively charged at both neutral and slightly acidic conditions (Jennings *et al.*, 2015). Pel is synthetized by the gene cluster/operon which contains 7 genes named *pelA* to *pelG*, the molecular processes behind the production of Pel are not yet fully understood (Franklin *et al.*, 2011). Pel, also has an important role in biofilm formation in *P. aeruginosa*, mostly in the PA14 strain, and it is the main polysaccharide secreted by this particular strain (Yang *et al*., 2011; Friedman and Kolter, 2004). However, it seems to be less important for biofilm formation in the *P. aeruginosa* PAO1 strain, since the loss of Pel does not cause a major biofilm disruption in this particular strain (Colvin *et al.*, 2011). Overall, Pel is still an important component because of its cationic charge it can be cross-linked with eDNA in the typical pH found in biofilms, unlike Psl (Jennings *et al.*, 2015). Pel can exist in two forms which may play different

roles during biofilm formation, a soluble low-molecular form (0.5 kDa) and a cell-bound high-molecular weight form (80 kDa)(Byrd *et al.*, 2009).

Interestingly, the contribution of Pel in biofilm formation varies from strain to strain. In PA14, Pel was found primarily in the periphery of the microcolonies whereas in PAO1 it was found accumulated in the stalk (Jennings *et al.*, 2015). Meanwhile, in PAO1 Psl polysaccharide was found in the periphery of the microcolonies. In the absence of Psl, Pel acts as a substitution in the periphery of mature biofilm, suggesting that Pel can compensate for the lack of Psl (Jennings *et al.*, 2015).

Overall, available data implies that Pel is important for the initiation and maintenance of cell-cell interactions and that it is the main provider of structural support of the biofilms (Colvin *et al*., 2013; Ma *et al*., 2009; Byrd *et al*., 2009). Pel is also responsible for the formation of pellicles in the air-liquid interface (Friedman and Kolter, 2004). Furthermore, Pel also protects *P. aeruginosa* biofilms, by forming a protective layer thus increasing resistance against certain aminoglycoside antibiotics (Colvin *et al.*, 2013).

As mentioned the levels of these polysaccharides within the matrix and their predominance in terms of structural stability fluctuates among *P. aeruginosa* strains (Passos da Silva *et al*., 2019).

Initial microcolony formation requires both Pel and Psl polysaccharides, the regulation of their production during the several stages of biofilm formation is complex and with multiple levels of sophisticated control (Schurr, 2013; Moradali *et al.*, 2017). Firstly, transcription of both *pel* and *psl* operons/gene clusters is repressed by the transcription regulator FleQ. Presence of the intracellular signalling molecule c-di-GMP is sensed directly by FleQ, which derepresses exopolysaccharide secretion (Starkey *et al.*, 2009). In addition, c-di-GMP can positively regulate Pel synthesis through allosteric binding of PelD (Lee *et al.*, 2007; Colvin *et al.*, 2013) Both QS and the Gac-Rsm signal transduction pathway have been suggested to control *pel* and *psl* expression as well (Gilbert *et al*., 2009; Irie *et al*., 2010; Sakuragi and Kolter, 2007; Goodman *et al.,* 2004; Ventre *et al*., 2006). Finally, the expression of *psl* gene is positively affected by the transcriptional regulator RpoS, whereas its translation is negatively affected by the RNA binding protein, RsmA (Gilbert *et al.*, 2009; Irie *et al.*, 2010).

Important factors for biofilm establishment include eDNA (Whitchurch *et al.*, 2002), which has multifaceted roles. At the early stage of biofilm formation, eDNA facilitates coordinated cell movements, though twitching motility, which promote initial attachment of cells to surfaces (Mann and Wozniak, 2012; Wei and Ma, 2013). In the mature biofilm eDNA (cross-linked with Pel) together with the flagella and the type 4 pili allow the formation of the stalk and the mushroom-shaped caps

seen in the microcolonies (Jennings *et al.*, 2015; Barken *et al.*, 2008; Mann and Wozniak, 2012). The stalk of mushroom-like microcolonies is the richest in eDNA, although present in the whole of the matrix, indicating that it has a role in the biofilm structure (Mann and Wozniak, 2012; Jennings *et al.*, 2015; Allesen-holm *et al.*, 2006). The release of eDNA, which appears to be from random fragments of the chromosome, is a poorly understood process, the *las* and *pqs* systems seem to be involved in the regulation of its release (Ma *et al*., 2009; Spoering and Gilmore, 2006; Wei and Ma, 2013; Turnbull *et al.,* 2016; Thomann *et al.,* 2016). Moreover, eDNA contributes to biofilm formation by creating gradients in the matrix which act as a nutrient reservoir during starvation and protect against antibiotics (Allesen-holm *et al*., 2006; Mulcahy *et al*., 2010; Gloag *et al*., 2013; Ma *et al*., 2009; Wilton *et al*., 2016).

The matrix also contains several components which are not considered as classical matrix biofilm constituents but instead have auxiliary functions, such as proteins, membrane vesicles (MVs), cyclic β-glucans, LPS, and motility appendages. The matrix proteasome contains protases (LasA, LasB or protease IV), oxidative stress response proteins, DNA-binding and iron acquisition proteins (Toyofuku *et al.*, 2012). A high fraction of these proteins are sorted into MVs along with LPS, fimbriae, peptidoglycan, nucleic acids, and various periplasmic proteins (Beveridge and Kadurugamuwa, 1995; Wai *et al.*, 2003; Bonnington and Kuehn, 2014; Schooling and Beveridge, 2006). Consequently, MVs play a wide array of roles in pathogenesis and immune modulation because they facilitate virulence factor secretion, cell-to-cell communication, nutrient acquisition, horizontal gene transfer, antibiotic resistance, etc (Schooling and Beveridge, 2006; Kulp and Kuehn, 2012). Interestingly, MV production and regulation is significantly different in PA14 compared to PAO1, differences in the extracellular matrix composition has been discussed previously (Florez *et al.*, 2017). Both the flagella and the type 4 pili mentioned above as well as Cup fimbriae are proteinaceous cell appendages and they play an important role in biofilm maturation (Vallet *et al.*, 2001; Ruer *et al.*, 2007). However, lectins are of proteinaceous nature and are considered components of the biofilm matrix (Diggle *et al.*, 2006). Each component of the matrix is interconnected with the rest and that shapes interactions with the surrounding environment and is crucial in maintaining homeostasis in the biofilm through all the steps of its development.

As mentioned previously, diagnosis and treatment of many biofilm infections are difficult. The persisting biofilm associated infection triggers a continuous inflammatory response from the host. The polarization to either T helper type 2 (antibodies) or T helper type 1 (cell-mediated) during the initial immune response to the microbe determines whether mononuclear cells or poly-morphonuclear neutrophil leucocytes will be dominating the infection site (Ozer *et al.,* 2014; Stover *et al.*, 2000).

Microcolonies start to develop, after the attachment and the loss of motility through clonal growth (Klausen *et al*., 2003). During maturation, subpopulations are formed within the biofilm which have significant differences in their transcriptome and proteome, these are also spatially separated (Rollet *et al.*, 2009). The non-motile cells reside at the inner layer and are mostly dormant, whereas metabolically active cells reside on the upper/outer layers (Klausen *et al.,* 2003; Chiang and Tolker-nielsen, 2012; Iii *et al*., 2003; Werner *et al.*, 2004). The limited nutrient and oxygen availability in the inner layers of the biofilm is hypothesized to cause the differences observed in activity. However, the signals that evoke the differentiation of motile and non-motile subpopulations are currently unknown. Interestingly, the dormant subpopulation is highly resilient to antibiotic treatment which target the metabolically active cells (Oliver *et al.*, 2017; Lewis, 2007; Wood *et al.*, 2013). The metabolically active subpopulation is also capable of adapting to membrane-targeting antibiotics by expressing a series of resistance genes. Dispersed cells are motile but they present a distinct stage of growth, it constitutes a third physiological state that differs to both planktonic and sessile cells (Sauer *et al.*, 2002; Chua *et al.*, 2014).

1.4 Regulatory mechanisms of pathogenicity in *P. aeruginosa*

As mentioned previously, *P. aeruginosa* is so successful in evading clearance and persisting due to the multiple virulence determinants it produces, which genes are under the control of a very sophisticated integrated global regulatory network (Girard and Bloemberg, 2008). One of the main regulatory networks is that controlled by QS which refers to a cell-to-cell communication mechanism (Williams, 2007; Williams and Camara, 2009). Apart from QS there are other regulatory mechanisms such as the extracytoplasmic function sigma factors, the GacA/S two component system, and various regulatory networks involving small non-coding RNAs (Girard and Bloemberg, 2008).

1.4.1 Quorum sensing systems in *P. aeruginosa*

QS is a cell-to-cell communication system mediated by small diffusible molecules in a population-density dependent manner in order to coordinate the physiology of the population in response to changes in their environment (Williams and Camara, 2009; Breidenstein *et al.*, 2011).

For full activation of the system, the signal molecules need to be accumulated beyond a threshold that is dependent on reaching a certain quorum (minimum number of members required to perform or approve a certain action), hence the name initially used by Fuqua *et al*., 1994 (Fuqua *et al.*, 1994). These signals that induce gene expression are subjected to a positive feedback loop, therefore they are often called autoinducers, resulting in a rapid activation of their own biosynthesis (Williams and Camara, 2009; Henke and Bassler, 2004; Whitehead *et al.*, 2001). QS systems present a widely used

regulatory mechanism found in Bacteria, Archaea and Eukarya (Montgomery *et al.*, 2013), and multiple systems may be found in the same species (Lee and Zhang, 2015).

The first QS system described was the LuxI-LuxR system of *Vibrio fischeri*, which regulates the population-density bioluminescence of this bacterium (Nealson *et al.*, 1970). When the autoinducer, N-(3-oxohexanoyl)- L-homoserine lactone (OHHL), which is produced by the LuxI synthase exceeds the threshold, it binds on the LuxR transcriptional factor which in turn activates the transcription of luminescence-related genes (Williams *et al.*, 1992; Hardman *et al.*, 1998). All QS systems are similarly organized, namely each system consists of at least two major functional elements: the autoinducer synthases and the cognate receptors, which sense the autoinducer. Upon accumulation of the diffusible small signal molecules (autoinducers), they bind their cognate receptor which in turn acts as transcriptional factor, which ultimately triggers gene expression.

It is proposed that these signals are transported by free diffusion, membrane transporters or membrane vesicles, although the exact mechanisms are not well understood (Mashburn and Whiteley, 2005; Martinez *et al.*, 2009; Alcalde-Rico *et al.*, 2016).

Several families of QS signal molecules exist based on their chemical structures. Gram-negatives mostly employ fatty acid molecules such as N-acyl-L-homoserine lactones (AHL) and 2-alkyl-4-quinolones (AQ) (Whitehead *et al.*, 2001; Heeb *et al.*, 2010). However, gram-positives usually rely on autoinducing oligopeptides and polypeptides (Garg and Manchanda, 2013; Reading and Sperandio, 2005). Gram-positives can produce another family of autoinducers the γ-butyrolactones (Polkade *et al.*, 2016), which for example regulate the production of antibiotics and spore formation in *Streptomyces sp.* (Polkade *et al.*, 2016).

At least three accepted QS systems, *las, rhl*, and *pqs* (Lee and Zhang, 2015) exist in *P. aeruginosa*, that are mediated by distinct diffusible signal molecules and exhibit a hierarchical organization in which they are interconnected (**Figure 1.2**) (Williams and Camara, 2009; Williams, 2007; Latifi *et al.*, 1996; Fuqua *et al.*, 1994). When QS systems get activated they drive the expression of around 10% of the genome in *P. aeruginosa*, including genes of the secretion machinery, efflux pumps, siderophores, proteases, exotoxins, lipases, rhamnolipids and hydrogen cyanide, amongst others (Heeb *et al.*, 2010; Girard and Bloemberg, 2008; Diggle *et al.*, 2003; Winzer and Williams, 2001; Hassett *et al.*, 1999), as well as genes implicated in social behaviours such as biofilm formation, motility, motility-sessility switch and antibiotic resistance mechanisms, among others (Venturi, 2006; Williams and Camara, 2009; Barr *et al.*, 2015; Winstanley and Fothergill, 2008; Girard and Bloemberg, 2008; Schuster and Greenberg, 2006). Hence, it is that QS is absolutely important for pathogenicity of *P. aeruginosa* and

it provides the bacterium with a great level of adaptability for colonization and survival of the community in many environments, particularly at early stages of infection (González and Keshavan, 2006).

However, QS-defective strains from the clinic are readily isolated due to fitness cost (Heurlier *et al.*, 2006). This does not necessarily mean that QS is not at all required during the course of an infection although it suggests that its role might diminish over time (Winstanley and Fothergill, 2008; Heurlier *et al.*, 2006).

This phenomenon is explained by the presence of a mixed population of *P. aeruginosa* in chronic infections so that the QS-defective strains, which are fitter exploit the QS-regulated goods contributed by the QS-functional members of the population, emerge (Williams *et al.*, 2007; Zhu and Kaufmann, 2013). However, a balance between the QS-defective "cheater" strains and the QS-functional bacterial populations is necessary for this cooperative behaviour to exist (Winstanley and Fothergill, 2008). It will be very beneficial understand how bacteria cooperate to control behaviours like "social cheating" involving the *las* and *rhl* QS systems (Wang *et al.*, 2015).

QS-deficient mutants cause considerably less tissue damage and pathological changes during infections, due to a significant decrease in the virulence and cytotoxicity (Nelson *et al.*, 2009; Feng *et al.*, 2016).

Lastly, QS facilitates evasion the host immune defences by impairing the immune responses and causes devastating injuries to the host tissues, worsening the clinical course of infections. The role of each QS in several aspects of *P. aeruginosa* physiology will be discussed below.

1.4.1.1 *las* and *rhl* systems

In *P. aeruginosa* there are two AHL-mediated QS systems named *las* and *rhl* which are interconnected (**Figure 1.2**)(Latifi *et al.*, 1996; Schuster and Greenberg, 2006). Both systems consist of LasI/RhlI synthases responsible for the production of *N*-3-oxododecanoyl homoserine lactone (3-oxo-C12-HSL) and *N*-butanoyl homoserine lactone (C4-HSL), respectively, which can bind to the LasR/RhlR transcriptional regulators, respectively (Latifi *et al.*, 1996; Schuster and Greenberg, 2006). The formed complex can activate transcription via binding to conserved *las*/*rhl* boxes residing near the promoters, upstream of the targeted genes (González-Valdez *et al.*, 2014; Lee and Zhang, 2015; Banerjee and Ray, 2016; Papenfort and Bonnie, 2014).

As previously mentioned, a hierarchy exists in QS systems and the *las* system, which is positioned/resides at the top of the cascade, is the most dominant QS system in *P. aeruginosa*, as the

LasR/3-oxo-C12-HSL complex can drive expression of genes integrated in the system itself as well as the other systems QS *rhl* and *pqs* (Lee and Zhang, 2015; Latifi *et al.*, 1996). Binding of 3-oxo-C12-HSL to LasR, allows for the formation of a dimeric structure that is capable of binding dsDNA and controlling gene expression. LasI synthetises N-(3-oxododecanoyl)-L-homoserine lactone (3OC12-HSL) early in the infection using two substrates, the oxo-C12-acyl group (attached to a carrier protein) and S-adenosyl-L-methionine (Pearson *et al.*, 1994; Gould *et al.*, 2004).
It is worth mentioning, that a fail-safe mechanism for LasR regulation is in place and is based on RsaL, the transcriptional repressor of *lasI*. A strong negative feedback loop is created after RsaL binds to the *lasI* promoter, which supersedes the positive one from LasR (hence the name). Expression of *lasR* implicates other important regulators as well but these will not be discussed here (Lee and Zhang, 2015).

The *rhl* system senses C4-HSL, its transcriptional regulator RhlR induces the expression of its own structural gene, in a classic positive feedback loop system (Lee and Zhang, 2015). The *rhl* system is activated in response to IFN-γ component of the innate/inflammatory immune and it causes upregulation of virulence-related genes, such as the *rhlAB* operon responsible for rhamnolipid biosynthesis (Schuster and Greenberg, 2006).

Both the *rhl* and *las* systems have some uniquely regulated genes, but the majority of them overlaps. As representative examples, the *las* system regulates elastase, alkaline protease and toxin A production, while the *rhl* system regulates pyocyanin, rhamnolipid as well as elastase and alkaline protease production (Brint and Ohman, 1995; Gambello *et al.*, 1993; Latifi *et al.*, 1996; Ochsner *et al.*, 1994; Pearson *et al.*, 1995; Pesci *et al.*, 1997). The redundancy observed might be buffering loss-of-function mutations in both systems ensuring a robust regulation (Lee and Zhang, 2015). The *las* and *rhl* systems mediates QS signalling at early stages of exponential growth phase (Choi *et al.*, 2011a).

As mentioned previously, a portion of CF isolates has mutations causing a *las* loss of QS function (LaFayette *et al.*, 2015). The absence of *las* or *rhl* does not impact the maintenance of biofilms, although the biofilms developed are thinner and flatter (Moradali *et al.*, 2017), therefore suggesting a pivotal role of these systems during the early stages of infection and during the establishment of biofilms, but a more limited role for maintenance of their structure. Hence, the contribution of QS to biofilm formation in *P. aeruginosa* is controversial.

1.4.1.2 *Pseudomonas* Quinolone Signal (PQS) QS

There is a third quorum sensing system identified in *P. aeruginosa* mediated by another class of QSSMs, the alkyl quinolones (AQ), principally the PQS (Pseudomonas quinolone signal, chemically 2-

heptyl-3-hydroxy-4(1*H*)-quinolone) (**Figure 1.2**) and its precursor HHQ (2-heptyl-4-quinolone) (Heeb *et al.*, 2010; Pesci, 1999; Williams and Camara, 2009). Both PQS and its precursor HHQ can bind the transcriptional regulator PqsR (also known as MvfR) and induce expression of the *pqsABCDE* operon, hence the reason they are also referred to as autoinducers or even coinducers (Xiao *et al.*, 2016; Williams *et al.*, 2007). However, PQS is a much more potent gene transcription activator than HHQ (Xiao *et al.*, 2006). Moreover, both autoinducers regulate their own production through a standard positive feedback loop (Cao *et al.*, 2001). Interestingly, the PQS biosynthetic pathway generates several byproducts, some of which have important biological functions of their own (Kesarwani *et al.*, 2011)(Gruber *et al.*, 2016).

PqsE is a puzzling component of the *pqs* system that controls a subset of genes that are not covered by PqsR. It is crucial for virulence in several infection models as well as biofilm formation although it is not necessary for PQS production (Rampioni *et al.*, 2010). A recent study has suggested that PqsE is responsible for the production of an alternative-autoinducer, which activates RhlR. Therefore, the PqsE and RhlR constitute a QS synthase–receptor pair, which is crucial for *P. aeruginosa* virulence and biofilm formation in several animal infection models as well (Mukherjee *et al.*, 2018).

The *las* system has positive effect on the expression of the *pqsABCDE* operon, while the *rhl* system has a negative effect (Williams and Camara, 2009; Xiao *et al.*, 2016; Deziel *et al.*, 2003; Wade *et al.*, 2005; Camilli and Bassler, 2006; Gallagher *et al.*, 2002). The *pqs* system controls the expression of many genes involved in virulence and biofilm formation and physiology such as pyocyanin, rhamnolipids, elastase, lectin *lecA* and also the biofilm formation, amongst other virulence traits (Smith and Iglewski, 2003; Camilli and Bassler, 2006; Long, 2012; Kim *et al.*, 2003; Zaborin *et al.*, 2009; Bains *et al.*, 2012; Lee *et al.*, 2013; Nguyen *et al.*, 2015; Choi *et al.*, 2011).

The *pqs* system is also capable of creating a low iron environment for *P. aeruginosa,* through iron chelation by activating a siderophore mechanism but it was also shown that PQS, but not HHQ, can chelate iron(III) under biological conditions. (Diggle *et al.*, 2007).

Moreover, PQS can activate the oxidative stress response in the presence of reactive oxygen species (ROS) derived usually from polymorphonuclear leukocytes (Haussler and Becker, 2008), hence, favouring *P. aeruginosa* immune evasion in the host environment.

Secretion of eDNA, a major component of the biofilm matrix is positively regulated by the *pqs* system, but the molecular mechanism has not been described yet (Argenio *et al.*, 2001; Allesen-holm *et al.*, 2006; Mashburn-warren *et al.*, 2008; Thomann *et al.*, 2016). Hence, the *pqs* system plays an important

role in biofilm formation and maintenance in a cyclic manner depending on oxygen availability within the biofilm (Borriello *et al.*, 2004; Maura and Rahme, 2017).

Overall, the PQS itself is obviously a multi-functional molecule and it can function via PqsR-dependent and PqsR-independent pathways, making the *pqs* system the most intricate and versatile QS system discussed (Rampioni *et al.*, 2016). Despite the extensive research done on this subject, the exact role of the PQS molecule remains poorly understood both *in vitro* and *in vivo*.

Another stress factor for *P. aeruginosa* during pathogenesis is oxygen depletion, also known as hypoxia. Reduced ventilation due to viscosity, chronic inflammation, and biofilm formation are all limiting factors that can create hypoxia/hypoxic conditions (Hassett, 1996; Worlitzsch *et al*., 2002; Yoon *et al*., 2002; Alvarez-Ortega and Harwood, 2007; Hassett *et al*., 2009). However, *P. aeruginosa* is capable of surviving under hypoxia stress to high cell densities through/by employing microaerobic respiration. It was proposed that nitrate respiration can occur in this case as well (Alvarez-Ortega and Harwood, 2007).

The QS regulon is in play at low oxygen conditions. A study showed that the 4-hydroxy-2-alkylquinolines (HAQ)-dependent QS pathway is active during hypoxia via the master transcriptional regulator of anaerobic respiration (ANR protein), then the PQS system takes over the regulation of virulence-related genes (Hammond *et al.*, 2015). Additionally, under hypoxia stress, hydrogen cyanide biosynthesis is being regulated by both the QS systems and ANR protein cooperatively (Castric, 1983, 1994; Pessi and Haas, 2000). The same study demonstrated that QS suppresses/has a negative effect on nitrate respiration (denitrification) under low oxygen conditions. In conclusion, cross-talking of the QS pathways contributes to the versatility of *P. aeruginosa* and facilitates establishment of acute and chronic infections (Moradali *et al.*, 2017).

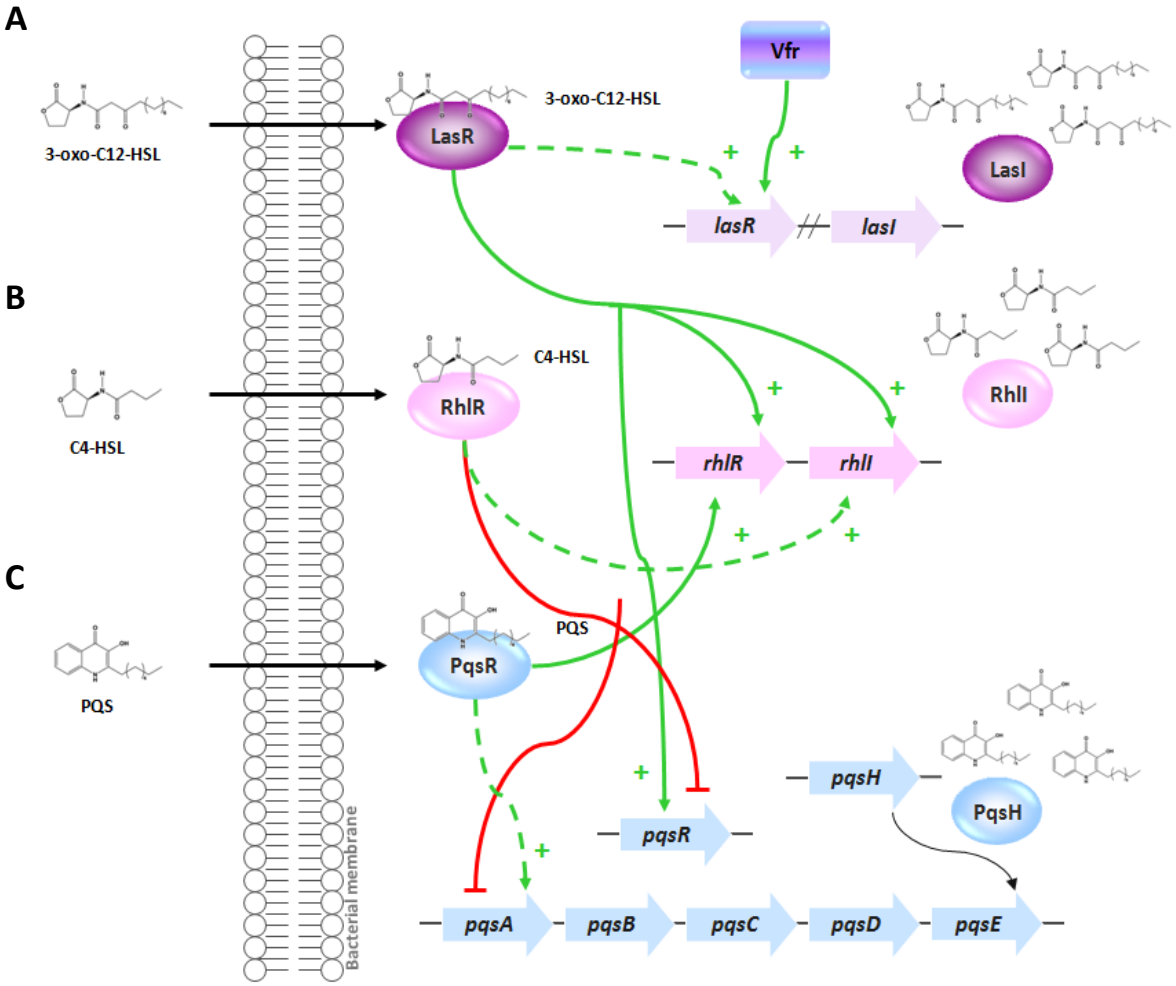


Figure 1.2. Schematic representation of AHL-dependent and AQ-dependent QS systems in *P. aeruginosa.*
Figure modified from Zhu and Kaufmann (Zhu and Kaufmann, 2013). **(A)** and **(B)** show the AHL-based QS systems *las* and *rhl* respectively. Vfr activates expression of *lasR* and then the AHL-LasR complex activates the expression of *lasI* to amplify production of the signalling molecule. The AHLs are synthesized by the LasI and RhlI synthases. When AHL extracellular concentration exceeds the threshold the AHL-binding transcriptional regulator (LasR or RhlR) complex forms, and it activates target gene expression, including virulence factors. Note that each system can activate gene expression to sustain itself (autoinduction) or to kick-start another system. For example, when the *las* system is activated it induces itself and it also activates both the second AHL-dependent system and the AQ-dependent system. **(C)** Shows the AQ-based system PQS which works similarly, PqsR is the transcriptional regulator and PqsH is the synthase. Pseudomonas quinolone signal (PQS) is produced after processing of its precursor 2-heptyl-4-quinolone (HHQ) by PqsH, which is a putative flavin-dependent monooxygenase (Girard and Bloemberg, 2008; Deziel *et al*., 2003). The *pqsE* gene of the *pqs* operon is of particular interest because although it is not required for AQ biosynthesis, it is crucial for virulence (Diggle *et al.*, 2003). There is cross-talk between the three systems. Solid green arrow with plus symbol (+) indicates positive regulation, dashed green arrow with plus symbol (+) indicates autoinduction and solid red bar indicates negative regulation.

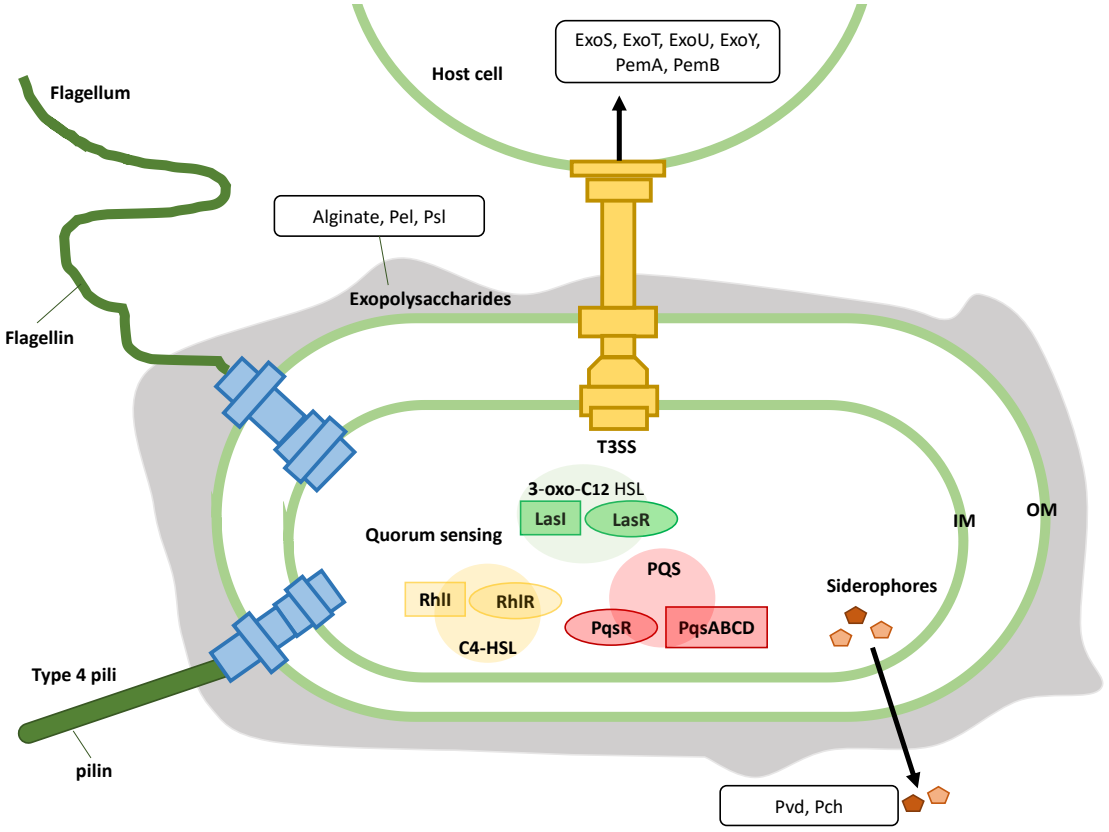


Figure 1.3 The virulence factors of *P. aeruginosa* discussed in this thesis.
The figure was adapted from (Liao *et al.*, 2022). The bacterial surface structures include the flagellum and type 4. Only T3SS systems from the 6 that exists in *P.aeruginosa* is depicted in this schematic for simplification purposes. The secreted factors are mentioned in black boxes. Note that none of he appendages are drawn to scale. The main Quorum sensing players are also shown in the schematic, but their in between interactions are not shown due to simplification purposes. More on that can be found in Figure 1.2.

1.5 Antibiotic resistance in *P. aeruginosa*

As mentioned previously, *P. aeruginosa* is a multi-drug resistant (MDR) microorganism and is emerging as a global health issue, due to a dramatic increase in the occurrence of nosocomial and chronic infections. Several resistance mechanisms were described, and each seems to contribute to a specific class of antibiotics, contribution of each mechanism varies from country to country (Lister *et al.*, 2009; Strateva and Yordanov, 2009; Sun *et al.*, 2014; Hong *et al.*, 2015; Potron *et al.*, 2015). Very briefly, each antibiotic class has different mechanisms of action. For example, Aminoglycosides (AGs) and tetracyclines inhibit bacterial protein synthesis. The β-lactam antibiotics interfere with bacterial cell wall biosynthesis by inhibiting transpeptidases responsible for peptidoglycan synthesis by penicillin-binding proteins (PBPs). Quinolones inhibit DNA synthesis via DNA manipulation enzymes such as topoisomerases and DNA gyrase (Obrecht *et al.*, 2011).

Resistance is mainly classified into intrinsic, acquired and adaptive mechanisms although more types exist. Here, the most frequent and well-understood mechanism *P. aeruginosa* employs to survive antibiotic treatments is reviewed.

Furthermore, the loss or reduced copy numbers of OprD and overproduction of active efflux pumps, AmpC β-lactamase and extended-spectrum β-lactamases have been mainly reported as main contributors to multi-drug resistance phenotypes of *P. aeruginosa* isolates.

1.5.1 Intrinsic resistance

P. aeruginosa itself has high intrinsic resistance to a narrow spectrum of antibiotics such as aminoglycosides, fluoroquinolones and β-lactams (Breidenstein *et al.,* 2011). Genes in bacterial genomes encoding inherent properties of cell structures and composition, which provide protection against antimicrobials, are the basis of intrinsic resistance mechanisms. For example, lower outer membrane permeability prevents the excessive penetration of the antibiotic molecules into the cell (Nicas and Hancock, 1983).

Moreover, *P. aeruginosa* possesses four well known active multidrug efflux pumps including MexAB-OprM, MexXY/OprM (OprA), MexCD-OprJ, and MexEF-OprN which greatly contribute to its antibiotic resistance.

Interestingly, these pumps can have an indirect effect on other physiological pathways as well. For instance, both MexEF-OprN and MexGHI-OpmD export the quinolone signalling molecule PQS, reducing its cellular concentration and resulting in the reduction of virulence factor production. This QS modulation seems to facilitate the establishment of chronic infections (Kohler *et al.*, 2001; Aendekerk *et al.*, 2005; Lamarche and De, 2011)

Furthermore, a gene encoding an inducible β-lactamase (AmpC) is another factor mediating intrinsic resistance and basal lower level antibiotic susceptibility of *P. aeruginosa*.

1.5.2 Acquired resistance

P. aeruginosa acquired resistance is mediated by the acquisition of antibiotic resistance genes via horizontal gene transfer or acquisition of mutations that affect the expression of the resistance genes (Breidenstein *et al.,* 2011) and it increases prevalence among clinical and environmental strains (Davies *et al.*, 1998; Davies and Davies, 2010)

Firstly, these mutations can result in overexpression of efflux pump encoding genes, for example, the derepression of the *mexAB-oprM* efflux pump genes due to mutations in *mexR* (Breidenstein *et al.,* 2011).

Secondly, these mutations can further reduce the uptake of the antibiotic, for example that of the antibiotic imipenem due to mutation in OprD specific porin (Walsh and Amyes, 2007). Thirdly, mutation in AmpD effector, indirectly controls the *ampC* gene encoding β-lactamase, leading to its upregulation (Hooper, 2001).

Acquired resistance occurs in the presence of antibiotic compounds, in contrast to intrinsic mechanisms and it leads to irreversible resistant population due to selective advantage (Lee *et al.*, 2016). However, acquired resistance similarly to intrinsic resistance, is stable and it can be transmitted to progeny. Acquired resistance is a potent mechanism which confers wide spectrum resistance due to the upregulation of resistance genes and the transmissibility by plasmids

1.5.3 Adaptive resistance

Adaptive resistance is an unstable and transient form of resistance, compared to other types of resistance mechanisms, the mechanisms behind it are not yet fully understood/are unclear. It is induced by specific antibiotics and other environmental stimuli and it involves modulation of genes associated with efflux pumps, the envelope and enzymes (Fernández *et al.*, 2010). Notably, the organism reverts to its default state of susceptibility once the inducing factor has been removed (Breidenstein *et al.,* 2011). Interestingly, the organism re-gains susceptibility upon removal of external stimuli (Barclay *et al.*, 1992; Xiong *et al.*, 1996; Fernández *et al.*, 2011). *P. aeruginosa* isolates have been presenting resistance to β-lactams, aminoglycosides, polymyxins and fluoroquinolones through this mechanism (Conesa *et al.*, 2016; Poole, 2005; Fernández *et al.*, 2011; Khaledi *et al.*, 2016) usually via adaptive multiple mutational mechanisms and genetic reversion (Lee *et al.*, 2016).

1.5.4 Biofilm-associated resistance

Biofilm is a functional community of microorganisms that is encased in an extracellular matrix composed of extracellular polysaccharide, eDNA and proteins (Breidenstein *et al.,* 2011; Geesey *et al.,* 1977; Costerton *et al*., 1995; Flemming *et al.,* 2007). The extracellular matrix itself presents the primary barrier to antibiotic penetration that adds to the antibiotic resistance. However, the cells organized in biofilms exhibit upregulation of efflux pumps, enzymes and various regulators that contribute to antibiotic resistance as well (Costerton *et al.,* 1995; O'Toole and Kolter, 1998; Groote *et al.*, 2009; Rollet *et al.,* 2009; Breidenstein *et al.,* 2011; Fitridge *et al.,* 2016). Resistance can also be

classified in terms of the molecular mechanism mediating it, it can be via mutations, via plasmids or QS associated. A gene promoter region or the gene sequence itself could be genetically altered via nucleotide deletion or insertion and point mutations. When a genetic alteration like this affects a regulatory pathway, it can boost resistance by increasing promoter activities of AmpC β-lactamase and multi-drug efflux pumps systems leading to their upregulation (Blair *et al.*, 2014). As a common mutational feature of *P. aeruginosa* isolates, resistant clinical mutants display a constitutive high level of AmpC production even in the absence of antibiotic inducers. In another example, mutational inactivation of *ampD* (repressor of *ampC*) can also have the same effect (Juan *et al.*, 2005).

Bacterial plasmids can also mediate resistance by/through transferring their genetic elements between bacteria in a process called horizontal gene transfer, which causes concern as its increasing treatment complications (Hong *et al.*, 2015). Resistance plasmids can be either narrow or broad host range, which signifies if it can be transferred within similar species or of unrelated species. For example, plasmid RP1 can transfer resistance genes to most Gram-negative bacteria (Brown, 1978). To date, *P. aeruginosa* resistance via horizontal gene transfer has been reported against β-lactams, fluoroquinolones and aminoglycosides (Bennett, 2008).

Interesting links between antibiotic resistance mechanism and the QS systems have been reported in *P. aeruginosa*. It was observed that some *lasR* mutants CF-infecting strains exhibited higher resistance to tobramycin, ciprofloxacin and ceftazidime, and the resistance was attributed to increased β-lactamase activity and bacterial metabolic adaptation shifts (D'Argenio *et al.*, 2007).

1.6. Non-traditional strategies to target Bacterial Infections with a focus on *P. aeruginosa*

1.6.1 Introduction: Challenges in fighting bacterial infections

The antibiotics revolution in medicine marked the 20th Century, it greatly contributed towards increase in longevity and quality of life by successful treatment in otherwise healthy individuals worldwide (Ó Muimhneacháin *et al.*, 2018).

Antimicrobial resistance has become a growing concern for public health globally (Pang *et al.*, 2019; Soukarieh *et al.*, 2018). Antibiotics currently in use aim on bacterial eradication, therefore very strong selective pressure is imposed on the bacterial communities (Defoirdt, 2018).

The overuse and misuse of antibiotics in enclosed clinical situations as well as in animal feed, resulted in accelerating development of drug-resistant bacterial strains (Pang *et al.*, 2019) due to increased evolutionary pressure and horizontal gene transfer (Ó Muimhneacháin *et al.*, 2018; Pang *et al.*, 2019). Overall, common bacterial infections are still being adequately treated by available antibiotics.

However, conventional antibiotics are not adequate treatment options in the case of the so-called ESKAPE pathogens (*Enterococcus faecium, Staphylococcus aureus, Klebsiella pneumoniae, Acinetobacter baumanii, P. aeruginosa,* and *Enterobacter* species), multidrug resistance pathogens causing nosocomial infections (Ó Muimhneacháin *et al.*, 2018).

Only very few novel classes of antibiotics have been discovered in the past 50 years, as development of antibiotic analogues is not sufficient to prevent the onset of resistance (Palumbi, 2001; Ó Muimhneacháin *et al.*, 2018) and there is a continuous need for new classes. As a consequence, a sharp decline in the development of new antimicrobials has been observed in recent years with the lack of investment by pharmaceutical companies (Ó Muimhneacháin *et al.*, 2018; Galdino *et al.*, 2019; Ventola, 2015; D'Angelo *et al.*, 2018). Unfortunately, *Pseudomonas aeruginosa* possesses numerous multi-faceted resistance mechanisms which make the development of new antipseudomonal antibiotics even more challenging (Veesenmeyer *et al.*, 2009).

Moreover, the high cost of drug development, the governmental pricing restrictions and the cost effectiveness of generic medicines present additional reasons affecting limited drug development (Ó Muimhneacháin *et al.*, 2018).

Therefore, the global challenges posed by the drug-resistant bacterial infections call on the development of new strategies to tackle those infections (Soukarieh *et al.*, 2018). At the moment, non-biocidal approaches, are rather appealing approaches since they aim at 'disarming' the pathogens, thereby preventing them from attacking their host (Defoirdt, 2013; Rasko and Sperandio, 2010; Clatworthy *et al.*, 2007; Defoirdt, 2018) rather than inhibiting growth or killing (or both) like traditional antibiotics (Theuretzbacher and Piddock, 2019). Hence, it is expected that this non-biocidal approach will not place such a strong evolutionary pressure on bacteria and would circumvent the bacteria from mutating and developing resistance (Ó Muimhneacháin *et al.*, 2018). However, more recent data indicates that approaches may still in fact carry a 'fitness cost' (Ó Muimhneacháin *et al.*, 2018).

1.6.2 The concept of antivirulence strategies, the potential targets

There is a growing body of literature describing anti-virulence strategies to combat infections caused by *P. aeruginosa*. The anti-virulence approach aims to disarm the *P. aeruginosa* infective arsenal through interference with the production or activity of virulence factors, in order to reduce the invasiveness of *P. aeruginosa* (Galdino *et al.*, 2019; Soukarieh *et al.*, 2018).

Therapies designed to attenuate virulence rather than killing bacteria may slow down or delay the emergence of resistance because they pose less selective pressure on the bacterial pathogen. Despite some reports on the emergence of resistance to these agents (García-Contreras *et al.*, 2013; Maeda *et al.*, 2012; Soukarieh *et al.*, 2018) they are still popular since it is a treatment that preserves commensal bacterial communities which are very important (Duménil, 2019; Galdino *et al.*, 2019).

Complex chemical signalling mechanisms of this opportunistic pathogen control virulence, hence they present potential targets in the development of novel therapeutic agents (Hurley *et al.*, 2012). These strategies include: inhibiting bacterial communication (inhibition of quorum sensing), targeting efflux pumps and lectins, impeding bacterial adhesion, and the use of iron chelators (Hurley *et al.*, 2012). Moreover, the use of bacteriophages for phage therapy, immunisation and immunotherapy as vaccine strategies, as well as targeting virulence via toxin production (Hurley *et al.*, 2012). In addition, antisenseRNA, nanoparticles, antimicrobial peptides, and microbiome-modifying therapies are discussed (Hurley *et al.*, 2012; Pang *et al.*, 2019; Theuretzbacher and Piddock, 2019)

Non-traditional treatment development also suffers hurdles that must be overcome. For example, they need to prove safety and efficacy for patient use. In the future, it is likely that most of these treatments, if approved, will not be replacing antibiotics it is more likely they will be used in combination with them (Theuretzbacher and Piddock, 2019). These therapies are known as Adjuvant therapies and they seem to have the potential to improve outcomes in *P. aeruginosa* infections (Veesenmeyer *et al.*, 2009). Numerous anti-virulence strategies are in discovery or preclinical development (Garland *et al.*, 2017; Theuretzbacher and Piddock, 2019).

Virulence factors can be variably conserved within species and among strains, therefore, any antimicrobials developed then will have high target specificity. Furthermore, the site of infection or the time course of the infection can play a role in the immune status of the host can shape/dictate the type of infection and the severity (Theuretzbacher and Piddock, 2019). Taken together, the high specificity of the antimicrobials and the complexity of the infection is a major challenge to predict the clinical presentation based on the early discovery. Hence, deeper understanding of host-pathogen interactions in *Pseudomonal* infections are necessary to develop both novel approaches and virulence factor antagonists (Veesenmeyer *et al.*, 2009)(Theuretzbacher and Piddock, 2019). Ideally, these strategies would yield more bioavailable and safe compounds which can move into clinical trials easily (D'Angelo *et al.*, 2018).

Bacterial surface virulent determinants such as flagella, pili and lipopolysaccharide as well as active processes such as the secretion of toxins (type III secretion), biofilm formation, and quorum sensing are some virulence "aspects" that are being targeted (Veesenmeyer *et al.*, 2009).

Disruption of QS by mimetic molecules, represents a primary target for the disruption of cooperative behaviour observed in in *P. aeruginosa* and provide an alternative approach to conventional antibacterial therapy (Ó Muimhneacháin *et al.*, 2018). Intriguingly, this approach which interferers with virulence regulatory mechanisms give a chance to interfere with multiple virulence factors at once (Defoirdt, 2018). However, whether targeting a master regulator of virulence is clinically beneficial still remains under question (Theuretzbacher and Piddock, 2019).

As an example, 5-fluorocytosine, an antifungal compound, inhibits virulence factor production in *P. aeruginosa* both *in vitro* and in a mouse lung infection model (D'Angelo *et al.*, 2018).

1.6.3 New antipseudomonal antibiotics

A novel class of antibiotics against *P. aeruginosa* named Protein epitope mimetic (PEM) molecules, have emerged. Compound POL7001 reduced bacterial burden and decreased the levels of inflammation in the lung of treated mice during *P. aeruginosa* acute and chronic infection. The side effects of POL7001 have not been reported yet (Pang *et al.*, 2019). However, with the new mode of action, the efficient pulmonary delivery and the potent *in vitro* and *in vivo* activity POL7001 is considered a novel therapeutic agent for future clinical trials.

A new carbapenem antibiotic, Doripenem demonstrated broad spectrum activity against Gram-negative and Gram-positive bacteria through inhibition of bacterial cell wall synthesis by binding to penicillin.

A next-generation, semisynthetic aminoglycoside antibiotic, Plazomicin which is synthetically derived from the natural product sisomicin (Aggen *et al.*, 2010) is able to resist a broad spectrum of aminoglycoside modifying enzymes, but not 16S rRNA ribosomal methyl-transferases (Cox *et al.*, 2018).

Therefore, Plazomicin demonstrates potent *in vitro* activity against both Gram-negative and Gram-positive bacterial pathogens. However, Plazomicin may cause mild to moderate nephrotoxic and ototoxic effects (Karaiskos *et al.*, 2015).

1.6.4 Virulence factor secretion targeting

Numerous toxins are secreted by *P. aeruginosa* into the extracellular environment, but a set of toxins are injected directly into host cells. Upon entry into the eukaryotic host cell, these secreted virulence factors responsible for pathogenesis elicit the symptoms in the infected individual (Lyons and Strynadka, 2019). Complex structures called Type III secretion systems (T3SS) are used to deliver the toxins into the host cell, therefore, they are obvious targets for anti-virulence therapies (Deng *et al.*, 2017; Anantharajah *et al.*, 2016b). Type III secretion systems form a macromolecular syringe (T3SS injectosome, T3SSi) embedded in both inner and outer membranes of *P. aeruginosa* and consists of 43 components (a simplistic schematic is shown on **Figure 1.3**). The development of small-molecule inhibitors which disrupt toxin secretion or the T3SSi, enhances as our understanding of different aspects of this machinery advances (Fasciano *et al.*, 2019; Aiello *et al.*, 2010). In addition, T3SS inhibitory monoclonal antibodies and peptides have been developed as well. Herein a briefly background on well-characterized classes and newly discovered classes of T3SS inhibitors is discussed.

Targeting the T3SS pathogenesis can occur by inhibiting the expression of T3SS genes in bacteria, by blocking the secretion of effectors into the extracellular environment or targeting the toxins/effectors themselves after secretion (Fasciano *et al.*, 2019).

Salicylidene acyl-hydrazides (SAHs) are a well-characterized class of T3SS small-molecule inhibitors across many bacterial species (Nordfelth *et al.*, 2005). An SAH, INP0341, mechanistic analysis has showed that it prevents T3SS gene expression in *P. aeruginosa* clinical isolates without affecting growth. Moreover, another SAH, INP0007 exhibits an impressive IC50 of 0.8 µM for T3SS-mediated secretion (Fasciano *et al.*, 2019).

Benzimidazole compounds have been shown to inhibit T3SS regulators such as ExsA in *P. aeruginosa* and provided protection from killing in models of *P. aeruginosa* infection (Veesenmeyer *et al.*, 2009). ExsA is a regulator necessary to express all T3SS genes (Marsden *et al.*, 2016; Lyons and Strynadka, 2019)

Several other classes of inhibitors have been identified and are known to inhibit the T3SS (Bowlin *et al.*, 2014). Phenoxyacetamide (PXA) was first discovered as an inhibitor of the T3SSi in *P. aeruginosa* and structure–activity relationship analysis demonstrated strict stereoselectivity suggesting an interaction with a specific target or site (Berube *et al.*, 2017).

HQ INP1855 reduces *P. aeruginosa* T3SS- mediated cytotoxicity in cultured cells, blocks secretion of ExoS effector protein, and enhances survival and reduces bacterial burden and lung pathology of mice infected intranasally with *P. aeruginosa* (Anantharajah *et al.*, 2016a; Fasciano *et al.*, 2019)

1.6.4.1 Immunotherapy

MEDI3902 and mAb A bispecific mAb monoclonal a (MEDI3902, Medimmune) targets the *P. aeruginosa* T3SS needle tip protein PcrV to prevent T3SS-mediated injection of toxins in host cells (Theuretzbacher and Piddock, 2019). This antibody was used in *P. aeruginosa* infected animal models and has shown efficacy in treating pneumonia.

A study has shown failure of this antibody in clinical use because only 11% of *P. aeruginosa* isolates of patients with chronic infections, produce a T3SS. However, Sawa and colleagues (Sawa *et al.*, 2014) suggested that the immunotherapy aspect was deemed to be safe and well tolerated in CF patients (Jain *et al.*, 2018) and may be useful in treatment of other pseudomonal nosocomial infections *in vivo* (Lyons and Strynadka, 2019).

Several derivatives also inhibit secretion of the *P. aeruginosa* effector protein ExoU, suggesting that they might target a conserved component of these two injectisome systems (Lam *et al.*, 2017; Fasciano *et al.*, 2019).

One proposed advantage of targeting the T3SS in *P. aeruginosa*, is that the injectisome is absent in many resident microbiota (Fasciano *et al.*, 2019). Hence, favourable members of the microbiome will be preserved, avoiding unwanted side effects from their elimination. Moreover, the likelihood of resistance development is kept minimal. However, a proposed disadvantage is that anti-T3SSi agents may need to be used in conjunction with antibiotics in infected immunocompromised patients (Fasciano *et al.*, 2019).

Novel anti-virulence compounds, can emerge by different methodologies, typically a defined compound library is screened *in vitro* for inhibitory effects on T3SS to the extracellular media. *In vivo* screening with infection models is possible, however, this can be difficult to accurately accomplish (Lyons and Strynadka, 2019).

Screening conditions should take into consideration biofilm formation in the case of *P. aeruginosa* (Totsika, 2016). Further challenges and considerations in anti- virulence drug design will not be discussed here. Overall, the main issues are that several identified inhibitors currently have no known mechanism of action, are not suitable in mammalian model systems due to their inability to cross membranes to reach their target or present bactericidal or general cytotoxicity (Lyons and Strynadka,

2019). Thus, we need to advance our knowledge of these compounds to be able to translate the potential of type III secretion neutralizing strategies to efficacy in the clinical setting (Veesenmeyer *et al.*, 2009).

Many candidates from different classes, and with different spectra of activity, that are effective in inhibition of the T3SS function show promise (Fasciano *et al.*, 2019). An ideal inhibitor would exhibit no bactericidal properties, no mammalian cell cytotoxicity, and no effect on the orthologous flagellar T3SS (Lyons and Strynadka, 2019).

1.6.5 Adhesion and Biofilm formation targeting

P. aeruginosa amongst other bacterial pathogens has evolved a number of surface-localized nanomachines that enable interactions with the host. Type IV Pili of the piliation system are considered nanomachines, that are being targeted as part of Innovative Antivirulence Therapeutics (Duménil, 2019).

Inhibitors of type IV pili have only been identified relatively recently and their potential applications are very broad (Duménil, 2019). For instance, Pilicides are an example of inhibitors that affect the biogenesis of the chaperone- usher class of pili (Duménil, 2019).

The P4MP4 (1-[(piperidin-4-yl)methyl]piperidin-4-ol), compound was identified by a phenotypic screening of bacteria by leading to reductions in the number of pili present at the bacterial surface. The effect of the compound was extremely rapid, and obvious within minutes, which highlighted the dynamic nature of type IV pili, which as it seems might be its weakness in this context (Duménil, 2019).

P4MP4 acts by targeting the PilF ATPase, which provides the energy required for pili assembly. P4MP4 actions basically locks the extension and retraction system, in a retraction-only mode which eventually leads to a bacterium without pili. Therefore, the drug has no effect on bacterial viability.

On the other hand phenothiazine derivatives exert their action differently, by affecting the function of the Na+-pumping NADH: quinone oxidoreductase (Na+-NQR) (Juárez and Barquera, 2012). The resulting trifluoroperazine concentration is partially toxic to bacteria and it triggers type IV pili disassembly.

Importantly, a study by Denis *et al*. (Denis *et al.*, 2019) demonstrated, that treatment with the phenothiazine family type IV pili inhibitor combined with antibiotic therapy in a humanized animal model, performs better than antibiotics alone. However, further work is necessary to optimize these drugs and understand in more depth their modes of action (Duménil, 2019) .

Biofilms are an obvious target for therapeutic interventions given their importance in *P. aeruginosa* pathogenesis. Specifically, the flagellum is a very important virulence factor of and is required for biofilm dispersal and adhesion to the surface of host cells. Therefore, immunization against flagellar antigens might be a suitable adjuvant therapy in individuals with CF as a preventive action for *P. aeruginosa* lung infection (Veesenmeyer *et al.*, 2009). However, such intervention might be futile since this bacterium downregulates the production of flagellin as it transitions to chronic infection in the CF lung (Wolfgang *et al.*, 2004; Palmer *et al.*, 2005)

1.6.6 Bacterial communication targeting

QS regulates the production of a multitude of virulence factors (Hurley *et al.*, 2012). 'Virulence factors' are compounds produced by pathogens that promote infection or evade the host immune system (Ó Muimhneacháin *et al.*, 2018).

When chronic biofilm infections are established by *P. aeruginosa*, permanent eradication is rarely achieved. *P. aeruginosa* infections are commonly difficult to eradicate with conventional antibiotics (Ó Muimhneacháin *et al.*, 2018). Therefore, new strategies such as 'antivirulence therapies' have emerged as a way to control *P. aeruginosa* infections by inhibiting QS signals (Ó Muimhneacháin *et al.*, 2018).This intervention does aim to kill bacteria, or to inhibit bacterial growth per se, but rather aims on blocking pathogenicity.

QS-interfering agents can be either natural or synthetic compounds which act by inhibiting the biosynthesis of the QS molecules, signal molecule detection, or signal transduction (Defoirdt, 2018). Other strategies include the promotion of QS molecule degradation or binding of QS signalling molecules by antibodies that sequester these and induce an immune response (Ó Muimhneacháin *et al.*, 2018).

As expected, such approaches come with their advances and challenges. For example, identification of such compounds needs evaluation though toxicity tests, which should be sensitive enough to identify the subtle toxic effects. Despite being subtle these toxic effects can have a significant impact on the expression of the reporter phenotype, without affecting growth (Defoirdt *et al.*, 2013).

However, it was shown that *P. aeruginosa* can become resistant to furanone C-30, a quorum-sensing inhibitor (Defoirdt, 2018).

Hence, mutations can arise that confer resistance to QS inhibitors (Defoirdt *et al.*, 2010) and, whether or not these mutants will likely lead to some degree of selection will depend on whether they would provide a fitness advantage under these conditions. Thus, the perceived advantages of antivirulence

strategies still need to be verified in order for these therapeutics to be brought into clinical use (Ó Muimhneacháin *et al.*, 2018).

In a relatively recent study, an *in silico* docking analysis was performed, and coupled with screening using a *P. aeruginosa* mCTX::P*pqsA*-*lux* chromosomal promoter fusion in order to identify new PqsR antagonists. A new class of *P. aeruginosa* PqsR antagonists was uncovered that inhibited pyocyanin and AQ signal molecule production in *P. aeruginosa* PAO1-L and PA14 strains (Soukarieh *et al.*, 2018). Importantly, the combined treatments had a synergistic effect with near complete biofilm eradication (Soukarieh *et al.*, 2018).

1.6.7 Counteraction of Immune evasion

Many bacteria employ their virulence factors to avoid detection or to escape the host immune response. Therefore, several strategies to neutralize such tactics are under development. For example, monoclonal antibodies targeting bacterial surface epitopes are hypothesized to increase bacterial clearance through enhancing antibody-dependent phagocytosis and/or complement-mediated bactericidal activity (Thanabalasuriar *et al.*, 2017).

1.6.8 Phage therapy (eg. As carriers, using phage-derived products)

Bacteriophages (phages) are naturally occurring viruses that infect bacterial cells, in many cases causing lysis of the bacterium. Synthetic biology amongst other modern tools have brought the field of phage research to the forefront (Pires *et al.*, 2016) as a response to the emergence of multidrug-resistant pathogens (Kortright *et al.*, 2019).

Generally, phages are considered safe because they do not infect mammalian cells. However, phage resistance can evolve quickly, usually within hours, regardless of the use of bacteriophage cocktail combinations. Overall, it is unlikely that phage therapy will replace the use of antibiotics (Rohde *et al.*, 2018), synergy with antibiotics seems like the most likely approach.

Bacteriophages produce endolysins which are peptidoglycan-degrading enzymes (Hurley *et al.*, 2012). They are encoded by phages in order to release the phage progeny from the inside of infected bacterial cells, resulting in bacterial cell death (Fischetti, 2018). Endolysins are highly specific bacteriolytic for a bacterial species or genus, and act independent of resistance pattern to conventional antibiotics (Fernandes and São-José, 2018; Theuretzbacher and Piddock, 2019). Overall, the recurrent failure of phage therapy due to the rise of phage resistance in the infecting bacterial population requires deeper

understanding of phage resistance for further development of phage therapy strategies that could be used in clinic (Chan *et al.*, 2018).

1.6.9 Novel therapeutic strategies for *P. aeruginosa* treatment

1.6.9.1 Lectin inhibitors

Lectins are outer membrane proteins which recognise sugar residues and allow bacterial cells to cross link. The two specific lectins, LecA and LecB have galactose- and fucose-specific specific binding sites, respectively, and so may be blocked by competitive inhibitors (galactose and fucose moieties, respectively)(Hurley *et al.*, 2012)

Lectins are bacterial outer membrane proteins that recognise host sugar residues and allow bacterial cells to crosslink to the host tissues. They also allow bacterial cells to aggregate and aid the formation of biofilm (Nilsson, 2003; Pang *et al.*, 2019). In the human airway, lectins interfere with normal ciliary beating and alter the host-mediated clearance of the organism (Hurley *et al.*, 2012).

1.6.9.2 Iron chelation

Iron is crucial for bacterial growth and is involved in many cellular processes, such as energy production, DNA replication and electron transport (Bullen *et al.*, 1978; Ma *et al.*, 2015). Iron metabolism in the respiratory tract is complex (Mateos *et al.*, 1998). Gallium is a non-redox iron III analogue that acts as an iron substitute in many biologic processes and thus it disrupts bacterial iron metabolism. It is a US FDA-approved drug for treatment of cancer-associated hypercalcemia (Minandri *et al.*, 2014). In addition, liposomal co-encapsulation preparations of gallium-gentamicin were shown to augment *in vitro* the activity of gentamicin against *P. aeruginosa* CF clinical isolates (Halwani *et al.*, 2008).

Kaneko *et al*. (Kaneko *et al.*, 2007) reported that gallium was able, by decreasing bacterial iron uptake and repressing transcriptional regulator PvdS-mediated pyoverdine synthesis, to inhibit *P. aeruginosa* growth, prevent biofilm formation, and manifest excellent bactericidal activity *in vitro*. Furthermore, gallium was tested in mouse infection model and it has been found able to effectively eradicate *P. aeruginosa* in bactericidal activity *in vivo* (DeLeon *et al.*, 2009; Kaneko *et al.*, 2007; Pang *et al.*, 2019)

1.6.9.3 Efflux pumps

It is crucial for the bacterium to be able to regulate its internal environment by removing toxic substances, including antibiotics (Alibert-Franco *et al.*, 2009), metabolites and QS signal molecules, and all that through the efflux pumps (Pearson *et al.*, 1999). Therefore, these structures are potential

targets of these non-conventional strategies as well. *P. aeruginosa* has a multitude of efflux pumps that are implicated in resistance to many antibiotics that render it multidrug resistant (Alcalde-Rico *et al.*, 2016). Efflux pump inhibitors (EPIs) have been utilized and it was revealed that intrinsic antibiotic resistance can be overcomed (Hurley *et al.*, 2012).

1.6.9.4 Vaccines

P. aeruginosa antigens elicit potent immune responses, and are responsible for pathogenesis (Lavoie *et al.*, 2011). Therefore, development of vaccines is another avenue that aims at preventing and reducing *P. aeruginosa* infections. However, no licensed vaccine is as yet available against this pathogen (Priebe and Goldberg, 2014). A novel *P. aeruginosa* vaccine PcrV28-294-OprI25-83-Hcp11-162 (POH), which contains PcrV, OprI and an important component of the type VI secretion system Hcp1, was tested in a mouse pneumonia and burn model. Interestingly, POH vaccination significantly triggered T-cell responses and proliferation, and protected mice against clinical *P. aeruginosa* strains (Yang *et al.*, 2017a; Pang *et al.*, 2019)

1.6.9.5 Pseudolysin

Pseudolysin is a 33-kDa neutral zinc-dependent metallopeptidase protein and is the most plentiful peptidase found in pseudomonal secretions. It contributes highly to *P. aeruginosa* invasiveness by disrupting the basolateral intercellular junctions present in the host tissues and cleaving several extracellular matrix proteins. This enzyme consists a promising target for the development of new anti-virulence compounds due to its multifaceted action. Several groups are focused on the development of pseudolysin-inhibitors that will downgrade pseudomonal infections by targeting of the proteolytic activity associated to this enzyme. Chelator agents have a great inhibitory action against pseudolysin since it belongs to the metallopeptidase class (Cathcart *et al.*, 2011; Kocabiyik *et al.*, 1995)

Therefore, the design of a therapeutic strategy that targets pseudolysin activity with natural and/or synthetic compounds, could be utilized to surpass the challenging antibiotic resistance concern (Galdino *et al.*, 2019).

1.6.9.6 Immunotherapy

Immunomodulating therapeutics refer to a great variety and diversity of drug classes which target a multitude of biological processes that modify host cell function (Chiang *et al.*, 2018). The most advanced immunomodulating agent/drug, is Reltecimod, which is in phase 3 clinical trials (AtoxB)(Theuretzbacher and Piddock, 2019).

Other strategies exist involving very immunogenic bacterial proteins, such as flagellin the protein that comprises the flagellum of *P. aeruginosa*, are currently in development. Some clinical trials of vaccine preparations were published suggesting a positive effect, however very few were of high quality in terms of randomisation and design (Hurley *et al.*, 2012). Much additional work is required to define the right dose and immunization schedule for optimal induction of long-lasting serum titers of antiflagellar IgG (Veesenmeyer *et al.*, 2009).

1.6.9.7 Antisense RNA

Antisense antimicrobial therapeutics are synthetic sequence-specific oligomers that silence expression of specific genes, in this case resistance genes (Sully and Geller, 2016). The idea is to target mRNA to prevent expression of a specific resistance gene and by doing so the gene product conferring resistance is no longer being made (Woodford and Wareham, 2009; Hurley *et al.*, 2012). Several functional genes are investigated as targets but there is still the need to be validated. The main challenge presented is that such agents need a delivery system to penetrate bacterial cells. Up to this point the main approach is coupling antisense oligomers to cell-penetrating peptides (Sully and Geller, 2016), but such conjugates have not progressed into clinical trials and more advanced research is necessary to deliver improved approaches (Theuretzbacher and Piddock, 2019).

1.6.10 Conclusions

In order to re-stock the insufficient antibiotic pipelines with new treatments, non-traditional therapies, such as "anti-virulence" therapies, have been proposed (Czaplewski *et al.*, 2016). Interestingly, approaches such as QS inhibition and phage therapy have shown significant antimicrobial effects against antibiotic-resistant strains of *P. aeruginosa in vitro* or in animal models (Pang *et al.*, 2019). However, it is highly unlikely that these non-conventional therapies will replace the use of antibiotics, in reality they will be used as adjuncts to conventional treatments (Czaplewski *et al.*, 2016). These combinatorial therapies are deemed more appropriate to battle *P. aeruginosa* infections because they utilize a multifaceted antibiotic resistance strategy (Pang *et al.*, 2019). Therefore, the drug-resistance problem will not be solved by these non-conventional therapies (Czaplewski *et al.*, 2016).

However, the major advantage of these therapies that aim to disarm *P. aeruginosa* virulence remains, and that is the delay of emergence of resistant strains due to no effect on bacterial viability and growth (Galdino *et al.*, 2019).

There are numerous challenges to translating anti-virulence strategies to new treatments for patients.

First of all the notion that they do not select for resistance has been challenged by experimental data (Allen *et al.*, 2014) and it seems that emergence of resistance depended on the importance of the specific targeted virulence factor to the pathogen (Totsika, 2016).

In addition, these treatments cannot use traditional MIC measurements of outcomes as they do not target bacterial growth or viability. Therefore, correlating outcome measures of non-traditional treatments in human does not apply to anti-virulence drugs (Theuretzbacher and Piddock, 2019). In most cases, alternative *in vitro* methods are not developed, and the predictability of animal models for clinical outcome are poorly described.

A huge challenge of late-stage clinical trials stems from the fact that non-traditional therapies must be administered with an active antibiotic. Hence, it would be very difficult to show a meaningful clinical benefit or to prove clinical efficacy in hospitalized patients for add-on in high-risk patient groups with a conventional non-inferiority clinical trial design (Theuretzbacher and Piddock, 2019). High-quality clinical trials are needed with fine selection of the appropriate indication, patient population and clinical endpoints (Theuretzbacher and Piddock, 2019).

Furthermore, production processes for biotherapeutic agents are not standardized or well-establish, same for quality control processes, which remain challenging. Identifying the right dose in the antibiotic field is a very well characterized process, however, in case of biotherapeutics it still remains elusive, further contributing to the challenges (Theuretzbacher and Piddock, 2019). One of the major obstacles with respect to practical applications is also finding adequate formulations and routes for delivery (Defoirdt, 2018).

Another enormous challenge has to do with choosing the optimal timing for the use of these agents, which remains uncertain. For example, some non-conventional therapies may be more suited for prophylaxis, while others may be more potent for clearance of chronic infection. However, there are other crucial aspects to consider that might present enormous challenges such as when and where are these non-conventional therapies active (Rathert *et al.*, 2008). Treatments would rely upon the expression of the targeted virulence factor gene in the particular strains of a species, the specific phase of infection etc. Therefore, such tailored approaches will require an in-depth understanding of the underlying mechanisms, the roles the targeted VFs have in disease processes and patient factors and thus it will require high financial resources.

Additionally, up to this point these agents have mainly been tested against pure cultures of pathogens therefore, it is unknown how other members of mixed communities could affect the outcome of the non-conventional therapies (Defoirdt, 2018). Last but not least, there is the possibility that any

interference with *P. aeruginosa* may potentially cause complications of infection in the patient due to indirect downstream effects in its cellular physiology (Pang *et al.*, 2019).

In conclusion, despite the interest in non-traditional approaches along with some encouraging results and what they could bring in treating bacterial infections, it is likely that effective treatments will be limited to healthcare settings with the best financial resources and healthcare systems that are able to financially support a strong growth of high-cost individual (personalized) medicines and thus to high-income countries (Theuretzbacher and Piddock, 2019).

The novel nature of each of these approaches combined with all the hurdles described above support that clinical application of these therapies may be slow and that it requires a better understanding of the host-bacteria as an integrated system in response to treatment for the development of innovative therapeutic strategies to fight against this extremely problematic human pathogen.

1.7 *P. aeruginosa* model strain genomic background

Generally, *P. aeruginosa* PAO1 model strain is extensively used in the field for illuminating the regulation of pathogenicity factors and of other exoproduct production (Girard and Bloemberg, 2008). *P. aeruginosa* PAO1, 6.3Mb genome was fully sequenced and it contains 5,570 predicted ORFs and 521 putative regulatory genes (Girard and Bloemberg, 2008; Stover *et al*., 2000). Interestingly, it has a relatively large genome and an unusually high proportion of regulatory genes (Girard and Bloemberg, 2008; Stover *et al*., 2000). Thereby, *P. aeruginosa* high environmental adaptability is reflected by its high genetic and functional diversity (Girard and Bloemberg, 2008; Stover *et al*., 2000).

1.8 Identification of novel putative antimicrobial targets in *P. aeruginosa*

The gene of interest investigated in this study was uncovered by an integrated whole genome screening using several disease models. The first step in the identification of antimicrobial target was the construction of a library of 57,360 random *P. aeruginosa* PAO1-Laussane Tn*5* transposants, representing approximately 95% of the genome (Miyata *et al.*, 2006). The library was constructed by using the pLM1 vector as it was proven highly efficient for this sole purpose (transposition) in *P. aeruginosa* (Larsen *et al.*, 2002). Subsequently, the library was assayed *in vitro* for reduced swarming, protease and pyocyanin production and 404 Tn*5* mutants were chosen and assayed further for reduced toxicity in non-vertebrates infection models *Drosophila melanogaster* and *Caenorhabditis elegans.*

The remaining Tn*5* targets were evaluated both *in vitro* and *in vivo* in mammalian cell lines and in mouse infection models, respectively (Dubern *et al.*, 2015). The proteins encoded by the evaluated 72

Tn*5* targets, which remained after removing any redundancies, were involved in antibiotic resistance, virulence factor delivery, biofilm formation and metabolism. The fact that no clear homologue was found for the majority of the selected targets is encouraging for their pharmaceutical applications. After the mammalian screenings were performed a total of 8 genes (*kdpB*, *pvdQ*, *bphO*, *crc*, PA2414, PA4916, PA5156, PA3613) which were found attenuated in both or at least one of the non-mammalian non-vertebrate infection models were published as targets. However, there were another 5 unpublished targets including the PA4803 gene, which is the center of this PhD project.

Significantly, more than 500 of *P. aeruginosa* genes are classified as uncharacterized thus suggesting that there is a gap in our knowledge in regards with the mechanisms and the array of virulence factors employed by *Pseudomonas* to cause disease waiting to be discovered (Dubern *et al.*, 2015). Finally, the screening revealed that pathogenicity exhibited by *Pseudomonas* Tn*5* transposants varied from model to model indicating that the environment in the host is the catalytic factor (Dubern *et al.*, 2015).

1.9 Aims of this study

The general aims of this PhD project were: (i) to investigate how the PA4803 gene, which is one of the novel antibacterial targets identified in the genome-wide screening, is regulated in *P. aeruginosa* (Dubern *et al.*, 2015); (ii) To unravel the mode of action of PA4803 in the control of virulence. This study also set out to characterize the PA4803 hypothetical protein with a methyltransferase predicted function. Crystallization of a protein is perquisite to solve the crystal structure, which is of great importance as it will provide an insight on how the particular protein functions, if it is an enzyme, its mechanisms of action and it might also reveal protein-protein interactions. Only then a structure-based drug design and development can be applied (Dessau and Modis, 2011).

Chapter 2 Materials and methods

2.10 Bacterial strains and growth conditions

2.10.1 Media and antibiotic concentrations

P. aeruginosa and *Escherichia coli* sublines were routinely grown in Lysogeny Broth (LB) liquid medium or on LB agar plates at 37 °C, supplemented with antibiotics when required as described on **Table 2.1.** IPTG was used at 1 mM concentration, to induce gene expression, unless otherwise stated.

Table 2.1. Overview of antibiotic concentration usage in this study.

Antibiotic	***E. coli***	***P. aeruginosa***
Ampicillin (Amp)	100 µg/mL Amp	-
Carbenicillin (Cb)	-	400 µg/mL
Chloroamphenicol (Cm)	20 µg/mL	-
Gentamicin (Gm)	20 µg/mL	20 µg/mL
Nalidixic Acid (Nal)	15 µg/mL	-
Spectinomycin (Sp)	-	1000 µg/mL
Tetracycline (Tc)	10 µg/mL	125 µg/mL

2.10.1.1 Chemically defined medium (CDM)

Chemically defined medium (CDM) used for growth assays. The CDM basic medium consisted of 20 mM D-glucose, 3 mM KCl, 3 mM NaCl, 12 mM $(NH_4)_2SO_4$, 3.2 mM $MgSO_4$, 0.02 mM $FeSO_4$, 1.2 mM K_2HPO_4 and 50 mM 3-(N-morpholino) propanesulfonicacid (MOPS), pH 7.8. A variation of the CDM medium, used for nutrient limitation consisted of 6 mM D-glucose, 0.9 mM $(NH_4)_2SO_4$.

2.10.1.2 Minimal M9 medium

M9 medium was used for the growth assays. 5 X M9 salt consisted 33.9 g/L Na_2HPO_4, 15 g/L KH_2PO_4, 2.5 g/L NaCl and 5 g/L NH_4Cl. M9 media was prepared by adding 1M $MgSO_4$ 2ml/L, 20% D-glucose and 1M $CaCl_2$ 0.1 ml/L to 5 X M9 salt solution diluted/dissolved with water.

2.10.1.3 Nutrient Broth

Nutrient Broth (NB), specifically NB No.2 (Oxoid) was used for motility assays. More details in the motility assays section below (Rashid and Kornberg, 2000).

2.10.1.4 *Pseudomonas* isolation agar

Pseudomonas isolation agar (PIA) was used to isolate *Pseudomonas* after conjugations. This medium was prepared as stated in the manufacturer's instructions. Namely, 45.03 g of powder were suspended in 1 L distilled water and 2 % (v/v) glycerol was supplemented after autoclaving and cool down.

2.10.1.5 Terrific Broth

Terrific broth is a highly enriched medium and it was used to improve yields in recombinant *E. coli* cultures used for protein production. It consisted of 0.17 M KH_2PO_4 (2.31 g), 0.72 M K_2HPO_4 (12.54 g), 24 g/L yeast extract and 20 g/L tryptone. 4 ml of glycerol were added after autoclaving and cool down.

2.10.1.6 Roswell Park Memorial Institute (RPMI) 1640 Medium

RPMI Media 1640 ready-to-use medium (Gibco) was used for growth assays.

2.10.2 Culture growth

Except otherwise stated, bacterial cultures were grown at 37 °C with 200 rpm shaking. When conical flasks were used they were filled to a 10 % of their total volume to allow good oxygenation. Culture growth was monitored by measuring optical density at 600 nm (OD_{600}) with a Spectrophotometer.

2.10.3 Bacterial storage/ Bacteria preservation

Bacterial overnight cultures were mixed in with 50-70 % (v/v) glycerol (1:1) and kept at -80°C for long-term storage.

2.11 General chemicals

Most chemical compounds were purchased from Sigma-Aldrich unless otherwise stated.

2.12 DNA manipulation

2.12.1 Strains and plasmids

Bacterial strains and plasmids used in this study are listed in **Table 2.2**.

Table 2.2. Bacterial strains and plasmids used in this study.

Strains or Plasmids	Description	Source/ Reference
E. coli strains		
DH5α	F– Φ80 *lacZ* Δ*M15* Δ*(lacZYA-argF) U169 recA1 endA1 hsdR17* (rK–, mK+) *phoA supE44 thi-1 gyrA96 relA1*	(Grant *et al.*, 1990)
S17-1 λ*pir*	*recA, thi, pro, hsdR*-M+RP4: 2-Tc:Mu: Km Tn*7* Tp^R Sm^R	(Simon *et al.*, 1983)
BL21	F^- *ompT gal dcm lon* $hsdS_B$ ($r_B^-m_B^-$) $[malB^+]_{K-12}(\lambda^S)$	(Paliy and Gunasekera, 2007)
S17-1 λ*pir* CTX-*lux*::P_{lasI} - Gm^r	S17-1 *λpir* strain carrying a copy of the *lasI* promoter linked to the *luxCDABE* genes (*lasI* transcriptional reporter); Gm^r	Matt Fletcher
S17-1 *λpir* CTX-*lux*::P_{rhlI} - Gm^r	S17-1 *λpir* strain carrying a copy of the *rhlI* promoter linked to the *luxCDABE* genes (*rhlI* transcriptional reporter); Gm^r	Matt Fletcher
S17-1 *λpir* CTX-*lux*::P_{pqsA} - Gm^r	S17-1 *λpir* strain carrying a copy of the *pqsA* promoter linked to the *luxCDABE* genes (*pqsA* transcriptional reporter); Gm^r	Matt Fletcher
S17-1 *λpir* CTX-*lux*::PA4802.1 - Gm^r	S17-1 λ*pir* strain carrying a copy of the PA4802.1 promoter linked to the *luxCDABE* genes (PA4802.1 transcriptional reporter); Gm^r	Ioanna Chatzigianni
P. aeruginosa strains		
PAO1-Lausanne (PAO1-L)	Wild-type/ prototroph /Parent strain	(Heurlier *et al.*, 2003)

PAO1-L CTX::P$_{PA4803}$[a]-*lux*	Wild type, carrying the transcriptional PA4803-*lux* reporter; Tc^R	This study
PAO1-L CTX::P$_{lasI}$-*lux*	Wild-type, carrying the *lasI lux*-based transcriptional reporter; Gm^r	This study
PAO1-L CTX::P$_{rhlI}$-*lux*	Wild-type, carrying the *rhlI lux*-based transcriptional reporter; Gm^R	This study
PAO1-L CTX::P$_{pqsA}$-*lux*	Wild-type, carrying the *pqsA lux*-based transcriptional reporter; Gm^R	This study
PAO1-L ΔPA4803[b] (Δ*samA*)[d]	Unmarked *samA* clean deletion mutant	Jean Dubern
PAO1-Lausanne (PAO1-L) pME3087-PA4803ind	Wild-type derivative carrying the pME3087- PA4803Ind construct in the chromosome (Before Cb enrichment); Tc^R , Sp^R/Sm^R	This study
PAO1-Lausanne (PAO1-L) PA4803ind candidates (No 1- No 16)	PAO1-L PA4803 Inducible strain (after Cb enrichment); Tc^S , Sp^R/Sm^R	This study
PAO1-L Δ*samA* CTX::P$_{lasI}$-*lux*[d]	Unmarked *samA* mutant, carrying the *lasI lux*-based transcriptional reporter; Gm^R	This study
PAO1-L Δ*samA* CTX::P$_{rhlI}$-*lux*[d]	Unmarked *samA* mutant, carrying the *rhlI lux*-based transcriptional reporter; Gm^R	This study
PAO1-L Δ*samA* CTX::P$_{pqsA}$-*lux*[d]	Unmarked *samA* mutant, carrying the *pqsA lux*-based transcriptional reporter; Gm^R	This study
PAO1-L *samA*Ind CTX::P$_{lasI}$-*lux*	*samA* inducible mutant, carrying the *lasI lux*-based transcriptional reporter; Gm^R	This study
PAO1-L *samA*Ind CTX::P$_{rhlI}$-*lux*	*samA* inducible mutant, carrying the *rhlI lux*-based transcriptional reporter; Gm^R	This study
PAO1-L *samA*Ind CTX::P$_{pqsA}$-*lux*	*samA* inducible mutant, carrying the *pqsA lux*-based transcriptional reporter; Gm^R	This study
PAO1-L CTX-*lux*::P$_{lasI}$	Wild-type, carrying the *lasI lux*-based transcriptional reporter; Gm^r	This study
PAO1-L CTX-*lux*::P$_{rhlI}$	Wild-type, carrying the *rhlI lux*-based transcriptional reporter; Gm^r	This study
PAO1-L CTX-*lux*::P$_{pqsA}$	Wild-type, carrying the *pqsA lux*-based transcriptional reporter; Gm^r	This study
PAO1-L CTX-*lux*::PA4802.1	Wild-type, carrying the PA4802.1 *lux*-based transcriptional reporter; Gm^r	This study
PAO1-L Δ*samA* CTX-*lux*::P$_{lasI}$[d]	Unmarked *samA* mutant, carrying the *lasI lux*-based transcriptional reporter; Gm^r	This study
PAO1-L Δ*samA* CTX-*lux*::P$_{rhlI}$[d]	Unmarked *samA* mutant, carrying the *rhlI lux*-based transcriptional reporter; Gm^r	This study
PAO1-L Δ*samA* CTX-*lux*::P$_{pqsA}$[d]	Unmarked *samA* mutant, carrying the *pqsA lux*-based transcriptional reporter; Gm^r	This study
PAO1-L Δ*samA* CTX-*lux*::PPA4802.1[d]	Unmarked *samA* mutant, carrying the PA4802.1 *lux*-based transcriptional reporter; Gm^r	This study

PAO1-L *samA*Ind	*samA* inducible mutant, in which transcription of the chromosomal *samA* gene is under the control of P_{tac} promoter and can be induced by IPTG; Sp^r	Ioanna Chatzigianni
PAO1-L *samA*Ind CTX-*lux*::P_{lasI}	*samA* inducible mutant, carrying the *lasI lux*-based transcriptional reporter; Gm^r	This study
PAO1-L *samA*Ind CTX-*lux*::P_{rhlI}	*samA* inducible mutant, carrying the *rhlI lux*-based transcriptional reporter; Gm^r	This study
PAO1-L *samA*Ind CTX-*lux*::P_{pqsA}	*samA* inducible mutant, carrying the *pqsA lux*-based transcriptional reporter; Gm^r	This study
PAO1-L *samA*Ind CTX-*lux*::PA4802.1	*samA* inducible mutant, carrying the PA4802.1 *lux*-based transcriptional reporter; Gm^r	This study
PAO1-L Δ*lasI*	Unmarked *lasI* in frame deletion mutant	James Lazenby
PAO1-L Δ*lasI* CTX-*lux*::PA4802.1	Unmarked *lasI* in frame deletion mutant, carrying the PA4802.1 *lux*-based transcriptional reporter; Gm^r	This study
PAO1-L Δ*rhlI*	Unmarked *rhlI* in frame deletion mutant	James Lazenby
PAO1-L Δ*rhlI* CTX-*lux*::PA4802.1	Unmarked *rhlI* in frame deletion mutant, carrying the PA4802.1 *lux*-based transcriptional reporter; Gm^r	This study
PAO1-L Δ*pqsA* CTX-*lux*::PA4802.1	Unmarked *pqsA* in frame deletion mutant, carrying the PA4802.1 *lux*-based transcriptional reporter; Gm^r	This study

Plasmids

pGEM®-T Easy	Linearized vector with a single 3´-terminal thymidine at both ends to improve the efficiency of ligation of PCR products, Blue/white screening; Amp^R	Promega Corporation
miniCTX-*lux*	Integration proficient vector with Ω FRT-*attP*, containing the *luxCDABE* operon downstream the multiple cloning site; Gm^R or Tc^R	(Hoang *et al.*, 2000)
miniCTX -*lux*:: $P_{PA4803/}$ CTX -*lux*:: P_{PA4803}	miniCTX vector carrying a copy of the PA4803 gene promoter linked to the *lux*CDABE genes (PA4803 *lux*-based transcriptional reporter); Tc^R	Jean Dubern
miniCTX-*lux* ::$P_{lasI /}$ CTX-*lux* ::P_{lasI}	miniCTX vector carrying a copy of the *lasI* gene promoter linked to the *lux*CDABE genes (*lasI lux*-based transcriptional reporter); Gm^r	Matt Fletcher
miniCTX-*lux*::$P_{rhlI /}$CTX-*lux*::P_{rhlI}	miniCTX vector carrying a copy of the *rhlI* gene promoter linked to the *lux*CDABE genes (*rhlI lux*-based transcriptional reporter); Gm^R	Matt Fletcher
miniCTX-*lux*::$P_{PA4802.1}$	miniCTX vector carrying a copy of the PA4802.1 promoter linked to the *luxCDABE* genes (PA4802.1 transcriptional reporter); Gm^r	Ioanna Chatzigianni
pME6032	pVS1-p15A shuttle expression vector; Tc^R	(Heeb *et al.*, 2002)
pME6032G-Gm^R	pVS1-p15A shuttle expression vector; Gm^R	Matt Fletcher

pME3087	ColE1 replicon-based suicide plasmid, IncP-1, Mob; Tc^R	(Voisard *et al.*, 1994)
pHP45Ω	Source of Ω Sm^R/Sp^R interposon	(Prentki and Krisch, 1984)
pBluescript KS II (+)	Cloning vector; ColE1 replicon; Amp^R	Stratagene[c]
pIC1 (pBS4803-1)	pBluescript KS II (+) derivative containing the 0.5 kb upstream region of PA4803 and the 1.5 kb *lacI*^{Q} fragment under the P_{tac} promoter; Amp^R	This study
pIC2 (pBS4803-2)	pBluescript KS II (+) derivative containing the 0.5 kb upstream region of PA4803, the 1.5 kb under the P_{tac} promoter and the 2.0 kb Ω cassette; Amp^R, Sp^R/Sm^R	This study
pIC3 (pBS4803-3)	pBluescript-II KS+ derivative containing the 0.5 kb upstream and 0.5 kb downstream regions of PA4803, the 1.5 kb under the P_{tac} promoter and the 2.0 kb Ω cassette; Amp^R, Sp^R/Sm^R	This study
pIC4 (pME3087-*PA4803*ind)	pME3087 derivative containing the 0.5 kb upstream and 0.5 kb downstream regions of PA4803, the 1.5 kb under the P_{tac} promoter and the 2.0 kb Ω cassette; Tc^R ; Sp^R/Sm^R	This study
pIC5 (pGEM®-T Easy-4803Compl)	pGEM®-T Easy vector derivative carrying the predicted PA4803 predicted promoter and PA4803 ORF region; Amp^R	This study
pIC6 (pME6032G-4803Compl)	Δ*lacI* pME6032 vector derivative carrying the predicted PA4803 predicted promoter and PA4803 ORF region; Gm^R	This study
pIC7 (pGEM®-T Easy-4803NToe)	pGEM®-T Easy vector derivative carrying the PA4803 ORF with an N-terminal His-tag; Amp^R	This study
pIC8 (pME6032-4803NToe)	pME6032 vector derivative carrying the PA4803 ORF with an N-terminal His-tag under the P_{tac} promoter; Tc^R	This study
pIC9a (PG-TEasytRNAUp) pGEM®-T Easy-PA4802.1Up	pGEM®-T Easy vector derivative containing the 0.5 kb upstream region of the PA4802.1 ($tRNA^{sec}$) gene; Amp^R	This study
pIC9b (PG-TEasytRNADw) pGEM®-T Easy-PA4802.1Down	pGEM®-T Easy vector derivative containing the 0.5 kb downstream region of the PA4802.1 ($tRNA^{sec}$) gene; Amp^R	This study
pIC11 (pGEM®-T Easy- $P_{PA4802.1}$)	pGEM®-T Easy vector derivative carrying a copy of the PA4802.1 gene and its predicted promoter; Amp^R	This study
pIC12 (miniCTX::$P_{PA4802.1}$-*lux*)	miniCTX vector carrying a copy of the PA4802.1 gene promoter linked to the *lux*CDABE genes (PA4802.1 *lux*-based transcriptional reporter); Tc^R	This study
pSK67-*samA*	pSK67 construct which expresses a SamA product with an N-terminal His-tag	Jean Dubern
pIC13 (pCOLD1-samA)	pCOLD1 construct which generates a SamA product with an extended N-terminal His-tag including an HRV 3C precision protease cleavage site	This study
pIC14 (pMALX(E)-samA)	pMALX(E) construct which generates a SamA product with an N-terminal Maltose Binding protein (MBP) fusion and a C-terminal His-tag	This study

pIC15 (pMALX(E)-(HRV 3C)-samA)	pMALX(E) construct which generates the same SamA product product with an N-terminal Maltose Binding protein (MBP) fusion and a C-terminal His-tag including an HRV 3C precision protease cleavage site after the MBP fusion partner	This study
pGEM®-T Easy- PA4802.1KO	pGEM®-T Easy vector derivative containing the 0.5 kb upstream and 0.5 kb downstream regions of the PA4802.1 ($tRNA^{sec}$) gene; Amp^R	This study
pME3087-PA4802.1KO	pME3087 derivative containing the 0.5 kb upstream and 0.5 kb downstream regions of the PA4802.1 ($tRNA^{sec}$) gene; Tc^R.	This study
pGEM®-T Easy-*samA*	pGEM®-T Easy vector derivative carrying a copy of the *samA* gene and its predicted promoter; Amp^R	This study
pME6032G-*samA* (complemantation plasmid)	Δ*lacI* pME6032 vector derivative carrying a copy of the *samA* gene and its predicted promoter; Gm^R	This study
pGEM®-T Easy-PA4802.1	pGEM®-T Easy vector derivative carrying a copy of the PA4802.1 gene and its predicted promoter; Amp^R	This study
pME6032G- PA4802.1 (complemantation plasmid)	Δ*lacI* pME6032 vector derivative carrying a copy of the PA4802.1 gene and its predicted promoter; Gm^R	This study
pGEM®-T Easy-*samA*-PA4802.1	pGEM®-T Easy vector derivative carrying a copy of both the samA and PA4802.1 genes including their predicted promoters; Amp^R	This study
pME6032G-*samA*-PA4802.1 (complemantation plasmid)	Δ*lacI* pME6032 vector derivative carrying a copy of both the samA and PA4802.1 genes including their predicted promoters; Gm^R	This study
pMini™ T 2.0 Vector	Cloning Vector of the NEB PCR Cloning Kit (NEB #E1202); Amp^R	New England Biolabs
pMini™ T 2.0 Vector-PA4812	pMini™ T 2.0 Vector derivative carrying 0.5 kb of the upstream 500 bp upstream and 500 bp downstream of the desired insertion point within the PA4812 gene sequence. In this case the insertion point is nucleotide 604; Amp^R	This study
pMini™ T 2.0 Vector-PA4812modified	pMini™ T 2.0 Vector derivative carrying 0.5 kb of the upstream 500 bp upstream and 500 bp downstream of the desired insertion point within the PA4812 gene sequence. A His-tag has been added at the insertion point which is nucleotide 604; Amp^R	This study
pME3087-4812-Tagged	pME3087 derivative containing the PA4812 His-tagged gene sequence; Tc^R	This study
CTX-*lux*::$P_{PA4802.1}$	miniCTX vector carrying a copy of the PA4802.1 promoter linked to the *luxCDABE* genes (PA4802.1 transcriptional reporter); Gm^r	This study

Antibiotic resistance abbreviations: Amp; ampicillin, Gm; gentamycin, Sm; streptomycin, Sp; spectinomycin Tc; tetracycline,

[a] miniCTX::P_{PAXXXX}-*lux* reporters were inserted in an intergenic region within the chromosome of *P. aeruginosa*.

[b] The PA4803 gene is also referred to as *samA* though out this thesis.

[c] http://www.genomics.agilent.com/en/home.jsp

[d] The marked strains are in reality in *Pseudomonas aeruginosa* PAO1-Nottingham strain background and not PAO1-Lausane, as it was discovered by RNA-seq in Chapter 6.

2.12.2 Molecular procedures

Genomic DNA was isolated using a Wizard Genomic DNA purification kit (Promega). Plasmid DNA was isolated using GenElute Plasmid Miniprep (Sigma-Aldrich) or a Midiprep Kit (Qiagen) according to the manufacturer's instructions. Oligonucleotides used in this study (Sigma-Aldrich) are listed in **Table 2.3**. PCR amplified fragments were obtained by using different systems/amplification programs, detailed in **Table 2.4**, and purified by Geneclean turbo kit (MP Biomedicals). Routine DNA sequencing was conducted using the Source BioScience, 1 Orchard Place, Nottingham Business Park, Nottingham, NG8 6PX, United Kingdom.

Further DNA manipulation techniques in the Molecular cloning context including restriction enzyme digestions, ligations (Promega enzymes) and agarose gel electrophoresis were performed as described by Sambrook and Russel (Sambrook and Russell, 2001). All agarose gels for electrophoresis were made at 1% agarose and stained with SYBR® Safe (Life Technologies). Band recovery was performed using the Monarch Gel extraction kit (New England Biolabs). When elevated concentrations of plasmid were required, the ligation reactions were dialyzed using 0.025 µm membrane filters (Merck Millipore).

Introduction of DNA into host cells by electroporation was carried out as described in Farinha and Kropinski (Farinha and Kropinski, 1990). Electrocompetent *E. coli* DH5α and S17 λ*pir* cells were prepared after several washes of the overnight (o/n) cultures with ice cold H_2O and 10% glycerol. A final volume of 50 µL of cells in glycerol was stored at -80°C and used for electroporation when required. Electrocompetent cells of *P. aeruginosa* were prepared from cultures grown overnight at 42 °C with several washes with 10% glycerol. In both cases, the MicroPulser (Bio-Rad) delivered 12.5 kV/cm per pulse in a 0.2 cm electroporation cuvette (Life Science).

During these procedures, DNA concentration and purity was assessed with the Nanodrop ND-1000 (Thermo Scientific).

Table 2.3. Primers used in this study.

Name	Sequence (5' → 3')	Restriction site [a] and or/tags
4803indFW1	ATAAAGCTTTGAGCATCGTCCTGCTGC	*Hin*dIII
4803indRV1	ATAGGATCCGACGACCTTCTCCGTGTT	*Bam*HI
4803indFW1-New	ATATCTAGATGAGCATCGTCCTGCTGC	*Xba*I
4803indFW2	ATAGAATTCATGTCCGAACGAGAGCAC	*Eco*RI
4803indRV2	ATAGGTACCTGCTCGGTGAGCTGGAAG	*Kpn*I

pSK67- 4803FW1	ATAGAATTCATG**CATCACCATCACCATCAC**TCCGAACGAGAGCACTGGCA	*Eco*RI, **His-tag**
pSK67- 4803RV1	ATAGAGCTCTCACAGGCGTTTCAGGCAAT	*Sac*I
Up4803Comp	TATGGATCCCATCTGCCTGTTCGTCGTCAC	*Bam*HI
Down4803Comp	TAT GAATTCCTCGAGACGGGAGCTTATCAGG	*Eco*RI
tRNA-UF1	ATAGGTACCAGGTGATGAAGGCGGTCC	*Kpn*I
tRNA-UR1	ATAGGATCCTCGAGACGGGAGCTTATCAG	*Bam*HI
tRNA-DF1	ATAGGATCCGTCTATCTCGGTCCGTTCCA	*Bam*HI
tRNA-DR1	ATATCTAGAGTCTATGCCAAGCAGCACCT	*Xba*I
tRNA-CTXF1	ATAGAATTCAGGTGATGAAGGCGGTCC	*Eco*RI
tRNA-CTXR1	ATAGGATCCGGATTTGAAGTCCGGCCAC	*Bam*HI
T7promoterFW[b]	TAATACGACTCACTATAGGG	-
T7terminalRV[b]	GCTAGTTATTGCTCAGCGG	-
M13FW[b]	TGTAAAACGACGGCCAGT	-
M13RV[b]	CAGGAAACAGCTATGAC	-
Tn13	CAGCAACACTTCTTCACGA	-
SamAoeSeqFw1	CTTTATGCTTGTAAACCGTTTTGTGAA	-
SamAoeSeqRev1	CCCGTCAAGTCAGCGTAATG	-
SamAComplSeqF	GTTAATGTGCCGTTAACGCCCT	-
SamAComplSeqR	AGGCAATGGCAGTAGACGAAGT	-
SamAoeSeqFw1	CTTATGCTTGTAAACCGTTTTGTGAA	-
		-
SamAoeSeqFw2	GCCACGGCCACTCGACCTT	-
SamAoeSeqRev4	AGGAATGGTGACGGCTTC	-
SamAoeSeqRev3	GCTGTGCAGGTCGTAAATCA	-
SamAoeSeqRev2	TTTCACATTCACCACCCTGA	-
SamAoeSeqRev1	CCCGTCAAGTCAGCGTAATG	-
fdhGFW1 (*Kpn*I)	ATAGGTACCGTGAAGGACAACTACCGGATG	*Kpn*I
fdhGRV1 (*Xba*I)	ATATCTAGATCTTGTCGTTTTCCAGCAGG	*Xba*I
fdhGRV2 (*Xba*I)	ATATCTAGATGACCCATTTGAATCCGCAC	*Xba*I
Q5SDM_fdhGFW1	**CACCATCAC**GTCCGCCACTTCAAGCTGG	**His-tag**
Q5SDM_fdhGRV1	**ATGGTGATG**CTGGTCGGCGAAGGCCTC	**His-tag**
FdhG-C-FW1	CCAGCATCACCATCACCATC	-
fdhG-C-RV1	TTCGGGCTGTGGATGTAGTC	-
FdhG-C-RV2	CTTCCTTCATCAGCTTGGCG	-

Primers used in this study for PA4803ind (*samA*ind) construct amplification and sequencing purposes

Name	Sequence (5' → 3')	Anneals in
*samA*indSeqFwd1	TAAGCTGATCCGGTGGATGACC	Omega cassette
*samA*indSeqRev1	GTTGAAAACCGGACATGGCACT	P_{tac} *lacI*^{Q}
*samA*indSeqFwd2	GGTGGTGTCGATGGTAGAACGA	P_{tac} *lacI*^{Q}
*samA*indSeqRev2	AGTGCTCTCGTTCGGACATGAA	PA4803 ORF
*samA*indSeqFwd3	CCGTCAACCACCATCAAACAGG	P_{tac} *lacI*^{Q}
*samA*indSeqRev3	AGGCAATGGCAGTAGACGAAGT	*samA* ORF (Not in construct)
*samA*indSeqFwd4	TTCATGTCCGAACGAGAGCACT	*samA* ORF
*samA*indSeqRev4	GCAGGAGTGCGTTTTGGAATGA	*samA* Downstream region

Abbreviations: FW; forward, RV; reverse.
Primers were designed using PAO1 as reference genome found in www.pseudomonas.org
[a] Restriction sites are underlined and tag encoding sequences are in bold in the primers sequences.
[b] Universal sequencing primers, their sequences were found in www.addgene.org

Table 2.4. Detailed PCR amplification programs used in this study.

Program 1				Program 2			Program 3			
Phases	**Temperature** (° C)	**Time**	**Cycles**	**Temp.** (° C)	**Time**	**Cycles**	**Phases**	**Temp.** (° C)	**Time**	**Cycles**
Initial denaturation	95	5 min	1x	98	1 min	1x	Initial denaturation	98 ° C	1 min	1x
Denaturation	95	30 sec	35 x	98	30 sec	35 x	Denaturation	98 ° C	10 sec	15 x
Annealing	60	45 sec	35 x	55 – 68	30 sec	35 x	Annealing	70 ° C	45 sec	15 x
Elongation	72	1 min	35 x	72	1 min	35 x	Elongation	72 ° C	45 sec	15 x
Final elongation	72	5 min	1x	72	5 min	1x	Denaturation	98 ° C	10 sec	20x
							Annealing	55 ° C	30 sec	20x
							Elongation	72 ° C	45 sec	20x
							Final elongation	72 ° C	5 min	1x
Cooling	4	∞	-	4	∞	1x	Cooling	4 ° C	∞	1x

Program 1: Routine PCR amplification program. **Program 2**: Adapted for the use of Phusion High Fidelity DNA polymerase (NEB). **Program 3**: Touchdown PCR amplification program, adapted for the use of Phusion High Fidelity DNA polymerase (NEB) as well.

2.12.3 Construction of biosensors

2.12.3.1 Construction of PA4802.1 transcriptional gene fusion reporter

A PA4802.1 reporter for *P. aeruginosa* was constructed as described in **Figure 2.1**, in order to assess PA4802.1 transcription under different growth phases and conditions. The upstream region of the PA4802.1 gene was analysed for a predicted promoter sequence using the BPROM software (http://linux1.softberry.com/berry). Using PAO1-L genomic DNA as template the promoter region of the PA4802.1 was amplified by PCR using primers tRNA-CTXF1/ tRNA-CTXR1 (**Table** 2.3. Primers used in **this study.**). The resulting PCR product was cloned in pGEM-T Easy and was excised with the *Bam*HI/*Eco*RI and cloned into pminiCTX-lux Gm^R (**Table 2.2**). The particular vector is able to insert in the chromosome due to the phase attachment site (attP) and Flp recombinase targets (FRTs) it contains, which are able to recombine with the attB sites in *P. aeruginosa.* The construct was confirmed by digestions and sequence analysis. The final construct was introduced in *E. coli* S17 λ*pir* donor strain and allelic exchange in *P. aeruginosa* PAO1-L occurred following conjugal mating. The light output during bacterial growth was then measured with an automated luminometer/spectrometer (TECAN GENios Pro).

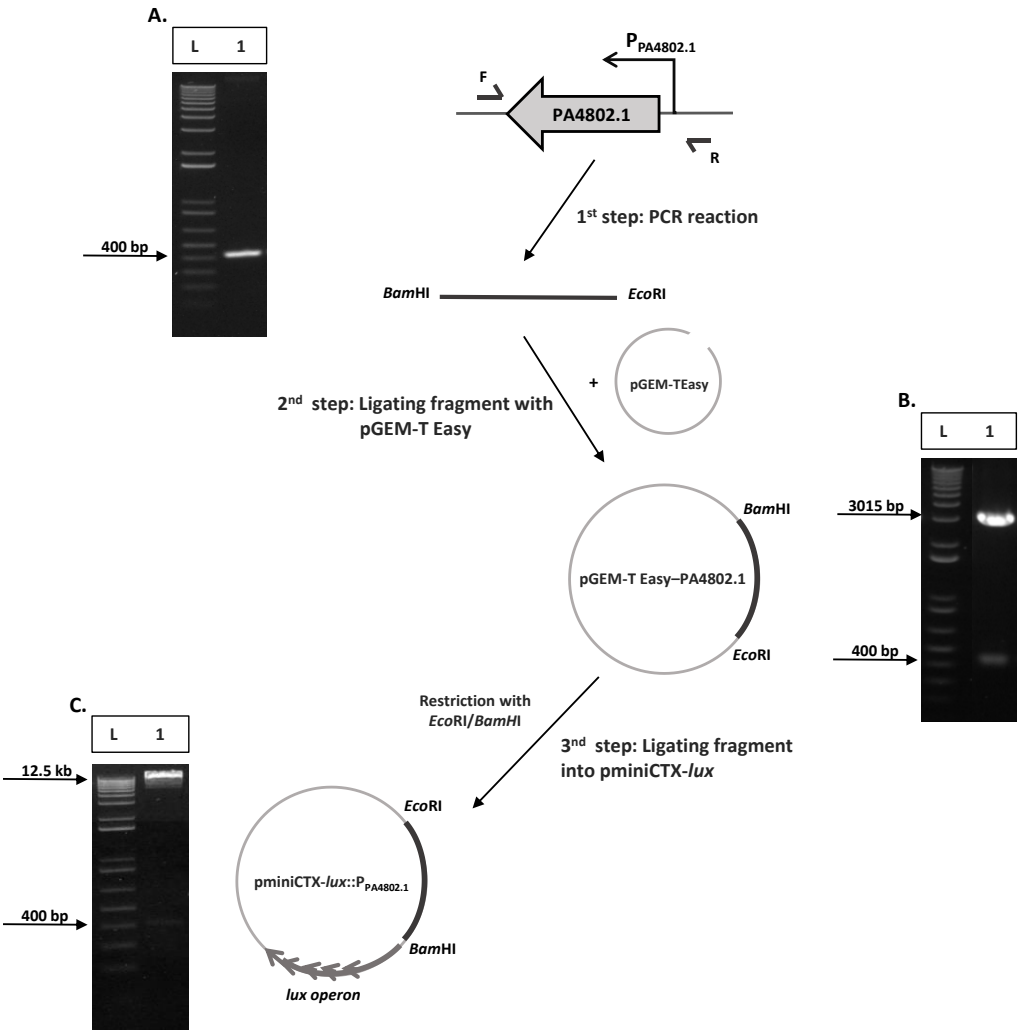


Figure 2.1. Schematic of the strategy used to construct the PA4802.1 biosensor.
Using PAO1-L genomic DNA as template PA4802.1 gene with its predicted promoter was amplified using the primer pairs tRNA-CTXF1/ tRNA-CTXR1 (Panel A). The resulting 400 bp PCR product was cloned in pGEM-T Easy. The sample was electroporated into competent *E. coli* S17 λ*pir* cells. Plasmid DNA from the transconjugants was extracted and analyzed by digestions with the same enzymes to confirm that both vector and insert were present, as seen in panel B. The *Eco*RI/*Bam*HI 400 bp fragment was extracted and cloned in pminiCTX-*lux* (Panel B). Sample was electroporated into competent *E. coli* S17 λ*pir* cells. Plasmid DNA from the transconjugants was extracted and analyzed by digestions with the same enzymes to confirm that both vector and insert were present, as seen in panel C. The final construct in pME3087 was introduced in *E. coli* S17 λ*pir* donor strain and allelic exchange in *P. aeruginosa* PAO1-L occurred following conjugal mating. ORFs and other elements are represented either by solid arrows or boxes. Letters F and R indicate forward and reverse primers. ORFs and other elements are represented either by solid arrows or boxes (Solovyev and Salamov, 2016; Groth and Calos, 2004).

2.12.4 Construction of deletion mutants and their complementation plasmids

2.12.4.1Construction of the *P. aeruginosa* PA4802.1 deletion mutant.

Using PAO1-L genomic DNA as template the upstream and downstream fragments of the PA4802.1 were amplified using the primer-pairs tRNA-UF1/tRNA-UR1 and tRNA-DF1/tRNA-DR1 (**Table 2.3**), respectively. The resulting PCR products were cloned in pGEM-T Easy, resulting in the plasmids PG-TEasytRNAUp and PG-TEasytRNADw (**Table 2.2**). The upstream and downstream fragments of each

gene were then excised with the *Kpn*I/*Bam*HI and *Bam*HI/*Xba*I restriction enzyme, respectively, and cloned in the suicide vector pME3087. The final construct was introduced in *E. coli* S17 λ*pir* donor strain and allelic exchange in *P. aeruginosa* PAO1-L occurred following conjugal mating. Putative PA4802.1 deletion mutants generated after the second recombination event were enriched by carbenicillin-treatment. Tc-susceptible clones were confirmed by PCR and sequence analysis.

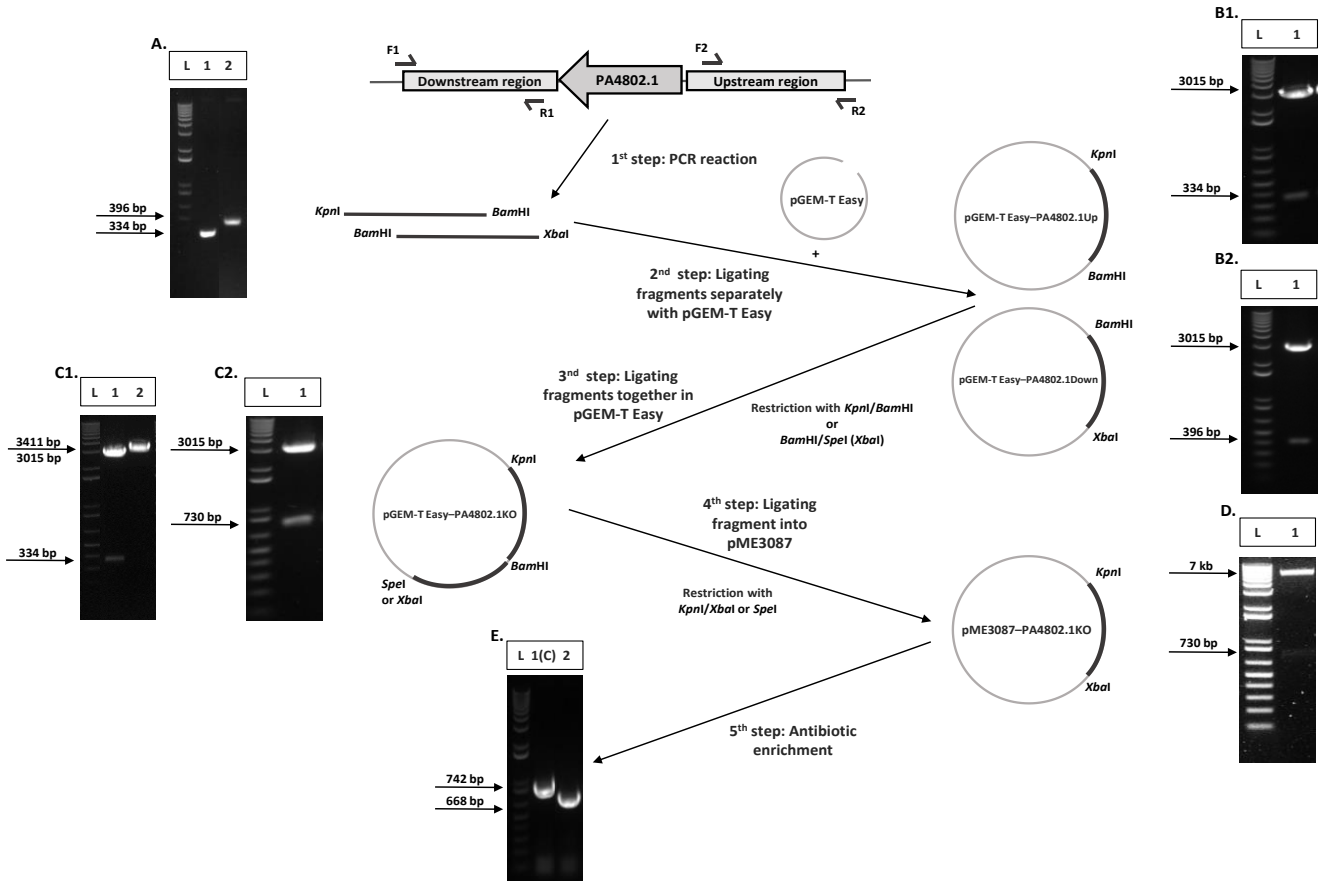


Figure 2.2. Schematic of the strategy used to construct the *P. aeruginosa* PA4802.1 deletion mutant.
Using PAO1-L genomic DNA as template the upstream and downstream fragments of the PA4802.1 were amplified using the primer pairs tRNA-UF1/tRNA-UR1 and tRNA-DF1/tRNA-DR1, respectively (Panel A). The resulting PCR products were cloned in pGEM-T Easy, resulting in the plasmids PG-TEasytRNAUp and PG-TEasytRNADw. The upstream and downstream fragments of each gene were then excised with the *Kpn*I/*Bam*HI and *Bam*HI/*Xba*I restriction enzymes and released a 334 bp and 396 bp fragment, respectively (Panel B). The orientation of the inserts was checked by a *Bam*HI/*Spe*I double digest as seen in panel C. The *Kpn*I/*Bam*HI 334 bp fragment from PG-TEasytRNAUp was extracted and cloned in the PG-TEasytRNADw next to the 396 bp fragment (Panel C2). The resulting 730 bp fragment was ligated in pME3087 and the sample was electroporated into competent *E. coli* S17 λ*pir* cells. Plasmid DNA from the transconjugants was extracted and analyzed by digestions with the same enzymes to confirm that both vector and insert were present, as seen in panel D. The final construct in pME3087 was introduced in *E. coli* S17 λ*pir* donor strain and allelic exchange in *P. aeruginosa* PAO1-L occurred following conjugal mating. Putative PA4802.1 mutants generated after the second recombination event were enriched by carbenicillin-treatment (Voisard *et al.*, 1994). Tc-susceptible clones were confirmed by PCR, see panel E, and sequence analysis. ORFs and other elements are represented either by solid arrows or boxes. For the PCR check tRNA-UF1/tRNA-DR1 primer pair was used with PAO1-L genomic DNA (C) and the PA4802.1 KO candidates (1-19) as template. ORFs and other elements are represented either by solid arrows or boxes. Letters F and R indicate forward and reverse primers. ORFs and other elements are represented either by solid arrows or boxes.

2.12.4.2 Construction of *samA* gene complementation plasmid

SamA gene ORF with its predicted promoter were amplified using the primer pair Up4803Comp/Down4803Comp (**Table 2.3**) with PAO1-L genomic DNA as template. The resulting PCR product was cloned in pGEM-T Easy and was excised with *Bam*HI/*Eco*RI and cloned into pME6032 which lacked the P_{tac} promoter. The construct was confirmed by digestions and sequence analysis. The final construct was introduced in *E. coli* S17 λ*pir* donor strain and allelic exchange in *P. aeruginosa* PAO1-L occurred following conjugal mating.

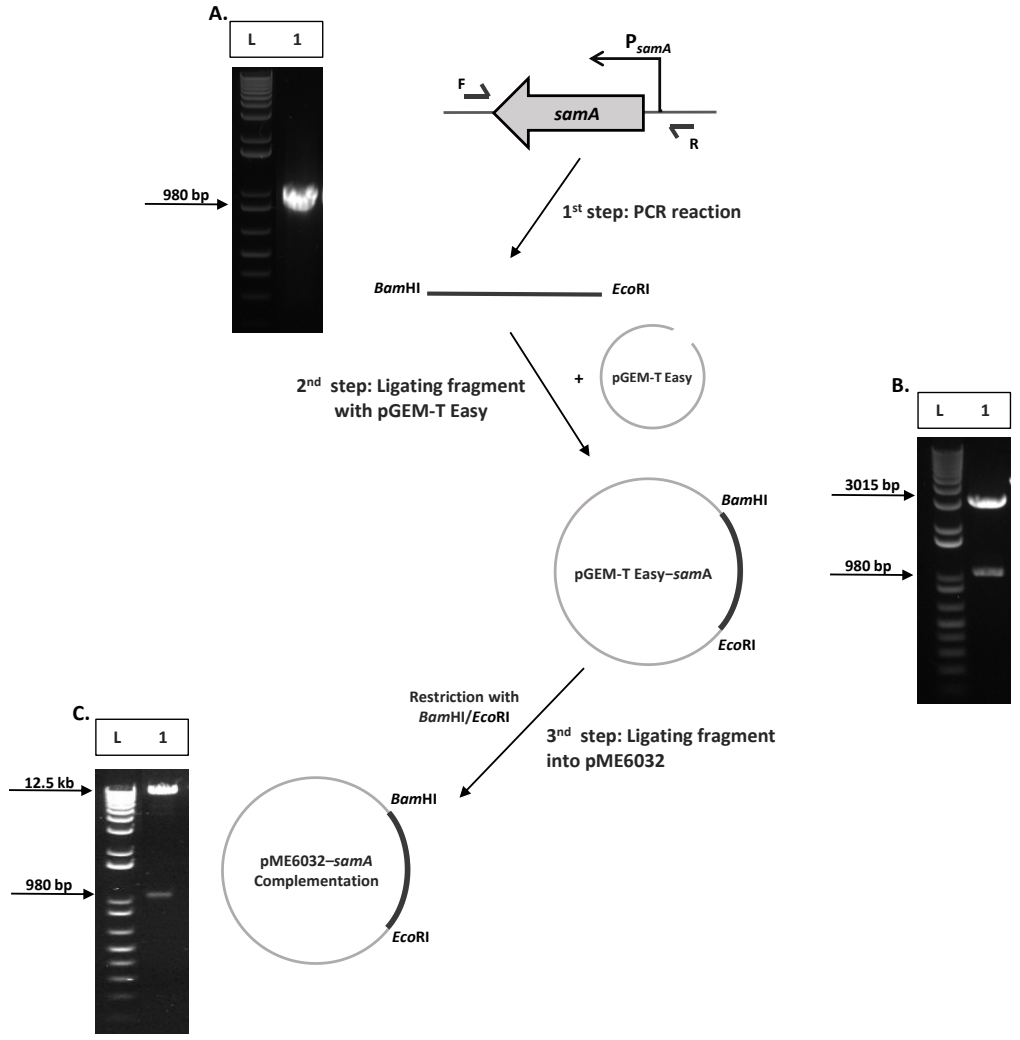


Figure 2.3. Schematic of the strategy used to construct the *P. aeruginosa samA* gene complementation plasmid.
The *samA* gene was amplified using the primer pair Up4803Comp/Down4803Comp with PAO1-L genomic DNA as template as seen in panels A. The resulting 271 bp PCR product with *Bam*HI/*Eco*RI restriction sites was cloned in pGEM-T Easy. The sample was electroporated into competent *E. coli* DH5α cells. Plasmid DNA from the transconjugants was extracted and analyzed by digestions with the same enzymes to confirm that both vector and insert were present, as seen in panel B. The insert was cloned into pME6032 (Gm^R). Plasmid DNA from the transconjugants was extracted and analyzed by digestions with the same enzymes to confirm that both vector and insert were present, as seen in panel C. ORFs and other elements are represented either by solid arrows or boxes. The putative *samA* transcriptional start site is represented by a thin black arrow. Letters F and R indicate forward and reverse primers.

2.12.4.3 Construction of PA4802.1 gene complementation plasmid

PA4802.1 gene with its predicted promoter were amplified using the primer pair Up4803Comp/Down4803Comp (**Table 2.3**) with PAO1-L genomic DNA as template. The resulting PCR product was cloned in pGEM-T Easy and was excised with *Eco*RI/*Kpn*I and cloned into pME6032 which lacked the P_{tac} promoter. The construct was confirmed by digestions and sequence analysis. The final construct was introduced in *E. coli* S17 λ*pir* donor strain and allelic exchange in *P. aeruginosa* PAO1-L occurred following conjugal mating.

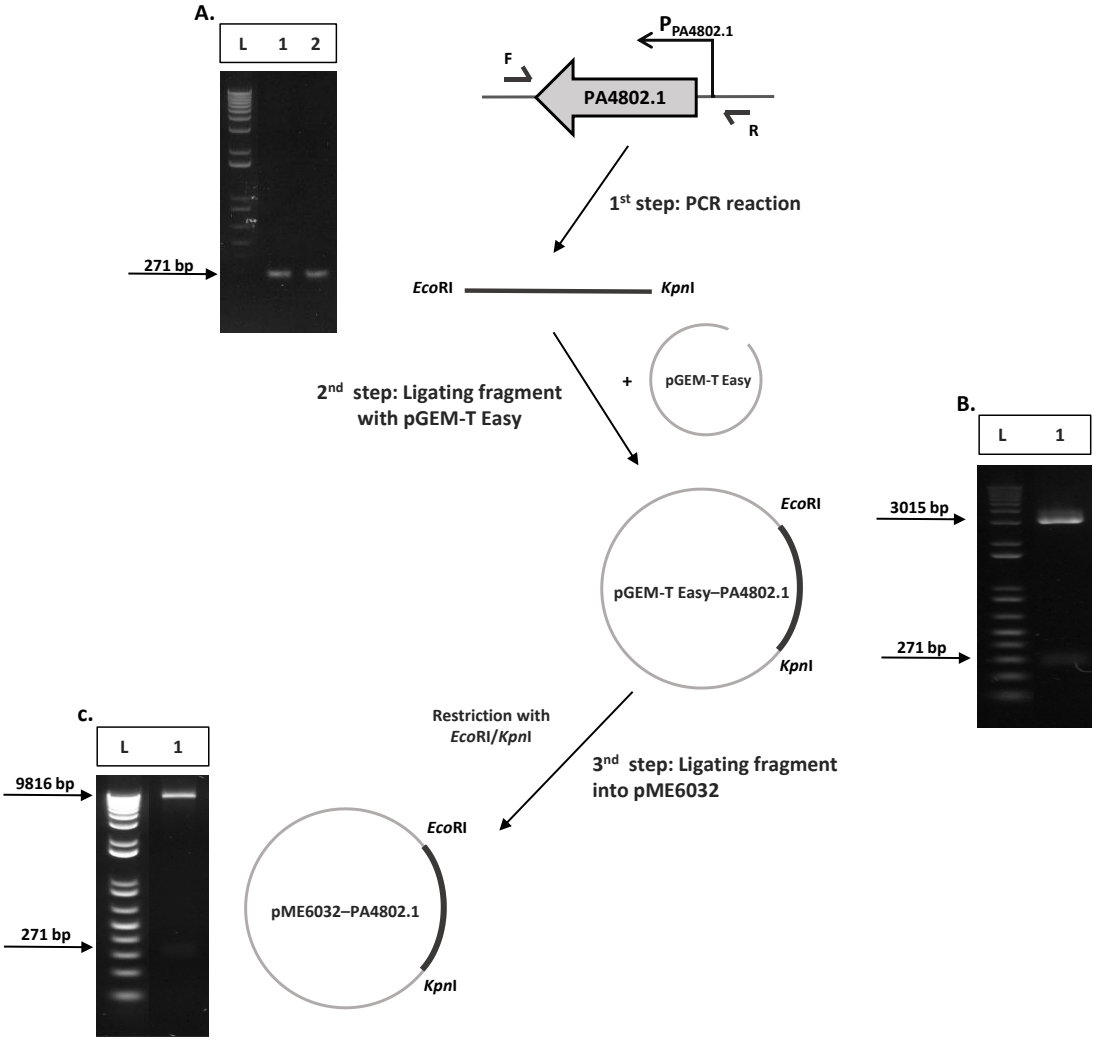


Figure 2.4. Schematic of the strategy used to construct the *P. aeruginosa PA4802.1* gene complementation plasmid
The PA4802.1 gene was amplified using the primer pair Up4802Compl/Down4802Compl with PAO1-L genomic DNA as template as seen in panels A. The resulting 271 bp PCR product with *Eco*RI/*Kpn*I restriction sites was cloned in pGEM-T Easy. The sample was electroporated into competent *E. coli* DH5α cells. Plasmid DNA from the transconjugants was extracted and analyzed by digestions with the same enzymes to confirm that both vector and insert were present, as seen in panel B. The insert was cloned into pME6032 (Gm^R). Plasmid DNA from the transconjugants was extracted and analyzed by digestions with the same enzymes to confirm that both vector and insert were present, as seen in panel C. ORFs and other elements are represented either by solid arrows or boxes. The putative PA4802.1 transcriptional start site is represented by a thin black arrow. Letters F and R indicate forward and reverse primers.

2.12.4.4 Construction of *samA* and PA4802.1 gene complementation plasmid

SamA and PA4802.1 genes with their predicted promoters were amplified using the primer pair Up480302Compl/Down480302Compl (**Table 2.3**) with PAO1-L genomic DNA as template. The resulting PCR product was cloned in pGEM-T Easy and was excised with *Eco*RI/*Kpn*I and cloned into pME6032 which lacked the P_{tac} promoter. The construct was confirmed by digestions and sequence analysis. The final construct was introduced in *E. coli* S17 λ*pir* donor strain and allelic exchange in *P. aeruginosa* PAO1-L occurred following conjugal mating.

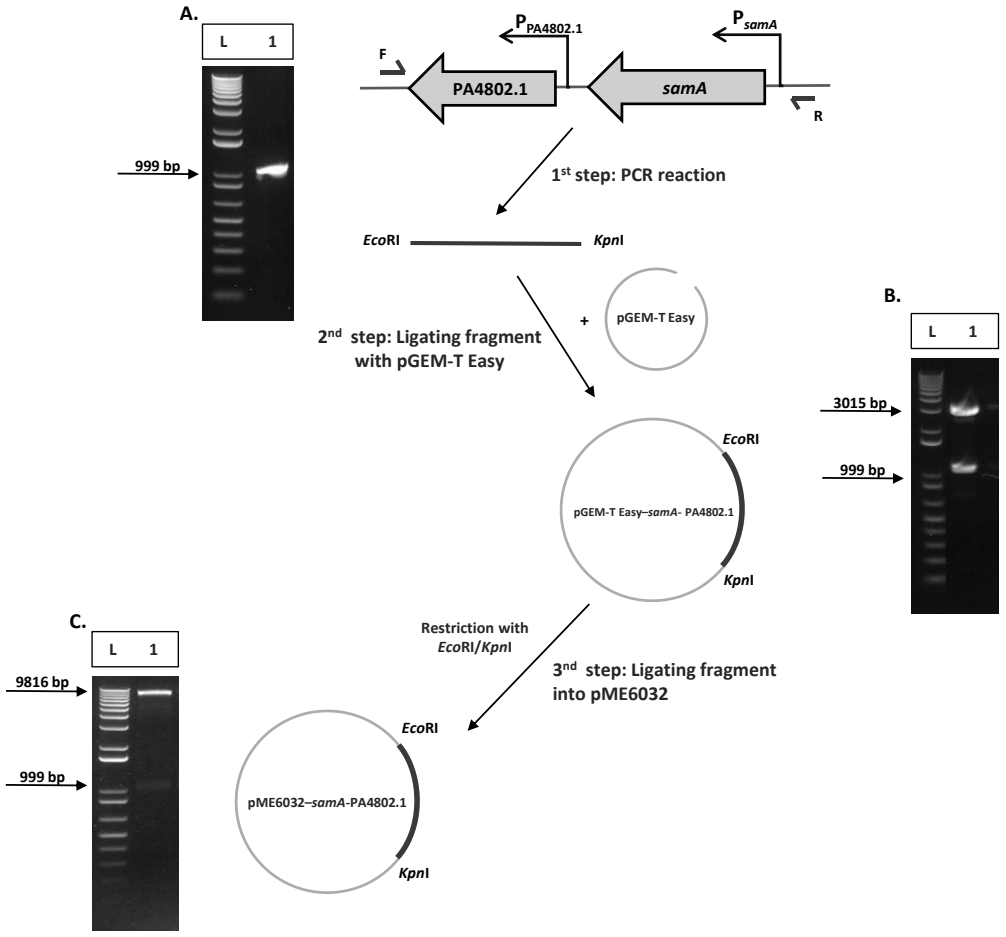


Figure 2.5. Schematic of the strategy used to construct the *P. aeruginosa samA* and PA4802.1 gene complementation plasmid.

Both PA4802.1 and PA4803 genes were amplified using the primer pair Up480302Compl/Down480302Compl with PAO1-L genomic DNA as template as seen in panel A. The resulting 999 bp PCR product with *Eco*RI/*Kpn*I restriction sites was cloned in pGEM-T Easy. The sample was electroporated into competent *E. coli* DH5α cells. Plasmid DNA from the transconjugants was extracted and analyzed by digestions with the same enzymes to confirm that both vector and insert were present, as seen in panel B. The insert was cloned into a derivative of pME6032 vector with Gm resistance. Plasmid DNA from the transconjugants was extracted and analyzed by digestions with the same enzymes to confirm that both vector and insert were present, as seen in panel C. ORFs and other elements are represented either by solid arrows or boxes. The putative *samA* and PA4802.1 transcriptional start sites are represented by a thin black arrow. Letters F and R indicate forward and reverse primers.

2.12.5 Construction of the *P. aeruginosa* conditional mutant PA4803ind (samA*Ind*) strain

Using PAO1-L genomic DNA as template the upstream fragment of the *samA* gene was amplified using the primers 4803indFW1 and 4803indRV1 (**Table 2.3**), while the downstream fragment was amplified using the primers 4803indFW2 and 4803indRV2-New (**Table 2.3**). The resulting PCR product for the Upstream PA4803 region and the 1.5 kb *Bam*HI-*Eco*RI *lacI*^{Q} P_{tac} inducible promoter fragment of pME6032 were cloned in pBluescript-II KS (+), resulting in the pIC1 plasmid. Then, the 2kb *Bam*HI Sm^{R}/Sp^{R} integron from pHP45Ω, was excised and cloned into the pIC1 plasmid digested with *Bam*HI resulting in the pIC2 plasmid. The resulting PCR product for the downstream PA4803 region was cloned into pIC2, resulting in pIC3. Then the whole construct was excised from PBlueScript-II KS (+) using *Xba*I and *Kpn*I and cloned into pME3087. The final construct in pME3087 was introduced in *E. coli* S17 λpir donor strain and allelic exchange in *P. aeruginosa* PAO1-L occurred following conjugal mating. Putative PA4803ind mutants generated after the second recombination event were enriched by carbenicillin-treatment. Tc-susceptible clones were confirmed by PCR, sequence analysis and phenotypic assays.

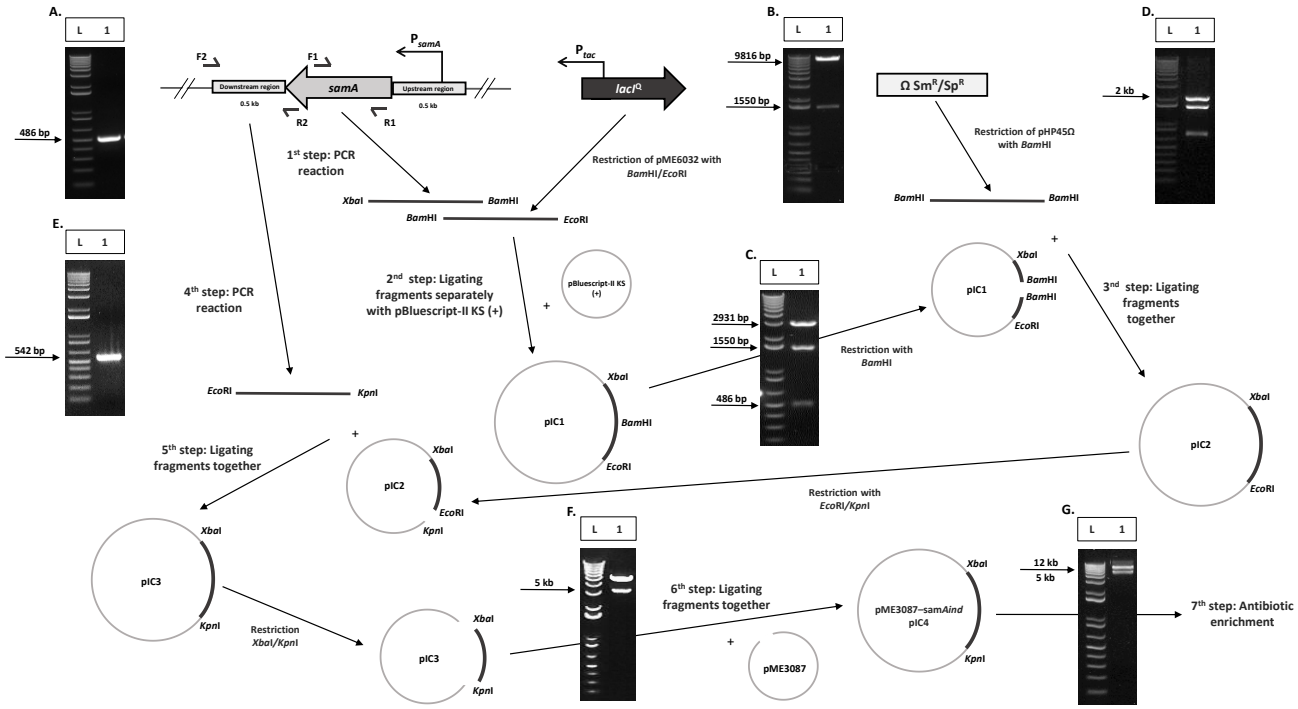


Figure 2.6. Schematic of the strategy used to construct the *P. aeruginosa samAInd* strain

Part of the *samA* gene was amplified using the primers 4803indFW1 and 4803indRV1. The resulting 486bp PCR product with *Xba*I/*Bam*HI restriction sites (PanelA) was cloned in pGEM-T Easy PBlueScript-II KS (+) with the 1.5 kb *Bam*HI-*Eco*RI *lacI*^{Q} P_{tac} inducible promoter fragment excised pME6032 (Panel B). The sample was electroporated into competent *E. coli* DH5α cells. Plasmid DNA from the transconjugants was extracted and analyzed by digestions with the same enzymes to confirm that both vector and insert were present, as seen in panel C. Then, the 2kb *Bam*HI Sm^{R}/Sp^{R} integron from pHP45Ω, was excised (Panel D) and cloned into the pIC1 vector digested with *Bam*HI resulting in the pIC2 plasmid. The downstream fragment was amplified using the primers 4803indFW2 and 4803indRV2-New. The resulting 542 bp PCR product for for the downstream *samA* region was cloned into pIC2, resulting in pIC3. Then the whole construct was excised from PBlueScript-II KS (+) using *Xba*I and *Kpn*I (Panel F) and cloned into pME3087. The final construct in pME3087 was analyzed by digestions (panel G) and was introduced in *E. coli* S17 λ*pir* donor strain and allelic exchange in *P. aeruginosa* PAO1-L occurred following conjugal mating. Putative *samA*ind mutants generated after the second recombination event were enriched by carbenicillin-treatment. Tc-susceptible clones were confirmed by PCR, sequence analysis and phenotypic assays. ORFs and other elements are represented either by solid arrows or boxes. The putative *samA* and PA4802.1 transcriptional start sites are represented by a thin black arrow. Letters F and R indicate forward and reverse primers.

2.12.6 Construction of chromosomal His-tagged *fdhG* gene strain in *P. aeruginosa.*

Part of the PA4812 *(fdhG)* gene was amplified using the primer-pair fdhGFW1/fdhGRV2 (**Table 2.3**) with PAO1-L genomic DNA as template. The resulting PCR product was cloned pMiniT 2.0 vector (**Table 2.2**). Primer pair Q5SDM_fdhGFW1/Q5SDM_fdhGRV1 (**Table 2.3**) was used in an inverse PCR of the entire plasmid, centred on the point we identified previously. The resulting PCR product (linearized vector with the insertion) was phosphorylated and circularized after the addition of a kinase and a ligase. The mix was transformed into *E. coli* cells, and the plasmid was isolated using the usual method in order to proceed to the next step. The generated plasmid was then digested with *Kpn*I /*Xba*I in order to obtain the insert, which was subclones in pME3087 suicide vector will be digested. The construct was confirmed by digestions and sequence analysis. The final construct was introduced in *E. coli* S17 λ*pir* donor strain and allelic exchange in *P. aeruginosa* PAO1-L occurred following conjugal mating.

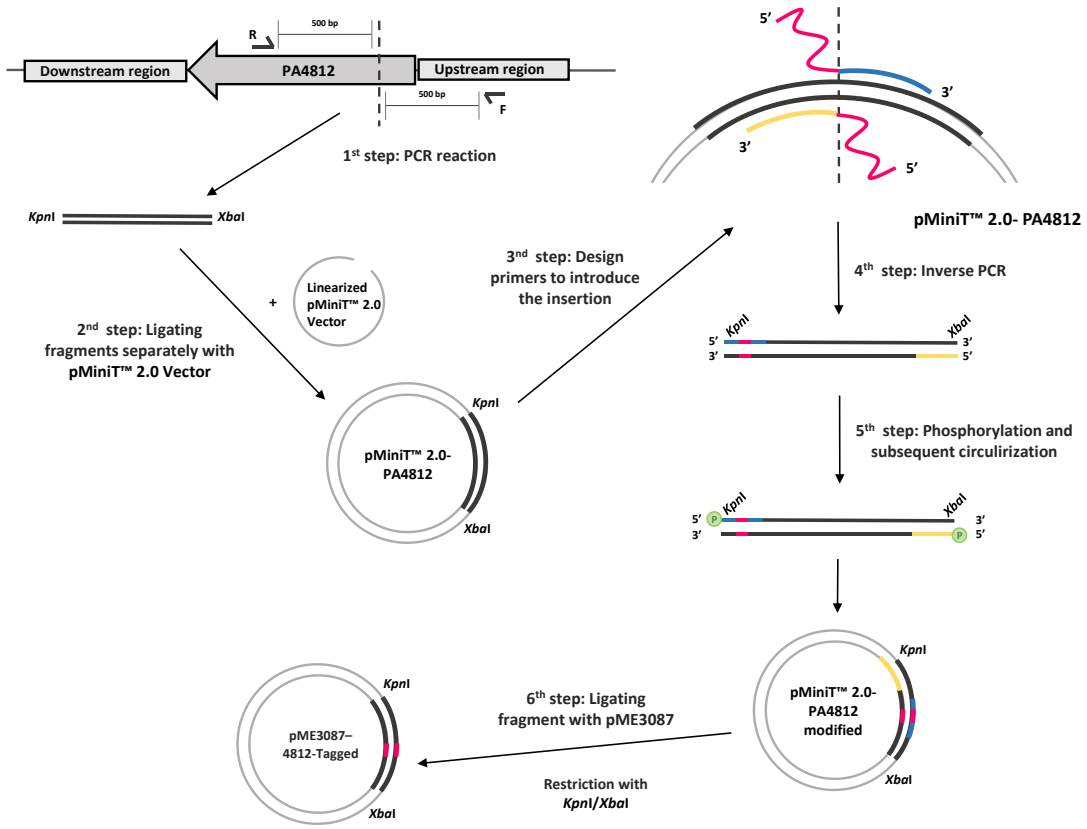


Figure 2.7. FdhG protein tagging through a chromosomal insertion – Cloning strategy
All the details are given in the section "2.3.6 Construction of chromosomal His-tagged *fdhG* gene strain in *P. aeruginosa*". ORFs and other elements are represented either by solid arrows or boxes. Letters F and R indicate forward and reverse primers. *Kpn*I restriction sequence is shown in blue line, *Xba*I restriction sequence is shown in yellow and the His-tag sequence is shown in pink.

2.13 Phenotypic characterization assays

2.13.1 Growth assays

Three types of growth curves were performed. Manual growth curves were performed by either inoculating liquid cultures in conical flasks or onto 96-well plates and aliquots were taken every hour to record OD_{600}/ absorbance values. Automated growth curves were performed by inoculating liquid cultures onto 96-well plates and measuring the OD_{600} with an automated spectrophotometer (TECAN Genios Pro).

2.13.2 Construction of strains by conjugation

P. aeruginosa PAO1-L derivative recipient and *E. coli* S17-1 λ*pir* donor cells containing the appropriate plasmid were grown in 5 mL LB liquid overnight cultures at 37 °C with or without antibiotic prior to conjugation. The saturated overnight bacterial cultures were centrifuged at 5,000x g for 5 min (Avanti 30; Beckman) and resuspended in 5 mL phosphate buffered saline (PBS). Following that, cultures of the donor and the recipient strains were mixed, centrifuged at 5,000x g for 5 min and again

resuspended in 5 mL of PBS. Approximately, 25 µL of the donor and recipient mixture (1:1) were inoculated on LB agar and incubated for 4-6 h at 37 °C. The transconjugants were selected on LB agar plates containing 15 µg/mL Nal and the antibiotic for which the plasmid has resistance to.

2.13.3 Motility assays

Motility assays media was prepared fresh on the day of the assay, autoclaved and allowed to cool down in a water bath at 50 °C for 30 min. Pictures of the motility were taken at the end of the assay, using a black background and indirect illumination.

2.13.3.1 Swarming motility

Swarming medium consisted of NB with a 0.5 % (wt/vol) Bacto Agar (BD). 20% Glucose was added to the media to final concentration of 0.5 (wt/vol) after cooling down because of temperature-sensitivity. 20 mL of molten medium were poured onto Petri dishes, allowed to settle at room temperature and dried for 30 min under laminar flow. 5 µL of overnight cultures were spotted on the surface of the plate. The plates were incubated at 37 °C for approximately 16 h.

2.13.3.2 Twitching motility

Twitching motility assay was performed as described by Rashid and Kornberg. The twitching medium consisted of 10 g/L tryptone (Oxoid), 5g/L yeast extract (Oxoid), 5g/L NaCl (Sigma) and 10g/L bacteriological agar (Oxoid). 10 mL of medium were poured in plates and dried for 15 min under laminar flow. A tip was used to stab inoculate the strains to be tested at the bottom of the twitching plates. Subsequently, the plates were incubated at 37 °C in a humidified container for 48 h. For better visualization of the twitching zone, the agar was removed, and the zone was stained with 1 % crystal violet.

2.13.4 Exoproduct quantification assays

Filtered supernatants of *P. aeruginosa* cultures in LB grown in flasks filled to a 10 % of their total volume, for 16 h at 37 °C and with 200 rpm shaking, were used to evaluate ability of the strains to produce pyocyanin as well as to assess elastase and protease activity.

The strains under investigation were evaluated for their ability to produce pyocyanin as described by Essar *et al.* (Essar *et al*., 1990) and elastase as described by Ohman *et al*. (Brint and Ohman, 1995). Protease production was evaluated in similar way like elastase as described by Ohman *et al*. but with some modifications.

2.13.4.1 Pyocyanin

Pyocyanin was first extracted from the culture supernatant with chloroform and re-extracted from the solvent with 0.2 M HCl. The aqueous phase after centrifugation was then measured at OD_{520}. The absorbance measurement was then multiplied by the extinction coefficient of the pigment, ε=17.072 m2/mol in order to calculate the quantitative data in µg/mL (Essar *et al*., 1990).

2.13.4.2 Alkaline protease, AprA

To assess alkaline protease activity, 0.25 mL of *P. aeruginosa* supernatant were mixed with 1 mL of a buffer composed of 20 mM Tris-HCl (pH 8.0), 1 mM $CaCl_2$ and 5 mg/mL of the azocasein. The mixture was incubated at 37 °C with 200 rpm shaking. The reaction was stopped after 15 minutes by the adding 500 µl of 10 % trichloroacetic acid (TCA). The supernatant phase after centrifugation was then measured at OD_{595}. The blank was a mixture of buffer and 0.25 mL fresh medium, to which the same treatment was applied.

2.13.4.3 Elastase, LasB

To assess elastase ability to cleave elastin, 100 µL of culture supernatant were mixed with 1 mL of buffer composed of 100 mM Tris-HCl (pH 7.5), 1 mM $CaCl_2$ 5, and supplemented with 5 mg/mL elastin-Congo red. The mixtures were incubated with 200 rpm shaking at 37 °C, The supernatant phase after centrifugation was then measured at OD_{495}. The blank was a mixture of buffer and 100 uL fresh medium, to which the same treatment was applied.

2.13.5 Alkyl quinolone extractions and LC-MS/MS quantification analysis

The strains under investigation were evaluated for their ability to produce *N*-acyl homoserine lactones (3-oxo-C12-HSL and C4-HSL) and alkyl quinolones (PQS) as described by Ortori (Ortori *et al.*, 2011). Bacterial overnight cultures were standardized to OD_{600nm} 0.01 and re-grown to stationary phase in 5ml of LB medium at 37°C. The culture supernatants were processed by centrifugation at 10000 × g for 5 min followed by filter-sterilization through a 0.22µm filter. Subsequently, 100 µl of supernatant was mixed with 390 µl of LB and 10 µl of appropriate internal standard to obtain a 1:5 dilution. The culture supernatants were extracted three times with acidified ethyl acetate (0.1% acetic acid) and 1.5 ml of extract was pooled for analysis by HPLC-coupled triple quadrupole mass spectrometry (LC-MS/MS). Chromatography was achieved using a Shimadzu series 10AD VP LC system. The MS system used for analyte detection was an Applied Biosystems Qtrap 4000 hybrid triple-quadrupole linear ion trap mass spectrometer equipped with an electrospray ionisation (ESI) interface.

2.14 Transposon mutagenesis

P. aeruginosa PAO1-L miniCTX-*lux*::PA4803 recipient was grown overnight in 5 mL LB liquid without antibiotic at 37 °C. *E. coli* S17-1 λ*pir* pME9978 carrying pLM1 donor was grown overnight in 5 mL LB liquid with 100 µg/mL Amp at 37 °C. Conjugation was carried out as described above. However, the incubation time was 8 h at 37 °C. The transconjugants were selected on LB agar plates containing 20 µg/mL Gm and 15 µg/mL Nal.

2.14.1 Transposon insertion locations

In order to determine the chromosomal insertion point of the transposon in the selected Tn*5* mutants total genomic DNA was isolated and digested with *Hind*III, *Eco*RI or *Eco*RV (Promega), because restriction sites for these enzymes are absent within pLM1. The resulted digested DNA fragments were recircularized and introduced in *E. coli* S17-1 λ*pir* by electroporation. The transformed clones were selected on 20 µg/ml Gm LB agar plates. DNA regions flanking the transposon were sequenced using primer Tn*13* at the Biopolymer synthesis and analysis department in QMC as mentioned above. The DNA sequences obtained were analyzed with the National Center for Biotechnology Information BLAST server by comparison with the PAO1 genome (www.pseudomonas.com) (Winsor *et al.*, 2016).

2.15 Gene expression analysis

2.15.1 Biosensor based gene expression assays / Microtiter plate assay

The optical density at 600nm (OD_{600}) of the bacterial overnight cultures was determined by a spectrophotometer (Thermo Scientific), after a washing step with fresh LB. Subsequently, the cultures were standardized to OD_{600} 0.05 and 200 µL of the re-standardized cultures were added onto a UV-light sterilized 96-well plate (Greiner) in triplicates. The unused wells of the plate were filled with medium to lower the evaporation of the samples. Absorbance and bioluminescence in relative light units (RLU) were recorded by a combined spectrophotometer/luminescence counter (TECAN GENios Pro) automatically every 30 min for 24 h.

2.15.2 RNA isolation (and reverse transcription)

Cultures of PAO1-L wt, ΔPA4803 and ΔPA4802.1 were inoculated in triplicates at starting OD_{600} of <0.01 and grown with aeration to an OD_{600} of 0.55-65 at 37 °C in LB and without aeration to an OD_{600} of 0.55-65 at 37 °C in LB supplemented with 100 mM KNO_3. Cells were then harvested and kept at –80 °C until RNA extraction.

RNA was isolated using two different protocols. 600 µl of culture were taken and mixed with 2 volumes of RNA Protect Bacteria Reagent (Qiagen). The pellets were processed further with the RNeasy Mini kit (Qiagen) following the manufacturer's instructions. Alternatively, pellets were resuspended in 1 mL of TRIzol (Invitrogen) and processed further following the manufacturer's instructions. DNA was removed from total RNA with Precision DNase kit (Primer design). RNA concentration was checked before and after DNAse treatment by spectrophotometry with NanoDrop™ 1000 (Thermo Fisher Scientific Inc., Waltham, MA USA). RNA integrity was checked using 2100 Agilent Bioanalyzer G2938B (Agilent Technologies Ltd., Santa Clara, CA USA) using the RNA 6000 Pico chip. Reverse transcription was performed by the Go-script reverse transcription system (Promega) according to the manufacturer's instructions. About 500ug of RNA were used per reaction.

2.15.3 (q)RT-PCR

The sequences of the genes studied were obtained from GenBank and the primers were designed with the aid of the Primer3Web (Available at: https://primer3.ut.ee/)(Koressaar and Remm, 2007; Kõressaar *et al.*, 2018; Untergasser *et al.*, 2012). The sequences of the primers are shown in **Table 2.5**. PCR was performed with PowerUp SYBR Green Master Mix (Applied Biosystems) according to the manufacturer's instructions. The final concentrations of cDNA and primers were respectively 1.3ng and 200 µm per reaction.

Table 2.5. Primers used in this study for qRT-PCR purposes.

Name	Sequence (5' → 3')
rpoDFW [a]	AAGGCCCTGAAGAAGCACGG
rpoDRV [a]	GATCGGCATGAACAGCTCGG
RT-PCRpscQFwd2 [b]	TGCACGAACTCGACCAACTGCC
RT-PCRpscQRev2 [b]	GGCACTGTCGAGATCGAGCAGC
RT-PCRfdnHFwd2 [b]	CCACAACCACGGCACCTACGAC
RT-PCRfdnHRev2 [b]	GATCAGCCACTCGAGGTTGCCG
RT-PCRoprMFwd1 [b]	GAGTTTCGACCTGACCCAGCGC
RT-PCRoprMRev1 [b]	AGCGCATTCTGGTCCTGGGCTA
RT-PCRcdrAFwd2 [b]	TCAACCTGTCCGGCGTGATCCT
RT-PCRcdrARev2 [b]	GTCGATCTTGCCGGCGATCTGG
RT-PCRfdnGFwd2 [b]	CGTCCGGACATCGCCATCATGG

RT-PCRfdnGRev2 [b]	CGTCGGGCTTGAGGTAGGACCA

Abbreviations: FW; forward, RV; reverse.
[a] Primer sequences were obtained from (Yoon *et al.*, 2011)
[b] Primers were designed using PAO1 as reference genome found in www.pseudomonas.org (Winsor *et al.*, 2016).

2.15.4 RNA-Seq library construction and sequencing

Following assessment of the quality of total RNA using Agilent 2100 bioanalyzer and RNA Nano Chip kit (Agilent Technologies, CA), rRNA was removed from X mg of RNA with RNAseq ribo depletion kit (Illumina). Quality of libraries were determined via Agilent 2100 Bioanalyzer using DNA High Sensitivity Chip kit and/or quantified using RT-PCR (No specifics on the kit used was given by the service company). Sequencing was performed using the NextSeq™ 500 platform resulting in 10 million total single-end 75-bp reads on average for each of the eighteen samples.

2.15.5 RNA-seq analysis

RNA-seq was performed previously by Novogene Ltd for *P. aeruginosa* PAO1-L cultures grown under two conditions: aerobic and anaerobic. The samples comprised of *P. aeruginosa* PAO1-L cultures in middle log phase (4 h), grown in LB. LB was supplemented with of 100 µM of KNO_3 for anaerobic growth. Independent triplicates were used for each condition. The analysis was done using the Galaxy server, (available at https://usegalaxy.org/)(Afgan *et al.*, 2018).

2.16 Bioinformatics/structure determination of PA4803 and PA4802.1 genes

2.16.1 Alignment of primary and secondary structures / Secondary structure predictions

The predicted secondary structure for PA4803 protein (also referred to as SamA) was obtained using four different online tools (SPIDER2, JPred4, Raghava and I-TASSER references available on **Table 2.6**). The ScanProsite tool was used to scan the PA4803 (SamA) protein sequence for the presence of SAM-dependent methyltransferase motifs.

The predicted secondary structure for PA4802.1 gene product ($tRNA^{sec}$) was obtained from two tools, the RNAComposer and the Vienna RNA-RNAfold (**Table 2.6**). Two different secondary structure prediction methods, the Centroid Fold and the Context Fold, were used.

2.16.2 Prediction of tertiary structures (and ligand binding sites)

The prediction of 3D protein structure for PA4803 (SamA) was determined with I-TASSER (**Table 2.6**), which first generates large ensemble of structural conformations, called decoys. The SPICKER program is used to give the final five models by clustering all the decoys based on the pair-wise structure

similarity. C-score is the confidence score of the prediction, it typically ranges from [-5, 2], where a higher score indicates a more reliable prediction. TM-score (ranking of structural alignment between the query structure and known structures in the PDB library) and Root mean square deviation (RMSD) between residues that are structurally aligned by TM-align, are estimated based on C-score and protein length following the correlation observed between these qualities. Possible binding ligands for the target protein were predicted by COFACTOR and COACH based on the I-TASSER structure prediction. The PA4802.1 $tRNA^{sec}$ tertiary structure prediction was obtained from the RNAComposer as well (data not shown).

Table 2.6. Summary of online servers and tools used for Protein and RNA Bionformatic analysis[a]

Server/Tool name	Access links	References
For Sequence alignment		
BLAST: Basic Local Alignment Search Tool (NCBI)	https://blast.ncbi.nlm.nih.gov/Blast.cgi	
EMBOSS Needle tool (EMBL-EBI)	http://www.ebi.ac.uk/Tools/psa/emboss_needle/	(Li *et al.*, 2015; Rice *et al.*, 2000)
For Secondary structure predictions (Protein)		
SPIDER2: Sequence-based Prediction of Local and Nonlocal Structural Features for Proteins	http://sparks-lab.org/server/SPIDER2/	(Heffernan *et al.*, 2015)
JPred4 : A Protein Secondary Structure Prediction Server	http://www.compbio.dundee.ac.uk/jpred/	(Gao *et al.*, 2016; Drozdetskiy *et al.*, 2015)
APSSP2: Advanced Protein Secondary Structure Prediction Server	http://www.imtech.res.in/raghava/apssp2/	(Raghava, 2002)
I-TASSER	http://zhanglab.ccmb.med.umich.edu/I-TASSER/	(Zhang, 2008; Roy *et al.*, 2011; Yang *et al.*, 2015)
For Secondary structure predictions (RNA)		
RNAComposer	http://rnacomposer.cs.put.poznan.pl/	(Popenda *et al.*, 2012)
Vienna RNA- RNAfold WebServer	http://rna.tbi.univie.ac.at/cgi-bin/RNAWebSuite/RNAfold.cgi	(Lorenz *et al.*, 2011; Hofacker *et al.*, 1994; Hofacker and Stadler, 2006; Zuker and Stiegler, 1980; McCaskill, 1990; Bompfünewerer *et al.*, 2008)
For Motif scanning		
ScanProsite	http://prosite.expasy.org/scanprosite/	(de Castro *et al.*, 2006)

[a]This is not an exhaustive list of Tools and Servers used in this study, many others were used and are mentioned in text.

2.1 PA4803 protein production, purification and crystallization

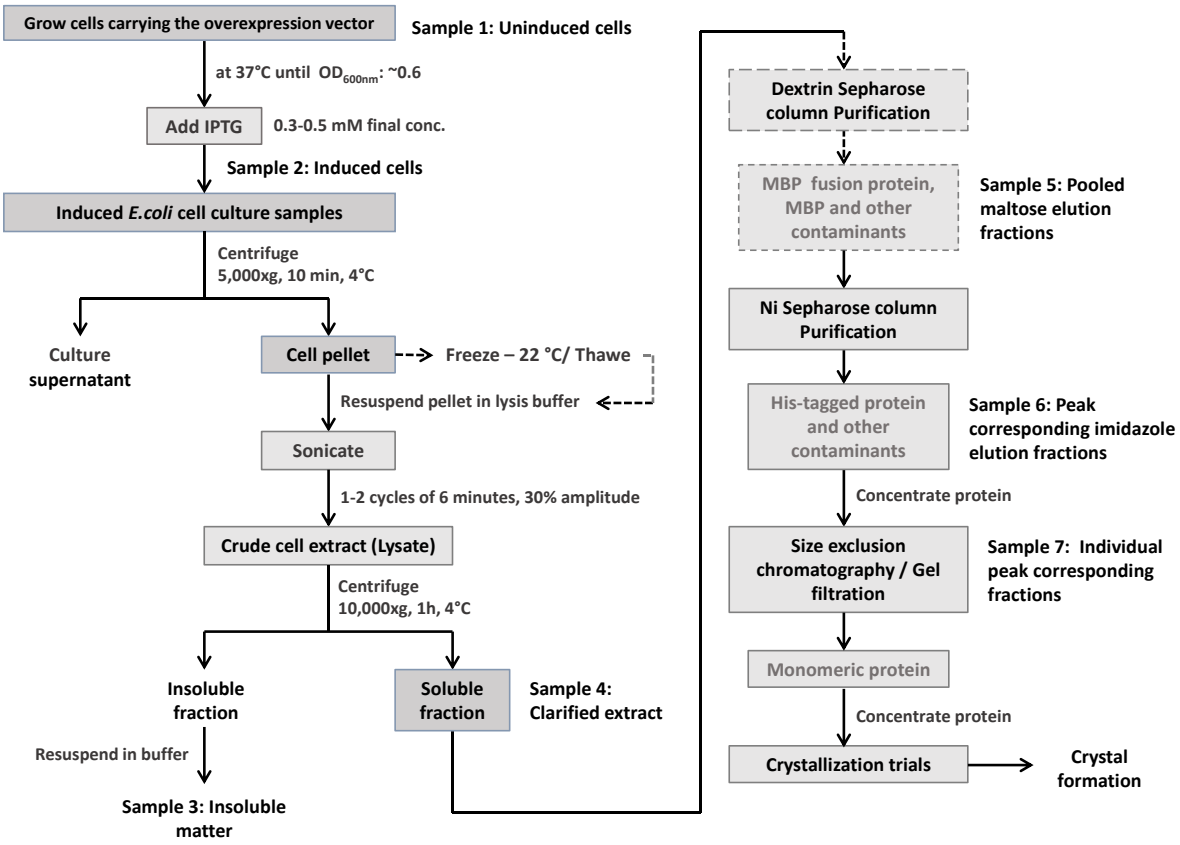


Figure 2.8. Protein purification protocol flowchart.
Figure modified from Rodriguez-Carmona (Rodríguez-Carmona *et al.*, 2010). This flow chart shows the process followed for PA4803 (SamA) protein purification produced by all the different constructs available. Different buffers were used dependent on the construct or the type of affinity column used for the purification. All the different buffer compositions are indicated in the text for simplification purposes. Dashed lines used in the flowchart indicate steps that were bypassed in some occasions.

2.16.3 PA4803 *(samA)* gene expression

A single *E. coli* colony containing the appropriate expression plasmid was picked from a fresh plate and inoculated in 10 mL of LB with the appropriate antibiotic and incubated overnight at 37 °C in a 50 mL flask. The next day 250 or 300 mL of Terrific broth (with the appropriate antibiotic) were inoculated with the overnight culture to OD_{600nm} 0.1 and grown at 37 °C with shaking (200 rpm) until OD_{600nm} of 0.6 was reached. The gene expression was induced by addition of isopropyl b-D-1-thiogalactopyranoside (IPTG) to final concentration of 0.3, 0.5 or 1 mM depending on the expression vector tested. The cultures were incubated with shaking and maximum aeration at a range of temperatures (18, 22, 30 and 37°C) for 24 h. Cell pellet samples were taken before and after the

induction at 4 h and 24 h and stored at –20 °C until expression analysis. The cells were harvested the next day by centrifugation at 5000 x g for 15 min. The pellet was stored overnight at -20°C.

2.16.4 Sample preparation and expression analysis by SDS-PAGE and Western Blotting

Total *E. coli* extracts were prepared after cell pellets collected from 0.1 mL of the o/n culture were resuspended in 100-200 µL of 1x SDS sample buffer, composed of 50 mM Tris-HCl (pH 6.8), 2% SDS, 10% Glycerol, 1% β-mercaptoethanol (β-ME), 12,5 mM EDTA, 0.02 % bromophenol blue and heated at 95 °C for 10 minutes. Total amount of 10 µL of the prepared samples, was separated in 12.5% or 15% SDS-PAGE at 200 V for 1 h. After separation, proteins were visualized using GelCode Blue stain reagent (Thermo Fisher Scientific). In some cases, the proteins were wet transferred at 150 V for 1h to a nitrocellulose membrane (GE Healthcare). The blot was blocked with 5% TBS-T/Skimmed milk powder (Sigma- Aldrich) overnight at 4°C. The next day the blot was washed with TBS-T twice for 7 min and incubated for 1h with the Penta-His antibody, contained in the Ni-NTA Fast Start Kit (Qiagen), in 1:10 dilution at room temperature. Finally, proteins were detected by chemiluminescence using ECL Plus (GE Healthcare) after the blot was washed with TBS-T twice for 5 min.

2.16.5 Purification of MBP and/or Hexahistidine tagged PA4803 (SamA)

Harvested cell pellets were washed with ice cold PBS and were resuspended in appropriate amount of Buffer (10 mL for each 1 g pellet). Depending on the column to be used the buffer composition varied. The resuspension was sonicated at Amplitude 30% for 6-12 minutes (15 sec-Pulse On, 15 sec-Pulse Off) with Sonic Dimembrator Model 705 (Fisher Scientific). After sonication the lysate was centrifugated at 10,000 x g for 1 h. The supernatant referred to as soluble fraction was stored for further processing and the sonication pellet was resuspended in another buffer composed of 8M Urea, 1.2% β-ME,50 mM Tris (pH 7,5) and 5% Glycerol, in the same amount as the lysis buffer used previously. Usually, 10 µL of each fraction was used for SDS-PAGE analysis after addition of 1:1 volume of 1x SDS-sample buffer (for composition see above).

The soluble fraction obtained was filtered using 0.22 µm filter and applied by the sample pump (flow rate 3 mL/min) onto a 5 mL MBPTrap HP columns (GE Healthcare) prepacked with Dextrin Sepharose already equilibrated with 5 column volumes (CV) of MBP buffer A of 300mM NaCl, 50 mM Tris (pH 7,5) and 5% glycerol. The column was then connected to an ÄKTA purification system (GE Healthcare) already washed and equilibrated with MBP buffer A. The purifier was programmed to collect 1-2.5 mL fractions of the eluted volume. Any unbound protein was washed from the resin and the bound

protein was eluted by addition of the MBP Buffer A with added 10 mM D(þ)-maltose (Sigma) referred to as MBP Buffer B.

The peak fractions that could contain the target protein were pooled and applied by the sample pump (flow rate 3 mL/min) onto a 5 mL HiTrap Chelating HP column (GE Healthcare) charged with 5 CV of 400 mM Ni+2 and equilibrated with 5 CV of Buffer A: 300 mM NaCl, 50 mM Tris (pH 7,5), 5% glycerol and 20 mM imidazole. The column was adapted to an ÄKTA purification system (GE Healthcare) washed and equilibrated with buffer A, followed by gradient imidazole elution of the His-tagged protein using increasing concentrations of buffer B: 500 mM instead of 20 mM imidazole (flow rate 2 mL/min). The final peak fractions and all solutions that could contain target protein were collected.

2.16.6 Size exclusion chromatography/Gel filtration

The eluted protein from the fractions was concentrated using Centricon Plus Centrifugal Filter Units (Millipore) and loaded onto a Superdex 200 30/10 size exclusion (GE Healthcare) equilibrated with degassed buffer composed of 300 mM NaCl, 20 mM Tris (pH 7,5), 2% glycerol and 40 mM D-(þ)-maltose. The monomeric protein peak fractions were pooled and concentrated to 3 mg/mL.

2.16.7 Crystallization trials and Optimization of conditions

Concentrated protein obtained was used for several commercially available 96-condition screens for protein crystallization. The hanging drop vapour diffusion method was performed. In which, equal amount of protein was mixed with each condition at a 200 µL final volume of drops, on MRC crystallization plates (Swissci) already containing Morpheus ® HT-96 (Molecular Dimensions) or another screen (85 mL in the main wells). Details of others screens can be found on **Table 4.1**. The dispensing was carried out using a Mosquito (TTP labtech) nanolitre liquid handler. Final assessments were made after one week by manual inspection using a high-powered Leica MZ12.5 stereomicroscope. When a probable protein crystal was detected in a screen tray, a crystallization optimization tray was set in which the ligand mixes, precipitant mixes and buffers (responsible for pH) fixed ratios were altered.

2.16.8 Pull down assays

Tagged PA4803 (SamA) was produced using *E. coli* BL21 containing the appropriate construct at 22 °C overnight. Cell pellet harvested from 150 mL of culture was resuspended in appropriate amount of buffer A: 50 mM, Tris (pH 7.5), 150 mM NaCl, 20 mM imidazole and 1% glycerol. The resuspension was sonicated, as described above, and the lysate of each strain after centrifugation was filter sterilized with 0.22 µm filters. Each *E.coli* lysate was mixed with PA PAO1-L lysate. After 2 h of incubation at 4

°C, 1 mL of the mixture was added to a 1.5 mL Eppendorf tube containing 100 µL of nickel beads previously washed 3 times with buffer buffer A. The tubes were kept on ice and constantly rolling for about 20 min and were washed 3 times with buffer A. The proteins were eluted with 200 µL of buffer B: 50 mM Tris (pH 7.5), 150 mM NaCl, 500mM imidazole and 1% glycerol. Samples of each individual lysate, of the mixture after incubation, and of each eluate were collected and analysed by SDS-PAGE (Fig. 4).

Alternatively, cell pellet harvested from 150 mL of culture was resuspended in appropriate amount of buffer A1: 50 mM Tris (pH 7.5), 500 mM NaCl, 50 mM imidazole and 1% glycerol. Each *E.coli* lysate was added to a 15 mL tube containing 500 µL of Nickel beads (GE Healthcare), previously washed 3 times with buffer A1. The tubes were kept cold and constantly rolling for about 20 min. After that, the tubes were centrifuged for 10 minutes at 10,000 x g and the supernatant was removed. The beads were washed 3 times by adding 15 mL of buffer A1 before PA PAO1-L lysate was added and incubated for 2 h at 4 °C shaking. After incubation, the tubes were centrifuged for 10 min at 10,000 x g the supernatant was removed. Then the beads were washed three times by adding 15 mL of buffer A2: 50 mM Tris pH 7.5, 150 mM NaCl, 50 mM imidazole and 1% glycerol. Lastly, the proteins were eluted with 500 µL of buffer B: 50 mM Tris (pH 7.5), 150 mM NaCl, 50 mM imidazole and 1% glycerol. Samples of each individual lysate before and after incubation, and after elution were collected and analysed by SDS-PAGE.

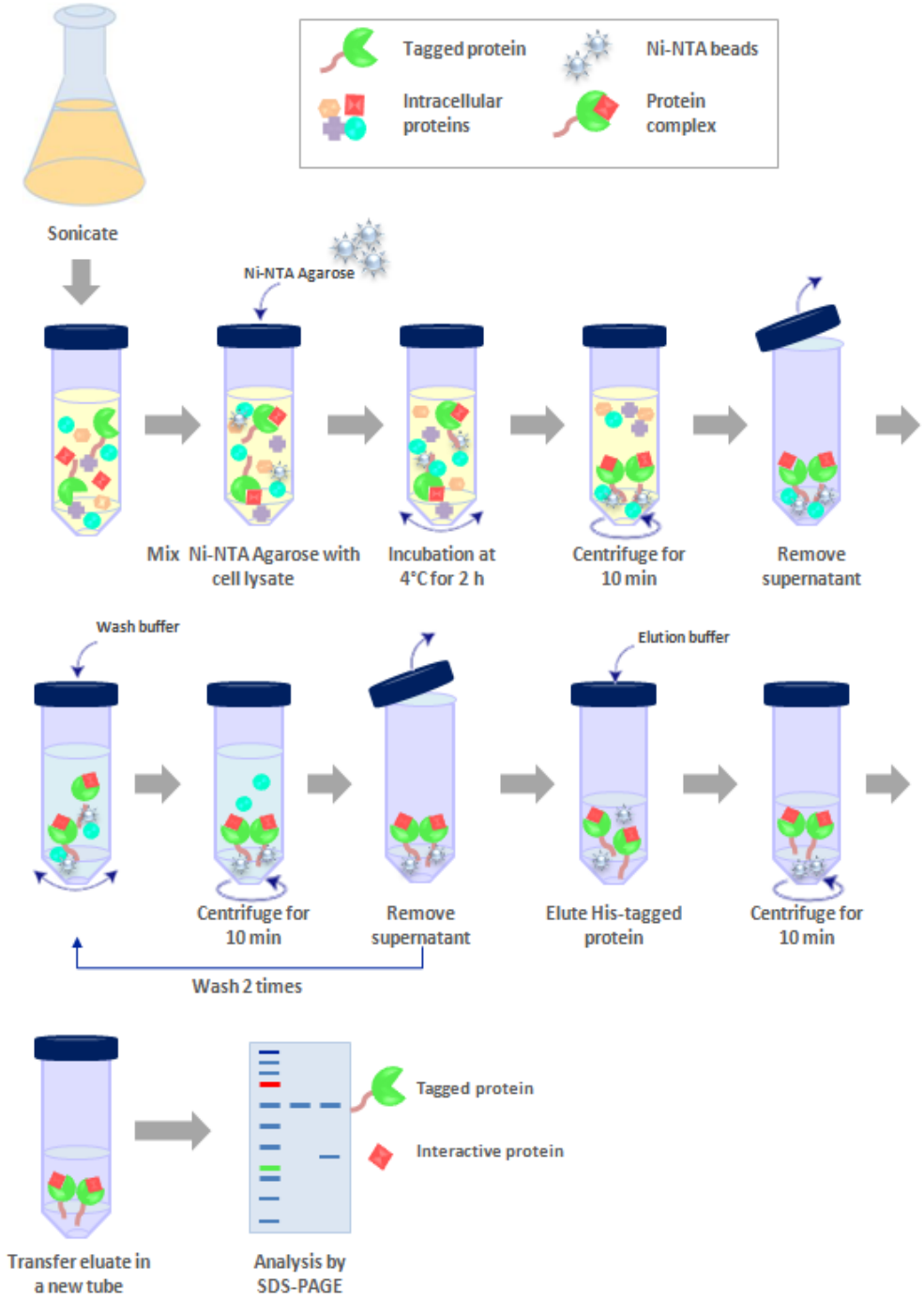


Figure 2.9. Pull down assay schematic.

Figure modified from MBL Life Science webpage, "Protein purification kit application note Vol.1" associated schematic. The schematic shows the general pull down assay process followed for identifying any PA4803 (SamA) protein binding partners. In this study, the presented process was modified slightly in some steps. Further details are found in the text.

2.17 Results analysis

2.17.1 Pixel integration analysis

The area colonized by cells in motility plates were quantified using sing GIMP2 image manipulation program by highlighting the target area with a distinctive colour, and then using the “Histogram” tool to count number of pixels occupied by that colour. The total area of each plate was used for normalization.

2.17.2 Statistical analysis

Significant differences between experimental groups were determined by using one-way ANOVA or one-way ANOVA Kruskal-Wallis test followed by Tukey’s multiple comparisons or by Dunn’s multiple comparisons test respectively, in Graph Pad Prism 7 on Windows, GraphPad Software, San Diego, California USA, www.graphpad.com. For all analyses, a P-value of 0.05 was considered statistically significant.

Unless otherwise stated, all data comparisons were completed using an unpaired two-tail t-test, or a one-way analysis of variance (ANOVA). ANOVA was followed by Tukey’s multiple comparison test in Graph Pad Prism. Data was considered statistically significant when the P value was 0.05 or less, between the groups.

Chapter 3 Initial characterisation of the impact of PA4803 (*samA*) and PA4802.1 in the biology of *P. aeruginosa*

3.1 Introduction

The following chapter will mainly deal with the impact of PA4803/*samA* and PA4802.1 deletions on some aspects of the regulation of the virulence of *P. aeruginosa in vitro*, with a view to gain some understanding of the role of this protein and this rare $tRNA^{sec}$ in the biology of *P. aeruginosa* and the networks in which they are involved.

3.1.1 Discovery of PA4803 (*samA*) as a putative antimicrobial target

As previously mentioned, *P. aeruginosa* is a multi-host opportunistic pathogen, which causes a range of severe diseases. Despite this, there is a lack of drugs with novel modes of action against this organism on the market (Page and Heim, 2009). Therefore, there is a real need to discover novel alternative strategies to combat *P. aeruginosa* infections such as those based on the targeting of virulence to reduce the emergence of resistance.

Hence, an integrated whole-genome approach was carried out in our laboratory to search for novel *P. aeruginosa* targets required for virulence in multiple hosts and which could be exploited for the development of novel anti-virulence interventions against this organism. A random library consisting of 57,360 mini-Tn*5* mutants in *P. aeruginosa* PAO1-L was constructed using the pLM1 mini-Tn*5* delivery vector (Fox *et al.*, 2008), a gentamicin-resistance derivative of pRL27 (Larsen *et al.*, 2002), due to its high transposition efficiency in *P. aeruginosa*. The constructed library represented an estimated mutation coverage of 95% of the genome (Dubern *et al.*, 2015). The process followed for candidate selection is summarised in **Figure 3.1.**

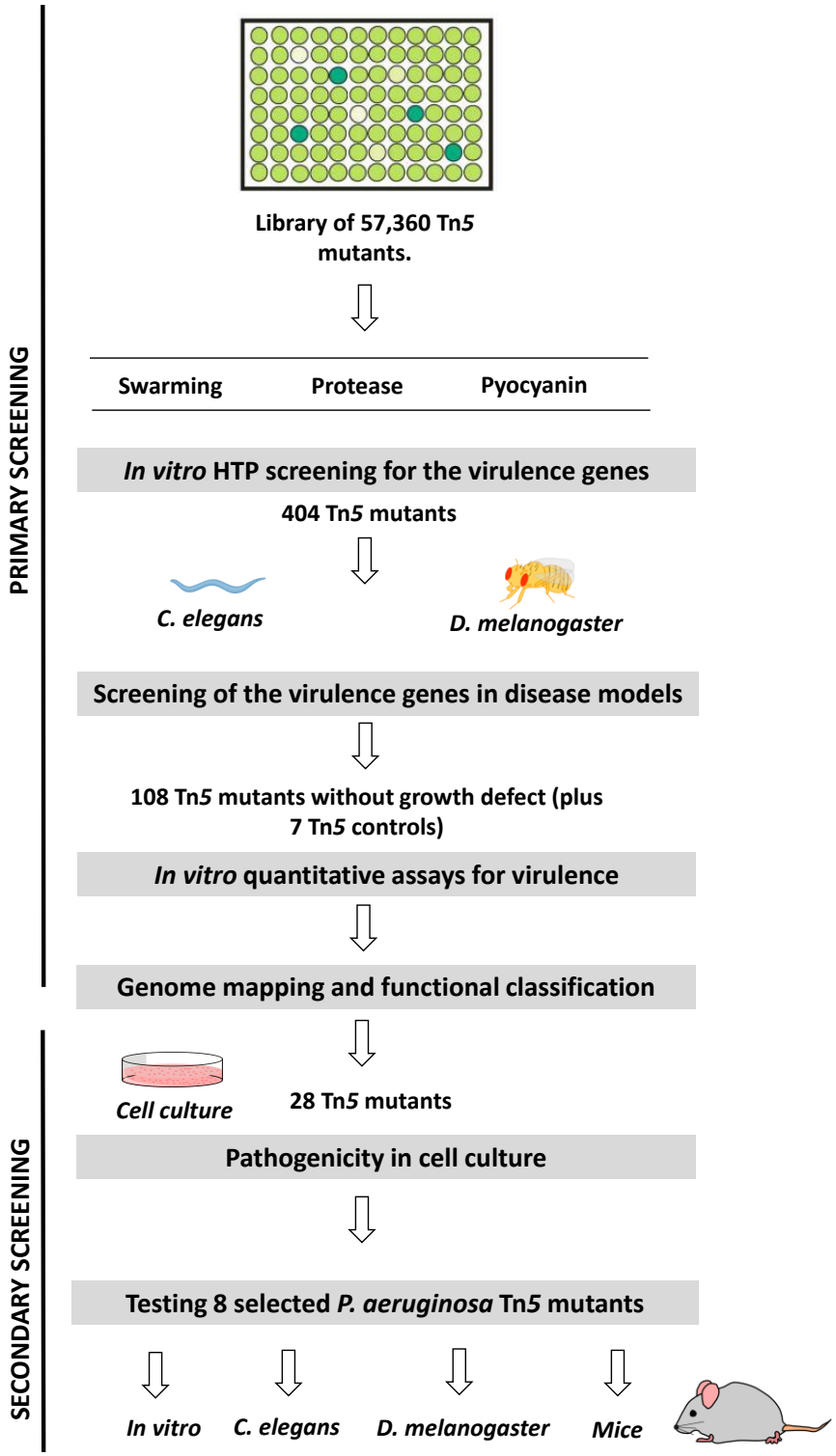


Figure 3.1. Schematic of the process followed to identify putative antimicrobial target genes.
The screening cascade is summarised in the figure adapted from Dubern *et al.*, (Dubern *et al.*, 2015).

In the primary *in vitro* screening, the mutants were assayed for attenuation in swarming motility and the production of protease and pyocyanin. A total of 404 putative virulence-related Tn*5* mutants showing pleiotropic effects on these phenotypes were selected for further testing in

Caenorhabditis elegans and *Drosophila melanogaster* disease models. From these, 275 Tn*5* mutants showed attenuation in at least one or both of the non-vertebrate disease models (Dubern *et al.*, 2015).

The screening consisted of several steps tested in a sequential fashion, which enabled further shortlisting of the Tn*5* mutants (Dubern *et al.*, 2015). Redundancies were identified during the process before proceeding to the secondary screening. Single insertions within a specific gene were found in 68 Tn*5* mutants, representing 1.2% of the ~5,570 coding sequences predicted in *P. aeruginosa* PAO1 (Stover *et al.*, 2000). The 68 open reading frames (ORFs) encoded proteins from almost all functional classes some of which had been previously shown to be virulence determinants in *P. aeruginosa* (Dubern *et al.*, 2015).

In the secondary screening 28 putative virulence-related Tn*5* mutants selected from the 68 shortlisted above were tested for their pathogenicity in human cell culture models (A549 pulmonary cell line). The final candidates were tested for virulence attenuation *in vivo,* in a murine model of acute pneumonia (Dubern *et al.*, 2015).

To recap, these *P. aeruginosa* mutants were subjected to quantitative *in vitro* analysis for the impairment on the production of virulence traits and attenuation of virulence on *C. elegans*, *D. melanogaster* and a murine model of pulmonary infection.

Surprisingly, the screening revealed that *P. aeruginosa* mutants behaved differently and the virulence of most of them varied between disease models, suggesting that virulence is dependent on the model used and hence the host environment. This study provided evidence that although *P. aeruginosa* is capable of infection of a wide range of hosts, many of the virulence determinants are host-specific (Dubern *et al.*, 2015).

The *samA* gene was identified using the above screening process and is the centre of this study. It has emerged as a very attractive novel anti-virulence target in *P. aeruginosa* because mice infected with the *samA* gene mutant strain had better survival than mice infected with the WT strain (Unpublished data, from Collaborators at IRCCS Ospedale San Raffaele).

3.1.2 Background information on PA4803 (*samA*) gene

The Pseudomonas Genome database (Available at: http://www.pseudomonas.com) (Winsor *et al.*, 2016), identified PA4803 as an hypothetical protein, a putative methyltransferase of 22.7 kDa encoded by a 618-bp ORF. It is predicted to be localised in the cytoplasm and it contains some conserved residues usually found in the S-Adenosyl-Methionine (SAM/AdoMet)-dependent methyltransferases. Hence, in this study it was renamed as *samA*. The SAM-dependent methyltransferases superfamily

enzymes catalyse the transfer of a methyl group from SAM to a variety of substrates such as proteins and nucleic acids (Schubert *et al.*, 2003a).

The *samA* gene has orthologs in numerous *P. aeruginosa* strains and other pseudomonads with sequenced genomes. The locus organization is very similar in all the *Pseudomonas* strains checked (**Figure 3.2**). Since little is known about PA4803 (*samA*), the study of its gene neighbourhood may contribute towards the understanding of its function. In the chromosome of *P. aeruginosa* strain PAO1, the *samA* appears to be forming an operon with the PA4804 and PA4805 genes. PA4804 encodes a predicted 50.3-kDa protein containing a polypeptide-transport-associated (POTRA)-like domain-containing usher, which makes it reminiscent to the 91.1-kDa outer membrane protein PA4084 (CupB3) involved in pili assembly (Ruer *et al.*, 2008). PA4805 encodes a putative 52.1-kDa class III aminotransferase, of still unknown biological function. A promoter region was identified for PA4803 gene (*samA*) by the use of SoftBerry software application executed on-line at www.softberry.com, and this information was used in the construction the *samA* transcriptional reporter (No reference available at website).

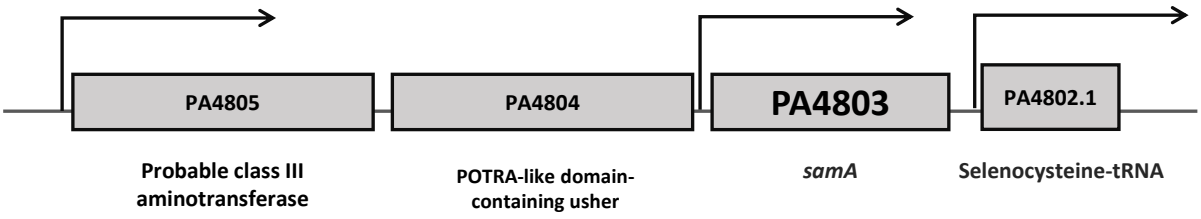


Figure 3.2. Genetic context of PA4803 (*samA*).
Schematic representation of the PA4803 locus genetic organization in *P. aeruginosa* PAO1, which is generally conserved between the other *P .aeruginosa* strains harbouring PA4803 orthologs, according to the Pseudomonas Genome Database (Winsor *et al.*, 2016). The PA4803 orthologs are usually located upstream of the $tRNA^{Sec}$ (selenocysteine-tRNA) gene, which is transcribed in the same direction. ORFs are represented by grey solid boxes and the direction of transcription by thin black arrows, respectively.

Using STRING (Search Tool for Recurring Instances of Neighbouring Genes) (Available at: https://string-db.org/)(Szklarczyk *et al.*, 2021), it was found that PA4803 (*samA*) may interact with its neighbours PA4804 and PA4805 (**Figure 3.3**). However, according to DOOR (Database of prOkaryotic OpeRons) (Available at: http://csbl.bmb.uga.edu/DOOR/)(Mao *et al.*, 2009) PA4803 (*samA*) is not included in the operon prediction.

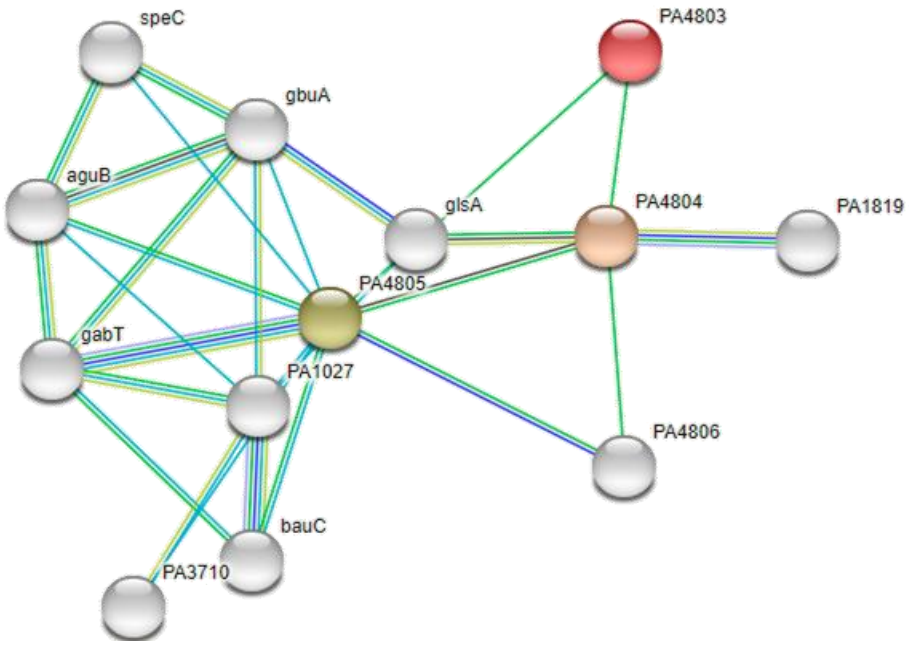


Figure 3.3. PA4803 *(samA*) predicted network by STRING.
Schematic representation of the PA4803 gene product predicted interactors, PA4804 and PA4805 due to gene neighbourhood (green line), according to STRING. The predicted interactions are based on several combinations of curated databases (light blue line), experimental evidence (pink line), gene neighbourhood (green line), gene co-occurrence (blue line), gene fusion (red line), co-expression (black line) and text mining (yellow line) evidence.

Determination of the PA4803 function and the mechanisms by which it modulates the disease process, may lead to the development of novel therapeutic interventions targeting these very mechanisms, which can result in the attenuation of virulence in *P. aeruginosa.*

3.1.3 Discovery of PA4802.1 in the vicinity of PA4803 (*samA*).

According to The Pseudomonas Genome database (Winsor *et al.*, 2016), the *samA* gene is also located, in all strains analysed, upstream of the unique tRNA encoded by PA4802.1, which is predicted to incorporate selenocysteine codons into selenoproteins. Therefore, in this study the production and potential role of this $tRNA^{Sec}$ has been investigated.

3.1.4 Aims of the study

The overall aims of the results reported in this chapter were (i) to gain some understanding on the role of SamA and the $tRNA^{Sec}$ in the biology of *P. aeruginosa* and (ii) to investigate how *samA* is regulated. More specifically, the aims were to:

- Assess the phenotypic impact of a *samA* deletion on the growth and production of virulence traits in *P. aeruginosa*.

- Use of transposon mutagenesis to elucidate potential regulators of *samA* in *P. aeruginosa*.
- Investigate any possible links between *samA* and quorum sensing.
- Assess the phenotypical impact of $tRNA^{Sec}$ on *P. aeruginosa* lifestyle.
- Investigate whether there is a link between the $tRNA^{sec}$ and quorum sensing.

3.2 Results

3.2.1 Phenotypic characterization of an in-frame *samA* deletion mutant

3.2.1.1 Impact of *samA* on *P. aeruginosa* growth

3.2.1.1.1 Aerobic conditions

The effect on growth of a *samA* deletion mutant in *P. aeruginosa* PAO1-L was assessed in liquid cultures of 10 ml under aerobic conditions (shaking at 200 rpm) in various growth media. Growth was monitored manually by measuring OD at 600 nm, using a spectrophotometer. The deletion of *samA* did not affect growth in LB, RPMI and CDM under the conditions used. However, it seemed to slightly negatively affect growth in M9 and positively in CDM nutrient limitation media, under these conditions (**Figure 3.4**).

Next, the effect of *samA* deletion on *P. aeruginosa* PAO1-L growth was assessed again in liquid cultures this time using microtitre plates instead, with 250 µl liquid culture volume, under aerobic conditions in various growth media. However, growth was monitored by measuring OD at 600 nm, using an automated spectrophotometer. The particular set up allowed the monitoring of three biological clones for each strain (**Figure 3.5**).

It was found that the *samA* deletion does not affect growth in CDM under the conditions used. However, it seemed to slightly affect growth negatively in LB, M9, RPMI and CDM nutrient limitation media. Growth in M9 was lower in the Δ*samA*, but this strain reached the same OD_{600} as the isogenic wt (wild type) after 25 h of growth (**Figure 3.5**). An inconsistency between the growth results in the CDM nutrient limitation between the manual and automatic set ups was observed where in the former the *samA* mutant reached higher ODs whereas the opposite was for the latter.

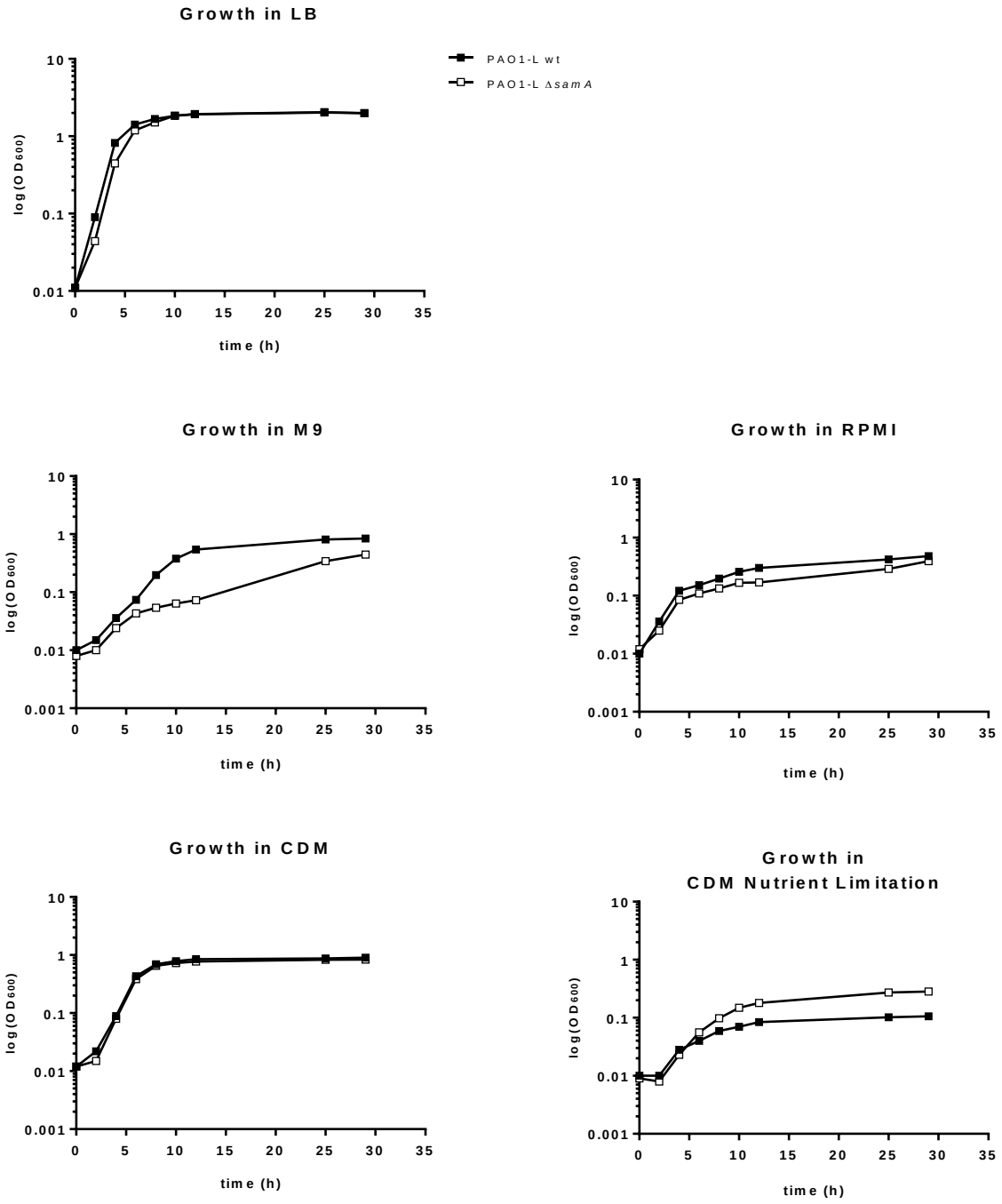


Figure 3.4. Growth curves determined manually for the wt and the *samA* mutant (Δ*samA*) under aerobic conditions in several growth media.

Samples were inoculated in flasks at OD_{600}, 0.005±0.010 and incubated at 37°C for more than 24 h, with shaking. The experiment was done once using only one clone for each strain tested. Standard deviation could not be applied for the above reason. This was a pilot experiment. Growth was determined manually by measuring the OD_{600} in a spectrophotometer. Readings were taken every 2 hours. The samA *mutant* Δsam A strain is in reality in *Pseudomonas aeruginosa* PAO1-Nottingham strain background and not PAO1-Lausanne, as it was discovered by RNA-seq in Chapter 6.

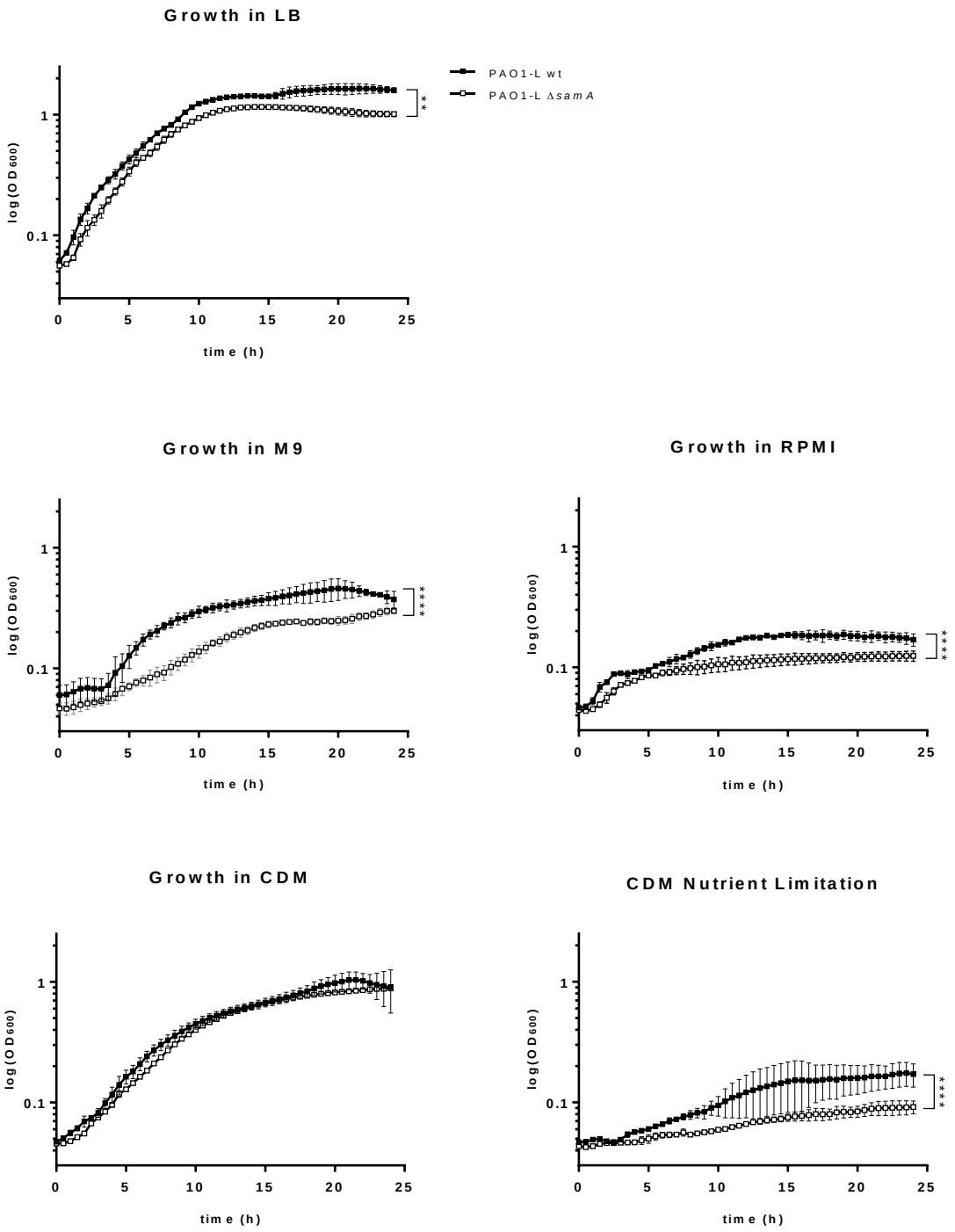


Figure 3.5. Growth curves determined automatically for the wt and the *samA* deletion (*ΔsamA*) under aerobic conditions in several growth media.

Samples were inoculated in 96-well plates at OD_{600}, 0.005±0.010 and incubated with shaking at 37°C for more than 24 h. The experiment was done once using three biological replicates for each strain tested. Error bars indicate standard deviation based on the mean values of biological clones. Growth was determined by the OD_{600} in an automated spectrophotometer. Readings were taken every 30 min. Statistical significance is depicted by: ns; P>0.05, *; P≤0.05, **; P≤0.01, ***; P≤0.001, ****; P≤0.0001. The samA *mutant* *Δ*samA strain is in reality in *Pseudomonas aeruginosa* PAO1-Nottingham strain background and not PAO1-Lausanne, as it was discovered by RNA-seq in Chapter 6.

3.2.1.1.2 Anaerobic conditions

The effect of *samA* deletion on *P. aeruginosa* PAO1-L growth was assessed in LB media liquid cultures under aerobic and anaerobic conditions, the latter in the presence of nitrate. Growth was monitored manually by measuring OD at 600 nm, using a spectrophotometer (**Figure 3.6**).

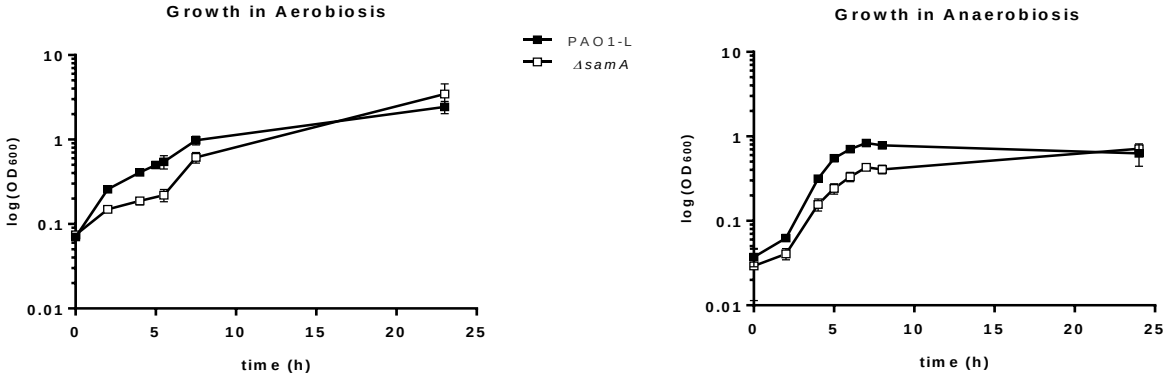


Figure 3.6. Growth curves determined manually for the wt and the Δ*samA* under aerobic conditions and anaerobic conditions.
Samples were inoculated in 96-well plates at OD_{600}, 0.005±0.010 and incubated at 37°C for more than 24 h. For the anaerobic conditions pre-culture was done under aerobic conditions and the media anoxic media was supplemented with 100 mM KNO_3. Error bars indicate standard deviation based on the mean values of three independent biological clones. The experiment was repeated three times with similar results. The samA *mutant Δ*samA strain is in reality in *Pseudomonas aeruginosa* PAO1-Nottingham strain background and not PAO1-Lausanne, as it was discovered by RNA-seq in Chapter 6.

The *samA* deletion slightly affected growth negatively under both aerobic and anaerobic conditions. The Δ*samA* reached the same OD_{600} as the isogenic PAO1-L WT after 25 h of growth (**Figure 3.6**). However, measurements were not taken for the whole course of this experiment. Overall, no important differences in growth were caused by the *samA* deletion.

3.2.1.2 Effect of *samA* deletion on motility and exoproduct production of *P. aeruginosa*

Cellular motility is key for *P. aeruginosa* virulence. Hence, as a first step in the investigation of *samA's* role, surface motilities such as swarming and twitching were next assessed. Swarming involves rapid movement of the flagellum and the secretion of rhamnolipids, across semi-solid surfaces (Kohler *et al.*, 2000), whereas twitching involves movement of the pili across solid surfaces (Burrows, 2012). The deletion was complemented with a pME6032-based construction expressing *samA*.

3.2.1.2.1 Swarming and Twitching

Compared to the WT, a less extended diameter occupied by swarming tendrils in the *samA* deletion strain was observed (**Figure 3.7, A**). However, complementation of the *sam*A deletion did not restore

the swarming motility impairment. All the following statistical analysis was carried out using either an unpaired two-tailed Student's t-test or Mann-Whitney test. The construction of the *samA* gene complementation plasmid is described in **2.12.4.2.**

As observed in **Figure 3.7 panel B**, *samA* deletion abolished twitching compared to the wt. Interestingly, complementation of the *samA* deletion in this case fully restored the twitching impairment. All the following statistical analysis was carried out using either an unpaired two-tailed Student's t-test or Mann-Whitney test.

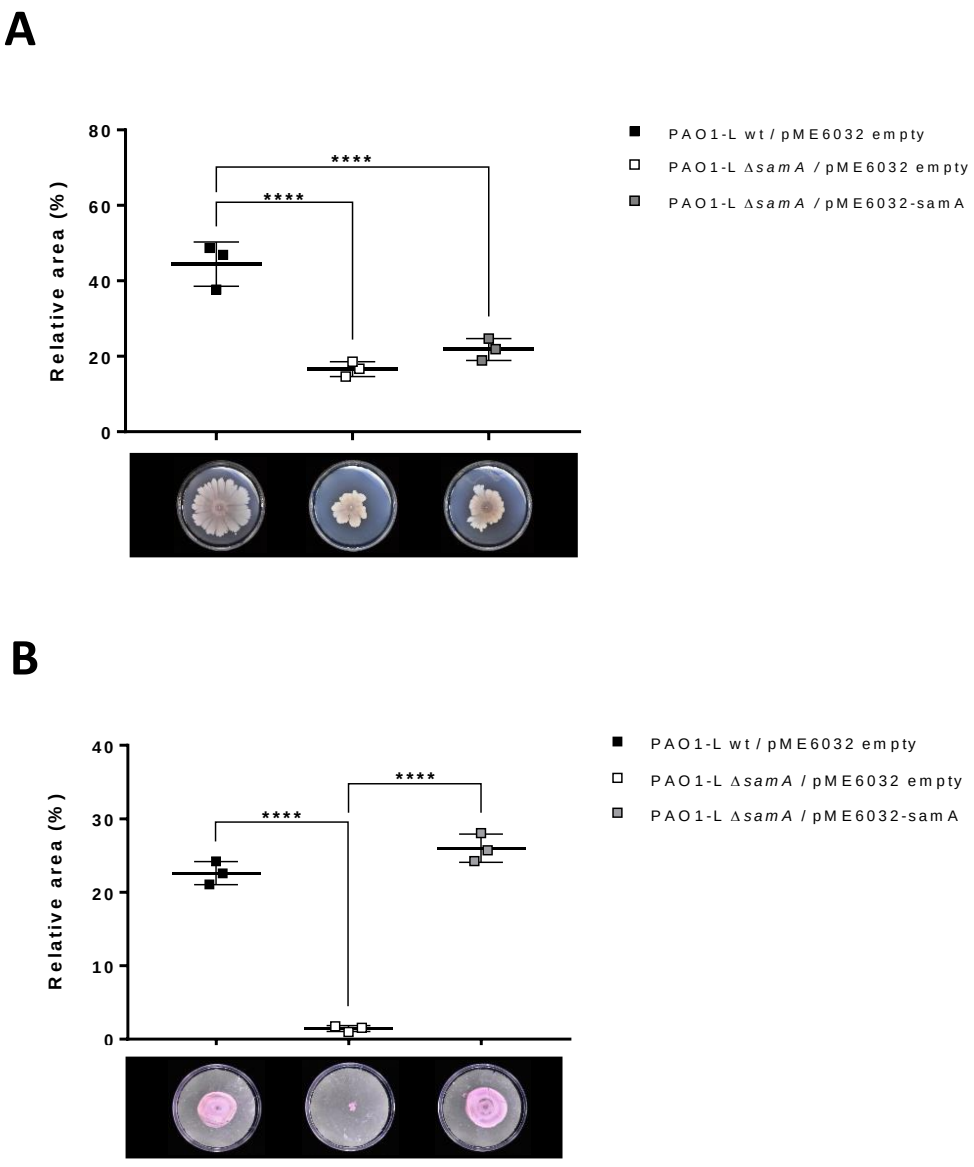


Figure 3.7. Effect of *samA* deletion on *P. aeruginosa* PAO1-L motilities.
A. Effect of *samA* deletion on *P. aeruginosa* PAO1-L swarming motility. Swarming was tested in the PAO1-L (WT), *samA* deletion (Δ*samA*) and Δ*samA* containing the pME6032 empty vector or the complementation plasmid pME6032-*samA*. Cells were inoculated on the surface of the plates, which were then incubated for 16 h at 37 °C. Pictures show representative results. The swarming area was quantified relative to the total area of the plates. Statistical significance is depicted by: ns; P>0.05, *; P≤0.05, **; P≤0.01, ***; P≤0.001, ****; P≤0.0001. **B. Effect of *samA* deletion on *P. aeruginosa* PAO1-L twitching**

motility. Twitching was tested in the PAO1-L (WT), *samA* (Δ*samA*) and Δ*samA* containing the pME6032 empty vector or the complementation plasmid pME6032-*samA*. Cells were inoculated on the bottom of the plates, which were then incubated for 16 h at 37 °C. Pictures show representative results. The twitching area was quantified relative to the total area of the plates. Statistical significance is depicted by: ns; P>0.05, *; P≤0.05, **; P≤0.01, ***; P≤0.001, ****; P≤0.0001. The samA *mutant* ΔsamA strain is in reality in *Pseudomonas aeruginosa* PAO1-Nottingham strain background and not PAO1-Lausanne, as it was discovered by RNA-seq in Chapter 6.

3.2.1.2.2 Pyocyanin, Elastase and Alkaline Protease production

As previously mentioned, exoproduct production is an important aspect of *P. aeruginosa* virulence during infection. Hence, the effect of *samA* deletion on the production of secreted virulence determinants was investigated next. As shown in **Figure 3.8** the *samA* in-frame deletion mutant did not seem to affect pyocyanin production or the proteolytic activity of alkaline protease. However, a *samA* deletion seemed to result in a reduction in elastase activity.

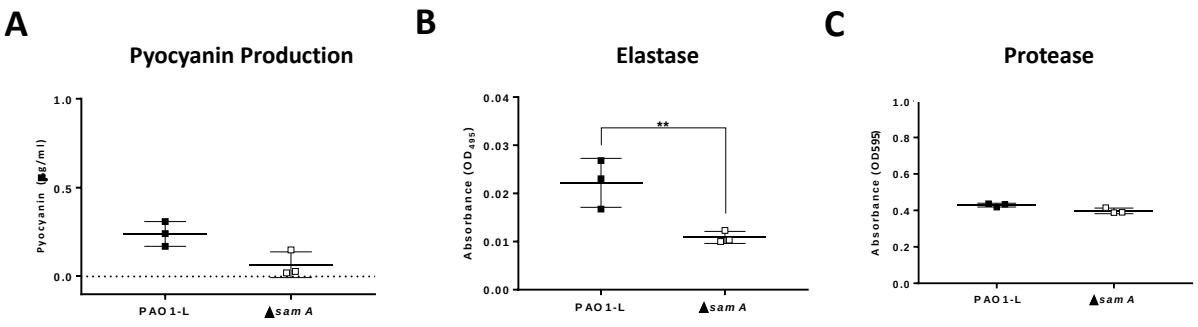


Figure 3.8. Impact of *samA* deletion on exoproduct production of *P. aeruginosa* PAO1-L.
A. Impact of *samA* deletion on pyocyanin production of *P. aeruginosa* PAO1-L. Supernatants from overnight cultures incubated for 16 h at 37 °C were subjected to chloroform-based pyocyanin extraction. Three biological replicates were used, and statistical significance is depicted by: *; P≤0.05, **; P≤0.01, ***; P≤0.001, ****; P≤0.0001**. B.C. Impact of *samA* deletion on the proteolytic activity of *P. aeruginosa* PAO1-L.** For the alkaline protease assay, supernatants of overnight cultures incubated for 16 h at 37 °C were mixed with azocasein and incubated for 1 h at 37 °C with 200 rpm shaking. The OD_{595} of the resulting suspension was determined. For the elastase assay, supernatants of overnight cultures incubated for 16 h at 37 °C were mixed with a suspension of elastin-Congo red, incubated at 37 °C with 200 rpm shaking for 2 h and centrifuged. The OD_{495} of the resulting suspension was determined. Three biological replicates were used, and statistical significance is depicted by: *; P≤0.05, **; P≤0.01, ***; P≤0.001, ****; P≤0.0001. In all the above experiments the *samA* deletion (Δ*samA*) used was not complemented. The samA *mutant* ΔsamA strain is in reality in *Pseudomonas aeruginosa* PAO1-Nottingham strain background and not PAO1-Lausanne, as it was discovered by RNA-seq in Chapter 6.

3.2.1.3 Initial investigation of the *samA* regulon

3.2.1.3.1 *samA* and quorum sensing (QS)

This study set out to identify regulators of the *samA* gene, either known regulators integrated within well studied regulatory circuits such as QS or novel regulators, in *P. aeruginosa* PAO1-L. Since some of the phenotypes affected in the original *samA* deletion mutant are controlled by QS, there is a possibility that *samA* may be linked to QS. Hence, the effect of QS on *samA* gene expression was

assessed by introducing the *samA* transcriptional reporter fusion, constructed as described in 2.12.3 ,into the QS mutant strains Δ*lasI*, Δ*rhlI* and Δ*pqsA*. It was found that activity of the *samA* promoter was upregulated in a Δ*pqsA* mutant, downregulated in a Δ*rhlI* mutant and exhibited no difference in a Δ*lasI* mutant compared to the parental PAO1-L. Furthermore, a mutation in *vfr* resulted in increased *samA* transcription compared to the parental PAO1-L (**Figure 3.9**). The *P. aeruginosa* virulence factor regulator Vfr has been shown to regulate exotoxin A production, *regA* transcription, and quorum sensing via control of lasR transcription (Beatson *et al*., 2002a)

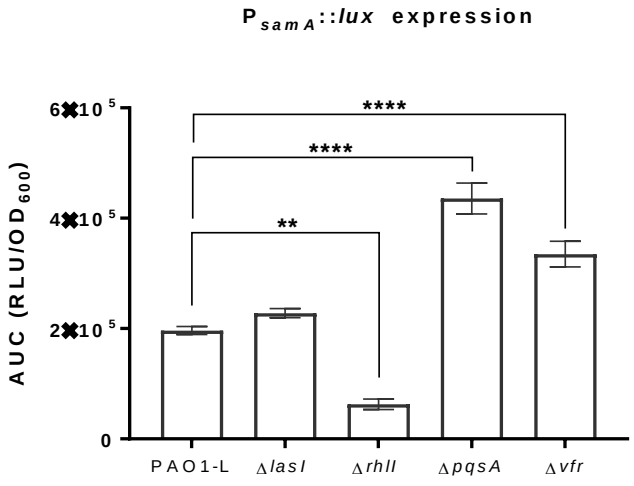


Figure 3.9. Effect of quorum sensing genes (*lasI*, *rhlI*, *pqsA* and *vfr*) on *samA* gene expression.
Growth of *P. aeruginosa* strains is shown on the above panel. Expression of *samA* gene in the *lasI* mutant (Δ*lasI*), *rhlI* mutant (Δ*rhlI*), *pqsA* mutant (Δ*pqsA*), and *vfr* mutant (Δ*vfr)* strains alongside the PAO1-L (WT) as control. Gene expression levels are represented as the area under the curve (AUC) of the normalized relative luminescent units (RLU).The experiment was repeated three times and error bars indicate standard deviation based on the mean values of three independent biological replicates. Statistical significance is depicted by: *; P≤0.05, **; P≤0.01, ***; P≤0.001, ****; P≤0.0001. The samA *mutant* ΔsamA strain is in reality in *Pseudomonas aeruginosa* PAO1-Nottingham strain background and not PAO1-Lausanne, as it was discovered by RNA-seq in Chapter 6.

The above experiments studied the impact of QS in *samA* expression. To establish whether the reverse was also the case, *lasI*, *rhlI* and *pqsA* expression was assessed by introducing their respective transcriptional reporter fusions into the Δ*samA* mutant (**Figure 3.10, A**) and *samA*Ind (with or without IPTG) backgrounds (**Figure 3.10, B**). The *samA*Ind is a *samA*-inducible mutant strain in *P. aeruginosa* in PAO1-L, which was constructed by the insertion of $lacI^Q$ and the P*tac* promoter upstream of *samA;* as described in **2.12.5***.* Addition of IPTG to this strain results in the induction of *samA* expression. To investigate the effect of *samA* overexpression or *samA* repression on the several phenotypes, discussed above. All the following statistical analysis were carried out using either an unpaired two-tailed Student's t-test or Mann-Whitney test. When there is no indication on the figure, no statistical significance was found.

Expression of all three QS genes was found upregulated in the Δ*samA* mutant compared to the WT with a statistical significance of $p<0.05$ (**Figure 3.10, A)**

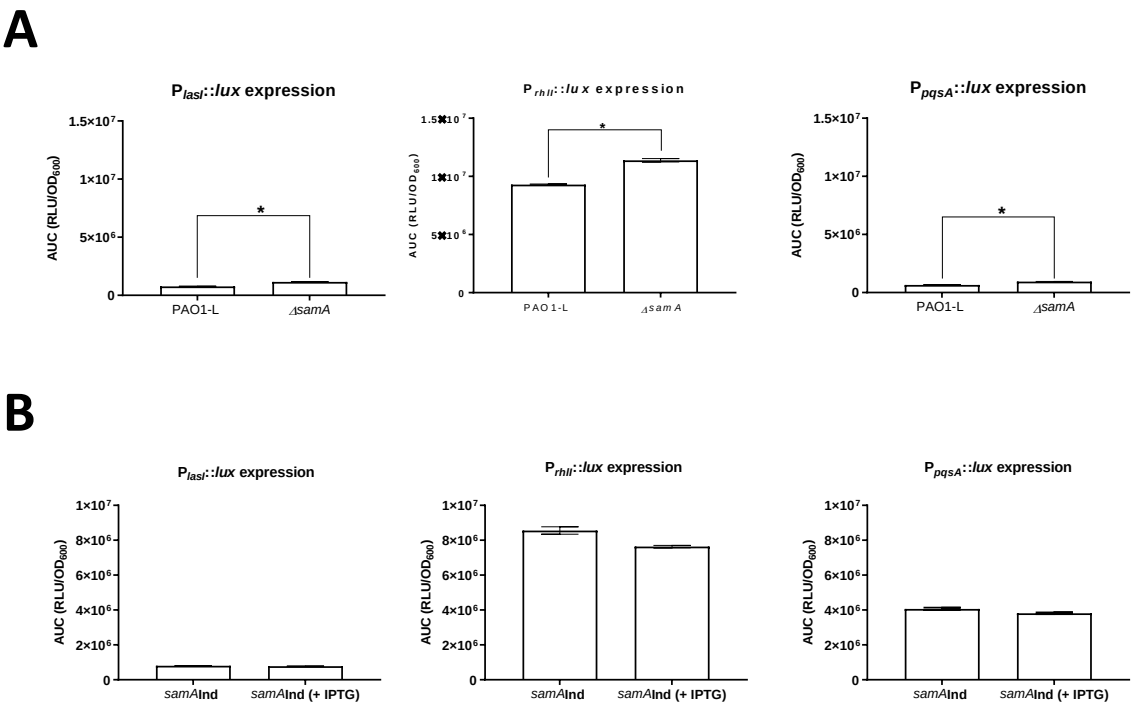


Figure 3.10. Promoter activity of the *lasI*, *rhlI* and *pqsA* quorum sensing genes in the *samA* mutant and the samAInd background.
A. Promoter activity of the *lasI*, *rhlI* and *pqsA* quorum sensing genes in the *samA* mutant background. Actvity of the *lasI, rhlI and pqsA* promoters in the *ΔsamA* strains alongside the PAO1-L (WT) as control, is represented as RLU/OD_{600nm}.The experiment was repeated three times and error bars indicate standard deviation based on the mean values of biological clones. **B. Promoter activity of the *lasI*, *rhlI* and *pqsA* quorum sensing genes in the *samA*Ind background.** Comparison of expression, represented as RLU/OD_{600nm}, of *lasI*, *rhlI* and *pqsA* genes between uninduced *samA*Ind strain and IPTG induced is shown above. Growth of *P. aeruginosa* strains in LB medium is not shown. The experiment was repeated three times and error bars indicate standard deviation based on the mean values of biological clones. The samA *mutant Δ*samA strain is in reality in *Pseudomonas aeruginosa* PAO1-Nottingham strain background and not PAO1-Lausanne, as it was discovered by RNA-seq in Chapter 6.

In contrast, the activity levels of the *lasI*, *rhlI* and *pqsA* promoters were not significantly different in IPTG-induced *samA*Ind strain (**Figure 3.10, B**) compared to uninduced *samA*Ind strain, which serves as the control, with $p>0.05$. Growth curves demonstrated similar growth for all the strains tested (data not shown). All the following statistical analysis was carried out using either an unpaired two-tailed Student's t-test or Mann-Whitney test. When there is no indication on the figure, no statistical significance was found.

3.2.1.3.2 Modulation of quorum sensing signalling molecules (QSSMs) production by SamA

The effect of SamA on QS was further assessed by quantification of the *N*-acylhomoserine lactones (3-oxo-C12-HSL and C4-HSL) and the alkyl quinolone (PQS) in PAO1-L, in Δ*samA* and *samA*Ind strains, respectively. Firstly, C4-HSL levels did not show significant differences in the Δ*samA* mutant strain (**Figure 3.11**) compared to PAO1-L, with $p>0.05$. Similarly, the C4-HSL levels were not significantly different in IPTG-induced *samA*Ind strain (**Figure 3.11**) compared to uninduced strain, with $p>0.05$. Secondly, PQS levels were reduced in the Δ*samA* strain compared to PAO1-L, with a statistical significance of $p<0.05$. In contrast, PQS levels were reduced in the IPTG-induced *samA*Ind strain (**Figure 3.11**) compared to uninduced strain, with a statistical significance of $p<0.05$. Lastly, 3-oxo-C12-HSL was not detected in any strain probably due to the low levels produced under the growth conditions used (data not shown). All the aforementioned statistical analysis was carried out using an unpaired two-tailed Student's t-test. When there is no indication on the figure, no statistical significance was found. These experiments were conducted by the MSc student Sakshi Lutrha under the supervision of Ioanna Chatzigianni.

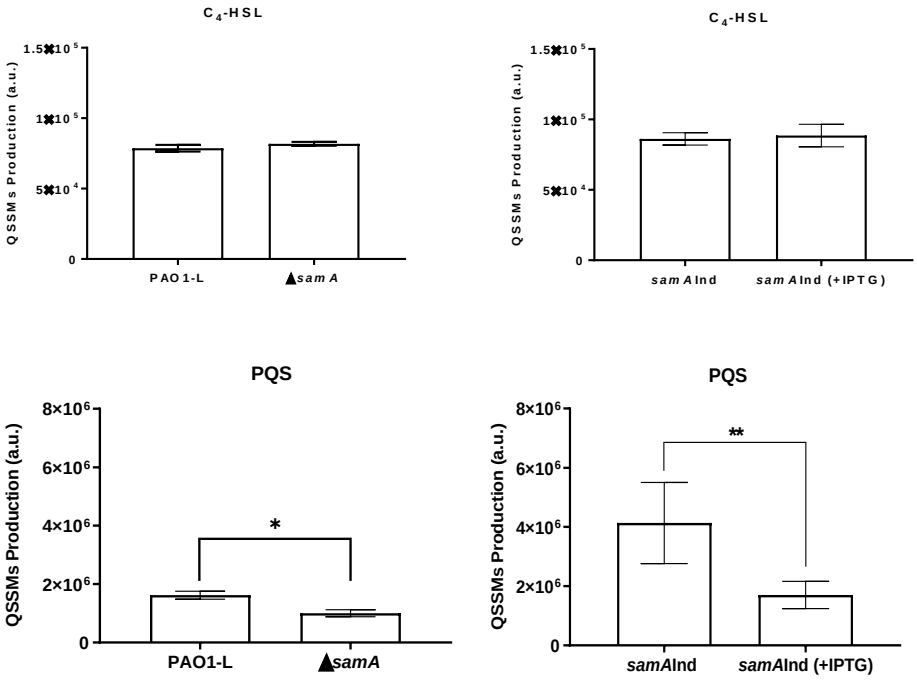


Figure 3.11. Quantitative profiling of QSSMs by LC-MS/MS.
Bar charts on the left show production of C4-HSL and PQS QSSMs by *P. aeruginosa* PAO1-L (WT) and Δ*samA* strains, represented with bars. Bar charts on the right show production of C4-HSL and PQS QSSMs by uninduced *samA*Ind and IPTG induced *samA*Ind strains represented, again represented with colorless bars. Production of each QSSM is represented in peak areas in each strain. The experiment was performed one time with three biological replicates and error bars indicate

standard deviation. The samA *mutant Δ*samA strain is in reality in *Pseudomonas aeruginosa* PAO1-Nottingham strain background and not PAO1-Lausanne, as it was discovered by RNA-seq in Chapter 6.

3.2.1.4 Identification of genes impacting on *samA* expression using a Tn*5*-based approach and study of their impact on virulence trait production.

A library of approximately 3,000 random mutants was constructed by introducing mini-Tn*5* in *P. aeruginosa* PAO1-L carrying the transcriptional reporter fusion miniCTX::P_{samA}-*lux* integrated in its chromosome. The primary screening of the library involved crude evaluation of bioluminescence production in the transposants on plate, under the Luminograph photon video camera (EG & G Berthhold). Higher bioluminescence production compared to the WT was an indication that the *samA* gene might be upregulated in that particular mutant. A secondary screening involved evaluation of light production using a combined spectrophotometer/luminometer to validate bioluminescence production differences of the transposants previously observed on the agar plates.

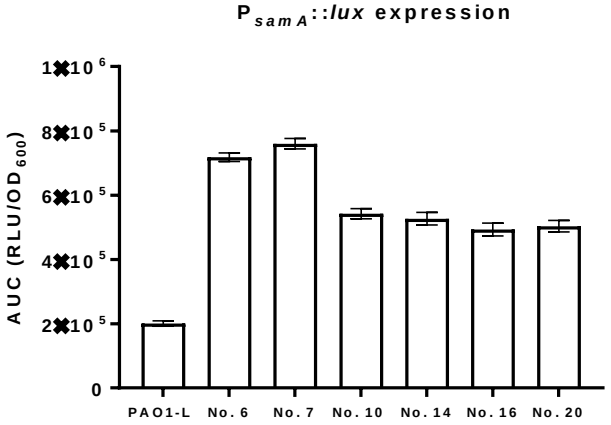


Figure 3.12. Effect of selected Tn5 chromosomal insertions on *samA* gene expression.
Expression of the *samA* gene in selected Tn*5* mutant strains alongside the PAO1-L (WT) as control, is represented as area under the curve (AUC) of RLU/OD_{600nm}. The experiment was repeated three times and error bars indicate standard deviation based on the mean values of biological clones. Statistical significance is stated in Table 3.1.

Determination of the sequences flanking the transposon revealed the chromosomal insertion points of the mini-Tn*5* element and the disrupted genes, were done as described in **2.14.1**. With this approach, four genes, *purD*, *faoA*, *mvaT* and *hmgA* were identified as novel potential negative regulators of *samA* transcription. Both, *faoA* and *mvaT* were found three and four times from the screening, respectively, whereas *purD* and *hmgA* were only scored once (**Table 3.1**). Disruption of all these identified genes resulted in *samA* upregulation.

PurD is a phosphoribosylamine-glycine ligase involved in nucleotide biosynthesis and metabolism in *E. coli* (Cheng *et al.*, 1990) but its exact function and contribution to the *P. aeruginosa* lifestyle has not yet been demonstrated. FaoA is the α-subunit of a multienzyme complex designated HDT, which has 2-enoyl-CoA hydratase and 3 hydroxyacyl-CoA dehydrogenase activities and is involved in fatty acid β-oxidation in *Pseudomonas fragi* (Sato *et al.*, 1992a)(Sato *et al.*, 1992b). In *P. aeruginosa* a predicted function of 3 hydroxyacyl-CoA dehydrogenase has been assigned to *faoA* according to the Pseudomonas Genome DB (Winsor *et al.*, 2016). MvaT acts as a transcriptional regulator and it controls the expression of several virulence genes in a growth phase-dependent manner (Diggle *et al.*, 2002).

Table 3.1. Identification of Tn*5* disrupted genes probably involved in the regulation of *samA* gene expression.

Mutant ID	Statistical Significance[b]	Locus ID[a]	Gene name or product[a]	Function classification (COG Prediction)
RM06	****	PA3014	***faoA***, fatty-acid oxidation complex alpha-subunit	3-hydroxyacyl-CoA dehydrogenase
RM14	****	PA3014	***faoA***[c], fatty-acid oxidation complex alpha-subunit	3-hydroxyacyl-CoA dehydrogenase
RM10	****	PA4315	***mvaT***, P16 subunit	Transcriptional regulator
RM16	****	PA4315	***mvaT***[c]„ P16 subunit	Transcriptional regulator
RM20	****	PA4315	***mvaT***[c]„ P16 subunit	Transcriptional regulator
RM07	****	PA4855	***purD***, phosphoribosylamine-glycine ligase	Phosphoribosylamine-glycine ligase
N/A	N/A	PA2009	***hmgA***, homogentisate 1,2-dioxygenase	homogentisate 1,2-dioxygenase

[a]Gene number, gene name and product name were obtained from the Pseudomonas Genome Database (http://www.pseudomonas.com)(Winsor *et al.*, 2016).
[b] Statistical significance of *samA* gene promoter transcriptional activity of the random mutants compared to the WT, is denoted with asterisks (ns, $p \geq 0.05$; ****, $p \leq 0.0001$ by using one-way ANOVA Kruskal-Wallis test
[c] The insertion sites between RM06 and RM16 were the same. The insertion sites for RM10 , RM16 and RM20 were the same as well. Therefore, they are considered redundancies.

HmgA is a homogentisate 1,2-dioxygenase which seems to be involved in tyrosine metabolism, L-phenylalanine catabolism, and oxidation reduction (Rodrıguez-Rojas *et al.*, 2016). Disruption of the *hmgA* gene resulted in *samA* upregulation and also overproduction of a dark brown pigment on plate.

Previous phenotypic characterization of the Δ*samA* strain has suggested a role for the gene in twitching motility and also in swarming motility, although complementation of Δ*samA* mutant could

not restore the latter. Hence, swarming and twitching motilities abilities were assessed for the potential regulators: *mvaT, faoA*, *purD* and *hmgA* (**Figure 3.13**). Swarming tendril pattern was slightly affected in Δ*samA*, *mvaT::*Tn*5* and *faoA::*Tn*5* compared with PAO1-L WT (**Figure 3.13, A**). Swarming was abolished in the *purD::*Tn*5* compared to the PAO1-L WT. The swarming tendrils of the *hmgA::*Tn*5* were radiating more from the inoculation Tn*5* compared to the PAO1-L WT.

Twitching was slightly affected in Δ*samA*, *mvaT::*Tn*5* and *faoA::*Tn*5* relative to PAO1-L. The most profound impairment was observed in the *purD::*Tn*5* compared to the PAO1-L WT. No effect was observed in the twitching ability of the *hmgA::*Tn*5* compared to the PAO1-L WT (**Figure 3.13, B**).

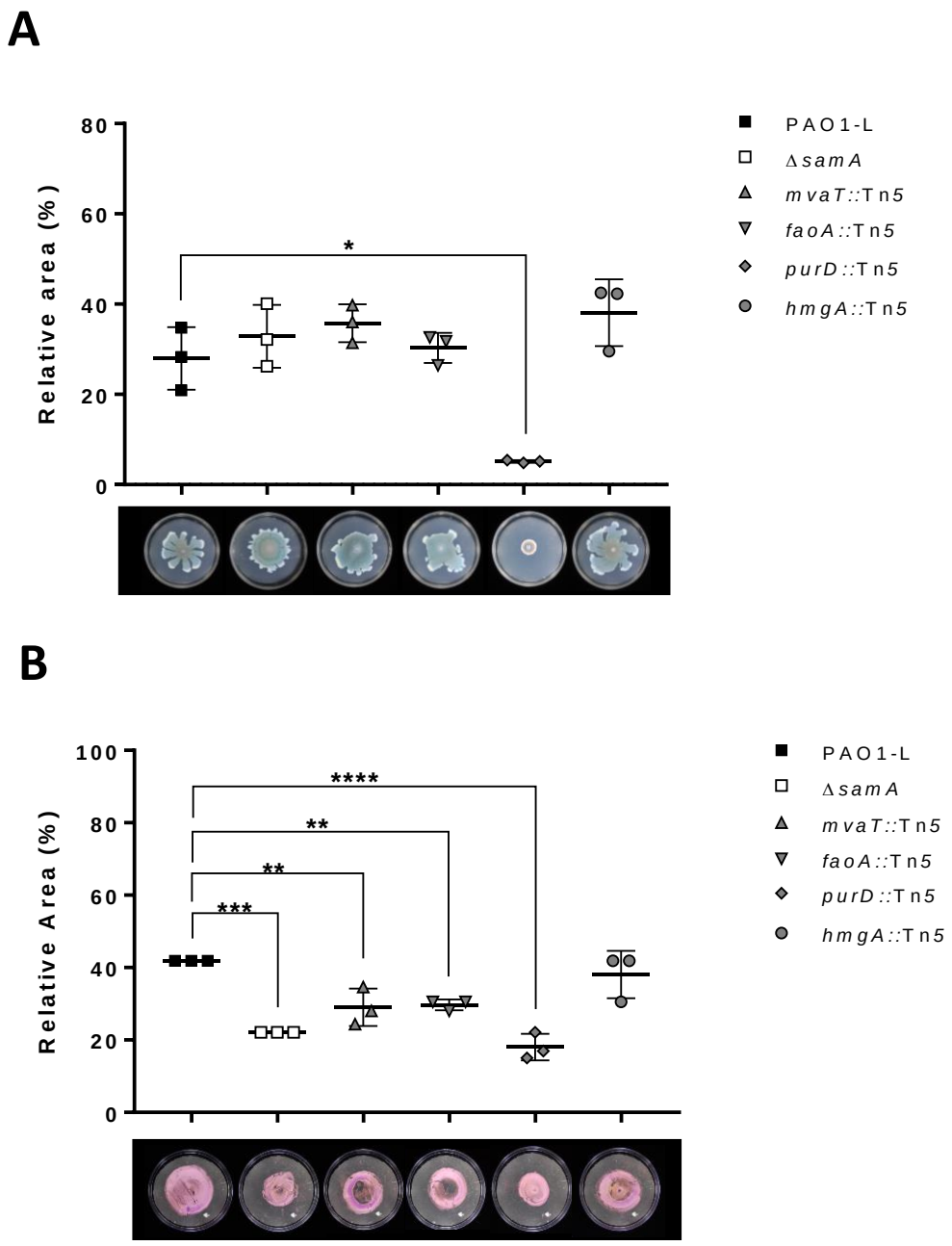


Figure 3.13. Motility profiles of selected *P. aeruginosa* PAO1-L Tn*5* mutants.
A. Swarming was tested in selected Tn*5* random mutant strains alongside the PAO1-L (WT), as control. Cells were inoculated on the surface of the plates, which were then incubated for 16 h at 37°C. Pictures show representative results. The swarming area was quantified relative to the total area of the plates and is represented as relative area (cm^2). Statistical significance is depicted by: ns; $p>0.05$, *; $p\leq0.05$, **; $p\leq0.01$, ***; $p\leq0.001$, ****; $p\leq0.0001$.**B. Twitching motility of selected *P. aeruginosa* PAO1-L Tn*5* mutants.** Twitching was tested in the Tn*5* Random mutant strains alongside the PAO1-L (WT), as control. Cells were inoculated on the bottom of the plates, which were then incubated for 16 h at 37 °C. Pictures show representative results. The twitching area was quantified relative to the total area of the plates represented relative area coverage in percent (%). Statistical significance is depicted by: ns; $p>0.05$, *; $p\leq0.05$, **; $p\leq0.01$, ***; $p\leq0.001$, ****; $p\leq0.0001$.

All three exoproducts, elastase, protease and pyocyanin (**Figure 3.14**) were quantified in the transposon mutant strains in *mvaT, faoA*, *purD* and *hmgA*. Pyocyanin production was unaffected in Δ*samA*, *purD::*Tn*5, and hmgA::*Tn*5* but it was found increased in the *mvaT::*Tn*5* and *faoA::*Tn*5* strains, compared to PAO1-L WT (**Figure 3.14, A**).

Elastase activity was unaffected in the *mvaT::*Tn*5* and *faoA::*Tn*5* strains. However, it was increased in the *hmgA::*Tn*5* and decreased in the Δ*samA* compared to PAO1-L WT (**Figure 3.14, B**).

Meanwhile, alkaline protease activity was unaffected in the Δ*samA and mvaT::*Tn*5* mutants (**Figure 3.14, C**), increased in the *faoA::*Tn*5* strains and decreased in the *hmgA::*Tn*5* compared to PAO1-L WT (**Figure 3.14, C**). Interestingly, the *purD::*Tn5 strain RM07 did not seem to produce any of the three exoproducts at all (**Figure 3.14**).

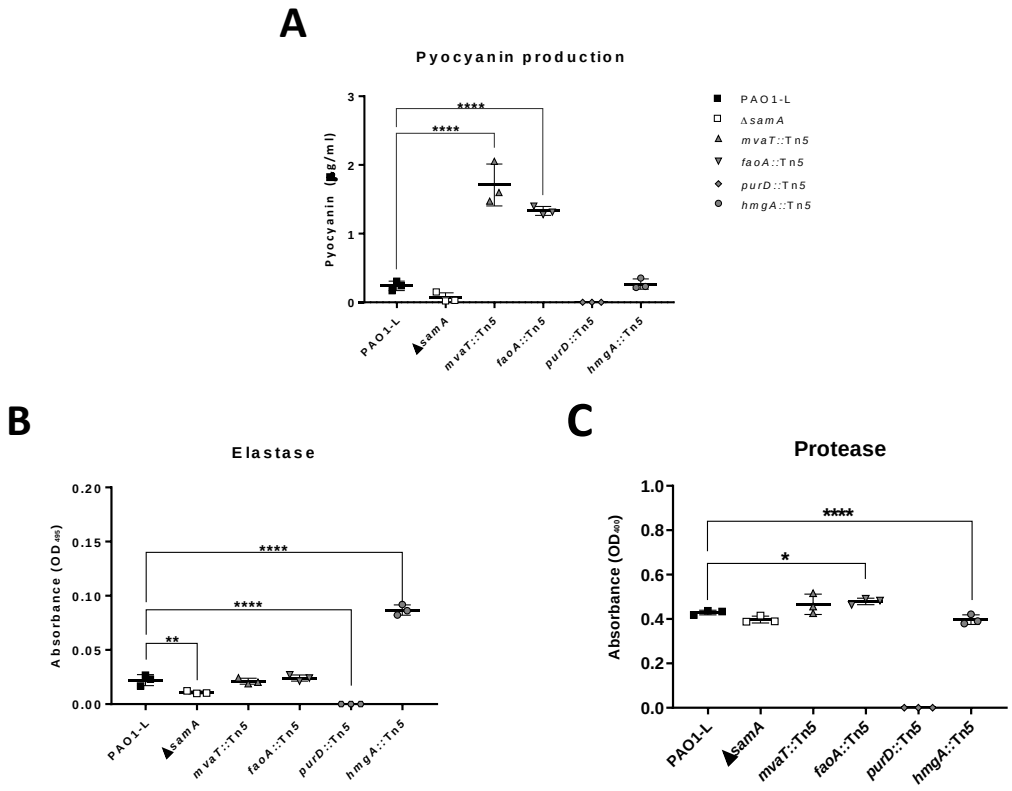


Figure 3.14. The effect of selected Tn*5* insertions on *P. aeruginosa* PAO1-L pyocyanin production and proteolytic activity. **A.** Chloroform-based pyocyanin extraction. **B.** Elastase assay using elastin-Congo red and OD_{495} measurement of the resulting suspension. **C.** Alkaline protease assay using azocasein and measuring OD_{400} of the resulting suspension. For each assay three biological replicates were used, and statistical significance is depicted by: ns; $p>0.05$, *; $p\leq0.05$, **; $p\leq0.01$, ***; $p\leq0.001$, ****; $p\leq0.0001$.

3.2.2 Phenotypic characterization of *PA4802.1* deletion mutant strain

3.2.2.1 Impact of PA4802.1 on *P. aeruginosa* growth

The effect of *samA* and PA4802.1 gene deletions on *P. aeruginosa* PAO1-L growth were compared in LB media liquid cultures under aerobic and anaerobic conditions. Growth was monitored manually by measuring OD at 600 nm, using a spectrophotometer. The PA4802.1 gene deletion strain was constracted as described in section **2.12.4.1**.

It was observed that the deletion of *samA* slightly affected growth negatively under both aerobic and anaerobic conditions. However, the Δ*samA* strain reached the same OD as the isogenic WT after 25 h of growth (**Figure 3.15**).

Growth of the PA4802.1 mutant was similar to that of the WT strain under aerobic conditions, and it was only slightly reduced under anaerobic conditions. The ΔPA4802.1 reached the same OD as the isogenic WT after 25 h of growth (**Figure 3.15**).

Overall, no drastic differences in growth were caused by *samA* or PA4802.1 deletions (**Figure 3.15**). However, measurements were not taken for the whole course of this experiment.

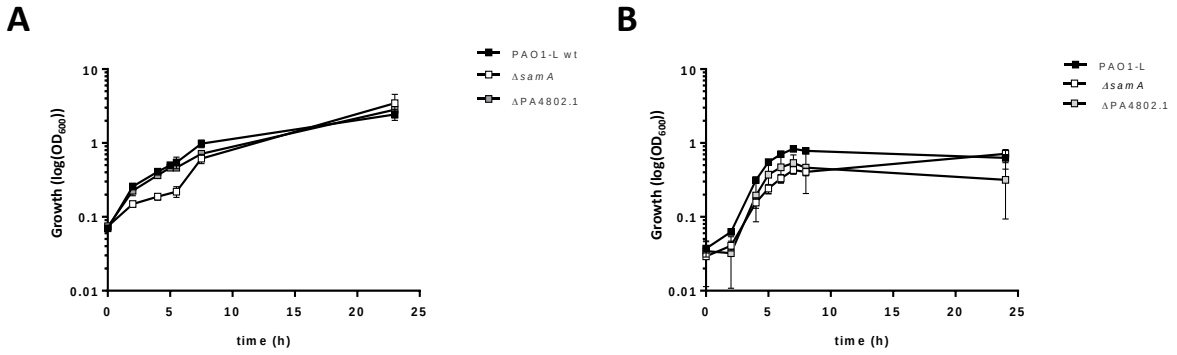


Figure 3.15. Manual Growth curves for the WT, the *ΔsamA* and PA4802.1 mutant (aka ΔtRNA^{sec}) under aerobic conditions and anaerobic conditions.
The mutant strains did not carry any complementation plasmids. Samples were inoculated in 96-well plates at OD_{600}, 0.005±0.010 and incubated at 37°C for more than 24 h. For the anaerobic conditions, pre-culture was done under aerobic conditions and the anoxic media was supplemented with 100 mM KNO_3. Error bars indicate standard deviation based on the mean values of three independent biological clones. The experiment was done three times with similar results. The *samA mutant (Δ*samA) strain is in reality in *Pseudomonas aeruginosa* PAO1-Nottingham strain background and not PAO1-Lausanne, as it was discovered by RNA-seq in Chapter 6.

3.2.2.2 Effect of a *PA4802.1* deletion on the motility of *P. aeruginosa*

3.2.2.2.1 Swarming and Twitching

When compared to the WT, the PA4802.1 mutant (with the empty pME6032 vector) was found to produce less swarming. The presence of pME6032 empty vector in the WT did not seem to affect the swarming and the pME6032::PA4802.1 complementation plasmid unexpectedly further decreased the swarming phenotype (**Figure 3.16, A**). As far as twitching is concerned, the deletion of PA4802.1 did not seem to affect twitching compared to the WT (**Figure 3.16, B)**. Interestingly, complementation of

the PA4802.1 unexpectedly reduced the twitching abilities of the strain. The pME6032::PA4802.1 complementation plasmid was constructed as described in section **2.12.4.3**.

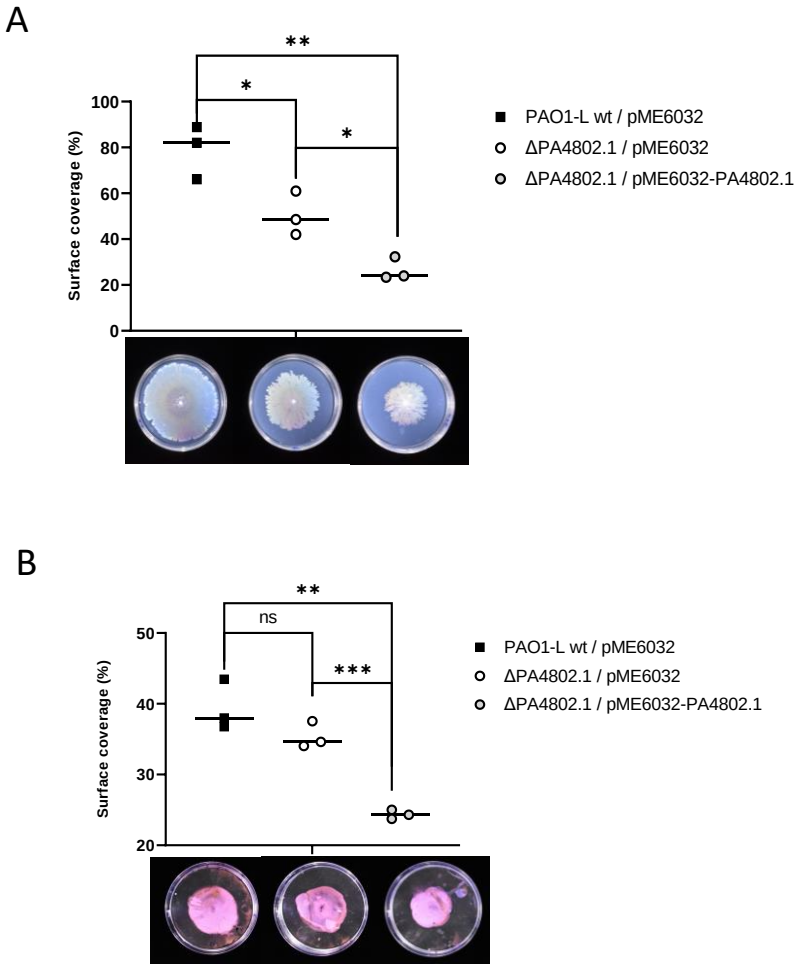


Figure 3.16. Role of PA4802.1 in *P. aeruginosa* PAO1-L swarming and twitching motilities.
A. Swarming was tested in the PAO1-L (WT), and ΔPA4802.1 mutant strains containing the pME6032 empty vector or the complementation plasmid pME6032-PA4802.1. Cells were inoculated on the surface of the plates, which were then incubated for 16 h at 37 °C. Pictures show representative results. The swarming area was quantified relative to the total area of the plates. Statistical significance is depicted by: ns; P>0.05, *; P≤0.05, **; P≤0.01, ***; P≤0.001, ****; P≤0.0001. B. Twitching was tested in the PAO1-L (WT), and PA4802.1 mutant strains containing the pME6032 empty plasmid or the complementation plasmid: pME6032-PA4802.1 Cells were inoculated on the surface of the plates, which were then incubated for 16 h at 37 °C. Pictures show representative results. The twitching area was quantified relative to the total area of the plates. Statistical significance is depicted by: ns; *p*>0.05, *; *p*≤0.05, **; *p*≤0.01, ***; *p*≤0.001, ****; *p*≤0.0001.

3.2.2.3 Initial investigation of PA4802.1 regulon

3.2.2.3.1 PA4802.1 and QS

If the *samA* and PA4802.1 regulons overlap due to the proximity of these two genes there is a possibility that PA4802.1 may also be linked to QS. To investigate this, the effect of QS on PA4802.1 promoter activity was assessed in the same way as for *samA*.

The miniCTX::$P_{PA4802.1}$-*lux* transcriptional reporter was introduced into the mutant strains Δ*lasI*, Δ*rhlI* and Δ*pqsA.* Both growth and bioluminescence were measured in LB, M9 and RPMI growth media. The miniCTX::$P_{PA4802.1}$-*lux* transcriptional reporter was constructed as described in section **2.12.3.1**.

The activity of the PA4802.1 promoter was upregulated in the Δ*lasI and* Δ*pqsA* backgrounds, compared to the WT in all three media tested (**Figure 3.17**). In more detail, PA4802.1 was more upregulated in Δ*lasI* when growing in M9 and RPMI media compared to the LB. The promoter of PA4802.1 was downregulated in Δ*rhlI* and in M9 and RPMI compared to the WT. However, no difference in its activity was observed in LB (**Figure 3.17**).

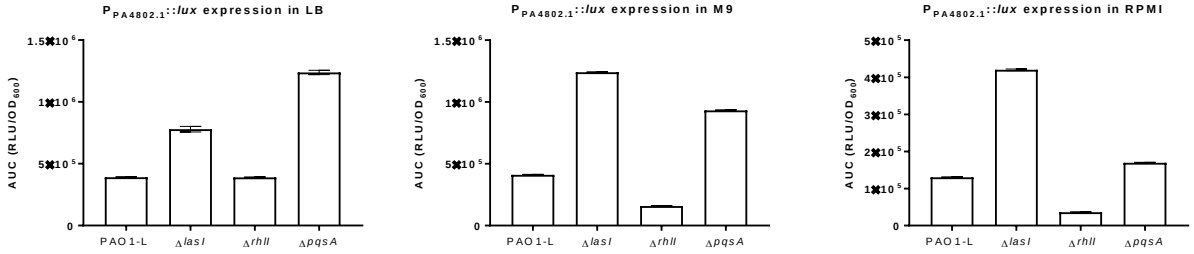


Figure 3.17. Effect of quorum sensing genes (*lasI*, *rhlI*, *pqsA* and *vfr*) on PA4802.1 gene expression.
Expression of PA4802.1 in the *lasI* mutant (Δ*lasI*), *rhlI* mutant (Δ*rhlI*) and *pqsA* mutant (Δ*pqsA*) alongside the PAO1-L (WT) as control, is represented as the area under the curve (AUC) of the normalized relative luminescent units (RLU). The experiment was repeated three times and error bars indicate standard deviation based on the mean values of three independent biological replicates. Statistical analysis was not feasible for these set of data.

3.2.3 Impact of SamA on PA4802.1 expression

To investigate whether SamA may affect PA4802.1 expression, the promoter activity of the latter was assessed in the Δ*samA* mutant (**Figure 3.18, A**) and *samA*ind (with or without IPTG) backgrounds (**Figure 3.18, B**). PA4802.1 gene expression was upregulated in Δ*samA* background compared to the WT strain in LB, M9 minimal and RPMI media, with statistical significance (p<0.001, p<0.05 and p<0.001, respectively). Growth was similar for all the strains tested in each medium (data not shown).

In contrast, the activity levels of the PA4802.1 promoter were not significantly different in IPTG-induced *samA*Ind strain (**Figure 3.18, B**) compared to uninduced condition which serves as the control, with p>0.05. Growth was found to be similar for all the strains tested (data not shown).

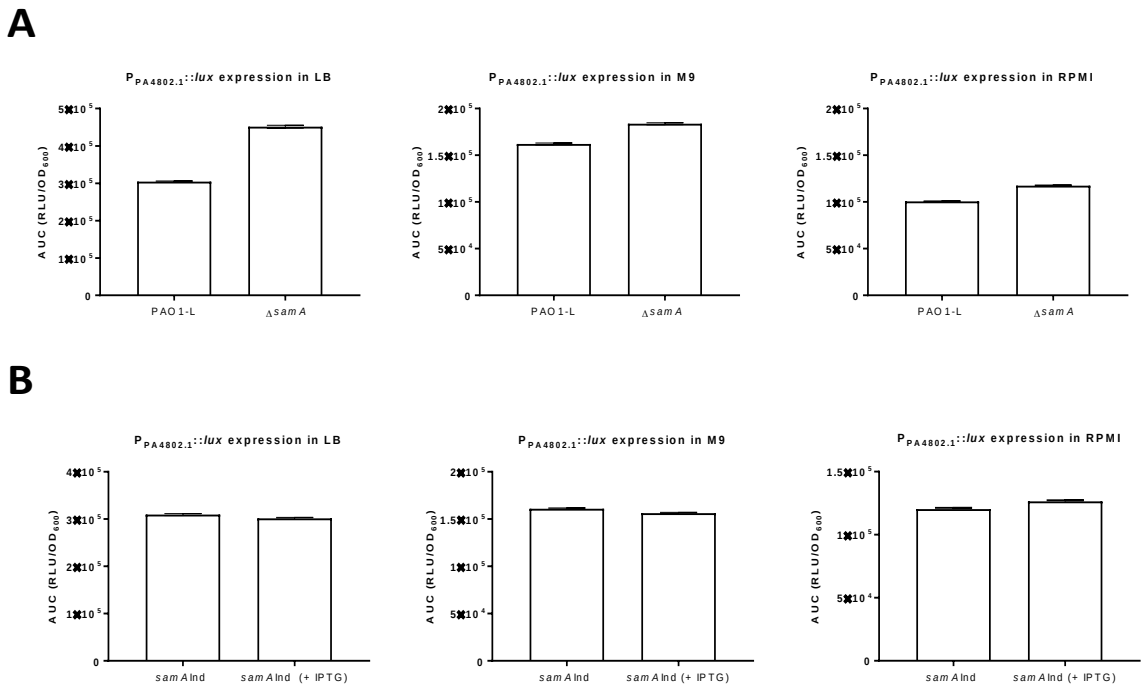


Figure 3.18. Role of *samA* on PA4802.1 promoter activity.
A. Expression of PA4802.1 in the Δ*samA* strain alongside the PAO1-L (WT) as control, is represented as the area under the curve (AUC) of the normalized relative luminescent units (RLU) (RLU/OD_{600nm}). The experiment was repeated three times and error bars indicate standard deviation based on the mean values of three biological clones**. B.** Expression of PA4802.1 between uninduced *samA*Ind strain and IPTG induced. Expression is represented as the area under the curve (AUC) of the normalized relative luminescent units (RLU) (RLU/OD_{600nm}). The experiment was repeated three times and error bars indicate standard deviation based on the mean values of biological clones. The samA *mutant Δ*samA strain is in reality in *Pseudomonas aeruginosa* PAO1-Nottingham strain background and not PAO1-Lausanne, as it was discovered by RNA-seq in Chapter 6.

3.3 Discussion

In an attempt to gain some insights into the mechanisms by which a *samA* mutant showed attenuation in several disease models, a wide genome mutant screening was used (Dubern *et al.*, 2015) (**Figure 3.2**). Phenotypic characterization of a *samA* mutant and identification of putative regulators of this gene were conducted as well.

Overall, no major differences in growth were caused by the deletion of *samA* (**Figure 3.4**) in different media. The general trend was for the *samA* mutant strain to show slightly slower growth earlier on than the WT but eventually it caught up. However, there are some limitations with these measurements as they were not taken for the whole course of this experiment and statistical analysis was not applied as logistic restrictions in some instances did not allow the use of more than one biological replicate for each strain. The manually collected sample data plots, using shaking flasks,

showed some discrepancies with the automatically measured ones, using static microtiter plates (**Figure 3.5**). This could be due to some differences in environmental parameters such as aeration although growing *samA* in anaerobiosis did not show any significant changes in growth compared to the WT (**Figure 3.6**).

The phenotypic characterization of the *samA* deletion mutant was the next step. Swarming in this mutant was affected (**Figure 3.7, A**). Attenuation of swarming motility is in agreement with findings in Dubern *et al*. (Dubern *et al.*, 2015). However, the impairment was not reverted with the *samA* complementation plasmid, which could not confirm a role for *samA* in *P. aeruginosa* swarming motility. This may be an effect of the multiple copies of the gene being expressed from the plasmid pME6032 construction. Alternatively, *samA* may not be responsible for the observed impairment and secondary mutations may take place in the mutant strains which could account for the lack of complementation. Sequencing of the chromosome of the *samA* mutant would be required to verify this.

A recent publication revealed that ToxR, a gene that was deleted in PAO1-Nottingham, ,which is the background of *samA* deletion, affects swarming positively by increasing the levels of C4-HSL and that of rhamnolipid surfactants. Hence, supporting that the reduction of swarming might be due to the *toxR* deletion and also contradicting opposite regulations for the rhl system and the rhamnolipids production (Dubern *et al.*, 2022).

Twitching in the *sam*A deletion strain (**Figure 3.7**,**B**) was severely affected and the impairment was reverted upon complementation of *samA* expressed from a plasmid verifying the impact of *samA* in *P. aeruginosa* twitching motility. Attenuation of twitching motility in a Δ*samA* in-frame deletion mutant has not been shown previously. It is a possibility that *samA* in *P. aeruginosa* affects twitching motility by affecting directly or indirectly the functionality of pili, or the adherence to solid surfaces or by affecting expression of genes involved in pili synthesis (Burrows, 2012) which deserves further investigation. Since twitching motility is a crucial action for *P. aeruginosa* to be able to break through the ciliated airway epithelium of the host and establish infection (Xia *et al.*, 2021).

The next step would be determination of levels of pilin protein produced and of the levels of surface piliation through Western blot analysis and ELISAs respectively (Geesey *et al.*, 1977). For instance, if reduced piliation is exhibited the *samA* gene might have a role in the assembly and functionality of the pili rather than their synthesis and that will be the basis of the attenuation observed.

Swimming motility was not followed as it was proved very difficult to prepare the media and replicate the same conditions for robust reproductions of the experiments.

Vfr regulates twitching motility although the mechanism has not been elucidated (Beatson *et al.*, 2002a, 2002b) It is speculated that Vfr is responsible for activating expression of genes that encode type IV pili components or other genes that coordinate twitching (Beatson *et al.*, 2002b). However, data presented here suggests that the c-AMP dependent regulator Vfr seems to suppress expression of the *samA* gene (**Figure 3.9**) which seems to have a positive role in twitching motility. Taken together, *samA* probably affects twitching through a different pathway than Vfr.

Exoproducts such as pyocyanin (**Figure 3.8, A**), elastase (**Figure 3.8, B**) and protease (**Figure 3.8, C**), are also important for *P. aeruginosa* virulence. Therefore, they were quantified in the *samA* deletion strain. Pyocyanin and protease production showed no differences between PAO1-L and the *ΔsamA* strain, whereas the levels of elastase produced were significantly reduced in the *samA* deletion strain. It is worth pointing out that these results would be more robust if they were repeated including a *samA* deletion strain carrying the *samA* complementation construct.

The above results contradict previous findings which suggest that reduced exoproduct production in *ΔsamA* was affected (Dubern *et al.*, 2015). However, this is probably due to the fact that exoproduct production assessments were carried out using the *samA::Tn5* random mutant and not the in frame deletion strain. In addition, in Dubern *et al*. the assays were performed in 96-microtitre well plates under microaerophilic conditions, whereas in this study the strains were grown in flasks under maximum aeration conditions. Moreover, the differences observed can be attributed to the exoproduct production regulation itself as it could be timely regulated.

This study set out to identify regulators of the *samA* gene in *P. aeruginosa*, either known regulators integrated within well studied regulatory circuits such as QS, or novel regulators of *samA*. Shedding light on the genetic regulation of *samA* is important to understand the mechanism behind the severe attenuation observed in a *samA* mutant *in vivo* (Dubern *et al.*, 2015). Moreover, the putative regulators uncovered by this study could potentially be exploited as antimicrobial targets upon further characterisation.

To sum up, *samA* gene expression is negatively affected by the *rhl* and PQS QS systems and by the Vfr global regulator (**Figure 3.9**), whereas, the *las* system does not seem to affect the expression of *samA* (**Figure 3.9)**. Since Vfr is a key modulator of the *las* system, and in turn the *las* system is the one to activate the *rhl* system (Latifi *et al.*, 1996; Lee and Zhang, 2015; Pesci *et al.*, 1997) an effect of the *las* system would be expected. However, it was not the case. Based on the aforementioned results, the global regulator Vfr seems to suppress expression of the *samA* gene. Moreover, the *las* system has a positive effect on the PQS system whereas the *rhl* system has a negative impact (Williams and Camara,

2009). Thus, when the *rhl* system is activated it negatively regulates the PQS system and drives *samA* expression. Therefore, the PQS system could indirectly suppress *samA* expression. However, the interactions between the different systems are intricate and further investigations are required. Specifically, to further investigate the interaction between *samA* and the PQS system the Δ*pqsA* strain could be complemented with PQS signalling molecule. If *samA* is still upregulated it would mean that PQS signalling molecule is not required to activate the system, and that the system is regulated via the *pqsR*/*pqsE* pathway rather than the *pqsR*/*pqsA* route (Williams and Camara, 2009).

Using a different approach to investigate any possible links between SamA and QS, transcriptional reporter fusions of genes constituting main components of these systems (e.g miniCTX:: *rhlI-lux*) were introduced in PAO1-L and Δ*samA* backgrounds and differences in their expression were evaluated (**Figure 3.10**). Expression of all three QS genes was found significantly (p<0.05) upregulated in Δ*samA* compared to the WT, suggesting that *samA* has a negative impact on all three *lasI, rhlI* and *pqsA* QS genes.

Given the fact that a methyltransferase is involved in the biosynthetic pathway of QSSMs (Bassler, 2002). There is a possibility that *samA*, which encodes a hypothetical protein with methyltransferase orthologs, can somehow impact directly or indirectly on the biosynthesis of the QSSMs. In order to determine if SamA affects QS post-transcriptionally, a step forward would be to quantify the several QSSMs such as 3-oxo-C12-HSL (*las* system), C4-HSL (*rhl* system), PQS and HHQ (PQS system) in PAO1-L, Δ*samA* and *samA*ind and evaluate differences between the different strains (**Figure 3.11**). In addition, the range of error bar for PQS quantification in the samAInd undiced strain could suggest the existence of an outlier. Further, suggesting that the difference although statistically significant it might not have biological significance in realuty.

The *samAind* mentioned above is the *P. aeruginosa samA* inducible strain in which the chromosomal *samA* gene is placed under the control of an IPTG-inducible promoter. It was created as an approach to avoid any side effect of complementing with plasmids. A similar approach was previously used in defining the interrelationship between the alkyl quinolone and the PqsE stimulons (Rampioni *et al.*, 2010).

Activity levels of the *lasI*, *rhlI* and *pqsA* promoters were not significantly different in the IPTG-induced *samA*Ind strain (**Figure 3.10**) compared to uninduced. This could be due to the inability to complement via overexpression or that there may be some post-transcriptional regulation taking place. To investigate the latter, the effect of SamA on QS was further assessed by quantifying the levels of the *N*-acylhomoserine lactones (3-oxo-C12-HSL and C4-HSL) and alkyl quinolones (PQS) in PAO1-L, Δ*samA*

and *samA*Ind strains. Firstly, C4-HSL levels did not show significant differences in Δ*samA,* uninduced *samA*Ind strain and IPTG induced *samA*Ind strain (**Figure 3.11**). However, PQS levels were reduced when the *samA* gene was absent although no reversal could be seen upon complementation (**Figure 3.11**) requiring further investigation.

The *samA*ind strain was largely verified by PCR, however, discrepancies between the Δ*samA* and the *samA*ind behaviour called for further validations. The first step was to verify that the P*tac* promoter was free of mutations. Sequencing of this promoter showed that there were no mutations present (data not shown). Ideally, the *samA*ind strain should be assessed for *samA* expression by qRT-PCR but this scenario was abandoned due to time constraints. It was suggested that strains like these might always have some "leaky" activity by the LacI repressor that cannot be completely suppressed under non-induced conditions. Nevertheless, this does not fully explain some of the results observed.

Another approach used towards identifying novel *samA* regulators was the construction of a transposon mutant library, in the WT PAO1-L having miniCTX::P_{samA}-*lux* inserted in its chromosome. Transposon mutants were selected for having either upregulated, downregulated or delayed *samA* expression, using bioluminescence as a reporter of transcriptional levels. However, this approach is sensitive to environmental conditions and time-dependent. This may explain why some of the strains that appeared to have attenuated light production during the primary screening ended up being false positives during the secondary screening. A solution would be to use a *samA*-fluorescent reporter fusion as indicator of expression, which would be more stable. Also, another way to overcome this limitation would be to fuse *samA* with the *lacZ* reporter gene for monitoring their expression, as production of the insoluble blue pigment from 5-bromo-4-chloro-3-indolyl-β-D-galactopyranoside is cumulative (Clark *et al.*, 2019).

Despite the efforts some random mutants were not able to be sequenced from the selected candidates. Probably, because the re-circularized fragments containing the transposon and its flanking chromosomal regions were too large to enable successful introduction into the *E. coli* S17 strain. With this mini-Tn*5* transposon insertion mutagenesis, four genes, *purD*, *faoA*, *mvaT* and *hmgA* were identified as novel putative negative regulators of *samA*, as their disruption resulted in *samA* upregulation (**Figure 3.12)** and are summarized on **Table 3.1**. Both, *faoA* and *mvaT* were uncovered several times but they were identified as redundancies, *purD* was only scored once. Therefore, the screening method can be considered reliable, however, changes in the way the method is carried out could be taken to reduce redundancies and to maximize the number of distinct genes identified.

MvaT, is an H-NS protein which acts as a transcriptional regulator and it controls the expression of several virulence genes in growth phase-dependent manner (Diggle *et al.*, 2002). Specifically, MvaT acts as a negative regulator for *cupA* gene cluster expression, which is required for biofilm formation on abiotic surfaces. Thus, MvaT negatively affects biofilm formation (Vallet *et al.*, 2004). Taken together, MvaT negatively regulates biofilm formation and *samA* gene expression, suggesting that indeed *samA* may positively affect biofilm formation, probably by affecting twitching motility. The possibility remains that *samA* may be part of the pathway controlling expression of *cupA* gene cluster which as previously mentioned is negatively regulated by MvaT (Vallet *et al.*, 2004).

HmgA is a homogentisate-1,2-dioxygenase and the dark brown pigment produced in the Δ*hmgA* strain is pyomelanin [103]. Its production seems to grant an adaptive advantage to *P. aeruginosa* in a chronic infection state due to increased resistance clearance by oxidative stress (Rodrıguez-Rojas *et al.*, 2016). Pyomelanin-producing *hmgA* mutated strains of *P. aeruginosa* are often isolated from CF patient lungs therefore an *hmgA* mutation could potentially increase *samA* expression. Given the preliminary results, increased *samA* expression might be further enhancing virulence of *P. aeruginosa* in the CF lung as shown in Dubern *et al*. through the use of a murine infection model (Dubern *et al.*, 2015; Rodrıguez-Rojas *et al.*, 2016).

PurD seems to be involved in nucleotide biosynthesis and FaoA seems to be involved in fatty acid β-oxidation, although their exact function and contribution to *P. aeruginosa* lifestyle has not been demonstrated.

Twitching (**Figure 3.13, B**) and swarming (**Figure 3.13, A**) were affected in ΔPA4803 (Δ*samA*), *ΔfaoA* and *ΔpurD* compared to PAO1-L. Whereas, twitching (**Figure 3.13, B**) but not swarming (**Figure 3.13, A**) were affected in *ΔmvaT* compared to PAO1-L. Briefly, this suggests that *samA* may act, directly or indirectly, by affecting expression of genes involved in pili synthesis or assembly. Since mutation of all three genes led to higher *samA* expression this makes them putative negative regulators of *samA* gene. The current suggestion is that *samA* is involved in twitching motility and biofilm formation. Therefore, disruption of the *faoA, purD, mvaT* should theoretically lead to higher *samA* expression and hence better swarming and twitching. However, disruption of a putative s*amA* negative regulator negatively affected these motilities. One explanation is that the network in which *samA* belongs is more complex than initially anticipated. All these contradictory results highlight the complexity of the regulation within which SamA is embedded in *P. aeruginosa*.

Significant differences in the production of all three exoproducts, elastase (**Figure 3.14, B**), protease (**Figure 3.14, C**) pyocyanin (**Figure 3.14, A**) between the PAO1-L WT and the mutant strains *samA*,

purD, faoA and *mvaT* were observed. In detail, PA4803 (*samA)*, *mvaT* and *faoA* seem to be involved particularly in pyocyanin and elastase production but not in protease production. Intriguingly, the phenotypes of the two *faoA* transposon mutants tested, RM06 and RM14 are not the same which was unexpected as the transposon insertion sites were identical (**Table 3.1**). One possibility is that there could be a secondary mutation in one of these two mutants affecting its phenotype. The same could apply for PurD strain, which does not seem to produce any of the three tested exoproducts. Ultimately, working with transposon mutants can have these effects. Finally, repetition of all the assays mentioned above with clean deletion mutants of *faoA, purD, mvaT* strains would be crucial to prove that all the attenuated phenotypes observed are indeed due to the specific gene disruption.

In conclusion, the results reported in this chapter indicate that in *P. aeruginosa*, *samA* plays a key role in twitching motility. Moreover, the data obtained suggests that expression of the gene is affected by *rhl* and PQS QS systems, as well as by the global regulator Vfr. However, further work is required to unravel the complicated regulatory network interplay between *samA* and the various systems. A number of mutants were isolated, all of which were affected in *samA* expression, and four genes, *purD*, *faoA* and *mvaT* were identified as putative *samA* negative regulators. Again, additional work will be required to consolidate a link between the putative regulators uncovered and *samA*. Finally, shedding light on *samA* function will be challenging but its exploitation as an antimicrobial target may contribute to the battle against chronic infections.

As mentioned, the results of the expression analyses have been particularly interesting and they suggest an intricate relationship between the *samA* gene and the QS systems in *P. aeruginosa*. At this point, complementation of all the strains used above with the appropriate plasmids and repetition of the expression analyses needs to be carried out next in order to confirm the results obtained before moving forwards into the unravelling of more in depth mechanisms.

The next step taken while preparing all the necessary complementation constructs was to investigate the role of the PA4802.1 gene and establish whether it has a link with *samA.*

Firstly, growth under aerobic and anaerobic conditions was assessed. Overall, no major differences in growth were caused by either *samA* or PA4802.1 deletions (**Figure 3.15**). PA4802.1 appeared to grow slightly more slowly but not significantly. However, measurements were not taken for the whole course of this experiment. Interestingly, the deletion of PA4802.1 seems to affect *P. aeruginosa* swarming, and complementation increases the attenuation (**Figure 3.16, A**). The deletion of PA4802.1 affected twitching motility slightly but again complementation enhanced the attenuation (**Figure 3.16, B**). This increase of the attenuation of swarming and twitching may be an effect of the multiple copies

of the gene being expressed from the plasmidic pME6032 construction. Therefore, a clear conclusion cannot be drawn by these results.

The next step was to investigate whether there were any links between PA4802.1 and QS. For that purpose, a CTX::$P_{PA4802.1}$-*lux* transcriptional reporter fusion, for PA4802.1 expression analyses was introduced into several strains: PAO1-L WT, Δ*samA, samAind,* Δ*lasI*, Δ*rhlI* and Δ*pqsA*.

Gene expression analysis showed significant downregulation of PA4802.1 in the Δ*rhlI* background and significant upregulation of gene expression in both Δ*lasI* as well as Δ*pqsA* strains compared to PAO1-L (**Figure 3.17**). Hence, the *las* and PQS system seems to have a negative impact on the expression of PA4802.1, whereas the *rhl* system seems to positively affect it. This is in contrast with the fact that the *las* system activates the *rhl* and the PQS systems. It seems that the *las* system is the first to inhibit the expression of PA4802.1 gene but then the suppression continues by the activation of the PQS system by the *las* system. In between, activation of *rhl* system could briefly inhibit the PQS system and drive the expression of PA4802.1 gene for a certain amount of time. Therefore, everything seems to be regulated in a time-dependent fashion.

To investigate whether SamA may affect PA4802.1 expression, the promoter activity of the latter was assessed in the Δ*samA* mutant (**Figure 3.18, A**) and *samA*ind (with or without IPTG) backgrounds (**Figure 3.18, B**). PA4802.1 gene expression was upregulated in Δ*samA* background compared to the WT strain in LB, M9 minimal and RPMI media. In contrast, the activity levels of the PA4802.1 promoter were not significantly different in IPTG-induced *samA*Ind strain (**Figure 3.18, B**) compared to uninduced condition. It can be speculated that PA4802.1 expression is lower in RPMI media compared to rich medium because these are growth-limiting conditions.

Absence of *samA* in the Δ*samA* background resulted in significant upregulation of PA4802.1 gene expression compared to PAO1-L. However, *samA* overexpression in the IPTG-induced *samA*Ind strain did not show significant differences in PA4802.1 expression compared to the uninduced strain.

Taken together, a regulatory link between *samA* and PA4802.1 gene expression cannot be established, based on the discrepancies observed between Δ*samA* and *samA*Ind strains. These discrepancies could indicate a potential disruption of the PA4802.1 promoter region resulting from deletion of *samA* gene in the Δ*samA* strain or it could be due to promoter leakage. The elevated PA4802.1 gene expression in the Δ*samA* strain could be explained if the promoter region of PA4802.1 contained a negative control element which was disrupted during the creation of the *samA* deletion.

It should be mentioned, that the QS systems in *P. aeruginosa* are regulated by several growth phase dependent regulators including: stationary-phase sigma factor RpoS (Kessel *et al.*, 2013; Schuster and Greenberg, 2006) and global post-transcriptional regulator RsmA (Heurlier *et al.*, 2001), amongst others. Hence, this may explain the differences in the relative timing and magnitude of PA4802.1 gene expression under different growth conditions. In conclusion, the regulation of PA4802.1 gene expression by QS is greatly influenced by environmental conditions. Further work is required to consolidate the links between the putative regulators uncovered and *samA* and to unravel the complicated regulatory network in play between *samA* and QS. Finally, shedding light into the biological function of *samA* is essential for its exploitation as an effective anti-virulence target against *P. aeruginosa* infections.

It should be mentioned that constitutive reporter control strains were not built. These are vectors which express *lux* constitutively thanks to the kanamycin promoter. This helps to detect and subtract potential undesired bias by unspecific interactions with the *lux* operon or with the bioluminescence metabolism.

Given the fact that the PA4802.1 gene is located downstream of *samA*, which probably encodes a hypothetical protein with SAM-dependent methyltransferase activity (Winsor *et al.*, 2016), the hypothesis that SamA probably plays an important role in tRNA modification to ensure translational fidelity in *P. aeruginosa* was formed. This hypothesis received the focus in this study but due to time constraints many avenues discussed above were not taken forward.

Overall, it is very important to take into consideration while looking at these results that wherever *samA* deletion strain was used, the strain was not in the PAO1-L background but in PAO1-N background; as it was discovered when the RNA-seq was perfomed. Therefore, any discrepancy observed could be due to this comparison of strains from different backgrounds.

Chapter 4 SamA protein crystallization and functionality

4.1 Introduction

The Pseudomonas Genome database (Available at: http://www.pseudomonas.com) (Winsor *et al.*, 2016), predicted PA4803 as a putative methyltransferase hypothetical protein of 22.7 kDa. This predicted protein contains some conserved residues usually found in the SAM/AdoMet dependent methyltransferases. Hence, it was renamed *samA* for this study. The S-Adenosyl-Methionine (SAM)-dependent methyltransferases superfamily of enzymes catalyse the transfer of a methyl group from SAM to a variety of substrates such as proteins and nucleic acids (Schubert *et al.*, 2003a).

4.1.1 S-adenosylmethionine (SAM) and its metabolism in bacteria

SAM (S-adenosylmethionine, also known as AdoMet) is the primary methyl donor in bacteria. This molecule contains the adenosine moiety of ATP and the amino acid methionine (Loenen, 2006). The recycling of the SAM pool is an important process in all cells and it happens via the Activated Methyl Cycle (AMC)(**Figure 4.1**).

Demethylation of SAM, mediated by SAM-dependent methyltransferase reactions, generates S-adenosylhomocysteine (SAH, also known as AdoHcy), which is a potent feedback inhibitor of SAM-dependent methyltransferases (Halliday *et al.*, 2010). In *P. aeruginosa*, SAH is hydrolysed into homocysteine (Hcy) and adenosine by a SAH hydrolase. SAM is also involved in the production of polyamines, thereby yielding 5'-methylthioadenosine (MTA). MTA is then converted to methylthioribose (MTR) and adenine by a SAH hydrolase (Winzer *et al.*, 2002). Several enzymes in the methionine cycle have unusual or even unique foldings.

SAM is generated through conversion of methionine, which is recycled from homocysteine. The conversion is catalysed by a SAM synthetase (MAT methionine adenosyltransferase) which uses the adenosine moiety of ATP. MATs are important enzymes for *de novo* SAM biosynthesis (Loenen, 2006). MAT also has an intrinsic polyphosphatase activity whereby it hydrolyses the remaining portion of ATP into Pi and PPi. Several steps within the cycle may differ between bacterial species. For example, in *E. coli*, homocysteine is produced in two steps rather than one, catalysed by methylthioadenosine/SAH nucleosidasev(MTA/SAH'ase) and S-ribosylhomocysteine (RH) cleavage enzyme (Winzer *et al.*, 2002).

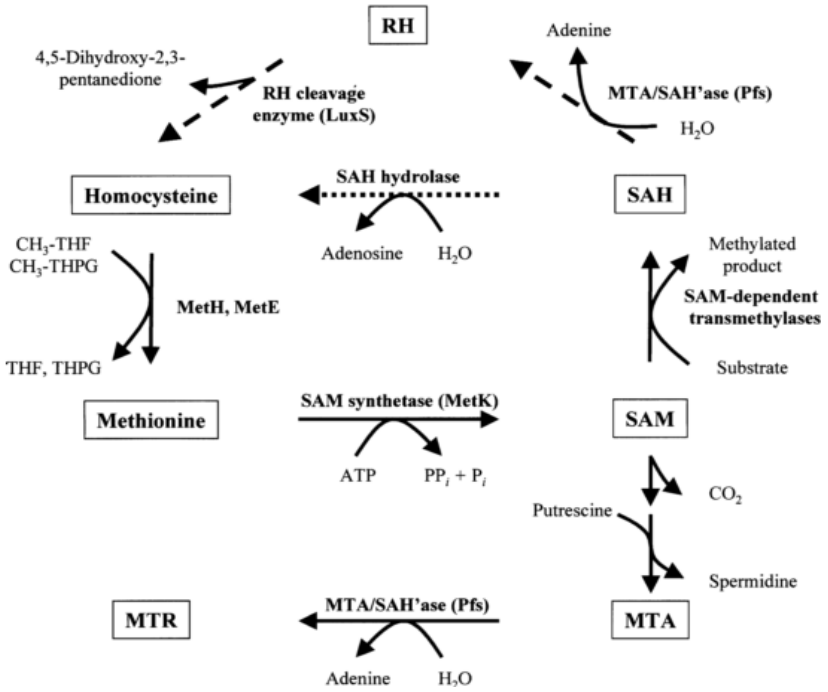


Figure 4.1. The S-adenosylmethionine (SAM) metabolism in bacteria.
Figure extracted from Winzer *et al*., 2002 (Winzer *et al.*, 2002). Arrows in the figure indicate the direction of metabolic conversions *in vivo*. Dotted arrow shows hydrolysis and dashed arrow a cleavage reaction. SAM; S-Adenosylmethionine, SAM synthetase; methionine adenosyltransferase, SAH; S- adenosylhomocysteine, MTA/SAH'ase; methylthioadenosine/SAH nucleosidase, RH; S-ribosylhomocysteine cleavage enzyme, CH3-THPG; N5-methyltetrahydropteroryl glutamate, CH3-THF; MetH cobalamin-dependent methionine synthase N5-methyltetrahydrofolate, MetE; cobalamin-independent methionine synthase and MTR, methylthioribose.

4.1.2 The versatility of S-adenosylmethionine (SAM) and the SAM-binding proteins

It is worth mentioning that the AMC contributes in the formation of quorum sensing signalling molecules (QSSMs), particularly, the *N*-acylhomoserine lactones (AHLs) made by Gram-negative bacteria including *P. aeruginosa* (Halliday *et al.*, 2010). AHLs are generated from S-adenosylmethionine (SAM) which provides the homoserine lactone moiety and from several components of the fatty acid metabolism (Winzer *et al.*, 2002).

So far, 15 superfamilies of SAM-binding proteins have been identified. The functions vary from methylation of many diverse substrates to the synthesis of polyamines as previously mentioned. Intriguingly, even within each family of SAM-binding proteins, the protein sequences themselves are not conserved (Loenen, 2006). Different domains and folds that perform all of these chemical reactions exist within these 15 superfamilies (Loenen, 2006).

In more detail, SAM serves as the methyl donor for the majority of methyltransferases, which catalyse a methyl transfer into a variety of substrates from DNA, RNA, proteins to small molecules. These modifications can dictate a number of important processes in both prokaryotes and eukaryotes (Loenen, 2006). Despite the lack of sequence conservation in their 3D structure, the majority of SAM-dependent MTases share a common conserved fold called the Rossmann fold. However, the residues which contact SAM, within the conserved fold, are not conserved (Loenen, 2006).

Particularly, methylation of bacterial DNA helps to protect endogenous DNA from digestion by restriction enzymes (Loenen, 2006). Moreover, SAM can also serve as a co-factor for nucleases such as the type I restriction enzyme *Eco*KI, as this multimeric modification/restriction enzyme is unable to bind and cut DNA in the absence of SAM (Loenen, 2006). Additionally, SAM can bind to certain RNA structures called riboswitches, which exist in bacteria such as *Bacillus subtilis* and control transcription or translation. In more detail, riboswitches, are highly structured RNA regions within the 5'-UTR (untranslated region) of certain mRNAs which SAM is able to bind causing alteration of the secondary loop formation, thereby affecting transcription or translation and controlling gene expression (Loenen, 2006).

4.1.3 SAM-dependent methyltransferases classifications

Members of the SAM-dependent methyltransferases superfamily can be classified into several classes (Classes I–V) depending on which of the five structural folds (I–V) they possess (**Figure 4.2**). The fold is able to bind SAM and catalyse the methyl transfer (Schubert *et al.*, 2003a). The majority of SAM-dependent MTases possess the Class I fold. As previously mentioned the amino-acid sequence similarity, even within the same MTase family, can be as low as 10%, supporting great flexibility in terms of the structural and catalytic requirements for methyl transfer from SAM to a variety of substrates (Schubert *et al.*, 2003a). Further classification of this large superfamily can be based on substrate specificity and the atomic targets for methylation (Loenen, 2006).

The Class I MTase structure is characterised by: seven stranded β sheets and a reversed β hairpin at the carboxyl end of the sheet, flanked by α helices (**Figure 4.2; A**). The first β strand typically ends in a GxGxG (or GxG) motif, which is a nucleotide-binding site, bending underneath SAM to initiate the first α helix. In addition, a conserved acidic residue is positioned at the end of β2, which forms hydrogen bonds to both hydroxyls of the SAM ribose. This structure is quite similar to that of the NAD(P)-binding Rossmann-fold domains (Schubert *et al.*, 2003a).

The Class II MTases possess the MetH reactivation domain, which is described as a long, central, antiparallel β-sheet flanked by groups of helices at either end (**Figure 4.2; B)**. SAM is bound to a shallow groove along the edges of the β strands through formation of hydrogen bonds to a conserved RxxxGY motif (Schubert *et al.*, 2003a).

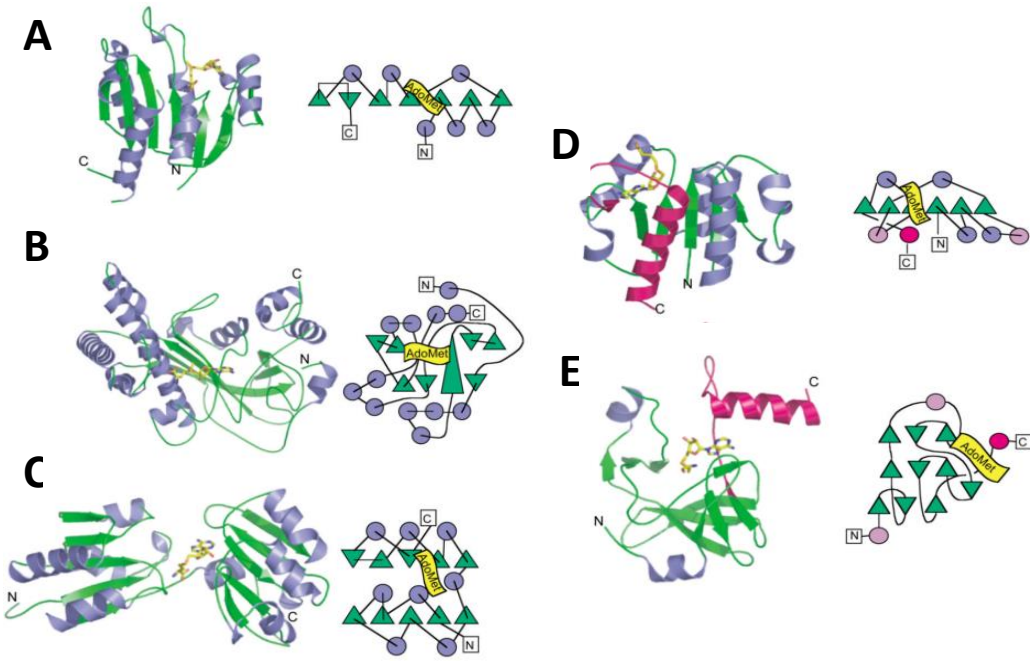


Figure 4.2. The tertiary structures of the five classes of SAM-dependent methyltransferases (MTases).
Figure extracted from Schubert *et al.*, 2003 (Schubert *et al.*, 2003a)**.** For each case a tertiary structure representation (left) and topology diagram (right) are shown**.** In the topology diagrams helices are represented by purple, magenta or lilac circles and beta-sheets as green triangles.

In Class III MTases the catalytic site is placed into a cleft between two αβα domains, each containing five strands and four helices (**Figure 4.2; C)**. SAM is tightly folded, and binds between the two domains (Schubert *et al.*, 2003a). However, SAM does not interact with the GxGxG motif found at the end of the first β strand.

The Class IV structure is only found in the SPOUT family of RNA MTases, which display a six-stranded parallel β sheet flanked by seven α helices (**Figure 4.2; D)**. The first three strands form half of a Rossman fold. Additionally, their active site is located near the subunit interface of a homodimer and, uniquely, the C terminus is tucked back into the structure in a 'knot' (Schubert *et al.*, 2003a).

Class V SAM-dependent MTases are the SET-domain proteins which contain a series of eight curved β strands forming three small sheets (**Figure 4.2; E)**, with the C terminus forming a knot-like structure similar to the Class IV MTases, but with an entirely different topology. SET-domain proteins have been

shown to methylate lysines in the flexible tails of histones etc. SAM binds to the enzyme near a conserved tyrosine residue, which seems to be involved in the catalytic reaction. The sequences flanking the SET domain may often be essential for MTase activity and might participate in substrate recognition and specificity (Schubert *et al.*, 2003a).

However, not all the proteins which possess a conserved fold/motif are active as MTases. For instance, DNMT3L (DNA MTase 3-like) which is required for imprinting in germ cells lacks MTase activity but it appears to accelerate the binding of DNA and SAM to other MTases (Loenen, 2006). In addition, spermidine synthase, an important enzyme in the polyamine pathway, lacks MTase activity although being highly identical with putrescine N-methyltransferase. Polyamines (putrescine, spermidine and spermine) are small positively charged molecules, which can bind tightly to DNA, RNA, proteins, phospholipids and many other negatively charged molecules. This enzyme is capable of fusing the methionine backbone of dcSAM to putrescine and, in that way, affect DNA bending, cause frameshifts and modulate signal transduction (Loenen, 2006).

4.1.4 SAM-dependent methyltransferases in the biology of *P. aeruginosa*

4.1.4.1 HemK (PrmC), a universally conserved SAM-dependent methyltransferase

HemK, is a conserved protein which shares the common signature of DNA-(adenine-N6) methyl transferases (MTases), the ([LIVMAC]-[LIVFYWA]-x-[DN]-P-P-[FYW], PROSITE accession no. PS00092) (Nakahigashi *et al.*, 2002). DNA-(adenine-N6) MTases methylate the exocyclic amino nitrogen attached to the C-6 position of adenine. Disruption of *hemK* led to downregulation of genes for aerobic respiration, and upregulation of genes for anaerobic respiration. It remains unknown whether this shift to anaerobic respiration was due to a translational defect, the demethylation of an unidentified HemK substrate(s), or due to the retarded growth of the particular mutant strain (Nakahigashi *et al.*, 2002).

PrmC, the HemK homolog in *P. aeruginosa*, is a SAM-dependent methyltransferase of peptide chain release factors (RFs), is essential for pyocyanin and rhamnolipids production in *P. aeruginosa* PA14 and it modulates motility (Pustelny *et al.*, 2013). Two class 1 Release factors (RFs) are responsible for recognizing the three stop codons UAG, UAA, and UGA in eubacterial cells. RF1, encoded by the *prfA* gene, recognizes the UAG stop codon. RF2 is encoded by *prfB* and recognizes the UGA stop codon. Both RF1 and RF2 recognize the UAA stop codon (Pustelny *et al.*, 2013).

RF1 and RF2 retain the GGQ conserved tripeptide motif. Studies have shown that the activity of RF2 is stimulated by Gln methylation within the conserved tripeptide motif, which interacts with the large ribosomal subunit, triggering release of the newly synthesized polypeptide from the ribosome.

Inactivation of PrmC reduces the termination activity of RF1 and RF2 (in a A246T background which is near the MeGln252) by 3 to 4-fold (Mora *et al.*, 2007). Interestingly, the PrmC mutant strain in PA14 is unable to grow under anoxic conditions (Pustelny *et al.*, 2013).

The PrmC crystal structure from *Thermotoga maritima,* in a complex with RF1 and SAM, was reported by Schubert and colleagues (Schubert *et al.*, 200b). A five-helix bundle exists in the N-terminal and a well-characterized class I AdoMet-dependent MTase fold is displayed in the C-terminal domain of PrmC. (Schubert *et al.*, 2003b).

4.1.4.2 PrmC and SamA relations

PrmC and PA4803 (SamA) share up to nine conserved residues (amino acids) when their sequences were aligned. A region of PrmC contains few conserved residues, which seem to be part of the SAM-MTase motif. Overall, there is no major conservation between the two proteins as expected.

In the cystic fibrosis lung, *P. aeruginosa* populations grow to high densities despite being in an environment that is depleted in oxygen (Pustelny *et al.*, 2013). It has been shown that *P. aeruginosa* can simultaneously carry out microaerobic respiration and nitrate respiration. However, it was not known which of the two respiration modes *P. aeruginosa* preferably uses in the lung and which genes contribute in each. No discrete set of genes was identified to be expressed upon exposure to low oxygen. Instead, an overlap between gene sets expressed depending on the amount of oxygen available (2%, 0.4% or none) was reported. The authors supported that *P. aeruginosa* might respond to low oxygen gradient, suggesting that it is able to respire in combinations of terminal electron acceptors that it may encounter (Alvarez-Ortega and Harwood, 2007).

Transcription of both the *prmC* and *samA* genes has been tested under hypoxic and anoxic conditions (Alvarez-Ortega and Harwood, 2007) Apparently, the differences in expression of each gene under the condition tested was not judged as significant to be mentioned in the paper. The data deposited in the Gene Expression Omnibus (GEO) database shows that abundance of s*amA* mRNA increases when there is reduction in oxygen levels whereas, levels of PA4664 (PrmC) seems to decrease under these conditions. However, the level of expression of both genes (in arbitrary expression units) under anoxic conditions is very similar. In addition, the s*amA* basal expression in the control is very low compared to PrmC (**Figure 4.3**). Comparisons can be made between the expressions of these genes since the results came from the same experiment. However, these data is to be taken merely as a trend. It will be very interesting to investigate whether *samA* expression confers an advantage to *P. aeruginosa* in the cystic fibrosis lung mainly under anaerobic conditions, given the fact that the *samA*

knockout strain of *P. aeruginosa* has a very attenuated virulence in a murine lung infection model (Unpublished data from our collaborators at IRCCS Ospedale San Raffaele).

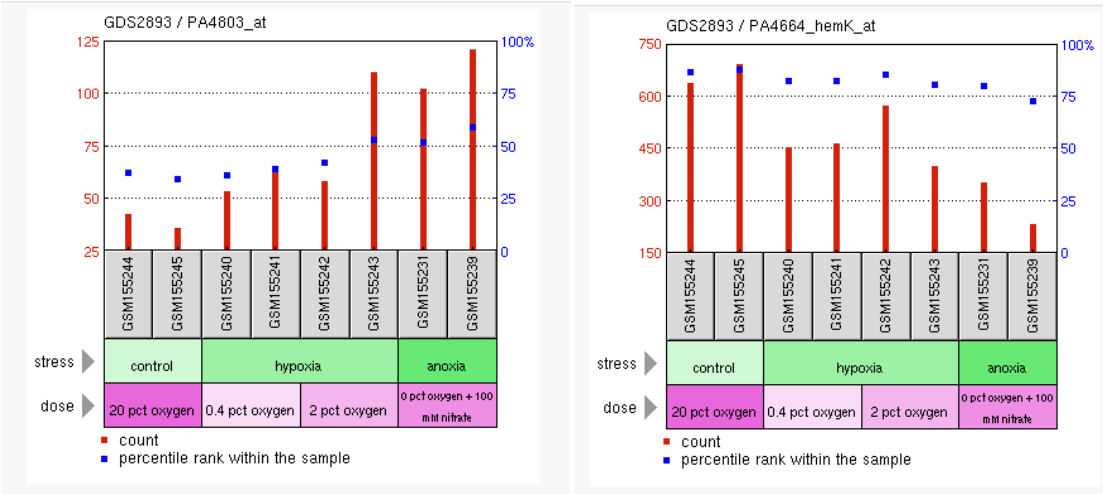


Figure 4.3. SamA (PA4803) and PrmC (PA4664) gene expression profiles under oxygen limitation conditions. Data extracted from GEO data base through http://www.pseudomonas.com/ (Winsor *et al.*, 2016).

4.1.5 Aims of the study

This research reported in this chapter aimed to study the structure and activity of SamA from *P. aeruginosa*. More specifically, this study is comprised of three main objectives:

- To analyse the SamA protein sequence bioinformatically.
- To assess the catalytic activity of SamA in *P. aeruginosa* and identify potential chaperone proteins.
- To elucidate the 3D structure of SamA to verify its predicted function.

4.2 Results

4.2.1 *In silico* characterization of *P. aeruginosa* SamA protein

The ultimate target of this part of the project was to determine the crystal structure of SamA to enable a more in-depth characterisation of this protein. To gain some initial information on the predicted structure of this protein both the primary aa sequence and the predicted secondary structure of the

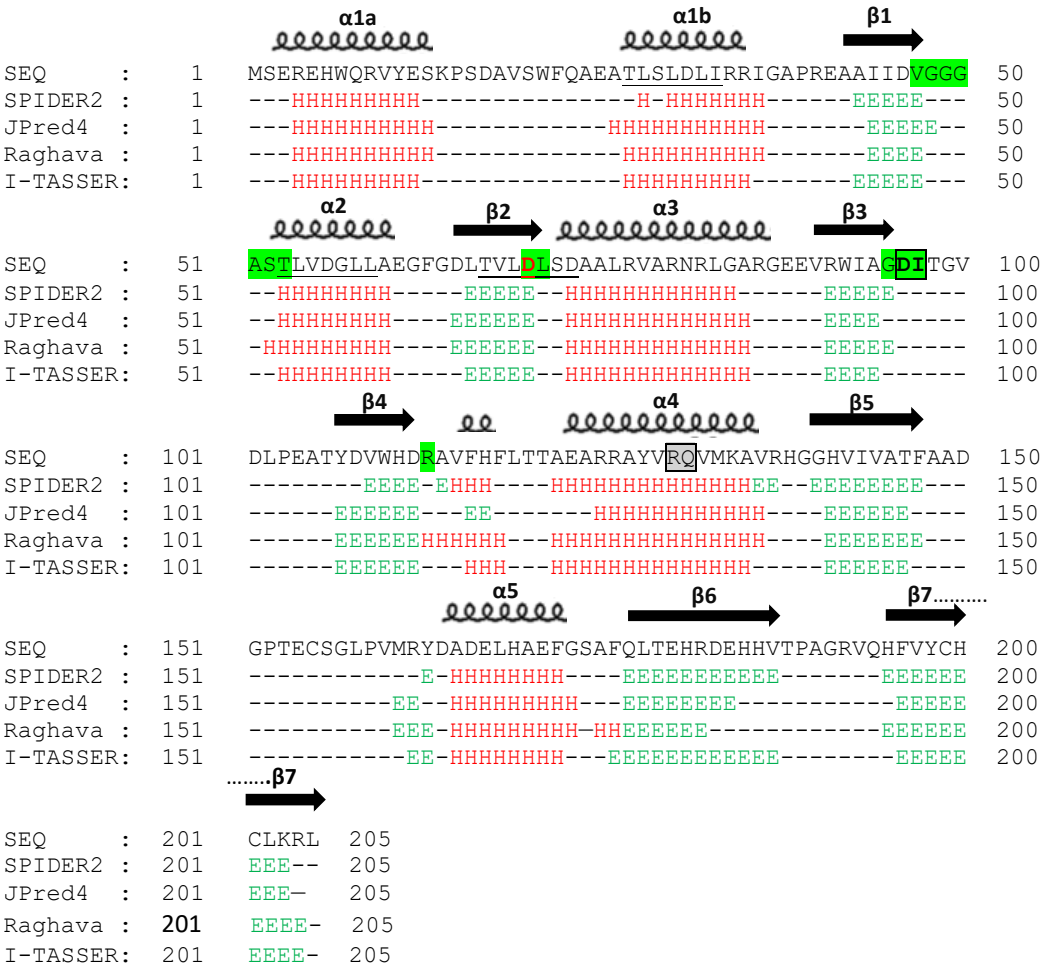


Figure 4.4. A graphical output of the predicted secondary structure of the SamA protein.
The SamA protein sequence [GenBank: AAG08189.1] follows the "SEQ" in the first row of each block. The prediction tools used (SPIDER2 (Yang *et al.*, 2017b), JPred4(Drozdetskiy *et al.*, 2015), Raghava(Raghava, 2002), I-TASSER(Zhang, 2008; Yang *et al.*, 2015; Roy *et al.*, 2011)) are shown on the left side. Red font H letter indicates that the above residue involved in α-Helices formation. Green font E letter indicates that the above residue is involved in β-strands formation. Coils are depicted with black dashes. A helix schematic or a solid black arrow, respectively above the sequence, indicates the number and extent of each helix (H) or strand (E). Green shading indicates conserved residues or motifs conserved within the SAM-dependent MTase family (as in NCBI CDD database) (Kozbial and Mushegian, 2005). Red font with green shading indicates conservation of an acidic residue (D) in Class I SAM-dependent-MTases positioned at the end of β2. Green shading in a red box indicates motif I GxG in Class I SAM-dependent-MTases which, marks the end of the first beta-sheet. Green shading in black box indicates Motif III (DI). Grey shading in black box indicates motif IX (RQ). Underlined residues indicate target recognition domains (TRDs). ScanProsite (de Castro *et al.*, 2006) identified the three patterns discussed above in the SamA sequence after manual entry.

SamA protein were analysed in detail. A number of conserved residues and motifs linked to the enzymatic activity of SAM-dependent MTases were identified in the protein sequence. The predicted secondary structure for SamA largely overlapped between the four prediction tools used (**Figure 4.4, Figure 4.5**). SamA appears to have six predicted helical structures (H) and seven beta-sheet structures (E) in the following order (-H1-H2-E1-H3-E2-H4-E3-E4-H5-E5-H6-E6-E7-) or (N – α1a – α1b- β1 – α2- β2- α3- β3 - β4 – α5 -β5 – α6 - β6 - β7 – C). The first β strand (β1/E1) ends with the GxG motif and the β2/E2 with a conserved acidic residue (**Figure 4.4, Figure 4.5**).

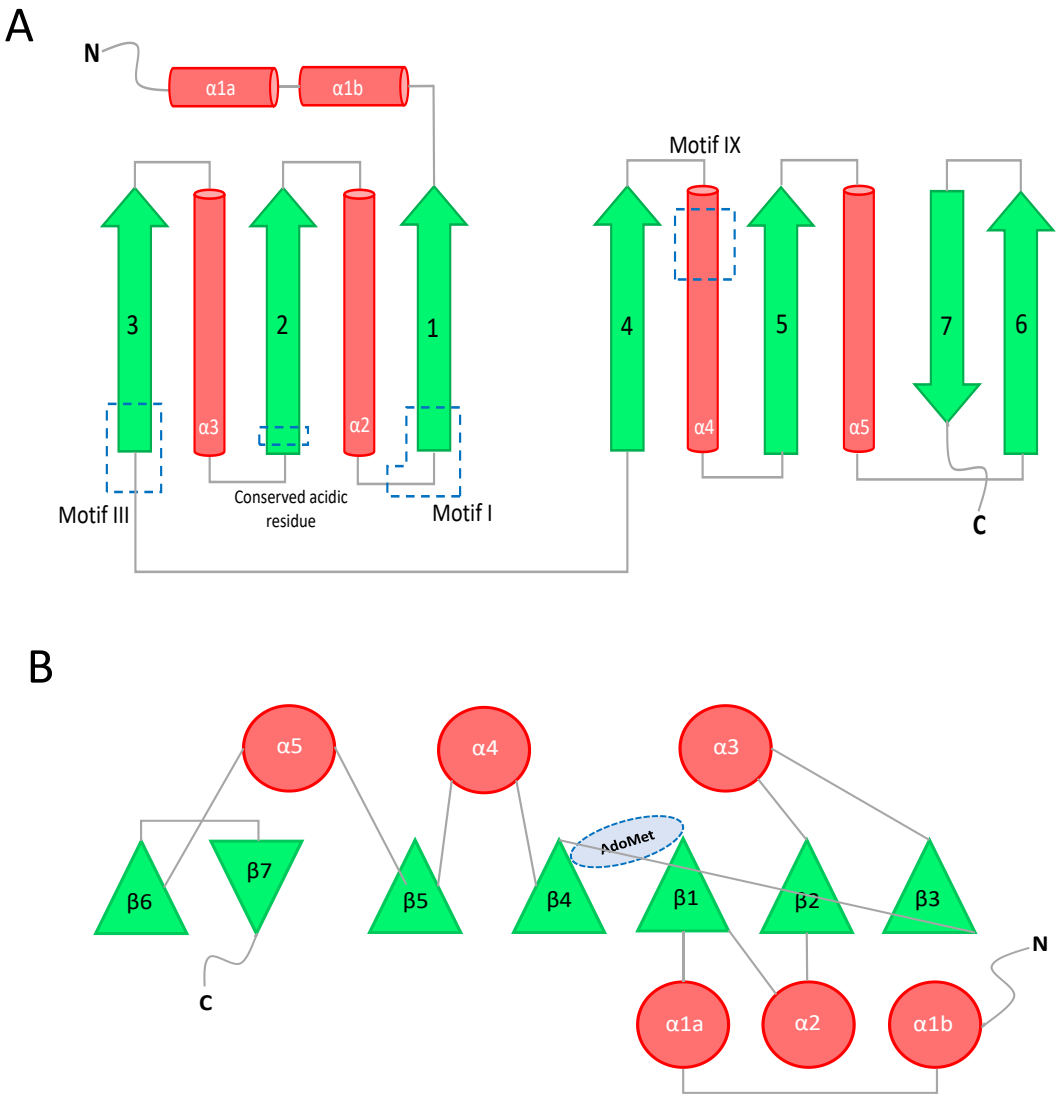
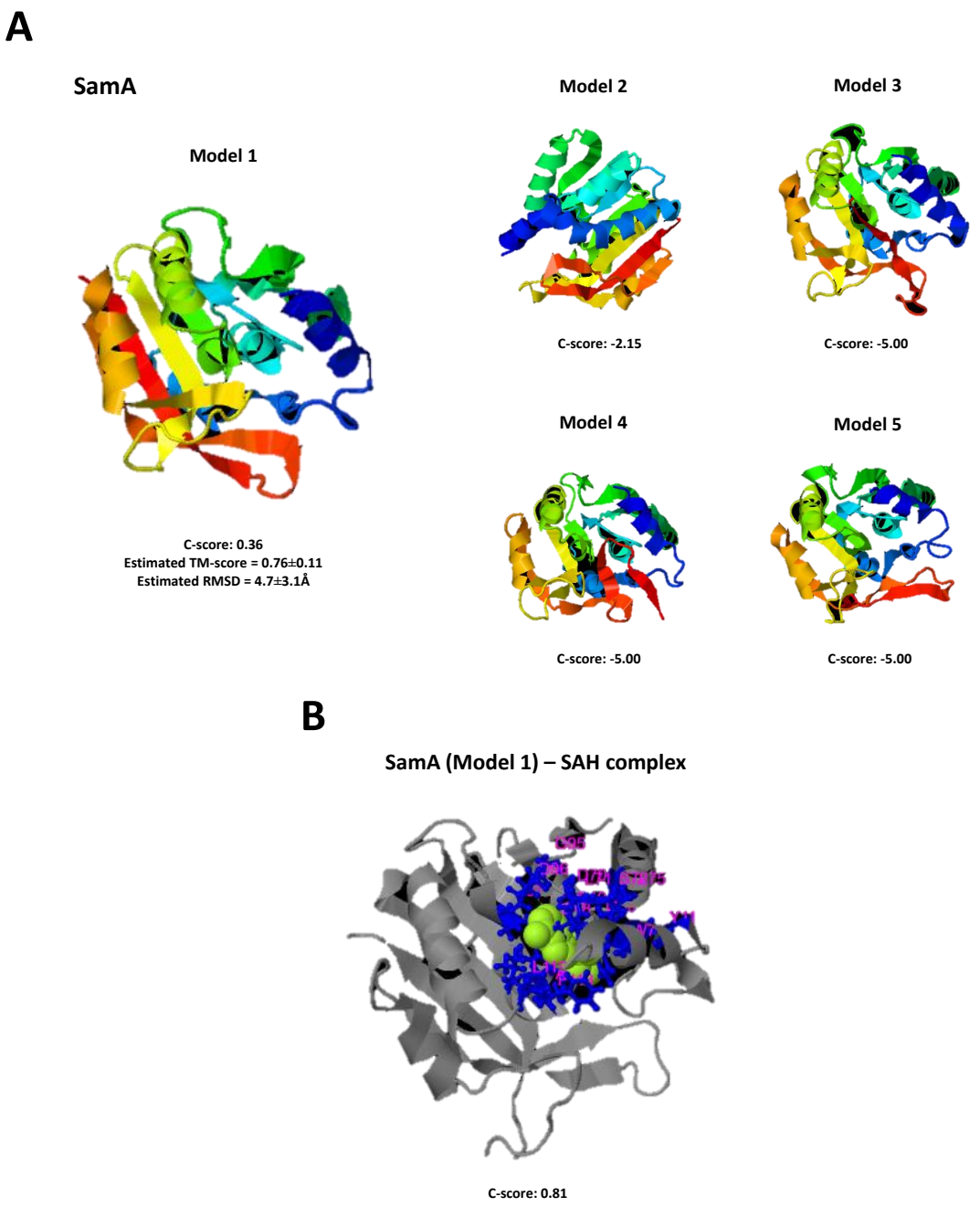


Figure 4.5. Schematic representation of the putative topology of SamA protein following the Class I methyltransferases fold.
The α-helices are depicted as red cylinders and beta sheets as green arrows. The β-strands are numbered (1-7) in the N-to-C direction. Connectors are shown in gray. **A.** The conserved hallmark motifs 'I' 'III' and 'IX' as well as the conserved acidic residue are indicated by blue dashed line boxes. The first two a-helices are named α1a and α1b for facilitating numbering**. B.** α-helices are depicted as red circles and beta sheets as green triangles. Normal triangles indicate β-sheets in parallel orientation, the inversed triangle indicates the antiparallel strand. Connectors are shown in gray. The putative AdoMet binding site is shown as well. Both schematic representations were created using Microsoft Powerpoint following the topology guidelines from Schubert *et al* (Schubert *et al.*, 2003a).

The Three-dimensional (3D) protein structure predictions for SamA were generated by the I-TASSER 3D protein structure prediction tool and are seen in **Figure 4.6.** The confidence of each model is quantitatively measured by C-score. C-score is typically in the range of [-5, 2], a C-score of higher value means a model with a higher confidence and vice-versa. C-score is calculated based on the significance of threading template alignments and the convergence parameters of the structure assembly simulations (Zhang, 2008; Yang *et al.*, 2015; Roy *et al.*, 2011). I-TASSER analysis offers probable ligands for the SamA protein (Model 1) which has the highest confidence (**Figure 4.6)**. Interestingly, SAH is one of those ligands with c-score of 0.81 and mentions that the ligand binding site residues are W7, Y11, G48, G49, G50, D70, L71, S72, D75, G95, D96, I97, R113, A114, V115, F118 and L119. The same analysis suggests that the binding pocket that binds SAH has the capacity to also bind SAM.




```
MSEREHWQRVYESKPSDAVSWFQAEATLSLDLIRRIGAPREAAIIDVGGGASTLVDGLLA   60
EGFGDLTVLDLSDAALRVARNRLGARGEEVRWIAGDITGVDLPEATYDVWHDRAVFHFLT   120
TAEARRAYVRQVMKAVRHGGHVIVATFAADGPTECSGLPVMRYDADELHAEFGSAFQLTE   180
HRDEHHVTPAGRVQHFVYCHCLKRL                                       205
```

Figure 4.6. **SamA predicted 3D protein structures as determined by the iterative threading assembly refinement.** **A.**The topologies are coloured in rainbow with the N-terminus denoted by blue and the C-terminus denoted by red. The secondary structures, α-Helices and β-Strands are represented as arrows and ribbons, respectively. C-score represents the confidence score for estimating the model quality. TM-score represents a scale for measuring the structural similarity between two structures. Root mean square deviation (RMSD) represents a quantitative measure of the distances between atoms. **B.** Shows the SamA protein Model 1 I-TASSER prediction in a complex with SAH. The SamA protein sequence coloured in rainbow with the N-terminus denoted by blue and the C-terminus is denoted by red is given as presented by SWISS-MODEL (Bienert *et al.*, 2017; Waterhouse *et al.*, 2018; Studer *et al.*, 2020; Bertoni *et al.*, 2017; Guex *et al.*, 2009).

4.2.2 PA4803 expression, protein purification and crystallization

4.2.2.1 PA4803 production and protein purification

Production of a C-terminal His-tagged SamA was tested first using the provided pSK67-SamA construct with C-terminal His-tag (This construct was kindly provided from Dr J. Dubern). Several incubation temperatures (22°C, 30°C and 37°C), times (4h and 24h) and media (Terrific Broth (TB) and Luria Broth (LB)) were tested in order to identify the optimal expression conditions in the presence and absence of IPTG (**Figure 4.7, A**). Protein production was similar at 30 °C and 37 °C but lower at 22°C as shown in the Western Blot (**Figure 4.7, B**). In addition, the production was similar after 4 h and 24 h incubation with IPTG at any given temperature (**Figure 4.7, A**). For the first trials both TB and LB media were used and protein production was only slightly higher when TB was used compared to LB. Fractionation of the cell pellet using a Nickel (Ni) purification column revealed that the SamA His-tagged product generated from this plasmid was Insoluble (**Figure 4.7, B**) restricting any further processing.

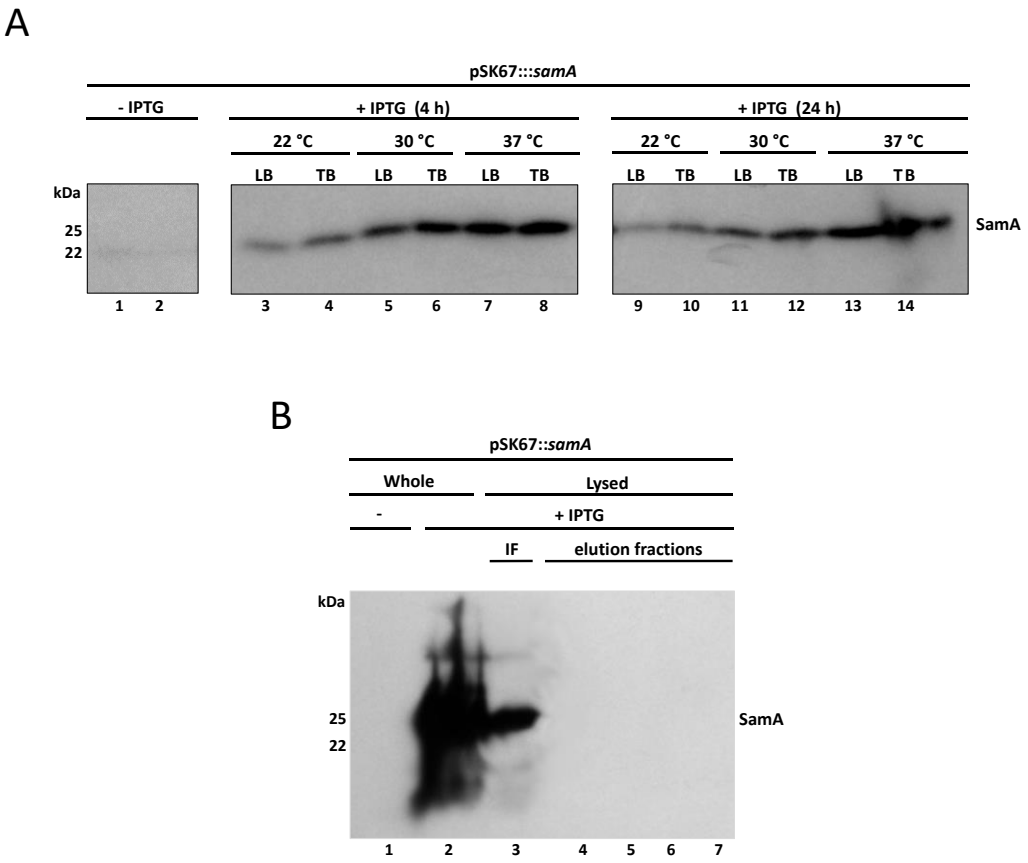


Figure 4.7. Western blot analysis of the SamA C-terminal His-tagged protein overexpressed using the pSK67 expression vector.

Whole cells extracts of *E. coli* harbouring the expression vector pSK67 are shown above uninduced (-) IPTG or induced by addition of 1mM IPTG (+) IPTG. A Pre-stained broad range molecular weight marker (NEB) was used, the sizes are given in kDa on the left. **A.** shows protein overexpression in LB media (lanes 3,5,7,9,11,13) and TB media (lanes 4,6,8,10,12,14) at three different temperatures (22°C, 30 °C and 37 °C). Samples were collected after 4 h and 24 h from the IPTG addition. **B.** shows solubility of the generated product. IF; Insoluble fraction (lane 3), elution fractions: of Nickel (Ni) purification obtained after gradient elution with imidazole (Lanes 4-7).

To bypass the solubility issue, three other constructs expressing *samA* were made: (i) pIC13 a pCOLD1 construct which, generates a SamA product with an extended N-terminal His-tag including an HRV 3C precision protease cleavage site; (ii) pIC14 a pMALX(E) construct which generates a SamA product with an N-terminal Maltose Binding protein (MBP) fusion and a C-terminal His-tag; and (iii) pIC15 another pMALX(E) construct which, generates the same SamA product described above but including an HRV 3C precision protease cleavage site after the MBP fusion partner. All constructs are shown schematically in **Figure 4.8**.

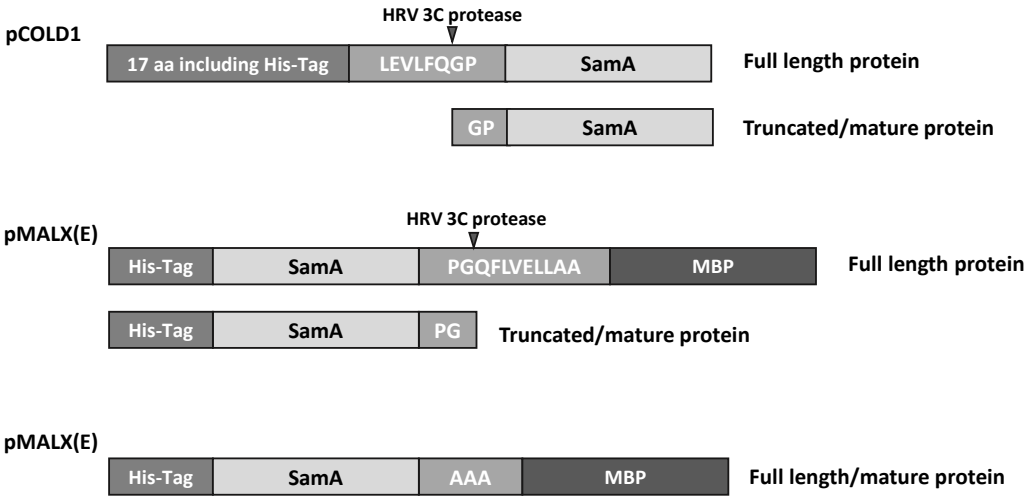


Figure 4.8. Schematic of the recombinant fusion constructs Histag-SamA-(MBP) products.
The top panel shows a SamA with cleavable N-terminus His-tag derived from pCOLD1 expression using pIC13. The middle panel shows a Histag-SamA-MBP recombinant protein, with cleavable MBP fused into the N-terminus of the target protein and a non-cleavable His-tag fused into the C-terminus derived from pIC15 (pMALX(E) expression vector). The lower panel shows a Histag-SamA-MBP recombinant protein, with cleavable MBP fused into the N-terminus of the target protein and a non-cleavable His-tag fused into the C-terminus of SamA derived from pIC14 (pMALX(E) expression vector). In the last two versions MBP (40.1 kDa) is genetically linked through a linker to the His-tagged SamA (23.7kDa). The sequences at the junction are highlighted and in the first two protein versions contain the HRV 3C-protease cleavage site. As mentioned, pCOLD1 and one of pMALX(E) constructed vectors bear an HRV 3C protease cleavage site which adds two artificial residues (PG or GP) on the N-terminus or the C-terminus of SamA, respectively.

Production and solubility of SamA from pIC14 (pMALX(E)::*samA*) was assessed by Western blot showing different band sizes for this His-tagged protein (**Figure 4.9**), with the more intense band just above 58 kDa. However, the SamA (22.7 kDa) with the MBP fusion (40.1 kDa) expressed from pIC14 was expected to run at approximately 63 kDa. In any case, the target protein was observed in the soluble fraction for the first time (**Figure 4.9**).

To verify the identity of the produced protein the lysate from 150 mL of *E. coli* BL21 pMALX(E) culture was purified in two steps, first using a Dextrin Purification column for its binding through MBP domain followed by Nickel affinity purification to select for the His-tag using the appropriate column. In every

step, the collected peak fractions were analysed (data not shown). The fusion protein was purified from the soluble fraction, showing a relatively high level of purity (data not shown), and was subjected to further purification.

The production and solubility of SamA obtained from pIC15 (pMALX(E)::*samA*) was assessed in the same manner as described for pIC14 above.

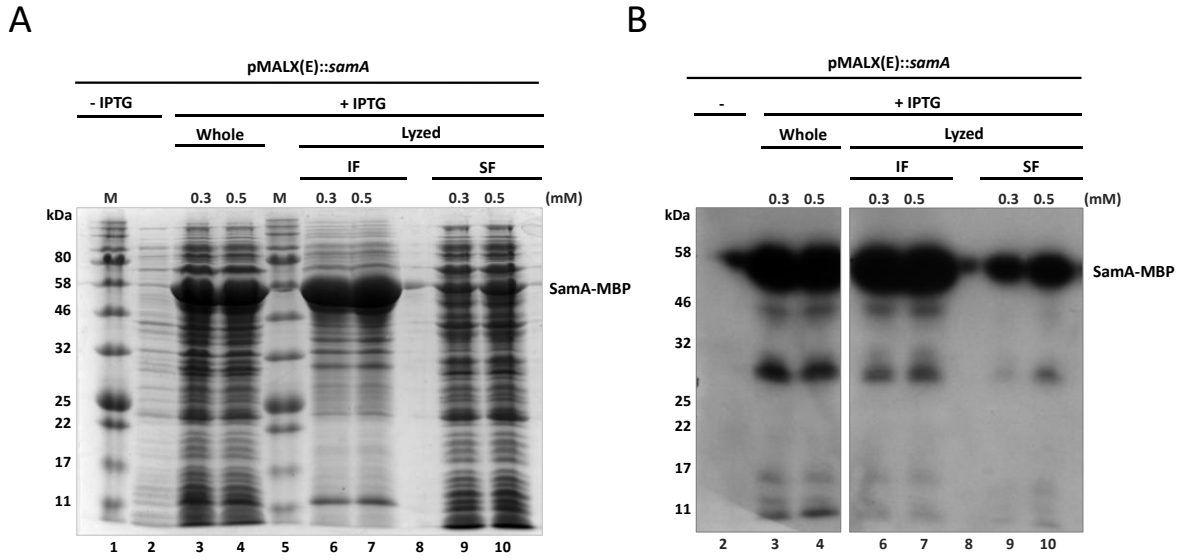


Figure 4.9. Expression analysis of the *samA*–MBP fusion C-terminal His-tagged protein overexpressed using the pMALX(E) vector.
Whole cells extracts of *E.coli* harbouring the expression vector pIC14 pMALX(E) are shown above uninduced - IPTG (lane 2) or induced by addition of 0.3 or 0.5 mM IPTG (+) (lanes 3,4,6,7,9,10). Lane M shows (top to bottom) the Pre-stained broad range molecular weight marker (NEB), the sizes are given in kDa on the left. **A**. shows protein overexpression and solubility using either 0.3 mM or 0.5 mM of IPTG in LB media after overnight incubation at 25°C by SDS-PAGE. **B.** shows the same samples analyzed by Western Blot. IF; Insoluble fraction (lanes 6,7), SF; soluble fraction (lanes 9,10).

4.2.2.2 Size exclusion chromatography

Size exclusion chromatography or Gel filtration (GF) using the concentrated protein obtained from the previous steps was performed for all SamA protein versions generated using each of the three constructs described above (**Figure 4.8**). Both SamA-MBP protein without and with the HRV 3C protease site were eluted in two peaks designated 1 and 2 in Figure 4.10. Peak 1) seems to be aggregated protein/High molecular weight species (HMWS) rather than void (particles too large to interact with the column) and the Peak 2 is the monomeric MBP-SamA fusion protein peak. Fraction samples analysis from each peak mainly showed an intense SamA-MBP band for both the cleavable and non-cleavable version (Figure **4.10, A**). Interestingly, a 40 kDa band which corresponds to the MBP

seems to appear in the monomeric peak fractions as well for the non-cleavable SamA-MBP (**Figure 4.11**).

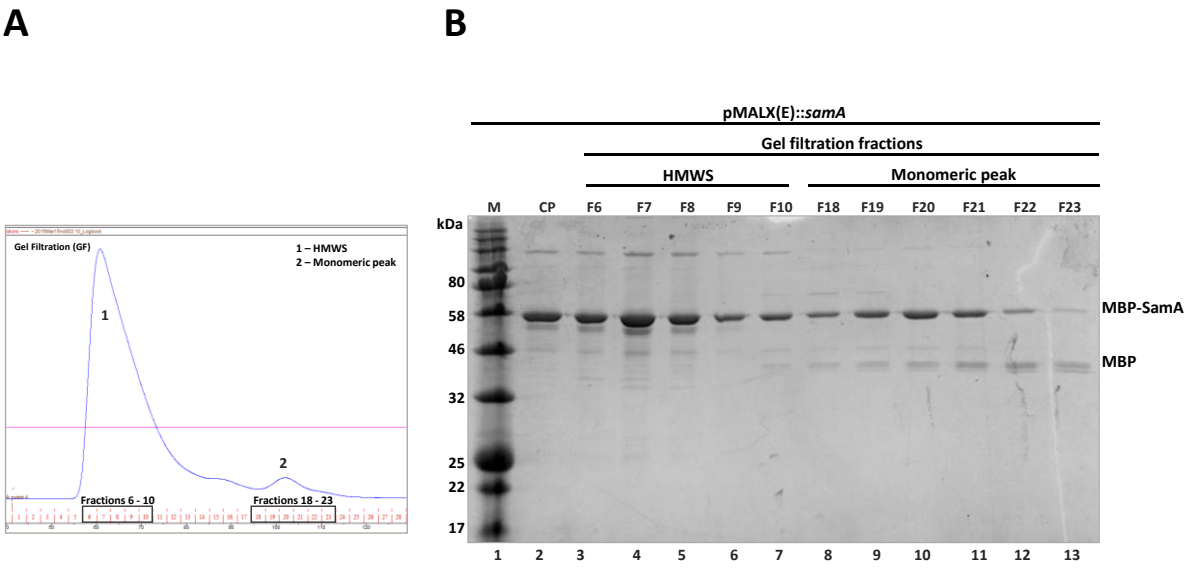


Figure 4.10. Gel filtration of the SamA-MBP fusion C-terminal His-tagged protein with no-cleavable tags overexpressed using the pIC14.
Dextrin and Nickel (Ni) purifications preceded, and all the elution fractions were pooled (lane 2 designated CP for Concentrated Protein) and were applied to the GF column. **A.**The chromatogram shows the His-tag-SamA-MBP Gel filtration profile. In each chromatogram, UV absorbance at 280 nm is plotted versus millilitres of buffer solution flow. **B**. shows analysis of the several peak corresponding fractions on an SDS-PAGE gel. Lane M shows (top to bottom) the Pre-stained broad range molecular weight marker (NEB), the sizes are given in kDa on the left (lane 1).

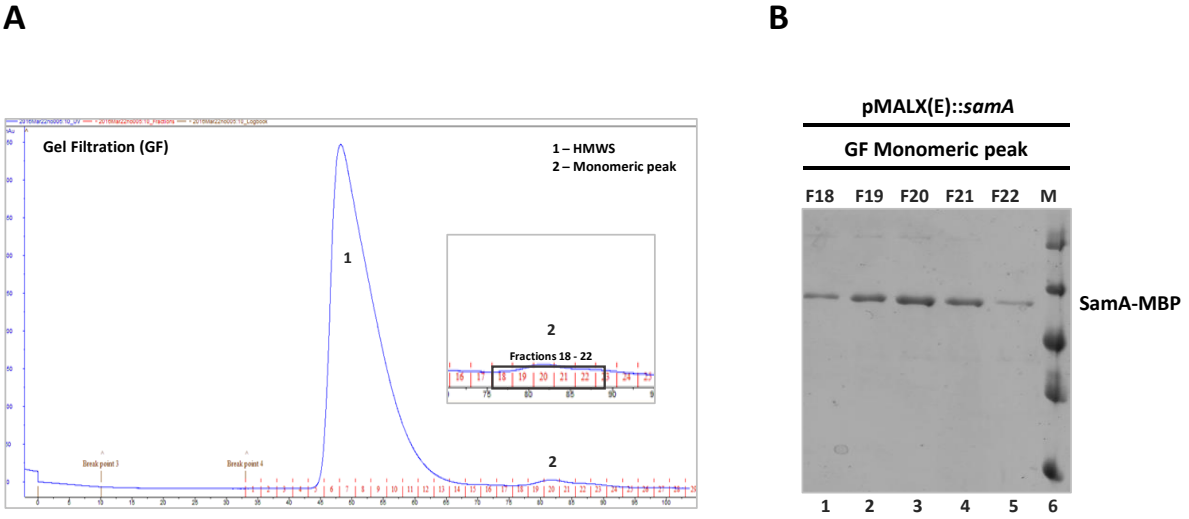


Figure 4.11. Gel filtration of the SamA-MBP fusion C-terminal His-tagged protein with cleavable MBP, overexpressed using the pIC15.
Dextrin and Nickel (Ni) purifications preceded and all the elution fractions from the Ni purification were applied to the GF column. **A.** The chromatogram shows the Histag-SamA-MBP (cleavable version) Gel filtration profile. In each chromatogram, UV absorbance at 280 nm is plotted versus millilitres of buffer solution flow. **B.** shows analysis of the several peak corresponding fractions on an SDS-PAGE gel. Lane M shows (top to bottom) the molecular weight marker.

In an attempt to remove the high molecular weight species (HMWS) and increase the purity of the monomer, further gel filtration using the Superdex 75 10/300 GL (GE Heatlhcare) column was performed with the addition of several reagents (SAH, EDTA, NaCl, MPD, Chaps, and cleaved SamA protein) (**Figure 4.12**). Limited proteolysis can sometimes be achieved using chymotrypsin, hence this approach was used to try reducing the size of the HMWS species. However, this approach did not visibly increase the levels of the monomer peak. The MBP product resulting from the digestion was visible, but the SamA cleaved product was not.

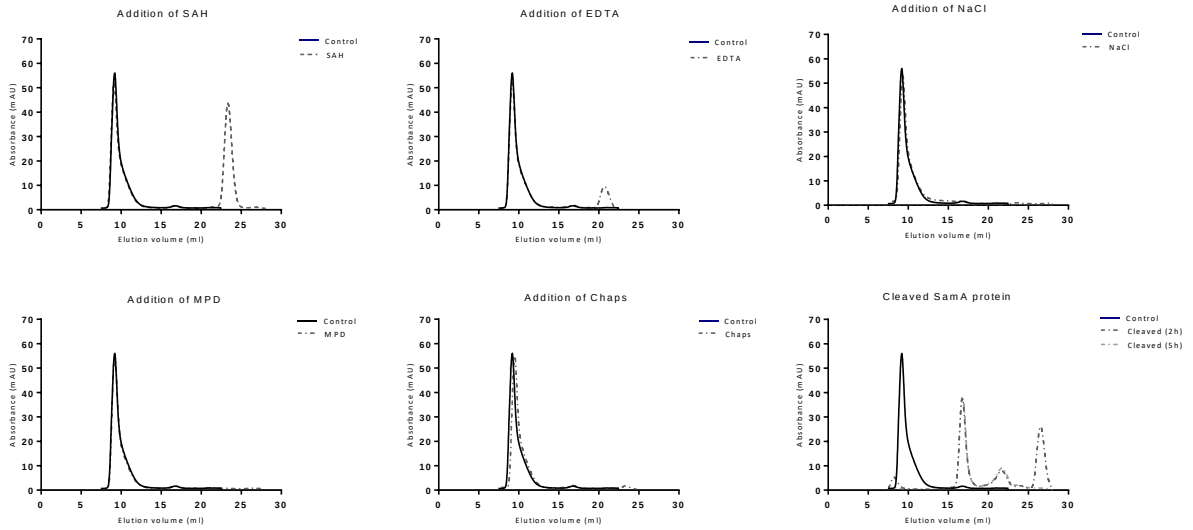


Figure 4.12. Additive Gel filtration of SamA-MBP fusion C-terminal His-tagged protein overexpressed using the pMALX(E). The chromatogram reveals the elution profile on Superdex 75 10/300 GL. Curve is plotted as absorption in milli-absorption units (mAU) at 280 nm versus volume in milliliters (ml). Each reagent used is indicated above the individual figures.

In an attempt to increase the monomer peak a larger scale purification of SamA from an *E. coli* BL21 from pIC15 (pMALX(E)-*samA*) culture was set up. Specifically, 1L instead of 150 mL of culture was used this time. Additionally, the culture was grown at 18 °C instead of 22 °C in an effort to minimize protein aggregation and aid protein folding. Unfortunately, gel filtration showed no increase in the monomer peak concentration (data not shown).

The C-terminal His-tagged SamA protein with cleavable MBP overproduced using the pIC15 plasmid was further processed as shown in **Figure 4.13; A**. The full-length protein was used in several crystallization screenings. This time cleavage of the MBP was attempted using the HRV 3C protease site. The cleaved protein was denatured and refolded which appeared to have worked successfully (**Figure 4.13; B and C**). However, an attempt to purify the cleaved SamA by Gel filtration failed to

collect a fraction with the SamA monomeric fraction as the protein precipitated overnight, further supporting an issue with SamA solubility.

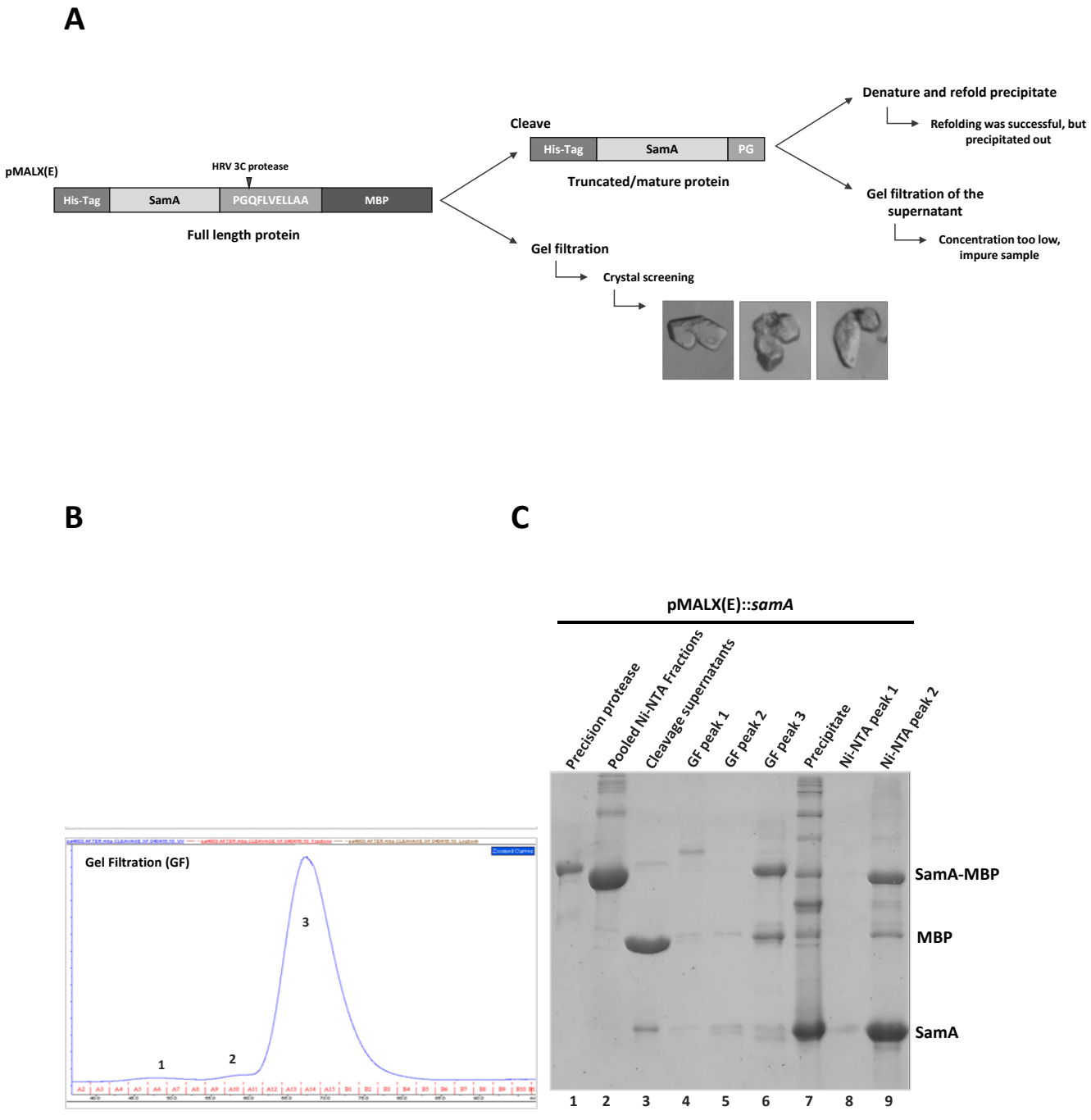


Figure 4.13. Summary of C-terminal His-tagged protein with cleavable MBP overexpressed using the pIC15 plasmid processing.
A.shows a Schematic explaining the different steps carried out with the C-terminal His-tagged SamA protein with cleavable MBP. The bottom left chromatogram reveals the cleaved and refolded Histag-SamA-(MBP) Gel filtration elution profile on Superdex 75 10/300 GL. In the chromatogram, UV absorbance at 280 nm is plotted versus milliliters of buffer solution flow. **C.** shows the SDS-PAGE analysis of the peaks corresponding to the fractions from the chromatogram (shown in **B**), as well as some control samples.

The 18°C overproduction of the C-terminal His-tagged Sam protein using the pIC13 (pCOLD1-*samA*) plasmid aided in producing a good quantity of soluble protein (**Figure 4.14**). The Gel filtration of the sample showed a monodisperse peak at the monomeric elution volume of the protein.

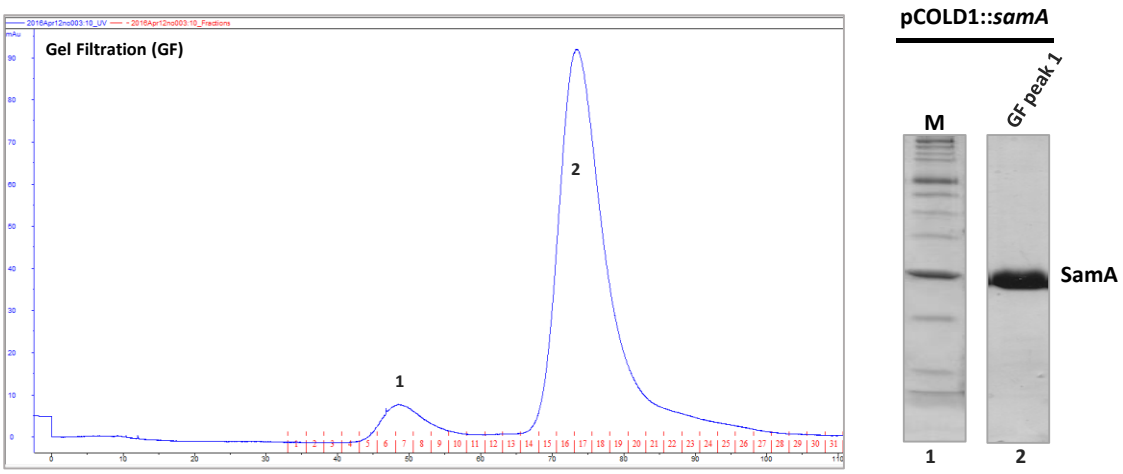


Figure 4.14. Gel filtration of the Histag-SamA overproduced using the pIC13 (pCOLD1*::samA*) plasmid.
The chromatogram on the left reveals the elution profile on Superdex 75 10/300 GL. Curve is plotted as absorption in milli-absorption units (mAU) at 280 nm versus volume in milliliters (ml). The right panel shows analysis of a peak corresponding fraction of the chromatograms on an SDS-PAGE. Lane M shows molecular weight marker.

4.2.2.3 Crystallization trials

The monomeric SamA protein recovered after Gel filtration that was obtained from either pIC13 (pCOLD1) or pIC14 and pIC15 (pMALX(E)) plasmids was concentrated and used for several crystallization screens (**Table 4.1**). S-Adenosyl-L-homocysteine (SAH), which is an amino acid derivative formed by the demethylation of SAM, was used in some cases. SAH could aid the formation of crystals. In some cases, cleavage attempts of SamA portion from the MBP fusion partner or the extended His-tag using the HRV 3C protease resulted in SamA protein precipitation which, did not permit further processing.

Some crystals appeared in a crystallisation screen (0.2M KF, 40% MPD) (**Figure 4.13, Table 4.1**). However, they did not diffract, and optimization of the conditions did not result in the formation of more crystals. Diffractable protein crystals were not identified in any of the crystallization screens performed yet.

Table 4.1 Summary of Crystallization screen conditions set up during this study.

Protein	Screen	Volumes	Temperature (°C)	Screen Results

MBP-SamA (monomeric peak) Concentration (~3 mg/ml)	Compass	4 µl + 4 µl with SAH	20	X
	Index	4 µl + 4 µl with SAH	20	X
	Classics	4 µl + 4 µl with SAH	20	X
	PEGSII	6 µl + 3 µl	20	X
	Classics	6 µl + 3 µl	20	X
	Index	6 µl + 3 µl	20	X
	SG1	6 µl + 3 µl	20	X
	Ammonium sulphate	4 µl + 2 µl	20	X
	MPD	4 µl + 2 µl	20	X
	PEGSII	4 µl + 2 µl	20	X
	Morpheus	4 µl + 2 µl	20	X
	Ammonium sulphate	4 µl + 2 µl with SAH	20	X
	MPD	4 µl + 2 µl with SAH	20	X
	PEGSII	4 µl + 2 µl with SAH	20	X
	Morpheus	4 µl + 2 µl with SAH	20	X
	Proplex	4 µl + 2 µl	10	X
	PEGSII	4 µl + 2 µl	10	X
	Morpheus	4 µl + 2 µl	10	X
	MIDAS	4 µl + 2 µl	10	X
	MPD	4 µl + 2 µl	10	X
	Morpheus	6 µl + 3 µl with SAH	10	X
	Ammonium sulphate	6 µl + 3 µl with SAH	10	X
	PEGSII	6 µl + 3 µl with SAH	10	X
MBP-SamA (HMWS peak)	Classics	6 µl + 3 µl	20	X
	SG1	6 µl + 3 µl	20	X
	PEGSII	6 µl + 3 µl	20	X
	Index	6 µl + 3 µl	20	X

MBP-HRV3C-SamA	Proplex	4 µl + 2 µl	10	✗
	MPD	4 µl + 2 µl	10	✗
	Morpheus	4 µl + 2 µl	10	✗
pCOLD SamA	PACT	4 µl + 2 µl	20	✗
	JCSG+	4 µl + 2 µl	20	✗
	Morpheus	4 µl + 2 µl	20	✗
	PEGSII	3 µl +1.5 µl	20	✗
	Classics	3 µl +1.5 µl	20	✗
	Index	3 µl +1.5 µl	20	✗
	Compass	3 µl +1.5 µl	20	✗
	SG1	6 µl + 3 µl	20	✗
	MIDAS	6 µl + 3 µl	20	✗
	Ammonium sulphate	6 µl + 3 µl	20	✗
	Wizard Cryo	6 µl + 3 µl	20	✗
	SG1	8 µl +4 µl	20	✗
	MPD	4+2	10	✗
	PEGSII	4+2	10	✗
	Index	4+2	10	✗
	Morpheus	4+2	10	✗
	Morpheus	4+2	10	✗
	Classics	4+2	10	✗
	PGA	4+2	10	✗
	Structure 1+2	4+2	10	✗
	MPD	4+2	10	✗
		Total	**51**	

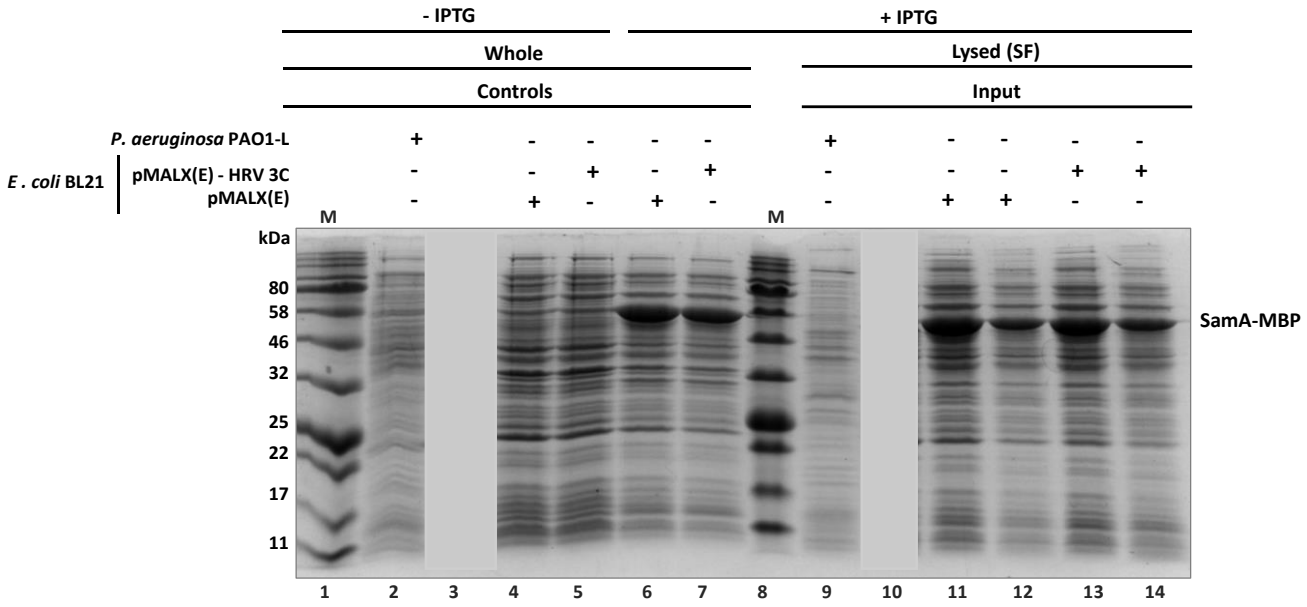
✓ Formation of a new crystalline phase; ✗ No crystalline phase.

4.2.2.4 Pull down assays

As previously mentioned, SamA protein solubility has been an issue. Therefore, the possibility that SamA has a binding partner that stabilizes it and assists with solubility was considered. In an effort to identify possible SamA binding partners pull down assays were performed.

During the first trial (pilot experiment), each of the *E. coli* expression lysates from the three plasmids used pIC13, pIC14 and pIC15 were individually mixed with PAO1-L wt lysates and incubated for 2 h (**Figure 4.15**). Samples of each individual lysate before (**Figure 4.15, A**) and after incubation, and after elution (**Figure 4.15, B**) were collected and analyzed by SDS-PAGE. A very faint SamA band appeared in the eluates although no other bands representing a possible binding partner appeared. During the second trial the process was changed *E.coli* lysates were first applied to the beads for some time and washed away. Then the PAO1-L wt lysate was added to the beads for 2 h. SDS-PAGE analysis showed too many faint bands of non-specific proteins. However, no SamA band was visible (**Figure 4.15, C**).

A



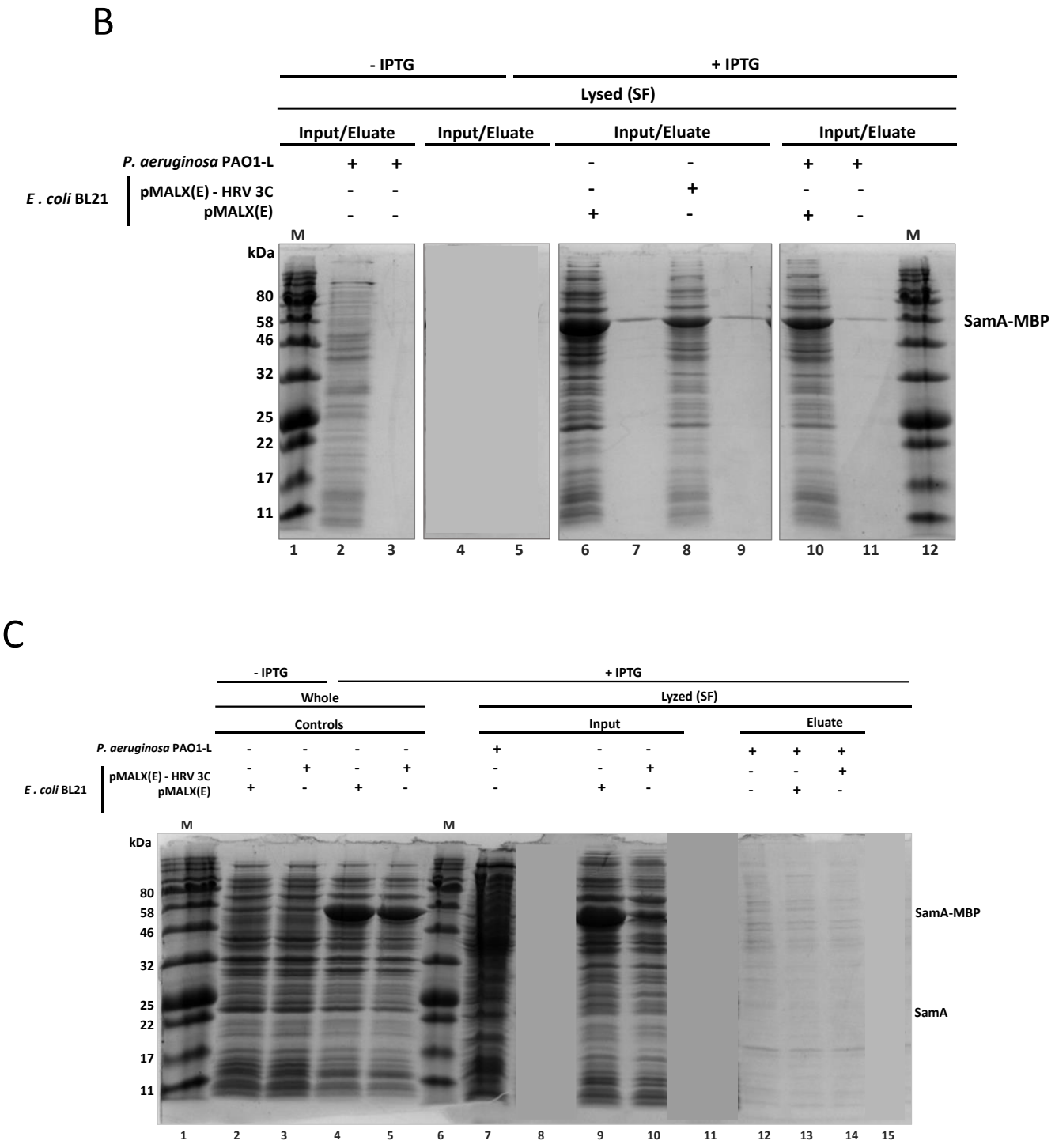


Figure 4.15. Pull down assays using SamA fusion His-tagged protein (with and without linker region) overproduced using the pMALX(E) vectors.

E.coli whole cell extracts induced by addition of 0.3 mM IPTG (+) harbouring the expression vector are shown above in LB media after overnight incubation at 22°C by SDS-PAGE/Staining. Lane M shows (top to bottom) the Pre-stained broad range molecular weight marker (NEB), the sizes are given in kDa on the left. The +/- symbols show which organisms and with which vector is present in the sample. **A.** shows expression and purification analysis after mixing the *E.coli* expression lysates and the *P. aeruginosa* lysates together and adding it to the Nickel beads. **B.** shows protein elution profiles in comparison to the samples of mixed *E.coli* and PA lysates. **C.** shows expression, purification and elution profile analysis after adding the *E.coli* expression lysates to the beads separately from the PA lysate. SF; soluble fraction.

4.3 Discussion

SamA has six predicted helical (H) and seven beta-sheet (E) structures and, according to the bioinformatics analysis (**Figure 4.4**), SamA appears to possess a distinctive Class I MTase structures (Schubert *et al.*, 2003a). The first β strand in Class I MTases typically ends in a GxGxG or GxG motif, which is a nucleotide-binding site, bending underneath SAM to initiate the first α helix (H1). Moreover, a conserved acidic residue is positioned at the end of β2/E2, which forms hydrogen bonds to both hydroxyls of the SAM ribose. Overall, the data supports that SamA possesses MTase characteristics such as the structure and the possible binding capacity of SAM (**Figure 4.6**) and that it could be an active MTase.

4.3.1 PA4803 production, purification and crystallization

Determination of the 3D structure of a protein is a multi-stage process, which requires gathering of a few milligrams of highly purified and soluble protein, which can result in quality crystals which can diffract (Moon *et al.*, 2010). Success in the crystallization of the purified protein is often the main obstacle for structure determination by X-ray crystallography (Chayen and Saridakis, 2008).

The C-terminal His-tagged SamA produced from the provided pSK67-PA4803 (PSK67-SamA) construct was found in the insoluble fraction in any given incubation temperature, time and media tested (**Figure 4.7**). This restricted any further processing. It is quite common that overproduction of many recombinant proteins in *E. coli* leads to the formation of highly aggregated protein referred to as inclusion bodies (Palmer and Wingfield, 2012). In this study, more effort was put into generating soluble protein mainly by modifying existing expression plasmids or using alternative expression vectors instead of solubilizing the inclusion bodies of the recombinant protein and then re-folding it (Esposito and Chatterjee, 2006).

Hence, *samA* was overexpressed using three other constructs, pCOLD1 (pIC13) and pMALX(E) (pIC14 pIC15), and the resulting protein state (soluble/insoluble) was assessed (**Figure 4.8**). The pMALX (E) plasmid which overproduces the SamA as a fusion with the MBP protein was employed. This was done because the MBP fusion partner, especially if it is positioned in the N-terminal, has been shown to increase protein solubility and aid folding by having a chaperone like effect (Moon *et al.*, 2010).

Expression of *samA* pMALX(E) as a SamA-MBP fusion with a C-terminal His-tag without the HRV 3C protease cleavage site resulted in a protein of 58 kDa (**Figure 4.9**) instead of the expected 63kDa. A possible explanation is that a small part of the protein may be missing due to the action of proteases released at the sonication step. In addition, the faint bands appearing on the SDS-PAGE analysis could

be fragments of the target protein caused by the released proteases in addition to some other contaminants. In any case, it was verified that the resulting protein had both the MBP fusion partner and the His-tag. The aforementioned plasmids constructed increased the solubility of SamA and enable to proceed to the next stages of purification.

The size exclusion chromatography or gel filtration performed revealed two peaks (**Figure 4.10**) one of which was a high molecular weight species (HMWS) and the other a monomeric MBP-PA4803 fusion (MBP-SamA) protein peak. Unfortunately, larger scale purification of *E. coli* BL21 pMALX(E) culture grown at lower temperature did not minimize protein aggregation. In addition, although chymotrypsin was able to reduce the size of the HMWS species, it did not visibly increase the SamA monomer peak (**Figure 4.11**). The MBP product of the cleavage was visible as a peak and on the gel in the corresponding fraction analysed. It may be that the SamA cleavage product was not visible because it was digested into smaller peptides, suggesting that it may not be folding properly making it more vulnerable to protease digestion.

Importantly, a single Nickel purification was shown to improve the HMWS peaks in gel filtration and it resulted in a bigger monomeric peak. Therefore, aggregation might be protein concentration dependent (**Figure 4.13**). As expected a fusion partner can be both advantageous and disadvantageous (Moon *et al.*, 2010). In this case, MBP increased the solubility and yield of the SamA protein. However according to the gel filtration results at least big part of the SamA-MBP population was not folding properly probably due to the bigger size and stability of the MBP fusion partner.

Another issue often faced by crystallographers is the production of non-diffractive quality crystals. A rescue approach is the use of the surface entropy reduction (SER) technique (Cooper *et al.*, 2007). This technique involves reduction of surface entropy, which drives protein crystallization, by mutating patches of surface-exposed large charged residues to small non-polar amino acids allowing crystal formation. Therefore, the pMALX(E) vector which retains the mutations D82A/K83A/E172A/N173A/K239A on the encoded MBP, instead of the target protein, is specifically designed to reduce surface entropy and aid crystals formation, and hence was used for SamA protein expression. Carrier driven crystallization was used previously to successfully solve the structures of three proteins when every other rescue strategies were failing (Moon *et al.*, 2010). As SamA was showing signs of a difficult protein for crystallisation, the MBP/SER system was employed. Cold production of SamA protein through the pCOLD1 vector was also employed but without much success as the SamA protein precipitated (**Figure 4.14**).

Another technique used to aid crystallization during crystal trials is additive screening (Moon *et al.*, 2010). In the present case, *S*-Adenosyl-L-homocysteine (SAH) was used as an additive based on the SAM-dependent methyltransferase characteristic conserved residues of the SamA protein. In theory, SAH could somehow stabilize the protein allowing crystalline formation. Use of SAM has been described before by Yang *et al* where they managed to get diffractable crystals and determine the 3D structure of the NSR protein in a complex with SAM (Yang *et al.*, 2010). However, no attempts were made so far to obtain a SAM-SamA complexes since a it was suggested that SAM turnover to SAH is rapid and it may not allow these complexes to form in a stable manner.

Taken together, there are numerous parameters which can affect protein crystallization, such as the nature of the protein, the possibilities of protein-protein interactions, the type of crystals obtained etc. Thus, all these need to be taken into consideration as it can generally take a significant amount of time to generate pure homogenous protein to enable several crystallization trials in a short time (Gorrec, 2013)

4.3.2 Pull down assays

Since SamA itself was not soluble it would mean that when it is produced in *P. aeruginosa*, its gene is either expressed in a smaller scale which favours solubility or it is stabilized by binding partners. Identifying a binding partner would be useful since crystallization of the target protein in complex with its endogenous binding partners could result in diffracting crystals. Simple pull down assays were performed in order to identify probable binding partners from *P. aeruginosa* by mixing lysates from *E. coli* overexpressing *samA* with lysates from *P. aeruginosa* (**Figure 4.15**). However, these simple experiments failed to identify any binding partners. It seemed as if SamA was not binding to the beads at all or binding very poorly, which makes it highly unlikely for a partner to bind and be visible on a gel. Further optimizations of the protocol are required to increase SamA protein binding and to increase the sensitivity. Regarding this, one of the next steps would be to try and overproduce the SamA protein in its natural host in order to favour the interaction with endogenous binding partners (Truan *et al.*, 2013). An alternative technique to try could have been the far-western blot, which is used to detect protein-protein interaction *in vitro. In* far-western the blot is covered by non-antibody proteins to probe the protein of interest on the blot. Thus, binding partners of the protein of interest (which is His-taged) may be identified (Machida and Mayer, 2009).

4.3.3 Conclusion and Future directions

Despite the successful purification of low levels of SamA, due to time constraints, the 3D Crystal structure of this protein could not be established due to the lack of diffracting crystals. This will require further work as new tools and technologies become available especially when dealing with a highly insoluble protein. Provisions were made during this study to assess the Methyltransferase activity of SamA protein directly. However, there was never enough quantity of SamA protein to carry out this part of the project and this possibility was worsened by the need to use radioactivity. Hence, this part of the work was abandoned to explore other avenues that could reveal the activity of SamA indirectly.

Chapter 5 Possible link between the selenocysteine-tRNA in *P. aeruginosa* encoded by PA4802.1 and SamA

5.1 Introduction

5.1.1 The unique process of selenocysteine incorporation into selenoproteins

Selenium is an essential trace element for many organisms, is present in proteins in the form of selenocysteine (Sec). Selenocysteine is known as the 21st amino acid and its translational insertion into proteins is directed by the UGA codon, which typically functions as stop codon. This is intriguing since the general rule is that a specific codon cannot have two different read-out meanings in the same organism (Yoshizawa and Böck, 2009). The UGA codon is recognized by a complex molecular machinery, known as selenosome, which competes with the normal translation machinery of the cell (Zhang *et al.*, 2006). The key components of the Sec-decoding trait are encoded by: the *selA*, *selB*, *selC* and *selD* genes. Selenium can also be found as a co-factor in certain molybdenum-containing enzymes (Zhang *et al.*, 2006), but this use of selenium will not be discussed further in this chapter. In most species, the four genes *selABCD* are not all part of one locus, although *selA* and *selB* are neighbouring genes in almost all species (Wassenaar and Meinersmann, 2006).

Selenoproteins appear to be widely distributed in nature, but are not ubiquitous (Birringer *et al.*, 2002). Studies have shown that selenocysteine is catalytically superior to its steric isomer cysteine (Cys) (Zhang *et al.*, 2006). Bacterial selenoproteins are mostly involved in catabolic processes and catalyse redox reactions (Hatfield and Gladyshev, 2002). Interestingly, only a small number of selenoproteins or even a single one can be detected in many Sec-encoding/Sec-utilizing organisms. Genetic manipulations of the $tRNA^{Sec}$, in order to study the role of selenoproteins, were possible because only small subset of proteins require this $tRNA^{Sec}$ molecule for their production (Yoshizawa and Böck, 2009).

Formation of a quaternary complex between the SelB dedicated translation factor (that binds GTP), the selenocysteyl-tRNASec (encoded by the *selC* gene) and a structural element of the mRNA termed SECIS (selenocysteine insertion element) are required for this alternative decoding of UGA of the mRNA at the ribosome (Yoshizawa and Böck, 2009) as shown in **Figure 5.1**. Hence, the regulation of translation in this case involves two species of RNA. Namely, the mRNA selenocysteine insertion

sequence (SECIS element) and a unique selenocysteyl-tRNA (Low and Berry, 1996). A unique feature of SelB is that it can interact with both RNA molecules (Yoshizawa and Böck, 2009). The sequence of the interaction with the two RNA molecules is random but cooperative (Yoshizawa and Böck, 2009).

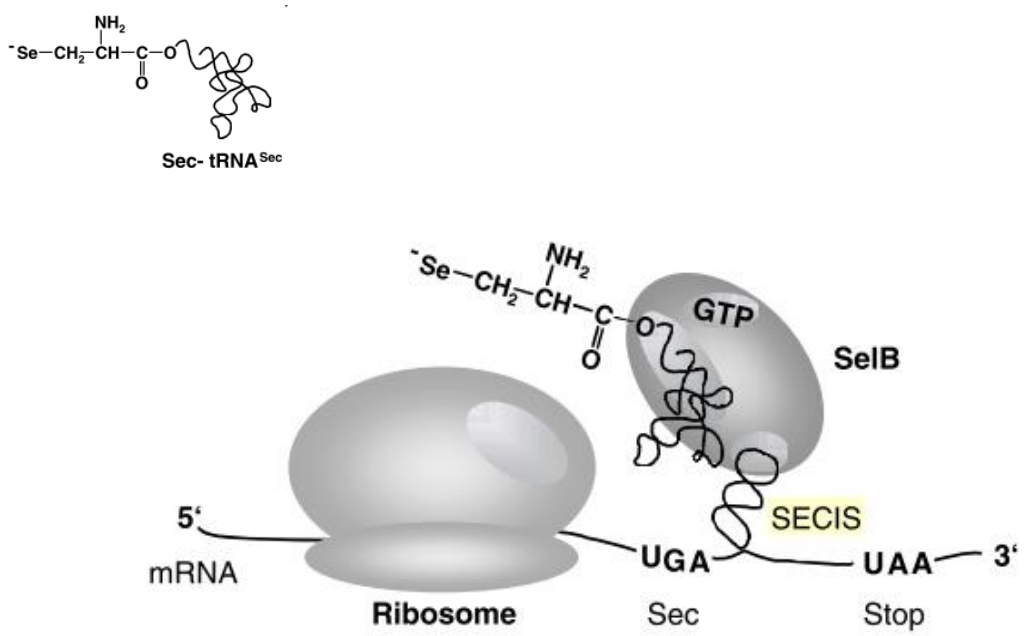


Figure 5.1. Interactions involved in the assembly of a functional quaternary complex SelB • GTP • mRNA • Sec-tRNA^{Sec} complex.
Figure extracted from Thanbichler and Bock (Thanbichler and Bock, 2002) .

SECIS elements fold into a stem-loop structure, which is comprised of the apical loop, upper and lower stems, internal loop, etc (Zhang and Gladyshev, 2005). The best characterised bacterial SECIS (bSECIS) elements are of *E. coli* genes encoding formate dehydrogenases H, N and O. FdhH (encoded by *fdhF*), FdhN (encoded by *fdnGHI*) and FdhO (encoded by *fdoGHI*) are distinct enzymes as they deliver electrons to different substrates (Hartwig *et al.*, 2015). The *fdoG* gene is expressed constitutively but *fdhF* and *fdnG* genes are only expressed under anaerobic conditions (Zinoni *et al*., 1990; Berg *et al*., 1991; Thanbichler and Bock, 2002) (more in **Section 5.1.6.1**).

5.1.2 The (bacterial) SECIS element and SECIS search-based identification of selenoproteins

Until recently systematic exploration of bSECIS elements, in order to gain better understanding on the Sec-decoding process and the selenoproteome of different organisms, had not been possible. The main reason behind this is that the UGA codon is interpreted as a stop codon by the available gene

annotation programs, which results in mis-annotation of selenoprotein genes (Kryukov and Gladyshev, 2004; Zhang and Gladyshev, 2005). Another limiting factor is the lack of consensus in bacterial SECIS elements, which precludes identification of bacterial selenoprotein genes in stem-loop structures (Kryukov and Gladyshev, 2004).

The bSECISearch computation tool was built specifically for identification of these structures and it has proven useful in the correct annotation of selenoprotein genes and the characterization of bacterial selenoproteomes. The bSECISearch searches for UGA codons followed by an RNA structure with a sliding window (39–100 bp) starting from each UGA codon in a query genome as shown in **Figure 5.2** (Zhang and Gladyshev, 2005). However, some support that SECIS elements can act at up to 2.7 kb from the site of selenocysteine insertion (Commans and Böck, 1999).

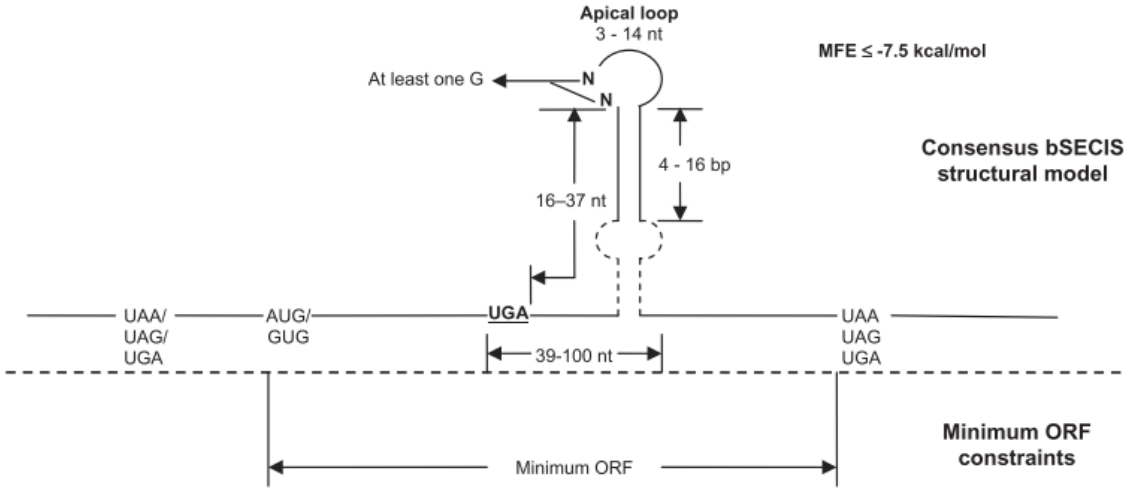


Figure 5.2. bSECIS consensus structural model and minimum ORF constraints.
Figure extracted from Zhang and Gladyshev (Zhang and Gladyshev, 2005). The Sec-UGA codon is shown in bold and is underlined. The consensus bSECIS model includes: (a) a 3–14 nt apical loop and a 4–16 bp upper-stem, (b) at least one guanosine (G) along the first two nucleotides in the apical loop, (c) a spacing of 16–37 nt between the UGA codon and the apical loop and (d) Minimum Free Energy, MFE ≤−7.5 kcal/mol. Minimum ORF constraint includes at least one AUG/GUG codon between the Sec UGA codon and the first upstream stop codon.

The common features between SECIS elements identified were: i) three consecutive adenosine residues in the terminal loop, ii) the sequence AUGA in the 5' arms and iii) UGA in the 3' arms of the stems (Low and Berry, 1996). Intriguingly, in *E. coli* a 'fourth base' effect in favour of termination over selenocysteine incorporation was observed. It was found that purines at this position increased the termination frequency substantially compared to pyrimidines (Low and Berry, 1996).

5.1.3 Biosynthesis and Identity of the tRNA^{Sec} in *E. coli*

The SECIS element binds the dedicated elongation factor SelB, and forms a complex with tRNA$^{Sec}_{UCA}$ (transcribed by *selC*). Initially, the tRNA^{Sec} is acylated with serine by a canonical seryl-tRNA synthetase. Then the seryl-tRNA^{Sec} intermediate is converted to Sec-tRNA^{Sec} by the Sec synthase SelA (Zhang *et al.*, 2006). The selenium donor utilized by SelA is monoselenophosphate ($SePO_3^{3-}$), which is synthesized from selenide (Se^{2-}) and ATP by the selenophosphate synthetase SelD (Zhang *et al.*, 2006). The *selD* gene from *E. coli* contains a putative ATP binding domain motif, GXGXXG. Discrimination of selenocysteyl-tRNA^{Sec} (Sec-tRNA^{Sec}) from its precursor seryl-tRNA^{Sec} (Sec[Ser]-tRNA^{Sec}) is a challenge faced by the elongation factor SelB. Most of the above process is summarised on **Figure 5.3**.

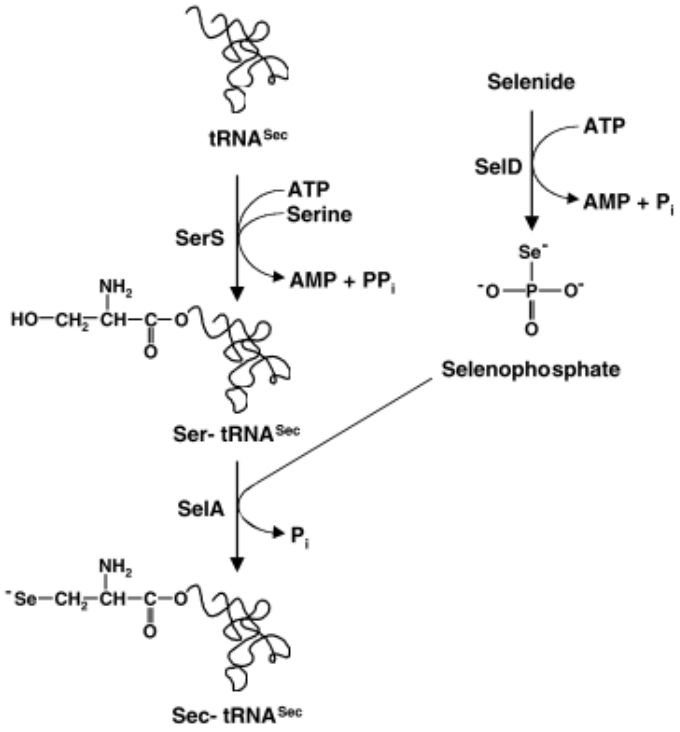


Figure 5.3. Reactions involved in the biosynthesis of selenocysteine tRNA in *E. coli.*
Figure extracted from Thanbichler and Bock (Thanbichler and Bock, 2002) .

A balanced ratio between SelB, selenocysteyl-tRNA^{Sec} and the SECIS of the mRNA is required for the quaternary complex formation (Yoshizawa and Böck, 2009). Also, the structure basis of rejection of canonical tRNAs by SelB is the length difference of the two tRNA classes (canonical elongator tRNAs and tRNA^{Sec}) which means that SelB measures the length of the A/T-arm (Yoshizawa and Böck, 2009). The tRNA^{Sec} has an extra base pair, G2-C71, within the amino acid acceptor stem compared to canonical tRNAs. It seems like there is a minor conformational difference between the SelB-GTP and the SelB-GDP form, which also plays a role in the correct tRNA binding.

It is speculated that prokaryotic SECIS elements located in the mRNA coding region might increase efficiency of selenoprotein synthesis in two ways. Firstly, by blocking ribosomal transit as the ribosome approaches the UGA codon, allowing increased time for selenocysteinyl-tRNA to bind. Alternatively, the secondary structure masks the UGA codon and prevents recognition by the 16S rRNA and/or by release factor 2 to cause translation termination (Zinoni *et al.*, 1990; Low and Berry, 1996; Murgola *et al.*, 1988).

5.1.4 The SECIS-like element function in *E. coli*

The genes s*elA and selB* are organised in an operon and are transcribed in a single mRNA. A SECIS-like element was detected into the 5' untranslated region of the *selA* mRNA. It is called SECIS-like element since it is located outside the reading frame (Thanbichler and Bock, 2002). This SECIS-like structure specifically binds to SelB and in the presence of Sec-tRNA^{Sec} the formation of a SelB-GTP-selenocysteyl-tRNA^{Sec} complex represses translation of *selA*, the gene encoding the selenocysteine biosynthetic enzyme (Thanbichler and Bock, 2002). By this specific mechanism, it adjusts the level of the gene products to the supply of the trace element selenium as shown in **Figure 5.4** (Thanbichler and Bock, 2002).

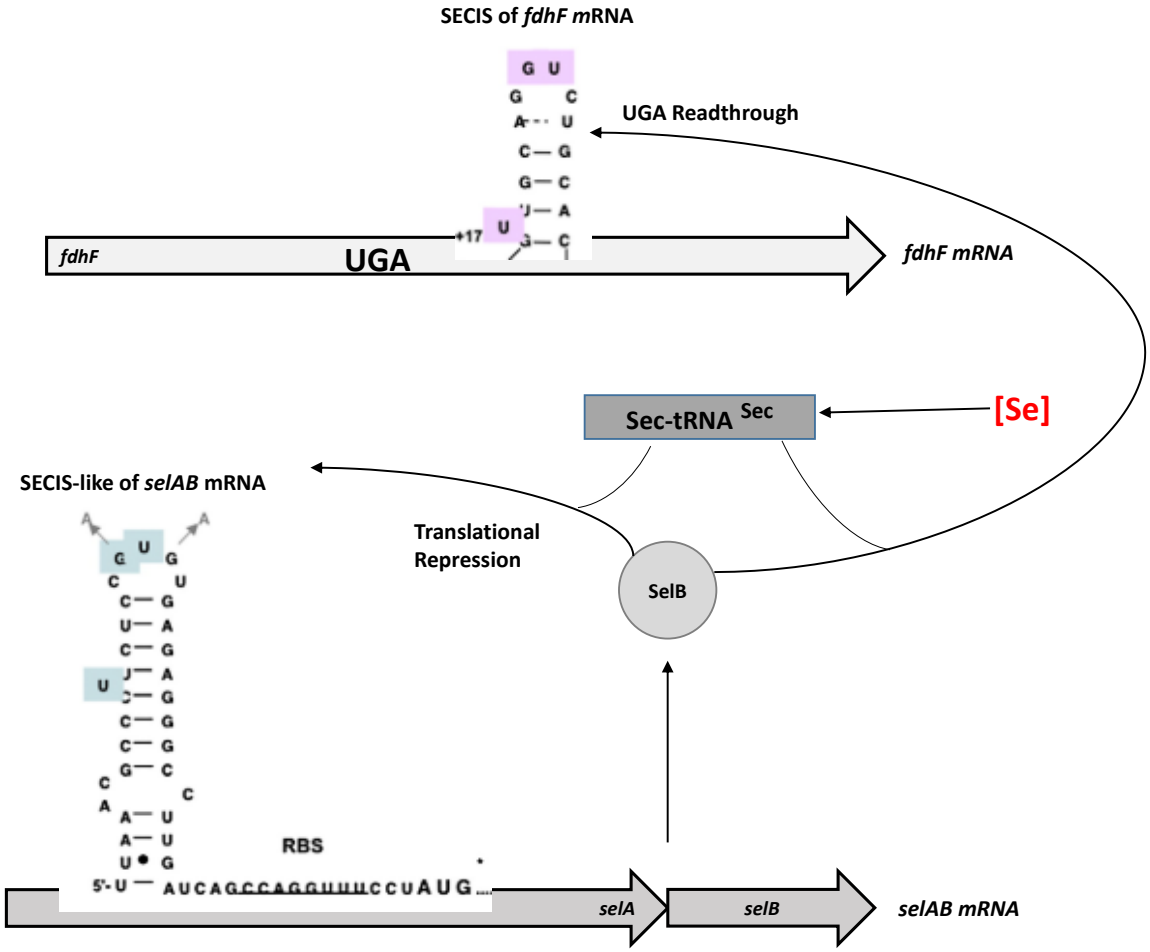


Figure 5.4. Interaction of SelB with the SECIS and the SECIS-like of the *fdhF* mRNA of the *selAB* mRNA, respectively. Figure adapted from Yoshizawa and Böck (Yoshizawa and Böck, 2009). The selenium (Se) status of the cells is reflected by the charging of $tRNA^{Sec}$ with selenocysteine. The affinity of SelB is higher for SECIS compared to the SECIS-like structure in the presence of selenium (Se) and therefore the read-through of UGA Sec is favored and the expression of *selAB* is increased. An excess of Sec though results into a downregulation of *selAB* expression.

In more detail, at adequate selenium supply selenocysteyl-$tRNA^{Sec}$ is able to bind SelB and form a complex with either the SECIS or SECIS-like structure. Since SelB has a higher affinity for SECIS compared to SECIS-like the read-through of UGA is favoured and expression of *selAB* is increased. However, at excess levels of selenium, there is an excess of $tRNA^{Sec}$ which forms a complex with SelB and the SECIS-like which causes reduction of *selA* expression (Yoshizawa and Böck, 2009). Hence, the $tRNA^{Sec}$ acts as sensor of selenium availability (Yoshizawa and Böck, 2009).

The interaction involves a 17 kDa peptide on the C-terminal domain of SelB, designated domain IVb, and the apical part of the SECIS hairpin. A GU doublet in the loop region is supposed to make contact with the SECIS-binding pocket of SelB (Thanbichler and Bock, 2002). This seems to be the only level of control since no regulation has been detected for *selD* expression. Competition between the SECIS-like and the SECIS elements might enable the cell to respond quickly to sudden changes in the intracellular concentration of selenoprotein mRNAs during aerobic and anaerobic growth shifts, and

regulate selenocysteine biosynthesis accordingly. This control mechanism might be necessary because of the high reactivity of the selenol group of selenocysteine which could be toxic if accumulated in the cell (Thanbichler and Bock, 2002).

5.1.5 Phylogenetic analysis of the selenocysteine decoding trait in bacteria

The formate dehydrogenase family had a particularly high representation in the selenoproteomes of most organisms investigated (Zhang and Gladyshev, 2005). In many of these organisms, formate dehydrogenase was the only selenoprotein. Interestingly, this study suggested that most selenoprotein-containing organisms uncovered were obligatory or facultative anaerobes that grow optimally at ambient temperatures and neutral pH (Zhang and Gladyshev, 2005).

Phylogenetic analysis placed *Pseudomonadale* sequences within the *Alphaproteobacteria-Betaproteobacteria* node, and not within the *Gammaproteobacteria* node, suggesting that a horizontal gene transfer (HGT) event rather than vertical descent was responsible for the acquirement of the Sec-decoding trait in these organisms (Zhang *et al.*, 2006). The topology of formate dehydrogenase α subunit (FdhA) tree, which is the only selenoprotein in *Pseudomonadales*, is consistent with an HGT event. In addition, the *fdhA* gene was very close to or even flanked the *selA-selB-selC* operon further suggesting that both the Sec-decoding trait (*selA*, *selB*, and *selC*) and *fdhA* of *Pseudomonadale*s were acquired by HGT (Zhang *et al.*, 2006). FdhA and SelD are the most widespread selenoproteins, and at least one of these proteins was present in each selenoprotein-containing organism (usually *fdhA*, or *selD* if *fdhA* is absent). High diversity of bacterial selenoproteomes was observed after analysing distribution of selenoprotein families in different bacterial phyla. Futhermore, Zhang and colleagues (Zhang *et al.*, 2006) give the sequence of *fdoG* as the selenoprotein of *P. aeruginosa* encoded by the *fdoG gene* (synonym fdnG/ fdhG, locus tag: PA4812)(Zhu *et al.*, 2006; Zhang and Gladyshev, 2005).

Interestingly, the PA4803 (*samA*) gene of interest of our study, which encodes for a putative S-adenosylmethionine (SAM)-dependent methyltransferase is positioned directly upstream of a $tRNA^{Sec}$ encoded by the PA4802.1 according to the Pseudomonas Genome Database (Winsor *et al.*, 2016). Upstream of *samA* in the same region, *selA*, *selB*, *fdhE, fdnGHI* genes are found for all of which the functions have been demonstrated in *E. coli*, but not yet in *P. aeruginosa*, and are being discussed below.

Environmental factors such as oxygen levels and optimal growth temperature fully correlated with changes in Sec utilization (Zhang *et al.*, 2006). Organisms possessing the Sec-decoding trait favour anaerobic and hyperthermic conditions. Thus, utilization of Sec seems to be stimulated in decreased

oxygen concentration and increased growth temperature (Zhang *et al.*, 2006). A possible explanation for this observation is that Sec generates reactive oxygen species under high oxygen conditions, which made it intolerable to cells. Hence, imposing a negative selection for this trait under the particular conditions (Zhang *et al.*, 2006).

5.1.6 Prokaryotic selenoproteins functions

5.1.6.1 Selenoproteins and Anaerobiosis

An active membrane-bound phenazine methosulfate-linked formate dehydrogenase (FDH-PMS) complex is formed in *E. coli* during the aerobic-anaerobic transition. This major anaerobic respiratory chain is composed of a formate dehydrogenase which transfers electrons from formate to nitrate and it requires the *fdhD* and *fdhE* genes (Berg *et al*., 1991; Schlindwein *et al*., 1990). The precise functions of FdhD and FdhE in formate dehydrogenase biosynthesis remain to be established, however, it is likely that they perform a function in post-translational maturation of the enzymes (Soboh *et al.*, 2011).

E. coli synthesizes three membrane-bound multi-subunit formate dehydrogenases (Fdh), each comprising of a large catalytic subunit, an electron-transfer subunit and a membrane-anchoring subunit (Soboh *et al.*, 2011). The large subunit contains both a selenocysteine residue and a molybdenum cofactor which are crucial for catalysis (Hartwig *et al.*, 2015). The Fdh enzymes are FdhH (H for hydrogen, associated with hydrogen production), FdhN (N for nitrate respiration) and FdhO (O for aerobic growth) (Hartwig *et al.*, 2015; Soboh *et al.*, 2011). Fdh enzymes are selenium-dependent, thus, impaired co-translational insertion of selenocysteine leads to truncated protein being produced without activity (Grundner-Culemann *et al.*, 2001).

Despite the high levels of amino acid sequence similarity, enzyme assays demonstrated that FdhH (encoded by *fdhF*), FdhN (encoded by *fdnGHI*) and FdhO (encoded by *fdoGHI*) are distinct enzymes as they deliver electrons to different substrates (Hartwig *et al.*, 2015).

FdhH enzyme activity is present at stationary phase and is dependent on oxygen but independent of the presence of either FdhO or FdhN (Hartwig *et al.*, 2015). Moreover, FdhH activity was shown to depend on formate and the machinery for incorporation of selenocysteine (Hartwig *et al.*, 2015). FdhH couples formate oxidation with proton reduction in the formate hydrogen lyase (FHL) complex (Hartwig *et al.*, 2015). FdhN is induced to maximal levels during growth in the presence of nitrate and the enzyme is also present at lower levels during fermentative growth. FdhO is synthesized constitutively and is present at low levels aerobically, during fermentative growth and nitrate

respiration (Soboh *et al.*, 2011). Moreover, FdhN and FdhO in *E. coli* have hydrogen-oxidizing activity and hence belong to new class of dihydrogen-oxidizing enzymes (Soboh *et al.*, 2011).

The *fdnGHI* genes are also found in the vicinity of the PA4803 (*samA*), PA4802.1 genes and the *selAB* operon in *P. aeruginosa*. It could be that the SamA SAM-Methyltranferase activity (which does not have a homolog in *E. coli*) adds a modification to a component in this pathway regulating the anaerobic respiration processes in which the above genes are involved in. Should this be the case, it is likely $tRNA^{Sec}$ transcribed by the PA4802.1 gene is the substrate of SamA since this is the case in mammalian cells, where Sec-tRNA[Ser]Sec mcm^5U is partially methylated by an unidentified Um34 methylase, and the level of methylation is dependent on selenium status (Schoenmakers *et al.*, 2016).

The *P. aeruginosa* FdnG protein contains a twin arginine motif RRXFL[KR] in the N-terminal signal sequence which makes it a substrate of the "twin-arginine translocation" (TAT) protein export system (Ochsner *et al.*, 2002; Lewenza *et al.*, 2005). The TAT system is capable of exporting folded proteins which are involved in pyoverdine-mediated iron-uptake, anaerobic respiration, osmotic stress defence, motility, and biofilm formation (Ochsner *et al.*, 2002). Hence, the TAT system has an effect on anaerobiosis by exporting periplasmic enzymes involved in the formation of multiprotein oxidation-reduction complexes involved in respiration or anaerobic growth such as FdnG (Ochsner *et al.*, 2002).

P. aeruginosa grows preferentially under aerobic respiration, however, is capable of growing under anaerobic conditions in the presence of nitrate, which can serve as terminal electron acceptor. There are four reductases which can catalyse the reduction of nitrate (Ochsner *et al.*, 2002). This TAT-dependent denitrification pathway may be significant in the context of *P. aeruginosa* cystic fibrosis (CF) lung infection, where this organisms encounters oxygen gradients and anaerobic pockets (Filiatrault *et al.*, 2006). The microaerobic or anaerobic environment is created by rapid depletion of oxygen by metabolically active cells and the alginate secreted by *P. aeruginosa* which further restricts oxygen availability (Ochsner *et al.*, 2002). Interestingly, the TAT system is an attractive potential target for development of novel antimicrobial agents because it not encoded in higher eukaryotes (Ochsner *et al.*, 2002).

Some overlaps in gene expression patterns were observed in *P. aeruginosa* according to oxygen levels, instead of a discrete set of genes (Alvarez-Ortega and Harwood, 2007). This suggests that *P. aeruginosa* does not have a clearly defined low oxygen regulon but it rather responds to changes in oxygen concentration along a continuum. Hence, this organism is ready to cope with sudden drops in oxygen without having to mount a transcriptional response (Alvarez-Ortega and Harwood, 2007). The

virulence of *P. aeruginosa* is influenced by anaerobic metabolism. Therefore, gaining further understanding of the anaerobic metabolism of *P. aeruginosa* may help to identify potential targets as possible candidates for antimicrobial therapy (Filiatrault *et al.*, 2006).

5.1.7 Modification of tRNA

The selenocysteine-incorporating trait is centred around the specific selenocysteine tRNA. Hence, an overview of tRNAs and their modifications capacities is necessary to understand how important they are, since modification have a direct link to their function. Transfer Ribonucleic Acids (tRNAs) are necessary for cellular viability because they provide an essential link between the genome and the proteome (Thüring *et al.*, 2016).

Transfer RNAs contain the highest density of modifications, more than 90 modified nucleosides have been found to date, in comparison to the other classes of RNA (Ross *et al.*, 2017; Hori, 2014). Such modifications create structural diversity and play significant functional roles since structure is intimately related to function (Meng and Limbach, 2006). This review focuses mainly on methylation, which can dictate a number of important processes such as gene regulation, stress-response, and RNA stabilization.

The biological role of many tRNA modifications is still unresolved, and understanding the role will be challenging because of synergistic effects among multiple modifications on the same tRNA or a selective advantage for particular conditions (Ross *et al.*, 2017). Modification enzymes such as tRNA guanine transglycosidase (Tgt) and tRNA ψ55 synthase (TruB) are essential factors for infection in *P. aeruginosa*. Thus, understanding the regulation of tRNA modifications and modification enzymes might be a powerful tool for controlling infectious organisms (Hori, 2014).

5.1.7.1 tRNA methytransferases and tRNA methylation

The majority of tRNA methyltransferases are S-adenosyl-methionine (SAM)-dependent and belong to two classes (classes I and IV) based on their catalytic domain (Hori, 2014). Class I enzymes possess a Rossmann fold in the catalytic domain, whereas class IV enzymes possess a topological-knot structure (Hori, 2014). Generally, tRNA methyltransferases recognize the local structure around the target site for methylation which is often embedded in the L-shaped tRNA structure (Hori, 2014).

The primary sequence and the predicted secondary structure of the PA4803 (SamA) protein were analysed in detail (See Chapter 4). A number of conserved residues and motifs linked to the enzymatic activity of SAM-dependent MTases were identified in the protein sequence. SamA seems to have six helical structures (H) and seven beta-sheet structures (E) in the following possible order (-H1-H2-E1-

H3-E2-H4-E3-E4-H5-E5-H6-E6-E7-). The first β strand (β1/E1) ends with the GxG motif and the β2/E2 with a conserved acidic residue. Taken together, SamA seems to be a Class I SAM-dependent MTase, and it could potentially target tRNA. However, structural studies are necessary in order to understand the reaction mechanisms, substrate specificity and protein-protein interactions etc (Hori, 2014).

5.1.8 Selenocysteine-inserting tRNAs

5.1.8.1 Bacterial selenocysteine-inserting tRNAs

Sec[Ser]-tRNA^{Sec} has additional features that distinguish it from all other tRNAs as shown in **Figure 5.5**. Firstly, it has an atypically long variable arm (**Figure 5.5**). Secondly, it has 13 nucleotides in the acceptor and TΨC stem helices (Ψ indicates pseudouridine) instead of the 12 normally found in canonical tRNAs. Thirdly, the Sec-tRNA^{Sec} contains relatively few modified nucleotides compared to other tRNAs, which may have as many as 15 to 17 modified nucleotides. Lastly, it may have up to six base pairs in the dihydrouracil stem instead (D stem) (**Figure 5.5**) of the three to four found in canonical tRNAs (Hatfield and Gladyshev, 2002).

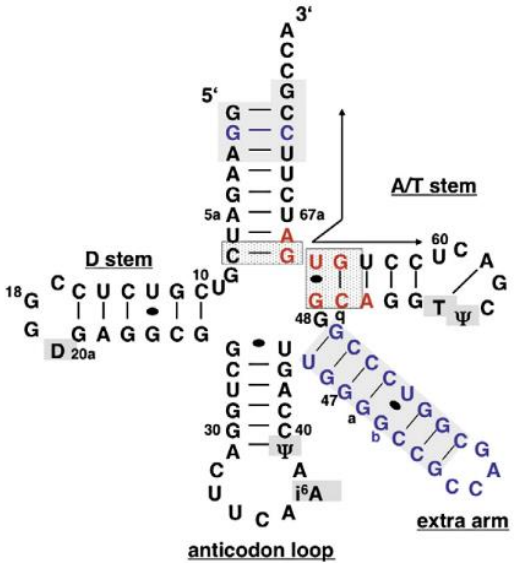


Figure 5.5. Secondary structure of tRNASec from *E. coli*.
Figure extracted from Yoshizawa and Böck (Yoshizawa and Böck, 2009). Bases involved in the recognition of tRNASer by seryl-tRNA synthetase are shown in blue. Bases suggested to participate in the interaction SelB are shown in red.

5.1.8.2 Eukaryal selenocysteine-inserting tRNAs

In mammals the Sec[Ser]-tRNA^{Sec} consists of two isoforms that differ from each other by a single modification at 2'-O-hydroxyl site at position 34 (Um34), which is the wobble position of the anticodon (Schoenmakers *et al.*, 2016). One isoform contains methylcarboxylmethyluridine (mcm^{5}U) at this site,

and the other contains methylcarboxymethyluridine-2'-O-methylribose (mcm^{5}Um) (Schoenmakers *et al.*, 2016). The ratio between the two isoforms is influenced by the intracellular selenium status (Hatfield *et al.*, 1991). Namely, under selenium deficiency the levels of mcm^{5}U are increased and the levels of mcm^{5}Um are reduced. The opposite occurs under adequate selenium concentration (Kim *et al.*, 2000).

The 5-methoxycar-bonylmethyluridine mcm^{5}U isoform is involved in the synthesis of a subclass of selenoproteins, called housekeeping selenoproteins (e.g. TR3), while the 5-methoxycarbonylmethyl-2'-O-methyluridine mcm^{5}Um isoform supports synthesis of stress-related selenoproteins (e.g. GPx1) (Schoenmakers *et al.*, 2016). This phenomenon is observed in mammals and is known as selenoprotein hierarchy (Kim *et al.*, 2000; Birringer *et al.*, 2002).

This methylation is a highly specialized event, it substantially affects Sec[Ser]-tRNA^{Sec} structure and it is the last step in its maturation (Carlson *et al.*, 2005). Whether the particular methylation event occurs as the result of a single enzyme or more than one enzymes is still unresolved (Kim *et al.*, 2000). The differences between the bacterial tRNA^{Sec} from *E. coli* and mammalian tRNA^{Sec} are shown in **Figure 5.6**.

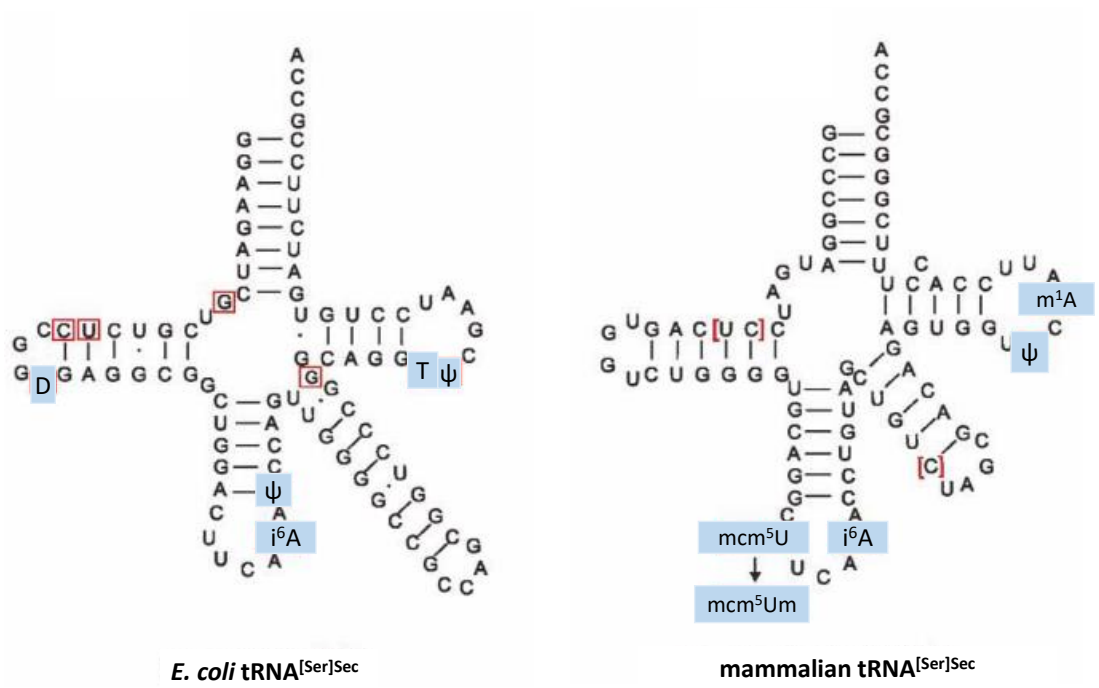


Figure 5.6. Cloverleaf tRNA(ser)sec models of *E. coli* (left panel) and mammalian (right panel).
Figure adapted from Birringer *et al* (Birringer *et al.*, 2002). Modified bases are highlighted in light blue (Ψ, pseudouridine; i^{6}A,N6-isopentenyladenosine; mcm5U, 5-methoxycarbonylmethyluridine; mcm^{5}Um, 5-methoxycarbonylmethyluridine-2'-O-methylribose; m^{1}A, 1-methyladenosine; D, dihydrouridine; T, ribothymidine). In *E. coli* tRNA$^{(ser)sec}$ boxed nucleotides indicate deviations from canonical elongator tRNA consensus. In mammalian tRNA$^{(ser)sec}$ brackets indicate variable bases.

The Sec[Ser]-tRNA^{Sec} contains only three other modifications as shown in **Figure 5.6**, namely, N6-isopentenyl-adenosine (i^{6}A) at position 37, pseudouridine (ψ) at position 55, and 1-methyladenosine (m^{1}A) at position 58, compared to most other tRNA which may contain up to 17 modifications (Kim *et al.*, 2000; Hatfield *et al.*, 1991). The role of ψ at position 55 and m1A at position 58 in the Sec[Ser]-tRNA^{Sec} function remain to be established (Kim *et al.*, 2000). Formation of each modified base mentioned and an intact tertiary structure is a prerequisite for mcm^{5}U to yield mcm^{5}Um (Kim *et al.*, 2000). In contrast, formation of both mcmU and i^{6}A does not have such strict requirements (Schoenmakers *et al.*, 2016). Prior aminoacylation of Sec[Ser]-tRNA^{Sec} is required for Um34 addition and Sec must be attached to its tRNA for subsequent Um34 methylation. Therefore, selenium seems crucial for Um34 methylase function and has implication in the selenoprotein hierarchy (Kim *et al.*, 2000).

The mcm^{5}Um34 seems to be involved in stabilization of the anticodon loop, as well as the I^{6}A37. In more detail, mcm^{5}Um34 restricts wobble base pairing (Hori, 2014). The m^{1}A58 seems to be involved in stabilization of the T-loop structures. Moreover, m^{1}A58 is part of the RNA quality control system. Therefore, it acts as the marker of maturation (Hori, 2014).

5.1.9 Main Hypothesis

It is hypothesized that in *P. aeruginosa* growing under anaerobic conditions, the SamA enzyme (encoded by PA4803) methylates the Sec[Ser]-tRNA^{Sec} (transcribed by PA4802.1) in the proximity of the anticodon. It is believed that this modification is a maturation step, which changes the tRNA^{Sec} tertiary which in turn drives translation of the *fdnGHI* genes found in the same locus (**Figure 5.7, A**). As mentioned above the *fdnGHI* genes products are involved in anaerobic respiration. If the SamA is absent then the unmodified Sec[Ser]-tRNA^{Sec} will not be able to drive translation of this multiprotein complex to completion, which will result in a truncated non-functional selenoprotein FdhG. Thereby, the switch to anaerobic respiration will not occur, or will be significantly hampered (**Figure 5.7, B)**.

This hypothesis is in agreement with the *in vivo* data, in which the SamA mutant was not as fit nor virulent in a mouse model of pulmonary infection (unpublished). As mentioned the CF lung is an environment which is mostly microaerophillic but with several anaerobic pockets and bacteria in this environment need to be able to rapidly switch from aerobic to anaerobic growth and *vice versa*. Hence, it is hypothesized that this mechanism in *P. aeruginosa* shares some resemblances to that found in *E. coli* and mammalian cells. In more detail, the FdhG, the only selenoprotein in *P. aeruginosa*

is involved in adaptation to anaerobic respiration as shown in *E. coli* and a methylation event in the Sec[Ser]-tRNA^{Sec} is critical for its full length translation as shown in mammalian cells.

One of the most crucial experiments in this study was designed to test the above hypothesis (**Figure 5.7**). The interest was focused in the length of the FdhG protein. The FdhG protein in *P. aeruginosa,* encoded by *fdhG/PA4812* was modified by the incorporation of a hexahistidine tag in order be able to visualise the protein under different conditions and in different strains. As explained previously and based on the study hypothesis (**Figure 5.7**), if the conditions are not favourable (fully aerobic environment, deleted SamA, assuming SamA adds the methylation on the tRNA^{sec}) the *fdhG* translation will stop at the UGA stop codon leading to the formation of a shorter transcript and a truncated protein. This UGA codon, which is located towards the middle of its sequence, gives the signalling for selenocysteine incorporation. Otherwise, under promoting conditions (e.g. reduced oxygen, anaerobic conditions and/or present SamA) the UGA codon will be read-out as a selenocysteine (Sec) incorporation codon leading to a full-length transcript and protein (**Figure 5.8**).

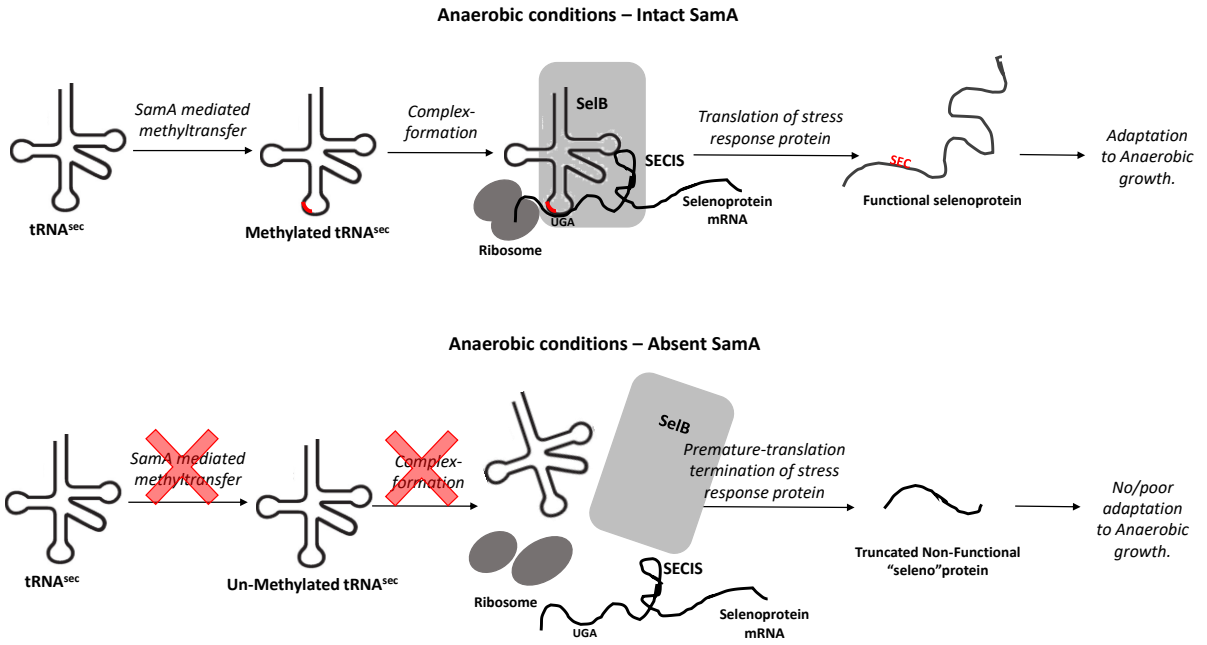


Figure 5.7. Current hypothesis.
The current hypothesis supports that A. *P. aeruginosa* under anaerobic conditions the SamA (encoded by PA4803) methylates the Sec[Ser]-tRNA^{Sec} (transcribed by PA4802.1) in the proximity of the anticodon. We believe this modification is a maturation step, which changes the tRNA^{Sec} tertiary which in turn drives translation of the *fdnGHI* genes found in the same locus. As mentioned above the *fdnGHI* genes products are involved in anaerobic respiration. B. If the SamA is absent then the unmodified Sec[Ser]-tRNA^{Sec} will not be able to drive translation of this multiprotein complex to completion, which will result in a truncated non-functional selenoprotein FdhG. Thereby, the switch to anaerobic respiration will not occur.

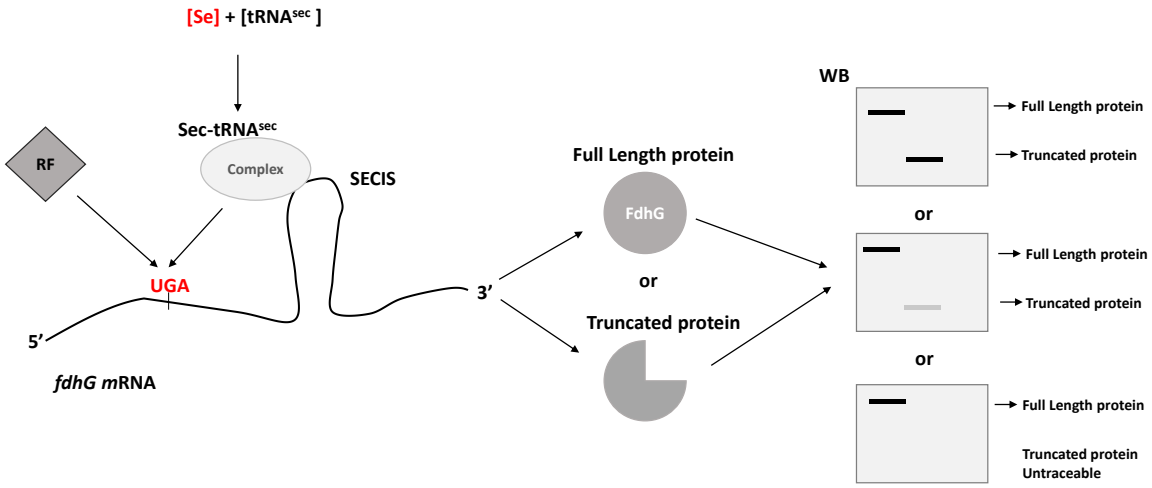


Figure 5.8. A model of UGA decoding during selenoprotein synthesis
Figure adapted from Chen *et al.*, 2017 (Chen *et al.*, 2017). The Sec-tRNA^{Sec} and Release Factors (RFs) compete for a UGA site. The abundance of Sec-tRNA^{Sec} is determined by both selenium (Se) and uncharged tRNA^{Sec}. When Sec-tRNA^{Sec} binds to the UGA site, the mRNA will be translated into full length selenoproteins. When RF binds to the UGA site, the mRNA will be translated into truncated proteins which maybe degraded quickly. WB; Western Blot films depictions denote the possible FdhG bands for each scenario: truncated protein fully traceable, truncated protein merely traceable and truncated protein not traceable.

5.1.10 Aims of the study

The *in silico* analysis reported in this chapter aimed to investigate the PA4802.1 and *fdhG* sequences from *P. aeruginosa* (amongst others) and their respective structures to assess their potential for a similar role to their equivalents in *E. coli.* In particular this study had as objectives to:

- Identify and assess the PA4802.1 tRNA structure
- Identify and assess *fdhG* regulatory elements and their structure

Of note, the predictions from this study could not be assessed experimentally due to health-related issues and the inability to travel to the laboratory of Prof Mark Helm at the University of Mainz in Germany where these validation experiments were going to be carried out.

5.2 Results

5.2.1 *In silico* characterisation of *P. aeruginosa* $tRNA^{sec}$

5.2.1.1 Alignment of the $tRNA_{sec}$ from *E. coli* with that from *P. aeruginosa*

Multiple alignment of the PA4802.1 $tRNA^{sec}$ sequence (through blastn suite) revealed hits with 100 % query cover and identity with the $tRNA^{sec}$. The hits included several *P. aeruginosa* strains: PAO1, PA14, PA7, LES and some other *Pseudomonas species* such as *P. pseudoalcaligenes*, *P. resinovorans*, *P. denitrificans*, *P. citronellolis* and *P. oryzihabitans*. The selected list of organisms was searched for the presence of the PA4803/*samA* gene ortholog. A total of 34 hits strains were found to have both genes and the results are summarized in **Table 5.1**.

Table 5.1. Summary of BLASTN hits for PA4802.1 (tRNA-Sec, from PAO1 reference strain) which overlapped with the 104 ortholog list for the *samA* gene (hypothetical protein, from PAO1 reference strain), which were all *P. aeruginosa* strains

Strain	PA4803 Ortholog Locus tag	Description	Presence of tRNA-Sec downstream	tRNA-Sec Locus tag
PAO1	PA4803	hypothetical protein	Yes	PA4802.1
UCBPP-PA14	PA14_63470	methyltransferase	Yes	PA14_63460
LESB58	PALES_51871	Putative methyltransferase	Yes	PALES_51862
DSM 50071	TU83_RS20620	methyltransferase	Yes	TU83_RS20625
PSE305	TY30_RS23070	hypothetical protein	Yes	TY30_RS23065
F22031	F22031_RS07650	hypothetical protein	Yes	F22031_RS07645
NCGM1984	NCGM1984_RS27380	hypothetical protein	Yes	NCGM1984_RS27375
PAO1-VE2	N296_4970	ubiE/COQ5 methyltransferase family protein	Yes	N296_4969
NCGM2.S1	NCGM2_RS03565	hypothetical protein	Yes	NCGM2_RS03570/ NCGM2_0729
PAO1-VE13	N297_4970	ubiE/COQ5 methyltransferase family protein	Yes	N297_4969
B136-33	G655_25335	Putative methyltransferase	Yes	G655_t29386
LESlike1	T225_RS26220	hypothetical protein	Yes	T225_RS26215/T225_26390

LESlike5	T227_RS57185	hypothetical protein	Yes	T227_RS57180/ T227_26505
PA1	PA1S_gp2723	SAM-dependent methyltransferase	Yes	PA1S_gp2722
FRD1	EG09_RS23615	hypothetical protein	Yes	EG09_RS23620/ EG09_23620 - UC33_RS17600 (Different assemblies)
MTB-1	U769_26365	NodS-like protein	Yes	U769_26360
C7447m	M802_4968	ubiE/COQ5 methyltransferase family protein	Yes	M802_4967
PA1R	PA1R_gp2723	SAM-dependent methyltransferase	Yes	PA1R_gp2722
PA96	PA96_RS25575	hypothetical protein	Yes	PA96_RS25570/PA 96_R0330
LESlike4	T226_RS56990	hypothetical protein	Yes	T226_RS56985
LESlike7	T228_RS56310	hypothetical protein	Yes	T228_RS56305
M18	PAM18_4912	Putative methyltransferase	Yes	PAM18_R071
PAO581	M801_4835	ubiE/COQ5 methyltransferase family protein	Yes	M801_4834
SCV20265	SCV20265_5459	SAM-dependent methyltransferase	Yes	SCV20265_6377
LESB65	T224_RS57095	hypothetical protein	Yes	T224_RS57090
YL84	AI22_RS07870	hypothetical protein	Yes	AI22_RS07875
PAO1H2O	OU9_04903	methyltransferase	Yes	OU9_04902
PA14	CIA_05872	Putative methyltransferase	Yes	CIA_05873
DK2	PADK2_25490	Putative methyltransferase	Yes	PADK2_t29711
NCGM1900	NCGM1900_RS27385	hypothetical protein	Yes	NCGM1900_RS2 7380
LES400	T222_RS57990	hypothetical protein	Yes	T222_RS57985
F9676	ADJ52_RS02010	hypothetical protein	Yes	ADJ52_RS02015
Carb01 63	YQ19_RS31140	hypothetical protein	Yes	YQ19_RS31135
LES431	T223_26560	NodS-like protein	Yes	(T223_26555)

As previously mentioned, tRNA^{sec} has been extensively studied in *E. coli*. Therefore, the *E. coli* and *P. aeruginosa* PAO1 tRNA^{sec} sequences were uncovered from the BioCyc Database Collection (Karp *et al.*, 2018) and the Pseudomonas Genome DB (Winsor *et al.*, 2016), respectively, and were aligned in a pairwise way (**Figure 5.9**) (Solovyev and Salamov, 2016)(Groth and Calos, 2004). The *E. coli* tRNA^{sec} is 95 nucleotides in length and the *P. aeruginosa* PAO1 tRNA^{sec} is 92, the latter missing the CCA tail at the end of the sequence.

Both the tRNA^{sec} DNA sequences from *E. coli* and *P. aeruginosa* were pairwise aligned as shown in **Figure 5.9.**

```
E. coli tRNA-Sec             1 GGAAG---AUCGUCGUCUCCGGUGAGGCGGCUGGACUUCAAAUCCAGUUGGG  49
                               ||||    ||| .||  .|||||||..|.|||.|||||||||||||.||.|||
P. aeruginosa tRNA-Sec       1 -GAAGGCAAUC-ACG--CCCGGUGGCGUGGCCGGACUUCAAAUCCGGUGGGG  48

E. coli tRNA-Sec            50 GCCGCCAG-CGGUCCCGGGCAGGUUCGACUC---CUGUGAUCUUCCGCCA    95
                                |.||.||| ||.|||.|||..||||||||||   |||   .||||||
P. aeruginosa tRNA-Sec      49 GACGGCAGCCGUUCCUGGGUGGGUUCGACUCCCACUG---CCUUCCG---    93
```

Figure 5.9. Sequence alignment between the tRNA-Sec of *E. coli* (encdoded by *selC*) and the tRNA-Sec of *P. aeruginosa* PAO1 (encoded by PA4802.1).
Grey highlights represent mismatches and hyphens represent gaps in comparison to the template sequence. The alignment was done in Benchling online platform.

Next, bioinformatic analysis of the PA4802.1 (tRNA^{sec}) generated three predicted secondary structures shown in **Figure 5.10**. The Centroid and Context fold predictions (**Figure 5.10**, upper structures), were generated automatically by prediction tools. Essentially, the only difference between the two is on the acceptor arm ends. In the Centroid fold prediction G1 is paired with C90 whereas in the Context fold prediction not. Thereby, C90 forms a small tail with C91 and G92. A manual *P. aeruginosa* tRNA^{sec} secondary structure prediction was attempted as well (**Figure 5.10**, lower structure).

The *P. aeruginosa* tRNA^{sec} is missing the first G present in the *E. coli* tRNA^{sec}, maybe this could explain why the acceptor stem is 7 instead of 8 nucleotides long. Through-out the *P. aeruginosa* tRNA^{sec} sequence there are several mismatches relative to the *E. coli* tRNA^{sec} but in such a way that base pairing is not affected (**Figure 5.9**). Another difference in this structure prediction is the generation of a 10 nucleotide variable arm loop instead of the 5 one given by the online prediction tools, which is more similar to the loop of the *E. coli* tRNA^{sec}.

Moreover, the *P. aeruginosa* tRNA^{sec} sequence is missing the CCA tail at the end of the acceptor arm, which is quite important for the amino acid loading and the process, which follows afterwards.

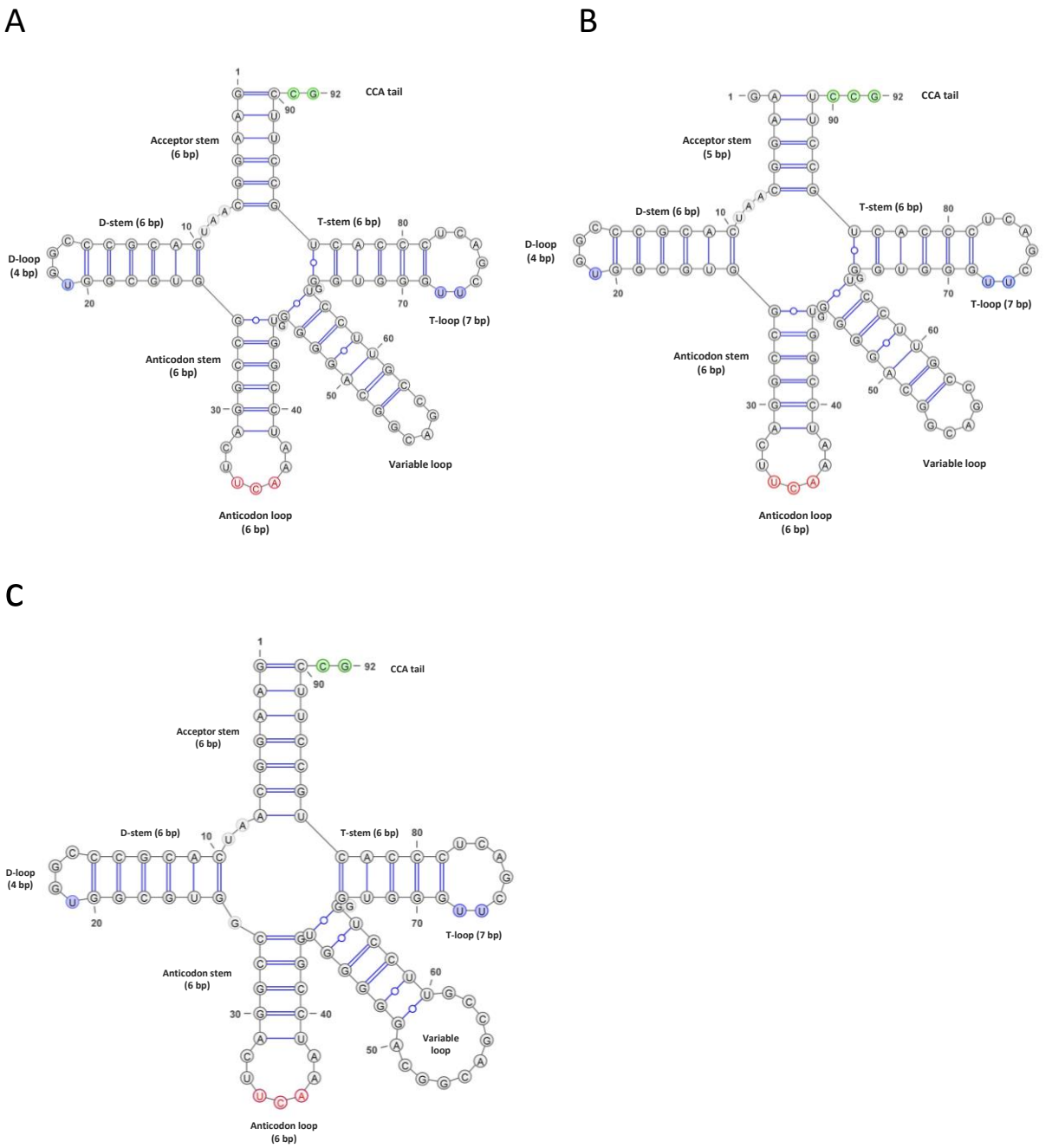


Figure 5.10. The different cloverleaf predicted structures of PA4802.1 tRNA$^{sec.}$

The upper structures were predicted by the RNAComposer (Table 2.6), with the centroid fold shown on the left and the context fold on the right. The lower structure was predicted manually following guidelines found in Commans and Bock (Commans and Böck, 1999) . Light grey circled nucleotides represent connector bases. Blue circled nucleotides represent modified bases such as the dihydrouridine in the D-loop and the pseudouridine and yet another modified uridine in the T-loop. Red outline circled nucleotides represent the anticodon. Green circled nucleotides represent the CCA tail. The methylation is predicted to take place in U34 of the anticodon shown with red circled nucleotides.

5.2.2 Biological function and regulation of PA4802.1

5.2.2.1 *In silico* characterisation of the regulatory elements involved in selenocysteine incorporation in *P. aeruginosa*

As previously mentioned, a SECIS-like element was detected into the 5' untranslated region of the *selA* mRNA. This SECIS-like structure specifically binds to SelB and in the presence of Sec-tRNA^{Sec} and the SelB-GTP-selenocysteyl-tRNA^{Sec} complex in turn represses translation of *selA*, the gene for the main selenocysteine biosynthetic enzyme (Thanbichler and Bock, 2002). Through this mechanism, the translation of the target gene can be tuned by the levels of the trace element selenium (Thanbichler and Bock, 2002).

Hence, the *selA* upstream region of *P. aeruginosa* was aligned with the *E. coli selA* SECIS-like sequence as an approach to better characterise this site. The results shown in **Figure 5.11** indicate that the sequences share 3.6% identity, with 93.4% of gaps. Overall, no significant sequence conservation could be inferred from this.

```
P.aeruginosa selA upstream region    201 CUGUCCCUGGAGCAUGACGGGCAGCCGGCGGAAAAAGCCGUGCUGCGCGC
250
                                                                    ..|||.|||.|.||.||.|
E.coli selA SECIS-like                 1 --------------------------------UUAAACGCCCUUCUCCGUG-
19

P.aeruginosa selA upstream region    251 CGAGACCUGCCCCAGUUGCCAGGGCUACCUGAAGCAGUUCUACCUGGAGU
300
                                                        ||..|||||  |.|||
E. coli selA SECIS-like                20 ----------------UGAGAGGGC--CUUGA------------------
33


P.aeruginosa           201 CUGUCCCUGGAGCAUGACGGGCAGCCGGCGGAAAAAGCCGUGCUGCGCGC    250
                                                     ..|||.|||.|.||.||.|
E.coli                   1 --------------------------------UUAAACGCCCUUCUCCGUG-     19

P.aeruginosa           251 CGAGACCUGCCCCAGUUGCCAGGGCUACCUGAAGCAGUUCUACCUGGAGU    300
                                         ||..|||||  |.|||
E. coli                 20 ----------------UGAGAGGGC--CUUGA------------------     33
```

Figure 5.11. SECIS alignment of PA4808/*selA* from *P. aeruginosa* upstream region and *selA* SECIS-like element from *E. coli.*
Mismatches are highlighted in grey and gaps by hyphen (-) symbol.

Alternatively, bioinformatic analysis of the *selA* upstream region of *P. aeruginosa* generated two predicted secondary structures shown in **Figure 5.12** Therefore, this analysis confirms that the sequence before *selA* has the potential of forming a SECIS-like structure. However, it cannot be concluded which structure is the most likely to be formed.

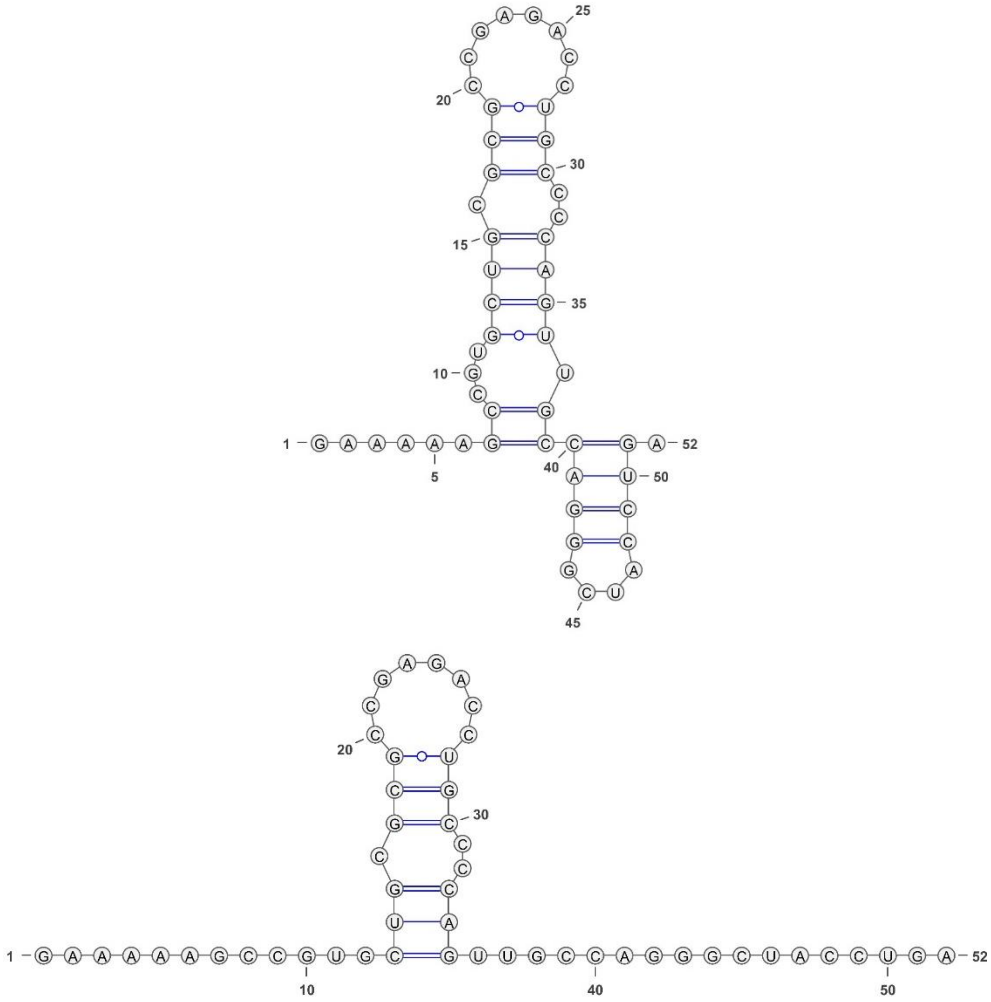


Figure 5.12. *P. aeruginosa* PA4808/*selA* SECIS-like element secondary structure predictions.
The predictions were obtained from the RNA Fold Web server (http://rna.tbi.univie.ac.at/cgi-bin/RNAWebSuite/RNAfold.cgi)(Gruber *et al.*, 2008) in the bracket dot RNA notation form. The secondary structure was visualised using the VARNA Visualization Applet for RNA (http://varna.lri.fr/)(Lorenz *et al.*, 2011).

5.2.2.2 *In silico* characterisation of the suspected *P. aeruginosa* selenoprotein FdoG

Zhang and colleagues (Zhang *et al.*, 2006) identified the sequence of *fdoG* as that encoding the selenoprotein of *P. aeruginosa* (also named as *fdnG/ fdhG*, locus tag: PA4812) which encodes the formate dehydrogenase-O, major subunit. This formate dehydrogenase is encoded next to the *selA-selB* and *selC* (PA4802.1) of *P. aeruginosa*, and the *samA* gene of interest. Analysis of the *fdnG* gene sequence for Sec insertion was carried out next. According to the Pseudomonas Genome DB, formate dehydrogenase-O contains a selenocysteine residue (^{197}U) followed by the bSECIS-binding element (^{198} HGPTVASLAPTF ^{208}) at the N-terminal region (**Figure 5.13**). The potential TAT signal peptide within the *fdhG* sequence was also predicted (Lewenza *et al.*, 2005; Ochsner *et al.*, 2002). Hence, the FdoG

protein localization seems to be extracellular, and it should be secreted by the TAT apparatus (Ochsner *et al.*, 2002).

MDMNRRQFFKVCGIGLGGSSLAALGMAPTEAFADQVRHFKLAHTVETRNTCTYCSVGCGLIMYSQGDGAKNVAQNIIHIEGDA
DHPVNRGTLCPKGAGLLDYIHSPNRLKYPEVREAGSSEWKRIEWDEALERIAKLMKEDRDANFVEKNEQGQTVNRWLTTGFLA
ASASSNEAGYITHKVMRSLGILGFDNQARVIHGPTVASLAPTFGRGAMTNHWTDIKNADLVLIMGGNAAEAHPCGFKWVTEAK
AHNKARLLVVDPRFTRSASVADYYAPIRTGTDIAFLGGLINYLLENDKIQHEYVRNYTDVSFIVKEGFSFEDGLFNGYDAEKR
TYPDKSSWGYEIGEDGYAKVDPTLTHPRCVFNLLKQHYSRYTPDVVSNICGTPKDMMLKVWAEIAETSKPGKVMTIMYALGWT
QHSVGAQMIRTGAMVQLLLGNIGMPGGGMNALRGHSNIQGLTDLGLLSNSLPGYLTLAMDAEQDYDAYIAKRTAKPLRPGQLS
YWQNYGKFHVSLMKAWFGKSATKENNWCYDWLPKLDMPGAGYDVLRYFDMMYQGKVNGYFCQGFNPIASFPNKAKVGAALARL
KWMVVMDPLVTETSEFWRNVGEYNDVDTASIKTTVFRLPTSCFAEEDGSIVNSGRWLQWHWKGAEPPGQARPDIAIMAGLFHR
LREMYRKDGGAFPDPILGLDWSYLKPDEPGPDELAREFNGKALSDLVDPANGMILAKAGEQLPGFALLRDDGSTASGCWIFAG
SWTQQGNQMGRRDNSDPYGMGQTLGWAWAWPANRRILYNRASADVSGKPWDPEKKRLVWWNGKSWGGTDVPDYKADVPPEAGM
NPFIMNPEGVARLFAVDKMAEGPFPEHYEPFETPIGVNPLHRDNRKAISNPAARVFKNDMELFGTADEFPYAATTYRLTEHFH
YWTKHCRLNAITQPEQFVEIGEALAKELGINAGDKVKVSSNRGYIKAVAVVTKRIRPLQVDGKTVHHVGIPIHWGFAGMARNG
FLANTLTPFVGDGNTQTPEFKSFLVNVEKA

Figure 5.13. Primary sequence of the *P. aeruginosa* PA4812/*fdhG* protein.
The PA4812 protein sequence is that of NCBI Reference Sequence WP_010895684, which is ubiquitous among *P. aeruginosa* isolates. Highlighted in green indicates the selenocysteine residue, in yellow the SECIS element, in pink the TAT signal for secretion, and in light blue the cleavage site.

The SECIS elements identified in the *E. coli fdnG, fdhF* and *fdoG* genes encoding for the formate-dehydrogenases were analysed first before proceeding with the analysis of the *fdhG* sequence from *P. aeruginosa*. The SECIS elements have been well studied in *E. coli* therefore, this analysis was aimed to assist in the identification of the *fdoG* gene SECIS element of *P. aeruginosa*.

The *E. coli* SECIS elements *fdnG, fdhF* and *fdoG* were aligned and the results are shown in **Figure 5.14**. The *fdnG* SECIS was 100% identical to the *fdoG* SECIS. Hence, both *fdnG* and *fdoG* SECIS sequences had 74.4% identity and similarity to the *fdhF* SECIS, the gap percentage was 11.6%. Overall, significant sequence conservation could be inferred between the SECIS elements compared.

```
fdnG   1 TGACACGGACCAACGGTAGCAAGTCTTGCTCCAACATTTGGT  42
         ||||||||||||||||||||||||||||||||||||||||
fdoG   1 TGACACGGACCAACGGTAGCAAGTCTTGCTCCAACATTTGGT  42
         ||||||||.|||.||||.|||.||||....|.|.|..|.
fdhF   1 TGACACGGCCCATCGGTTGCAGGTCTGCACCAATCGGTC---  39 (ClustalW)


fdnG   1 TGACACGGACCAACGGTAGCAAGTCTTGCTCCAACATTTGGT- 42
         ||||||||.|||.||||.|||.||| |||.||||   |.|||
fdhF   1 TGACACGGCCCATCGGTTGCAGGTC-TGCACCAA---TCGGTC 39
         ||||||||.|||.||||.|||.||| |||.||||   |.|||
fdoG   1 TGACACGGACCAACGGTAGCAAGTCTTGCTCCAACATTTGGT- 42 (EMBOSS)
```

Figure 5.14. SECIS alignment of the *fdnG*, *fdhF* and *fdoG* genes of *E. coli*, encoding formate dehydrogenase isoenzymes.
Mismatches are highlighted in grey and gaps by hyphen (-) symbol. Two programmes were used, ClustalW (Thompson *et al.*, 1994) and EMBOSS (Rice *et al.*, 2000) with parameters set to default.

To identify the potential secondary structures following the UGA codon in the mRNAs from *fdhF* and *fdoG/fdnG* responsible for the selenocysteine incorporation, bioinformatic and manual analysis of the sequences were performed . The results are shown in **Figure 5.15**. The predicted structures show how two slightly different structures could be employed for selenocysteine addition to protein as long as they are within the consensus structure mentioned in the main text before **Figure 5.2** and as shown in **Figure 5.2**. This analysis also shows how very closely related genes could have different SECIS element to achieve selenocysteine incorporation into protein.

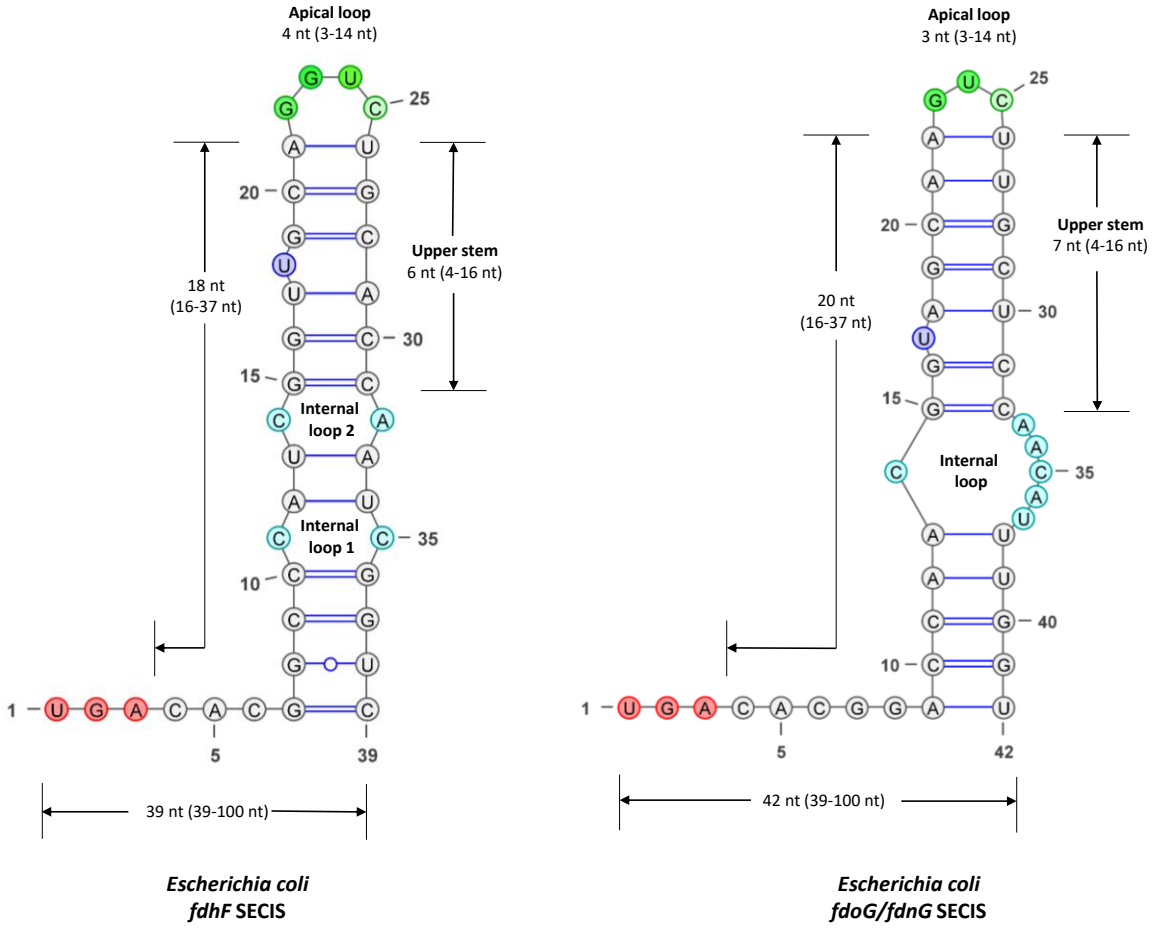


Figure 5.15. *E. coli fdnG*, *fdhF* and *fdoG* SECIS elements secondary structure predictions.
The predictions were obtained from the RNA Fold Web server (http://rna.tbi.univie.ac.at/cgi-bin/RNAWebSuite/RNAfold.cgi)(Gruber *et al.*, 2008) in the bracket-dot RNA notation form. The secondary structure was vizualized using the VARNA Visualisation Applet for RNA (http://varna.lri.fr/)(Lorenz *et al.*, 2011). The Sec-UGA codon is shown in red. The length constraint of each component is shown in a parenthesis on the figure (Zhang and Gladyshev, 2005).

The SECIS element of PA4812/*fdhG* of *P. aeruginosa* was then aligned with the SECIS element of the *E. coli fdoG*-like sequence to assess conservation. The results indicated that the sequences shared 78.6% identity and 78.6% similarity, with 7.1% gaps (**Figure 5.16**).

```
P. aeruginosa fdhG      1 UGACACGGCCCGACGGUGGCAAGUCUUGCCCCGACGUUU---      39
                          |||||||||.||.||||||.||||||||||||.|||.||.|||
E. coli fdoG            1 UGACACGGACCAACGGUAGCAAGUCUUGCUCCAACAUUUGGU      42
```

Figure 5.16. SECIS alignment of PA4812/*fdhG* from *P. aeruginosa* and *fdoG* from *E. coli.*
Mismatches are highlighted in grey and gaps by hyphen (-) symbol. The EMBOSS tool was used (Rice *et al.*, 2000).

To identify and compare the predicted secondary structures of the SECIS element of PA4812/*fdhG* from *P. aeruginosa* and *fdoG* from *E. coli.* These predictions were done manually for the *P. aeruginosa* bSECIS element and by using the RNA Fold Web server (http://rna.tbi.univie.ac.at/cgi-bin/RNAWebSuite/RNAfold.cgi) for the *E. coli* bSECIS element (Gruber *et al.*, 2008). The predicted structures are shown in **Figure 5.17**. As indicated above bSECIS elements share some common sequence and structural features essential for Sec insertion (Heider *et al.*, 1992; Alexander *et al.*, n.d.; Liu *et al.*, 1998; Thanbichler and Bock, 2002)(Zinoni *et al.*, 1990; Thanbichler and Bock, 2002).

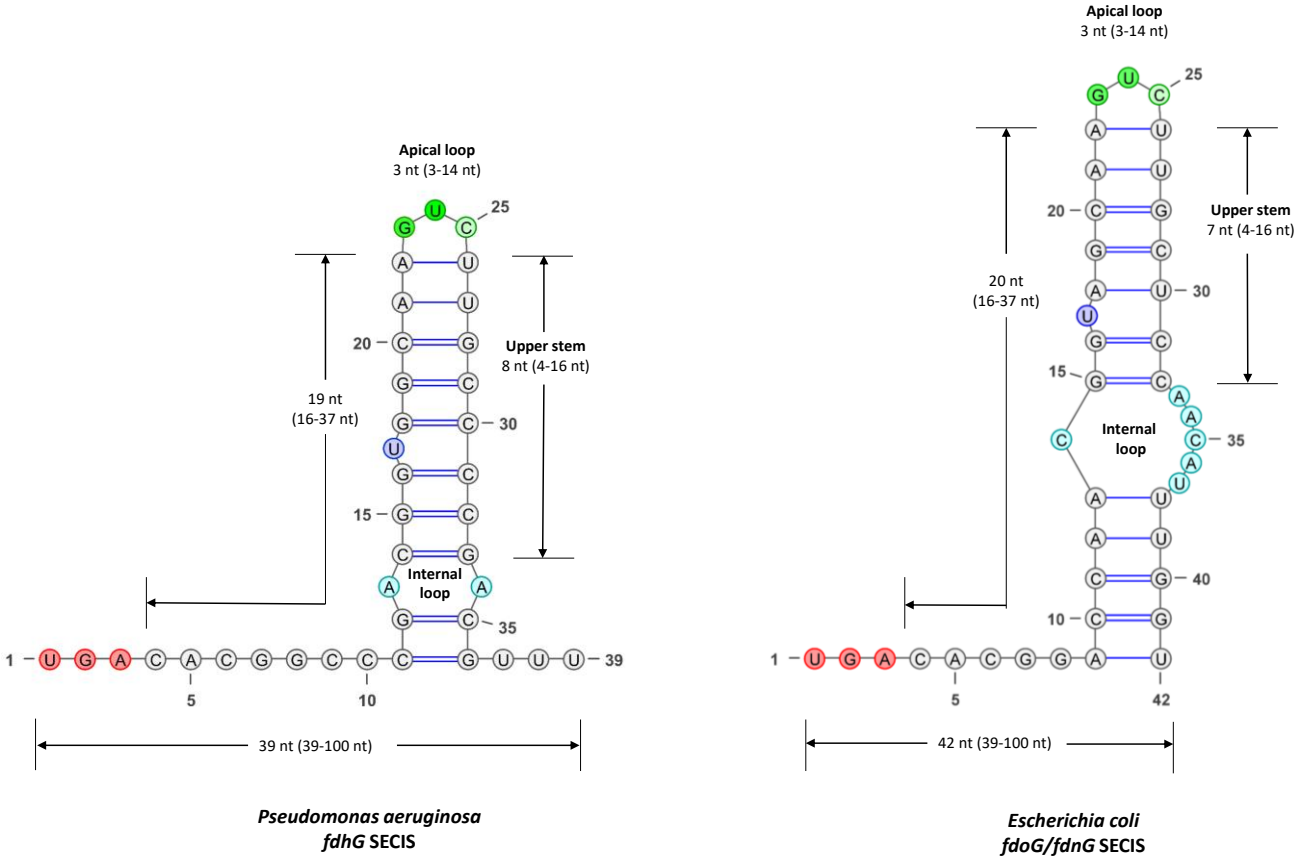


Figure 5.17. Comparison of *P. aeruginosa* PA4812/*fdhG* and *E. coli fdoG* SECIS elements secondary structure predictions.
The Sec-UGA codon is shown in red. Both *fdhG* and *fdoG* SECIS follows the consensus bSECIS model presented by Zhang and Gladyshev; the length constraint of each component is shown in a parenthesis on the figure (Zhang and Gladyshev, 2005) (Zhang and Gladyshev, 2005). The RNA secondary structure was obtained from the VARNA Visualization Applet for RNA (http://varna.lri.fr/)(Lorenz *et al.*, 2011).

This predicted 2D structure analysis revealed several interesting points. Firstly, a fixed spacing of 19 nt (some of them are paired) between the UGA codon and the apical loop (Inouyes, 1993), which exists in both structures (**Figure 5.16**). Secondly, at least one G is present among the first two nucleotides in the apical loop. In some occasions the G is followed with a U, which is supposed to interact with SelB, but this nucleotide is not strictly conserved (Zhang and Gladyshev, 2005; Thanbichler and Bock, 2002)(Fourmy *et al.*, 2002). Lastly, a bulged U is present in the upper stem, positioned at about 17 nucleotides relative to the selenocysteine-encoding UGA codon. However, this feature is absent in most other bSECISes (Alexander *et al.*, n.d.).

The length of the SECIS elements of the *P. aeruginosa fdhG* and the *E. coli fdoG* was 39 nt and 42 nt respectively, which is within the constraints of 39 -100 nt. The distance between the UGA codon and the apical loop observed in both structures was 19 nt, which is well within the 16-37 nt constraint. The apical loop in both structures was 3 nt, which is the minimum length as it can be up to 14 nt

The adjacent stem was 8 nt for *P. aeruginosa* and 7 nt in *E. coli*, respectively. The upper stem is usually 4-16 nt. The two structures did not share other SECIS structural features such as number and composition of internal loops and lower stems. In more detail, the *E. coli* SECIS has an asymmetric internal loop, whereas the *P. aeruginosa* SECIS has a mismatch which may not be considered as an internal loop. Moreover, the *E. coli SECIS* has a lower stem, which is not observed in the *P. aeruginosa* SECIS. However, overall the general key characteristics between the two SECIS elements are being conserved as shown in ***Figure 5.18*.**

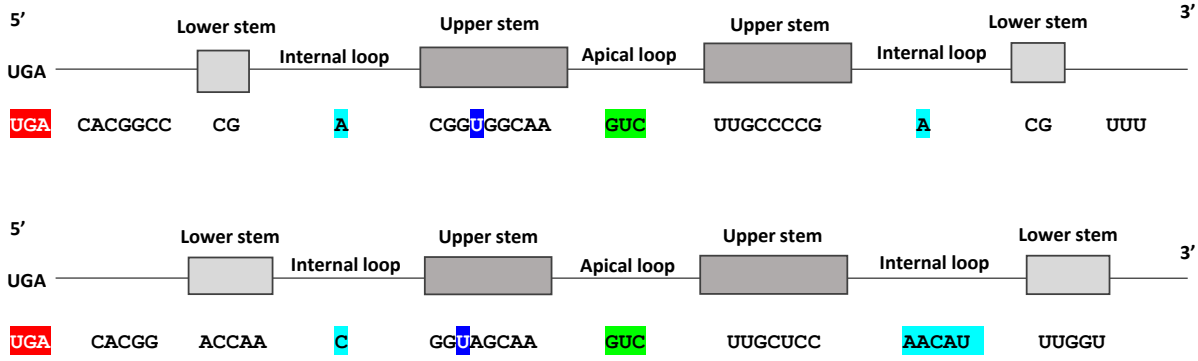


Figure 5.18. SECIS element component organization of the *P. aeruginosa fdhG* gene (upper schematic) and *E. coli fdoG* gene (lower schematic).
Both f*dhG* and *fdoG* genes encode for the selenoprotein formate dehydrogenase-major subunit O. Conserved nucleotides in bacterial SECIS element are highlighted. The UGA codon is highlighted in red, the internal loop nucleotides in light blue, the bulged U base in the upper stem in blue and the apical loop in green. The G of the apical loop is in bold.

The next step was to test the study hypothesis. The FdhG protein in *P. aeruginosa,* encoded by *fdhG/PA4812* was tagged with a hexahistidine tag in order to visualise the protein under different conditions and in different strains. The construction of this strain is decribed in section **2.12.6**. The rationale of this experiment is explained in the Introduction (See Section **5.1.9**) and summarised in **Figure 5.8.** A potential 6XH-FdhG band was found when the wild type was grown in both aerobic and anaerobic conditions full length proteins, with slightly less intense signal in the aerobic fraction. The protein was not found in wt samples which serve as the controls.

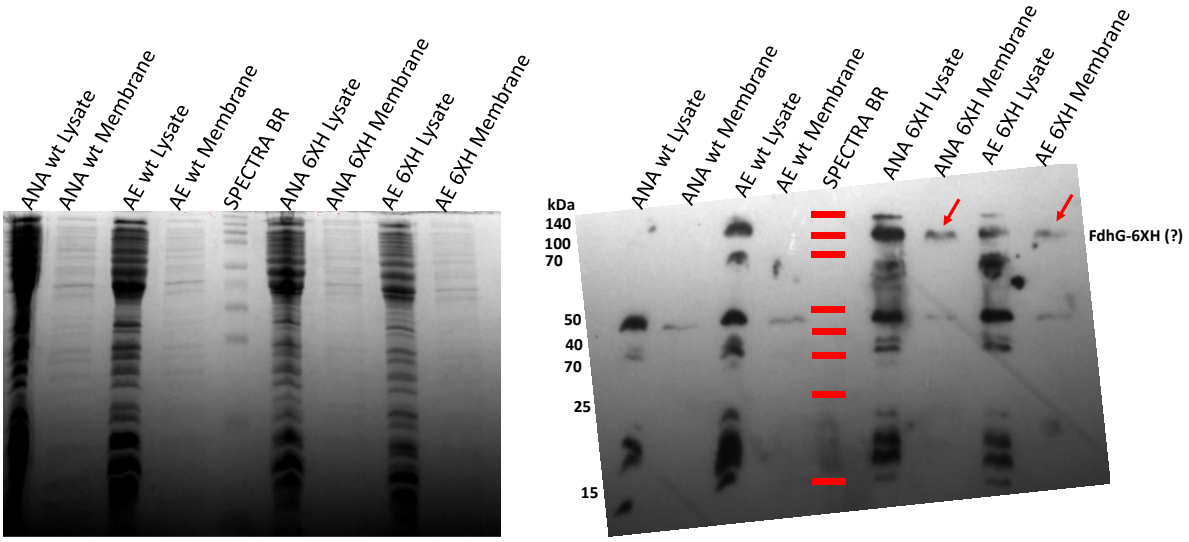


Figure 5.19. SDS-PAGE and Western blot analysis of the chromosomally His-tagged FdhG protein under aerobic and anaerobic conditions.
Whole cells extracts of *P. aeruginosa* were separated to the lysate and membrane fractions for each condition. A Spectra BR molecular weight marker was used indicated on the Western blot as red lines, the sizes are given in kDa. The possible FdhG-6XH bands are pointed by red arrows. ANA; anaerobic conditions, AE; aerobic conditions, 6XH; Strain with chromosomally His-tagged FdhG.

5.3 Discussion

The selenocysteine decoding trait enabling the incorporation of selenocysteine into an UGA codon, was deciphered in the 1960s. In recent years, remarkable progress has been made in understanding the mechanism by which selenocysteine is synthesized and inserted into nascent peptides in mammals (Carlson *et al.*, 2005). However, as noted in the introduction, the Sec-decoding mechanism in *P. aeruginosa* has not yet been described. The studies reported in this chapter aimed to identify all the possible players involved in this mechanism in *P. aeruginosa* based on what was demonstrated in *E. coli* and in mammals.

All components involved in selenoprotein biosynthesis in *E. coli* have been isolated and characterized, and can therefore serve as a paradigm for related systems (Yoshizawa and Böck, 2009). This was the reasoning behind comparing *E. coli* with *P. aeruginosa* sequences throughout this study.

Firstly, a list was compiled (See **Table 5.1**) to show that *samA gene* orthologs in other strains are followed by a $tRNA^{sec}$, with 100 % query cover (the query cover is a number that describes how much of the query sequence is covered by the target sequence.) and identity to the *P. aeruginosa* PA4802.1 $tRNA^{sec}$ sequence. This is particularly encouraging since gene proximity can result in a possible functional link (Junier and Rivoire, 2016).

Secondly, both the $tRNA^{sec}$ DNA sequences from *E. coli* and *P. aeruginosa* PAO1 were compared (**Figure 5.8**) and scored high identity (68.9%) between the two sequences, which suggests high similarity in folding and therefore in function, further supporting the hypothesis under investigation.

In more detail, Identity refers to the percentage of identical residues. Similarity is the percentage of residues conserved with similar physicochemical properties. Both calculations consider the length of the alignment. Commonly, two sequences are considered homologous if they share 30% identity over their entire lengths. However, 30% identity cut-off is not ideal when aligning of short sequences because higher identities result by chance (Pearson, 2013). Therefore the 68.9% value given above suggests the existence of a real functional conservation.

In addition, the alignment has shown that the $tRNA^{sec}$ sequence of *P. aeruginosa* is missing the CCA tail at the end of the sequence. However, this should not have a significant impact since the CCA nucleotides could be added during processing, in which case these would not appear in the tRNA gene sequence (Aebi *et al.*, 1990).

The next step was the bioinformatic analysis of the PA4802.1 ($tRNA^{sec}$) folding, which generated three predicted secondary structures (**Figure 5.9**). The prediction tools used did not take into account the $tRNA^{sec}$ features given by Commans and Böck, which deviate from that of canonical tRNAs (Commans and Böck, 1999)(Commans and Böck, 1999). In more detail, in a $tRNA^{sec}$ the acceptor stem is extended by one base pair (8 bp) compared to 7 bp long acceptor arm of canonical tRNAs. The D-stem should be 6 bp long instead of 3-4 bp long as in canonical tRNAs, which minimizes the D-loop to 4 nucleotides instead of 8-10 nt. The length of both the anticodon and the T-stem is 5 bp. Also, canonical tRNAs can be characterized as Class I if they have short variable sequences (4-5 bp) or Class II if their variable regions are 10-24 bp long. Both the *E. coli* and the *P. aeruginosa* $tRNA^{sec}$ have long variable arms.

In the 2D predictions (**Figure 5.9**, upper structures), the acceptor arm is 5-6 bp long which is not in agreement with the $tRNA^{sec}$ features mentioned. However, the D-stem (Stem D2) is 6 bp long and the D-loop (Loop L2) 4 bp, which agrees with the $tRNA^{sec}$ features mentioned. Taken together, the manual *P. aeruginosa* $tRNA^{sec}$ secondary structure prediction (**Figure 5.9**, lower structure) is preferable over the others as it follows features given by Commans and Böck.

The nucleotides, which indicate the deviation from the canonical tRNAs, are the G9, U14, C15 and G48 in the *E. coli* $tRNA^{sec}$. In the *P. aeruginosa* $tRNA^{sec}$ only C15 and G48 remain the same G9 becames U9 and U14 becomes G14. Therefore, further review of the literature is necessary to identify those nucleotides in the *P. aeruginosa* $tRNA^{sec}$.

The next step was to compare the upstream region of *selA* of *P. aeruginosa* with the *E. coli selA* SECIS-like sequence as an approach to identify the *selA* SECIS-like sequence in *P. aeruginosa* (**Figure 5.10**). Overall, no significant sequence conservation could be inferred in *P. aeruginosa.* Although PA4808/*selA* SECIS-like element secondary structure predictions are shown, the lack of additional information could not provide robust support of one structure over the other. However, this is not a negative finding since SECIS and SECIS-like elements do not often have conservation at the nucleotide sequence but rather at their secondary folding characteristics (Jean-jean *et al.*, 2009).

A study mentioned that FdhA and SelD are the most widespread selenoproteins, and at least one of these proteins was present in each selenoprotein-containing organism. However, Zhang and colleagues (Zhang *et al*., 2006) give the sequence of *fdoG* as the only selenoprotein of *P. aeruginosa*, encoded by the *fdoG gene* (synonym *fdnG*/ *fdhG*, locus tag: PA4812).

Hence, the next regulatory element to be investigated was the SECIS element of the *P. aeruginosa fdnG*, by comparing it with the *E. coli* SECIS elements in *fdhF and fdoG* (**Figure 5.11**). Overall, significant sequence conservation could be inferred between the SECIS elements compared, which is again

encouraging. It is plausible that the high conservation scored could be due to the short length of the query sequence (42 nucleotides)**.** In any case**,** it is of interest to note that SECIS elements in this analysis are quite conserved in contrast to the *selA* SECIS-like element.

The *fdhF* SECIS structure predicted in this study agrees with the one presented in Zinoni *et al*., 1990 (Zinoni *et al.*, 1990). The *fdnG* SECIS sequence is identical to the *fdoG* SECIS sequence, therefore, the folding is identical and agrees with the one presented in by Thanbichler and Bock as well (Thanbichler and Bock, 2002).

However, it is crucial to mention that individual bSECIS elements may have additional functionally important features. Overall, the *P. aeruginosa fdhG* follows the consensus bSECIS structural model and the associated constraints described by Zhang and Gladyshev (**Figure 5.16**) (Zhang and Gladyshev, 2005).

Unfortunately, further investigations of the FdhG selenoprotein that were planned did not progress further than a pilot trial (**Figure 5.19**). The right protein FdhG-HX6 seems to have been identified at full length size in both aerobic and anaerobic samples. However, overloading of the SDS-Page with sample has resulted in multiple bands appearing in the Western blot. If the protein identified is indeed N-terminally hexahistidine-tagged FdhG these results challenge the study hypothesis, as full length protein should be visible only during growth in anaerobic and not in aerobic conditions. This experiment should have been repeated, however, due to time constraints that was not possible.

Finally, it should be emphasized that every selenoprotein is unique, and the specific features of any given selenoprotein in terms of architecture for instance, serve a specific function which in many cases has not yet been discovered (Arnér, 2020)(Arner 2020).

Interestingly, literature on the bacterial Sec-decoding trait does not mention extensively the modifications that occur on the $tRNA^{sec}$ and which should play a role in its maturation. However, there is extensive research on these modifications in the mammalian $tRNA^{sec}$. It is not thought to be a coincidence that a methyltransferase gene is located right next to this highly unique $tRNA^{sec}$ in *P. aeruginosa*. The current hypothesis states that a methylation event is involved in the mechanism of maturation and activation of this $tRNA^{sec}$ and identifying the nucleotides modified is of considerable interest. However, due to time constraints and other unforeseen circumstances the validation of the methylation of the $tRNA^{sec}$ by SamA as well as the identification of the methylated nucleotide could not be carried out during this PhD project.

5.3.1 Future directions

Overall, in this chapter evidence is given to support that all the elements necessary for the Sec-decoding traits identified in *E. coli* are present in *P. aeruginosa* and it is therefore highly likely that this mechanism is also active in this organism as well. Also, SamA appears to have the structure that would allow it to modify a tRNA. However, no other link or proof of interaction could be established between SamA and the *P. aeruginosa* $tRNA^{sec}$.

There were provisions to investigate further the hypothesis and establish directly a link between SamA protein and the $tRNA^{sec}$. However, several unfortunate circumstances did not allow these efforts to continue. A collaboration with Professor Mark Helm, based in Johannes Gutenberg University Mainz in Germany, was initiated. One of the approaches was to analyze the tRNA pool from each of the strains of interest grown under aerobic and anaerobic conditions and obtain the modification profiles (**Figure 5.20**). Comparison of the profiles in between strains and conditions would have shed some light on the hypothesis. Another approach, was to isolate enough $tRNA^{sec}$ and detect its modification, which is a much more direct approach. One of the issues first identified by Prof. Helm was gathering enough $tRNA^{sec}$, as this type of tRNA is rare compared to the rest and not very abundant.

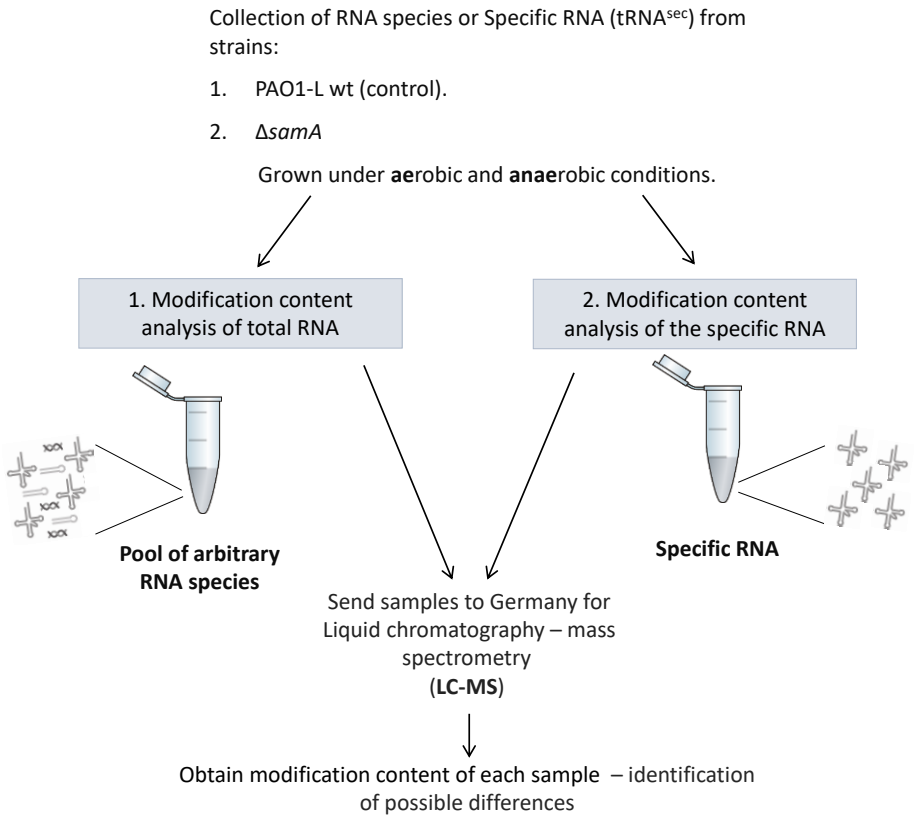


Figure 5.20. Experimental design for the identification of modifications on the specific tRNAsec under investigation.

Liquid chromatography tandem mass spectrometry (LC–MS/MS), was the tool of choice to analyse and gain further understanding of these functions, due to its high sensitivity and accuracy in the detection and quantification of modified nucleosides (Thüring *et al.*, 2016).

The most common techniques are the dynamic multiple reaction monitoring (DMRM) and the neutral loss scan (NLS). Dynamic multiple reaction monitoring (DMRM) enables the highly sensitive analysis of modifications for which the mass transitions and retention times are known (Thüring *et al.*, 2016). In contrast, Neutral loss scans (NLS) enables the analysis of modifications, for which mass transitions and retention time are unknown, and the analysis of novel modified nucleosides. More on the workflow and the use of these technique is given by Thüring and colleagues (Thüring *et al.*, 2016).

Quantitative and qualitative analysis or RNA through a MS-based approach involves total hydrolysis of RNA to nucleosides and subsequent analysis using LC/MS (Meng and Limbach, 2006). However, the above methodology is unable to determine the positions of the modified nucleosides detected, because the sequence context of a modification within the RNA is lost after digestion (Thüring *et al.*, 2016).

A method has been described for sequence mapping of modified nucleosides in transfer RNA, it was used successfully for the sequence specific placement of modified nucleosides in tRNAs obtained from the *Thermus thermophilus* as well as human placenta (Medsker *et al.*, 2016). This approach is able to locate modifications sites-specifically in the tRNA sequence by combining the modified nucleosides profile with the genome-derived tRNA sequence. This approach requires isolation of the tRNA of interest, which, is in turn digested to nucleosides and oligonucleotides. Both samples are analysed by LC-MS/MS and the data sets are then combined to yield the modification profile of the tRNA.

Chapter 6 Impact of *samA* and PA4802.1 on global gene expression in *P. aeruginosa*

6.1 Introduction

The PA4803 (*samA*) gene product has been assigned the predicted function of a methyltransferase due to some conserved residues usually found in the SAM/AdoMet dependent methyltransferases (See Analysis in **Chapter 4**). S-Adenosyl-Methionine (SAM)-dependent methyltransferases superfamily enzymes catalyse transfer of a methyl group from SAM to a variety of substrates such as proteins and nucleic acids (Schubert *et al.*, 2003a) hence the gene was named as *samA*. Interestingly, *samA* is positioned upstream of a unique $tRNA^{Sec}$ in *P. aeruginosa*, transcribed by the PA4802.1 gene in the same orientation. This $tRNA^{Sec}$ is homologous to the *selC* gene in *E. coli* (Commans and Böck, 1999). In the surrounding area are the *selA*, *selB*, *fdhE, fdnGHI* genes, the function of all of which have been demonstrated in *E. coli* (Yoshizawa and Böck, 2009; Berg *et al.*, 1991). In more detail, the *fdnGHI* operon of *E. coli* encodes a nitrate-inducible formate dehydrogenase-N, which is comprised of three subunits: FdnG, FdnH and FdnI, also called the major, beta and gamma subunits, respectively. The *fdnG* mRNA contains a signal for selenocysteine incorporation during protein elongation and also encodes a cysteine cluster, FdnH contains 4 cysteine clusters typical of iron-sulfur centers, and lastly, FdnI encodes a putative unique cytochrome b that absorbs at 556 nm (Fdn556) based on spectral analyses (Berg *et al*., 1991) .

In *E. coli*, selenocysteine incorporation during mRNA translation requires the formation of a quaternary complex between: the dedicated translation elongation factor SelB, GTP, the selenocysteyl-$tRNA^{Sec}$ (product of the *selC* gene) and a structural element of the mRNA termed SECIS (selenocysteine-inserting sequences) (Yoshizawa and Böck, 2009)

The formate dehydrogenase family has a particularly high representation in the selenoproteomes of most organisms investigated (Zhang and Gladyshev, 2005). *E. coli* synthesizes three membrane-bound multi-subunit formate dehydrogenases (Fdh), each comprising of a large catalytic subunit, an electron-transfer subunit and a membrane-anchoring subunit (Soboh *et al.*, 2011). The large subunit contains both a selenocysteine residue and a molybdenum cofactor, which are crucial for catalysis. In *E. coli* the three Fdh enzymes are called FdhH (involved in hydrogen production), FdhN (involved in anaerobic respiration on nitrate) and FdhO (involved in aerobic respiration on oxygen) (Hartwig *et al.*, 2015).

The prokaryotic and eukaryotic Sec[Ser]-tRNA^{Sec} (See more in **Chapter** 5) have additional features that distinguish them from all other tRNAs (Hatfield and Gladyshev, 2002). In mammals the Sec[Ser]-tRNA^{Sec} consists of two isoforms that differ from each other by a single modification at the uridine at position 34, which is the wobble nucleotide of the anticodon (Diamond *et al.*, 1993; Schoenmakers *et al.*, 2016). Both isoforms are methylcarboxy-methyl-5' derivatives of uridine (mcm5U), but one is further methylated at the 2'-O-hydroxyl site of the ribosyl moiety (producing mcm5Um)(Moustafa *et al.*, 2001; Diamond *et al.*, 1993). This last methylation step in the maturation of Sec[Ser]-tRNA^{Sec} (designated Um34), is a highly specialised process, requiring pre-maturation of the tRNA and the presence of selenium (Moustafa *et al.*, 2001). Modification of this position has the ability to stabilize the anticodon (Hori, 2017). Each isoform is individually involved in the synthesis of one of the two subclasses of selenoproteins, designated housekeeping and stress-related selenoproteins (Kim *et al.*, 2011; Schoenmakers *et al.*, 2016).

It is here hypothesized that the mechanism of selenocysteine addition to protein in *P. aeruginosa* is an intermediate step in the adaptation process to environmental changes as it occurs in *E. coli* and mammalian cells. In more detail, the FdhG is the only stress-related selenoprotein in *P. aeruginosa* (See **Chapter 5**) and its homologue in *E. coli* is involved in adaptation to anaerobic respiration, with a methylation event being critical for its production as shown in mammalian cells (Diamond *et al.*, 1993).

Based on the above hypothesis, it is expected that in *P. aeruginosa*, growing under anaerobic conditions, SamA methylates the Sec[Ser]-tRNA^{Sec} (encoded by PA4802.1) in the proximity of the anticodon. This modification is considered as a maturation step that changes the tRNA^{Sec} tertiary structure, which in turn enables the translation of the *fdnGHI* genes (Berg *et al*., 1991). As mentioned above, the *fdnG* gene product in *P. aeruginosa* is expected to help the bacteria to switch from aerobic to anaerobic growth rapidly. It is therefore postulated that if the SamA methylase is absent, then the unmodified Sec[Ser]-tRNA^{Sec} will not be able to drive translation of this multiprotein complex, and the switch to anaerobic respiration will be perturbed.

The work described in this chapter aimed to explore the profile of Differentially Expressed Genes (DEGs), as assessed by RNA-seq, of cultures of the widely used strain PAO1-Lausanne (PAO1-L) growing exponentially. Specifically, sequences of the total mRNA from a PA4803 (*samA)* deletion mutant ((ΔPA4803)(*ΔsamA*)) and PA4802.1 deletion mutant (ΔPA4802.1) strains, when grown aerobically and anaerobically in the presence of nitrate. In order to establish the effect of these conditions on PAO1-L transcriptome the aforementioned mutant strains were compared to the wild type strains.

Previous work in this study demonstrated that *samA* might be involved in a variety of regulating pathways (See **Chapter 3**), many of which are implicated in the virulence of *P. aeruginosa*. As far as the PA4802.1 gene is concerned, a role in anaerobic adaptation of *P. aeruginosa* is expected, as mentioned above. However, the extent of the *samA* and PA4802.1 regulons are unknown. Hence, transcriptional profiling via RNA-Seq was attempted in order to achieve this.

6.1.1 Aims of this research

The aims of this study were to unravel the roles of PA4803 (*samA*) and PA4802.1 *in P. aeruginosa*, defining their potential regulons, under aerobic and anaerobic conditions. More specifically,

The two main objectives were:

- To use transcriptomics to determine if there is a link between *samA* and PA4802.1.
- To use transcriptomics to uncover novel regulatory networks that *P. aeruginosa* uses when switching from aerobic to anaerobic growth and *vice versa*.

6.2 Results

The collection of all the transcripts in a population of cells at certain stage of growth and under particular environmental conditions can be identified by RNA sequencing via Illumina platforms, based on a sequencing by synthesis mechanism. Transcriptomic analysis helps to study distinct cell populations and identify differentially expressed genes between them. Firstly, the original image data file from high-throughput sequencing is transformed into sequenced reads (called Raw Data or Raw Reads) by CASAVA base recognition (Base Calling). Raw data are stored in FASTQ (fq) format files, which contain sequences of reads and corresponding base read quality.

The sequenced reads/raw reads often contain low quality reads or reads with adaptors, which will affect the quality of downstream analysis. Therefore, Quality Control (QC) in every step is crucial, data filtering is required to avoid those raw reads and get the clean reads. For example, reads with adaptor contamination are removed. Every strain tested was sent to the company in biological triplicates (Sample names on **Table 6.1** were used for identification purposes but they are not needed for the purpose of understanding the analysis). The Data Quality Control Summary is provided on the table below as it was provided by Novogene Co Ltd (**Table 6.2**)

Table 6.1. Strain nomenclature.

Sample name	Sample strain	Sample name	Sample strain
ICA11[a]	*P. aeuriginosa* PAO1-L wt, clone a, aerobic conditions	ICN11	*P. aeuriginosa* PAO1-L wt, clone a, anaerobic conditions
ICA12	*P. aeuriginosa* PAO1-L wt, clone b, aerobic conditions	ICN12	*P. aeuriginosa* PAO1-L wt, clone b, anaerobic conditions
ICA13	*P. aeuriginosa* PAO1-L wt, clone c, aerobic conditions	ICN13	*P. aeuriginosa* PAO1-L wt, clone c, anaerobic conditions
ICA21	*P. aeuriginosa* PAO1-L ΔPA4802.1, clone a, aerobic conditions	ICN21	*P. aeuriginosa* PAO1-L ΔPA4802.1, clone a, anaerobic conditions
ICA22	*P. aeuriginosa* PAO1-L ΔPA4802.1, clone b, aerobic conditions	ICN22	*P. aeuriginosa* PAO1-L ΔPA4802.1, clone b, anaerobic conditions
ICA23	*P. aeuriginosa* PAO1-L ΔPA4802.1, clone c, aerobic conditions	ICN23	*P. aeuriginosa* PAO1-L ΔPA4802.1, clone c, anaerobic conditions

ICA31	*P. aeuriginosa* PAO1-L Δ*samA*, clone a, aerobic conditions	ICN31	*P. aeuriginosa* PAO1-L Δ*samA*, clone a, anaerobic conditions
ICA32	*P. aeuriginosa* PAO1-L Δ*samA*, clone b, aerobic conditions	ICN32	*P. aeuriginosa* PAO1-L Δ*samA*, clone b, anaerobic conditions
ICA33	*P. aeuriginosa* PAO1-L Δ*samA*, clone c, aerobic conditions	ICN33	*P. aeuriginosa* PAO1-L Δ*samA*, clone c, anaerobic conditions

[a]Sample names on Table 6.1 and Table 6.2 were used for identification purposes but they are not needed for the purpose of understanding the analysis.

Table 6.2. Data Quality Control Summary.

Sample name	Raw reads	Clean reads	Raw bases	Clean bases	Error rate(%)	Q20(%)	Q30(%)	GC content(%)
ICA11	8997509	8934596	2.7	2.7	0.03	97.6	93.41	62.19
ICA12	10035332	9969873	3	3	0.03	97.41	92.98	62.31
ICA13	8703703	8622434	2.6	2.6	0.03	97.73	93.65	62.29
ICA21	9467943	9408869	2.8	2.8	0.03	97.61	93.4	62.63
ICA22	8745051	8676343	2.6	2.6	0.02	98.02	94.22	62.36
ICA23	7052748	6992188	2.1	2.1	0.02	98.35	95.02	62.36
ICA31	9966360	9916967	3	3	0.03	97.97	94.11	62.2
ICA32	8567683	8523879	2.6	2.6	0.03	97.44	93.02	62.28
ICA33	10448951	10396771	3.1	3.1	0.03	97.6	93.39	61.85
ICN11	8639775	8602616	2.6	2.6	0.03	97.13	92.57	61.33
ICN12	9342319	9298416	2.8	2.8	0.03	97.28	92.75	61.36
ICN13	11566479	11499660	3.5	3.4	0.03	97.59	93.43	61.68
ICN21	9711606	9656154	2.9	2.9	0.03	97.31	92.86	60.91
ICN22	9057718	9009920	2.7	2.7	0.03	97.4	93.07	61.04
ICN23	9105239	9023368	2.7	2.7	0.03	97.3	92.89	60.69
ICN31	9076590	9023496	2.7	2.7	0.03	97.15	92.65	61.34
ICN32	7207232	7166669	2.2	2.2	0.03	97.55	93.24	61.47
ICN33	6952993	6917054	2.1	2.1	0.03	97.59	93.35	61.6

(1) Sample name: sampleID; (2) Raw reads: reads count from the raw data, four rows as an unit, with statistics of reads count for every sequencing; (3) Clean reads: Clean data is reads count filtered from raw data. Statistics method is similar with raw reads. All the following analysis is based on clean data; (4) Raw bases: Base number of raw data. (number of raw reads) * (sequence length), converting unit to G; (5) Clean bases: Base number of raw data after filtering. (number of clean reads) * (sequence length), converting unit to G; (6) Error rate(%): base error rate of whole sequencing; (7) Q20(%): Phred values greater than 20 base number contain the percentage of total bases. (Base number of Phred value > 20) / (Total base number)*100; (8) Q30(%): Phred values greater than 30 base number contain the percentage of total bases. (Base number of Phred value > 30) / (Total base number)*100; (9) GC content(%): The percentage of G&C base numbers of total bases.(G&C base number) / (Total base number)*100.

The next step was mapping the reads to a reference genome, which in this study was the approximate genome sequence of PAO1-N as described in Romero *et al.* 2018 (Romero *et al.*, 2018) and which essentially consists of the reference genome of subline PAO1-UW (Stover *et al.*, 2000) with the addition of Region of Genomic Plasticity 42 (RGP42)(Klockgether *et al.*, 2010; Mathee *et al.*, 2008). An algorithm for this process is chosen according to the characteristics of the reference genome (**Table 6.3**). In general, the total mapped rate should be more than 70%, and the percentage of reads that can be mapped to multiple sites in the reference genome should be less than 10%, if there is no contamination and a correct reference genome is chosen.

Table 6.3. Overview of Mapping Status.

Aerobic samples									
Sample_name	**ICA11**	**ICA12**	**ICA13**	**ICA21**	**ICA22**	**ICA23**	**ICA31**	**ICA32**	**ICA33**
Total reads	17869192	19939746	17244868	18817738	17352686	13984376	19833934	17047758	20793542
Total mapped reads	17762888	19824371	17148168	18301321	17197630	13823536	19704692	16914357	20184546
Uniquely mapped reads	17383132	19397810	16767743	17849338	16866029	13593120	19361157	16558192	19565162
Multiple mapped reads	379756	426561	380425	451983	331601	230416	343535	356165	619384
Total mapping rate	99.41%	99.42%	99.44%	97.26%	99.11%	98.85%	99.35%	99.22%	97.07%
Uniquely mapping rate	97.28%	97.28%	97.23%	94.85%	97.20%	97.20%	97.62%	97.13%	94.09%
Multiple mapping rate	2.13%	2.14%	2.21%	2.40%	1.91%	1.65%	1.73%	2.09%	2.98%
Anaerobic samples									
Sample_name	**ICN11**	**ICN12**	**ICN13**	**ICN21**	**ICN22**	**ICN23**	**ICN31**	**ICN32**	**ICN33**
Total reads	17205232	18596832	22999320	19312308	18019840	18046736	18046992	14333338	13834108
Total mapped reads	17067325	18213888	22830647	19092030	17879365	17893645	17915983	14241941	13737517
Uniquely mapped reads	16671183	17830403	11260977	18772975	17603536	17586835	17514998	13993757	13516410
Multiple mapped reads	396142	383485	11569670	319055	275829	306810	400985	248184	221107
Total mapping rate	99.20%	97.94%	99.27%	98.86%	99.22%	99.15%	99.27%	99.36%	99.30%
Uniquely mapping rate	96.90%	95.88%	48.96%	97.21%	97.69%	97.45%	97.05%	97.63%	97.70%
Multiple mapping rate	2.30%	2.06%	50.30%	1.65%	1.53%	1.70%	2.22%	1.73%	1.60%

(1) Total reads: total number of filtered reads (Clean data); (2) Total mapped reads: total number of reads mapped to the reference genome; (3) Uniquely mapped reads: number of reads uniquely mapped to the reference genome; (4) Multiple mapped reads: number of reads mapped to multiple sites in the reference genome; (5) Total mapping rate: the mapping rate of total reads mapped to the reference genome. In general, this number should be larger than 70% when there is no contamination and the correct reference genome is chosen; (6) Uniquely mapping rate: the uniquely mapping rate of mapped to the reference genome; (7) Multiple mapping rate: the multiple mapping rate of mapped to the reference genome. This number is usually less than 10% of the total.

Mapped regions in the reference genome were classified based on the structural annotation of the reference genome and then visualization of Mapping status of the reads became available by providing files in BAM format, a standard file format. Then the BAM files were used in a software such as DeSeq2 in order to obtain differential expression data. More about the next steps of the process followed in this study can be found in **Chapter 2, section 2.15.5**.

Estimated Fold-change (FC) was assessed by the level of expression of the genes, DEGs were considered significantly regulated with at least $\log_2$(FC) value > 1 and with Benjamini-Hochberg adjusted *p* value <0.05. The total number of genes found affected, either downregulated or upregulated in every condition are summarised in **Table 6.4**.

Table 6.4. Numbers of DEGs affected in each comparison between strains, performed by RNA-seq.

Gene PA4803/*samA*	Genes per List DOWN	UP	Gene PA4802.1	Genes per list DOWN	UP
Main comparisons			**Main comparisons**		
Δ*samA*[a] vs WT aerobic conditions	107	174	ΔPA4802.1 vs WT aerobic conditions	38	48
Δ*samA*[a] vs WT anaerobic conditions	877	676	ΔPA4802.1 vs WT anaerobic conditions	5	2
Supporting comparisons			**Supporting comparisons**		
WT aerobic vs WT anaerobic conditions	462	737	WT aerobic vs WT anaerobic conditions	462	737
Δ*samA* aerobic vs Δ*samA* anaerobic conditions	787	828	ΔPA4802.1 aerobic vs ΔPA4802.1 anaerobic conditions	683	789

[a] The *samA mutant (Δ*samA) strain is in reality in *Pseudomonas aeruginosa* PAO1-Nottingham strain background and not PAO1-Lausanne, as it was discovered by RNA-seq in Chapter 6.

The Supporting comparisons: (1) WT aerobic vs WT anaerobic conditions, (2) Δ*samA* aerobic vs Δ*samA* anaerobic conditions and (3) ΔPA4802.1 aerobic vs ΔPA4802.1 anaerobic conditions, were performed to allow exclusion of genes that were found differentially expressed due to the presence or absence of oxygen. This enabled a focus on uncovering those genes affected by the deletion of *samA* and PA4802.1 genes.

6.2.1 Impact of *samA* on global gene expression in *P. aeruginosa* grown under aerobic and anaerobic conditions

The volcano plots (**Figure 6.1**) resulting from the RNAseq display the pattern of gene expression values resulting from the comparison of *ΔsamA* (ΔPA4803) vs WT strains grown under aerobic and anaerobic

conditions. There is a tendency for DEGs with higher values under anaerobic conditions compared to aerobic conditions.

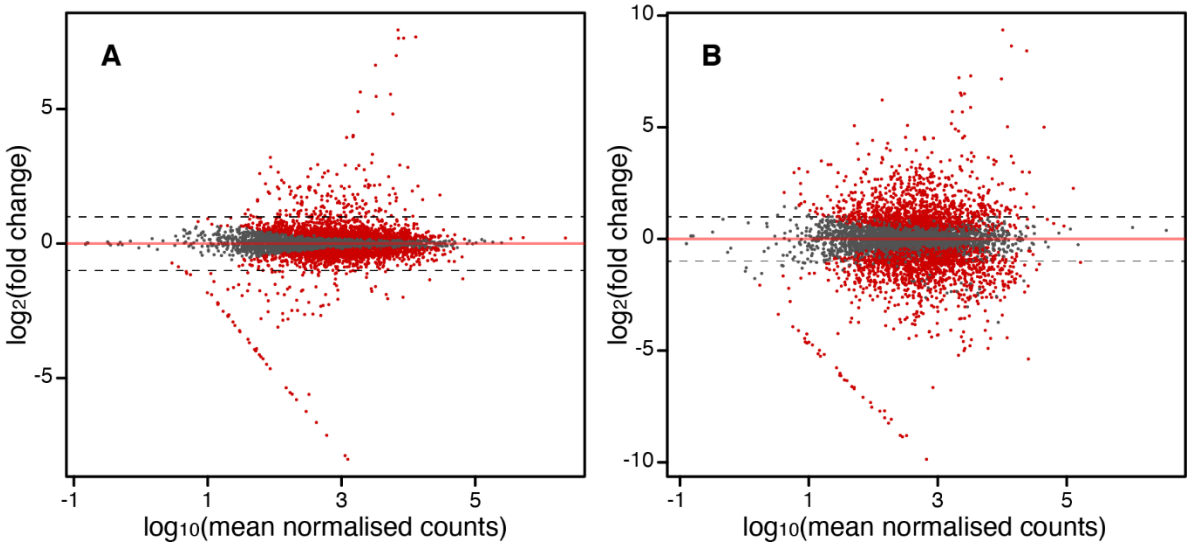


Figure 6.1. Volcano plot of RNA-seq transcriptome data displaying the pattern of gene expression values for Δ*samA*. The comparison is relative to WT strain under aerobic (A panel) and anaerobic (right B panel) conditions. Significantly differentially expressed genes (p <0.05) are highlighted in red. Grey coloured points show genes that have a fold-change less than 2 (log_2 = 1). Thresholds of genes having 2-fold changes in RNA abundance, either increased (positive values) or decreased (negative values) in the mutant compared to the WT are indicated by the dashed lines. The *samA mutant (Δ*samA) strain is in reality in *Pseudomonas aeruginosa* PAO1-Nottingham strain background and not PAO1-Lausanne, as it was discovered by RNA-seq in Chapter 6.

6.2.1.1 Impact of *samA* on global gene expression in *P. aeruginosa* by RNA-seq grown under aerobic conditions.

According to the DeSeq2 data obtained from gene expression level analysis, a total of 281 significantly differentially expressed genes (DEGs) with log_2 (FoldChange) value > 2 and p-value < 0.05 were identified between *P. aeruginosa ΔsamA* vs WT strains under **aerobic conditions**. Specifically, there were 174 down regulated genes 107 upregulated genes and in *ΔsamA* sample vs WT sample.

During the RNA-seq experiment, it was uncovered that the *ΔsamA* strain was not in the PAO1-L background as initially thought but in PAO1-Nottingham (PAO1-N). However, as data of aerobically grown *P. aeruginosa* PAO1-N was already available in the laboratoy, this allowed the subline specific genes to be identified and removed from the initial list of DEGs. The author would like to acknowledge Maria Papangeli for giving permission to use her data for this analysis.

An additional analysis was performed to further reduce the number of differentially expressed genes to only those candidates that were affected by the specific gene deletion (**Figure 6.2**). In more detail, the four comparisons obtained by RNA-seq concerning the ***samA*** gene, which are shown in **Table 6.4**

were analysed using a Venn diagram (**Figure 6.2**). The reasoning was to enable the identification of genes affected (downregulated or upregulated) by the deletion *sam*A under **aerobic conditions**, differentiating them from those affected solely by the transition from aerobic to anaerobic conditions. Only certain areas from the 15 areas created by the Venn diagram were chosen for this purpose aand are **highlighted in red** as shown on **Figure 6.2**. The chosen categories are listed below:

- Genes affected by the deletion in **aerobic** conditions.
- Genes affected by the deletion in **anaerobic** conditions.
- Genes affected by oxygen in the mutant.
- Genes affected by the deletion in **aerobic** conditions and the deletion in **anaerobic** conditions.
- Genes affected by the deletion in **aerobic** conditions and oxygen in the mutant.
- Genes affected by the deletion in **anaerobic** conditions and oxygen in the mutant.
- Genes affected by the deletion in **aerobic** conditions, the deletion in **anaerobic** conditions and oxygen in the mutant.

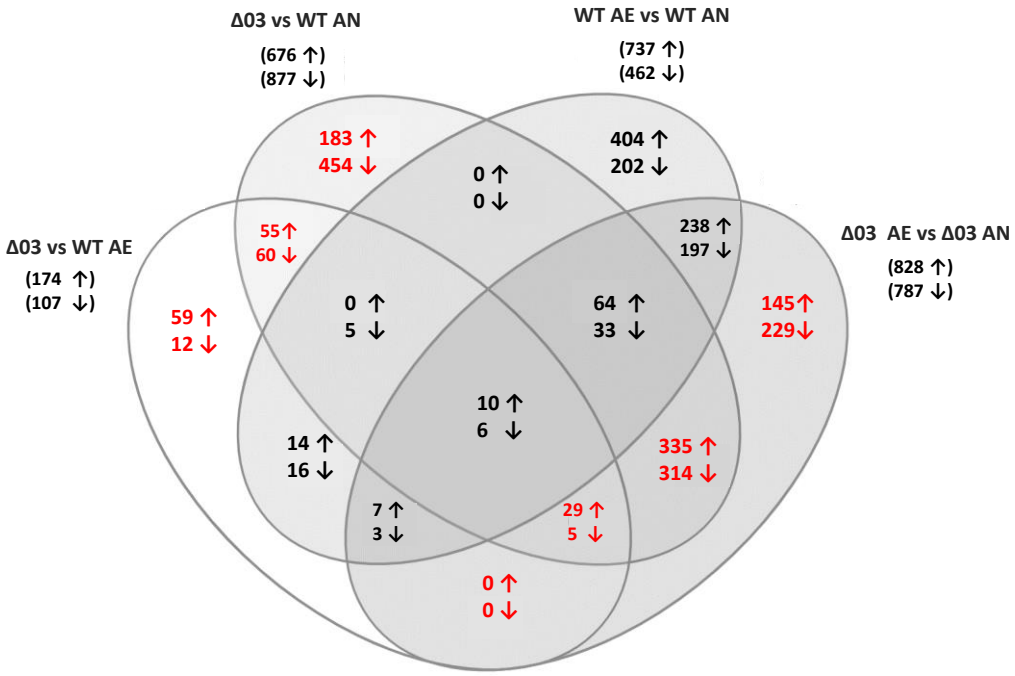


Figure 6.2. Venn diagram showing the overlap of DEGs among the four comparisons.
The *samA* in this schematic depicted as Δ03 for simplification purposes. Upregulated genes are depicted with an arrow going upwards next to the number. Downregulated genes are depicted with an arrow going downwards next to the number. The areas that contain red font are the areas chosen to identify genes affected solely by the deletion of *samA* (in this schematic depicted as Δ03). AE; aerobic, AN; anaerobic.

6.2.1.1.1 Identification of Downregulated DEGs by *samA* deletion under aerobic conditions

The deletion of *samA* results in downregulation of 11 genes (excluding PA4803 (*samA*)) in total listed in **Table 6.5** under **aerobic conditions.**

Table 6.5. Summary of genes found downregulated due to samA deletion under aerobic conditions.

GeneID	log2(FC)	P-adj	Gene name	Gene Ontology (GO)
PA4803	-5.60	$3E^{-131}$	*samA*	hypothetical protein
PA1719	-1.75	$5.24E^{-11}$	*pscF*	type III export protein PscF
PA1718	-1.41	0.000113	*pscE*	type III export protein PscE
PA0958	-1.34	$2.85E^{-83}$	*oprD*	Basic amino acid, basic peptide and imipenem outer membrane porin OprD precursor
PA5471.1	-1.18	$1.82E^{-17}$		PA5471 leader peptide
PA5471	-1.12	$4.08E^{-33}$	*armZ*	ArmZ
PA4307	-1.11	$4.43E^{-25}$	*pctC*	chemotactic transducer PctC
PA1699	-1.11	0.003047	*pcr1*	Pcr1
PA5139	-1.09	$3.96E^{-21}$		hypothetical protein
PA4892	-1.06	$1.6E^{-06}$	*ureF*	urease accessory protein UreF
PA0616	-1.05	$3.64E^{-21}$		hypothetical protein
PA0911	-1.03	$4.27E^{-07}$	*alpE*	AlpE

Firstly, *samA* was downregulated -48.5 fold (-5.60 log2) as expected since this gene was deleted in the strain under investigation.

The PA1718 type III export protein PscE and PA1719/pscF type III export protein PscF, were also downregulated. Type III secretion systems (T3SS) are employed to inject toxins directly into the cytoplasm of target cells and therefore play a key role in the pathogenicity of many Gram-negative bacteria. Both, PscE and PscF are part of the PscE-PscF-PscG complex which controls Type III secretion and needle biogenesis in *P. aeruginosa*, with PscF being the main component of needle (Quinaud *et al.*, 2005).

Furthermore, the PA1699 (*pcr1*) gene involved in T3 Secretion (T3S) was also downregulated. Pcr1 specifically interacts with PopN, and they form a complex that functions as a T3SS repressor. Both PopN and Pcr1 are secreted in a T3 secretion-dependent manner, which implies that these components may hold regulatory roles in controlling this mechanism (Yang *et al.*, 2007).

The PA0958 (*oprD*) precursor was found downregulated. In a study, OprD was found localized on the outer membrane of *P. aeruginosa* and it was also found in abundance in the biofilm matrix. In addition,

it was also associated with outer membrane vesicles, which are spherical bilayered phospholipid nanostructures, which various Gram-negative bacteria secrete in the environment. They have important biological functions and contribute to pathogenesis (Toyofuku *et al.*, 2012).

Moreover, both the PA5471 and PA5471.1 were found downregulated. PA5471 was previously shown to be required for upregulation of the *mexXY* genes during exposure to ribosome inhibitors(Caughlan *et al.*, 2009). The MexXY multidrug efflux pump is responsible for the majority of intrinsic aminoglycoside resistance observed in *P. aeruginosa*. Further studies revealed that PA5471 is implicated in the control of *mexXY* expression, as an anti-repressor hence the name ArmZ (for anti-repressor MexZ). The interaction between MexZ and ArmZ was confirmed using a bacterial 2-hybrid assay (Hay *et al.*, 2013).

The PA4307 (*pctC*) gene was also downregulated. Both PctC and PctB are chemotactic transducers in *P. aeruginosa* and respond to seven L-amino acids (alanine, arginine, glutamate, glutamine, lysine, methionine and tyrosine) and two D-amino acids (histidine and proline) when present in the environment (Shitashiro *et al.*, 2005)(Taguchi *et al.*, 1997).

Furthermore, the PA0911 (*alpE*) gene was downregulated. AlpE is encoded by the *alpBCDE* lysis locus and is a part of a potential Programmed Cell Death (PCD pathway) in *P. aeruginosa*. Activation of the system can occur in response to DNA damage inflicted by the host immune system, and seems to enhance the ability of the bacterial population as a whole to cause disease in a lung infection model (McFarland *et al.*, 2015).

6.2.1.1.2 Identification of Upregulated DEGs by *samA* deletion under aerobic conditions

The *samA* gene deletion results in upregulation of 104 genes under **aerobic** conditions. The genes selected out of the 104 are listed on **Table 6.6**.

Table 6.6. Summary of genes found upregulated due to *samA* deletion under aerobic conditions.

GeneID	log2(FC)	P-adj	Gene name	Gene Ontology (GO)
PA0999	1.228825	$3.97E^{-43}$	*pqsD; fabH1*[a]	3-oxoacyl-[acyl-carrier-protein] synthase III
PA2385	2.065084	$2.69E^{-30}$	*pvdQ*	3-oxo-C12-homoserine lactone acylase PvdQ
PA2386	2.699838	$9.08E^{-87}$	*pvdA*	L-ornithine N5-oxygenase
PA2391	1.010164	$2.47E^{-12}$	*opmQ*	probable outer membrane protein precursor
PA2392	1.22814	$9.15E^{-12}$	*pvdP*	PvdP
PA2393	2.263022	$5.76E^{-30}$		putative dipeptidase
PA2394	1.052717	$1.05E^{-08}$	*pvdN*	PvdN
PA2395	1.952861	$4.51E^{-27}$	*pvdO*	PvdO

PA2396	1.336834	$3.7E^{-28}$	*pvdF*	pyoverdine synthetase F
PA2397	1.011196	$3.82E^{-09}$	*pvdE*	pyoverdine biosynthesis protein PvdE
PA2398	1.711973	$1.92E^{-54}$	*fpvA*	ferripyoverdine receptor
PA2399	1.041369	$5.38E^{-19}$	*pvdD*	pyoverdine synthetase D
PA2400	1.04514	$8.38E^{-26}$	*pvdJ;*	PvdJ
PA2402	1.365285	$7.03E^{-48}$	*pvdI*	pyoverdine peptide synthetase
PA2403	1.765136	$3.99E^{-67}$	*fpvG*	FpvG
PA2404	1.712775	$1.78E^{-23}$	*fpvH*	FpvH
PA2405	1.663103	$2.89E^{-15}$	*fpvJ*	FpvJ
PA2406	1.784592	$7.96E^{-27}$	*fpvK*	FpvK
PA2407	1.629702	$3.11E^{-36}$	*fpvC*	FpvC
PA2408	1.371642	$1.03E^{-30}$	*fpvD*	FpvD
PA2409	1.721088	$1.22E^{-33}$	*fpvE*	FpvE
PA2410	1.483568	$7.63E^{-43}$	*fpvF*	FpvF
PA2411	2.482698	$4.17E^{-63}$		probable thioesterase
PA2413	1.836191	$4.92E^{-26}$	*pvdH*	L-2,4-diaminobutyrate:2-ketoglutarate 4-aminotransferase, PvdH
PA2424	2.116248	$7.1E^{-102}$	*pvdL*	PvdL
PA2425	2.221843	$3.88E^{-18}$	*pvdG*	PvdG
PA2426	1.633286	$2.51E^{-09}$	*pvdS*	sigma factor PvdS
PA3058	1.436914	$2.39E^{-22}$	*pelG*	PelG
PA3059	2.110022	$2.84E^{-54}$	*pelF*	PelF
PA3060	1.115231	$1.52E^{-12}$	*pelE*	PelE
PA3061	2.046602	$1.99E^{-48}$	*pelD*	PelD
PA3062	2.106054	$7.05E^{-32}$	*pelC*	PelC
PA3064	1.583131	$8.79E^{-39}$	*pelA*	PelA
PA4210	2.102832	$1.7E^{-23}$	*phzA1*	probable phenazine biosynthesis protein
PA4211	2.935785	$2.1E^{-103}$	*phzB1*	probable phenazine biosynthesis protein
PA4624	1.825967	$6.88E^{-95}$	*cdrB*	cyclic diguanylate-regulated TPS partner B, CdrB
PA4625	1.486173	$4.3E^{-99}$	*cdrA*	cyclic diguanylate-regulated TPS partner A, CdrA

[a] In various cases one PA number has been given 2 or even 3 different names in the literature, which are all given on the above table under “gene name” separated by a Semicolon.

Numerous genes involved in pyoverdine (PVD) synthesis were found upregulated in this analysis. Pyoverdines or pseudobactins are yellow-green siderophores secreted by fluorescent pseudomonads. Siderophores are iron chelators produced by bacteria to access iron, which is an essential nutriment. Pyoverdine, the major siderophore produced by *P. aeruginosa* PAO1, consists of a fluorescent chromophore linked to an octapeptide. At first, six genes that encode proteins required for pyoverdine synthesis (*pvd* genes) in *P. aeruginosa* strain PAO1 were identified, their expression required an

alternative sigma factor PvdS. However, eight new *pvd* genes were identified as well (Cunliffe *et al.*, 1995; Lamont and Martin, 2003). It is obvious that several clusters and their gene products are involved in the biosynthesis of pyoverdine and not all of them will be discussed here. For example, the *pvdF* gene product catalyses the formylation of N5 -hydroxyornithine to give N5 -formyl-N5 -hydroxyornithine, which is present in the type I pyoverdine (pyoverdinePAO) made by *P. aeruginosa* PAO1 (McMorran *et al.*, 2001).

FpvA is also important as it acts as an outer membrane transporter, which transports the ferric form of PVDI from the extracellular environment into the periplasm (Ganne *et al.*, 2017). Overall, there is a requirement for the *FpvWXYZCDEF* ABC Transporter Complex in order for *P. aeruginosa* to grow and maintain virulence under iron-limiting conditions (Gao *et al.*, 2018).

Six out of the seven genes of the *pel* gene cluster, previously identified by Friedman and Kolter (2004a), were upregulated in this analysis (Friedman and Kolter, 2004a). The seven *pel* genes encode proteins with similarity to components involved in polysaccharide biogenesis. Friedman and Kolter suggested that: PelA, PelC, PelD, PelE and PelF have sequence similarities with proteins involved in carbohydrate processing (Vasseur *et al.*, 2005). While, PelF is a putative glycosyltransferase and PelG a putative component of the polysaccharide transporter (PST) family. Interestingly, biofilm-deficient *P. aeruginosa* PAK strains were affected in the seven-gene *pel* cluster. These mutants were severely defective in the attachment process on solid surfaces and they could not form strong biofilms on a solid surface (Vasseur *et al.*, 2005). Therefore, loss of the *pel* cluster can jeopardize chronic bacterial infections, which are increasingly associated with the biofilm lifestyle.

The PA4210 (*phzA1*) and PA4211 (*phzB1*) were also upregulated. In *P. aeruginosa* PAO1 these genes are part one of the two identical seven-gene phenazine biosynthetic loci designated *phzA1B1C1D1E1F1G1* and *phzA2B2C2D2E2F2G2*, which are redundantly responsible for the synthesis of phenazine-1-carboxylic acid (PCA)(Mavrodi *et al*., 2001). Two additional genes, *phzS* and *phzM*, are required to convert PCA to pyocyanin during the final steps of its biosynthesis (Ho Sui *et al.*, 2012) These secondary metabolites are thought to confer an advantage to the producer bacteria when in competition with other microflora in the soil habitat (Khan *et al.*, 2005).

Moreover, PA4624 (*cdrB*) and PA4625 (*cdrA*) were upregulated. CdrB is a putative outer membrane transporter. CdrA is a putative adhesion and shares structural similarities to extracellular adhesins that belong to two-partner secretion systems. Both *cdrB* and *cdrA* gene are in the same operon and their expression was found to promote auto-aggregation in liquid culture and biofilm formation. It was shown that CdrA-mediated aggregation is dependent on the Psl polysaccharide. CdrA promotes

increased biofilm structural stability by either cross-linking Psl polysaccharide polymers or by tethering Psl to the cell surface (Borlee *et al.*, 2010).

6.2.1.1.3 Functional classification of downregulated and upregulated DEGs found under aerobic conditions, identified due to *samA* deletion

To further investigate the DEGs identified under these conditions, a KEGG pathway enrichment analysis was performed. All the enriched pathways are listed in **Table 6.7.** The downregulated DEGs were enriched in 18 pathways whereas the upregulated DEGs were enriched in 44 pathways. The most enriched pathway for downregulated DEGs was the "Bacterial secretion systems" with 25 genes. The most enriched pathway for upregulated DEGs is "Metabolic Pathways" with 26 genes. Three more pathways were also found highly upregulated: (i) the biosynthesis of secondary metabolites, (ii) biofilm formation and (iii) quorum sensing. The hypothetical proteins upregulated do not belong in any predicted pathways and hence were omitted from every KEGG enrichment analysis presented in this study for simplification purposes.

According to the DeSeq2 data obtained from gene expression level analysis, a total of 1552 significantly DEGs with $\log_2$(FoldChange) value > 4 and p-value < 0.05 were identified between the *P. aeruginosa* Δ*samA* and the *WT* strain under anaerobic conditions. Specifically, there were 876 down regulated and 676 upregulated genes. In this occasion, the PAO1-N data was not available under anaerobic conditions to enable the removal of genes differentially expressed due to the subline effects between this strain and PAO1-L. A Venn diagram analysis like the one shown in **Figure 6.2** enabled the reduction of the number of differentially expressed genes to only those that were affected by the specific gene deletion. This showed that there were 833 down regulated genes and 602 upregulated genes in Δ*samA* samples vs WT samples.

Table 6.7. KEGG Pathway Enrichment Summary of downregulated and upregulated DEGs found under aerobic conditions, identified due to *samA* deletion.

Pathway ID	KEGG Pathway	Number of Genes/Count
Down		
[PATH:ko00970]	Aminoacyl-tRNA biosynthesis	1
[PATH:ko00627]	Aminobenzoate degradation	1
[PATH:ko00330]	Arginine and proline metabolism	1
[PATH:ko02030]	Bacterial chemotaxis	1
[PATH:ko03070]	Bacterial secretion system	25
[PATH:ko01501]	beta-Lactam resistance	3
[PATH:ko02025]	Biofilm formation - P. aeruginosa	2
[PATH:ko01110]	Biosynthesis of secondary metabolites	1
[PATH:ko01040]	Biosynthesis of unsaturated fatty acids	2

[PATH:ko01212]	Fatty acid metabolism	2
[PATH:ko00260]	Glycine, serine and threonine metabolism	1
[PATH:ko01100]	Metabolic pathways	4
[PATH:ko01120]	Microbial metabolism in diverse environments	1
[PATH:ko00360]	Phenylalanine metabolism	1
[PATH:ko00860]	Porphyrin and chlorophyll metabolism	2
[PATH:ko00643]	Styrene degradation	1
[PATH:ko00380]	Tryptophan metabolism	1
[PATH:ko02020]	Two-component system	4
Up		
[PATH:ko01210]	2-Oxocarboxylic acid metabolism	1
[PATH:ko02010]	ABC transporters	7
[PATH:ko00592]	alpha-Linolenic acid metabolism	1
[PATH:ko00520]	Amino sugar and nucleotide sugar metabolism	1
[PATH:ko00330]	Arginine and proline metabolism	1
[PATH:ko02030]	Bacterial chemotaxis	2
[PATH:ko03070]	Bacterial secretion system	1
[PATH:ko00362]	Benzoate degradation	4
[PATH:ko00410]	beta-Alanine metabolism	1
[PATH:ko01501]	beta-Lactam resistance	1
[PATH:ko02025]	Biofilm formation - P. aeruginosa	12
[PATH:ko01230]	Biosynthesis of amino acids	1
[PATH:ko01110]	Biosynthesis of secondary metabolites	18
[PATH:ko01053]	Biosynthesis of siderophore group nonribosomal peptides	2
[PATH:ko00650]	Butanoate metabolism	2
[PATH:ko00930]	Caprolactam degradation	1
[PATH:ko01200]	Carbon metabolism	2
[PATH:ko01503]	Cationic antimicrobial peptide (CAMP) resistance	3
[PATH:ko00460]	Cyanoamino acid metabolism	2
[PATH:ko00061]	Fatty acid biosynthesis	1
[PATH:ko00071]	Fatty acid degradation	4
[PATH:ko01212]	Fatty acid metabolism	4
[PATH:ko00281]	Geraniol degradation	2
[PATH:ko00480	Glutathione metabolism]	1
[PATH:ko00260]	Glycine, serine and threonine metabolism	1
[PATH:ko00630]	Glyoxylate and dicarboxylate metabolism	1
[PATH:ko00903]	Limonene and pinene degradation	1
[PATH:ko00540]	Lipopolysaccharide biosynthesis	1
[PATH:ko00310]	Lysine degradation	4
[PATH:ko01100]	Metabolic pathways	26
[PATH:ko01120]	Microbial metabolism in diverse environments	8
[PATH:ko00261]	Monobactam biosynthesis	1
[PATH:ko00190]	Oxidative phosphorylation	1
[PATH:ko00405]	Phenazine biosynthesis	8

[PATH:ko00640]	Propanoate metabolism	1
[PATH:ko00620]	Pyruvate metabolism	4
[PATH:ko02024]	Quorum sensing	10
[PATH:ko00920]	Sulfur metabolism	1
[PATH:ko00900]	Terpenoid backbone biosynthesis	1
[PATH:ko00380]	Tryptophan metabolism	3
[PATH:ko02020]	Two-component system	8
[PATH:ko00350]	Tyrosine metabolism	1
[PATH:ko00130]	Ubiquinone and other terpenoid-quinone biosynthesis	1
[PATH:ko00280]	Valine, leucine and isoleucine degradation	3

6.2.1.2 Impact of *samA* on global gene expression in *P. aeruginosa* by RNA-seq grown under anaerobic conditions.

6.2.1.2.1Identification of Downregulated DEGs by the *samA* deletion under anaerobic conditions

The *samA* gene deletion resulted in downregulation of 833 genes under **anaerobic conditions**. For the purpose of simplification, only a selection of genes out of the 833 differentially regulated were chosen for discussion and shown in **Table 6.8** below. These genes showed high alteration in expression levels.

Table 6.8. Summary of genes found downregulated due to *samA* deletion under anaerobic conditions.

GeneID	log2(FC)	P-adj	Gene name	Gene Ontology (GO)
PA0280	-4.78	$3.64E^{-10}$	*cysA*	sulfate transport protein CysA
PA0281	-4.28	$9.86E^{-09}$	*cysW*	sulfate transport protein CysW
PA0282	-4.30	$1.03E^{-07}$	*cysT*	sulfate transport protein CysT
PA0292	-1.02	$5.45E^{-06}$	*aguA*	agmatine deiminase
PA0297	-1.09	0.000921908	*spuA ycjL*	probable glutamine amidotransferase
PA0298	-2.05	$5.02E^{-07}$	*spuB*	Glutamylpolyamine synthetase
PA0299	-2.03	0.00033948	*spuC*	Polyamine:pyruvate transaminase
PA0300	-1.88	$2.52E^{-05}$	*spud; potF2*[a]	polyamine transport protein
PA0301	-1.16	0.000117532	*spuE; potF3*	polyamine transport protein
PA0302	-1.48	$9.24E^{-05}$	*spuF; potG*	polyamine transport protein PotG
PA0303	-1.17	0.000140071	*spuG; potH*	polyamine transport protein PotH
PA0304	-1.38	$6.64E^{-05}$	*spuH; potI*	polyamine transport protein PotI
PA0411	-1.34	$2.12E^{-13}$	*pilJ*	twitching motility protein PilJ
PA0412	-1.12	$2.18E^{-06}$	*pilK*	methyltransferase PilK
PA0413	-1.56	$5.46E^{-06}$	*chpA pilL*	component of chemotactic signal transduction system
PA0414	-1.91	$9.59E^{-07}$	*chpB*	probable methylesterase
PA0415	-1.72	$1.59E^{-06}$	*chpC*	probable chemotaxis protein
PA0416	-1.97	$8.93E^{-07}$	*chpD*	probable transcriptional regulator
PA0417	-1.36	0.000710939	*chpE*	probable chemotaxis protein

PA0603	-2.57	$1.44E^{-30}$	*agtA*	AgtA
PA0604	-2.54	$6.65E^{-13}$	*agtB*	AgtB
PA0605	-1.09	$7.41E^{-06}$	*agtC*	AgtC
PA0609	-1.09	0.000578926	*trpE*	anthranilate synthetase component I
PA0746	-2.34	0.000379149		probable acyl-CoA dehydrogenase
PA1054	-1.42	$5.05E^{-12}$	*shaA;phaA*	ShaA
PA1055	-1.92	$1.34E^{-10}$	*shaB;phaC*	ShaB
PA1056	-1.33	$1.94E^{-15}$	*shaC;phaD*	ShaC
PA1057	-1.80	$6.38E^{-14}$	*shaD;phaE*	ShaD
PA1058	-1.91	$4.44E^{-10}$	*shaE;phaF*	ShaE
PA1059	-1.39	$2.19E^{-06}$	*shaF;phaG*	ShaF
PA1696	-1.53	0.026971806	*pscO*	translocation protein in type III secretion
PA1698	-1.75	$2.86E^{-06}$	*popN*	Type III secretion outer membrane protein PopN precursor
PA1700	-1.09	0.031625117	*pcr2*	Pcr2
PA1701	-1.54	0.05548232	*pcr3*	Pcr3
PA1705	-3.73	$1.53E^{-11}$	*pcrG*	regulator in type III secretion
PA1706	-3.09	$3.22E^{-09}$	*pcrV*	type III secretion protein PcrV
PA1707	-3.07	$9.43E^{-06}$	*pcrH*	regulatory protein PcrH
PA1708	-2.61	$3.96E^{-09}$	*popB;pepB*	translocator protein PopB
PA1709	-3.23	$2.63E^{-12}$	*popD;pepD*	Translocator outer membrane protein PopD precursor
PA1710	-1.80	$1.07E^{-06}$	*exsC*	ExsC, exoenzyme S synthesis protein C precursor.
PA1711	-2.27	$3.70E^{-09}$	*exsE*	ExsE
PA1712	-1.15	0.000109981	*exsB*	exoenzyme S synthesis protein B
PA1713	-2.27	$9.75E^{-10}$	*exsA*	transcriptional regulator ExsA
PA1714	-2.04	$1.01E^{-11}$	*exsD*	ExsD
PA1716	-1.25	$1.34E^{-06}$	*pscC*	Type III secretion outer membrane protein PscC precursor
PA1719	-1.84	0.024792994	*pscF*	type III export protein PscF
PA1721	-2.04	$9.05E^{-06}$	*pscH*	type III export protein PscH
PA1722	-1.63	$5.24E^{-06}$	*pscI*	type III export protein PscI
PA1723	-1.85	$2.33E^{-08}$	*pscJ*	type III export protein PscJ
PA1724	-2.33	$1.03E^{-06}$	*pscK*	type III export protein PscK
PA1725	-1.99	0.000335421	*pscL*	type III export protein PscL
PA1946	-2.07	$1.29E^{-06}$	*rbsB*	binding protein component precursor of ABC ribose transporter
PA1947	-3.24	3.64E-10	*rbsA*	ribose transport protein RbsA
PA1948	-1.61	0.018075538	*rbsC*	membrane protein component of ABC ribose transporter
PA1949	-1.60	*NA*	*rbsR*	ribose operon repressor RbsR
PA1973	-1.06	0.000559118	*pqqF*	pyrroloquinoline quinone biosynthesis protein F
PA1975	-2.13	$7.53E^{-07}$		hypothetical protein
PA1976	-1.07	0.001435039	*ercS'*	ErcS'
PA1978	-2.56	$5.58E^{-09}$	*erbR; agmR*	response regulator ErbR
PA1979	-1.84	$1.48E^{-06}$	*eraS; exaD*	sensor kinase, EraS
PA1980	-1.23	0.083463295	*eraR; exaE*	response regulator EraR

PA1986	-2.47	$1.15E^{-10}$	*pqqB*	pyrroloquinoline quinone biosynthesis protein B
PA1987	-1.55	$3.63E^{-08}$	*pqqC*	pyrroloquinoline quinone biosynthesis protein C
PA1988	-1.41	0.003021725	*pqqD*	pyrroloquinoline quinone biosynthesis protein D
PA1991	-1.49	$2.21E^{-11}$		probable iron-containing alcohol dehydrogenase
PA1992	-2.82	$6.47E^{-42}$	*ercS*	ErcS
PA3931	-3.64	$2.68E^{-09}$		putative methionine-binding protein
PA3932	-1.59	0.017872082		probable transcriptional regulator
PA3935	-2.28	0.001379101	*tauD*	taurine dioxygenase
PA3936	-2.82	$2.48E^{-05}$	*tauC*	probable permease of ABC taurine transporter
PA3937	-2.97	$5.04E^{-06}$	*tauB*	probable ATP-binding component of ABC taurine transporter
PA3938	-2.53	$2.12E^{-05}$	*tauA*	probable periplasmic taurine-binding protein precursor

[a] In various cases one PA number has been given 2 or even 3 different names in the literature, which are all given on the above table under "gene name" separated by a Semicolon.

Firstly, the PA0280 (*cysA*), PA0281 (*cysW*) and PA0282 (cyst) were downregulated. The PA0280 (*cysA*) gene is thought to encode a membrane-associated transport component and is deemed essential for sulfate and thiosulfate transport (Sirko *et al.*, 1990).

All genes that belong to *spuABCDEFGH*, a multiple-gene locus for polyamine uptake and utilization in *P. aeruginosa* PAO1, were downregulated. *Pseudomonas* species, including *P. aeruginosa*, can utilize polyamines (putrescine, spermidine and spermine) as the sole source of carbon and nitrogen (Lu *et al.*, 2002; Nishijyo *et al.*, 2001; Stanier *et al.*, 1966). The *spuABCDE* are putrescine and spermidine biosynthetic genes (Yao *et al.*, 2011). Both s*puA* and *spuB* encode putative enzymes with homology to glutamine amidotransferase and glutamine synthetase, respectively, and the *spuDEFGH* cluster specifies a transport system of spermidine (Lu *et al.*, 2002).

Genes from the Sha system were also downregulated in the *samA* mutant. In *P. aeruginosa*, the homologues of the Sha system (Na^+/H^+ antiporter, also known by the names of Mrp, Mnh or Pha) exist as a cluster of six genes *sha*ABCDEFG , PA1054 to PA1059, encoding a Na^+/H^+ antiporter. Homeostasis of H^+, Na^+, and other monovalent cations is conferred by Sha. In addition, this system is also critical for Na^+ extrusion in *P. aeruginosa* and has a role in infection (Kosono *et al.*, 2005). We propose to designate PA1054 to PA1059 as the sha (sodium hydrogen antiporter) genes to avoid confusion.

In addition, more than 20 genes associated with protein secretion were downregulated, these genes belonged to the translocation apparatus (*pcr*, *pop*) or had a regulatory function (*exs*), while the T3SS needle complex itself, encoded by the *psc* genes, was also downregulated, somewhat as under aerobic conditions. Some examples are the PA1696 (*pscO*) encoding the translocation protein in type III secretion, The PA1697 (*pscN*) gene encoding the T3SS ATPase and the PA1698 (*popN*) encoding the

type III secretion outer membrane protein PopN. PopN, is a component of the T3SS that is readily detectable on the bacterial cell surface. PopN and Pcr1 interact and form a complex that functions as a T3SS repressor (Yang *et al.*, 2007).

Twitching motility in *P. aeruginosa* allows it to respond to stimuli by extending and retracting its type IV pili (TFP). PilJ is a protein necessary for this surface-associated twitching motility through full TFP assembly/extension(DeLange *et al.*, 2007). The *pilK*, encodes a chemotactic methyltransferase (CheR) homologue (Darzins and State, 1993). Both *pilJ* and *pilK* were downregulated in the *samA* mutant. Other components of the Twitching motility in *P. aeruginosa* pathway are ChpA, ChpB, ChpC, ChpD and ChpE which are controlled in part by the Chp chemosensory system (Whitchurch *et al.*, 2004)(Bertrand *et al.*, 2010).

The *agtA*, *agtB* and *agtC* genes were also found downregulated. The *agt*ABCD locus have been shown to be involved in δ-aminovalerate (AMV) and γ-aminobutyrate (GABA) uptake. Interestingly, a link between AMV/GABA metabolism and polymicrobial infection has been made through the recently reported function of *agtR* in sensing of peptidoglycan shed by gram-positive bacteria(Chou *et al.*, 2014) (Chou *et al.*, 2014)(Chou *et al.*, 2014).

Moreover, the *trpE* gene, which in *P. aeruginosa* encodes an anthranilate synthase enzyme was downregulated. The *trpE* gene product is capable of providing some anthranilate for pyocyanin synthesis (Essar *et al*., 1990).

Five conserved genes, *pqqA-E*, were found downregulated in the *samA* mutant. These genes are responsible for pyrroloquinoline quinone (PQQ) biosynthesis. PqqE is a radical S-adenosyl methionine (RS) protein with a C-terminal SPASM domain (so called as it is present in the maturases of subilitosin, PQQ, anaerobic sulfatases, and mycofactocin) and is proposed to catalyze the formation of a carbon-carbon bond between the glutamate and tyrosine side chains of the peptide substrate PqqA. PqqD is a 10-kDa protein with an unknown function, but is essential for PQQ production (Latham *et al.*, 2015).

The RNAseq analysis also found the PA3935 (*tauD*), PA3936 (*tauC*), PA3937 (*tauB*) and PA3938 (*tauA)* genes involved in taurine metabolism downregulated. In *E. coli*, sulfate starvation-induces the expression of the *tauABCD* genes, which are required for utilization of taurine as sulfur source for growth (Van Der Ploeg *et al.*, 1997). Synthesis of TauD is repressed in the presence of sulfate or cysteine in the growth medium and is dependent on two very similar LysR-type transcriptional activators, CysB and Cbl (Kertesz *et al.*, 1999).

6.2.1.2.2 Identification of Upregulated DEGs by PA4803 (*samA*) deletion under anaerobic conditions

The PA4803 (*samA*) gene deletion results in upregulation of 602 genes under **anaerobic** conditions. For purposes of simplification, only a selection of genes was chosen for discussion below. Hence, the genes discussed out of the 602 are listed on **Table 6. *9*.**

Table 6. 9 Summary of genes found upregulated due to *samA* deletion under anaerobic conditions.

GeneID	log2(FC)	P-adj	Gene name	Gene Ontology (GO)
PA0996	1.97	1.99E^{-05}	*pqsA*	PqsA
PA0997	1.47	0.007489496	*pqsB*	PqsB
PA0998	1.26	3.71E^{-08}	*pqsC*	PqsC
PA0999	1.66	0.000463954	*pqsD fabH1*	3-oxoacyl-[acyl-carrier-protein] synthase III
PA1000	1.53	0.003391727	*pqsE*	Quinolone signal response protein
PA1001	1.17	0.002157861	*phnA*	anthranilate synthase component I
PA1130	1.77	5.32E^{-12}	*rhlC*	rhamnosyltransferase 2
PA1861	2.23	7.70E^{-09}	*modC*	molybdenum transport protein ModC
PA1862	2.40	6.42E^{-08}	*modB*	molybdenum transport protein ModB
PA1863	3.02	3.51E^{-11}	*modA*	molybdate-binding periplasmic protein precursor ModA
PA1864	2.63	0.00018118		probable transcriptional regulator
PA1898	1.90	1.84E^{-10}	*qscR phzR*	quorum-sensing control repressor
PA1899	3.33	2.47E^{-09}	*phzA2*	probable phenazine biosynthesis protein
PA1900	2.96	1.08E^{-08}	*phzB2*	probable phenazine biosynthesis protein
PA2231	1.12	7.99E^{-10}	*pslA*	PslA
PA2232	1.00	7.58E^{-07}	*pslC*	PslC
PA2234	1.15	2.61E^{-06}	*pslD*	PslD
PA2237	1.14	6.14E^{-05}	*pslG*	PslG
PA2302	2.06	2.98E^{-15}	*ambE*	AmbE
PA2303	2.28	7.15E^{-18}	*ambD*	AmbD
PA2304	1.77	1.40E^{-12}	*ambC*	AmbC
PA2305	1.31	2.95E^{-10}	*ambB*	AmbB
PA2306	1.10	0.032080681	*ambA*	AmbA
PA2361	2.75	3.09E^{-20}	*icmF3*	IcmF3
PA2362	2.56	1.13E^{-06}	*dotU3*	DotU3
PA2363	2.50	5.27E^{-23}	*hsiJ3*	HsiJ3
PA2364	1.79	6.11E^{-06}	*lip3*	Lip3
PA2365	2.74	8.82E^{-25}	*hsiB3*	HsiB3
PA2366	2.76	3.10E^{-17}	*hsiC3 puuD*	HsiC3
PA2367	2.66	1.09E^{-09}	*hcp3*	Hcp3
PA2368	4.26	1.09E^{-15}	*hsiF3*	HsiF3
PA2369	4.01	2.34E^{-20}	*hsiG3*	HsiG3
PA2370	4.06	3.17E^{-16}	*hsiH3*	HsiH3

PA2371	3.64	$2.79E^{-61}$	*clpV3*	ClpV3
PA2373	2.17	$2.21E^{-07}$	*vgrG3*	VgrG3
PA2374	2.26	$2.26E^{-07}$	*tseF*	TseF
PA2376	1.94	$5.91E^{-09}$		probable transcriptional regulator
PA2395	1.01	0.093677226	*pvdO*	PvdO
PA2399	1.09	$2.19E^{-05}$	*pvdD*	pyoverdine synthetase D
PA2402	1.17	$4.40E^{-06}$	*pvdI*	pyoverdine peptide synthetase
PA2411	1.72	0.003260996		probable thioesterase
PA2413	1.65	$2.92E^{-07}$	*pvdH*	L-2,4-diaminobutyrate:2-ketoglutarate 4-aminotransferase, PvdH
PA2414	1.75	0.000339806		L-sorbosone dehydrogenase
PA2416	1.75	0.000168116	*treA*	periplasmic trehalase precursor
PA2426	1.38	0.025759834	*pvdS*	sigma factor PvdS
PA3476	1.56	$9.76E^{-15}$	*rhlI*	autoinducer synthesis protein RhlI
PA3477	2.48	$8.65E^{-21}$	*rhlR*	transcriptional regulator RhlR
PA3478	2.91	$1.10E^{-23}$	*rhlB*	rhamnosyltransferase chain B
PA3479	4.60	$3.57E^{-44}$	*rhlA*	rhamnosyltransferase chain A

The *pqsABCDE* operon, required for PQS biosynthesis, was upregulated. The Pseudomonas quinolone signal (PQS) is a 3-hydroxy-4-quinolone with a 2-alkyl substitution, which is synthesized by the condensation of anthranilic acid with a 3-keto-fatty acid. Hence, anthranilic acid is the precursor to both PQS and HHQ. The PqsA protein in *P. aeruginosa* is an Anthranilate-Coenzyme A Ligase and is responsible for anthranilate activation. The anthranilate precursor can be produced by the *phnAB* operon, from tryptophan (*trpE*) via the kynurenine pathway, or from exogenous anthranilate (Coleman *et al.*, 2008). PqsB, PqsC, and PqsD are designated as condensing enzymes. PqsBC catalyzes the condensation of octanoyl-coenzyme A and 2-aminobenzoylacetate (2-ABA) to form the signal molecule 2-heptyl-4(1*H*)-quinolone (Drees *et al.*, 2016). Moreover, *pqsD* Is responsible for the synthesis of 2,4-Dihydroxyquinoline DHQ, an extracellular metabolite produced by *P. aeruginosa* (Zhang *et al.*, 2008). All of the gene products in the *pqsABCD* gene cluster are thought to be essential for the formation of PQS and HHQ (Zhang *et al.*, 2008). Lastly, although PqsE is dispensable for AQ biosynthesis there is a requirement for it in the regulation of diverse genes coding for key virulence determinants and biofilm development in response to PQS (Rampioni *et al.*, 2016).

Moreover, the genes *phzA2* and *phzB2*, which belong to the two seven-gene phenazine biosynthetic loci designated *phzA1B1C1D1E1F1G1* and *phzA2B2C2D2E2F2G*2 from *P. aeruginosa* PAO1, were also downregulated. Each biosynthetic operon is sufficient for the production of phenazine-1-carboxylic acid (PCA). Subsequently, PCA is converted to to pyocyanin by two phenazine-modifying genes, PhzM and PhzS (Mavrodi *et al*., 2001). The gene *phzR/qscR* was also downregulated, its product QscR it is a third LuxR-type protein found in *P. aeruginosa*, which adds further complexity to this regulatory

network. QscR represses transcription of three QS-controlled gene clusters, the two *phz* and the *hcn* operons, essential for phenazine and hydrogen cyanide production, respectively (Ledgham *et al.*, 2003).

Additionally, the genes *ampA-E* are required for the production of L-2-amino-4-methoxy-*trans*-3-butenoic acid (AMB) were downregulated. AMP is an antimetabolite produced by *P. aeruginosa* that is a non-proteinogenic amino acid belonging to a small group of natural compounds known as oxyvinylglycines (Berkowitz *et al.*, 2006). AmbA is a putative LysE-type transporter, AmbB and AmbE are two non-ribosomal peptide synthetases, and AmbC and AmbD are two iron(II)/α-ketoglutarate-dependent oxygenases (Murcia *et al.*, 2015).

Moreover, four genes from the *psl* locus (polysaccharide synthesis locus) were upregulated. Namely, *pslA, pslC, pslD, pslG*. Exopolysaccharides such as the Psl polysaccharide contribute significantly to surface attachment and biofilm formation in *P. aeruginosa* (Byrd *et al.*, 2009).

In *P. aeruginosa* three Type VI Secretion System (T6SS) coexist with the loci called H1- to H3-T6SS. There is a possibility that the H2-T6SS during the host infection is connected to the H3-T6SS but other than that very little is known about the latter. Apparently, H3-T6SS is required for *P. aeruginosa* PAO1 virulence in the worm model (Sana *et al.*, 2013). Interestingly, several genes that encode H3-T6SS secretion functions were upregulated.

As mentioned previously, pyoverdines, the main siderophores produced by fluorescent *Pseudomonads,* are of importance to pathogens during infection due to iron sequestration by host iron-binding proteins (Vandenende *et al.*, 2004). Genes *pvdO, pvdD, pvdI, pvdH* and *pvdS* are upregulated and some of their functions are discussed below. Under conditions of iron starvation, repression of the *pvdS* promoter by Fur is relieved and *pvdS* is expressed, reprogramming the cells to start pyoverdine synthesis (Cunliffe *et al.*, 1995). The PvdO iron (III) reductase is involved in pyoverdine maturation (Yeterian *et al.*, 2010). The conversion of aspartyl phosphate to l-2,4-diaminobutyrate requires the enzymatic activity of an aminotransferase, PvdH, (Vandenende *et al.*, 2004)(Merriman *et al.*, 1995).

Rhamnolipids are tenso-active glycolipids containing one (mono-rhamnolipid) or two (di-rhamnolipid) L-rhamnose molecules. Rhamnolipids (RL) produced by *P. aeruginosa* are the most studied biosurfactants (Toribio *et al.*, 2010). RhlA and RhlB proteins together comprise the rhamnosyltransferase 1 which catalyzes the synthesis of this surfactant. The genes *rhlA* and *rhlB* were upregulated in these conditions. The precise role that rhamnolipids play in *P. aeruginosa* life cycle and pathogenicity is not well known, but it is suggested that they are involved hydrophobic nutrient

uptake, swarming motility, and pathogenesis (Zhu and Rock, 2008)(Soberón-Chávez *et al.*, 2005). The *rhlC*, gene encodes the rhamnosyltransferase involved in di-rhamnolipid production from mono-rhamnolipids in *P. aeruginosa* (Rahim *et al.*, 2001)(Soberón-Chávez *et al.*, 2005).

The genes *rhlR* and *rhlI* were upregulated, *RhlR-RhlI* represent the second autoinducer-responsive regulatory mechanism found in *P. aeruginosa* that controls expression of multiple virulence factor exoproducts (Brint and Ohman, 1995).

Interestingly, an operon associated with molybdenum was found upregulated under these conditions. Namely, PA1861 (*modC*), PA1862 (*modB*) and PA1863 (*modA*) genes. This *modABCD* operon encodes genes of a high-affinity uptake system for molybdate. The *modA* product has a signal peptide at the N-terminus therefore, it probably is the periplasmic binding-protein for molybdate. The products of *modB* and *modC* have been described as the inner membrane protein and the ATP-binding protein of the molybdate transport system, respectively. No further information on the *modD* function is available. (Walkenhorst *et al.*, 1995).

6.2.1.2.3 Functional classification of downregulated and upregulated DEGs found under anaerobic conditions, identified due to *samA* deletion

To further investigate the DEGs identified under these conditions, a KEGG pathway enrichment analysis was performed. All the enriched pathways are listed in **Table 6.10**. There was enrichment in 100 pathways for the downregulated DEGs, for simplification purposes only the top 20 enriched pathways are listed on the table below. Similarly, there was enrichment in 76 pathways for the upregulated DEGs but for simplification purposes, only the top 20 enriched pathways are listed on the table. The most affected ones were the “metabolic pathways” with 217 genes downregulated and 86 upregulated in these. Therefore, these will not be discussed in great detail.

Table 6.10. KEGG Pathway Enrichment Summary of downregulated and upregulated DEGs found under anaerobic conditions, identified due to *samA* deletion.

Pathway ID	KEGG Pathway	Number of Genes/Count
Down		
[PATH:ko02010]	ABC transporters	64
[PATH:ko00330]	Arginine and proline metabolism	12
[PATH:ko03070]	Bacterial secretion system	19
[PATH:ko02025]	Biofilm formation - P. aeruginosa	14
[PATH:ko01230]	Biosynthesis of amino acids	30
[PATH:ko01240]	Biosynthesis of cofactors	26
[PATH:ko01110]	Biosynthesis of secondary metabolites	74

[PATH:ko01200]	Carbon metabolism	35
[PATH:ko01212]	Fatty acid metabolism	15
[PATH:ko00010]	Glycolysis / Gluconeogenesis	14
[PATH:ko00630]	Glyoxylate and dicarboxylate metabolism	17
[PATH:ko01100]	Metabolic pathways	217
[PATH:ko01120]	Microbial metabolism in diverse environments	71
[PATH:ko00640]	Propanoate metabolism	23
[PATH:ko00230]	Purine metabolism	18
[PATH:ko00620]	Pyruvate metabolism	22
[PATH:ko02024]	Quorum sensing	20
[PATH:ko03010]	Ribosome	30
[PATH:ko00920]	Sulfur metabolism	27
[PATH:ko02020]	Two-component system	37
[PATH:ko00280]	Valine, leucine and isoleucine degradation	20
Up		
[PATH:ko02010]	ABC transporters	12
[PATH:ko00970]	Aminoacyl-tRNA biosynthesis	15
[PATH:ko02030]	Bacterial chemotaxis	12
[PATH:ko03070]	Bacterial secretion system	10
[PATH:ko02025]	Biofilm formation - P. aeruginosa	32
[PATH:ko01230]	Biosynthesis of amino acids	8
[PATH:ko01240]	Biosynthesis of cofactors	23
[PATH:ko01110]	Biosynthesis of secondary metabolites	52
[PATH:ko00270]	Cysteine and methionine metabolism	5
[PATH:ko00790]	Folate biosynthesis	8
[PATH:ko00260]	Glycine, serine and threonine metabolism	5
[PATH:ko01100]	Metabolic pathways	86
[PATH:ko01120]	Microbial metabolism in diverse environments	14
[PATH:ko00405]	Phenazine biosynthesis	9
[PATH:ko00860]	Porphyrin and chlorophyll metabolism	7
[PATH:ko02024]	Quorum sensing	21
[PATH:ko00500]	Starch and sucrose metabolism	11
[PATH:ko04122]	Sulfur relay system	7
[PATH:ko02020]	Two-component system	25
[PATH:ko00280]	Valine, leucine and isoleucine degradation	5

6.2.2 Impact of PA4802.1 on global gene expression in *P. aeruginosa* by RNAseq grown under both aerobic and anaerobic conditions.

The volcano plots (**Figure 6.3**) are displaying the pattern of gene expression values for the comparisons of ΔPA4802.1 vs WT under **aerobic** and **anaerobic conditions**. There were much less DEGs identified under anaerobic than aerobic conditions.

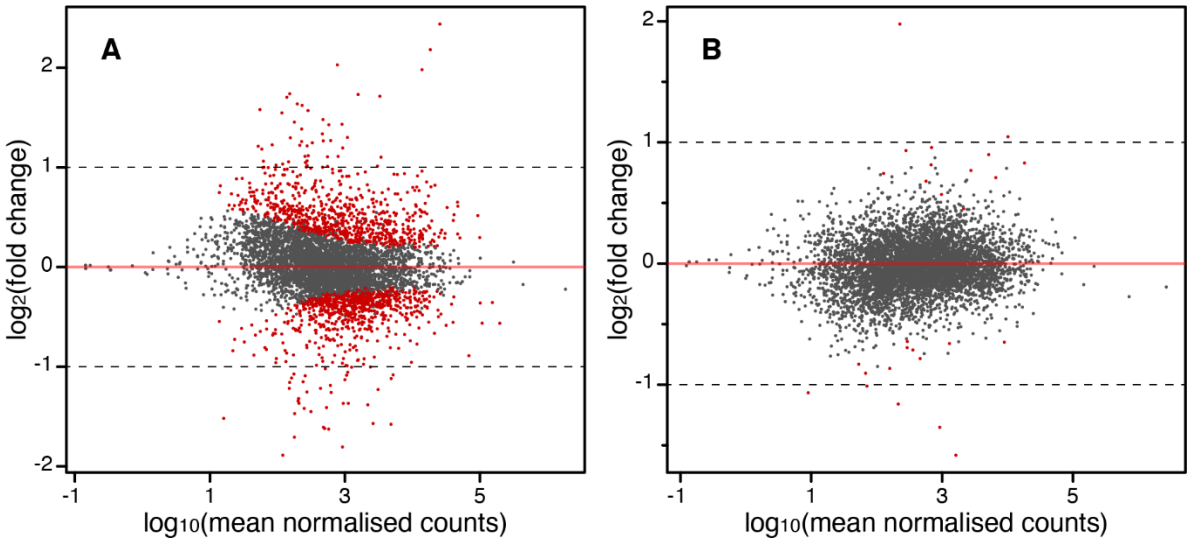


Figure 6.3. Volcano plot of RNA-seq transcriptome data displaying the pattern of gene expression.
Values for ΔPA4802.1 relatively to the WT strain under aerobic (A) and anaerobic (B) conditions. Significant differentially expressed genes ($p \leq 0.05$) are highlighted in red. Genes having a fold-change of less than 2 ($\log_2 = 1$) are shown in grey. Thresholds of genes having 2-fold changes in RNA abundance, either increased (positive values) or decreased (negative values) in the mutant compared to the WT are indicated by the dashed lines.

6.2.2.1 Impact of PA4802.1 on global gene expression in *P. aeruginosa* by RNAseq under both aerobic conditions

Comparisons between the Δ*PA402.1* vs *WT* strains under aerobic conditions and anaerobic conditions were established. In more detail, the four comparisons obtained by RNA-seq in the ***PA4802.1*** mutant, which are explained on **Table 6.4** and **Figure 6.2** were analysed by a Venn diagram to aid identifying those genes affected (downregulated or upregulated) by the deletion of this gene under both aerobic and anaerobic conditions (**Figure 6.2**.) Under anaerobic conditions a total of 86 significantly differentially expressed genes DEG with log2 (FoldChange) value > 2 and q-value < 0.05 were identified. Specifically, 48 up regulated and 38 down regulated genes in the Δ*PA4802.1* vs the WT strains. After a series of removals and curations, 38 out of the 48 genes and 16 out of the initial 38 genes were selected for further analysis and are presented below.

6.2.2.1.1Identification of Downregulated DEGs by PA4802.1 deletion under aerobic conditions

The absence of gene PA4802.1 resulted in downregulation of the genes listed in **Table 6.11** under **aerobic** conditions. The results confirmed that signals corresponding to expression of PA4802.1 were almost abolished in the deletion strain most likely noise due to unspecific mapping.

Table 6.11. Summary of genes found downregulated due to PA4802.1 deletion under aerobic conditions.

GeneID	log2(FC)	P-adj	Gene name	Gene Ontology (GO)
PA0531	-1.02	$4.26E^{-14}$		probable glutamine amidotransferase
PA1698	-1.21	$1.13E^{-06}$	*popN*	Type III secretion outer membrane protein PopN precursor
PA1705	-1.88	$4.15E^{-19}$	*pcrG*	regulator in type III secretion
PA1706	-1.45	$7.82E^{-16}$	*pcrV*	type III secretion protein PcrV
PA1708	-1.21	$5.68E^{-11}$	*popB; pepB*	translocator protein PopB
PA1710	-1.18	$2.38E^{-17}$	*exsC*	ExsC, exoenzyme S synthesis protein C precursor.
PA1714	-1.13	$3.71E^{-22}$	*exsD*	ExsD, ExsD is classified as an anti-activator.
PA1725	-1.07	$2.65E^{-06}$	*pscL*	type III export protein PscL
PA2259	-1.08	$2.39E^{-21}$	*ptxS*	transcriptional regulator PtxS
PA2260	-1.70	$3.25E^{-19}$	*kguE*	hypothetical protein
PA2261	-1.31	$1.18E^{-13}$	*kguK ; kgk*[a]	probable 2-ketogluconate kinase
PA3842	-1.15	$1.26E^{-09}$	*spcS;orf1*	specific Pseudomonas chaperone for ExoS, SpcS
PA4802.1	-1.51	$9.80E^{-08}$		tRNA-Sec
PA4810	-1.62	$1.06E^{-32}$	*fdnI; fdhI*	nitrate-inducible formate dehydrogenase, gamma subunit
PA4811	-1.80	$5.33E^{-46}$	*fdnH; fdhH*	nitrate-inducible formate dehydrogenase, beta subunit
PA4878	-1.38	$6.39E^{-27}$	*brlR*	BrlR

[a]In various cases one PA number has been given 2 or even 3 different names in the literature, which are all given on the above table under "gene name" separated by a Semicolon.

PopN and some other proteins associated with type III secretion system were downregulated. PopN, was discussed previously. In *P. aeruginosa*, regulation and biogenesis of the T3SS needle structure implicates almost 30 genes. These genes are clustered in a locus and form five operons, including the *pscL*, *popN*, *pcrV*, *exsC*, and *exsD* operons. In *P. aeruginosa*, a chromosomal operon, *pcrGVH-popBD*, encodes five proteins, PcrG, PcrV, PcrH, PopB and all of them are downregulated under these conditions (Allmond *et al.*, 2003). Part of the locus for exoenzyme S synthesis, e*xsC*, and *exsD*, were also downregulated.

In addition, PA2260 (*kguE*) of uknown function, and PA2261 (*kguK/kgk*) encoding a 2-ketogluconate kinase were downregulated. A study suggested that these ORFs constitute the 2-ketogluconate

utilization operon *kgu* in *P. aeruginosa*. Therefore, ORFs were designated *kguE* and *kguK* (Swanson *et al.*, 2000).

Lastly, the *fdnH* and *fdnI* of *P. aeruginosa* were downregulated. The *fdnH* and *fdnI* genes are part of the *fdnGHI* operon of *E. coli* encoding a nitrate-inducible formate dehydrogenase. Each of the genes encodes one of the three subunits of the formate dehydrogenase-N (Berg *et al*., 1991).

6.2.2.1.2 Identification of Upregulated DEGs by PA4802.1 deletion under aerobic conditions

The PA4802.1 gene absence results in upregulations of all the genes listed in **Table 6.12** under **aerobic** conditions.

Table 6.12. Summary of genes found upregulated due to PA4802.1 deletion under aerobic conditions.

GeneID	log2(FC)	P-adj	Gene name	Gene Ontology (GO)
PA0171	1.01	$6.68E^{-11}$		hypothetical protein
PA0203	1.02	0.000319		probable binding protein component of ABC transporter
PA0425	1.98	$2.18E^{-118}$	*mexA*	Resistance-Nodulation-Cell Division (RND) multidrug efflux membrane fusion protein MexA precursor
PA0426	2.43	$1.20E^{-158}$	*mexB*	Resistance-Nodulation-Cell Division (RND) multidrug efflux transporter MexB
PA0427	2.18	$1.71E^{-77}$	*oprM*	Major intrinsic multiple antibiotic resistance efflux outer membrane protein OprM precursor
PA0978	1.58	$1.17E^{-08}$		conserved hypothetical protein
PA1416	1.11	$5.15E^{-06}$		conserved hypothetical protein
PA1417	1.05	0.000139		probable decarboxylase
PA1797	1.10	$2.30E^{-08}$		hypothetical protein
PA1893	1.24	$1.51E^{-08}$		hypothetical protein
PA1932	1.06	$1.31E^{-07}$		probable hydroxylase molybdopterin-containing subunit
PA2235	1.01	$2.70E^{-18}$	*pslE*	PslE, psl cluster plays a role in cell-cell and/or cell-surface interaction in biofilm formation.
PA2284	1.73	$3.27E^{-13}$		hypothetical protein
PA2286	1.33	$5.17E^{-06}$		hypothetical protein
PA2398	1.73	$1.93E^{-49}$	*fpvA*	ferripyoverdine receptor
PA2403	1.43	$1.78E^{-30}$	*fpvG*	FpvG, part ABC transporter complex FpvWXYZCDEF coded by operons *fpvWXYZCDEF* and *fpvF*.
PA2404	1.45	$1.30E^{-12}$	*fpvH*	FpvH
PA2405	1.54	$1.30E^{-12}$	*fpvJ*	FpvJ
PA2407	1.48	$4.16E^{-21}$	*fpvC*	FpvC
PA2408	1.26	$2.27E^{-14}$	*fpvD*	FpvD
PA2409	1.57	$1.13E^{-21}$	*fpvE*	FpvE
PA2410	1.19	$4.43E^{-17}$	*fpvF*	FpvF

PA2780	1.00	$4.24E^{-09}$	*bswR*	bacterial swarming regulator BswR
PA2835	1.06	0.000178		probable major facilitator superfamily (MFS) transporter
PA3059	1.38	$3.12E^{-12}$	*pelF*	PelF
PA3061	1.22	$1.00E^{-08}$	*pelD*	PelD
PA4136	1.00	$7.54E^{-07}$	*sur; bcr*	probable major facilitator superfamily (MFS) transporter
PA4261	1.10	$3.36E^{-18}$	*rplW*	50S ribosomal protein L23
PA4582	1.26	$3.44E^{-10}$		conserved hypothetical protein
PA4583	1.42	$1.11E^{-12}$	*rtcB*	conserved hypothetical protein
PA4802	2.02	3.14E-53		hypothetical protein
PA5181	1.30	9.95E-19		probable oxidoreductase

The *mexA*, *mexB* and *oprM* genes are upregulated. OprM is the Major intrinsic multiple antibiotic resistance efflux outer membrane protein. The OprM precursor is on the outer membrane and is part of the MexAB-OprM efflux pump associated with antibiotic resistance in *P. aeruginosa*. MexAB-OprM extrude quinolones, macrolides, tetracyclines, lincomycin, chloramphenicol, novobiocin, β-lactams except imipenem and novobiocin, cefsulodin, and flomoxef (Masuda *et al.*, 2000).

Furthermore, *pelF* and *pelD,* part of the *pel* operon responsible for the production of glucose-rich biofilm matrix exopolysaccharide in strain *P. aeruginosa* PA14, were upregulated (Sakuragi and Kolter, 2007)(Baraquet *et al.*, 2012) PelD and PelF have sequence similarities with proteins involved in carbohydrate processing (Vasseur *et al.*, 2005) with PelF being a putative glycosyltransferase. Thus, affecting pel gene expression can jeopardize chronic bacterial infections, which are increasingly associated with the biofilm lifestyle.

Iron is an essential nutrient and bacteria have developed sophisticated systems to acquire it. Several genes of the *fpv* operons were upregulated under these conditions. FpvA is important as it acts as an outer membrane transporter, which transports the ferric form of PVDI from the extracellular environment into the periplasm (Ganne *et al.*, 2017). Overall, the *fpvCDE*F (PA2407-2410) genes have been suggested to encode an ABC transporter implicated in pyoverdine-Fe uptake. Overall, the *fpvWXYZCDEF* operon is involved in iron uptake and seems to play important roles in growth, oxidative stress resistance, and the virulence of *P. aeruginosa* (Gao *et al.*, 2018).

6.2.2.1.3 Functional classification of downregulated and upregulated DEGs found under aerobic conditions, identified due to the PA4802.1 deletion

To further investigate the DEGs identified under these conditions, a KEGG pathway enrichment analysis was performed. All the enriched pathways are listed in **Table 6.12**. There was enrichment in 18 pathways for the downregulated DEGs, with the most enriched ones being the "Metabolic pathways" with 9 genes. There was enrichment in 25 pathways for the upregulated DEGs with the most enriched pathway being for "ABC transporters" with 8 genes involved.

6.2.2.2 Impact of PA4802.1 on global gene expression in *P. aeruginosa* by RNAseq grown under anaerobic conditions

Moreover, a total of 5 significantly differentially expressed genes DEG with $\log_2$(FoldChange) value > 2 and q-value < 0.05 were identified between strain *P. aeruginosa ΔPA4802.1 vs WT* under anaerobic conditions. Specifically, there were 2 up regulated genes and 3 down regulated genes in Δ*PA4802.1* samples vs WT samples.

6.2.2.2.1 Identification of Downregulated DEGs by PA4802.1 deletion under anaerobic conditions

The PA4802.1 gene absence results in downregulation of all the genes listed in **Table 6.13** under anaerobic conditions.

Table 6.13. Summary of genes found downregulated due to the PA4802.1 deletion under anaerobic conditions.

GeneID	log2(FC)	P-adj	Gene name	Other names
PA4811	-1.58	$4.16E^{-09}$	*fdnH* *fdhH*	nitrate-inducible formate dehydrogenase, beta subunit
PA4810	-1.35	$9.41E^{-05}$	*fdnI* *fdhI*	nitrate-inducible formate dehydrogenase, gamma subunit
PA4802.1	-1.06	0.005754		tRNA-Sec

Previously mentioned, *fdnH* and *fdnI* of *P. aeruginosa* are downregulated. The PA4802.1 encoding the tRNA-^{sec} was also downregulated, which is normal since it is deleted in this strain.

6.2.2.2.2 Identification of Upregulated DEGs by PA4802.1 deletion under anaerobic conditions

The deletion of PA4802.1 results in upregulation of all the genes listed in **Table 6.14** under anaerobic conditions.

Table 6.14. Summary of genes found upregulated due to PA4802.1 deletion under anaerobic conditions.

GeneID	log2(FC)	P-adj	Gene name	Gene Ontology (GO)
PA4802	1.976665	$1.49E^{-13}$		hypothetical protein
PA0427	1.046868	0.013305	*oprM*	Major intrinsic multiple antibiotic resistance efflux outer membrane protein OprM precursor

The *oprM* gene is once again upregulated. This gene was also upregulated in the absence of the tRNA-sec even under aerobic conditions. As a reminder, OprM is the major intrinsic multiple antibiotic resistance efflux outer membrane protein OprM part of the MexAB-OprM efflux pump associated with antibiotic resistance in *P. aeruginosa* (Masuda *et al.*, 2000). The PA4802 encoding a hypothetical protein and next to PA4802.1 is also upregulated.

6.2.2.2.3 Functional classification of downregulated and upregulated DEGs found under anaerobic conditions in the PA4802.1 deletion mutant.

To further investigate the DEGs identified under these conditions, a KEGG pathway enrichment analysis was performed. All the enriched pathways are listed in **Table 6.15.** For downregulated DEGs 10 pathways were found enriched and all of them involved a maximum of 2 genes. For the upregulated DEGs, 2 pathways were found enriched both involving 1 gene.

Table 6.15. KEGG Pathway Enrichment Summary of downregulated and upregulated DEGs found under anaerobic conditions, identified due to PA4802.1 deletion.

Pathway ID	KEGG Pathway	Number of Genes/Count
Down		
[PATH:ko00970]	Aminoacyl-tRNA biosynthesis	1
[PATH:ko02025]	Biofilm formation - P. aeruginosa	2
[PATH:ko01110]	Biosynthesis of secondary metabolites	2
[PATH:ko01200]	Carbon metabolism	2
[PATH:ko00630]	Glyoxylate and dicarboxylate metabolism	2

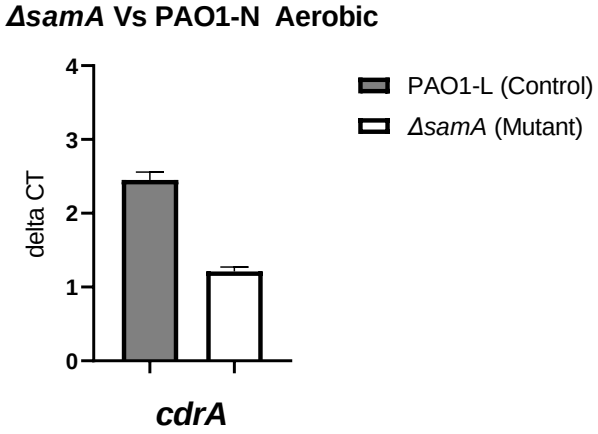
[PATH:ko01100]	Metabolic pathways	2
[PATH:ko00680]	Methane metabolism	2
[PATH:ko01120]	Microbial metabolism in diverse environments	2
[PATH:ko00405]	Phenazine biosynthesis	2
[PATH:ko02024]	Quorum sensing	2
Up		
[PATH:ko01501]	beta-Lactam resistance	1
[PATH:ko02024]	Quorum sensing	1

6.2.3 qRT-PCR Validation of the RNA-seq data

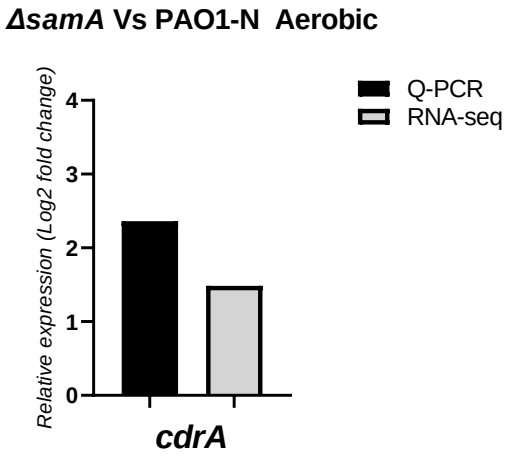
A few of the most significant DEGs including *cdrA, pscQ, oprM, fdhG* and *fdhH* were further evaluated by quantitative real-time polymerase chain reaction (qRT-PCR) in different deletion strains (Δ*samA* and ΔPA4802.1) under different conditions (aerobic and anaerobic) because of their key functionalities. The levels of all the above mentioned- transcripts were determined by RT-qPCR using the primer pairs from (**Chapter 2**, **Table 2.5**) and after normalization to the *rpoD* mRNA level.

Firstly, the cyclic diguanylate-regulated TPS partner A (*cdrA)* gene promotes increased biofilm structural stability by either cross-linking Psl polysaccharide polymers or by tethering Psl to the cell surface, as previously mentioned (Borlee *et al.*, 2010). Therefore, the *cdrA* gene is considered very important for *P. aeruginosa* virulence and hence it was selected as one of the genes to be tested further by RT-PCR. In this analysis *cdrA* was upregulated in the qRT-PCR and upregulated in RNA-seq when ΔPA4803 *(ΔsamA*) was compared to the wt under aerobic conditions (**Figure 6.4**)

A


ΔsamA Vs PAO1-N Aerobic
PAO1-L (Control)
ΔsamA (Mutant)
delta CT
4
3
2
1
0
cdrA

B


ΔsamA Vs PAO1-N Aerobic
Q-PCR
RNA-seq
Relative expression (Log2 fold change)
4
3
2
1
0
cdrA

B

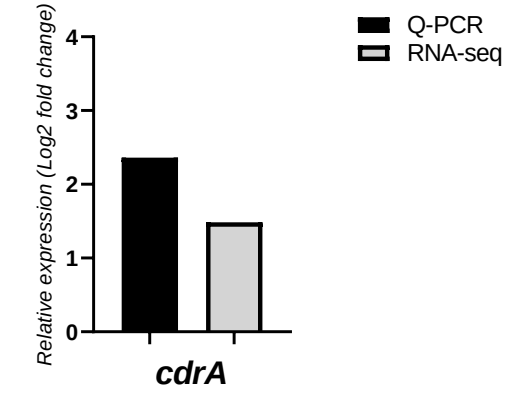

ΔsamA Vs PAO1-N Aerobic
Q-PCR
RNA-seq
Relative expression (Log2 fold change)
4
3
2
1
0
cdrA

Figure 6.4. Expression analysis for *cdrA* gene.
The strain comparison and the conditions are indicated on the figure. Three technical replicates were tested for each sample. A. shows the CT delta values of *cdrA* expression analysed by qRT–PCR between the wt and the *samA* mutant. While associated error bars denote the s.e.m. B. Shows the comparison of fold change of *cdrA* between the Q-PCR (qRT–PCR) and RNA-seq. The height of each box represents the mean average of sample-specific 2−△△ct values.

Secondly, the *pscQ* gene encodes a translocation protein in type III secretion, as mentioned, protein secretion through Type III system is crucial for virulence (Quinaud *et al.*, 2005) hence *pscQ* was selected as one of the genes to be tested further by RT-PCR. In this analysis *pscQ* was downregulated when ΔPA4802.1 was compared to the WT under aerobic conditions (**Figure 6.5**). Major intrinsic multiple antibiotic resistance efflux outer membrane protein OprM precursor (*oprM*), which is a key gene in *P. aeruginosa* virulence (Uwate *et al.*, 2013) was also selected to be tested further by qRT-PCR. Basically, *oprM* was upregulated in the qRT-PCR and upregulated in RNA-seq when ΔPA4802.1 was compared to the WT under aerobic conditions.

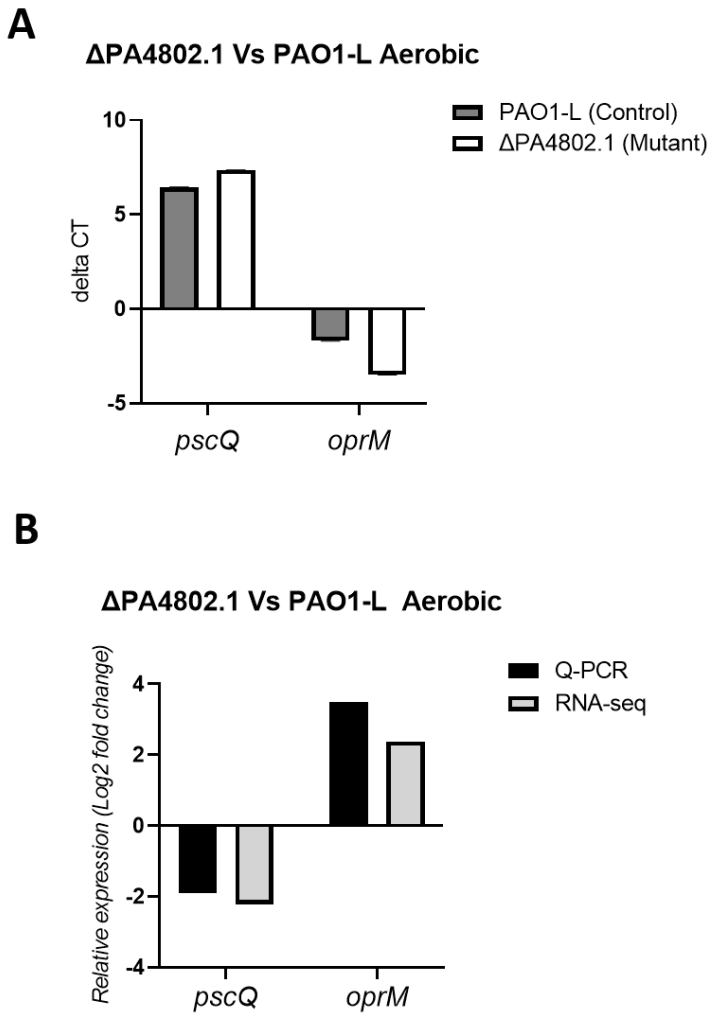


Figure 6.5. Expression analysis for *pscQ* and *oprM* genes.
The strain comparison and the conditions are indicated on the figure. Three technical replicates were tested for each sample. A. shows the CT delta values of *pscQ* and *oprM* expression analysed by qRT–PCR between the wt and the PA4802.1 mutant. Associated error bars denote the s.e.m. B. Shows the comparison of fold change of *pscQ* and *oprM* between the Q-PCR (qRT–PCR) and RNA-seq. The height of each box represents the mean average of sample-specific 2−△△ct values.

Furthermore, expression of *fdhG* and *fdhH* genes under specific conditions was evaluated further, as well, by RT-PCR because of the key functionality in the mechanism this study was set to investigate. In more detail, FdhG is the only stress-related selenoprotein in *P. aeruginosa* and FdhN is the nitrate-inducible formate dehydrogenase, beta subunit which is part of a bigger complex formed with FdhG (Zhang and Gladyshev, 2005; Soboh *et al.*, 2011).The RT-qPCR confirmed that expression *fdhG* and *fdhH* were downregulated as expected and this was consistent with the RNA-seq result for *fdhH* in the PA4802.1 mutant background under anaerobic conditions (**Figure 6.6**). The RT-qPCR confirmed that expression of *fdhG* and *fdhH* was unaffected in the *samA* mutant strain under both aerobic and anaerobic conditions (data not shown).

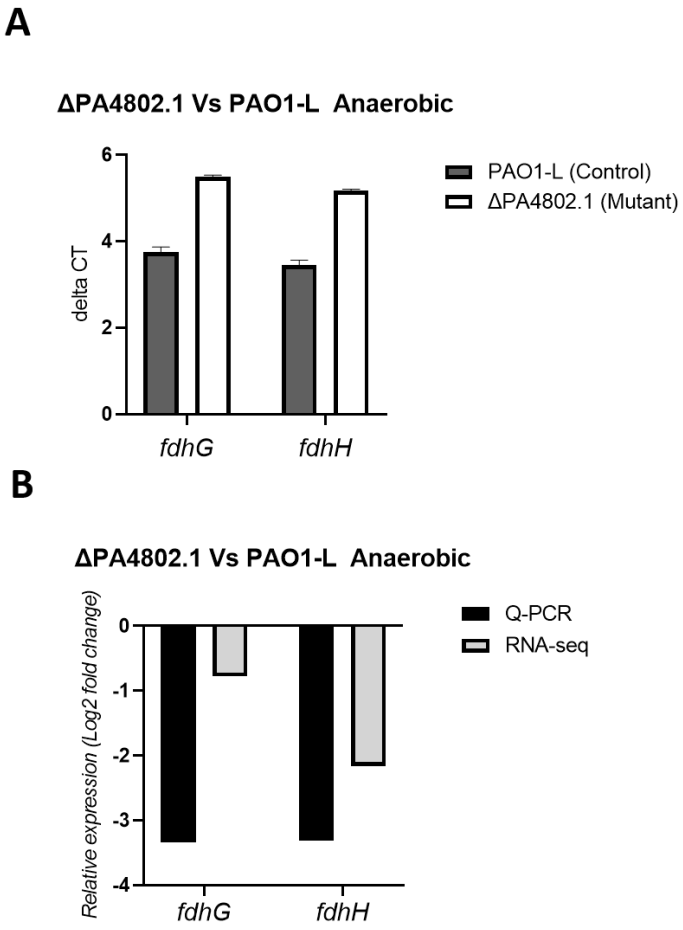


Figure 6.6. Expression analysis for *fdhG a*nd *fdhH* genes.

The strain comparison and the conditions are indicated on the figure. Three technical replicates were tested for each sample. A. shows the CT delta values of *fdhG a*nd *fdhH* expression analysed by qRT–PCR between the wt and the PA4802.1 mutant. While associated error bars denote the s.e.m. B. Shows the comparison of fold change in expression of *fdhG a*nd *fdhH* between the Q-PCR (qRT–PCR) and RNA-seq. The height of each box represents the mean average of sample-specific 2−△△ct values

Overall, qRT-PCR analysis on the few selected genes showed similar expression patterns to those observed in RNA-seq. Due to time constraints no further validation by qRT-PCR was possible.

6.3 Discussion

Understanding how bacteria respond to varying conditions in the environment and during infection is of high importance for identifying new anti-virulence targets, which is critical to fight infections. This part of the study investigated the effect of the deletions of the *samA* and PA4802.1 genes in *P. aeruginosa* and developed a transcriptional profile by transcriptome analysis (RNA-seq). The power of this technique lies on its genome-wide application. Results obtained from such a comprehensive

experiment would provide insights into discerning the regulons of these genes. However, a big proportion of genes identified remains uncharacterised.

Firstly, **Table 6.2** shows that all the necessary data quality control was done further supported by **Table 6.3** which confirms that the total mapped rate was more than 70% as expected, and the percentage of reads that can be mapped to multiple sites in the reference genome were less than 10%, as it should be. Hence, the robustness of the RNA-seq analysis was confirmed.

Then**, Table 6.4** summarizes the comparisons performed and analysed in this study and how many differentially expressed genes DEGs (upregulated or downregulated) were uncovered after comparing each deletion strain and condition with the WT. To uncover which genes were differentially expressed due to the presence/absence of oxygen, gene expression profiles were also compared between isogenic deletion strains.

The volcano plots (**Figure 6.1**) display the pattern of gene expression values for the comparisons of *ΔsamA* (ΔPA4803) vs WT under aerobic and anaerobic conditions. There is a tendency for DEGs with higher values under anaerobic conditions compared to aerobic conditions. Therefore, it seems as if deletion of *samA* has a higher impact under anaerobic conditions. This may suggest that the role of *samA* is broader and more important under these conditions. This is also reflected on the number DEGs identified under aerobic conditions (274 in total) compared to those identified under anaerobic conditions (1553 in total). It is rather interesting to observe that the *samA* deletion affects nearly 10% of the genome.

6.3.1 Impact of SamA and PA4802.1 under aerobic conditions

The *samA* deletion under aerobic conditions led to downregulation of 107 genes and upregulation of 174, these numbers were diminished after a series of criteria that were applied. For the purpose of simplification, 11 downregulated genes and 37 upregulated genes were presented (**Table 6.5** and **Table 6.6**). Therefore, *samA* could be considered a positive regulator of those 11 genes and a negative regulator of those 37 genes however unravelling the pathways leading to this overall impact would require significant further work. Overall, a role for *samA* under aerobic conditions was not really anticipated as the hypothesis of this study focused on its role under anaerobic conditions.

Downregulation was observed in TIII secretion genes, and some efflux pumps genes and efflux pump associated genes. This could suggest that *samA* when present elevates Type III secretion, which will be interesting as TIII secretion is linked with pathogenicity and in particular acute infection since the

machinery is used to translocate toxins from the bacteria to the host cells (Jin *et al.*, 2011)(Thanabalasuriar *et al.*, 2017). In addition, the effect on efflux pumps and their partners gives rise to the possibility that *samA* positively affects antimicrobial resistance in *P. aeruginosa* (Wang and Liu, 2004). It could be that *samA* upregulates type III secretion system components and allows for the secretion of virulence factors which enables the bacterium to establish an infection. Intriguingly, *samA* seems to positively affect a mechanism of bacterial Programmed Cell Death (PCD) this contributes to the damage *P. aeruginosa* can cause to the host (McFarland *et al.*, 2015). In more detail, it is proposed that activation of the Alp cell lysis pathway, in response to bacterial DNA damage inflicted by the host immune system, in *P. aeruginosa* cells is lethal to a subset of bacteria but it benefits the general population of the bacterium (McFarland *et al.*, 2015).

Interestingly, numerous genes involved in either pyoverdine synthesis, phenazine synthesis, *pel* and/or *cdrAB* loci were all upregulated in *samA* absence. This suggests that *samA* is negatively affecting iron acquisition, phenazine biosynthesis and biofilm formation in *P. aeruginosa.* Such an effect was not anticipated for this gene, which is considered crucial for *P. aeruginosa* virulence. This discrepancy may stem from the difference in environmental conditions which are encountered during infection and in the laboratory-setting/*in vitro* setting. Therefore, it would be interesting to further define the timing in which *samA* acts by enhancing the virulence of the bacterium under aerobic conditions. Perhaps, *samA* may be supressing phenotypes associated with the later stages of infection. Another possibility is that *samA* may mainly exerts its function through different mechanisms of pathogenicity and is also keeping under control the effects of other pathways. Further investigation will be required to find the precise timings of the *samA* gene's action.

Functional annotation of these upregulated and downregulated DEGs in aerobic conditions due to the PA4802.1 gene mutation, revealed that indeed there was downregulation of genes involved in "Metabolic pathways" and an upregulation of genes involved in "ABC transporters". The mutation of PA4802.1 showed many less genes affected compared to the *samA* mutant. For upregulated DEGs 10 pathways were enriched and each pathway had 2 genes, so there is an equal distribution. Therefore, there was no evidence of any particular pathways enriched. Moreover, the PA4802.1 mutation affected even less genes under anaerobic conditions, which is not surprising since PA4802.1 encodes for a very specific tRNA. Intrerestingly, PA4802.1 deletion seems to affect keys genes under anaerobic conditions but more on that is discussed below. Overall, the KEGG analysis revealed that most DEGs contributed to metabolism related pathways.

Overall, it was rather anticipated that *samA* gene deletion would affect quite a few pathways more than PA4802.1 because it encodes for a protein. It is very interesting that we got some clues on how *samA* maybe affecting virulence in *P. aeruginosa* however that will not be discussed further, and more focus will be given to PA4802.1 in this instance. PA4802.1 having such a narrow effect supports our hypothesis in the sense that the hypothesis proposes every specific mechanism with a very specific purpose.

6.3.2 Impact of SamA and PA4802.1 under anaerobic conditions

Under anaerobic conditions deletion of *samA* has caused downregulation of TIIIS and twitching by affecting many genes involved in these phenotypes (**Table 6.8** and **Table 6. *9***). TIIIS Secretion was also affected under aerobic conditions. In more detail, under aerobic conditions three genes were downregulated that are associated with TIIIS; namely, *pscE*, *pscf* and *pcr1* (table). However, under anaerobic conditions the effect on TIIIS was bigger with with 13 genes downregulated; namely, *psco*, *popN*, *pcr2*, *pcr3*, *pcrG*, *pcrV* , *pcrH*, *pscF*, *pscH*, *pscI*, *pscJ*, *pscK* and *pscL*. Strengthening the assumption that under both aerobic and anaerobic conditions *samA* positively affects TIIIS is a positive regulator of type III secretion system. In contrast, under the same conditions *samA* seems to negatively affect T4 secretion. Interestingly, *samA* positive effect on twitching is shown under aerobic conditions when *samA* deletion completely abolishes twitching of *P. aeruginosa* (See **Chapter 3, Section 3.2.1.2.1, Figure 3.7**).

Furthermore, some loci such as *spu* and *sha* involved in metabolism were downregulated. The multiple-gene locus for polyamine uptake and utilization as the sole source of carbon and nitrogen in *P. aeruginosa* PAO1, *spu* (*spuABCDE* genes) was downregulated (Stanier *et al.*, 1966; Nishijyo *et al.*, 2001; Lu *et al.*, 2002). Taken together, these data indicate that the *samA* gene, when present, seems to positively affect transport of many different compounds/metabolites.

Interestingly, genes involved in fatty acid metabolism and homeostasis of H, Na, and other monovalent cations, which is critical for many functions, were downregulated as well. Cumulatively, de-repression of these genes in *P. aeruginosa* could massively modify its metabolism in response to infection.

Intriguingly, under anaerobic conditions *samA* deletion negatively affects the production of anthranilate from gene *trpE*. Anthranilate is key for the generation of PQS signalling molecule. At the same time *samA* deletion seems to upregulate the PQS system, which raises the questions of which pathway is the anthranilate sourced from to enable a functional PQS system under these conditions. Overall, it seems as if *samA* enhances anthranilate production while repressing the PQS system under

anaerobic conditions. Further investigations will be required to shed light to this paradox the reason being the complexity of the PQS system due to multi-functionality of the PQS molecule. PQS can interact with several key virulence pathways through several PqsR-dependent and PqsR-independent pathways (Rampioni *et al.*, 2016) but by directly binding hundreds of protein partners in the cell. These observations are the first to demonstrate that PQS can function trough many pathways (Hodgkinson *et al.*, 2016; Baker *et al.*, 2017; Dandela *et al.*, 2018).

Additionally, a large repertoire of iron responsive genes and *phz* genes were upregulated again under anaerobic conditions in the absence of SamA. Therefore, it is safe to speculate that *samA* maybe negatively affecting iron acquisition through the pyoverdine pathway. An explanation could be that *samA* may be favouring non-pyoverdine mediated iron-sourcing. Another explanation is that, *P. aeruginosa* presents a complex network of integrated stimuli sensing and physiological responses. Future studies would be necessary to explore the relationship of *samA* and iron acquisition during infection, as well as the involvement of *samA* in phenazine biosynthesis.

Furthermore, the *pel* operon, which was previously upregulated under aerobic conditions was no longer upregulated under anaerobic conditions in the *samA* mutant. Therefore, *samA* might be negatively affecting polysaccharide production in a regulated manner to control the transition from acute to chronic infections. As mentioned before the function of *samA* may very well depend on the context and timing of the infection. However, under anaerobic conditions *psl* gene associated with polysaccharide production is upregulated in *samA* mutant. This could mean that under anaerobic conditions *samA* favours *psl* production instead of *pel*, which is very interesting. In a study Psl showed to play an important role in surface attachment for all the isolates whereas, Pel did not appear to be an important attachment determinant (Colvin *et al.*, 2013). Therefore, one can speculate that Psl is more important in the initial stages of infection rather than Pel. Another aspect to consider is the timepoint of the infection and in which stage of the transition from acute to chronic are the bacteria in.

Finally, the PQS system and the *RhlR-RhlI* were all positively affected in the absence of *samA*. Therefore, *samA* could be considered a positive modulator of these players of these QS systems. This is in line with the work presented in this thesis where *samA* deletion showed upregulation of the *rhl* system (**Figure 3.10**). In addition, overexpression of SamA was shown to supress PQS signal production (**Figure 3.11**).

In addition, production of rhamnolipids is also positively affected in the absence of *samA* under anaerobic conditions. Therefore, *samA* could be considered a negative regulator of rhamnolipid production. Rhamnolipids are important for the organization of swarming tendrils (Caiazza *et al.*, 2005). This contradicts the results in **Chapter 3**, **Figure 3.7** which shows that absence of *samA* affects swarming negatively. The positive impact on the *rhl* system and the negative impact on rhamnolipids accounts for another contradiction. One explanation could be that these differences stem from the differences in the experiment conditions. Another explanation would be that these systems in *P. aeruginosa* are very complex and intricate and the timepoint in the infection timeline is crucial. However, a recent publication revealed that ToxR, a gene that was deleted in PAO1-Nottingham, ,which is the background of *samA* deletion, affects swarming positively by increasing the levels of C4-HSL and that of rhamnolipid surfactants. Hence, supporting that the reduction of swarming might be due to the *toxR* deletion and also contradicting opposite regulations for the rhl system and the rhamnolipids production (Dubern *et al.*, 2022).

Overall, it is consisted that under both aerobic and anaerobic conditions *samA* seems to negatively affect phenazine production, iron sourcing, the PQS system and its actions, biofilm formation (through *pel* and *psl*) and also the production of rhamnolipids. As mentioned before all these systems in *P. aeruginosa* are very intricate and interconnected and further investigation will be required to identify the usefulness of *samA* gene in different stages of infection.

Interestingly, several genes that were upregulated under anaerobic conditions in the absence of *samA* were associated with molybdate. Namely, PA1860, PA1861 (*modC*), PA1862 (*modB*), PA1863 (*modA*) of the *modABCD* operon. In anaerobic environments, *P. aeruginosa* utilizes nitrate reduction for energy production, a process dependent on the availability of the oxyanionic form of molybdenum, molybdate (MoO_4^{2-}). This evidence suggests that *samA* might negatively regulated molybdate processing and the molybdate transport system when present. This contradicts in part our hypothesis that expects that *samA* protein modifies the PA4802.1 $tRNA^{sec}$ in order to help adaptation to anaerobic conditions. The only explanation is that *P. aeruginosa* is very adaptable in diverse and dynamic environments, and sometimes changes in expression patterns of genes happening might fall into that transitional stage making it difficult to identify the role of a particular gene during that window.

Before concluding the discussion about the *samA* regulon, it should be noted that *samA* deletion used in this RNA-seq analysis was discovered to have been made in the *P. aeruginosa* PAO1 Nottingham strain. This was discovered from the RNA-seq DEGs analysis. Hence, during the RNA-seq experiment comparisons were made with the Wild type *P. aeruginosa* PAO1 Lausanne strain. This is not the ideal

scenario, but it does not discredit these results. After this discovery, the correct WT strains were used during the RT-PCR validations to in order to correct this error. Overall, the comparison between isogenic strains ΔPA4803 (*ΔsamA)* aerobic vs ΔPA4803 *(ΔsamA)* anaerobic was more appropriate since the comparison was between strains of the same background that is *P. aeruginosa* PAO1 Nottingham. A recent study compared Genome sequence data which, revealed fundamental differences between these sublines, *P. aeruginosa* PAO1 Nottingham strain and *P. aeruginosa* PAO1 Lausanne strain. The *P. aeruginosa* PAO1-N subline used which exhibits a reduction in swarming motility compared to PAO1-Lausanne, due to a substantial deletion of 59-kb in its chromosome which includes the regulatory gene toxR, could explain the reduction in swarming seen in the *samA* mutant which until now it was attributed on the specific gene deletion and not the massive subline deletion of *P. aeruginosa* Nottingham.

Functional annotation of these upregulated and downregulated DEGs in anaerobic conditions due to PA4802.1 mutation, revealed that indeed there was downregulation of genes involved as many as 10 pathways (**Table 6.15**), but a specific pathway did not stand out. Therefore, functional analysis done under anaerobic conditions placed the downregulated DEGs in numerous pathways indicating a diverse range of biological processes. Overall, KEGG analysis revealed that upregulated DEGs contributed to "beta-lactam resistance" and "quorum sensing" showing a more narrow effect of PA4802.1 positive impact. However, some DEGs were associated with more than one metabolic pathway indicating their overlapping functions in different metabolic activities.

The PA4802.1 deletion under aerobic conditions led to downregulation of 42 genes and upregulation of 50, always in comparison with the WT (**Table 6.11** and **Table 6.12**). However, after a series of criteria that were applied the numbers of affected genes were diminished. For simplification purposes, only selected genes were discussed. Comparison of the effects of *samA* deletion and tRNA-sec deletion is striking. Not many genes were affected by the tRNA-sec mutation. The most likely explanation for this effect is that *samA* encodes a protein which may be involved in many more pathways than this very specific $tRNA^{sec}$ encoded by the PA4802.1 gene.

Overall, it is very interesting that we got some clues on how *samA* maybe affecting virulence in *P. aeruginosa* under anaerobic conditions but due to the multitude of pathways enriched no more will be discussed here. The focus would rather be on PA4802.1 gene.

6.3.3 Impact of PA4802.1 on *fdnH* and *fdhI*

Amongst the downregulated transcripts in the PA4802.1 mutant under aerobic conditions, were the *fdnH* and *fdhI* genes (**Table 6.14**). These genes encode a nitrate-inducible formate dehydrogenase beta subunit and a nitrate-inducible formate dehydrogenase gamma subunit, respectively. This is a very encouraging result regarding the hypothesis of this study (See Introduction of chapter), because it links the PA4802.1 gene with the expression of genes *fdnH* and *fdnI* genes. Specifically, it suggests that the PA4802.1 deletion itself has a negative impact on the expression of these genes. What is of extreme interest in this study is that PA4802.1 deletion under anaerobic conditions also causes downregulation of genes *fdnH* and *fdnI.*

Interestingly, it was anticipated that the *fdnG* gene, which is also a focus in this study, seems to be in the same operon as f*dnH* and *fdnI* but it was not shown as downregulated as the other genes, after the DEGs list was curated. However, because of its importance of the *fdhG* in the mechanisms under investigation it was included in the RT-PCR validation experiments, which followed the RNA-seq analysis. The RT-PCR confirmed downregulation of *fdhG* in the conditions tested (aerobic and anaerobic). Therefore, this supports the hypothesis of this study. The *fdhG* transcript possesses the secondary structure potentially involved in selenocysteine addition post transcriptionally (analysis can be found in). Based on the available literature it was assumed that if the complex between the methylated $tRNA^{sec}$ and *fdhG* transcript is stabilized then this mRNA would get translated with a selenocysteine residue incorporated into the FdhG protein. Conversely, if the complex would not be formed then the translation would stop and a short-length FdhG protein would be released without modification **Figure 5.8**).

Since it is thought that the mechanisms that involve all these genes must have a post-transcriptional modification as an output, high changes in the expression of these genes in the RNA-seq analysis would not necessarily reflect the final phenotypic outcome. There is a possibility that a small production of the FdhF protein incorporating selenocysteine is enough to assist the *P. aeruginosa* adaptation to anaerobic conditions, mostly encountered in the CF lung.

Another observation is that *samA* does not seem to affect PA4802.1 expression and vice versa at least directly based on the results of the RNA-seq. Also, under anaerobic conditions a PA4802.1 deletion downregulated the PA4802 gene next to it encoding a hypothetical protein, but this is not the case under aerobic conditions. Hence, we cannot assume that the PA4802.1 deletion had any polar effect on PA4802 expression. Moreover, it is interesting that deletion of PA4802.1 under aerobic conditions

seems to affect negatively T3S and positively *psl*, *pel* and *fvp* loci just like the effects of *samA* deletion under the same conditions.

Generally, this tRNA-sec has a very specific role in *E. coli* were it was extensively studied and we expect that it will also has a much more narrow effects in *P. aeruginosa*.

Finally, the expression levels of chosen DEGs *cdrA* (**Figure 6.4**), *pscQ* (**Figure 6.5**)*, oprM* (**Figure 6.5**)*, fdhG* and *fdhH* (**Figure 6.6**) generated from RNA–Seq analysis were verified by qPCR. Almost all showed similar expression patterns to those observed in RNA-seq. Statistical analysis was not performed for the above figures due to the way the calculations were done when the delta-delta Ct method was performed, in order to calculate the relative fold gene expression of samples after performing real-time polymerase chain reaction. Instead of the 3 biological measurement values used separately for the calculation, the the SD of them was calculated first and just the average of the 3 values was used for the delta-delta Ct method.

6.4 Future directions

Future studies should identify whether the PA4802.1 product $tRNA^{sec}$ gets methylated by SamA, if so which base is methylated and whether this affects the modification of the FdhG protein directly. It is worth mentioning that tagging of the selenoprotein identified in *P. aeruginosa,* FdhG was performed in this study in order to assess if it exists in different lengths under different experimental conditions (aerobic vs anaerobic conditions). As previously mentioned, it would be expected that if the conditions are not favourable *fdhG* translation will stop at the UGA stop codon which exists in the middle of its sequence leading to the formation of a shorter peptide and hence a truncated protein. Otherwise, under promoting conditions such as reduced oxygen levels, the UGA codon will be read-out as a selenocysteine (Sec) incorporation codon leading to a full-length transcript and protein. Unfortunately, initial experiments performed to study this effect failed to detect enough protein FdhG protein in cell extracts and due to time constraints could not be optimised.

6.5 Summary

The RNA-Seq data indicated that *samA* and PA4802.1 strongly, though indirectly, repress many genes involved in an array of different functions (T3SS, T6SS, iron acquisition, metabolism etc) and numerous common virulence factors. The *samA* and PA4802.1 regulons did have some parallel effects but it is not believed that they belong in an operon. Overall, further experiments are needed to understand if the two genes are linked in any way. In addition, further experiments will be necessary to dissect the complex role of *samA* at different stages of infection and its relationships with nutrient availability and

regulation of virulence, to facilitate the development of novel therapeutics targeting it. The results obtained for PA4802.1 were encouraging for the hypothesis around the $tRNA^{sec}$ and adaptation to anaerobic conditions. Although more investigations are required in the case of PA4802.1 and the exact experiments needed to uncover its mechanism of action have already been designed and they will be performed in the future when circumstances allow (See **Chapter 5, Section 5.1.9, Figure 5.7**).

6.6 Conclusions

- SamA seems to have diverse functions in *P. aeruginosa*.
- Complete analysis of the *samA* regulon indicates that it mainly exerts its virulence through T3SS contributing to establishment of infection in *P. aeruginosa.*
- Further experiments are required to understand the links between iron acquisition and expression of Pel and Psl genes, and how they contribute to virulence.
- PA4802.1 regulon results are supportive of our hypothesis about the PA4802.1 mechanism of action.
- No clear links were established between *samA* and PA4802.1

Chapter 7 General Discussion

P. aeruginosa is a Gram-negative bacterium that is widespread in the environment (Girard and Bloemberg, 2008). It is an opportunistic human pathogen, causing a variety of life-threatening acute and chronic infections in patients with compromised immune defences (Moradali *et al.*, 2017). *P. aeruginosa* has striking environmental versatility due to the arsenal of virulence factors it produces and secretes. Hence, is capable of not only surviving but thriving in the unfavourable conditions encountered in these diverse environments (Stover *et al.*, 2000; Trunk *et al.*, 2010).

P. aeruginosa belongs to the so-called ESKAPE pathogens, an acronym which groups multidrug resistance pathogens (*Enterococcus faecium*, *Staphylococcus aureus*, *Klebsiella pneumoniae*, *Acinetobacter baumannii*, *P. aeruginosa*, and *Enterobacter* spp) that frequently lead to nosocomial infections (Ó Muimhneacháin *et al.*, 2018). Antimicrobial resistance has become a global concern for public health, highlighting the need for the development of new strategies to tackle these infections (Pang *et al.*, 2019; Soukarieh *et al.*, 2018). Non-biocidal approaches, or "anti-virulence" approaches that exert less selective pressure are rather appealing since they aim at 'striping' the pathogens virulence unlike traditional antibiotics that aim at killing (Defoirdt, 2013; Rasko and Sperandio, 2010; Clatworthy *et al.*, 2007; Defoirdt, 2018) (Theuretzbacher and Piddock, 2019). Therefore, there is the notion that non-biocidal approaches will limit development of resistance (Ó Muimhneacháin *et al.*, 2018).

A library of 57,360 random *P. aeruginosa* PAO1-Lausanne Tn*5* transposants, covering approximately 95% of the genome (Miyata *et al.*, 2006) was the first step taken for the identification of novel putative antimicrobial targets in *P. aeruginosa.* The gene of interest investigated in this study, PA4803 (*samA*) was uncovered by this integrated whole genome screening using several disease models. In preliminary experiments the disruption of the *samA* gene had shown promising indications of it being a potential novel anti-microbial target, as in a murine infection model with the deletion of *samA* increased mice survival significantly compared with the infection with the wild type strain (unpublished data).

Therefore, the aim of this PhD project, reported in Chapter 3 was to advance the knowledge on the impact of the *samA* gene on the growth and production of virulence traits in *P. aeruginosa*, with special attention to the effects that this gene has on the production of key virulence factors such as

pyocyanin, elastase and protease(s). To this end, a *samA* clean deletion mutant was utilized in a multitude of assays and compared to the wild type strain. No effect was observed following the disruption of *samA* on the growth of *P. aeruginosa* or on the production of protease and pyocyanin. Some reduction in elastase production due to *samA* deletion could be observed but this was not confirmed.

Interestingly, the deletion of *samA* seemed to impair both swarming and twitching motilities. However, it was not until the RNA-seq analysis came to light (reported in Chapter 6) that it was realized that the *samA* deletion was made in the *P. aerurignosa* PAO1-Nottingham background strain rather than in the PAO1-Lausanne as it was initially thought. Based on a recent publication by Dubern and colleagues, the PAO1-Nottingham strain is impaired for swarming motility due to a substantial 59 kb deletion in its chromosome and point mutation affecting c-di-GMP signalling (Dubern *et al*., 2022). Therefore, it is possible that the swarming impairment observed is not exclusively due to *samA* absence. However, it is still possible that the twitching impairment observed is due to *samA* being deleted because the complementation rescued the impaired phenotype.

Furthermore, Chapter 3 also reports a thorough investigation of any possible links between *samA* and quorum sensing. Transcriptional reporter strains were constructed for *lasI, pqsA* and *rhlI,* as a first step to unravel the intricacies of the expression of these genes. Expression of all three QS genes was found significantly (p<0.05) upregulated in Δ*samA* background compared to the WT, suggesting that *samA* has a negative impact on all three QS genes. In an opposite approach *samA* gene expression was found to be positively affected by the *rhl* and PQS QS systems and by the Vfr global regulator, whereas, the *las* system did not seem to affect the expression of *samA.* However, Quorum sensing is a very complex and intricate network and it was exceptionally difficult to extract any conclusions from the analysis. It would be very interesting in the future if additional work was done in quantifying the Quorum Sensing Signaling Molecules (QSSMs) and trying to see if the differences observed in the expression of these genes are translated as changes in the quantity of these QSSMs. Interestingly, the RNA-seq reported in Chapter 6 revealed upregulation of several *rhl* genes (*rhlI* included) in the absence of *samA* under anaerobic conditions, which agrees with the results of the reporter assays. Moreover, the RNA-seq analysis revealed upregulation of several *pqs* genes (*pqsA* included) in the absence of *samA* but under anaerobic conditions, which also agrees with the results of the reporter assays.

Another aim reported in Chapter 3 was the identification of potential regulators of *samA* in *P. aeruginosa* with the use of transposon mutagenesis. Few putative negative regulators of *samA* were uncovered (*purD*, *faoA*, *mvaT* and *hmgA*) and these were investigated for their abilities to produce

certain virulence factors and also their motility capabilities. The results of these assays were rather puzzling which can be attributed to the fact that the transposon mutants were used instead of clean deletions strains. In any case, these genes were not investigated further as another avenue for *samA* function came into play.

To recapitulate, the most striking result found during Chapter 3 was the twitching impairment in the *samA* gene deletion mutant and a possible role of *samA* in *P. aeruginosa* surface attachment, which could have implications in the transition from acute into chronic infection state.

Overall, is important to highlight that a lot of the results obtained could be explained by the fact that the *samA* mutant was in the *P. aeruginosa* PAO1 Nottingham background instead of the Lausane and the fact that it was always compared with other PAO1 Lausane strains.

According to genome sequence (Winsor *et al.*, 2016), the *samA* gene is located upstream of the unique tRNA encoded by PA4802.1, which is predicted to incorporate selenocysteine codons into selenoproteins. In addition, other genes involved in the selenocysteine incorporation mechanism, namely *fdnGHI,* as it was described in *E. coli* (Abaibou, et al.,1995) were found in the vicinity of *samA*. It was thought that samA might be acting as a methyltransferase adding a modification on this $tRNA^{Sec}$. At which point, this PhD project took another direction by investigating this $tRNA^{Sec}$. Assessments of the phenotypical impact of $tRNA^{Sec}$ deletion on *P. aeruginosa* lifestyle and investigations of a possible link between the $tRNA^{sec}$ and quorum sensing were all reported in Chapter 3.

To this end, a $tRNA^{Sec}$ clean deletion mutant was utilized in a various assays along with the WT strain. No effect was observed on the growth of *P. aeruginosa* under aerobic or anaerobic conditions. Anaerobic conditions were investigated because the $tRNA^{Sec}$ in *E. coli* is involved in adaptation of the bacterium to anaerobiosis. Again quorum sensing is a very complex and intricate network and it was exceptionally difficult to extract any conclusions from the analysis for any solid links between QS and $tRNA^{Sec}$. It is worth mentioning that RNA-seq reported in Chapter 6 did not show any links between the *P. aeruginosa* $tRNA^{Sec}$ and any QS genes of any of the three main systems.

Given the fact that the PA4802.1 gene is located downstream of *samA*, several genes (6 to be exact) required for selenocysteine addition to protein are found in the vicinity of *samA* and the fact that *samA* probably encodes a hypothetical protein with SAM-dependent methyltransferase activity (Winsor *et al.*, 2016) a strong hypothesis was formed that became the focus of the study. From this point onwards, this PhD project set out to investigate whether the SamA protein is involved in this $tRNA^{Sec}$ mechanism in *P. aeruginosa*.

Selenocysteine is known as the 21st amino acid and its translational insertion into proteins is directed by the UGA codon, which typically functions as stop codon (Yoshizawa and Böck, 2009). The UGA codon is recognized by a complex molecular machinery, known as selenosome (Zhang *et al.*, 2006). In *E. coli* formation of a quaternary complex between the SelB dedicated translation factor, the selenocysteyl-tRNASec (transcribed from the *selC* gene) and a structural element of the mRNA termed SECIS (selenocysteine insertion element) are required for this alternative decoding of UGA of the mRNA at the ribosome (Yoshizawa and Böck, 2009). The best characterised bacterial SECIS (bSECIS) elements are of *E. coli* genes encoding formate dehydrogenases H, N and O. FdhH (encoded by *fdhF*), FdhN (encoded by *fdnGHI*) and FdhO (encoded by *fdoGHI*) are distinct respiration enzymes as they deliver electrons to different substrates (Hartwig *et al.*, 2015). The enzymes are the selenoproteins in *E. coli* (Zinoni *et al*., 1990).

It is hypothesized that in *P. aeruginosa* growing under anaerobic conditions, the SamA enzyme (encoded by PA4803) methylates the Sec[Ser]-tRNA^{Sec} (transcribed by PA4802.1) in the proximity of the anticodon. It is thought that this modification is a maturation step, which changes the tRNA^{Sec} tertiary structure which in turn drives translation of the *fdnGHI* genes found in the same locus. As mentioned above the *fdnGHI* genes products are involved in anaerobic respiration. If the SamA is absent then the unmodified Sec[Ser]-tRNA^{Sec} will not be able to drive translation of this multiprotein complex to completion, which will result in a truncated non-functional selenoprotein FdhG. Thereby, the switch to anaerobic respiration will not occur, or will be significantly hampered.

This hypothesis is in agreement with the *in vivo* data obtained, in which the *samA* mutant strain lacked fitness and virulence when tested in a mouse model of pulmonary infection (unpublished data from collaborators at Ospedale San Raffaele). The CF lung is an environment with several anaerobic pockets and bacteria in this environment need to be able to rapidly switch from aerobic to anaerobic growth and *vice versa*. Hence, it is hypothesized that this mechanism of selenocysteine incorporation into protein in *P. aeruginosa* combines characteristics of the mechanisms described for *E. coli* and mammalian cells. In more detail, it is hypothesized that FdhG, the only selenoprotein in *P. aeruginosa* is involved in adaptation to anaerobic respiration as shown in *E. coli* and a methylation event in the Sec[Ser]-tRNA^{Sec} is critical for its full length translation as shown in mammalian cells.

With the aim to better understand the function of *samA* in *P. aeruginosa*, the research reported in Chapter 4 primarily sought to analyse SamA bioinformatically, and secondly, to assess the catalytic activity of SamA in *P. aeruginosa* and identify potential chaperone proteins. Lastly, it was aimed to elucidate the 3D structure of SamA in order to verify its predicted function. Results shown in this chapter indicate that SamA protein appears to possess a distinctive Class I Methytransferase (MTase)

structure (Schubert *et al.*, 2003a). In addition, data supports that SamA has a possible binding capacity of SAM therefore, it could be an active MTase. Several assays were explored to verify the activity of SamA as an MTase but they were not explored further as another experiment was designed to test the activity indirectly.

Further along, numerous efforts were made to crystallize the SamA protein but up to date no diffractable crystals have been obtained, mainly due to solubility issues that could not be overcome despite the numerous different approaches used. A significant amount of time was taken to generate pure homogenous protein to enable several crystallization trials in a short time. Future work in the field of protein crystallization might provide new avenues to be explored in order for a protein with solubility issues, such as SamA, to produce diffractable crystals. In any case, verifying the activity of SamA as MTase was not abandoned but a rather indirect approach was pursued which will be explained further below.

Since it was hypothesized that SamA modifies the $tRNA^{Sec}$ Chapter 5 reports the *in silico* analysis of the $tRNA^{Sec}$ and *fdhG* sequences from *P. aeruginosa* (amongst others) and their respective structures to assess their potential for a similar role to their equivalents in *E. coli.* In more detail, Chapter 5 reports identification and assessment of the $tRNA^{Sec}$ structure and *fdhG* regulatory elements and their structure.

The analysis performed in Chapter 5 demonstrated that the $tRNA^{sec}$ DNA sequences from *E. coli* and *P. aeruginosa* PAO1 when compared had high identity, which suggests high similarity in folding and function. The next step was the bioinformatic analysis of the PA4802.1 ($tRNA^{sec}$) secondary structure prediction which supported a folding according to features given by Commans and Bock about non-canonical tRNAs (Commans and Bock, 1999). In addition, the *P. aeruginosa fdnG* SECIS sequence is identical to the *fdoG* SECIS sequence of *E. coli*, therefore, the folding is identical and agrees with the one presented in by Thanbichler and Bock as well (Thanbichler and Bock, 2002). All these results support the hypothesis under investigation.

Identifying the nucleotides modified is of high interest. However, due to time constraints and other unforeseen circumstances (health-related issues) the validation of the methylation of the $tRNA^{sec}$ by SamA as well as the identification of the methylated nucleotide could not be carried out during this project. Mainly, because of inability to travel to the laboratory of Prof Mark Helm at the University of Mainz in Germany where these validation experiments were going to be carried out.

The approaches were primarily to analyze the tRNA pool from each of the strains of interest grown under aerobic and anaerobic conditions and obtain the modification profiles. Comparison of the profiles in between strains and conditions would have shed some light on the model and verified the hypothesis. Secondly, the idea was to isolate enough $tRNA^{sec}$ and detect its modified nucleotides, which is a much more direct approach. One of the issues first identified by Prof. Helm, when a pilot experiment was run, was gathering enough $tRNA^{sec}$ as this type of tRNA is rare compared to the rest.

Overall, this study showed that all the elements necessary for the Sec-decoding traits identified in *E. coli* are present in *P. aeruginosa* and it is therefore highly likely that this mechanism is also active in this organism as well. Also, SamA appears to have the structure that would allow it to modify a tRNA. Hence, the findings reported in this thesis constitute a strong basis that supports the hypothesis. However, no other link or proof of interaction could be established between SamA and the *P. aeruginosa* $tRNA^{sec}$ during this project.

With the aim to better understand the functions and unravel the roles of PA4803 (*samA*) and PA4802.1 ($tRNA^{sec}$) *in P. aeruginosa* Chapter 6 sought to use transcriptomics. Because the hypothesis supports a function for these players when switching from aerobic to anaerobic growth and *vice versa* the RNA-seq analysis was carried out in aerobic and anaerobic conditions.

A whole transcriptome study performed with Δ*samA* and ΔPA4802.1 analysed led to the identification of interesting targets for further research. However, a big proportion of genes identified remains uncharacterised.

In particular, results presented in Chapter 6 show that *samA* gene has a much bigger effect under anaerobic conditions compared to aerobic conditions which suggests a more important role for *samA* under those conditions, which is in line with the hypothesis that SamA plays a role in *P. aeruginosa* adaptation to anaerobic growth.

Results obtained suggested that *samA*, when present under aerobic conditions, elevates Type 3 secretion (T3S), which is interesting as T3S is linked with pathogenicity and in particular with acute infection since the machinery is used to translocate toxins from the bacteria to the host cells (Jin *et al.*, 2011)(Thanabalasuriar *et al.*, 2017). It is possible that SamA upregulates the T3S system components and allows for the secretion of virulence factors which enables the bacterium to establish an infection.

Interestingly, the deletion of PA4802.1 under aerobic conditions seems to affect negatively T3S and positively *psl*, *pel* and *fvp* loci just like the effects of *samA* deletion under the same conditions. It would be very interesting to explore this area where the functions of the two genes of interest seem to overlap.

It was puzzling to observe that *samA* under both aerobic and anaerobic conditions is negatively affecting iron acquisition, phenazine biosynthesis and biofilm formation in *P. aeruginosa.* Such an effect was not anticipated for this gene, which is considered crucial for *P. aeruginosa* virulence (unpublished data). However, this discrepancy may stem from the difference in environmental conditions which are encountered during infection and in the laboratory-setting/*in vitro* setting.

Overall, both under aerobic and anaerobic conditions *samA* seems to be a positive regulator of type 3 secretion system. In addition, a large repertoire of iron responsive genes and *phz* genes were upregulated again under anaerobic conditions in the absence of *samA*. Therefore, it is safe to speculate that SamA maybe negatively affecting iron acquisition through the pyoverdine pathway. These results offer new insights in the function of SamA but the relevance of these findings is still not well understood. Definitely, there is a scope for future experiments to investigate these indications.

However, the most striking results of Chapter 6 in relation to the previously formed hypothesis concern the PA4802.1 gene. Interestingly, amongst the downregulated transcripts in the PA4802.1 mutant growing under both aerobic and anaerobic conditions, were the *fdnH* and *fdhI* genes. These genes encode nitrate-inducible formate dehydrogenase beta and gamma subunits, respectively. This is a very encouraging result regarding the hypothesis of this study because it links the PA4802.1 gene with the expression of *fdnH* and *fdnI* genes, which are part of the sec-decoding trait mechanism. Specifically, it suggests that the PA4802.1 deletion itself has a negative impact on the expression of these genes.

Another observation is that *samA* does not seem to affect PA4802.1 expression and vice versa, at least directly based on the results of the RNA-seq. Therefore, a solid link between *samA* and the *PA4802*.1 remains to be established.

To this end, an experiment was designed to investigate the link between SamA and the $tRNA^{sec}$ of *P. aeruginosa* and their involvement in selenocysteine incorporation in FdhG. The FdhG protein in *P. aeruginosa,* encoded by *fdhG/PA4812* was modified by the incorporation of an N-terminal hexahistidine tag in order be able to visualise the protein under different conditions and in different

strains. As explained previously and based on the study hypothesis if the conditions are not favourable (fully aerobic environment, deleted *samA*, and assuming SamA adds an essential methylation on the $tRNA^{sec}$) the *fdhG* translation will stop at the UGA stop codon leading to the formation of a truncated protein. This UGA codon, which is located towards the middle of the *samA* coding sequence, gives under promoting conditions (e.g. reduced oxygen, anaerobic conditions and/or present SamA) the signalling for selenocysteine (Sec) incorporation leading to a full-length protein, otherwise translation is halted, and transcription might as well following this.

At this stage we the data gathered suggests that *samA* exerts it's function mostly during the acute state of the infection rather than the chronic state. If the infection progression is as shown belown in **Figure 7.1** *samA* acts at the beginning of time.

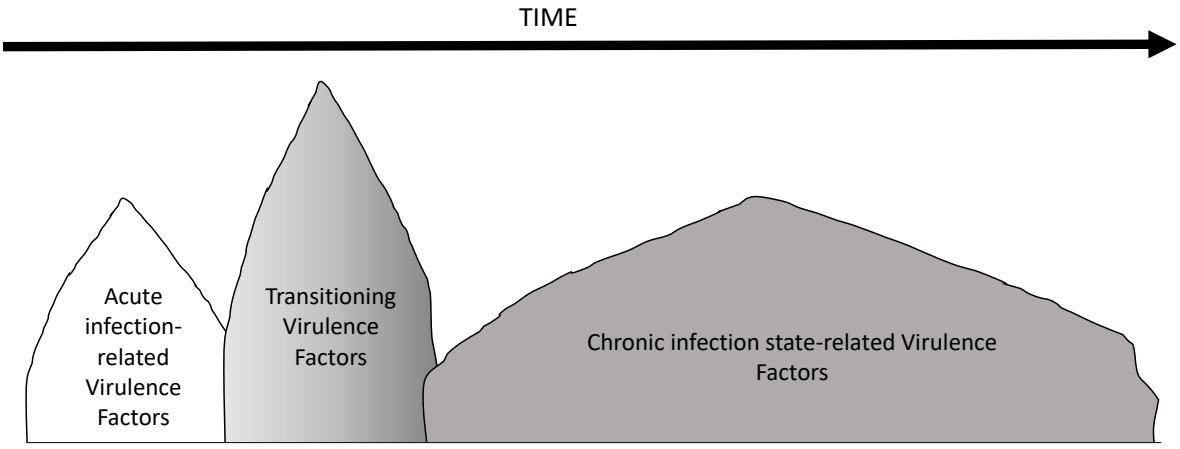


Figure 7.1. Schematic of the Infection Progression in relation to Time.

All in all, from this work future avenues have arisen in the investigation of the function of SamA in the lifestyle of *P. aeruginosa.* These have been thoroughly discussed in the discussions from the previous chapters. The data also provided a strong basis for the main hypothesis on focus key experiments are pending for the elucidation of the mechanism.

Bibliography

Aebi, M., Kirchner, G., Martins, N.C., *et al*. (1990) Isolation of a temperature-sensitive mutant with an altered tRNA nucleotidyltransferase and cloning of the gene encoding tRNA nucleotidyltransferase in the Yeast *Saccharomyces cerevisiae*. *Journal of Biological Chemistry*, 265 (27): 16216–16220.

Aendekerk, S., Diggle, S.P., Song, Z., *et al*. (2005) The MexGHI-OpmD multidrug efflux pump controls growth , antibiotic susceptibility and virulence in *Pseudomonas aeruginosa* via 4-quinolone-dependent cell-to-cell communication., *Microbiology (Reading, England), 151*(Pt 4), pp. 1113–1125. doi:10.1099/mic.0.27631-0.

Afgan, E., Baker, D., Batut, B., *et al*. (2018) The Galaxy platform for accessible, reproducible and collaborative biomedical analyses: 2018 update. *Nucleic Acids Research*, 46 (W1): W537–W544. doi:10.1093/nar/gky379.

Aggen, J.B., Armstrong, E.S., Goldblum, A.A., *et al*. (2010) Synthesis and spectrum of the neoglycoside ACHN-490. *Antimicrobial Agents and Chemotherapy*, 54 (11): 4636–4642. doi:10.1128/AAC.00572-10.

Aiello, D., Williams, J.D., Majgier-Baranowska, H., *et al*. (2010) Discovery and characterization of inhibitors of *Pseudomonas aeruginosa* type III secretion. *Antimicrobial agents and chemotherapy*, 54 (5): 1988—1999. doi:10.1128/aac.01598-09.

Alcalde-Rico, M., Hernando-Amado, S., Blanco, P., *et al*. (2016) Multidrug efflux pumps at the crossroad between antibiotic resistance and bacterial virulence. *Frontiers in Microbiology*, 7 (SEP): 1–14. doi:10.3389/fmicb.2016.01483.

Alibert-Franco, S., Pradines, B., Mahamoud, A., *et al*. (2009) Efflux mechanism, an attractive target to combat multidrug resistant Plasmodium falciparum and *Pseudomonas aeruginosa*. *Current Medicinal Chemistry*, 16 (3): 301–317. doi:10.2174/092986709787002619.

Allen, H.K., Trachsel, J., Looft, T., *et al*. (2014) Finding alternatives to antibiotics. *Annals of the New York Academy of Sciences*, 1323 (1): 91–100. doi:10.1111/nyas.12468.

Allesen-holm, M., Barken, K.B., Yang, L., *et al*. (2006) A characterization of DNA release in *Pseudomonas aeruginosa* cultures and biofilms. *Molecular microbiology*, 59: 1114–1128. doi:10.1111/j.1365-2958.2005.05008.x.

Allmond, L.R., Karaca, T.J., Nguyen, V.N., *et al*. (2003) Protein binding between PcrG-PcrV and PcrH-PopB/PopD encoded by the pcrGVH-popBD operon of the *Pseudomonas aeruginosa* type III secretion system. *Infection and Immunity*, 71 (4): 2230–2233. doi:10.1128/IAI.71.4.2230-2233.2003.

Alvarez-Ortega, C. and Harwood, C.S. (2007) Responses of *Pseudomonas aeruginosa* to low oxygen indicate that growth in the cystic fibrosis lung is by aerobic respiration. *Molecular Microbiology*, 65 (1): 153–165. doi:10.1111/j.1365-2958.2007.05772.x.

Amiel, E., Lovewell, R.R., Toole, G.A.O., *et al*. (2010) *Pseudomonas aeruginosa* evasion of phagocytosis is mediated by loss of swimming motility and is independent of flagellum expression. *Infection and Immunity*, 78 (7): 2937–2945. doi:10.1128/IAI.00144-10.

Anantharajah, A., Faure, E., Buyck, J.M., *et al*. (2016a) Inhibition of the injectisome and flagellar type III secretion systems by INP1855 impairs *Pseudomonas aeruginosa* pathogenicity and inflammasome activation. *The Journal of infectious diseases*, 214 (7): 1105–1116. doi:10.1093/infdis/jiw295.

Anantharajah, A., Mingeot-Leclercq, M.-P. and Van Bambeke, F. (2016b) Targeting the type three secretion system in *Pseudomonas aeruginosa*. *Trends in pharmacological sciences*, 37 (9): 734–749. doi:10.1016/j.tips.2016.05.011.

Anderson, G.G., Moreau-Marquis, S., Stanton, B.A., *et al*. (2008) *In vitro* analysis of tobramycin-treated *Pseudomonas aeruginosa* biofilms on cystic fibrosis-derived airway epithelial cells. *Infection and immunity*, 76 (4): 1423–1433. doi:10.1128/IAI.01373-07.

Andrejko, M., Zdybicka-barabas, A., Janczarek, M., *et al*. (2013) Three *Pseudomonas aeruginosa* strains with different protease profiles. *Acta biochimica Polonica*, 60 (1).

Anyan, M.E., Amiri, A., Harvey, C.W., *et al*. (2014) Type IV pili interactions promote intercellular association and moderate swarming of *Pseudomonas aeruginosa*. *Proceedings of the National Academy of Sciences of the United States of America*, 111 (50). doi:10.1073/pnas.1414661111.

Argenio, D.A.D., Gallagher, L.A., Berg, C.A., *et al*. (2001) *Drosophila* as a Model Host for *Pseudomonas aeruginosa* Infection., *Journal of bacteriology*, 183 (4): 1466–1471. doi:10.1128/JB.183.4.1466.

Arnér, E.S.J. (2020) Common modifications of selenocysteine in selenoproteins. *Essays in Biochemistry*, 64 (1): 45–53. doi:10.1042/ebc20190051.

Aspedon, A., Palmer, K. and Whiteley, M. (2006) Microarray analysis of the osmotic stress response in *Pseudomonas aeruginosa*. *Journal of Bacteriology*, 188 (7): 2721–2725. doi:10.1128/JB.188.7.2721-2725.2006.

Bagge, N., Schuster, M., Hentzer, M., *et al*. (2004) *Pseudomonas aeruginosa* biofilms exposed to imipenem exhibit changes in global gene expression and beta-lactamase and alginate production. *Antimicrobial agents and chemotherapy*, 48 (4): 1175–1187. doi:10.1128/AAC.48.4.1175-1187.2004.

Bains, M., Fernández, L. and Hancock, R.E.W. (2012) Phosphate starvation promotes swarming motility and cytotoxicity of *Pseudomonas aeruginosa*. *Applied and Environmental Microbiology*, 78 (18): 6762–6768. doi:10.1128/AEM.01015-12.

Baker, Y.R., Hodgkinson, J.T., Florea, B.I., *et al*. (2017) Identification of new quorum sensing autoinducer binding partners in: *Pseudomonas aeruginosa* using photoaffinity probes. *Chemical Science*, 8 (11): 7403–7411. doi:10.1039/c7sc01270e.

Balasubramanian, D., Kumari, H., Jaric, M., *et al*. (2014) Deep sequencing analyses expands the *Pseudomonas aeruginosa* AmpR regulon to include small RNA-mediated regulation of iron acquisition, heat shock and oxidative stress response. *Nucleic Acids Research*, 42 (2): 979–998. doi:10.1093/nar/gkt942.

Ball, C.A., Dolinski, K., Dwight, S.S., *et al*. (2000) Integrating functional genomic information into the *Saccharomyces* Genome Database., *Nucleic acids research,* 28 (1): 77–80.

Balsalobre, C. (2012) Biofilm infections , their resilience to therapy and innovative treatment strategies., *Journal of internal medicine,* pp. 541–561. doi:10.1111/joim.12004.

Banerjee, G. and Ray, A.K. (2016) The talking language in some major Gram-negative bacteria. *Archives of Microbiology*, 198 (6): 489–499. doi:10.1007/s00203-016-1220-x.

Baraquet, C., Murakami, K., Parsek, M.R., *et al*. (2012) The FleQ protein from *Pseudomonas aeruginosa* functions as both a repressor and an activator to control gene expression from the Pel operon promoter in response to c-di-GMP. *Nucleic Acids Research*, 40 (15): 7207–7218. doi:10.1093/nar/gks384.

Barclay, M.L., Begg, E.J. and Chambers, S.T. (1992) Adaptive Resistance Following Single Doses of Gentamicin in a Dynamic *In Vitro* Model., *Antimicrobial agents and chemotherapy,* 36 (9): 1951–1957.

Barken, K.B., Pamp, S.J., Yang, L., *et al*. (2008) Roles of type IV pili , flagellum-mediated motility and extracellular DNA in the formation of mature multicellular structures in *Pseudomonas aeruginosa biofilms*., *Environmental microbiology,* 10: 2331–2343. doi:10.1111/j.1462-2920.2008.01658.x.

Baron, S.S. and Rowe, J.J. (1981) Antibiotic action of pyocyanin. *Antimicrobial agents and chemotherapy*, 20 (6): 814–820. doi:10.1128/AAC.20.6.814.

Barr, H.L., Halliday, N., Cámara, M., *et al*. (2015) *Pseudomonas aeruginosa* quorum sensing molecules correlate with clinical status in cystic fibrosis. *European Respiratory Journal*, 46 (4): 1046–1054. doi:10.1183/09031936.00225214.

Bassler, B.L. (2002) Small talk: Cell-to-cell communication in bacteria. *Cell*, 109 (4): 421–424. doi:10.1016/S0092-8674(02)00749-3.

Basso, P. (2017) *Pseudomonas aeruginosa* Pore-Forming exolysin and type IV pili cooperate to induce host cell lysis, *mBio, 8*(1), e02250-16.

Beatson, S.A., Whitchurch, C.B., Sargent, J.L., *et al*. (2002a) Differential regulation of twitching motility and elastase production by Vfr in *Pseudomonas aeruginosa*. *Journal of Bacteriology*, 184 (13): 3605–3613. doi:10.1128/JB.184.13.3605.

Beatson, S.A., Whitchurch, C.B., Semmler, A.B.T., *et al*. (2002b) Quorum Sensing is not required for twitching motility in *Pseudomonas aeruginosa*. *Journal of Bacteriology*, 184 (13): 3598–3604. doi:10.1128/JB.184.13.3598.

Bennett, P.M. (2008) Plasmid encoded antibiotic resistance : acquisition and transfer of antibiotic resistance genes in bacteria., *British journal of pharmacology*, S347–S357. doi:10.1038/sj.bjp.0707607.

Berg, B.L., Baron, C. and Stewart, V. (1991) Nitrate-inducible formate dehydrogenase in *Escherichia coli K-12 II*. Evidence that a mRNA stem-loop structure is essential for decoding opal (UGA) as selenocysteine. *Journal of Biological Chemistry*, 266 (33): 22386–22391.

Berkowitz, D.B., Charette, B.D., Karukurichi, K.R., *et al*. (2006) α-Vinylic amino acids: occurrence, asymmetric synthesis, and biochemical mechanisms. *Tetrahedron Asymmetry*, 17 (6): 869–882. doi:10.1016/j.tetasy.2006.02.026.

Bertoni, M., Kiefer, F., Biasini, M., *et al*. (2017) Modeling protein quaternary structure of homo- and hetero-oligomers beyond binary interactions by homology. *Scientific Reports*, 7 (1): 1–15. doi:10.1038/s41598-017-09654-8.

Bertrand, J.J., West, J.T. and Engel, J.N. (2010) Genetic analysis of the regulation of type IV pilus function by the Chp chemosensory system of *Pseudomonas aeruginosa*. *Journal of Bacteriology*, 192 (4): 994–1010. doi:10.1128/JB.01390-09.

Berube, B.J., Murphy, K.R., Torhan, M.C., *et al*. (2017) Impact of type III secretion effectors and of Phenoxyacetamide inhibitors of type III secretion on abscess formation in a mouse model of *Pseudomonas aeruginosa* infection. *Antimicrobial agents and chemotherapy*, 61 (11). doi:10.1128/AAC.01202-17.

Beveridge, T.J. and Kadurugamuwa, J. (1995) Virulence Factors Are Released from *Pseudomonas aeruginosa* in Association with Membrane Vesicles during Normal Growth and Exposure to Gentamicin : a Novel Mechanism of Enzyme Secretion., *Journal of bacteriology,* 177 (14): 3998–4008.

Bhattacharjee, A., Nusca, T.D. and Hochbaum, A.I. (2016) *Rhamnolipids Mediate an Interspecies Bio fi lm Dispersal Signaling Pathway*. *ACS chemical biology.* doi:10.1021/acschembio.6b00750.

Bianchi, S.M., Prince, L.R., McPhillips, K., *et al*. (2008) Impairment of apoptotic cell engulfment by pyocyanin, a toxic metabolite of *Pseudomonas aeruginosa*. *American Journal of Respiratory and Critical Care Medicine*, 177 (1): 35–43. doi:10.1164/rccm.200612-1804OC.

Bienert, S., Waterhouse, A., De Beer, T.A.P., *et al*. (2017) The SWISS-MODEL Repository-new features and functionality. *Nucleic Acids Research*, 45 (D1): D313–D319. doi:10.1093/nar/gkw1132.

Billings, N., Millan, M.R., Caldara, M., *et al*. (2013) The Extracellular matrix component Psl provides fast- acting antibiotic defense in *Pseudomonas aeruginosa* biofilms., *PLOS Pathogens*, 9 (8). doi:10.1371/journal.ppat.1003526.

Birringer, M., Pilawa, S. and Flohé, L. (2002) Trends in selenium biochemistry. *Natural product reports*, 19 (6): 693–718. doi:10.1039/B205802M.

Bjarnsholt, T., Jensen, P.Ø., Burmølle, M., *et al*. (2005) *Pseudomonas aeruginosa* tolerance to tobramycin , hydrogen peroxide and polymorphonuclear leukocytes is quorum-sensing dependent. *Microbiology*, 151: 373–383. doi:10.1099/mic.0.27463-0.

Bjarnsholt, T., Jensen, P.Ø., Fiandaca, M.J., *et al*. (2009) *Pseudomonas aeruginosa* biofilms in the respiratory tract of Cystic Fibrosis patients., *Pediatric pulmonology,* 558 (August 2008): 547–558. doi:10.1002/ppul.21011.

Blair, J.M.A., Webber, M.A., Baylay, A.J., *et al*. (2014) Molecular mechanisms of antibiotic resistance. *Nature Publishing Group*, (December): 1–10. doi:10.1038/nrmicro3380.

Bleves, S., Viarre, V., Salacha, R., *et al*. (2010) Protein secretion systems in *Pseudomonas aeruginosa* : A wealth of pathogenic weapons. *International Journal of Medical Microbiology*, 300 (8): 534–543. doi:10.1016/j.ijmm.2010.08.005.

Bodey, G.P., Bolivar, R., Fainstein, V., *et al*. (1983) Infections Caused by *Pseudomonas aeruginosa*., *Reviews of infectious diseases,* 5 (2): 279–313.

Bodman, S.B. Von, Willey, J.M. and Diggle, S.P. (2008) Cell-Cell Communication in Bacteria : United We Stand. *Journal of Bacteriology*, 190 (13): 4377–4391. doi:10.1128/JB.00486-08.

Boles, B.R., Thoendel, M. and Singh, P.K. (2005) Rhamnolipids mediate detachment of *Pseudomonas aeruginosa* from biofilms. *Molecular microbiology*, 57 (5): 1210–1223. doi:10.1111/j.1365-2958.2005.04743.x.

Bompfünewerer, A.F., Backofen, RolfBernhart, S.H., Hertel, J., *et al*. (2008) Variations on RNA folding and alignment lessons from Benasque. *Journal of Mathematical Biology*, 56 (1): 129–144. doi:10.1007/s00285-007-0107-5.

Bonneau, A., Roche, B. and Schalk, I.J. (2020) Iron acquisition in *Pseudomonas aeruginosa* by the siderophore pyoverdine: an intricate interacting network including periplasmic and membrane proteins. *Scientific Reports*, 10 (1): 1–11. doi:10.1038/s41598-019-56913-x.

Bonnington, K.E. and Kuehn, M.J. (2014) Protein selection and export via outer membrane vesicles. *BBA - Molecular Cell Research*, 1843 (8): 1612–1619. doi:10.1016/j.bbamcr.2013.12.011.

Borlee, B.R., Goldman, A.D., Murakami, K., *et al*. (2010) *Pseudomonas aeruginosa* uses a cyclic-di-GMP-regulated adhesin to reinforce the biofilm extracellular matrix. *Molecular Microbiology*, 75 (4): 827–842. doi:10.1111/j.1365-2958.2009.06991.x.

Borriello, G., Werner, E., Roe, F., *et al*. (2004) Oxygen Limitation Contributes to Antibiotic Tolerance of *Pseudomonas aeruginosa* in Biofilms., *Antimicrobial agents and chemotherapy,* 48 (7): 2659–2664. doi:10.1128/AAC.48.7.2659.

Botzenhart, K. and Doring, G. (1947) Ecology and Epidemiology of *Pseudomonas aeruginosa.* In: Campa, M., Bendinelli, M., Friedman, H. (eds) *Pseudomonas aeruginosa* as an Opportunistic Pathogen. Infectious Agents and Pathogenesis. Springer, Boston, MA. https://doi.org/10.1007/978-1-4615-3036-7_1

Bowlin, N.O., Williams, J.D., Knoten, C.A., *et al*. (2014) Mutations in the *Pseudomonas aeruginosa* Needle Protein Gene pscF Confer Resistance to Phenoxyacetamide Inhibitors of the Type III Secretion System., *Antimicrobial agents and chemotherapy,* 58 (4): 2211–2220. doi:10.1128/AAC.02795-13.

Bradley, D.E. (1980) A function of *Pseudomonas aeruginosa* PAO polar pili: twitching motility. *Canadian journal of microbiology*, 26 (2): 146–154. doi:10.1139/m80-022.

Breidenstein, E.B.M., Fuente-Nunez, C. de la and Hancock, R.E.W. (2011) *Pseudomonas aeruginosa* : all roads lead to resistance. *Trends in Microbiology*, 19 (8): 419–426. doi:10.1016/j.tim.2011.04.005.

Briard, B., Bomme, P., Lechner, B.E., *et al*. (2015) *Pseudomonas aeruginosa* manipulates redox and iron homeostasis of its microbiota partner *Aspergillus fumigatus* via phenazines. *Scientific reports,* pp. 1–13. doi:10.1038/srep08220.

Brint, J.M. and Ohman, D.E. (1995) Synthesis of Multiple Exoproducts in *Pseudomonas aeruginosa* Is under the Control of RhlR-RhlI , Another Set of Regulators in Strain PAO1 with Homology to the Autoinducer-Responsive LuxR-LuxI Family. *Journal of Bacteriology*, 177 (24): 7155–7163.

Brown, K. (1978) Influence of R-Plasmid RP1 of *Pseudomonas aeruginosa* on Cell Wall Composition , Drug Resistance , and Sensitivity to cold shock. *Antimicrobial agents and chemotherapy,* 13 (3): 446–453.

Bullen, J.J., Rogers, H.J. and Griffiths, E. (1978) Role of iron in bacterial infection. *Current topics in microbiology and immunology*, 80: 1–35. doi:10.1007/978-3-642-66956-9_1.

Burns, J.L., Gibson, R.L., Mcnamara, S., *et al*. (2001) Longitudinal assessment of *Pseudomonas aeruginosa* in young children with Cystic Fibrosis. *The Journal of infectious diseases*, (3): 444–452.

Burrows, L.L. (2012) *Pseudomonas aeruginosa* twitching motility: type IV pili in action. *Annual review of microbiology*, 66: 493–520. doi:10.1146/annurev-micro-092611-150055.

Byrd, M., Sadovskaya, I., Vinogradov, E., *et al*. (2009) Genetic and biochemical analyses of the *Pseudomonas aeruginosa* Psl exopolysaccharide reveal cverlapping roles for polysaccharide synthesis enzymes in Psl and LPS Product. *Physiology & behavior*, 176 (12): 139–148. doi:10.1111/j.1365-2958.2009.06795.x.Genetic.

Caci, E., Scudieri, P., Carlo, E. Di, *et al*. (2015) Upregulation of TMEM16A protein in bronchial epithelial cells by bacterial pyocyanin. *PLoS ONE,* pp. 1–13. doi:10.1371/journal.pone.0131775.

Caiazza, N.C., Shanks, R.M.Q. and Toole, G.A.O. (2005) Rhamnolipids modulate swarming motility patterns of *Pseudomonas aeruginosa*. *Journal of Bacteriology*, 187 (21): 7351–7361. doi:10.1128/JB.187.21.7351.

Camilli, A. and Bassler, B.L. (2006) Bacterial Small-Molecule Signaling Pathways. *Science*, 311: 1113–1116.

Campodonico, V.L., Llosa, J., Grout, M., *et al*. (2010) Evaluation of Flagella and Flagellin of *Pseudomonas aeruginosa* as Vaccines*. Infection and immunity,* 78 (2): 746–755. doi:10.1128/IAI.00806-09.

Cantin, A.M., Hartl, D., Konstan, M.W., *et al*. (2015) Inflammation in cystic fibrosis lung disease : pathogenesis and therapy. *Journal of Cystic Fibrosis*, 14 (4): 419–430. doi:10.1016/j.jcf.2015.03.003.

Cao, H., Krishnan, G., Goumnerov, B., *et al*. (2001) *A* quorum sensing-associated virulence gene of *Pseudomonas aeruginosa* encodes a LysR-like transcription regulator with a unique self-regulatory mechanism. *Proceedings of the National Academy of Sciences of the United States of America*, 98 (25): 10–15.

Carlson, B.A., Xu, X.M., Gladyshev, V.N., *et al*. (2005) Selective rescue of selenoprotein expression in mice lacking a highly specialized methyl group in selenocysteine tRNA. *Journal of Biological Chemistry*, 280 (7): 5542–5548. doi:10.1074/jbc.M411725200.

Casilag, F., Lorenz, A., Krueger, J., *et al*. (2016) The LasB Elastase of Pseudomonas aeruginosa Acts in Concert with Alkaline Protease AprA To Prevent Flagellin-Mediated Immune. *Infection and immunity,* 84 (1): 162–171. doi:10.1128/IAI.00939-15.Editor.

Castric, A. (1983) Hydrogen cyanide production by *Pseudomonas aeruginosa* at reduced oxygen levels. *Canadian journal of microbiology, 29*(10), 1344–1349.

Castric, P. (1994) Microbiology Influence of Oxygen on the *Pseudomonas aeruginosa* Hydrogen Cyanide Synthase. *Current Microbiology*, 29: 2–4.

de Castro, E., Sigrist, C.J.A., Gattiker, A., *et al*. (2006) ScanProsite: Detection of PROSITE signature matches and ProRule-associated functional and structural residues in proteins. *Nucleic Acids Research*, 34: 362–365. doi:10.1093/nar/gkl124.

Cathcart, G.R.A., Quinn, D., Greer, B., *et al*. (2011) Novel inhibitors of the *Pseudomonas aeruginosa* virulence factor LasB: a potential therapeutic approach for the attenuation of virulence mechanisms

in pseudomonal infection. *Antimicrobial agents and chemotherapy*, 55 (6): 2670–2678. doi:10.1128/AAC.00776-10.

Caughlan, R.E., Sriram, S., Daigle, D.M., *et al*. (2009) Fmt bypass in *Pseudomonas aeruginosa* causes induction of MexXY efflux pump expression. *Antimicrobial Agents and Chemotherapy*, 53 (12): 5015–5021. doi:10.1128/AAC.00253-09.

Chan, B.K., Turner, P.E., Kim, S., *et al*. (2018) Phage treatment of an aortic graft infected with *Pseudomonas aeruginosa*. *Evolution, Medicine and Public Health*, 2018 (1): 60–66. doi:10.1093/emph/eoy005.

Chayen, N.E. and Saridakis, E. (2008) Protein crystallization: from purified protein to diffraction-quality crystal. *Nature Methods*, 5 (2): 147–153.

Chen, L., Zou, Y., She, P., *et al*. (2015) Composition , function , and regulation of T6SS in *Pseudomonas aeruginosa*. *Microbiological Research*, 172: 19–25. doi:10.1016/j.micres.2015.01.004.

Chen, Y.-F., Lin, H.-C., Chuang, K.-N., *et al*. (2017) A quantitative model for the rate-limiting process of UGA alternative assignments to stop and selenocysteine codons. *PLOS Computational Biology*, 13 (2): e1005367.

Cheng, Y.S., Shen, Y., Rudolph, J., *et al*. (1990) Glycinamide ribonucleotide synthetase from Escherichia coli: cloning, overproduction, sequencing, isolation, and characterization. *Biochemistry*, 29 (1): 218–227. doi:10.1021/bi00453a030.

Chiang, C.-Y., Uzoma, I., Moore, R.T., *et al*. (2018) Mitigating the Impact of Antibacterial Drug Resistance through Host-Directed Therapies: Current Progress, Outlook, and Challenges. *mBio*, 9 (1). doi:10.1128/mBio.01932-17.

Chiang, W. and Tolker-nielsen, C.T. (2012) The metabolically active subpopulation in *Pseudomonas aeruginosa* biofilms survives exposure to membrane-targeting antimicrobials via distinct molecular mechanisms. *FEMS immunology and medical microbiology,* 65: 245–256. doi:10.1111/j.1574-695X.2012.00929.x.

Choi, D.-S., Kim, D.-K., Choi, S.J., *et al*. (2011a) Proteomic analysis of outer membrane vesicles derived from *Pseudomonas aeruginosa*. *Proteomics*, 11 (16): 3424–3429. doi:10.1002/pmic.201000212.

Choi, Y., Park, H., Park, S.J., *et al*. (2011b) Growth Phase-differential Quorum Sensing regulation of anthranilate metabolism in *Pseudomonas aeruginosa*. *Molecules and cells,* pp. 57–65. doi:10.1007/s10059-011-2322-6.

Chou, H.T., Li, J.Y. and Lu, C.D. (2014) Functional characterization of the *agtABCD* and *agtSR* operons for 4-aminobutyrate and 5-aminovalerate uptake and regulation in *Pseudomonas aeruginosa* PAO1. *Current Microbiology*, 68 (1): 59–63. doi:10.1007/s00284-013-0446-y.

Chow, S., Gu, K., Jiang, L., *et al*. (2011) Salicylic acid affects swimming , twitching and swarming motility in *Pseudomonas aeruginosa* , resulting in decreased Biofilm Formation. *Journal of Experimental Microbiology and Immunology (JEMI)*, 15 (April): 22–29.

Chua, S.L., Liu, Y., Kuok, J., *et al*. (2014) Dispersed cells represent a distinct stage in the transition from bacterial biofilm to planktonic lifestyles. *Nature Communications*, 5: 1–12. doi:10.1038/ncomms5462.

Cirz, R.T., O'Neill, B.M., Hammond, J.A., *et al*. (2006) Defining the *Pseudomonas aeruginosa* SOS response and its role in the global response to the antibiotic ciprofloxacin. *Journal of bacteriology*, 188 (20): 7101–7110. doi:10.1128/JB.00807-06.

Clark, D.P., Pazdernik, N.J. and McGehee, M.R. (2019) *Chapter 21 - Analysis of Gene Expression*. In Clark, D.P., Pazdernik, N.J. and McGehee, M.R.B.T.-M.B. (Third E. (eds.) Academic Cell. pp. 654–690. doi:https://doi.org/10.1016/B978-0-12-813288-3.00021-5.

Clatworthy, A.E., Pierson, E. and Hung, D.T. (2007) Targeting virulence: a new paradigm for antimicrobial therapy. *Nature chemical biology*, 3 (9): 541–548. doi:10.1038/nchembio.2007.24.

Cogen, A.L., Nizet, V. and Gallo, R.L. (2009) Skin microbiota: a source of disease or defence? *British journal of dermatology,* 158 (3): 442–455. doi:10.1111/j.1365-2133.2008.08437.x.Skin.

Coleman, J.P., Hudson, L.L., McKnight, S.L., *et al*. (2008) *Pseudomonas aeruginosa* PqsA is an anthranilate-coenzyme A ligase. *Journal of Bacteriology*, 190 (4): 1247–1255. doi:10.1128/JB.01140-07.

Colvin, K.M., Gordon, V.D., Murakami, K., *et al*. (2011) The Pel polysaccharide can serve a structural and protective role in the biofilm matrix of *Pseudomonas aeruginosa*. *PLOS Pathogens*, 7 (1). doi:10.1371/journal.ppat.1001264.

Colvin, K.M., Irie, Y., Tart, C.S., *et al*. (2013) The Pel and Psl polysaccharides provide *Pseudomonas aeruginosa* structural redundancy within the biofilm matrix. *Environmental Microbiology*, 14 (8). doi:10.1111/j.1462-2920.2011.02657.x.

Colwell, R.R. (1964) A Study of Features used in the Diagnosis of *Pseudomonas aeruginosa*., *Microbiology.*

Commans, S. and Böck, A. (1999) Selenocysteine inserting tRNAs: An overview. *FEMS Microbiology Reviews*, 23 (3): 335–351. doi:10.1016/S0168-6445(99)00011-X.

Conesa, A., Madrigal, P., Tarazona, S., *et al*. (2016) A survey of best practices for RNA-seq data analysis. *Genome Biology*, pp. 1–19. doi:10.1186/s13059-016-0881-8.

Cooper, D.R., Boczek, T., Grelewska, K., *et al*. (2007) Protein crystallization by surface entropy reduction: optimization of the SER strategy. *Acta Crystallographica Section D*, *Biological crystallography,* 63 (5): 636–645. doi:10.1107/S0907444907010931.

Cooper, V.S. and Lenski, R.E. (2000) The population genetics of ecological specialization in evolving *Escherichia coli* populations*. Nature*, 407 (October): 10–13.

Cornelis, G.R. (2010) The type III secretion injectisome, a complex nanomachine for intracellular "toxin" delivery. *Biological Chemistry*, 391 (7): 745–751. doi:10.1515/BC.2010.079.

Costerton, J.W., Irvin, R.T. and Cheng, K.J. (1981) The bacterial glycocalyx in nature and disease. *Annual review of microbiology*, 35: 299–324. doi:10.1146/annurev.mi.35.100181.001503.

Costerton, J.W., Lewandowski, Z., Caldwell, D.E., *et al*. (1995) Microbial biofilms. *Annual Reviews of Microbiology*, 49: 711–745.

Cox, G., Ejim, L., Stogios, P.J., *et al*. (2018) Plazomicin Retains Antibiotic Activity against Most Aminoglycoside Modifying Enzymes. *ACS infectious diseases*, 4 (6): 980–987. doi:10.1021/acsinfecdis.8b00001.

Cullen, L., Weiser, R., Olszak, T., *et al*. (2019) Phenotypic characterization of an international *Pseudomonas aeruginosa* reference panel : strains of cystic fibrosis (CF) origin show less in vivo virulence than non-CF strains. *Microbiology*, (2015): 1961–1977. doi:10.1099/mic.0.000155.

Cunliffe, H.E., Merriman, T.R. and Lamont, I.L. (1995) Cloning and characterization of pvdS, a gene required for pyoverdine synthesis in *Pseudomonas aeruginosa*: PvdS is probably an alternative sigma factor. *Journal of Bacteriology*, 177 (10): 2744–2750. doi:10.1128/jb.177.10.2744-2750.1995.

Czaplewski, L., Bax, R., Clokie, M., *et al*. (2016) Alternatives to antibiotics-a pipeline portfolio review. *The Lancet. Infectious diseases*, 16 (2): 239–251. doi:10.1016/S1473-3099(15)00466-1.

Dandela, R., Mantin, D. and Meijler, M.M. (2018) Chemical Science proteome-wide mapping of PQS-interacting proteins in *Pseudomonas aeruginosa. Chemical Science*, pp. 2290–2294. doi:10.1039/c7sc04287f.

D'Angelo, F., Baldelli, V., Halliday, N., *et al*. (2018) Identification of FDA-approved drugs as antivirulence agents. *Journal of American Society Microbiology,* pp. 1–20. doi:10.1128/AAC.01296-18.

D'Argenio, D.A., Wu, M., Hoffman, L.R., *et al*. (2007) Growth phenotypes of *Pseudomonas aeruginosa* lasR mutants adapted to the airways of cystic fibrosis patients. *Molecular microbiology*, 64 (2): 512–533. doi:10.1111/j.1365-2958.2007.05678.x.

Darzins, A. and State, T.O. (1993) The pilG gene product , required for *Pseudomonas aeruginosa* pilus production and twitching motility , is homologous to the enteric , single-domain Response Regulator CheY. *Journal of Bacteriology*, 175 (18): 5934–5944.

Das, T., Kutty, S.K., Kumar, N., *et al*. (2013) Pyocyanin facilitates extracellular DNA binding to *Pseudomonas aeruginosa* influencing cell surface properties and aggregation. *PLoS ONE,* 8 (3): 1–11. doi:10.1371/journal.pone.0058299.

Das, T., Kutty, S.K., Tavallaie, R., *et al*. (2015) Phenazine virulence factor binding to extracellular DNA is important for *Pseudomonas aeruginosa* biofilm. *Scientific Reports*, pp. 1–9. doi:10.1038/srep08398.

Das, T. and Manefield, M. (2012) Pyocyanin promotes extracellular DNA release in *Pseudomonas aeruginosa*. *PLoS ONE*, 7 (10). doi:10.1371/journal.pone.0046718.

Dasgupta, N., Arora, S.K. and Ramphal, R. (2004) "The Flagellar System of *Pseudomonas aeruginosa*." In Ramos, J.-L. (ed.) *Pseudomonas: Volume 1 Genomics, Life Style and Molecular Architecture*. Boston, MA: Springer US. pp. 675–698. doi:10.1007/978-1-4419-9086-0_22.

Davey, M.E., Caiazza, N.C. and Toole, G.A.O. (2003) Rhamnolipid Surfactant Production Affects Biofilm Architecture in *Pseudomonas aeruginosa PAO1*. *Journal of Bacteriology*, 185 (3): 1027–1036. doi:10.1128/JB.185.3.1027.

Davies, D.G., Parsek, M.R., Pearson, J.P., *et al*. (1998) The involvement of cell-to-cell signals in the development of a bacterial biofilm. *Science (New York, N.Y.)* 280 (April): 295–298.

Davies, J. and Davies, D. (2010) Origins and evolution of antibiotic resistance. *Microbiology and molecular biology reviews : MMBR*, 74 (3): 417–433. doi:10.1128/MMBR.00016-10.

Defoirdt, T. (2013) Antivirulence Therapy for Animal Production : Filling an Arsenal with Novel Weapons for Sustainable Disease Control. *PLoS Pathogens*, 9 (10): 1–4. doi:10.1371/journal.ppat.1003603.

Defoirdt, T. (2018) Quorum-Sensing systems as targets for antivirulence therapy. *Trends in Microbiology*, 26 (4): 313–328. doi:10.1016/j.tim.2017.10.005.

Defoirdt, T., Boon, N. and Bossier, P. (2010) Can bacteria evolve resistance to Quorum Sensing Disruption*? PLos Pathogens*, 6 (7): 2–7. doi:10.1371/journal.ppat.1000989.

Defoirdt, T., Brackman, G. and Coenye, T. (2013) Quorum sensing inhibitors: how strong is the evidence? *Trends in microbiology*, 21 (12): 619–624. doi:10.1016/j.tim.2013.09.006.

DeLange, P.A., Collins, T.L., Pierce, G.E., *et al*. (2007) PilJ localizes to cell poles and is required for type IV pilus extension in *Pseudomonas aeruginosa*. *Current microbiology*, 55 (5): 389–395. doi:10.1007/s00284-007-9008-5.

DeLeon, K., Balldin, F., Watters, C., *et al*. (2009) Gallium maltolate treatment eradicates *Pseudomonas aeruginosa* infection in thermally injured mice. *Antimicrobial agents and chemotherapy*, 53 (4): 1331–1337. doi:10.1128/AAC.01330-08.

Deng, W., Marshall, N.C., Rowland, J.L., *et al*. (2017) Assembly, structure, function and regulation of type III secretion systems. *Nature reviews. Microbiology*, 15 (6): 323–337. doi:10.1038/nrmicro.2017.20.

Denis, K., Le Bris, M., Le Guennec, L., *et al*. (2019) Targeting Type IV pili as an antivirulence strategy against invasive meningococcal disease. *Nature microbiology*, 4 (6): 972–984. doi:10.1038/s41564-019-0395-8.

Dessau, M.A. and Modis, Y. (2011) Protein Crystallization for X-ray Crystallography. *Journal of Visualized Experiments*, 9: 190–195. doi:10.3791/2285.

Déziel, E., Lépine, F., Milot, S., *et al*. (2003) rhlA is required for the production of a novel biosurfactant promoting swarming motility in *Pseudomonas aeruginosa*: 3-(3-hydroxyalkanoyloxy)alkanoic acids (HAAs), the precursors of rhamnolipids. *Microbiology*, 149 (8): 2005–2013. doi:10.1099/mic.0.26154-0.

Deziel, E., Lepine, F., Milot, S., *et al*. (2003) rhlA is required for the production of a novel biosurfactant promoting swarming motility in *Pseudomonas aeruginosa :* the precursors of rhamnolipids. *Microbiology*, 149: 2005–2013. doi:10.1099/mic.0.26154-0.

Diamond, A.M., In Shon Choi, Crain, P.F., *et al*. (1993) Dietary selenium affects methylation of the wobble nucleoside in the anticodon of selenocysteine tRNA([Ser]Sec). *Journal of Biological Chemistry*, 268 (19): 14215–14223.

Diggle, S.P., Matthijs, S., Wright, V.J., *et al*. (2007) The *Pseudomonas aeruginosa* 4-Quinolone signal molecules HHQ and PQS play multifunctional roles in Quorum Sensing and Iron entrapment. *Cell Press*, 14: 87–96. doi:10.1016/j.chembiol.2006.11.014.

Diggle, S.P., Stacey, R.E., Dodd, C., *et al*. (2006) The galactophilic lectin, LecA, contributes to biofilm development in *Pseudomonas aeruginosa*. *Environmental Microbiology*, 8 (6): 1095–1104. doi:10.1111/j.1462-2920.2006.001001.x.

Diggle, S.P., Winzer, K., Chhabra, S.R., *et al*. (2003) The *Pseudomonas aeruginosa* quinolone signal molecule overcomes the cell density-dependency of the quorum sensing hierarchy, regulates rhl-dependent genes at the onset of stationary phase and can be produced in the absence of LasR. *Molecular Microbiology*, 50 (1): 29–43. doi:10.1046/j.1365-2958.2003.03672.x.

Diggle, S.P., Winzer, K., Lazdunski, A., *et al*. (2002) Advancing the Quorum in *Pseudomonas aeruginosa* : MvaT and the regulation of N -Acylhomoserine Lactone production and virulence gene expression. *Journal of Bacteriology*, 184 (10): 2576–2586. doi:10.1128/JB.184.10.2576.

Dobler, L., Vilela, L.F., Almeida, R. V, *et al*. (2016) Rhamnolipids in perspective : gene regulatory pathways , metabolic engineering , production and technological forecasting. *New Biotechnology*, 33 (1): 123–135. doi:10.1016/j.nbt.2015.09.005.

Drees, S.L., Li, C., Prasetya, F., *et al*. (2016) PqsBC, a condensing enzyme in the biosynthesis of the *Pseudomonas aeruginosa* quinolone signal: Crystal structure, inhibition, and reaction mechanism. *Journal of Biological Chemistry*, 291 (13): 6610–6624. doi:10.1074/jbc.M115.708453.

Drozdetskiy, A., Cole, C., Procter, J., *et al*. (2015) JPred4 : a protein secondary structure prediction server. *Nucleic Acids Research*, 43: 389–394. doi:10.1093/nar/gkv332.

Dubern, J.F., Cigana, C., Simone, M. De, *et al*. (2015) Integrated whole genome screening for *Pseudomonas aeruginosa* virulence genes using multiple disease models reveals that pathogenicity is host specific. *Environmental Microbiology*, 17 (11): 4379–4393. doi:10.1111/1462-2920.12863.

Dubern, J.F., Romero, M., Mai-Prochnow, A., *et al*. (2022) ToxR is a c-di-GMP binding protein that modulates surface-associated behaviour in *Pseudomonas aeruginosa*. *npj Biofilms and Microbiomes*, 8 (1). doi:10.1038/s41522-022-00325-9.

Duménil, G. (2019) Type IV Pili as a Therapeutic Target. *Trends in Microbiology*, 27 (8): 658–661. doi:10.1016/j.tim.2019.05.005.

Elliott, B.W., Jr, S. and Cohen, C. (1986) Isolation and characterization of a Lysine-specific protease from *Pseudomonas aeruginosa*. *The Journal of biological chemistry*, *261*(24), 11259–11265.

Engel, L.S., Hill, J.M., Caballero, A.R., *et al*. (1998) Protease IV , a unique extracellular protease and virulence factor from *Pseudomonas aeruginosa. The Journal of biological chemistry*, 273 (27): 16792–16797.

Esposito, D. and Chatterjee, D.K. (2006) Enhancement of soluble protein expression through the use of fusion tags. *Current Opinion in Biotechnology*, 17: 353–358. doi:10.1016/j.copbio.2006.06.003.

Essar, D.W., Eberly, L., Hadero, A., *et al*. (1990) Identification and characterization of genes for a second anthranilate synthase in *Pseudomonas aeruginosa*: Interchangeability of the two anthranilate synthase and evolutionary implications. *Journal of Bacteriology*, 172 (2): 884–900. doi:10.1128/jb.172.2.884-900.1990.

Farinha, M.A. and Kropinski, A.M. (1990) High efficiency electroporation of *Pseudomonas aeruginosa* using frozen cell suspensions. *FEMS Microbiology Letters*, 70 (2): 221–225.

Farrow, J.M. 3rd, Sund, Z.M., Ellison, M.L., *et al*. (2008) PqsE functions independently of PqsR-*Pseudomonas* quinolone signal and enhances the rhl quorum-sensing system. *Journal of bacteriology*, 190 (21): 7043–7051. doi:10.1128/JB.00753-08.

Fasciano, A.C., Shaban, L. and Mecsas, J. (2019) Promises and challenges of the type three secretion system injectisome as an antivirulence target. *Protein Secretion in Bacteria*, pp. 261–276. doi:10.1128/ecosalplus.esp-0032-2018.

Feldman, M., Bryan, R., Rajan, S., *et al*. (1998) Role of flagella in pathogenesis *of Pseudomonas aeruginosa* pulmonary infection. *Infection and immunity*, 66 (1): 43–51. doi:10.1128/IAI.66.1.43-51.1998.

Feng, L., Xiang, Q., Ai, Q., *et al*. (2016) Effects of Quorum Sensing systems on regulatory T Cells in catheter-related *Pseudomonas aeruginosa* biofilm infection rat models. *Mediators of Inflammation*, 2016. doi:10.1155/2016/4012912.

Fernandes, S. and São-José, C. (2018) Enzymes and mechanisms employed by tailed Bacteriophages to breach the bacterial cell barriers. *Viruses*, 10 (8). doi:10.3390/v10080396.

Fernández, L., Breidenstein, E.B.M. and Hancock, R.E.W. (2011) Creeping baselines and adaptive resistance to antibiotics. *Drug resistance updates : reviews and commentaries in antimicrobial and anticancer chemotherapy*, 14: 1–21. doi:10.1016/j.drup.2011.01.001.

Fernández, L., Gooderham, W.J., Bains, M., *et al*. (2010) Adaptive resistance to the “last hope” antibiotics polymyxin B and colistin in *Pseudomonas aeruginosa* is mediated by the novel two-component regulatory system ParR-ParS. *Antimicrobial Agents and Chemotherapy*, 54 (8): 3372–3382. doi:10.1128/AAC.00242-10.

Feuillet, V., Medjane, S., Mondor, I., *et al*. (2006) Involvement of Toll-like receptor 5 in the recognition of flagellated bacteria. *Proceedings of the National Academy of Sciences of the United States of America*, *103*(33), 12487–12492.

Filiatrault, M.J., Picardo, K.F., Ngai, H., *et al*. (2006) Identification of *Pseudomonas aeruginosa* genes involved in virulence and anaerobic growth. *Infection and Immunity*, 74 (7): 4237–4245. doi:10.1128/IAI.02014-05.

Fischetti, V.A. (2018) Development of Phage Lysins as Novel Therapeutics: A Historical Perspective. *Viruses*, 10 (6). doi:10.3390/v10060310.

Fitridge, I., Dempster, T., Guenther, J., *et al*. (2016) The impact and control of biofouling in marine aquaculture : a review. *Biofouling*, 28 (7): 649–669. doi:10.1080/08927014.2012.700478.

Flemming, H., Neu, T.R. and Wozniak, D.J. (2007) The EPS Matrix : The “House of Biofilm Cells.” *Journal of Bacteriology*, 189 (22): 7945–7947. doi:10.1128/JB.00858-07.

Flemming, H. and Wingender, J. (2010) The biofilm matrix. *Nature Publishing Group*, 8 (9): 623–633. doi:10.1038/nrmicro2415.

Florez, C., Raab, J.E., Cooke, A.C., *et al*. (2017) Membrane distribution of the Pseudomonas Quinolone Signal modulates outer membrane vesicle production in *Pseudomonas aeruginosa*. *mBio*, 8 (4). doi:10.1128/mBio.01034-17.

Folkesson, A., Jelsbak, L., Yang, L., *et al*. (2012) Adaptation of *Pseudomonas aeruginosa* to the cystic fibrosis airway: An evolutionary perspective. *Nature Reviews Microbiology*, 10 (12): 841–851. doi:10.1038/nrmicro2907.

Fourmy, D., Guittet, E. and Yoshizawa, S. (2002) Structure of Prokaryotic SECIS mRNA hairpin and its interaction with elongation factor SelB. *Journal of molecular biology*, 2836 (02): 137–150. doi:10.1016/S0022-2836(02)01030-6.

Fox, Á., Haas, D., Reimmann, C., *et al*. (2008) Emergence of secretion-defective sublines of *Pseudomonas aeruginosa* PAO1 resulting from spontaneous mutations in the vfr global regulatory gene. *Applied and Environmental Microbiology*, 74 (6): 1902–1908. doi:10.1128/AEM.02539-07.

Franklin, M.J., Nivens, D.E., Weadge, J.T., *et al*. (2011) Biosynthesis of the *Pseudomonas aeruginosa* extracellular polysaccharides, Alginate, Pel, and Psl. *Frontiers in microbiology*, 2 (August): 1–16. doi:10.3389/fmicb.2011.00167.

Friedman, L. and Kolter, R. (2004) Genes involved in matrix formation in *Pseudomonas aeruginosa* PA14 biofilms. *Molecular Microbiology*, 51 (3): 675–690. doi:10.1046/j.1365-2958.2003.03877.x.

Frølund, B. (1996) Extraction of extracellular polymers from activated sludge using a cation exchange resin, *Water Research*.

Fuqua, C., Parsek, M. R., & Greenberg, E. P. (2001). Regulation of gene expression by cell-to-cell communication: acyl-homoserine lactone quorum sensing. *Annual review of genetics*, *35*, 439–468.

Fuqua, W.C., Winans, S.C. and Greenberg, E.P. (1994) Quorum Sensing in Bacteria : the LuxR-LuxI family of cell density-responsive transcriptional regulators. *Journal of Bacteriology*, 176 (2): 269–275.

Galdino, A.C.M., de Oliveira, M.P., Ramalho, T.C., *et al*. (2019) Anti-Virulence Strategy against the Multidrug-Resistant Bacterial Pathogen *Pseudomonas aeruginosa*: Pseudolysin (Elastase B) as a Potential Druggable Target. *Current Protein & Peptide Science*, 20 (5): 471–487. doi:10.2174/1389203720666190207100415.

Gallagher, L.A., Mcknight, S.L., Kuznetsova, M.S., *et al*. (2002) Functions Required for Extracellular Quinolone Signaling by *Pseudomonas aeruginosa*. *Journal of Bacteriology*, 184 (23): 6472–6480. doi:10.1128/JB.184.23.6472.

Gambello, M.J., Kaye, S. and Iglewski, B.H. (1993) LasR of *Pseudomonas aeruginosa* Is a transcriptional activator of the alkaline protease gene (apr) and an enhancer of Exotoxin A expression. *Infection and Immunity*, 61 (4): 1180–1184.

Ganne, G., Brillet, K., Basta, B., *et al*. (2017) Iron release from the siderophore Pyoverdine in *Pseudomonas aeruginosa* involves three new actors: FpvC, FpvG, and FpvH. *ACS Chemical Biology*, 12 (4): 1056–1065. doi:10.1021/acschembio.6b01077.

Gao, J., Yang, Y. and Zhou, Y. (2016) Structural bioinformatics predicting the errors of predicted local backbone angles and non-local solvent- accessibilities of proteins by deep neural networks. *Bioinformatics*, 32 (24): 3768–3773. doi:10.1093/bioinformatics/btw549.

Gao, L., Guo, Z., Wang, Y., *et al*. (2018) The Two-Operon-Coded ABC transporter complex FpvWXYZCDEF is required for *Pseudomonas aeruginosa* growth and virulence under Iron-limiting conditions. *Journal of Membrane Biology*, 251 (1): 91–104. doi:10.1007/s00232-017-9979-5.

García-Contreras, R., Maeda, T. and Wood, T.K. (2013) Resistance to quorum-quenching compounds. *Applied and environmental microbiology*, 79 (22): 6840–6846. doi:10.1128/AEM.02378-13.

Garg, N. and Manchanda, G. (2013) Bacterial quorum sensing : circuits and applications. *Antonie van Leeuwenhoek,* doi:10.1007/s10482-013-0082-3.

Garland, M., Loscher, S. and Bogyo, M. (2017) Chemical Strategies to target b acterial virulence. *Chemical reviews*, 117 (5): 4422–4461. doi:10.1021/acs.chemrev.6b00676.

Geesey, G.G., Richardson, W.T., Yeomans, H.G., *et al*. (1977) Microscopic examination of natural sessile bacterial populations from an alpine stream. *Canadian Journal of Microbiology*, 23 (12): 1733–1736.

Gellatly, S.L. and Hancock, R.E.W. (2013) *Pseudomonas aeruginosa* : new insights into pathogenesis and host defenses. *Pathogens and disease*, pp. 159–173. doi:10.1111/2049-632X.12033.

Van Gennip, M., Christensen, L.D., Alhede, M., *et al*. (2009) Inactivation of the rhlA gene in *Pseudomonas aeruginosa* prevents rhamnolipid production, disabling the protection against polymorphonuclear leukocytes. *APMIS : acta pathologica, microbiologica, et immunologica Scandinavica*, 117 (7): 537–546. doi:10.1111/j.1600-0463.2009.02466.x.

Van Gerven, N., Waksman, G. and Remaut, H. (2011) Pili and flagella biology, structure, and biotechnological applications. *Progress in molecular biology and translational science*, 103: 21–72. doi:10.1016/B978-0-12-415906-8.00005-4.

Ghafoor, A., Hay, I.D. and Rehm, B.H.A. (2011) Role of Exopolysaccharides in *Pseudomonas aeruginosa* Biofilm Formation and Architecture. *Applied and environmental microbiology,* 77 (15): 5238–5246. doi:10.1128/AEM.00637-11.

Gibiansky, M.L., Conrad, J.C., Jin, F., *et al*. (2010) *Bacteria Use Type IV Pili to Walk Upright and Detach from Surfaces*. *Science (New York, N.Y.)*, (October): 8–10.

Gilbert, K.B., Kim, T.H., Gupta, R., *et al*. (2009) Global position analysis of the *Pseudomonas aeruginosa* quorum-sensing transcription factor LasR. *Molecular microbiology*, 73 (6): 1072–1085. doi:10.1111/j.1365-2958.2009.06832.x.

Girard, G. and Bloemberg, G. V (2008) Central role of quorum sensing in regulating the production of pathogenicity factors in *Pseudomonas aeruginosa*. *Future Microbiology*, 3 (1): 97–106.

Gloag, E.S., Turnbull, L., Huang, A., *et al*. (2013) Self-organization of bacterial biofilms is facilitated by extracellular DNA. *Proceedings of the National Academy of Sciences of the United States of America*, 110 (28): 11541–11546. doi:10.1073/pnas.1218898110.

González, J.E. and Keshavan, N.D. (2006) Messing with bacterial quorum sensing. *Microbiology and molecular biology reviews : MMBR*, 70 (4): 859–875. doi:10.1128/MMBR.00002-06.

González-Valdez, A., Servín-González, L., Juárez, K., *et al*. (2014) The effect of specific rhlA-las-box mutations on DNA binding and gene activation by *Pseudomonas aeruginosa* quorum-sensing transcriptional regulators RhlR and LasR. *FEMS Microbiology Letters*, 356 (2): 217–225. doi:10.1111/1574-6968.12505.

Goodman, A.L., Kulasekara, B., Rietsch, A., *et al*. (2004) A signaling network reciprocally regulates genes associated with acute infection and chronic persistence in *Pseudomonas aeruginosa*. *Developmental cell*, 7 (5): 745–754. doi:10.1016/j.devcel.2004.08.020.

Gorrec, F. (2013) The current approach to initial crystallization screening of proteins is under-sampled. *Journal of Applied Crystallography*, 46: 795–797. doi:10.1107/S0021889813008030.

Gould, T.A., Schwelzer, H.P. and Churchill, M.E.A. (2004) Structure of the *Pseudomonas aeruginosa* acyl-homoserilactone synthase LasI. *Molecular Microbiology*, 53 (4): 1135–1146. doi:10.1111/j.1365-2958.2004.04211.x.

Grant, S.G.N., Jesseet, J., Bloomt, F.R., *et al*. (1990) Differential plasmid rescue from transgenic mouse DNAs into *Escherichia coli* methylation-restriction mutants. *Proceedings of the National Academy of Sciences of the United States of America. USA*, 87: 4645–4649.

Groote, V.N. De, Verstraeten, N., Fauvart, M., *et al*. (2009) Novel persistence genes in *Pseudomonas aeruginosa* identified by high-throughput screening. *FEMS Microbiology Letters*, 297: 73–79. doi:10.1111/j.1574-6968.2009.01657.x.

Grosso-Beccera, M.-V., Santos-medellín, C., González-valdez, A., *et al*. (2014) *Pseudomonas aeruginosa* clinical and environmental isolates constitute a single population with high phenotypic diversity. *BMC Genomics,* doi:10.1186/1471-2164-15-318.

Groth, A.C. and Calos, M.P. (2004) Phage integrases: Biology and applications. *Journal of Molecular Biology*, 335 (3): 667–678. doi:10.1016/j.jmb.2003.09.082.

Gruber, A.R., Lorenz, R., Bernhart, S.H., *et al*. (2008) The Vienna RNA websuite. *Nucleic acids research*, 36 (Web Server issue): 70–74. doi:10.1093/nar/gkn188.

Gruber, J.D., Chen, W., Parnham, S., *et al*. (2016) The role of 2,4-dihydroxyquinoline (DHQ) in *Pseudomonas aeruginosa* pathogenicity. *PeerJ*, 2016 (1): 1–23. doi:10.7717/peerj.1495.

Grundner-Culemann, E., Martin, G.W., Tujebajeva, R., *et al*. (2001) Interplay between termination and translation machinery in eukaryotic selenoprotein synthesis. *Journal of Molecular Biology*, 310 (4): 699–707. doi:10.1006/jmbi.2001.4809.

Guex, N., Peitsch, M.C. and Schwede, T. (2009) Automated comparative protein structure modeling with SWISS-MODEL and Swiss-PdbViewer: a historical perspective. *Electrophoresis*, 30 Suppl 1: S162-73. doi:10.1002/elps.200900140.

Guttenplan, S.B. and Kearns, D.B. (2014) Regulation of flagellar motility during biofilm formation. *FEMS microbiology reviews,* 37 (6): 849–871. doi:10.1111/1574-6976.12018.

Haenni, M., Hocquet, D., Ponsin, C., *et al*. (2015) Population structure and antimicrobial susceptibility of *Pseudomonas aeruginosa* from animal infections in France. *BMC veterinary research,* pp. 1–5. doi:10.1186/s12917-015-0324-x.

Hall, S., McDermott, C., Anoopkumar-Dukie, S., *et al*. (2016) Cellular effects of pyocyanin, a secreted virulence factor of *Pseudomonas aeruginosa*. *Toxins*, 8 (8): 1–14. doi:10.3390/toxins8080236.

Halliday, N.M., Hardie, K.R., Williams, P., *et al*. (2010) Quantitative liquid chromatography-tandem mass spectrometry profiling of activated methyl cycle metabolites involved in LuxS-dependent

quorum sensing in *Escherichia coli*. *Analytical Biochemistry*, 403 (1–2): 20–29. doi:10.1016/j.ab.2010.04.021.

Hall-Stoodley, L., Costerton, J.W. and Stoodley, P. (2004) Bacterial biofilms: from the natural environment to infectious diseases. *Nature reviews Microbiology*, 2 (2): 95–108. doi:10.1038/nrmicro821.

Halwani, M., Yebio, B., Suntres, Z.E., *et al*. (2008) Co-encapsulation of gallium with gentamicin in liposomes enhances antimicrobial activity of gentamicin against *Pseudomonas aeruginosa*. *The Journal of antimicrobial chemotherapy*, 62 (6): 1291–1297. doi:10.1093/jac/dkn422.

Hammond, J.H., Dolben, E.F., Smith, T.J., *et al*. (2015) Links between Anr and Quorum Sensing in *Pseudomonas aeruginosa* biofilms. *Journal of bacteriology*, 197 (17): 2810–2820. doi:10.1128/JB.00182-15.

Hansen, S.K., Rau, M.H., Johansen, H.K., *et al*. (2012) Evolution and diversification of *Pseudomonas aeruginosa* in the paranasal sinuses of cystic fibrosis children have implications for chronic lung infection. *The ISME journal*, 6 (1): 31–45. doi:10.1038/ismej.2011.83.

Hardman, A.M., Stewart, G.S. and Williams, P. (1998) Quorum sensing and the cell-cell communication dependent regulation of gene expression in pathogenic and non-pathogenic bacteria. *Antonie van Leeuwenhoek*, 74 (4): 199–210. doi:10.1023/a:1001178702503.

Harmsen, M., Yang, L., Pamp, J., *et al*. (2010) An update on *Pseudomonas aeruginosa* biofim formation, tolerance, and dispersal. *FEMS immunology and medical microbiology,* doi:10.1111/j.1574-695X.2010.00690.x.

Hartwig, S., Pinske, C. and Sawers, R.G. (2015) Chromogenic assessment of the three molybdo-selenoprotein formate dehydrogenases in *Escherichia coli. Biochemistry and Biophysics Reports*, 1: 62–67. doi:10.1016/j.bbrep.2015.03.006.

Häse, C.C. and Finkelstein, R.A. (1993) Bacterial extracellular zinc-containing metalloproteases. *Microbiological reviews*, 57 (4): 823–837. doi:10.1128/mr.57.4.823-837.1993.

Hassett, D.J. (1996) Anaerobic Production of Alginate by *Pseudomonas aeruginosa*: Alginate Restricts Diffusion of Oxygen. *Journal of bacteriology,* 178 (24): 7322–7325.

Hassett, D.J., Ma, J., Elkins, J.G., *et al*. (1999) Quorum sensing in *Pseudomonas aeruginosa* controls expression of catalase and superoxide dismutase genes and mediates biofilm susceptibility to hydrogen peroxide. *Molecular microbiology,* 34: 1082–1093.

Hassett, D.J., Sutton, M.D., Schurr, M.J., *et al*. (2009) *Pseudomonas aeruginosa* hypoxic or anaerobic biofilm infections within cystic fibrosis airways. *Trends in microbiology*, (February). doi:10.1016/j.tim.2008.12.003.

Hatfield, D., Lee, B.J., Hampton, L., *et al*. (1991) Selenium induces changes in the selenocysteine tRNA[Ser]Sec population in mammalian cells. *Nucleic acids research*, 19 (4): 939–43. doi:10.1093/nar/19.4.939.

Hatfield, D.L. and Gladyshev, V.N. (2002) How Selenium has altered our understanding of the Genetic code. *Society*, 22 (11): 3565–3576. doi:10.1128/MCB.22.11.3565.

Haussler, S. and Becker, T. (2008) The Pseudomonas Quinolone Signal (PQS) balances life and death in *Pseudomonas aeruginosa* populations. *PLoS Pathogens*, 4 (9): e1000166. doi:10.1371/journal.ppat.1000166.

Hay, T., Fraud, S., Lau, C.H.F., *et al*. (2013) Antibiotic Inducibility of the mexXY Multidrug Efflux operon of *Pseudomonas aeruginosa*: involvement of the MexZ Anti-Repressor ArmZ. *PLoS ONE*, 8 (2): 20–23. doi:10.1371/journal.pone.0056858.

Haynes, W.C. (2009) *Pseudomonas aeruginosa*---its Characterization and identification. *Journal of General Microbiology*, 5 (5): 939–950. doi:10.1099/00221287-5-5-939.

Heck, L. (1986) *Specific* Cleavage of Human Type III and IV Collagens by *Pseudomonas aeruginosa* Elastase. *Infection and immunity*, 51 (1): 115–118.

Heck, L.W., Morihara, K. and Abrahamson, D.R. (1986) Degradation of soluble laminin and depletion of tissue-associated basement membrane laminin by *Pseudomonas aeruginosa* elastase and alkaline protease. *Infection and immunity*, 54 (1): 149–153. doi:10.1128/iai.54.1.149-153.1986.

Heeb, S., Blumer, C. and Haas, D. (2002) Regulatory RNA as mediator in GacA / RsmA-Dependent global control of exoproduct formation in *Pseudomonas fluorescens* CHA0. *Journal of Bacteriology*, 184 (4): 1046–1056. doi:10.1128/JB.184.4.1046.

Heeb, S., Fletcher, M.P., Chhabra, S.R., *et al*. (2010) Quinolones : from antibiotics to autoinducers. *FEMS Microbiology Reviews*, 35: 247–274. doi:10.1111/j.1574-6976.2010.00247.x.

Heffernan, R., Dehzangi, A., Lyons, J., *et al*. (2015a) Structural bioinformatics Highly accurate sequence-based prediction of half-sphere exposures of amino acid residues in proteins. *Bioinformatics*, 32 (6): 843–849. doi:10.1093/bioinformatics/btv665.

Heffernan, R., Paliwal, K., Lyons, J., *et al*. (2015b) Improving prediction of secondary structure , local backbone angles , and solvent accessible surface area of proteins by iterative deep learning. *Nature Publishing Group*, 5: 1–11. doi:10.1038/srep11476.

Heider, J., Baron, C. and Bockn, A. (1992) Coding from a distance : dissection of the mRNA determinants required for the incorporation of selenocysteine into protein. *The EMBO journal*, 1 (1): 3759–3766.

Hemmati, F., Salehi, R., Ghotaslou, R., *et al*. (2020) Quorum Quenching: A potential target for antipseudomonal therapy. *Infection and drug resistance*, 13: 2989–3005. doi:10.2147/IDR.S263196.

Henke, J.M. and Bassler, B.L. (2004) Bacterial social engagements. *Trends in cell biology*, 14 (11). doi:10.1016/j.tcb.2004.09.012.

Henrichsen, J. (1972) Bacterial Surface Translocation : a Survey and a Classification. *Bacteriological Reviews*, 36 (4): 478–503.

Heurlier, K., Denervaud, V. and Haas, D. (2006) Impact of quorum sensing on fitness of *Pseudomonas aeruginosa*. *International Journal of Medical Microbiology*, 296: 93–102. doi:10.1016/j.ijmm.2006.01.043.

Heurlier, K., Denervaud, V., Pessi, G., *et al*. (2003) Negative control of Quorum Sensing by RpoN (σ54) in *Pseudomonas aeruginosa* PAO1. *Journal of Bacteriology*, 185 (7): 2227–2235. doi:10.1128/JB.185.7.2227.

Heurlier, K., Pessi, G., Williams, F., *et al*. (2001) The Global Posttranscriptional regulator RsmA modulates production of virulence determinants and N- Acylhomoserine Lactones *in Pseudomonas aeruginosa*. *Journal of Bacteriology*, 183 (22): 6676–6683. doi:10.1128/JB.183.22.6676.

Heurlier, K., Williams, F., Heeb, S., *et al*. (2004) Positive control of Swarming , rhamnolipid synthesis , and lipase production by the Posttranscriptional RsmA / RsmZ System in *Pseudomonas aeruginosa PAO1*. *Journal of bacteriology,* 186 (10): 2936–2945. doi:10.1128/JB.186.10.2936.

Hilker, R., Munder, A., Klockgether, J., *et al*. (2015) Interclonal gradient of virulence in the *Pseudomonas aeruginosa* pangenome from disease and environment. *Environmental Microbiology*, 17 (1): 29–46. doi:10.1111/1462-2920.12606.

Ho Sui, S.J., Lo, R., Fernandes, A.R., *et al*. (2012) Raloxifene attenuates *Pseudomonas aeruginosa* pyocyanin production and virulence. *International Journal of Antimicrobial Agents*, 40 (3): 246–251. doi:10.1016/j.ijantimicag.2012.05.009.

Hoang, T.T., Kutchma, A.J., Becher, A., *et al*. (2000) Integration-proficient plasmids for *Pseudomonas aeruginosa*: Site-Specific integration and use for engineering of reporter and expression strains. *Plasmid*, 43 (1): 59–72. doi:10.1006/plas.1999.1441.

Hobbs, M. and Mattick, J.S. (1993) Common components in the assembly of type 4 fimbriae, DNA transfer systems, filamentous phage and protein-secretion apparatus: a general system for the formation of surface-associated protein complexes. *Molecular microbiology*, 10 (2): 233–243. doi:10.1111/j.1365-2958.1993.tb01949.x.

Hodgkinson, J.T., Gross, J., Baker, Y.R., *et al*. (2016) *A new Pseudomonas* quinolone signal *(PQS) binding partner : MexG*. *Chemical Science*, pp. 2553–2562. doi:10.1039/c5sc04197j.

Hofacker, I.L., Fontana, W., Stadler, P.F., *et al*. (1994) Fast Folding and comparison of RNA Secondary Structures. *Monatshefte für Chemie*, 125: 167–188.

Hofacker, I.L. and Stadler, P.F. (2006) Memory efficient folding algorithms for circular RNA secondary structures. *Bioinformatics*, 22 (10): 1172–1176. doi:10.1093/bioinformatics/btl023.

Hoge, R., Pelzer, A., Rosenau, F., *et al*. (2010) Weapons of a pathogen : Proteases and their role in virulence of *Pseudomonas aeruginosa.* 45: 383–395.

Høiby, N., Bjarnsholt, T., Moser, C., *et al*. (2015) ESCMID* guideline for the diagnosis and treatment of biofilm infections 2014. *Clinical Microbiology and Infection*, 21 (S1): S1–S25. doi:10.1016/j.cmi.2014.10.024.

Holder, K.K. and Bull, J.J. (2001) Profiles of adaptation in two similar viruses. *Genetics*, 159 (4): 1393–1404. doi:10.1093/genetics/159.4.1393.

Hong, D.J., Bae, I.K., Jang, I., *et al*. (2015) Epidemiology and Characteristics of Metallo- β - Lactamase-Producing *Pseudomonas aeruginosa*. *Infection and Chemotherapy*, 47 (2): 81–97.

Hong, Y. (1992) Effect of *Pseudomonas aeruginosa* elastase and elkaline protease on serum complement and isolated Components Clq and C3. *Clinical immunology and immunopathology,* 62 (2): 133–138.

Hooper, D.C. (2001) Emerging mechanisms of fluoroquinolone resistance. *Emerging Mechanisms of Fluoroquinolone Resistance*, 7 (2): 337–341. doi:10.3201/eid0702.010239.

Hori, H. (2014) Methylated nucleosides in tRNA and tRNA methyltransferases. *Frontiers in Genetics*, 5 (MAY): 1–26. doi:10.3389/fgene.2014.00144.

Hori, H. (2017) Transfer RNA methyltransferases with a SpoU-TrmD (SPOUT) fold and their modified nucleosides in tRNA. *Biomolecules*, 7 (1): 1–24. doi:10.3390/biom7010023.

Hüttenhofer, A., Westhof, E., & Böck, A. . (1996) Solution structure of mRNA hairpins promoting selenocysteine incorporation in *Escherichiia coli* and their base specific interaction with special elongation factor SELB. RNA *(New York, N.Y.)*, *2*(4), 354–366.

Hurley, M.N., Cámara, M. and Smyth, A.R. (2012) Novel approaches to the treatment of *Pseudomonas aeruginosa* infections in cystic fibrosis. *European Respiratory Journal*, 40 (4): 1014–1023. doi:10.1183/09031936.00042012.

Iii, M.C.W., Roe, F., Bugnicourt, A., *et al*. (2003) Contributions of Antibiotic Penetration, Oxygen Limitation , and Low Metabolic Activity to Tolerance of *Pseudomonas aeruginosa* Biofilms to Ciprofloxacin and Tobramycin. *International journal of molecular sciences*, 47 (1): 317–323. doi:10.1128/AAC.47.1.317.

Inouyes, M. (1993) Effect of the Relative Position of the UGA Codon to the Unique. *Biochemistry*, *The Journal of biological chemistry*, 268 (31): 23128–23131.

Irie, Y., Starkey, M., Edwards, A.N., *et al*. (2010) *Pseudomonas aeruginosa* biofilm matrix polysaccharide Psl is regulated transcriptionally by RpoS and post-transcriptionally by RsmA. *Molecular Microbiology*, 78 (September): 158–172. doi:10.1111/j.1365-2958.2010.07320.x.

Jackowski, G. (1996) Senescence-Related Changes in the Subcomplex Arrangement of the Major Light-Harvesting Chlorophyll a / b -Protein Complex of Photosystem II (LHCII) as Influenced by Cytokinin, *Zeitschrift für Naturforschung C.*

Jackowski, J.T., Szepfalusi, Z., Wanner, D.A., *et al*. (1991) Effects of *P. aeruginosa*-derived bacterial products on tracheal ciliary function: role of O2 radicals. *The American journal of physiology*, 260 (2 Pt 1): L61-7. doi:10.1152/ajplung.1991.260.2.L61.

Jackson, K.D., Starkey, M., Kremer, S., *et al*. (2004) Identification of psl , a Locus Encoding a Potential Exopolysaccharide That Is Essential for *Pseudomonas aeruginosa* PAO1 Biofilm Formation. *Journal of bacteriology*, 186 (14): 4466–4475. doi:10.1128/JB.186.14.4466.

Jain, R., Chmiel, J.F. and Group, K.S. (2018) KB001-A , a novel antinflammatory, found to be safe and well-tolerated in cystic fibrosis patients infected with Pseudomonas aeruginosa. *Journal of Cystic Fibrosis*, 17 (4): 484–491. doi:10.1016/j.jcf.2017.12.006.

Jeffries, J.L., Jia, J., Choi, W., *et al*. (2016) *Pseudomonas aeruginosa* pyocyanin modulates mucin glycosylation with sialyl-Lewis(x) to increase binding to airway epithelial cells. *Mucosal immunology*, 9 (4): 1039–1050. doi:10.1038/mi.2015.119.

Jennings, L.K., Storek, K.M., Ledvina, H.E., *et al*. (2015a) Pel is a cationic exopolysaccharide that cross-links extracellular DNA in the *Pseudomonas aeruginosa* biofilm matrix. *Proceedings of the National Academy of Sciences of the United States of America*, 112 (36): 11353–11358. doi:10.1073/pnas.1503058112.

Jensen, P., Givskov, M., Bjarnsholt, T., *et al*. (2010) The immune system vs . *Pseudomonas aeruginosa* biofilms. *FEMS immunology and medical microbiology*, 59: 292–305. doi:10.1111/j.1574-695X.2010.00706.x.

Jimenez, P.N., Koch, G., Thompson, J.A., *et al*. (2012) The multiple signaling systems regulating virulence in *Pseudomonas aeruginosa*. *Microbiology and molecular biology reviews : MMBR* pp. 46–65. doi:10.1128/MMBR.05007-11.

Jin, Y., Yang, H., Qiao, M., *et al*. (2011) Mext regulates the type III secretion system through mexs and ptrc in *Pseudomonas aeruginosa*. *Journal of Bacteriology*, 193 (2): 399–410. doi:10.1128/JB.01079-10.

Johansen, H.K., Aanaes, K., Pressler, T., *et al*. (2012) Colonisation and infection of the paranasal sinuses in cystic fibrosis patients is accompanied by a reduced PMN response. *Journal of cystic fibrosis : official journal of the European Cystic Fibrosis Society*, 11 (6): 525–531. doi:10.1016/j.jcf.2012.04.011.

Jones, A.K., Fulcher, N.B., Balzer, G.J., *et al*. (2010) Activation of the *Pseudomonas aeruginosa* AlgU regulon through mucA mutation inhibits cyclic AMP/Vfr signaling. *Journal of bacteriology*, 192 (21): 5709–5717. doi:10.1128/JB.00526-10.

Juan, C., Gutie, O., Vidal, C., *et al*. (2005) Molecular Mechanisms of beta-Lactam Resistance Mediated by AmpC Hyperproduction in *Pseudomonas aeruginosa* Clinical Strains. *Frontiers in Cellular and Infection Microbiology*, 49 (11): 4733–4738. doi:10.1128/AAC.49.11.4733.

Juárez, O. and Barquera, B. (2012) Insights into the mechanism of electron transfer and sodium translocation of the Na(+)-pumping NADH:quinone oxidoreductase. *Biochimica et biophysica acta*, 1817 (10): 1823–1832. doi:10.1016/j.bbabio.2012.03.017.

Junier, I. and Rivoire, O. (2016) Conserved Units of Co-Expression in Bacterial Genomes : An Evolutionary Insight into Transcriptional Regulation., *PLoS ONE*, pp. 1–25. doi:10.1371/journal.pone.0155740.

Kanehisa, M., Furumichi, M., Tanabe, M., *et al*. (2017) KEGG: new perspectives on genomes, pathways, diseases and drugs. *Nucleic acids research*, 45 (D1): D353–D361. doi:10.1093/nar/gkw1092.

Kaneko, Y., Thoendel, M., Olakanmi, O., *et al*. (2007) The transition metal gallium disrupts *Pseudomonas aeruginosa* iron metabolism and has antimicrobial and antibiofilm activity. *Journal of Clinical Investigation*, 117 (4): 877–888. doi:10.1172/JCI30783.

Karaiskos, I., Souli, M. and Giamarellou, H. (2015) Plazomicin: an investigational therapy for the treatment of urinary tract infections. *Expert opinion on investigational drugs*, 24 (11): 1501–1511. doi:10.1517/13543784.2015.1095180.

Karp, P.D., Billington, R., Caspi, R., *et al*. (2018) The BioCyc collection of microbial genomes and metabolic pathways. *Briefings in Bioinformatics*, 20 (4): 1085–1093. doi:10.1093/bib/bbx085.

Kato, J., Kim, H., Takiguchi, N., *et al*. (2008) *Pseudomonas aeruginosa* as a Model Microorganism for Investigation of Chemotactic Behaviors in Ecosystem. *Journal of bioscience and bioengineering,* 106 (1): 1–7. doi:10.1263/jbb.106.1.

Kertesz, M.A., Schmidt-Larbig, K. and Wüest, T. (1999) A novel reduced flavin mononucleotide-dependent methanesulfonate sulfonatase encoded by the sulfur-regulated msu operon of *Pseudomonas aeruginosa*. *Journal of Bacteriology*, 181 (5): 1464–1473. doi:10.1128/jb.181.5.1464-1473.1999.

Kesarwani, M., Hazan, R., He, J., *et al*. (2011) A quorum sensing regulated small volatile molecule reduces acute virulence and promotes chronic infection phenotypes. *PLoS Pathogens*, 7 (8). doi:10.1371/journal.ppat.1002192.

Kessel, J.C. Van, Rutherford, S.T., Shao, Y., *et al*. (2013) Individual and combined roles of the master Regulators AphA and LuxR in control of the *Vibrio harveyi* Quorum-Sensing regulon. *Journal of bacteriology*, 195 (3): 436–443. doi:10.1128/JB.01998-12.

Kessler, E., Safrin, M., Abrams, W.R., *et al*. (1997) Inhibitors and Specificity of *Pseudomonas aeruginosa LasA. The Journal of biological chemistry,* 272 (15): 9884–9889.

Kessler, E., Safrin, M., Gustin, J.K., *et al*. (1998) Elastase and the LasA protease of *Pseudomonas aeruginosa* are secreted with their propeptides. *Journal of Biological Chemistry*, 273 (46): 30225–30231. doi:10.1074/jbc.273.46.30225.

Kessler, E., Safrins, M., Olsonll, J.C., *et al*. (1993) Secreted LasA of *Pseudomonas aeruginosa* is a staphylolytic protease. T*he Journal of biological chemistry,* 268 (10): 7503–7508.

Khaledi, A., Schniederjans, M., Pohl, S., *et al*. (2016) Transcriptome profiling of antimicrobial resistance in *Pseudomonas aeruginosa*. *Antimicrobial agents and chemotherapy*, 60 (8): 4722–4733. doi:10.1128/AAC.00075-16.Address.

Khan, S.R., Mavrodi, D. V., Jog, G.J., *et al*. (2005) Activation of the phz operon of *Pseudomonas fluorescens* 2-79 requires the LuxR homolog PhzR, N-(3-OH-hexanoyl)-L-homoserine lactone produced by the LuxI homolog PhzI, and a cis-acting phz box. *Journal of Bacteriology*, 187 (18): 6517–6527. doi:10.1128/JB.187.18.6517-6527.2005.

Kim, E.J., Sabra, W. and Zeng, A.P. (2003) Iron deficiency leads to inhibition of oxygen transfer and enhanced formation of virulence factors in cultures of *Pseudomonas aeruginosa* PAO1. *Microbiology*, 149 (9): 2627–2634. doi:10.1099/mic.0.26276-0.

Kim, J.Y., Carlson, B.A., Xu, X.M., *et al*. (2011) Inhibition of selenocysteine tRNA[Ser]Sec aminoacylation provides evidence that aminoacylation is required for regulatory methylation of this tRNA. *Biochemical and Biophysical Research Communications*, 409 (4): 814–819. doi:10.1016/j.bbrc.2011.05.096.

Kim, L.K., Matsufuji, T., Matsufuji, S., *et al*. (2000) Methylation of the ribosyl moiety at position 34 of selenocysteine tRNA [Ser] Sec is governed by both primary and tertiary structure . Methylation of the ribosyl moiety at position 34 of selenocysteine tRNA [Ser] Sec is governed by both primary and *te. Molecular Biology, pp. 1306–1315.*

Klausen, M., Aaes-jørgensen, A., Molin, S., *et al*. (2003) Involvement of bacterial migration in the development of complex multicellular structures in *Pseudomonas aeruginosa* biofilms. *Molecular microbiology*, 50: 61–68. doi:10.1046/j.1365-2958.2003.03677.x.

Klockgether, J., Munder, A., Neugebauer, J., *et al*. (2010) Genome diversity of *Pseudomonas aeruginosa* PAO1 laboratory strains. *Journal of Bacteriology*, 192 (4): 1113–1121. doi:10.1128/JB.01515-09.

Kocabiyik, S., Ergin, E. and Turkoglu, S. (1995) Effects of metals on elastase from *Pseudomonas aeruginosa* SES-938-1. *Biological trace element research*, 50 (1): 25–31. doi:10.1007/BF02789146.

Kohler, T., Curty, L.K., Barja, F., *et al*. (2000) Swarming of *Pseudomonas aeruginosa* is dependent on Cell-to-Cell siignaling and requires Flagella and Pili. *Journal of Bacteriology*, 182 (21): 5990–5996.

Kohler, T., Delden, C.V.A.N., Curty, L.K., *et al*. (2001) *Overexpression of the MexEF-OprN Multidrug Efflux System Affects Cell-to-Cell Signaling in Pseudomonas aeruginosa*. *Journal of bacteriology,* 183 (18): 5213–5222. doi:10.1128/JB.183.18.5213.

Kolpen, M., Hansen, C.R., Bjarnsholt, T., *et al*. (2009) Polymorphonuclear leucocytes consume oxygen in sputum from chronic *Pseudomonas aeruginosa* pneumonia in cystic fibrosis. *Thorax*, 65 (1): 0–1. doi:10.1136/thx.2009.114512.

Kon, Y., Tsukada, H., Hasegawa, T., *et al*. (1999) The role of *Pseudomonas aeruginosa* elastase as a potent inflammatory factor in a rat air pouch inflammation model. *FEMS Immunology & Medical Microbiology,* 25: 313–321.

Kõressaar, T., Lepamets, M., Kaplinski, L., *et al*. (2018) Primer3-masker: Integrating masking of template sequence with primer design software. *Bioinformatics*, 34 (11): 1937–1938. doi:10.1093/bioinformatics/bty036.

Koressaar, T. and Remm, M. (2007) Enhancements and modifications of primer design program Primer3. *Bioinformatics*, 23 (10): 1289–1291. doi:10.1093/bioinformatics/btm091.

Kortright, K.E., Chan, B.K., Koff, J.L., *et al*. (2019) Phage Therapy: A Renewed Approach to Combat Antibiotic-Resistant Bacteria. *Cell host & microbe*, 25 (2): 219–232. doi:10.1016/j.chom.2019.01.014.

Kosono, S., Haga, K., Tomizawa, R., *et al*. (2005) *Characterization of a Multigene-Encoded Sodium / Hydrogen Antiporter (Sha) from Pseudomonas aeruginosa :* Its Involvement in Pathogenesis. *Journal of bacteriology,* 187 (15): 5242–5248. doi:10.1128/JB.187.15.5242.

Kozbial, P.Z. and Mushegian, A.R. (2005) Natural history of S-adenosylmethionine-binding proteins. *BMC Structural Biology*, 5 (19). doi:10.1186/1472-6807-5-19.

Kryukov, G. V. and Gladyshev, V.N. (2004) The prokaryotic selenoproteome. *EMBO Reports*, 5 (5): 538–543. doi:10.1038/sj.embor.7400126.

Kulp, A. and Kuehn, M.J. (2012) Biological functions and biogenesis of secreted bacterial outer membrane vesicles. *Annual review of microbiology,* pp. 163–184. doi:10.1146/annurev.micro.091208.073413.

Laarman, A.J., Bardoel, B.W., Ruyken, M., *et al*. (2019) *Pseudomonas aeruginosa* alkaline protease Blocks complement activation via the classical and lectin pathways. *Journal of immunology,* doi:10.4049/jimmunol.1102162.

Latrèche, L.,Jean-jean, O., Driscoll, D.M., Chavatte, L., *et al*. (2009) Novel structural determinants in human SECIS elements modulate the translational recoding of UGA as selenocysteine. *Nucleic acids research,* 37 (17): 5868–5880. doi:10.1093/nar/gkp635.

LaFayette, S.L., Houle, D., Beaudoin, T., *et al*. (2015) Cystic fibrosis–adapted *Pseudomonas aeruginosa* quorum sensing lasR mutants cause hyperinflammatory responses. *Science Advances*, 1 (6): 1–16. doi:10.1126/sciadv.1500199.

Lam, H., Schwochert, J., Lao, Y., *et al*. (2017) Synthetic Cyclic Peptomers as Type III Secretion System Inhibitors. *Antimicrobial agents and chemotherapy*, 61 (9). doi:10.1128/AAC.00060-17.

Lamarche, M.G. and De, E. (2011) MexEF-OprN Efflux Pump Exports the Pseudomonas Quinolone Signal (PQS) Precursor HHQ (4-hydroxy-2- heptylquinoline). *PLoS ONE*, 6 (9). doi:10.1371/journal.pone.0024310.

Lamont, I.L. and Martin, L.W. (2003) Identification and characterization of novel pyoverdine synthesis genes in *Pseudomonas aeruginosa*. *Microbiology*, 149 (4): 833–842. doi:10.1099/mic.0.26085-0.

Larsen, R.A., Wilson, M.M., Guss, A.M., *et al*. (2002) Genetic analysis of pigment biosynthesis in Xanthobacter autotrophicus Py2 using a new , highly efficient transposon mutagenesis system that is functional in a wide variety of bacteria. *Archives of Microbiology*, 178: 193–201. doi:10.1007/s00203-002-0442-2.

Latham, J.A., Iavarone, A.T., Barr, I., *et al*. (2015) PqqD is a novel peptide chaperone that forms a ternary complex with the radical S-adenosylmethionine protein PqqE in the pyrroloquinoline quinone biosynthetic pathway. *Journal of Biological Chemistry*, 290 (20): 12908–12918. doi:10.1074/jbc.M115.646521.

Latifi, A., Foglino, M., Williams, P., *et al*. (1996) A hierarchical quorum-sensing cascade in Pseudomonas aeruginosa links the transcriptional activators LasR and RhlR (VsmR) to expression of the stationary-phase sigma factor RpoS. *Molecular Microbiology*, 21 (6): 1137–1146.

Lau, G.W., Hassett, D.J., Ran, H., *et al*. (2004) The role of pyocyanin in *Pseudomonas aeruginosa* infection. *Trends in Molecular Medicine*, 10 (12): 599–606. doi:10.1016/j.molmed.2004.10.002.

Lavoie, E.G., Wangdi, T. and Kazmierczak, B.I. (2011) Innate immune responses to *Pseudomonas aeruginosa* infection. *Microbes and infection*, 13 (14–15): 1133–1145. doi:10.1016/j.micinf.2011.07.011.

Ledgham, F., Ventre, I., Soscia, C., *et al*. (2003) Interactions of the quorum sensing regulator QscR: Interaction with itself and the other regulators of *Pseudomonas aeruginosa* LasR and RhlR. *Molecular Microbiology*, 48 (1): 199–210. doi:10.1046/j.1365-2958.2003.03423.x.

Lee, J., Park, Y.K., Chung, E.S., *et al*. (2016) Evolved resistance to colistin and its loss due to genetic reversion in *Pseudomonas aeruginosa*. *Nature Publishing Group*, (April): 1–13. doi:10.1038/srep25543.

Lee, J., Wu, J., Deng, Y., *et al*. (2013) Erratum: A cell-cell communication signal integrates quorum sensing and stress response (Nature Chemical Biology (2013) 9 (339-343)). *Nature Chemical Biology*, 9 (6): 406. doi:10.1038/nchembio0613-406a.

Lee, J. and Zhang, L. (2015) The hierarchy quorum sensing network in *Pseudomonas aeruginosa*. *Protein & cell,* 6 (1): 26–41. doi:10.1007/s13238-014-0100-x.

Lee, V.T., Matewish, J.M., Kessler, J.L., *et al*. (2007) A cyclic-di-GMP receptor required for bacterial exopolysaccharide production. *Molecular microbiology*, 65 (6): 1474–1484. doi:10.1111/j.1365-2958.2007.05879.x.

Lewenza, S., Gardy, J.L., Brinkman, F.S.L., *et al*. (2005) Genome-wide identification of *Pseudomonas aeruginos*a exported proteins using a consensus computational strategy combined with a laboratory-based PhoA fusion screen. *Genome Research*, 15 (2): 321–329. doi:10.1101/gr.3257305.

Lewis, K. (2007) Persister cells , dormancy and infectious disease. *Nature reviews Microbiology*, (January): 48–56. doi:10.1038/nrmicro1557.

Li, W., Cowley, A., Uludag, M., *et al*. (2015) The EMBL-EBI bioinformatics web and programmatic tools framework. *Nucleic Acids Research*, 43: 580–584. doi:10.1093/nar/gkv279.

Liao, C., Huang, X., Wang, Q., *et al*. (2022) Virulence Factors of *Pseudomonas aeruginosa* and antivirulence strategies to combat its drug resistance. *Frontiers in Cellular and Infection Microbiology*, 12 (July): 1–17. doi:10.3389/fcimb.2022.926758.

Lister, P.D., Wolter, D.J. and Hanson, N.D. (2009) Antibacterial-Resistant *Pseudomonas aeruginosa :* Clinical Impact and Complex Regulation of Chromosomally Encoded Resistance Mechanisms. *Clinical microbiology reviews,* 22 (4): 582–610. doi:10.1128/CMR.00040-09.

Liu, B., Hassler, D.F., Smith, G.K., *et al*. (1998) Purification and characterization of a membrane bound neutral pH Optimum magnesium-dependent and Phosphatidylserine-stimulated Sphingomyelinase from rat brain. *Journal of Biological Chemistry*, 273 (51): 34472–34479. *doi*:10.1074/jbc.273.51.34472.

Loenen, W.A.M. (2006) S-adenosylmethionine: jack of all trades and master of everything? *Biochemical Society transactions*, 34 (2): 330–3. doi:10.1042/BST20060330.

Long, J. (2012) Depletion of intestinal phosphate following surgical injury activates the virulence of *P. aeruginosa* causing lethal Gut-derived sepsis. *Bone*, 23 (1): 1–7. doi:10.1016/j.surg.2008.03.045.Depletion.

Lopes, S.P., Ceri, H., Azevedo, N.F., *et al*. (2012) Antibiotic resistance of mixed biofilms in cystic fibrosis: impact of emerging microorganisms on treatment of infection. *International journal of antimicrobial agents*, 40 (3): 260–263. doi:10.1016/j.ijantimicag.2012.04.020.

Lorenz, R., Bernhart, S.H., Höner, C., *et al*. (2011) ViennaRNA Package 2.0. *Algorithms for Molecular Biology*, 6 (26): 1–14.

Low, S.C. and Berry, M.J. (1996) Knowing when not to stop: Selenocysteine incorporation in eukaryotes. *Trends in Biochemical Sciences*, 21 (6): 203–208. doi:10.1016/0968-0004(96)10025-6.

Lu, C., Itoh, Y., Nakada, Y., *et al*. (2002) Functional analysis and regulation of the divergent spuABCDEFGH-spuI operons for polyamine uptake and utilization in *Pseudomonas aeruginosa* PAO1 functional analysis and regulation of the divergent spuABCDEFGH-spuI operons for polyamine uptake and utilization. *Society*, 184 (14): 3765–3773. doi:10.1128/JB.184.14.3765.

Lyons, B.J.E. and Strynadka, N.C.J. (2019) On the road to structure-based development of anti-virulence therapeutics targeting the type III secretion system injectisome. *Medicinal Chemistry Communications*, 10 (8): 1273–1289. doi:10.1039/c9md00146h.

Ma, L., Conover, M., Lu, H., *et al*. (2009) Assembly and development of the *Pseudomonas aeruginosa* biofilm matrix. *PLoS Pathogens*, 5 (3). doi:10.1371/journal.ppat.1000354.

Ma, L., Lu, H., Sprinkle, A., *et al*. (2007) *Pseudomonas aeruginosa* Psl is a galactose- and mannose-rich exopolysaccharide. *Journal of bacteriology*, 189 (22): 8353–8356. doi:10.1128/JB.00620-07.

Ma, L., Terwilliger, A. and Maresso, A.W. (2015) Iron and zinc exploitation during bacterial pathogenesis. *Metallomics : integrated biometal science*, 7 (12): 1541–1554. doi:10.1039/c5mt00170f.

Maeda, T., García-Contreras, R., Pu, M., *et al*. (2012) Quorum quenching quandary: resistance to antivirulence compounds. *The ISME journal*, 6 (3): 493–501. doi:10.1038/ismej.2011.122.

Mah, T., Pitts, B., Pellock, B., *et al*. (2003) A genetic basis for *Pseudomonas aeruginosa* biofilm antibiotic resistance. *Nature,* 426 (November): 1–5. doi:10.1038/nature02090.1.

Mahenthiralingam, E., Campbell, M.E. and Speert, D.P. (1994) Nonmotility and Phagocytic Resistance of *Pseudomonas aeruginosa* Isolates from Chronically Colonized Patients with Cystic Fibrosis. *Infection and immunity,* 62 (2): 596–605.

Mann, E.E. and Wozniak, D.J. (2012) *Pseudomonas* biofilm matrix composition and niche biology. *FEMS microbiology reviews,* 36: 893–916. doi:10.1111/j.1574-6976.2011.00322.x.

Mansfeld, R. van, Jongerden, I., Bootsma, M., *et al*. (2010) The population genetics *of Pseudomonas aeruginosa* isolates from different patient populations exhibits high-level host specificity. *PLoS ONE*, 5 (10): 1–7. doi:10.1371/journal.pone.0013482.

Mao, F., Dam, P., Chou, J., *et al*. (2009) DOOR : a database for prokaryotic operons. *Nucleic Acids Research*, 37 (November 2008): 459–463. doi:10.1093/nar/gkn757.

Mariencheck, W.I., Alcorn, J.F., Palmer, S.M., *et al*. (2003) *Pseudomonas aeruginosa* elastase degrades surfactant proteins A and D. *American Journal of Respiratory Cell and Molecular Biology*, 28 (4): 528–537. doi:10.1165/rcmb.2002-0141OC.

Marsden, A.E., King, J.M., Spies, M.A., *et al*. (2016) Inhibition of *Pseudomonas aeruginosa* ExsA DNA-Binding Activity by N-Hydroxybenzimidazoles. *Antimicrobial agents and chemotherapy*, 60 (2): 766–776. doi:10.1128/AAC.02242-15.

Martinez, J.L., Sánchez, M.B., Martínez-Solano, L., *et al*. (2009) Functional role of bacterial multidrug efflux pumps in microbial natural ecosystems. *FEMS Microbiology Reviews*, 33 (2): 430–449. doi:10.1111/j.1574-6976.2008.00157.x.

Mashburn, L.M. and Whiteley, M. (2005) Membrane vesicles traffic signals and facilitate group activities in a prokaryote. *Nature*, 437 (7057): 422–425. doi:10.1038/nature03925.

Mashburn-warren, L., Howe, J., Garidel, P., *et al*. (2008) Interaction of quorum signals with outer membrane lipids : insights into prokaryotic membrane vesicle formation. *Molecular Microbiology*, 69 (June): 491–502. doi:10.1111/j.1365-2958.2008.06302.x.

Masuda, N., Sakagawa, E., Ohya, S., *et al*. (2000) Substrate specificities of MexAB-OprM, MexCD-OprJ, and MexXY-OprM efflux pumps in *Pseudomonas aeruginosa*. *Antimicrobial Agents and Chemotherapy*, 44 (12): 3322–3327. doi:10.1128/AAC.44.12.3322-3327.2000.

Mateos, F., Brock, J.H. and Pérez-Arellano, J.L. (1998) Iron metabolism in the lower respiratory tract. *Thorax*, 53 (7): 594–600. doi:10.1136/thx.53.7.594.

Mathee, K., Narasimhan, G., Valdes, C., *et al*. (2008) Dynamics of *Pseudomonas aeruginosa* genome evolution. *Proceedings of the National Academy of Sciences of the United States of America,* doi:10.1073/pnas.0711982105.

Matsumoto, T., Tateda, K., Furuya, N., *et al*. (1998) Efficacies of alkaline protease, elastase and exotoxin A toxoid vaccines against gut-derived *Pseudomonas aeruginosa* sepsis in mice. *Journal of Medical Microbiology*, 47 (4): 303–308. doi:10.1099/00222615-47-4-303.

Matz, C., Moreno, A.M., Alhede, M., *et al*. (2009) *Pseudomonas aeruginosa* uses type III secretion system to kill biofilm-associated amoebae. *The ISME journal*, 2 (8): 843–852. doi:10.1038/ismej.2008.47.

Maura, D. and Rahme, L.G. (2017) Pharmacological inhibition of the formation and potentiates antibiotic-mediated biofilm disruption. *Antimicrobial agents and chemotherapy,* 61 (12): 15–17.

Mavrodi, D. V, Bonsall, R.F., Delaney, S.M., *et al*. (2001) Functional Analysis of Genes for Biosynthesis of Pyocyanin and Phenazine-1-Carboxamide from *Pseudomonas aeruginosa* PAO1. *Journal of bacteriology,* 183 (21): 6454–6465. doi:10.1128/JB.183.21.6454.

McCaskill, J.S. (1990) The Equilibrium Partition Function and Base Pair Binding Probabilities for RNA Secondary Structure. *Biopolymers*, 29: 1105–1119.

McFarland, K.A., Dolben, E.L., LeRoux, M., *et al*. (2015) A self-lysis pathway that enhances the virulence of a pathogenic bacterium. *Proceedings of the National Academy of Sciences of the United States of America*, 112 (27): 8433–8438. doi:10.1073/pnas.1506299112.

McKnight, S.L.M.C. and Iglewski, B.H. (2000) The Pseudomonas Quinolone Signal Regulates rhl Quorum Sensing in *Pseudomonas aeruginosa*. *Journal of bacteriology,* 182 (10): 2702–2708.

McMorran, B.J., Shantha Kumara, H.M.C., Sullivan, K., *et al*. (2001) Involvement of a transformylase enzyme in siderophore synthesis in *Pseudomonas aeruginosa*. *Microbiology*, 147 (6): 1517–1524. doi:10.1099/00221287-147-6-1517.

Medsker, B., Forno, E., Simhan, H., *et al*. (2016) Prenatal stress, prematurity, and asthma. *Obstetrical & gynecological survey*, 70 (12): 773–779. doi:10.1097/OGX.0000000000000256.

Melville, S. and Craig, L. (2013) Type IV pili in Gram-positive bacteria. *Microbiology and molecular biology reviews : MMBR*, 77 (3): 323–341. doi:10.1128/MMBR.00063-12.

Mendes, R., Garbeva, P. and Raaijmakers, J.M. (2013) The rhizosphere microbiome: significance of plant beneficial, plant pathogenic, and human pathogenic microorganisms. *FEMS Microbiology Reviews* 37: 634–663. doi:10.1111/1574-6976.12028.

Meng, Z. and Limbach, P.A. (2006) Mass spectrometry of RNA: Linking the genome to the proteome. *Briefings in Functional Genomics and Proteomics*, 5 (1): 87–95. doi:10.1093/bfgp/ell012.

Merriman, T.R., Merriman, M.E. and Lamont, I.L. (1995) Nucleotide sequence of pvdD, a pyoverdine biosynthetic gene from *Pseudomonas aeruginosa*: PvdD has similarity to peptide synthetases. *Journal of Bacteriology*, 177 (1): 252–258. doi:10.1128/jb.177.1.252-258.1995.

Michalska, M. and Wolf, P. (2015) *Pseudomonas* Exotoxin A : optimized by evolution for effective killing. F*rontiers in microbiology,* 6 (September): 1–7. doi:10.3389/fmicb.2015.00963.

Minandri, F., Bonchi, C., Frangipani, E., *et al*. (2014) Promises and failures of gallium as an antibacterial agent. *Future microbiology*, 9 (3): 379–397. doi:10.2217/fmb.14.3.

Mishra, M., Mcphail, L., Schlesinger, L.S., *et al*. (2015) *Pseudomonas aeruginosa* Psl polysaccharide reduces neutrophil phagocytosis and the oxidative response by limiting complement-mediated opsonizat*ion*. *mBio,* 14 (1): 95–106. doi:10.1111/j.1462-5822.2011.01704.x.

Miyata, S., Lee, D.G., Drenkard, E., *et al*. (2006) An ordered , nonredundant library of *Pseudomonas aeruginosa* strain PA14 transposon insertion mutants. *Proceedings of the National Academy of Sciences*, 103 (52): 2833–2838.

Montgomery, K., Charlesworth, J.C., LeBard, R., *et al*. (2013) Quorum sensing in extreme environments. *Life (Basel, Switzerland)*, 3 (1): 131–148. doi:10.3390/life3010131.

Moon, A.F., Mueller, G.A., Zhong, X., *et al*. (2010) A synergistic approach to protein crystallization : Combination of a fixed-arm carrier with surface entropy reduction. *Protein Science*, 19: 901–913. doi:10.1002/pro.368.

Mora, L., Heurgué-Hamard, V., De Zamaroczy, M., *et al*. (2007) Methylation of bacterial release factors RF1 and RF2 is required for normal translation termination in vivo. *Journal of Biological Chemistry*, 282 (49): 35638–35645. doi:10.1074/jbc.M706076200.

Moradali, M.F., Ghods, S. and Rehm, B.H.A. (2017) *Pseudomonas aeruginosa* Lifestyle: A Paradigm for Adaptation, Survival, and Persistence. *Frontiers in cellular and infection microbiology*, 7 (February): 39. doi:10.3389/fcimb.2017.00039.

Morrison, A.J.J. and Wenzel, R.P. (1984) Epidemiology of infections due to *Pseudomonas aeruginosa. Reviews of infectious diseases*, 6 Suppl 3: S627-42. doi:10.1093/clinids/6.supplement_3.s627.

Moustafa, M.E., Carlson, B. a, Muhammad, a, *et al*. (2001) Selective inhibition of Selenocysteine tRNA maturation and selenoprotein synthesis in transgenic mice expressing isopentenyladenosine-deficient selenocysteine tRNA. *Molecular and cellular biology*, sopenten., 21 (11): 3840–3852. doi:10.1128/MCB.21.11.3840.

Mowat, E., Paterson, S., Fothergill, J.L., *et al*. (2010) *Pseudomonas aeruginosa* Population Diversity and Turnover in Cystic Fibrosis Chronic Infections. *American journal of respiratory and critical care medicine*, 183(12), 1674–1679. doi:10.1164/rccm.201009-1430OC.

Mukherjee, S., Moustafa, D.A., Stergioula, V., *et al*. (2018) The PqsE and RhlR proteins are an autoinducer synthase-receptor pair that control virulence and biofilm development in *Pseudomonas aeruginosa*. *Proceedings of the National Academy of Sciences of the United States of America*, 115 (40): E9411–E9418. doi:10.1073/pnas.1814023115.

Mulcahy, H., Charron-mazenod, L. and Lewenza, S. (2010) *Pseudomonas aeruginosa* produces an extracellular deoxyribonuclease that is required for utilization of DNA as a nutrient source. *Environmental microbiology,* 12: 1621–1629. doi:10.1111/j.1462-2920.2010.02208.x.

Murcia, N.R., Lee, X., Waridel, P., *et al*. (2015) The *Pseudomonas aeruginosa* antimetabolite L -2-amino-4-methoxy-trans-3-butenoic acid (AMB) is made from glutamate and two alanine residues via

a thiotemplate-linked tripeptide precursor. *Frontiers in Microbiology*, 6 (MAR): 1–13. doi:10.3389/fmicb.2015.00170.

Murgola, E.J., Hijazi, K.A., Goringer, H.U., *et al*. (1988) Mutant 16S ribosomal RNA: A codon-specific translational suppressor. *Proceedings of the National Academy of Sciences of the United States of America*, 85 (12): 4162–4165. doi:10.1073/pnas.85.12.4162.

Murray, T.S. and Kazmierczak, B.I. (2008) *Pseudomonas* aeruginosa Exhibits Sliding Motility in the Absence of Type IV Pili and Flagella. *Journal of bacteriology,* 190 (8): 2700–2708. doi:10.1128/JB.01620-07.

Nakahigashi, K., Kubo, N., Narita, S., *et al*. (2002) HemK, a class of protein methyl transferase with similarity to DNA methyl transferases, methylates polypeptide chain release factors, and hemK knockout induces defects in translational termination. *Proceedings of the National Academy of Sciences of the United States of America*, 99 (3): 1473–1478. doi:10.1073/pnas.032488499.

Nealson, K.H., Platt, T. and Hastings, J.W. (1970) Cellular control of the synthesis and activity of the bacterial luminescent system. *Journal of Bacteriology*, 104 (1): 313–322. doi:10.1128/jb.104.1.313-322.1970.

Nelson, L.K., D'Amours, G.H., Sproule-Willoughby, K.M., *et al*. (2009) *Pseudomonas aeruginosa* las and rhl quorum-sensing systems are important for infection and inflammation in a rat prostatitis model. *Microbiology*, 155 (8): 2612–2619. doi:10.1099/mic.0.028464-0.

Nguyen, A.T., Jones, J.W., Ruge, M.A., *et al*. (2015) Iron depletion enhances production of antimicrobials *by Pseudomonas aeruginosa*. *Journal of Bacteriology*, 197 (14): 2265–2275. doi:10.1128/JB.00072-15.

Nicas, T.I. and Hancock, R.E. (1983) Alteration of susceptibility to EDTA, polymyxin B and gentamicin in Pseudomonas aeruginosa by divalent cation regulation of outer membrane protein H1. *Journal of general microbiology*, 129 (2): 509–517. doi:10.1099/00221287-129-2-509.

Nickzad, A., Déziel, E., Nickzad, A., *et al*. (2015) The involvement of rhamnolipids in microbial cell adhesion and biofilm development – an approach for control? *Letters in applied microbiology*, doi:10.1111/lam.12211.

Nilsson, C. (2003) Lectins: Proteins That Interpret the Sugar Code. *Analytical chemistry*, 75: 348A-353A. doi:10.1021/ac031373w.

Nishijyo, T., Haas, D. and Itoh, Y. (2001) The CbrA-CbrB two-component regulatory system controls the utilization of multiple carbon and nitrogen sources in *Pseudomonas aeruginosa*. *Molecular Microbiology*, 40 (4): 917–931. doi:10.1046/j.1365-2958.2001.02435.x.

Nogales, J., Domínguez-ferreras, A., Amaya-gómez, C. V, *et al*. (2010) Transcriptome profiling of a *Sinorhizobium meliloti* fadD mutant reveals the role of rhizobactin 1021 biosynthesis and regulation genes in the control of swarming. *BMC Genomics*.

Nordfelth, R., Kauppi, A.M., Norberg, H.A., *et al*. (2005) Small-molecule inhibitors specifically targeting type III secretion. *Infection and immunity*, 73 (5): 3104–3114. doi:10.1128/IAI.73.5.3104-3114.2005.

Notti, R.Q. and Stebbins, C.E. (2016) The structure and function of type iii secretion systems. *Virulence Mechanisms of Bacterial Pathogens*, pp. 241–264. doi:10.1128/9781555819286.ch9.

Ó Muimhneacháin, E., Reen, F.J., O'Gara, F., *et al*. (2018) Analogues of *Pseudomonas aeruginosa* signalling molecules to tackle infections. *Organic and Biomolecular Chemistry*, 16 (2): 169–179. doi:10.1039/c7ob02395b.

Obrecht, D., Bernardini, F., Dale, G., *et al*. (2011) Emerging New Therapeutics Against Key Gram-Negative Pathogens. 1st ed. Elsevier Inc. doi:10.1016/B978-0-12-386009-5.00012-6.

Ochsner, U. (2000) Role of the *Pseudomonas aeruginosa* oxyR-recG Operon in Oxidative Stress Defense and DNA Repair : OxyR-Dependent Regulation of katB-ankB , ahpB , and ahpC-ahpF. *Journal of bacteriology,* 182 (16): 4533–4544.

Ochsner, U. a, Snyder, A., Vasil, A.I., *et al*. (2002) Effects of the twin-arginine translocase on secretion of virulence factors, stress response, and pathogenesis. *Proceedings of the National Academy of Sciences of the United States of America*, 99 (12): 8312–8317. doi:10.1073/pnas.082238299.

Ochsner, U., Koch, A., Fiechter, A., *et al*. (1994) Isolation and Characterization of a Regulatory Gene Affecting Rhamnolipid Biosurfactant Synthesis in. *Journal of Bacteriology*, 176 (7): 2044–2054.

Ołdak, E. and Trafny, A. (2005) Secretion of Proteases by *Pseudomonas aeruginosa* Biofilms Exposed to Ciprofloxacin. *Antimicrobial agents and chemotherapy*, 49 (8): 3281–3288. doi:10.1128/AAC.49.8.3281.

Oliver, A., Ciofu, O., Rojo-molinero, E., *et al*. (2017) Antibiotic treatment of biofilm infections. *APMIS: acta pathologica, microbiologica, et immunologica Scandinavica,* (June 2016): 304–319. doi:10.1111/apm.12673.

O'Malley, Y.Q., Reszka, K.J., Spitz, D.R., *et al*. (2004a) *Pseudomonas aeruginosa* pyocyanin directly oxidizes glutathione and decreases its levels in airway epithelial cells. *American journal of physiology. Lung cellular and molecular physiology*, 287 (1): L94-103. doi:10.1152/ajplung.00025.2004.

O'Malley, Y.Q.O., Reszka, K.J., Spitz, D.R., *et al*. (2004b) *Pseudomonas aeruginosa* pyocyanin directly oxidizes glutathione and decreases its levels in airway epithelial cells. *American journal of physiology. Lung cellular and molecular physiology*, pp. 94–103.

Ortori, C.A., Dubern, J.-F., Chhabra, S.R., *et al*. (2011) Simultaneous quantitative profiling of N-acyl-L-homoserine lactone and 2-alkyl-4(1H)-quinolone families of quorum-sensing signaling molecules using LC-MS/MS. *Analytical and bioanalytical chemistry*, 399 (2): 839–850. doi:10.1007/s00216-010-4341-0.

O'Sullivan, B.P. and Freedman, S.D. (2009) Cystic fibrosis. *The Lancet*, 373 (9678): 1891–1904. doi:10.1016/S0140-6736(09)60327-5.

O'Toole, G.A. and Kolter, R. (1998) Flagellar and twitching motility are necessary for *Pseudomonas aeruginosa* biofilm development. *Molecular Microbiology*, 30 (2): 295–304.

Overhage, J., Bains, M., Brazas, M.D., *et al*. (2008) Swarming of *Pseudomonas aeruginosa* is a complex adaptation leading to increased production of virulence factors and antibiotic resistance. *Journal of bacteriology*, 190 (8): 2671–2679. doi:10.1128/JB.01659-07.

Overhage, J., Schemionek, M., Webb, J.S., *et al*. (2005) Expression of the psl operon in *Pseudomonas aeruginosa* PAO1 biofilms: PslA performs an essential function in biofilm formation. *Applied and environmental microbiology*, 71 (8): 4407–4413. doi:10.1128/AEM.71.8.4407-4413.2005.

Ozer, E.A., Allen, J.P. and Hauser, A.R. (2014) Characterization of the core and accessory genomes of Pseudomonas aeruginosa using bioinformatic tools Spine and AGEnt. *BMC Genomics*, 15 (1): 1–17. doi:10.1186/1471-2164-15-737.

Page, M.G. and Heim, J. (2009) Prospects for the next anti-*Pseudomonas* drug. *Current Opinion in Pharmacology*, 9 (5): 558–565. doi:10.1016/j.coph.2009.08.006.

Paliy, O. and Gunasekera, T.S. (2007) Growth of *E . coli* BL21 in minimal media with different gluconeogenic carbon sources and salt contents. *Applied Microbiology and Biotechnology*, 73: 1169–1172. doi:10.1007/s00253-006-0554-8.

Palmer, I. and Wingfield, P.T. (2012) Preparation and Extraction of Insoluble (Inclusion-Body) Proteins from *Escherichia coli*. *Current Protocols in Protein Science*, pp. 1–25. doi:10.1002/0471140864.ps0603s38.Preparation.

Palmer, K.L., Mashburn, L.M., Singh, P.K., *et al*. (2005) Cystic fibrosis sputum supports growth and cues key aspects of *Pseudomonas aeruginosa* physiology. *Journal of bacteriology*, 187 (15): 5267–5277. doi:10.1128/JB.187.15.5267-5277.2005.

Palumbi, S.R. (2001) Humans as the World's Greatest Evolutionary Force. *Science (New York, N.Y.)* 293 (5536): 1786–1790.

Pang, Z., Raudonis, R., Glick, B.R., *et al*. (2019) Antibiotic resistance in *Pseudomonas aeruginosa*: mechanisms and alternative therapeutic strategies. *Biotechnology Advances*, 37 (1): 177–192. doi:10.1016/j.biotechadv.2018.11.013.

Papenfort, K. and Bonnie, B. (2014) Quorum-Sensing Signal-Response Systems in Gram-Negative Bacteria. *Saber Ciencia Y Libertad*, 9 (2): 91–108. doi:10.1038/nrmicro.2016.89.Quorum-Sensing.

Parmely, M., Gale, A., Clabaugh, M., *et al*. (1990) Proteolytic Inactivation of Cytokines by *Pseudomonas aeruginosa*. *Infection and immunity,* 58 (9): 3009–3014.

Passos da Silva, D., Matwichuk, M.L., Townsend, D.O., *et al*. (2019) The *Pseudomonas aeruginosa* lectin LecB binds to the exopolysaccharide Psl and stabilizes the biofilm matrix. *Nature Communications*, pp. 1–11. doi:10.1038/s41467-019-10201-4.

Paulsen, I.T., Press, C.M., Ravel, J., *et al*. (2005) Complete genome sequence of the plant commensal *Pseudomonas fluorescens* Pf-5. *Nature Biotechnology*, 23 (7): 873–878. doi:10.1038/nbt1110.

Pavlovskis, O.R., Edman, D.C., Leppla, S.H., *et al*. (1981) Protection against experimental Pseudomonas aeruginosa infection in mice by active immunization with exotoxin A toxoids. *Infection and immunity*, 32 (2): 681–689. doi:10.1128/iai.32.2.681-689.1981.

Pearson, J.P., Van Delden, C. and Iglewski, B.H. (1999) Active efflux and diffusion are involved in transport of *Pseudomonas aeruginosa* cell-to-cell signals. *Journal of Bacteriology*, 181 (4): 1203–1210. doi:10.1128/JB.181.4.1203-1210.1999.

Pearson, J.P., Gray, K.M., Passador, L., *et al*. (1994) Structure of the autoinducer required for expression of Pseudomonas aeruginosa virulence genes. *Proceedings of the National Academy of Sciences of the United States of America*, 91 (1): 197–201. doi:10.1073/pnas.91.1.197.

Pearson, J.P., Passador, L., Iglewski, B.H., *et al*. (1995) A second N-acylhomoserine lactone signal produced by Pseudomonas aeruginosa. *Proceedings of the National Academy of Sciences of the United States of America*, 92: 1490–1494.

Pearson, J.P., Pesci, E.C. and Iglewski, B.H. (1997) Roles of *Pseudomonas aeruginosa* las and rhl Quorum-Sensing Systems in Control of Elastase and Rhamnolipid Biosynthesis Genes. *Journal of bacteriology*, 179 (18): 5756–5767.

Pearson, W.R. (2013) An Introduction to Sequence Similarity ("Homology") Searching. *International Journal of Research*, 1 (10): 1286–1292. doi:10.1002/0471250953.bi0301s42.An.

Pesci, E.C. (1999) Quinolone signaling in the cell-to-cell communication system of *Pseudomonas aeruginosa*. *Proceedings of the National Academy of Sciences of the United States of America,* 96 (September): 11229–11234.

Pesci, E.C., Pearson, J.P., Seed, P.C., *et al*. (1997) Regulation of las and rhl Quorum Sensing in *Pseudomonas aeruginosa. Journal of Bacteriology*, 179 (10): 3127–3132.

Pessi, G. and Haas, D. (2000) Transcriptional Control of the Hydrogen Cyanide Biosynthetic Genes hcnABC by the Anaerobic Regulator ANR and the Quorum-Sensing Regulators LasR and RhlR in *Pseudomonas aeruginosa*. *Journal of bacteriology,* 182 (24): 6940–6949.

Peters, J.E., Park, S.J., Darzins, A., *et al*. (1992) Further studies *on Pseudomonas aeruginosa* LasA : analysis of specificity. *Molecular microbiology,* 6: 1155–1162.

Peterson, J.W. (1996) *Bacterial Pathogenesis.* In S. Baron (Ed.), *Medical Microbiology*. (4th ed.). University of Texas Medical Branch at Galveston.

Pires, D.P., Cleto, S., Sillankorva, S., *et al*. (2016) Genetically Engineered Phages: a Review of Advances over the Last Decade. *Microbiology and molecular biology reviews : MMBR*, 80 (3): 523–543. doi:10.1128/MMBR.00069-15.

Van Der Ploeg, J.R., Iwanicka-Nowicka, R., Kertesz, M.A., *et al*. (1997) Involvement of CysB and Cbl regulatory proteins in expression of the *tauABCD* operon and other sulfate starvation-inducible genes in Escherichia coli. *Journal of Bacteriology*, 179 (24): 7671–7678. doi:10.1128/jb.179.24.7671-7678.1997.

Polkade, A. V, Mantri, S.S., Patwekar, U.J., *et al*. (2016) Quorum Sensing : An Under-Explored Phenomenon in the Phylum *Actinobacteria*. *Frontiers in microbiology,* 7 (February): 1–13. doi:10.3389/fmicb.2016.00131.

Pollack, M. (1983) The role of exotoxin A in *Pseudomonas* disease and immunity. *Reviews of infectious diseases*, 5 Suppl 5: S979-84. doi:10.1093/clinids/5.supplement_5.s979.

Poole, K. (2005) Aminoglycoside Resistance in *Pseudomonas aeruginosa*. *Antimicrobial agents and chemotherapy*, 49 (2): 479–487. doi:10.1128/AAC.49.2.479.

Popenda, M., Szachniuk, M., Antczak, M., *et al*. (2012) Automated 3D structure composition for large RNAs. *Nucleic Acids Research*, 40 (14): 1–12. doi:10.1093/nar/gks339.

Potron, A., Poirel, L. and Nordmann, P. (2015) Emerging broad-spectrum resistance in *Pseudomonas aeruginosa* and *Acinetobacter baumannii* : Mechanisms and epidemiology. *International Journal of Antimicrobial Agents*, 45 (6): 568–585. doi:10.1016/j.ijantimicag.2015.03.001.

Prentki, P. and Krisch, H.M. (1984) In vitro insertional mutagenesis with a selectable DNA fragment. *Gene*, 29: 303–313.

Price-whelan, A., Dietrich, L.E.P. and Newman, D.K. (2007) Pyocyanin Alters Redox Homeostasis and Carbon Flux through Central Metabolic Pathways in *Pseudomonas aeruginosa PA14* . *Journal of bacteriology*, 189 (17): 6372–6381. doi:10.1128/JB.00505-07.

Priebe, G.P. and Goldberg, J.B. (2014) Vaccines for Pseudomonas aeruginosa: a long and winding road. *Expert review of vaccines*, 13 (4): 507–519. doi:10.1586/14760584.2014.890053.

Pustelny, C., Brouwer, S., Müsken, M., *et al*. (2013) The peptide chain release factor methyltransferase PrmC is essential for pathogenicity and environmental adaptation of *Pseudomonas aeruginosa* PA14. *Environmental Microbiology*, 15 (2): 597–609. doi:10.1111/1462-2920.12040.

Quinaud, M., Chabert, J., Faudry, E., *et al*. (2005) The PscE-PscF-PscG complex controls type III secretion needle biogenesis in *Pseudomonas aeruginosa*. *Journal of Biological Chemistry*, 280 (43): 36293–36300. doi:10.1074/jbc.M508089200.

Raghava, G.P. (2002) A combination method for protein secondary structure prediction based on neural network and example based learning.

Rahim, R., Ochsner, U.A., Olvera, C., *et al*. (2001) Cloning and functional characterization of the *Pseudomonas aeruginosa* rhlC gene that encodes rhamnosyltransferase 2, an enzyme responsible for di-rhamnolipid biosynthesis. *Molecular Microbiology*, 40 (3): 708–718. doi:10.1046/j.1365-2958.2001.02420.x.

Raidt, L. (2015) Increased prevalence and resistance of important pathogens recovered from respiratory specimens of Cystic Fibrosis patients during a decade. *The Pediatric Infectious Disease Journal*, 34 (7).

Rasamiravaka, T. and Jaziri, M. El (2016) Quorum-Sensing Mechanisms and Bacterial Response to Antibiotics in *P . aeruginosa*. *Current Microbiology*.. doi:10.1007/s00284-016-1101-1.

Rampioni, G., Falcone, M., Heeb, S., *et al*. (2016) Unravelling the Genome-Wide Contributions of Specific 2-Alkyl-4-Quinolones and PqsE to Quorum Sensing in *Pseudomonas aeruginosa*. *PLoS Pathogens*, 12 (11): 1–25. doi:10.1371/journal.ppat.1006029.

Rampioni, G., Pustelny, C., Fletcher, M.P., *et al*. (2010) Transcriptomic analysis reveals a global alkyl-quinolone-independent regulatory role for PqsE in facilitating the environmental adaptation of *Pseudomonas aeruginosa* to plant and animal hosts. *Environmental Microbiology*, 12 (6): 1659–1673. doi:10.1111/j.1462-2920.2010.02214.x.

Rashid, M.H. and Kornberg, A. (2000) Inorganic polyphosphate is needed for swimming , swarming , and twitching motilities of *Pseudomonas aeruginosa*. *Proceedings of the National Academy of Sciences of the United States of America*, 97 (9): 4885–4890.

Rasko, D.A. and Sperandio, V. (2010) Anti-virulence strategies to combat bacteria-mediated disease. *Nature Reviews Drug Discovery*, 9 (2): 117–128. doi:10.1038/nrd3013.

Rathert, P., Dhayalan, A., Ma, H., *et al*. (2008) Specificity of protein lysine methyltransferases and methods for detection of lysine methylation of non-histone proteins. *Molecular BioSystems*, 4 (12): 1186. doi:10.1039/b811673c.

Ravel, J. and Cornelis, P. (2003) Genomics of pyoverdine-mediated iron uptake in pseudomonads Jacques. *Trends in Microbiology*, 11 (5): 192–195. doi:10.1016/S0966-842X(03)00100-8.

Read, R.C., Roberts, P., Munro, N., *et al*. (1992) Effect of *Pseudomonas aeruginosa* rhamnolipids on mucociliary transport and ciliary beating. *Journal of applied physiology (Bethesda, Md. : 1985)*, 72 (6): 2271–2277. doi:10.1152/jappl.1992.72.6.2271.

Reading, N.C. and Sperandio, V. (2005) Quorum sensing : the many languages of bacteria. *FEMS Microbiology Letters*, doi:10.1111/j.1574-6968.2005.00001.x.

Regamey, N., Jeffery, P.K., Alton, E.W.F.W., *et al*. (2011) Airway remodelling and its relationship to inflammation in cystic fibrosis. *Thorax*, 66 (7): 624–629. doi:10.1136/thx.2009.134106.

Rice, P., Longden, I. and Bleasby, A. (2000) EMBOSS: the European Molecular Biology Open Software Suite. *Trends in genetics : TIG*, 16 (6): 276—277. doi:10.1016/s0168-9525(00)02024-2.

Rodríguez-Carmona, E., Cano-garrido, O., Seras-franzoso, J., *et al*. (2010) Isolation of cell-free bacterial inclusion bodies. *Microbial Cell Factories*, 9 (71): 1–9.

Rodrıguez-Rojas, A., Mena, A., Martın, S., *et al*. (2016) Inactivation of the *hmgA* gene of *Pseudomonas aeruginosa* leads to pyomelanin hyperproduction , stress resistance and increased persistence in chronic lung infection. *Microbiology*, 115: 1050–1057. doi:10.1099/mic.0.024745-0.

Rohde, C., Wittmann, J. and Kutter, E. (2018) Bacteriophages: A Therapy Concept against Multi-Drug-Resistant Bacteria. *Surgical infections*, 19 (8): 737–744. doi:10.1089/sur.2018.184.

Rohmer, L. (2012) Are pathogenic bacteria just looking for food? Metabolism and microbial pathogenesis. *Trends in microbiology*, 19 (7): 341–348. doi:10.1016/j.tim.2011.04.003.Are.

Rollet, C., Gal, L. and Guzzo, J. (2009) Biofilm-detached cells , a transition from a sessile to a planktonic phenotype : a comparative study of adhesion and physiological characteristics in Pseudomonas aeruginosa. *FEMS Microbiology Letters*, 290: 135–142. doi:10.1111/j.1574-6968.2008.01415.x.

Romero, M., Silistre, H., Lovelock, L., *et al*. (2018) Genome-wide mapping of the RNA targets of the *Pseudomonas aeruginosa* riboregulatory protein RsmN. *Nucleic Acids Research*, 46 (13): 6823–6840. doi:10.1093/nar/gky324.

Ross, R.L., Cao, X. and Limbach, P.A. (2017) Mapping post-transcriptional modifications onto transfer ribonucleic acid sequences by liquid chromatography tandem mass spectrometry. *Biomolecules*, 7 (1). doi:10.3390/biom7010021.

Roy, A., Kucukural, A. and Zhang, Y. (2011) I-TASSER: a unified platform for automated protein structure and function prediction. *Nature Protocols*, 5 (4): 725–738. doi:10.1038/nprot.2010.5.I-TASSER.

Ruer, S., Ball, G., Filloux, A., *et al*. (2008) The “P-usher”, a novel protein transporter involved in fimbrial assembly and TpsA secretion. *The EMBO journal*, 27 (20): 2669–80. doi:10.1038/emboj.2008.197.

Ruer, S., Stender, S., Filloux, A., *et al*. (2007) Assembly of Fimbrial Structures in *Pseudomonas aeruginosa :* Functionality and Specificity of Chaperone-Usher Machineries*. Journal of Bacteriology*, 189 (9): 3547–3555. doi:10.1128/JB.00093-07.

Rutherford, S.T. and Bassler, B.L. (2012) Bacterial quorum sensing: Its role in virulence and possibilities for its control. *Cold Spring Harbor Perspectives in Medicine*, 2 (11): 1–26. doi:10.1101/cshperspect.a012427.

Sakuragi, Y. and Kolter, R. (2007) Quorum-sensing regulation of the biofilm matrix genes (pel) of *Pseudomonas aeruginosa*. *Journal of bacteriology*, 189 (14): 5383–5386. doi:10.1128/JB.00137-07.

Sambrook, J. and Russell, D.W. (2001) Molecular Cloning: A laboratory Manual. 4th ed. Cold Spring Harbor Laboratory Press.

Sampedro, I., Parales, R.E., Krell, T., *et al*. (2015) *Pseudomonas* chemotaxis. *FEMS Microbiology Reviews*, 39 (1): 17–46. doi:10.1111/1574-6976.12081.

Sana, T.G., Soscia, C., Tonglet, C.M., *et al*. (2013) Divergent Control of Two Type VI Secretion Systems by RpoN in *Pseudomonas aeruginosa*. *PLoS ONE*, 8 (10): 1–10. doi:10.1371/journal.pone.0076030.

Sass, G., Miller Conrad, L.C., Nguyen, T.T.H., *et al*. (2020) The *Pseudomonas aeruginosa* product pyochelin interferes with *Trypanosoma* cruzi infection and multiplication in vitro. *Transactions of the Royal Society of Tropical Medicine and Hygiene*, 114 (7): 492–498. doi:10.1093/trstmh/trz136.

Sato, H., Frank, D.W., Hillard, C.J., *et al*. (2003) The mechanism of action of the *Pseudomonas aeruginosa*-encoded type III cytotoxin, ExoU. *EMBO Journal*, 22 (12): 2959–2969. doi:10.1093/emboj/cdg290.

Sato, S., Hayashi, M., Imamura, S., *et al*. (1992a) Primary Structures of the Genes , faoA and faoB , from *Pseudomonas frag*i B-0771 Which Encode the Two Subunits of the HDT Multienzyme Complex Involved in Fatty Acid β-Oxidation. *Journal Biochemistry*, 15 (1): 8–15.

Sato, S., Imamura, S., Ozeki, Y., *et al*. (1992b) Induction of Enzymes Involved in Fatty Acid β-Oxidation in *Pseudomonas frag*i B-0771 Cells Grown in Media Supplemented with Fatty acid. *Journal Biochemistry*, 111 (1): 16–19.

Sauer, K., Camper, A.K., Ehrlich, G.D., *et al*. (2002) *Pseudomonas aeruginosa* displays multiple phenotypes during development as a biofilm. *Journal of bacteriology*, 184 (4): 1140–1154. doi:10.1128/JB.184.4.1140.

Sawa, T., Ito, E., Nguyen, V.H., *et al*. (2014) Anti-PcrV antibody strategies against virulent *Pseudomonas aeruginosa*. *Human vaccines & immunotherapeutics*, 10 (10): 2843–2852. doi:10.4161/21645515.2014.971641.

Scaccabarozzi, L., Leoni, L., Ballarini, A., *et al*. (2015) *Pseudomonas aeruginosa* in Dairy Goats : genotypic and phenotypic comparison of intramammary and environmental isolates. *PLoS ONE*, doi:10.1371/journal.pone.0142973.

Schaber, J.A., Carty, N.L., McDonald, N.A., *et al*. (2004) Analysis of quorum sensing-deficient clinical isolates of *Pseudomonas aeruginosa*. *Journal of medical microbiology*, 53 (Pt 9): 841–853. doi:10.1099/jmm.0.45617-0.

Schlindwein, C., Giordano, G., Santini, C.-L., *et al*. (1990) Identification and expression of the Escherichia coli fdhD and fdhE genes, which are involved in the formation of respiratory formate dehydrogenase. *Journal of Bacteriology*, 172 (10): 6112–6121.

Schoenmakers, E., Carlson, B., Agostini, M., *et al*. (2016) Mutation in human selenocysteine transfer RNA selectively disrupts selenoprotein synthesis. *Journal of Clinical Investigation*, 126 (3): 992–996. doi:10.1172/JCI84747.

Schooling, S.R. and Beveridge, T.J. (2006) Membrane Vesicles : an Overlooked Component of the Matrices of Biofilms. *Journal of bacteriology*, 188 (16): 5945–5957. doi:10.1128/JB.00257-06.

Schooling, S.R., Charaf, U.K., Allison, D.G., *et al*. (2013) A role for rhamnolipid in biofilm dispersion A role for rhamnolipid in biofilm. *Biofilms* , (September 2004). doi:10.1017/S147905050400119X.

Schubert, H.L., Blumenthal, R.M. and Cheng, X. (2003a) Many paths to methyltransfer- a chronic of convergence. *Trends in Biomedical Sciences*, 28 (6): 329–335. doi:10.1016/S0968-0004(03)00090-2.

Schubert, H.L., Phillips, J.D. and Hill, C.P. (2003b) Structures along the catalytic pathway of PrmC/HemK, an N5-glutamine AdoMet-dependent methyltransferase. *Biochemistry*, 42 (19): 5592–5599. doi:10.1021/bi034026p.

Schultz, D.R. and Miller, K.D. (1974) Elastase of *Pseudomonas aeruginosa* : Inactivation of complement components and complement-derived chemotactic and phagocytic factors. *Infection and immunity* , 10 (1): 128–135.

Schurr, M.J. (2013) Which bacterial biofilm exopolysaccharide Is preferred , Psl or Alginate? *Journal of Bacteriology*, 195 (8): 1623–1626. doi:10.1128/JB.00173-13.

Schuster, M. and Greenberg, E.P. (2006) A network of networks : Quorum-sensing gene regulation in *Pseudomonas aeruginosa*. *International Journal of Medical Microbiology*, 296 (2–3): 73–81. doi:10.1016/j.ijmm.2006.01.036.

Shigematsu, T., Fukushima, J., Oyama, M., *et al*. (2001) Iron-Mediated Regulation of Alkaline Proteinase Production in *Pseudomonas aeruginosa*. *Microbiology and immunology,* 45 (8): 579–590.

Shitashiro, M., Tanaka, H., Hong, C.S., *et al*. (2005) Identification of chemosensory proteins for trichloroethylene in *Pseudomonas aeruginosa*. *Journal of Bioscience and Bioengineering*, 99 (4): 396–402. doi:10.1263/jbb.99.396.

Shrout, J.D., Chopp, D.L., Just, C.L., *et al*. (2006) The impact of quorum sensing and swarming motility on *Pseudomonas aeruginosa* biofilm formation is nutritionally conditional. *Molecular Microbiology*, 62 (5): 1264–1277. doi:10.1111/j.1365-2958.2006.05421.x.

Silander, O.K., Tenaillon, O. and Chao, L. (2007) Understanding the Evolutionary Fate of Finite Populations : *The Dynamics of Mutational Effects*. *PLos Biology*, 5 (4). doi:10.1371/journal.pbio.0050094.

Silby, M.W., Winstanley, C., Godfrey, S.A.C., *et al*. (2011) *Pseudomonas* genomes : diverse and adaptable. *FEMS Microbiology Reviews,* 35: 652–680. doi:10.1111/j.1574-6976.2011.00269.x.

Silverman, M. and Simon, M. (1974) Flagellar rotation and the mechanism of bacterial motility. *Nature*, 249 (452): 73–74. doi:10.1038/249073a0.

Simon, R., Priefer, U. and Pühler, A. (1983) A Broad Host Range Mobilization System for *In Vivo* Genetic Engineering: Transposon Mutagenesis in Gram Negative Bacteria. *Nature Biotechnology*, 1: 784–791.

Sirko, A., Hryniewicz, M., Hulanicka, D., *et al*. (1990) Sulfate and thiosulfate transport *in Escherichia coli K-12:* Nucleotide sequence and expression of the cysTWAM gene cluster. *Journal of Bacteriology*, 172 (6): 3351–3357. doi:10.1128/jb.172.6.3351-3357.1990.

Skerker, J.M. and Berg, H.C. (2001) Direct observation of extension and retraction of type IV pili. *Proceedings of the National Academy of Sciences of the United States of America*, *98*(12), 6901–6904.

Smith, R.S. and Iglewski, B.H. (2003) *P . aeruginosa* quorum-sensing systems and virulence. *Current Opinion in Microbiology*, 6: 56–60. doi:10.1016/S1369-5274(03)00008-0.

Soberón-Chávez, G., Aguirre-Ramírez, M. and Sánchez, R. (2005) The *Pseudomonas aeruginosa* RhlA enzyme is involved in rhamnolipid and polyhydroxyalkanoate production. *Journal of Industrial Microbiology and Biotechnology*, 32 (11–12): 675–677. doi:10.1007/s10295-005-0243-0.

Soboh, B., Pinske, C., Kuhns, M., *et al*. (2011) The respiratory molybdo-selenoprotein formate dehydrogenases of Escherichia coli have hydrogen: benzyl viologen oxidoreductase activity. *BMC Microbiology*, 11 (1): 173. doi:10.1186/1471-2180-11-173.

Solovyev, V. and Salamov, A. (2016) Automatic Annotation of Microbial Genomes and Metagenomic Sequences. *Metagenomics and its Applications in Agriculture, Biomedicine and Environmental Studies*, (January 2011): 61–78.

Sonawane, A., Jyot, J. and Ramphal, R. (2006) *Pseudomonas aeruginosa* LecB is involved in pilus biogenesis and protease IV activity but not in adhesion to respiratory mucins. *Infection and Immunity*, 74 (12): 7035–7039. doi:10.1128/IAI.00551-06.

Soukarieh, F., Oton, E.V., Dubern, J.F., *et al*. (2018) *In silico* and *in vitro*-guided identification of inhibitors of alkylquinolone-dependent quorum sensing in *Pseudomonas aeruginosa*. *Molecules*, 23 (2). doi:10.3390/molecules23020257.

Spoering, A.L. and Gilmore, M.S. (2006) Quorum sensing and DNA release in bacterial biofilms. *Current opinion in microbiology*, 9(2), 133–137. doi:10.1016/j.mib.2006.02.004.

Stanier, R.Y., Palleroni, N.J. and Doudoroff, M. (1966) The aerobic *pseudomonads*: a taxonomic study. *Journal of general microbiology*, 43 (2): 159–271. doi:10.1099/00221287-43-2-159.

Starkey, M., Hickman, J.H., Ma, L., *et al*. (2009) *Pseudomonas aeruginosa* Rugose Small-Colony Variants Have Adaptations That Likely Promote Persistence in the Cystic fibrosis lung. *Journal of bacteriology*, 191 (11): 3492–3503. doi:10.1128/JB.00119-09.

Stoodley, P., Sauer, K., Davies, D.G., *et al*. (2002) Biofilms as complex differentiated communities. *Annual review of microbiology*, 56: 187–209. doi:10.1146/annurev.micro.56.012302.160705.

Stover, C.K., Pham, X.Q., Erwin, A.L., *et al*. (2000) Complete genome sequence of *Pseudomonas aeruginos*a PAO1 , an opportunistic pathogen. *Nature*, 406: 959–964.

Strateva, T. and Yordanov, D. (2009) *Pseudomonas aeruginosa* – a phenomenon of bacterial resistance. *Journal of medical microbiology* ,pp. 1133–1148. doi:10.1099/jmm.0.009142-0.

Strempel, N., Neidig, A., Nusser, M., *et al*. (2013) *Human host defense peptide LL-37 stimulates virulence factor production and adaptive resistance in Pseudomonas aeruginosa*. *PLoS ONE,* 8 (12). doi:10.1371/journal.pone.0082240.

Studer, G., Rempfer, C., Waterhouse, A.M., *et al*. (2020) QMEANDisCo—distance constraints applied on model quality estimation. *Bioinformatics*, 36 (6): 1765–1771. doi:10.1093/bioinformatics/btz828.

Sully, E.K. and Geller, B.L. (2016) Antisense antimicrobial therapeutics. *Current opinion in microbiology*, 33: 47–55. doi:10.1016/j.mib.2016.05.017.

Sulochana, M.B., Jayachandra, S.Y., Kumar, S.A., *et al*. (2014) Siderophore as a potential plant growth-promoting agent produced by *Pseudomonas aeruginosa* JAS-25. *Applied biochemistry and biotechnology*, 174 (1): 297–308. doi:10.1007/s12010-014-1039-3.

Sun, J., Deng, Z. and Yan, A. (2014) Biochemical and biophysical research communications bacterial multidrug efflux pumps : Mechanisms , physiology and pharmacological exploitations. *Biochemical and Biophysical Research Communications*, 453 (2): 254–267. doi:10.1016/j.bbrc.2014.05.090.

Sundin, C., Henriksson, M.L., Hallberg, B., *et al*. (2001) Exoenzyme T of *Pseudomonas aeruginosa* elicits cytotoxicity without interfering with Ras signal transduction. *Cellular Microbiology*, 3 (4): 237–246. doi:10.1046/j.1462-5822.2001.00108.x.

Swanson, B.L., Hager, P., Phibbs, P., *et al*. (2000) Characterization of the 2-ketogluconate utilization operon in *Pseudomonas aeruginosa* PAO1. *Molecular Microbiology*, 37 (3): 561–573. doi:10.1046/j.1365-2958.2000.02012.x.

Szklarczyk, D., Gable, A.L., Nastou, K.C., *et al*. (2021) The STRING database in 2021 : customizable protein – protein networks , and functional characterization of user-uploaded gene / measurement sets. *Nucleic acids research*, *49*(D1), D605–D612.

Taguchi, K., Fukutomi, H., Kuroda, A., *et al*. (1997) Genetic identification of chemotactic transducers for amino acids in *Pseudomonas aeruginosa*. *Microbiology*, 143 (10): 3223–3229. doi:10.1099/00221287-143-10-3223.

Tan, M.-W. (1999) Killing of Caenorhabditis elegans *by Pseudomonas aeruginosa* used to model mammalian bacterial pathogenesis*. The Proceedings of the National Academy of Sciences*, 96 (January): 715–720. doi:10.1073/pnas.96.2.715.

Thanabalasuriar, A., Digiandomenico, A., Kubes, P., *et al*. (2017) Bispecific antibody targets multiple *Pseudomonas aeruginosa* evasion mechanisms in the lung vasculature. *The Journal of clinical investigation,* 127 (6): 2249–2261.

Thanbichler, M. and Bock, A. (2002) The function of SECIS RNA in translational control of gene expression in *Escherichia coli. Embo Journal*, 21 (24): 6925–6934. doi:10.1093/emboj/cdf673.

Theuretzbacher, U. and Piddock, L.J.V. (2019) Non-traditional Antibacterial Therapeutic Options and Challenges. *Cell Host and Microbe*, 26 (1): 61–72. doi:10.1016/j.chom.2019.06.004.

Thomann, A., de Mello Martins, A.G.G., Brengel, C., *et al*. (2016) Application of Dual Inhibition Concept within Looped Autoregulatory Systems toward Antivirulence Agents against *Pseudomonas aeruginosa* Infections. *ACS chemical biology*, 11 (5): 1279–1286. doi:10.1021/acschembio.6b00117.

Thomas, J., Thanigaivel, S., Vijayakumar, S., *et al*. (2014) Colloids and Surfaces B : Biointerfaces pathogenecity of *Pseudomonas aeruginosa* in *Oreochromis mossambicus* and treatment using lime oil nanoemulsion. *Colloids and Surfaces B: Biointerfaces*, 116: 372–377. doi:10.1016/j.colsurfb.2014.01.019.

Thompson, J.D., Higgins, D.G. and Gibson, T.J. (1994) CLUSTAL W: Improving the sensitivity of progressive multiple sequence alignment through sequence weighting, position-specific gap penalties and weight matrix choice. *Nucleic Acids Research*, 22 (22): 4673–4680. doi:10.1093/nar/22.22.4673.

Thüring, K., Schmid, K., Keller, P., and Helm, M. (2016). Analysis of RNA modifications by liquid chromatography-tandem mass spectrometry. *Methods*, 107, 48–56. doi:10.1016/j.ymeth.2016.03.019.

Tian, M., Wu, Z., Zhang, R., *et al*. (2022) A new mode of swimming in singly flagellated *Pseudomonas aeruginosa*. *Proceedings of the National Academy of Sciences of the United States of America*, 119 (14): 1–10. doi:10.1073/pnas.2120508119.

Toribio, J., Escalante, A.E. and Soberón-Chávez, G. (2010) Rhamnolipids: Production in bacteria other than *Pseudomonas aeruginosa*. *European Journal of Lipid Science and Technology*, 112 (10): 1082–1087. doi:10.1002/ejlt.200900256.

Totsika, M. (2016) Benefits and Challenges of Antivirulence Antimicrobials at the Dawn of the Post-Antibiotic Era. *Current Medicinal Chemistry*, pp. 30–37. doi:10.2174/2210303106666161605061200.

Toyofuku, M., Roschitzki, B., Riedel, K., *et al*. (2012) Identification of proteins associated with the pseudomonas aeruginosa biofilm extracellular matrix. *Journal of Proteome Research*, 11 (10): 4906–4915. doi:10.1021/pr300395j.

Tremblay, J., Richardson, A., Lépine, F., *et al*. (2007) Self-produced extracellular stimuli modulate the *Pseudomonas aeruginosa* swarming motility behaviour. *Environmental microbiology,* 9: 2622–2630. doi:10.1111/j.1462-2920.2007.01396.x.

Tripathy, S., Kumar, N., Mohanty, S., *et al*. (2007) *Characterisation of Pseudomonas aeruginosa* isolated from freshwater culture systems. *Microbiological Research*, 162. doi:10.1016/j.micres.2006.08.005.

Truan, D., Vasil, A., Stonehouse, M., *et al*. (2013) High-level over-expression , purification , and crystallization of a novel phospholipase C / sphingomyelinase from *Pseudomonas aeruginosa*. *Protein Expression and Purification*, 90 (1): 40–46. doi:10.1016/j.pep.2012.11.005.

Trunk, K., Benkert, B., Quäck, N., *et al*. (2010) Anaerobic adaptation *in Pseudomonas aeruginosa:* Definition of the Anr and Dnr regulons. *Environmental Microbiology*, 12 (6): 1719–1733. doi:10.1111/j.1462-2920.2010.02252.x.

Turnbull, L., Toyofuku, M., Hynen, A.L., *et al*. (2016) Explosive cell lysis as a mechanism for the biogenesis of bacterial membrane vesicles and biofilms. *Nature communications*, doi:10.1038/ncomms11220.

Untergasser, A., Cutcutache, I., Koressaar, T., *et al*. (2012) Primer3-new capabilities and interfaces. *Nucleic Acids Research*, 40 (15): 1–12. doi:10.1093/nar/gks596.

Uwate, M., Ichise, Y., Shirai, A., *et al*. (2013) Two routes of MexS-MexT-mediated regulation of MexEF-OprN and MexAB-OprM efflux pump expression in *Pseudomonas aeruginosa*. *Microbiology and immunology*, 57 (4): 263–272. doi:10.1111/1348-0421.12032.

Vallet, I., Diggle, S.P., Stacey, R.E., *et al*. (2004) Biofilm formation in *Pseudomonas aeruginosa* : fimbrial cup gene clusters are controlled by the transcriptional regulator MvaT. *Journal of Bacteriology*, 186 (9): 2880–2890. doi:10.1128/JB.186.9.2880.

Vallet, I., Olson, J.W. and Lory, S. (2001) The chaperone usher pathways of *Pseudomonas aeruginosa* : Identification of fimbrial gene clusters (cup) and their involvement in biofilm formation. *Proceedings of the National Academy of Sciences of the United States of America, 98*(12), 6911–6916.

Vandenende, C.S., Vlasschaert, M. and Seah, S.Y.K. (2004) Functional characterization of an aminotransferase required for pyoverdine siderophore biosynthesis in *Pseudomonas aeruginosa* PAO1. *Journal of Bacteriology*, 186 (17): 5596–5602. doi:10.1128/JB.186.17.5596-5602.2004.

Vasseur, P., Vallet-Gely, I., Soscia, C., *et al*. (2005) The pel genes of the *Pseudomonas aeruginosa* PAK strain are involved at early and late stages of biofilm formation. *Microbiology*, 151 (3): 985–997. doi:10.1099/mic.0.27410-0.

Veesenmeyer, J.L., Hauser, A.R., Lisboa, T., *et al*. (2009) *Pseudomonas aeruginosa* virulence and therapy. *Critical care medicine*, 37 (5): 1777–1786. doi:10.1097/CCM.0b013e31819ff137.

Ventola, C.L. (2015) The antibiotic resistance crisis: part 1: causes and threats. *P & T : a peer-reviewed journal for formulary management*, 40 (4): 277–283.

Ventre, I., Goodman, A.L., Vallet-gely, I., *et al*. (2006) Multiple sensors control reciprocal expression of *Pseudomonas aeruginosa* regulatory RNA and virulence genes. *Proceedings of the National Academy of Sciences of the United States of America*, 103 (1): 171–176.

Venturi, V. (2006) Regulation of quorum sensing in *Pseudomonas*. *FEMS Microbiology Reviews*, 30: 274–291. doi:10.1111/j.1574-6976.2005.00012.x.

Vleesschauwer, D. De, Cornelis, P. and Höfte, M. (2006) Redox-active pyocyanin secreted by *Pseudomonas aeruginosa* 7NSK2 triggers systemic resistance to *Magnaporthe grisea* but enhances *Rhizoctonia solani* susceptibility in rice. *Molecular plant-microbe interactions : MPMI*, 19 (12): 1406–1419.

Voisard, C., Bull, C.T., Keel, C., et al. (1994) Biocontrol of root diseases by *Pseudomonas fluorescens*, *Plant Pathology and Environmental Microbiology*.

Voynow, J. (2009) Proteases and cystic fibrosis. *The international journal of biochemistry & cell biology* 40: 1238–1245.

Wade, D.S., Calfee, M.W., Rocha, E.R., *et al*. (2005) Regulation of *Pseudomonas* Quinolone Signal synthesis in *Pseudomonas aeruginosa*. *Journal of Bacteriology*, 187 (13): 4372–4380. doi:10.1128/JB.187.13.4372.

Wagner, S., Sommer, R., Hinsberger, S., *et al*. (2016) Novel Strategies for the Treatment of *Pseudomonas aeruginosa* Infections. *Journal of Medicinal Chemistry*, 59 (13): 5929–5969. doi:10.1021/acs.jmedchem.5b01698.

Wai, S.N., Westermark, M., Oscarsson, J., *et al*. (2003) Characterization of dominantly negative mutant ClyA cytotoxin proteins in *Escherichia coli*. *Journal of Bacteriology*, 185 (18): 5491–5499. doi:10.1128/JB.185.18.5491.

Walkenhorst, H.M., Hemschemeier, S.K. and Eichenlaub, R. (1995) Molecular analysis of the molybdate uptake operon, *modABCD*, of *Escherichia coli* and *modR*, a regulatory gene. *Microbiological Research*, 150 (4): 347–361. doi:10.1016/S0944-5013(11)80016-9.

Walker, T.S., Bais, H.P., De, E., *et al*. (2004) *Pseudomonas aeruginosa* -plant root interactions . Pathogenicity , biofilm formation , and root exudation. *Plant Physiology*, 134 (January): 320–331. doi:10.1104/pp.103.027888.such.

Walsh, F. and Amyes, S. (2007) Carbapenem resistance in clinical isolates of *Pseudomonas aeruginosa*. *Journal of Chemotherapy*, 19 (4): 376–381.

Wang, J. and Liu, J.H. (2004) Mutations in the chloramphenicol acetyltransferase (S61G, Y105C) increase accumulated amounts and resistance in *Pseudomonas aeruginosa*. *FEMS Microbiology Letters*, 236 (2): 197–204. doi:10.1016/j.femsle.2004.05.037.

Wang, M., Schaefer, A.L., Dandekar, A.A., *et al*. (2015) Quorum sensing and policing of *Pseudomonas aeruginosa* social cheaters. *Proceedings of the National Academy of Sciences*, 112 (7): 2187–2191. doi:10.1073/pnas.1500704112.

Wang, Y., Kern, S.E. and Newman, D.K. (2010) Endogenous phenazine antibiotics promote anaerobic survival of *Pseudomonas aeruginosa* via extracellular electron transfer. *Journal of bacteriology*, 192 (1): 365–369. doi:10.1128/JB.01188-09.

Wassenaar, T.M. and Meinersmann, R.J. (2006) The TGA stop codon and the phylogeny of the selenocysteine pathway. *Genome Letters*, 2 (4): 127–138. doi:10.1166/gl.2004.030.

Waterhouse, A., Bertoni, M., Bienert, S., *et al*. (2018) SWISS-MODEL: homology modelling of protein structures and complexes. *Nucleic Acids Research*, 46 (W1): W296–W303. doi:10.1093/nar/gky427.

Wei, Q. and Ma, L.Z. (2013*)* Biofilm Matrix and Its Regulation in *Pseudomonas aeruginosa*. *International journal of molecular sciences*, pp. 20983–21005. doi:10.3390/ijms141020983.

Werner, E., Roe, F., Bugnicourt, A., *et al*. (2004) Stratified growth in *Pseudomonas aeruginosa* biofilms. *Applied and environmental microbiology*, 70 (10): 6188–6196. doi:10.1128/AEM.70.10.6188.

Whitchurch, C.B., Leech, A.J., Young, M.D., *et al*. (2004) Characterization of a complex chemosensory signal transduction system which controls twitching motility in *Pseudomonas aeruginosa*. *Molecular Microbiology*, 52 (3): 873–893. doi:10.1111/j.1365-2958.2004.04026.x.

Whitchurch, C.B., Tolker-Nielsen, T., Ragas, P.C., *et al*. (2002) Extracellular DNA required for bacterial biofilm formation. *Science (New York, N.Y.)*, 295 (5559): 1487. doi:10.1126/science.295.5559.1487.

Whitehead, N.A., Barnard, A.M.L., Slater, H., *et al*. (2001) Quorum-sensing in Gram-negative bacteria. *FEMS Microbiology Letters*, 25: 365–404.

Wilderman, P.J., Vasil, A.I., Johnson, Z., *et al*. (2001) Characterization of an endoprotease (PrpL) encoded by a PvdS-regulated gene in *Pseudomonas aeruginosa*. *Infection and immunity,* 69 (9): 5385–5394. doi:10.1128/IAI.69.9.5385.

Williams, B.R.J., Dehnbostel, J.O. and Blackwell, T.I.S. (2010) *Pseudomonas aeruginosa :* host defence in lung diseases. *Respirology* , 2010 (May). doi:10.1111/j.1440-1843.2010.01819.x.

Williams, P. (2007) Quorum sensing , communication and cross-kingdom signalling in the bacterial world. *Microbiology*, 153: 3923–3938. doi:10.1099/mic.0.2007/012856-0.

Williams, P., Bainton, N.J., Swift, S., *et al*. (1992) Small molecule-mediated density-dependent control of gene expression in prokaryotes: bioluminescence and the biosynthesis of carbapenem antibiotics. *FEMS Microbiology Letters*, 100 (1–3): 161–167. doi:10.1016/0378-1097(92)90204-2.

Williams, P. and Camara, M. (2009) Quorum sensing and environmental adaptation in *Pseudomonas aeruginosa* : a tale of regulatory networks and multifunctional signal molecules. *Current Opinion in Microbiology*, 12: 182–191. doi:10.1016/j.mib.2009.01.005.

Williams, P., Fletcher, M.P., Diggle, S.P., *et al*. (2007) Biosensor-based assays for PQS , HHQ and related 2-alkyl-4-quinolone quorum sensing signal molecules. *Nature Protocols*, 2 (5): 1254–1262. doi:10.1038/nprot.2007.158.

Wilton, M., Charron-Mazenod, L., Moore, R., *et al*. (2016) Extracellular DNA acidifies biofilms and induces aminoglycoside resistance in *Pseudomonas aeruginosa*. *Antimicrobial agents and chemotherapy*, 60 (1): 544–553. doi:10.1128/AAC.01650-15.

Winsor, G.L., Griffiths, E.J., Lo, R., *et al*. (2016) Enhanced annotations and features for comparing thousands of *Pseudomonas* genomes in the *Pseudomonas* genome database. *Nucleic Acids Research*, 44 (November 2015): 646–653. doi:10.1093/nar/gkv1227.

Winstanley, C. and Fothergill, J.L. (2008) The role of quorum sensing in chronic cystic fibrosis *Pseudomonas aeruginosa* infections. *FEMS Microbiology Letters*, 290: 1–9. doi:10.1111/j.1574-6968.2008.01394.x.

Winzer, K., Hardie, K.R., Burgess, N., *et al*. (2002) LuxS : its role in central metabolism and the *in vitro* synthesis of 4-hydroxy-5-methyl-3 (2H)-furanone. *Microbiology*, 148: 909–922.

Winzer, K. and Williams, P. (2001) Quorum sensing and the regulation of virulence gene expression in pathogenic bacteria. *International journal of medical microbiology : IJMM*, 291 (2): 131–143. doi:10.1078/1438-4221-00110.

Wolfgang, M.C., Jyot, J., Goodman, A.L., *et al*. (2004) *Pseudomonas aeruginosa* regulates flagellin expression as part of a global response to airway fluid from cystic fibrosis patients. *Proceedings of the National Academy of Sciences of the United States of America*, 101 (17): 6664–6668. doi:10.1073/pnas.0307553101.

Wolfgang, M.C., Kulasekara, B.R., Liang, X., *et al*. (2003) Conservation of genome content and virulence determinants among clinical and environmental isolates of *Pseudomonas aeruginosa*. *The Proceedings of the National Academy of Sciences*, 100 (14).

Wood, T.K., Knabel, S.J. and Kwan, W. (2013) Bacterial persister cell formation and dormancy., *Applied and environmental microbiology,* 79 (23): 7116–7121. doi:10.1128/AEM.02636-13.

Woodford, N. and Wareham, D.W. (2009) Tackling antibiotic resistance: a dose of common antisense? *The Journal of antimicrobial chemotherapy*, 63 (2): 225–229. doi:10.1093/jac/dkn467.

Worlitzsch, D., Tarran, R., Ulrich, M., *et al*. (2002) Effects of reduced mucus oxygen concentration in airway *Pseudomonas* infections of cystic fibrosis patients. *The Journal of clinical investigation,* 109 (3): 317–325. doi:10.1172/JCI200213870.Introduction.

Wu, W., Badrane, H., Arora, S., *et al*. (2004) MucA-mediated coordination of type III secretion and alginate synthesis in *Pseudomonas aeruginosa*. *Journal of Bacteriology*, 186 (22): 7575–7585. doi:10.1128/JB.186.22.7575-7585.2004.

Xia, A., Qian, M., Wang, C., *et al*. (2021) Optogenetic modification of *Pseudomonas aeruginosa* enables controllable twitching motility and host infection. *ACS Synthetic Biology*, 10 (3): 531–541. doi:10.1021/acssynbio.0c00559.

Xiao, G., Déziel, E., He, J., *et al*. (2006) MvfR, a key *Pseudomonas aeruginosa* pathogenicity LTTR-class regulatory protein has dual ligands. *Molecular Microbiology*, 62 (6): 1689–1699. doi:10.1111/j.1365-2958.2006.05462.x.

Xiao, G., He, J. and Rahme, L.G. (2016) Mutation analysis of the *Pseudomonas aeruginosa mvfR* and *pqsABCDE* gene promoters demonstrates complex quorum-sensing circuitry. *Microbiology*, 152 (2006): 1679–1686. doi:10.1099/mic.0.28605-0.

Xiong, Y., Caillon, J., Drugeon, H., *et al*. (1996) Influence of pH on adaptive resistance of *Pseudomonas aeruginosa* to aminoglycosides and their postantibiotic effects. *Antimicrobial Agents Chemotherapy,* 40 (1): 35–39.

Yahr, T.L., Goranson, J. and Frank, D.W. (1996) Exoenzyme S of *Pseudomonas aeruginosa* is secreted by a type III pathway. *Molecular microbiology*, 22 (5): 991–1003. doi:10.1046/j.1365-2958.1996.01554.x.

Yahr, T.L., Vallis, A.J., Hancock, M.K., *et al*. (1998) ExoY, an adenylate cyclase secreted by the *Pseudomonas aeruginosa* type III system. *Proceedings of the National Academy of Sciences of the United States of America*, 95 (23): 13899–13904. doi:10.1073/pnas.95.23.13899.

Yang, F., Gu, J., Yang, L., *et al*. (2017) Protective efficacy of the trivalent *Pseudomonas aeruginosa* vaccine candidate PcrV-OprI-Hcp1 in murine pneumonia and burn models. *Scientific reports*, 7 (1): 3957. doi:10.1038/s41598-017-04029-5.

Yang, H., Shan, Z., Kim, J., *et al*. (2007) Regulatory role of PopN and its interacting partners in type III secretion of *Pseudomonas aeruginosa*. *Journal of Bacteriology*, 189 (7): 2599–2609. doi:10.1128/JB.01680-06.

Yang, H., Wang, Z., Shen, Y., *et al*. (2010) Crystal structure of the nosiheptide-resistance methyltransferase of *Streptomyces actuosus*. *Biochemistry*, 49 (30): 6440–6450. doi:10.1021/bi1005915.

Yang, J., Yan, R., Roy, A., *et al*. (2015) The I-TASSER Suite: protein structure and function prediction. *Nature Methods*, 12 (1): 7–8. doi:10.1038/nmeth.3213.

Yang, L., Hu, Y. and Liu, Y. (2011a) Distinct roles of extracellular polymeric substances in *Pseudomonas aeruginosa* biofilm development. *Environmental microbiology,* (May). doi:10.1111/j.1462-2920.2011.02503.x.

Yang, L., Jelsbak, L., Lykke, R., *et al*. (2011b) Evolutionary dynamics of bacteria in a human host environment. *The Proceedings of the National Academy of Sciences*, 108 (18): 7481–7486. doi:10.1073/pnas.1018249108.

Yang, Y., Heffernan, R., Paliwal, K., *et al*. (2017) SPIDER2: a package to predict secondary structure, accessible surface area, and main-chain torsional angles by Deep Neural Networks. *Methods in molecular biology,* 1484: 55—63. doi:10.1007/978-1-4939-6406-2_6.

Yao, X., He, W. and Lu, C.D. (2011) Functional characterization of seven γ-glutamylpolyamine synthetase genes and the *bauRABCD* locus for polyamine and β-alanine utilization in *Pseudomonas aeruginosa* PAO1. *Journal of Bacteriology*, 193 (15): 3923–3930. doi:10.1128/JB.05105-11.

Yeterian, E., Martin, L.W., Guillon, L., *et al*. (2010) Synthesis of the siderophore pyoverdine in *Pseudomonas aeruginosa* involves a periplasmic maturation. *Amino Acids*, 38 (5): 1447–1459. doi:10.1007/s00726-009-0358-0.

Yeung, A.T.Y., Parayno, A. and Hancock, R.E.W. (2012) Mucin promotes rapid surface motility in *Pseudomonas aeruginosa*. *mBio*, 3 (3): 1–12. doi:10.1128/mBio.00073-12.Editor.

Yeung, A.T.Y., Torfs, E.C.W., Jamshidi, F., *et al*. (2009) Swarming of *Pseudomonas aeruginosa* is controlled by a broad spectrum of transcriptional regulators , including MetR. *Journal of bacteriology*, 191 (18): 5592–5602. doi:10.1128/JB.00157-09.

Yoon, M.Y., Lee, K.M., Park, Y., *et al*. (2011) Contribution of cell elongation to the biofilm formation of *Pseudomonas aeruginosa* during anaerobic respiration. *PLoS ONE*, 6 (1): 1–11. doi:10.1371/journal.pone.0016105.

Yoon, S.S., Hennigan, R.F., Hilliard, G.M., et al. (2002) *Pseudomonas aeruginosa* anaerobic respiration in biofilms : relationships to cystic fibrosis pathogenesis. *Developmental cell*, 3: 593–603.

Yoshizawa, S. and Böck, A. (2009) The many levels of control on bacterial selenoprotein synthesis. *Biochimica et Biophysica Acta - General Subjects*, 1790 (11): 1404–1414. doi:10.1016/j.bbagen.2009.03.010.

Zaborin, A., Romanowski, K., Gerdes, S., *et al*. (2009) Red death in *Caenorhabditis elegans* caused by *Pseudomonas aeruginosa* PAO1. *Proceedings of the National Academy of Sciences of the United States of America*, 106 (15): 6327–6332. doi:10.1073/pnas.0813199106.

Zegans, M.E., Wozniak, D., Griffin, E., *et al*. (2012) *Pseudomonas aeruginosa* exopolysaccharide Psl promotes resistance to the biofilm inhibitor Polysorbate *80*. *Antimicrobial agents and Chemotherapy*, 56 (8): 4112–4122. doi:10.1128/AAC.00373-12.

Zhang, Y. (2008) I-TASSER server for protein 3D structure prediction. *BMC Bioinformatics*, 9 (40): 1–8. doi:10.1186/1471-2105-9-40.

Zhang, Y. and Gladyshev, V.N. (2005) An algorithm for identification of bacterial selenocysteine insertion sequence elements and selenoprotein genes. *Bioinformatics*, 21 (11): 2580–2589. doi:10.1093/bioinformatics/bti400.

Zhang, Y., Romero, H., Salinas, G., *et al*. (2006) Dynamic evolution of selenocysteine utilization in bacteria: A balance between selenoprotein loss and evolution of selenocysteine from redox active cysteine residues. *Genome Biology*, 7 (10). doi:10.1186/gb-2006-7-10-r94.

Zhang, Y.M., Frank, M.W., Zhu, K., *et al*. (2008) PqsD is responsible for the synthesis of 2,4-dihydroxyquinoline, an extracellular metabolite produced by *Pseudomonas aeruginosa*. *Journal of Biological Chemistry*, 283 (43): 28788–28794. doi:10.1074/jbc.M804555200.

Zhao, K., Tseng, B.S., Beckerman, B., *et al*. (2014) Psl trails guide exploration and microcolony formation in early *P. aeruginosa* biofilms. *Nature,* 497 (7449): 388–391. doi:10.1038/nature12155.

Zhu, J. and Kaufmann, G.F. (2013) Quo vadis quorum quenching ? *Current Opinion in Pharmacology*, 13 (5): 688–698. doi:10.1016/j.coph.2013.07.003.

Zhu, K., Choi, K.H., Schweizer, H.P., *et al*. (2006) Two aerobic pathways for the formation of unsaturated fatty acids in *Pseudomonas aeruginosa*. *Molecular Microbiology*, 60 (2): 260–273. doi:10.1111/j.1365-2958.2006.05088.x.

Zhu, K. and Rock, C.O. (2008) RhlA converts β-hydroxyacyl-acyl carrier protein intermediates in fatty acid synthesis to the β-hydroxydecanoyl-β-hydroxydecanoate component of rhamnolipids in *Pseudomonas aeruginosa*. *Journal of Bacteriology*, 190 (9): 3147–3154. doi:10.1128/JB.00080-08.

Zinoni, F., Heider, J. and Böck, A. (1990) Features of the formate dehydrogenase mRNA necessary for decoding of the UGA codon as selenocysteine. *Proceedings of the National Academy of Sciences of the United States of America*, 87 (12): 4660–4. doi:10.1073/PNAS.87.12.4660.

Zuker, M. and Stiegler, P. (1980) Optimal computer folding of large RNA sequences using thermodynamics and auxiliary information. *Nucleic Acids Research*, 9 (11981): 133–148.

Zulianello, L., Canard, C., Köhler, T., *et al*. (2006) Rhamnolipids are virulence factors that promote early infiltration of primary human airway epithelia by *Pseudomonas aeruginosa*. *Infection and immunity*, 74 (6): 3134–3147. doi:10.1128/IAI.01772-05.